LA-12908-MS

Status of Volcanism Studies for the Yucca Mountain Site Characterization Project

Los Alamos
NATIONAL LABORATORY

Los Alamos National Laboratory is operated by the University of California for the United States Department of Energy under contract W-7405-ENG-36.

DISTRIBUTION OF THIS DOCUMENT IS UNLIMITED

Edited by Susan H. Klein, Group CIC-1

This work was supported by the Yucca Mountain Site Characterization Office as part of the Civilian Radioactive Waste Management Program. This project is managed by the U.S. Department of Energy, Yucca Mountain Site Characterization Project. A list of notebooks and samples used to obtain data cited in this report will be included as an appendix to this report. The appendix will be issued by December 31, 1995; its unique identifier assigned to this appendix is LA-EES-13-LV-12-95-002. To obtain references before the appendix is issued, contact Kean Finnegan at (702)-794-7273. The Los Alamos data tracking number for this work is LA000000000093.001.

An Affirmative Action/Equal Opportunity Employer

This report was prepared as an account of work sponsored by an agency of the United States Government. Neither The Regents of the University of California, the United States Government nor any agency thereof, nor any of their employees, makes any warranty, express or implied, or assumes any legal liability or responsibility for the accuracy, completeness, or usefulness of any information, apparatus, product, or process disclosed, or represents that its use would not infringe privately owned rights. Reference herein to any specific commercial product, process, or service by trade name, trademark, manufacturer, or otherwise, does not necessarily constitute or imply its endorsement, recommendation, or favoring by The Regents of the University of California, the United States Government, or any agency thereof. The views and opinions of authors expressed herein do not necessarily state or reflect those of The Regents of the University of California, the United States Government, or any agency thereof.

DISCLAIMER

Portions of this document may be illegible in electronic image products. Images are produced from the best available original document.

LA-12908-MS

UC-802
Issued: February 1995
Revised: March 1995

Status of Volcanism Studies for the Yucca Mountain Site Characterization Project

B. Crowe
F. Perry
*J. Geissman**
*L. McFadden**
*S. Wells***
M. Murrell
J. Poths
G. A. Valentine
L. Bowker†
K. Finnegan†

Los Alamos National Laboratory, Los Alamos, New Mexico
**University of New Mexico*
***University of California, Riverside*
†*University of Nevada, Las Vegas*

MASTER

DISTRIBUTION OF THIS DOCUMENT IS UNLIMITED

Los Alamos
NATIONAL LABORATORY
Los Alamos, New Mexico 87545

STATUS OF VOLCANISM STUDIES FOR

THE YUCCA MOUNTAIN SITE CHARACTERIZATION PROJECT

by

B. Crowe, F. Perry, J. Geissman, L. McFadden, S. Wells, M. Murrell, J. Poths, G. A. Valentine, L. Bowker, and K. Finnegan

ABSTRACT

Chapter 1 introduces the volcanism issue for the Yucca Mountain site and provides the reader with an overview of the organization, content, and significant conclusions of this report. The risk of future basaltic volcanism is the primary topic of concern including both events that intersect a potential repository and events that occur near or within the waste isolation system of a repository. Future volcanic events cannot be predicted with certainty but instead are estimated using formal methods of probabilistic volcanic hazard assessment. Chapter 2 describes the volcanic history of the Yucca Mountain region (YMR) and emphasizes the Pliocene and Quaternary volcanic record, the interval of primary concern for volcanic risk assessment. The distribution, eruptive history, and geochronology of Plio-Quaternary basalt centers are described by individual center emphasizing the two cycles of the Postcaldera basalt, the Older postcaldera basalt and the Younger postcaldera basalt. The Lathrop Wells volcanic center is described in detail because it is the youngest basalt center in the YMR; it has been problematic to establish the geochronology of the center; and it probably formed during multiple, time-separate eruptive events, an unexpected difference from typical monogenetic basaltic volcanic centers. Chapter 3 describes the tectonic setting of the YMR and presents and assesses the significance of multiple alternative tectonic models. The Crater Flat volcanic zone is defined and described as one of many alternative models of the structural controls of the distribution of Plio-Quaternary basalt centers in the YMR. Geophysical data are described for the YMR and are used as an aid to understand the distribution of basaltic volcanic centers. Chapter 4 discusses the petrologic and geochemical features of basaltic volcanism in the YMR, the southern Great Basin and the Basin and Range province. Geochemical and isotopic data are described that indicate basalt of the southern Great Basin was derived from ancient lithospheric mantle. The long time of activity and characteristic small volume of the Postcaldera basalt of the YMR result in one of the lowest eruptive rates in a volcanic field in the southwest United States. Quaternary lavas of the YMR lack plagioclase phenocrysts and fractionated at high pressure in the lower crust or upper mantle before ascent and eruption. The compositional variation of the Lathrop Wells center provides strong evidence of formation from separate and unrelated magma batches. Chapter 5 summarizes current concepts of the segregation, ascent, and eruption of basalt magma. Magma ascending as dikes probably followed northwest-trending structure at depth and diverted at shallow depths following the direction of maximum compressive stress. Chapter 6 summarizes the history of volcanism studies (1979 through early 1994), including work for the Yucca Mountain Site Characterization Project and overview studies by the state of Nevada and the Nuclear Regulatory Commission. Chapter 7 summarizes probabilistic volcanic hazard assessment using a three-part conditional probability model. Revised probability estimates are presented for the recurrence rate (E1), the disruption probability (E2), and the probability of magmatic disruption of the Yucca Mountain site, the controlled area, and a volcanic event in the YMR. Simulation modeling is applied to describe the uncertainty of these estimates using minimum, maximum, and midpoint estimates and multiple alternative models of E1. Sensitivity analyses using simulation modeling show that E1 is well constrained, E2 shows more variability, and 50 percentile estimates (median) of the probability of magmatic disruption of the Yucca Mountain site are about 2×10^{-8} events yr^{-1}. These estimates are similar to most published probability estimates. Chapter 8 describes remaining volcanism work judged to be needed to complete characterization studies for the YMP. Chapter 9 summarizes the conclusions of this volcanism status report.

I. Preface

Use this preface as a reading guide to this volcanism status report, a lengthy report that describes a complex topic, and summarizes a wide range of work covering more than a decade of volcanism studies. The report is not designed to be read in sequence. Rather, it is split into distinct topics that can be read independently. The introduction (Chapter 1) provides an overview of the scope of the report and can be used as a guide to the content of the different chapters and the major conclusions of the report. Chapter 2 describes the background geology of the record of basaltic volcanism in the Yucca Mountain region and site characterization data for basaltic volcanic centers in order of decreasing age. A large part of the chapter discusses the geology, eruptive models, and chronology of the Lathrop Wells center. Those readers interested in this at times controversial topic should focus on this chapter. It also covers current applications of a range of geochronology methods to a topical problem of establishing, with an acceptable degree of confidence, the timing of Quaternary volcanic events. Chapter 3 is concerned primarily with the tectonic setting of the Yucca Mountain region. The current tectonic models for the area, ranging from detachment, to caldera, to pull-apart basins are described. The relationship of basaltic volcanic activity to the different tectonic models, both real and possibly nonreal, are discussed. The wide range of geophysical data for the site region is summarized and examined with respect to its implications for understanding the tectonic setting of volcanism in this region. Chapter 4 provides an overview of basaltic volcanism in the Great Basin and Basin and Range province from a geochemical and petrologic perspective. Patterns of small volume basaltic volcanism in the interior of the province are contrasted with much larger volume and more active fields at the province boundaries. Consideration is given to the evolutionary patterns of basaltic volcanism both at the scale of a volcanic field and at individual volcanic centers. Chapter 5 reviews the dynamics of magma segregation, migration, storage, and eruption of basaltic magma. There has been much progress in quantifying processes of magmatism in the last decade, and some of this progress can be applied to the timing, setting, and location of sites of basaltic volcanism in the Yucca Mountain region. Chapter 6 summarizes, in chronological order, the history of volcanism studies associated with the Yucca Mountain Project. This should prove to be a useful chapter for readers attempting to gain an overview perspective on the scope and logic of volcanism studies. Chapter 7 is concerned entirely with a probabilistic assessment of the risk of future volcanism for the Yucca Mountain site. This is the suggested chapter to read for those who want, without wading through the accompanying details, to find out what the volcanism problem is, how it is being studied, and what it means. We present the results of the most recent and comprehensive assessment of the conditional probability of magmatic disruption of the repository, the controlled area, and the Yucca Mountain region. Chapter 8 attempts to present in abbreviated form what future work needs to be accomplished to complete volcanism studies and why conclusions concerning the probability of magmatic disruption are unlikely to change. Finally, Chapter 9 presents the conclusions of the report, chapter by chapter. Those readers with limited time should read the introduction and the conclusions. Hopefully, some of the information may catch your attention and lead you to read other parts of the report.

II. Changes In The Final Version Of The Report

The preliminary version of this volcanism status report was reviewed by many people from many different organizations, and we attempted to accommodate as many of the review suggestions as possible. In the hope of saving time and reducing the reading load of those who read the preliminary version, we have provided the following brief comments on the major changes between the preliminary and final versions. Chapter 1 received only minor editing, and the most significant changes were made in the conclusions. Chapter 2 was extensively rewritten, and new data were provided from several sources. First, the results of continuing chronology studies were incorporated throughout the text including new $^{40}Ar/^{39}Ar$ results for several basalt centers. This method shows considerable promise for basalt centers older than a few hundred

thousand years, and it has given us considerably more confidence that the chronology task is nearly complete. Second, the results of trenching, field mapping, geomorphology, and particularly geochemistry studies for the Lathrop Wells center have at last converged. We have high confidence that the eruptive sequences of the volcanic center are correctly identified. The chronostratigraphic subdivisions have remained firm through repeated tests against insights provided from extremely detailed geochemical data and over 30 additional trenches. Also, there appears to be convergence between the results of our studies at Lathrop Wells and the results of trenching studies for the tectonics program conducted by the U.S. Geological Survey. Trench exposures of basaltic ash at multiple trench sites almost certainly were derived from the Lathrop Wells center and provide some additional support for polygenetic volcanism at the center. We are still not quite sure exactly how old the ashes are or which chronostratigraphic unit correlates with which ash, but the number of possibilities has narrowed, and will be constrained in the future using geochemical correlation tools. We also made a change in terminology for referring to eruption models for the basalt centers of the Yucca Mountain region. The preliminary versions of the volcanism status report used the term "polycyclic" volcanism to describe small volume, basaltic volcanic centers that exhibit multiple, time-separate volcanic events. This usage resulted in confusion over the semantics of the term and that confusion has obscured the more important underlying conceptual distinctions between eruption models. We therefore have changed the term "polycyclic" to the more widely accepted term "polygenetic". Finally, new results have been obtained using step-heating $^{40}Ar/^{39}Ar$ age measurements of silicic tuff fragments in volcanic units of the Lathrop Wells center. This is new work being conducted by W. McIntosh and M. Heizler, at the New Mexico Bureau of Mines. The results are too preliminary to report in this paper but may suggest somewhat younger ages for chronostratigraphic units I and II than are reported herein. Just prior to the last revision of this report (March, 1995), final U-Th disequilibrium age determinations were obtained. These results are similar to the step-heating $^{40}Ar/^{39}Ar$ and support younger ages for chronostratigraphic units II and III. The data also strongly support age differences between chronostratigraphic units I and III.

Most changes in Chapter 3 were minor, but a major advancement that could only be incorporated in part is the new results from tectonic studies of Crater Flat conducted by Chris Fridrich and others with the U.S. Geological Survey. His tectonic model brings together many different observations on the origin of Crater Flat and will be the subject of future papers. Chapter 4 received extensive rewrites with new insights provided by the major and trace-element data for the Lathrop Wells center. These results provide increased support for the interpretation that the volcanic center is *not* a simple monogenetic center. That an alternative model of multiple, time-separate eruptions at the Lathrop Wells center must be considered for volcanic risk assessment remains valid despite numerous tests designed to disprove the model. We are fully (and sometimes painfully) aware that the polygenetic model is not widely accepted in the volcanological community, but popularity should not be the criterion for judging scientific models and we cannot dismiss field, geochemical, geomorphic, and soil data supporting the model. Not accepting and assessing this admittedly controversial eruption model would be equivalent to a Type II statistical error and possibly lead to underestimation of the risk of volcanism for the Yucca Mountain site. Chapter 5 also received only minor editing. A new section was added at the end of this chapter, on future applications of studies from magma dynamics and a cross section was drawn showing magma sources in the southern Great Basin. Chapter 6 was updated to add results from new papers, most of which were presented at the 1993 High Level Waste and *Focus '93* conferences.

Chapter 7 was extensively rewritten and simulation modeling was completed for E1, E2, and E1 given E2. The new results have led to significant advances in understanding of the results of probabilistic volcanic hazard assessment. These data show conclusively that there is *little difference* between competing recurrence models. Moreover, estimated values of the probability of magmatic disruption of the potential repository show surprising agreement among different workers despite the use of somewhat different perspectives and assumptions. That agreement has not and probably will not curtail lively

debates over the significance of future volcanism, but hopefully future discussions will encompass the more pertinent topics of the eruptive and subsurface effects of volcanic events near a repository. Chapters 8 and 9 have been changed to reflect the changes in the rest of the chapters of the volcanism status report.

III. Acknowledgments

The idea of developing an overview document covering all volcanism studies was developed with David Dobson, now with Golder Associates. The volcanism studies have involved a team effort that crosses a range of disciplines. The report is the product of contributions from the following people:

Les McFadden, Soil Studies
Stephen Wells, Geomorphic Studies
Jane Poths, Cosmogenic Helium
John Geissman, Paleomagnetism
Mike Murrell, U-Th Disequilibrium
Frank Perry, Field/Petrology
Greg Valentine, Volcanic Effects
Bruce Crowe, Field/Probability Studies
Andrew Burningham, Quality Assurance
Lynn Bowker, Field Studies and Trenching
W. Zeitler, Ar/Ar Studies
Kean Finnegan, Field Studies and Trenching

We are grateful to Jeanne Nesbit, Department of Energy (DOE), for her encouragement, persistence, and patience in supporting the completion of this report. Carl Gertz, DOE, was the Project Manager of YMP during important years of the volcanism work. Our studies were facilitated greatly by his support of focused science, and his commitment to quality and integrity in scientific studies. Don DePaolo served as scientific advisor to the geochronology studies. We benefited substantially from his insightful advice and his willingness to allow us to use his reflective comments in our report. Over the years, there have been many important discussions with many other researchers. The researchers who have contributed substantially are W. J. Carr, Gary Dixon, David Vaniman, Scott Sinnock, David Dobson, Chris Fridrich, Chris Menges, Steve Nelson, John Whitney, and Jeanne Nesbit. The draft report was reviewed by too many people to list. Craig Scherschel provided support in field studies and in scanning figures, assembling maps, tracing down references, digging trenches, and filing safety plans. Allison Inglett's support in graphics was invaluable. Kelly Quintana compiled, typed, edited, proofread, and assembled the preliminary draft of the report. Susan Klein edited the Preface, Chapters 1 and 2, and provided assistance and essential advice in assembling the final draft of the document. Jesse Peel assisted in editing of the final version of the report. The records and quality assurance requirements of the YMP can be intimidating. Andrew Burningham's support in quality assurance and Alice Thompson's support in records management were essential. Allyn Pratt performed miracles to purchase and deliver our 4 x 4 backhoe truck needed to expose contacts and test alternative eruptive models at the Lathrop Wells center. Finally, special thanks go to Ernie Selman of Cind-R-Lite Block Company for graciously providing permission to wander through his property, dig trenches, lead field trips, argue over outcrops, and especially for assistance in construction of trenches on private property.

STATUS OF VOLCANISM STUDIES FOR THE YUCCA MOUNTAIN SITE CHARACTERIZATION PROJECT

CONTENTS

CHAPTER 1: INTRODUCTION TO THE VOLCANISM ISSUE 1-1
- I. Summary 1-1
- II. Introduction 1-2
- III. References 1-10

CHAPTER 2: GEOLOGIC SETTING OF BASALTIC VOLCANISM IN THE YUCCA MOUNTAIN REGION 2-1
- I. Summary 2-1
- II. Introduction 2-4
- III. Basaltic Volcanism: Yucca Mountain Region 2-8
  - A. Basalt of the Silicic Episode 2-9
    1. Mafic Lavas of Dome Mountain 2-9
    2. Basaltic Rocks of the Black Mountain Caldera 2-10
    3. Basaltic Volcanic Rocks, Yucca Mountain Area 2-11
  - B. Postcaldera Basalt of the Yucca Mountain Region 2-12
    1. Older Postcaldera Basalt 2-12
    2. Younger Postcaldera Basalt 2-15
- IV. The Lathrop Wells Center 2-31
  - A. Introduction 2-31
    1. Chronostratigraphic unit I 2-33
    2. Chronostratigraphic unit II 2-33
    3. Chronostratigraphic unit III 2-34
    4. Chronostratigraphic unit IV 2-34
  - B. Chronostratigraphic Unit I 2-34
    1. The Qs1/Ql1 Unit 2-37
  - C. Chronostratigraphic Unit II 2-42
    1. Unit Qs2/Ql2 2-42
  - D. Chronostratigraphic Unit III 2-49
    1. Unit Qs3/Ql3 2-49
  - E. Chronostratigraphic Unit IV 2-54
    1. Unit Qs4 2-54
  - F. Application of Multiple Geochronology Methods: The Chronology of the Lathrop Wells Center 2-60
    1. K-Ar Age Determinations 2-60
    2. $^{40}Ar/^{39}Ar$ Age Determinations 2-63
    3. Summary 2-66
    4. U-Th Disequilibrium Age Determinations 2-66
    5. Cosmogenic Helium Surface Exposure Ages 2-68
    6. Thermoluminescence Age Determinations 2-73
    7. Geomorphic Studies 2-74
    8. Soil Studies 2-75
    9. Paleomagnetic Studies 2-77

G. Alternative Models of the Eruptive History of the Lathrop Wells Volcanic Center....2-85
1. Model A....2-90
2. Model B....2-90
3. Model C....2-90
V. References....2-91

CHAPTER 3 TECTONIC SETTING OF THE YUCCA MOUNTAIN REGION: RELATIONSHIP TO EPISODES OF BASALTIC VOLCANISM....3-1
I. Summary....3-1
II. Introduction....3-2
III. Southern Great Basin....3-5
IV. Tectonic Setting: Yucca Mountain Region....3-11
V. Tectonic Setting: Time-space Patterns of the Distribution of Basaltic Volcanism....3-17
A. Silicic Episode....3-18
B. Postcaldera Basalt....3-19
C. Older Postcaldera Basalt....3-22
D. Younger Postcaldera Basalt....3-24
VI. Geophysical Studies: Yucca Mountain Region....3-29
A. Seismic Studies....3-29
B. Gravity Investigations....3-31
C. Magnetic Investigations....3-32
D. Geoelectric Surveys....3-34
E. Seismic Investigations....3-34
1. Seismic Refraction Surveys....3-34
2. Seismic Reflection....3-35
F. Teleseismic Studies....3-35
VII. Tectonic Models of Basaltic Volcanism in the Yucca Mountain Region....3-38
A. Detachment Systems....3-39
B. Caldera Models....3-40
C. North/Northeast-Trending Rifts....3-40
D. Pull-Apart Basins....3-40
E. Crater Flat Volcanic Zone....3-41
F. North-Northeast-Trending Structures....3-41
G. Alluvial Basins....3-41
VIII. References....3-41

CHAPTER 4 PETROLOGIC AND GEOCHEMICAL CONSTRAINTS ON BASALTIC VOLCANISM IN THE GREAT BASIN....4-1
I. Summary....4-1
II. Introduction....4-1
III. Time-Space Trends in the Location, Composition, and Volume of Basaltic Volcanism....4-3
IV. The Role of the Mantle in Basaltic Volcanism....4-5
V. Evolution of Basaltic Volcanic Fields....4-7
VI. Geochemical Evidence for Polygenetic Volcanism in the Crater Flat Volcanic Zone....4-8
VII. References....4-18

CHAPTER 5 SEGREGATION, TRANSPORT, AND LOCAL STORAGE OF BASALTIC MAGMA 5-1
I. Summary 5-1
II. Introduction.....5-1
III. Melt Generation And Segregation 5-2
IV. Magma Ascent 5-6
V. Eruption or Intrusion of Basaltic Magma 5-10
VI. Future Work.....5-15
VII. References.....5-17

CHAPTER 6 HISTORY OF VOLCANISM STUDIES 6-1
I. Summary 6-1
II. Introduction.....6-5
III. Progress Before The Site Characterization Plan.....6-5
A. Publications in 1979.....6-5
1. Silicic Volcanism 6-5
B. Publications in 1980.....6-6
1. Development of Methods of Risk Assessment for Future Basaltic Volcanism 6-6
C. Publications in 1981.....6-7
1. Geology, Petrology, and Geochemical Studies of Basaltic Volcanism in Crater Flat 6-7
D. Publications in 1982.....6-8
1. Origin of Trace Element Enriched, Hawaiite Lava of Crater Flat 6-8
2. Revised Probability Calculations; Probability Bounds.....6-8
3. Results of the First Volcanism Drill Hole.....6-8
4. K-Ar Age Determinations: The First Glimpse of a Long-Lived Controversy 6-9
E. Publications in 1983.....6-9
1. Volcanism Status Report, Death Valley-Pancake Range Volcanic Zone, Basaltic Volcanic Fields of the Southern Great Basin, Tectonic Setting, Uncertainty of Volcanism Risk Assessment.....6-9
2. Scenario Development for Consequence Analysis 6-10
3. Completion of Consequence Analysis for Basaltic Volcanism: The First Radiological Release Calculations for Magmatic Disruption of the Repository 6-11
F. Publications in 1984.....6-11
1. Structural and Tectonic Setting of the YMR.....6-11
G. Publications in 1985.....6-12
1. Second Volcanism Drill Hole 6-12
H. Publications in 1986.....6-12
1. Volcanism Summary Report in a Book Published by the National Research Council Entitled *Active Tectonics: Impact on Society*.....6-12

2. Second Volcanism Status Report; Discussion of the Issues of the Mechanism of Emplacement of Shallow Intrusions, the Possibility of Future Bimodal Volcanism, the Origin of Trace-Element Enriched Basalt, and the Likelihood of Hydrovolcanic Activity....6-12
3. Environmental Assessment....6-14
I. Publications in 1988....6-14
1. Site Characterization Report....6-14
IV. Progress Since The Site Characterization Report....6-15
A. Publications in 1988
1. Reassessment of the Chronology of the Lathrop Wells Volcanic Center; New Geomorphic and Soils Studies....6-15
2. Revised Geologic Map of the Lathrop Wells Volcanic Center....6-15
B. Publications in 1989....6-15
1. New Development in Concepts of Basaltic Volcanism, Evidence of Complex Evolution of the Lathrop Wells Center, New K-Ar Age Determinations, Definition of Polygenetic Volcanism, Revised Volcanic Risk Assessment Using Multiple Volcanic-Eruption Scenarios....6-15
2. Recurrence Rate of Volcanic Events; Cumulative Magma Volume Versus Time, Recognition of the Crater Flat Volcanic Zone....6-17
3. Isotopic Composition of Strontium, Neodymium, and Lead for Basalt of the YMR, Preservation of Ancient Lithospheric Mantle....6-18
C. Publications in 1990....6-19
1. Volcanic Patterns of the YMR; Time-Space Migration of Volcanism, Multiple Chronology Models for the Lathrop Wells Volcanic Center....6-19
2. Study Plan 8.3.1.8.5.1 Characterization of Volcanic Features; Data Gathering Activities for Volcanism Studies....6-20
3. First Publication of Technical Overview of Volcanism Studies by the State of Nevada....6-20
D. Publications in 1991....6-21
1. Alternative Views by the U.S. Geological Survey; Monogenetic Versus Polygenetic Eruption Models....6-21
2. Alternative Views by the U.S. Geological Survey; Age of the Lathrop Wells Volcanic Center....6-22
3. Geologic Map of the Sleeping Butte Volcanic Centers; Possible Polygenetic Eruptions of the Hidden Cone Center....6-22
4. Alternative Views by the US Geological Survey; The Lathrop Wells Volcanic Center....6-22
5. Volcanism Probability Studies; State of Nevada....6-23
6. Study Plan 8.3.1.8.1.1 Probability of Magmatic Disruption of the Repository....6-24
E. Publications in 1992....6-25
1. Resumption of Surface Disturbing Activities for Site Characterization Studies; Status of Field and Geochronolgy studies of the Lathrop Wells Volcanic Center....6-25

2. Recurrence Models of Volcanic Events; Definition of the Tripartite Probability, Application of a Simple Poisson Model, Revised Values of the Recurrence of Volcanic Events 6-27
3. Monte Carlo Technique for Estimation of the Probability of Disruption of a Repository by Propagation of Volcanic Dikes 6-29
4. Teleseismic Tomography of the YMR; Applications to Volcanism Studies 6-29
5. Geochemical Evidence of Waning Magmatism; Polygenetic Volcanism 6-29
6. Revised Assessment of the Consequences of Magmatic Disruption of the Potential Repository, Perspectives from Modeling of Intrusion and Eruption Processes 6-30
7. Structural Controls of Volcanic Activity 6-31
8. Estimations of Volcanic Disruption, Continued Probability Studies by the State of Nevada. 6-32
9. Comment and Response to the Article Published in *Science* on the Age of the Lathrop Wells Volcanic Center 6-34

F. Publications in 1993 6-36
1. Alternative Age Determinations of the Lathrop Wells Volcanic Center Using the Cosmogenic ^{36}Cl Method 6-36
2. Geophysical Investigations of Buried Volcanic Centers: Studies by the U.S. Geological Survey 6-36
3. Assessment of Volcanic Hazards for the Yucca Mountain site by Golder Associates Using the Repository Integration Program (RIP) 6-37
4. Alternative Calculations of the Probability of Magmatic Disruption of the Potential Repository: Work by the Center for Nuclear Waste Regulatory Analyses 6-38
5. An Alternative Method for Calculating the Probability of Dikes Intersecting a Repository: Continuing Studies by Golder Associates Inc. 6-39
6. Continuing Field and Computational Studies of the Effects of ..... Magmatic Activity on the Yucca Mountain site 6-39
7. Continuing Revisions of the Probability of Magmatic Disruption of the Potential Yucca Mountain: The First Results of Simulation Modeling 6-40

V. References 6-41

CHAPTER 7 VOLCANIC RISK ASSESSMENT FOR THE YUCCA MOUNTAIN SITE 7-1
I. Summary 7-1
II. Introduction 7-4
III. Probability Model 7-8
IV. Strategy For Assessing The Volcanism Issue 7-11
V. Revised Probability Calculations 7-23
A. Volcanic Record: Assumptions and Physical Models 7-23
1. Time Perspective of Probability Calculations 7-24
2. Definition of Volcanic Events 7-25
3. Polygenetic Volcanism 7-27

B. Quaternary Volcanic Centers in the Yucca Mountain Region (Oldest to Youngest) 7-29
1. 1.0 Ma Centers: Quaternary Basalt of Crater Flat 7-29
2. 0.32 Ma Centers: Basalt of Sleeping Butte 7-29
3. 0.1 Ma Center: Lathrop Wells Center 7-30
C. Pliocene Volcanic Events in the Yucca Mountain Region (Oldest to Youngest) 7-30
1. 4.8 Ma Centers: Basalt of Thirsty Mesa 7-30
2. 3.8 Ma Center: Basalt of the Amargosa Valley 7-30
3. Undrilled Aeromagnetic Anomalies: Basalt of Central Amargosa Valley 7-31
4. 3.7 Ma Centers: Basalt of Southeast Crater Flat 7-31
5. 2.9 Ma Center: Basalt of Buckboard Mesa 7-31
D. Revised Calculations of E1: The Recurrence Rate of Volcanic Events 7-31
1. Time-Series Analysis 7-32
2. Homogeneous Poisson Models (Event Counts) 7-35
3. Nonhomogeneous Poisson Models 7-40
4. Volume-Predictable Recurrence Rates 7-43
5. Simulation Modeling: E1 the Recurrence Rate 7-51
E. Revised Calculations of E2: the Disruption Probability 7-58
1. Published Estimates of E2 7-62
2. Spatial Distribution Models 7-62
3. Structural Models for E2 7-71
4. Analog Basaltic Volcanic Fields of the Basin and Range Province 7-80
5. Simulation Modeling: E2 the Disruption Probability 7-82
F. Probability of Magmatic Disruption of the Potential Repository 7-86
G. Discussion: Probability of Magmatic Disruption 7-91
V. References 7-95

CHAPTER 8: STATUS AND IMPLICATIONS OF FUTURE STUDIES 8-1
I. Introduction 8-1
II. Study Plan 8.3.1.8.5.1, Characterization of Volcanic Features 8-1
A. Activity 8.3.1.8.1.1., Volcanism Drill holes 8-1
B. Activity 8.3.1.8.5.1.2, Geochronology Studies 8-2
1. Basalt of Thirsty Mesa 8-2
2. Basalt of Amargosa Valley (Aeromagnetic Anomaly) 8-2
3. Basalt of Southeast Crater Flat (3.7 Ma) 8-2
4. Basalt of Buckboard Mesa 8-3
5. Quaternary Basalt of Crater Flat 8-3
6. Basalt of Sleeping Butte 8-4
7. Lathrop Wells Volcanic Center 8-4
C. Activity 8.3.1.8.5.1.3, Field Volcanism Studies 8-5
D. Activity 8.3.1.8.5.1.4, Geochemistry Studies of Eruptive Sequences 8-5
E. Activity 8.3.1.8.5.1.5, Evolutionary Cycles of Basaltic Volcanic Fields 8-6
III. Study Plan 8.3.1.8.1.1, Probability of Magmatic Disruption of the Repository 8-6
A. Activity 8.3.1.8.1.1, Age and Location of Volcanic Centers 8-6

B. Activity 8.3.1.8.1.1.2, Evaluation of the Structural Controls of Sites of Basaltic Volcanism 8-6
C. Activity 8.3.1.8.1.1.3, Presence of Magma Bodies in the Site Vicinity 8-7
D. Activity 8.3.1.8.1.1.4, Revised Probability Calculations and Assessment 8-8
1. Areas of Controversy 8-9

CHAPTER 9 CONCLUSIONS 9-1
Chapter 1 9-1
Chapter 2 9-1
Chapter 3 9-5
Chapter 4 9-7
Chapter 5 9-8
Chapter 6 9-8
Chapter 7 9-9
Chapter 8 9-12

FIGURES

CHAPTER 1: INTRODUCTION TO THE VOLCANISM ISSUE 1-1
Figure 1.1 Schematic diagrams of eruption and intrusion scenarios for potential magmatic activity in the Yucca Mountain region 1-8

CHAPTER 2: GEOLOGIC SETTING OF BASALTIC VOLCANISM IN THE YUCCA MOUNTAIN REGION 2-1
Figure 2.1 Digital satellite image showing the location of the Yucca Mountain site and Quaternary volcanic centers in the YMR 2-5
Figure 2.2 The Southwest Nevada Volcanic Field 2-6
Figure 2.3 Time-transgressive, mid-Cenozoic volcanism of the Basin and Range province 2-7
Figure 2.4 Distribution of the BSE 2-10
Figure 2.5 Postcaldera Basalt of the YMR 2-13
Figure 2.6 Generalized geologic map of the Little Black Peak volcanic center of the basalt of Sleeping Butte compiled on an uncorrected aerial photograph 2-27
Figure 2.7 Generalized geologic map of the Hidden Cove volcanic center of the basalt of Sleeping Butte 2-29
Figure 2.8 Geologic setting of the Lathrop Wells volcanic center 2-31
Figure 2.9 Generalized map of the outlines of the Lathrop Wells volcanic center showing the informal names of the lava units 2-35
Figure 2.10 Geologic map of the distribution of volcanic subunits of chronostratigraphic unit I of the Lathrop Wells volcanic center 2-36

Figure 2.11 Spidergram of elemental compositions normalized to an average composition for all analyzed samples of the volcanic units of the Lathrop Wells center 2-37
Figure 2.12 Geologic map of the distribution of volcanic subunits of chronostratigraphic unit II of the Lathrop Wells volcanic center 2-43
Figure 2.13 Spidergram of elemental compositions normalized to an average composition for all analyzed samples of the volcanic units of the Lathrop Wells center 2-44
Figure 2.14 Digitized image of aerial photograph of the Lathrop Wells volcanic center showing the outcrop distribution of the Lathrop lava flow 2-46
Figure 2.15 Geologic map of the distribution of volcanic subunits of chronostratigraphic unit III of the Lathrop Wells volcanic center 2-50
Figure 2.16 Spidergram of elemental compositions normalized to an average composition for all analyzed samples of the volcanic units of the Lathrop Wells center 2-51
Figure 2.17 Geologic map of the distribution of volcanic subunits of chronostratigraphic unit IV of the Lathrop Wells volcanic center 2-55
Figure 2.18 Spidergram of elemental compositions normalized to an average composition of all analyzed samples of the volcanic units of the Lathrop Wells center 2-56
Figure 2.19 Historic photograph of the south flank of the Lathrop Wells volcanic center 2-59
Figure 2.20 Probability and box plots of the conventional whole-rock, K-Ar data of Turrin et al. 2-62
Figure 2.21 Probability and box plots of the conventional whole-rock, K-Ar data of Turrin et al. with outliers removed 2-63
Figure 2.22 Plot of percentage of radiogenic argon versus age by the conventional K-Ar age determinations of Turrin et al. 2-64
Figure 2.23 Probability and box plots of the $^{40}Ar/^{39}Ar$ data set of Turrin et al 2-65
Figure 2.24 Probability and box plots of the $^{40}Ar/^{39}Ar$ data set of Turrin et al. with outliers removed 2-65
Figure 2.25 Plot of percentage radiogenic argon versus age for the $^{40}Ar/^{39}Ar$ age determinations of Turrin et al 2-66
Figure 2.26 U-Th isochron plot for the Q13 lava 2-67
Figure 2.27 U-Th isochron for the Ql1d lava 2-68
Figure 2.28 Cosmogenic ^{3}He ages of chronostratigraphic unit I plotted with minimum estimated thickness of scoria-fall deposits of chronostratigraphic unit II 2-72
Figure 2.29 Locations of the 23 paleomagnetic sampling site at the Lathrop Wells volcanic center 2-78
Figure 2.30 Representative modified orthogonal demagnetization diagrams showing the endpoint of the magnetization vector projected onto the horizontal plane and the true vertical plane for samples from lava flows (Fig. 2.30A) and scoria mounds (Fig. 2.30b) from the Lathrop Wells volcanic center 2-81
Figure 2.31 Examples of site-level dispersion of paleomagnetic data from lava flows at the Lathrop Wells volcanic center 2-82
Figure 2.32 Summary of paleomagnetic data from the Lathrop Wells volcanic center 2-85

Figure 2.33 Geologic map of the Lathrop Wells volcanic center showing the distribution of all chronostratigraphic units of the center 2-89

CHAPTER 3 TECTONIC SETTING OF THE YUCCA MOUNTAIN REGION: RELATIONSHIP TO EPISODES OF BASALTIC VOLCANISM 3-1
Figure 3.1 Physiographic subdivisions of North America 3-5
Figure 3.2 Distribution of late Cenozoic faults in the western United States 3-6
Figure 3.3 Subdivisions of the Basin and Range province 3-7
Figure 3.4 Seismicity map of the western United States 3-10
Figure 3.5 Proposed caldera complexes and the distribution of Quaternary basaltic volcanic rocks of the Crater Flat area 3-14
Figure 3.6 Kawich-Greenwater rift zone 3-15
Figure 3.7 ADRZ superimposed on the Bouguer gravity map 3-16
Figure 3.8 Distribution of the BSE 3-18
Figure 3.9 Post-Caldera Basalts of the YMR 3-20
Figure 3.10 Alternative geographic subdivisions of the PCB episode of the YMR 3-21
Figure 3.11 Histogram of ages for the PCB of the YMR 3-22
Figure 3.12 Location of the distribution centroid by basalt cycle for the PCB 3-23
Figure 3.13 Least squares linear regression fit of the distribution of Quaternary basalt vents of the CFVZ 3-25
Figure 3.14 Least squares linear regression fit of the distribution of Pliocene and Quaternary basalt centers of the CFVZ 3-25
Figure 3.15 Three-dimensional plot of magma volume versus location of the Quaternary basalt centers of the CFVZ 3-26
Figure 3.16 Three-dimensional plot of the log of the magma volume versus the location of Pliocene and Quaternary basalt centers of the CFVZ 3-27
Figure 3.17 Distance-weighted least squares surface fit of the volume/location data of the Pliocene and Quaternary basalt centers of the CFVZ 3-28

CHAPTER 4 PETROLOGIC AND GEOCHEMICAL CONSTRAINTS ON BASALTIC VOLCANISM IN THE GREAT BASIN 4-1
Figure 4.1 Map of the western United States showing the distribution of basalt erupted during the past 16-5 and 5-0 Ma 4-3
Figure 4.2 Estimated volume versus eruption duration for late Cenozoic basaltic volcanic fields in the southwestern United States 4-4
Figure 4.3 MgO versus saturation index for basalts of the Basin and Range province 4-5
Figure 4.4 Location of samples collected for geochemistry studies at the Lathrop Wells volcanic center 4-10
Figure 4.5 Geologic map of the Lathrop Wells volcanic center 4-11
Figure 4.6 Summary spidergram plot comparing compositions of four major eruptive episodes of the Lathrop Wells volcanic center 4-12
Figure 4.7 Histogram of magnesium numbers of samples from the Lathrop Wells volcanic center 4-12
Figure 4.8 Lanthanum (INAA determination)/samarium (isotope dilution determination) ratio versus magnesium number for eruptive units of the Lathrop Wells volcanic center 4-13
Figure 4.9 Thorium/potassium ratio versus magnesium number of major lava flows and main cinder cone of the Lathrop Wells volcanic center 4-13

Figure 4.10 Neodymium versus lead for eruptive units of the Lathrop Wells volcanic center 4-14
Figure 4.11 La/Sm, Th/K, thorium and TiO_2 versus eruptive episode for the Lathrop Wells volcanic center 4-16
Figure 4.12 Lanthanum versus rubidium for basalts of the Black Cone volcanic center 4-17
Figure 4.13 Lanthanum versus rubidium for samples encompassing the 9-yr. eruptive history of Paricutin 4-17

CHAPTER 5 SEGREGATION, TRANSPORT, AND LOCAL STORAGE OF BASALTIC MAGMA 5-1
Figure 5.1 Schematic cross-section of the southern Great Basin showing the distribution of the crust, lithospheric mantle, and asthenospheric mantle 5-16

CHAPTER 7 VOLCANIC RISK ASSESSMENT FOR THE YUCCA MOUNTAIN SITE 7-1
Figure 7.1 Diagram of logic used to study the risk of volcanism for the YMR 7-14
Figure 7.2 Distribution area of Pliocene and Quaternary volcanic events, including aeromagnetic anomalies, in the YMR 7-21
Figure 7.3 Schematic cross section of a volcanic event penetrating a repository 7-26
Figure 7.4 Plot of volcanic events versus age for the Pliocene and Quaternary volcanic record of the YMR 7-35
Figure 7.5 Plot of clustered volcanic events versus age for the Pliocene and Quaternary volcanic record of the YMR 7-36
Figure 7.6 Plot of cumulative volume versus age for the Pliocene and Quaternary volcanic record of the YMR 7-37
Figure 7.7 Plot of repose interval versus age for the Pliocene and Quaternary volcanic record of the YMR 7-37
Figure 7.8 Bivariate plot of magma volume (DRE) versus age for the Pliocene and Quaternary volcanic events of the YMR 7-45
Figure 7.9 Bivariate plot of magma volume (DRE) versus age for the Pliocene and Quaternary volcanic events of the YMR with the basalt of southeast Crater Flat combined with the aeromagnetic anomalies of the Amargosa Valley 7-46
Figure 7.10 Plot of log-transformed magma volume (DRE) versus age for the Pliocene and Quaternary volcanic events of the YMR with the basalt of southeast Crater Flat combined with the aeromagnetic anomalies of the Amargosa Valley 7-47
Figure 7.11 Distribution of estimates of E1 in probability space 7-52
Figure 7.12 Results of simulation modeling of the column variation of the simulation matrix of Table 7.10 for the homogenous Poisson distribution models 7-57
Figure 7.13 Results of simulation modeling of the column variation of the simulation matrix of Table 7.10 for the nonhomogeneous Poisson distribution model 7-57
Figure 7.14 Results of simulation modeling showing the row variation in the simulation matrix of Table 7.10 for simulation three 7-58
Figure 7.15 Results of simulation modeling showing the row variation in the simulation matrix of Table 7.10 for simulation three 7-59

Figure 7.16 Distribution of Pliocene and Quaternary volcanic centers in the YMR 7-64
Figure 7.17 Distribution centroids for combinations of Pliocene and Quaternary volcanic centers in the YMR 7-65
Figure 7.18 Cluster patterns using simple visual clustering of different combinations of Pliocene and Quaternary volcanic centers in the YMR 7-66
Figure 7.19 Visual clustering of Quaternary volcanic centers in the YMR following the same steps as Figure 7.18 7-67
Figure 7.20 Plot of the sequence of Pliocene and Quaternary volcanic events in the YMR 7-71
Figure 7.21 Distribution of volcanic vents in the Lunar Crater Volcanic field 7-81
Figure 7.22 Distribution of volcanic vents in the Cima volcanic field 7-82
Figure 7.23 Plot of the distribution of Pliocene and Quaternary volcanic events in the YMR (excluding the basalt of Buckboard mesa) with the event centroid drawn at a 90% confidence interval 7-83
Figure 7.24 Distribution of E2, the disruption probability in probability space 7-84
Figure 7.25 Cumulative probability curves for E2 generated from the simulation matrix of Table 7.16 7-87
Figure 7.26 Variability in the probability of disruption for published, spatial, and structural models of E2 (published and spatial models shown with and without outliers) 7-87
Figure 7.27 Cumulative probability distribution curves for the simulation matrix of Table 7.18 7-89
Figure 7.28 Cumulative probability distribution curves for the probability of magmatic disruption of the repository using a fixed estimate of E1 and varying models for E2 7-91

TABLES

CHAPTER 2: GEOLOGIC SETTING OF BASALTIC VOLCANISM IN THE YUCCA MOUNTAIN REGION 2-1
Table 2.1 $^{40}Ar/^{39}Ar$ ages of basaltic volcanic centers in the YMR 2-17
Table 2.2 K-Ar and $^{40}Ar/^{39}Ar$ age determinations for the Quaternary Basalt of Crater Flat 2-25
Table 2.3 Descriptive statistics for conventional K-Ar and $^{40}Ar/^{39}Ar$ data sets of Turrin et al. (1991) 2-61
Table 2.4 Cosmogenic ^{3}He age determinations for the Lathrop Wells Center 2-70
Table 2.5 Paleomagnetic data for the Lathrop Wells Volcanic Center 2-79
Table 2.6 Summary table of all geochronology data for the Lathrop Wells Volcanic Center 2-87

CHAPTER 7 VOLCANIC RISK ASSESSMENT FOR THE YUCCA MOUNTAIN SITE 7-1
Table 7.1 Eruption characteristics of Pliocene and Quaternary volcanic centers in the YMR 7-19
Table 7.2 Structural and Topographic Setting of Pliocene and Quaternary volcanic centers/events in the YMR 7-20
Table 7.3 Published estimates of the recurrence Rate (E1) of Volcanic Events in the YMR 7-33
Table 7.4 Age, volume, cumulative volume and repose intervals for Pliocene and Quaternary volcanic events of the YMR 7-34
Table 7.5 Table of Homogeneous Poisson Models for Volcanic Events (E1) in the YMR 7-38
Table 7.6 Nonhomogeneous recurrence models (E1) for the YMR 7-43
Table 7.7 Results of simple regression fits for seven combinations (cases) of Pliocene and Quaternary volcanic centers of the YMR 7-48
Table 7.8 Regression residuals for the seven regression cases of Table 7.7 7-49
Table 7.9 Age, Cumulative Volume, Magma-Output Rates, Magma-Generation Rates, and Event Rates for Pliocene and Quaternary Volcanic Centers 7-50
Table 7.10 Simulation matrix, expected values and matrix statistics for E1, the recurrence rate 7-54
Table 7.11 Results of simulation modeling using the simulation matrix of Table 7.10 7-56
Table 7.12 Published values of E2, the disruption ratio 7-60
Table 7.13 Spatial Distribution models for E2 7-69
Table 7.14 Alternative structural models for the distribution of Pliocene and Quaternary volcanic centers in the YMR 7-72
Table 7.15 Estimations of E2 for structural models of the YMR 7-79
Table 7.16 Simulation matrix for E2, the disruption probability 7-85
Table 7.17 Simulation results for E2, the probability of magmatic disruption 7-86
Table 7.18 Simulation matrix for homogeneous and nonhomogeneous Poisson recurrence models of E1 using fixed estimates of E2 7-88
Table 7.19 Simulation results of homogeneous Poisson models for the probability of magmatic disruption of the repository 7-88
Table 7.20 Simulation matrix for the probability of magmatic disruption of the repository using median, minimum and maximum estimates of E2 and a fixed estimate of E1 7-89
Table 7.21 Simulation results for the probability of magmatic disruption of a repository using the probability matrix of Table 7.20 7-90
Table 7.22 Probability of magmatic disruption of the repository where the recurrence rate (E1) is adjusted for individual spatial and structural models of E2 7-92

CHAPTER 1: INTRODUCTION TO THE VOLCANISM ISSUE

I. Summary

An assessment of the risk of future volcanic activity is one of many site characterization studies that must be completed to evaluate the Yucca Mountain site for potential long-term storage of high-level radioactive waste. There are two topics for volcanism that require study. The first is the risk of silicic volcanism. This risk is judged to be negligible primarily because of the absence of silicic volcanism in the region for the last 8.5 million years (Ma). The second topic is the risk of basaltic volcanism. The presence of multiple basaltic volcanic centers in the Yucca Mountain region (YMR) of Pliocene and Quaternary age indicates that there is a finite risk of a future volcanic event occurring during the 10,000-yr isolation period of a potential repository. The risk is that magma feeding a surface eruption could ascend directly through a repository or erupt/intrude near a repository and modify the waste isolation system.

Four scenarios have been identified with respect to the risk of future basaltic volcanic events. The first scenario, which is the most important event from the perspective of disqualification of the potential repository site, is penetration of a repository by ascending magma that erupts at the surface. Such an event could possibly lead to eruptive (direct) release of radionuclides to the accessible environment. The second scenario includes volcanic eruptions *through* the controlled area, or the YMR. The third scenario includes intrusion of magma *near* a repository *without* accompanying eruptions. The fourth scenario includes intrusion of magma *into* the controlled area, or the YMR, also *without* accompanying eruptions. The latter three scenario classes may not lead to immediate releases of radionuclides; their effects are primarily on the waste isolation system. The latter two scenarios, the intrusion scenarios without eruptions, may be unlikely in the YMR. All basaltic eruptions are accompanied by the formation of minor to significant intrusions (dikes, conduit plugs, sills). However, intrusion of magma into the shallow crust (<1 km) without an associated eruption appears unlikely. All known occurrences of shallow basalt intrusions in the YMR were associated with eruptions. Each scenario component of volcanic risk is studied from the perspective of suitability of the Yucca Mountain site as well as the contribution of future volcanic processes to radiological releases from the waste isolation system (system performance). *The emphasis of this report is on assessment of the likelihood of occurrence of the first two scenarios: the probability of basaltic eruptions through or near a potential repository.* The timing and location of future volcanic events in the YMR cannot be predicted with certainty because of the small number of Pliocene and Quaternary volcanic events. A *probabilistic assessment of the risk* of future volcanic events can be modeled as a conditional probability comprising the recurrence rate of volcanic events, the probability of disruption, and the probability of volcanic-driven, radiological releases exceeding regulatory requirements. This volcanism status report summarizes work through April 1994 on probabilistic assessment of magmatic disruption of a potential repository at the Yucca Mountain site.

The major conclusions of the report include:

(1) the recurrence probability of silicic volcanism is so low that it is not a significant issue for the potential Yucca Mountain site;
(2) the most current estimate of the probability of future volcanic events directly penetrating the repository and erupting at the surface are low (slightly greater than 10^{-8} events per yr or about 1 chance in 10,000 during the 10,000-yr period of required waste isolation);
(3) the low estimate of the probability of repository disruption continues to support the previous judgments that the Yucca Mountain site is not disqualified *solely* on the basis of volcanic risk;

(4) the uncertainty of the estimates of the probability of magmatic disruption is constrained through development of cumulative probability distributions using multiple eruptive, chronological and structural models, and comparison with analog basaltic volcanic fields; and

(5) the uncertainty of probability estimates is sufficiently great that no classes of volcanic scenarios can be *excluded* from consideration with respect to their contribution to the cumulative releases from the waste isolation system.

II. Introduction

An evaluation of the risk of future volcanic activity with respect to geologic isolation of high-level radioactive waste is an important part of studies for the Yucca Mountain Site Characterization Project (YMP). The issues generated by questions about future volcanic activity are among a number of issues requiring resolution, either positively or negatively, for assessing the suitability of the Yucca Mountain site (Department of Energy [DOE] 1988). Volcanism studies have been ongoing for over a decade (Crowe and Carr 1980; Crowe et al. 1992, 1993). Future volcanism is a natural geologic process that could pose a risk to the integrity of a repository's waste isolation system (*risk is used as a general term to describe attempts to quantify an identified hazard; volcanic risk assessment refers to attempts to quantify the occurrence probability and consequences of a future volcanic or intrusive event).* Volcanic risk assessment must be performed for the 10,000-yr period required for isolation of high-level radioactive waste. Penetration of a repository by ascending magma followed by surface eruption of waste contaminated volcanic rocks could, under some conditions, lead to direct releases of radionuclides to the accessible environment. Also, intrusion of magma through or near an underground repository could alter the integrity of the waste isolation system even if no magma erupts at the surface. If the risk of volcanism from future eruptions of magma through or near a repository is judged to exceed the regulatory requirements for licensing of such a repository, the Yucca Mountain site cannot be found acceptable. If the risk of magmatic intrusion accompanied or not by eruptions exceeds regulatory requirements, the Yucca Mountain site cannot be found acceptable as a repository. Alternatively, if the risk of volcanism or intrusion is judged to be acceptable, the Yucca Mountain site still may not be suitable for a repository. The site must also meet regulatory requirements that limit the allowable releases of radionuclides over the next 10,000 yr. The DOE is charged with the responsibility of assessing the significance of issues that could potentially disqualify the Yucca Mountain site.

There are two aspects to an assessment of the risk of future volcanism. The first is the risk of future silicic volcanic activity. The rocks that were uplifted by faulting in the Miocene to form Yucca Mountain were deposited as outflow facies of large volume, explosive eruptions of silicic magma. These eruptions produced hot pyroclastic flows (ignimbrites) and formed multiple, coalesced caldera complexes. The age of this silicic activity ranges from about 15 to 11 Ma. Silicic volcanism in a related but spatially separated caldera complex occurred about 8.5 Ma (in the Black Mountain caldera complex). There are no Pliocene or younger silicic centers within a 50-km radius of the Yucca Mountain site. The nearest young silicic center is the Mount Jackson rhyolite dome (2.9 Ma). It is located 105 km to the northwest of Yucca Mountain. Quaternary centers of silicic volcanic activity occur at the eastern and western margins of the Great Basin, more than 100 km from Yucca Mountain. The absence of post-Miocene silicic volcanism in the YMR provides the major basis for the interpretation that the likelihood of recurrence of a large volume, explosive silicic eruption is very low, perhaps extremely low. Accordingly, it is judged not to be a significant issue for isolation of high-level radioactive waste isolation at the potential Yucca Mountain site (Crowe et al. 1983a; National Research Council 1992).

A second more critical issue for studies of the Yucca Mountain site is an evaluation of the risk of future basaltic volcanism. There are five small-volume Quaternary basalt centers within a 25-km radius centered at the exploratory block of the Yucca Mountain site. The closest Quaternary volcanic center is the 1.0-Ma Black Cone center. It is 9 km from the southwestern edge of the exploratory block. The youngest volcanic center in the region, the Lathrop Wells center, is 20 km south of the exploratory block. Other basalt sites of Pliocene or Quaternary age include two centers of the basalt of Sleeping Butte (0.32 Ma) and that of Buckboard Mesa (2.9 Ma). These centers are located, respectively, 47 km northwest and 35 km northeast of the potential site. A north-trending alignment of eroded basalt centers (five or six centers), which are about 3.7 Ma, is present in the southeast part of Crater Flat. A 4.8-Ma basalt mesa is located south of Black Mountain. It is 35 km northwest of Yucca Mountain. A 3.8-Ma basalt center is buried beneath alluvial deposits several kilometers south of the town of Amargosa Valley and 25 km southeast of the central part of Yucca Mountain.

Stated simply, the risk represented by the Quaternary record of volcanism is the possible recurrence of basaltic eruptive activity during the 10,000-yr performance period of a potential repository at Yucca Mountain. The nature of the future risk of volcanism can be summarized in the context of four questions:

1. Could a future pulse of basaltic magma penetrate through or near the repository, erupt, and release waste radionuclides to the accessible environment (eruption scenario)?

2. Could intrusion of magma into or around the repository perturb the waste isolation system and cause increased or accelerated release of waste radionuclides (subsurface scenario)?

3. Is the risk *of eruption, subsurface magmatic effects, or combined eruption and subsurface effects* sufficient to disqualify the Yucca Mountain site from consideration for underground storage of high-level radioactive waste?

4. Is the contribution of accelerated radiological releases from possible future magmatic processes (eruptive and subsurface) significant for the integrated performance of a repository system over a 10,000-yr period?

Several types of data are required to answer these questions. The recurrence rate or the frequency of occurrence of basaltic eruptions and subsurface intrusions needs to be established for the YMR. Possible future sites of eruptions or intrusions need to be identified or bounded. An evaluation of subsurface intrusion effects requires estimating the likelihood of intrusions and their effect on both the repository and the waste isolation system encompassing the repository. A subset of the first question, the eruption scenario, is that an identified event could directly affect the suitability of the potential Yucca Mountain site. The volcanic event of concern is disruption of a repository by ascending magma followed by eruption of waste-contaminated magma at the surface. This scenario could lead to immediate release of radionuclides along pathways that may bypass the multiple natural barriers of the waste isolation system.

Acquisition of the data needed to answer these questions has been the focus of volcanism studies for the last decade. The emphasis of current volcanism studies includes completion of field and geochronology studies, assessment of geochemical models of basalt centers, studies of the evolutionary patterns of basaltic volcanic fields, and a recent emphasis on studies of the effects of basaltic eruptions and intrusions on the repository and the waste isolation system (Valentine et al. 1992, 1993a). However, two principal areas of progress have been in gathering the data needed for site characterization studies (Crowe 1990; Perry and Crowe, 1992; Crowe et al. 1993) and estimating the occurrence probability of magmatic

disruption of a potential repository (Crowe 1986; Crowe et al. 1992, 1993). There has been sufficient progress in these studies to bound the range of possible events (minimum and maximum values) and estimate the cumulative probability distribution for the case of intersection of the repository by ascending magma and eruption at the surface (intrusion-eruption scenario). This subset of volcanic scenarios has been examined in a series of papers and reviews both external and internal to the YMP. The conclusions reached in the papers and reviews have been that *current data* indicate the probability of magmatic disruption of a repository with accompanying eruption is *too low to disqualify* the potential Yucca Mountain site (Crowe et al. 1983a; Link et al. 1983; Crowe 1986; DOE 1986, 1988; Younker et al. 1992; National Research Council 1992; Wallmann et al. 1993; Crowe et al. 1993). The DOE will make the formal assessment of the potential disqualification of the Yucca Mountain site with respect to the issue of future volcanism.

The Nuclear Regulatory Commission (NRC) has evaluated the conclusions concerning the volcanism studies for the YMP. They have neither refuted nor accepted conclusions about the significance of volcanism for the potential Yucca Mountain site. The NRC has provided questions and comments about the methods used for probability calculations, the uncertainty of the probability calculations, and the completeness of information used in risk assessment. The state of Nevada has argued in both oral and written form that volcanism is an unresolved issue with respect to the safety of the Yucca Mountain site. Their arguments were derived from qualitative judgments of the risk of volcanism and from uncertainty in evaluations of volcanic risk. The potential risk of future volcanism with respect to underground storage of radioactive waste at the Yucca Mountain site is an issue of considerable interest and some difference of opinion.

The view that future volcanic events are not a significant issue for the disqualification of the potential Yucca Mountain site requires clarification. There can be apprehension from the simple perception of a finite probability of a future volcanic event. An erupting volcano invokes images of explosions accompanied by ejection of towering columns of ash, and devastation of the surrounding areas, destruction of forests and wildlife, lost lives, and ruined property. This imagery is reinforced by media dramatizations of volcanic eruptions, filled with photography of the eruptions and zones of destruction. The series of well publicized major eruptions in the last 12 years (Mount St. Helens 1980; El Chichon 1982; Mount Pinatubo 1991–1992) have made the public more aware of the potential effects of explosive volcanic eruptions.

However, the public is generally unfamiliar with the wide range in the eruptive energy, particle fragmentation, and eruptive volume, and of the mechanisms of dispersal of volcanic materials in different types of volcanic eruptions. Additionally, critics of the Yucca Mountain site often exaggerate publicly sensitive issues, such as, the risks of volcanic eruptions and earthquakes. The Pliocene and Quaternary volcanic centers (basaltic volcanoes) in the YMR comprise relatively small scoria and spatter cones with associated low-volume, blocky aa lava flows. The nature of the deposits of the basalt centers requires that they were formed from mildly explosive, hawaiian and strombolian eruptions and more explosive, but less common, hydrovolcanic eruptions of basaltic magma. The depth of the water table at the potential Yucca Mountain site (0.6 km) should limit but not preclude the occurrence of hydrovolcanic eruptions (Crowe et al. 1986). The expected type of volcanic eruption with magma penetrating a potential repository at Yucca Mountain should have a limited capability to carry radioactive waste from depth and disperse the material long distances at the surface of the earth. There is a finite risk to storage of high-level radioactive waste from future basaltic volcanic events, but the risks are limited by the established geologic record of mildly explosive, small volume eruptions of basaltic magma at locations well removed from the Yucca Mountain site. Future basaltic volcanic events would have to intersect or erupt near a potential repository under most conditions to release radionuclides *directly* into the accessible environment.

An important, perhaps critical, aspect of geologic predictions concerned with future volcanic events is the uncertainty associated with the predictions. A common misconception is that comprehensive studies will lead to highly precise predictions of the time and location of future volcanic eruptions. That is impossible for two reasons. First, predictions of future events are based on the assumption that the record of volcanism provides a suitable indicator of the rates and style of future volcanic activity, or simply that the history of eruptive activity can be used to predict the most likely patterns of future volcanic activity. However, rates and processes of volcanic activity can change, and moreover, the record of past volcanic processes may be incomplete or hard to decipher, particularly with increasing age of the deposits. Second, there is a limited record of volcanic events in the YMR, providing only a small number of past events to forecast future volcanic events.

These uncertainties markedly constrain both the formulation and accuracy of volcanic predictions. We have a limited ability to predict the location in space and time of future volcanic activity. In fact, such predictions are probably not possible for the types of volcanoes and the small number of past volcanic events in the YMR. Currently, volcanic eruptions have been predicted only for special conditions at historically active volcanoes (UNESCO 1971; Bolt et al. 1975; Tazieff and Sabroux 1983; Swanson et al. 1985), in which a relatively large number of recent events or a consistent pattern of past events provides the basis for predictions.

The problem of prediction of eruptions is much more difficult for spatially isolated, small-volume basalt centers, because there is insufficient data to statistically define or test distribution models for the timing of future volcanic events. We can bound models of how often volcanoes might occur but cannot predict the *specific time* of a future eruption. Equally, we can define the general area where volcanic events might occur but cannot define *specific sites* of future volcanic events. We currently lack, and are unlikely to develop during the next few decades, predictive models of the triggering mechanisms of generation, ascent, or eruption of magma for areas of intermittent volcanic activity like the southern Great Basin.

Further, the recently evolving ideas of chaos and nonlinear dynamics arising in complex natural systems provide a new perspective of how unpredictable complex processes may be through time (Briggs and Peat, 1989; Stewart 1989; Devaney 1990; Peitgen et al. 1992). The processes controlling the intermittent generation, ascent, and eruption of magma at the surface exhibit many properties of chaotic systems (Shaw 1987; Dubois and Cheminee 1991; Sornette et al. 1991; Turcotte 1992) and may be particularly applicable to the relatively new field of spatiotemporal chaotic dynamics (Moon 1992). Studies applying these ideas suggest currently that accurate predictions of future volcanic events over an extended period may, like weather forecasts, be impossible. The record of scientists at predicting the future across a range of disciplines is marginal at best (Casti 1990). These difficulties appear, on first examination, disconcerting. But the questions posed for the volcanism studies at Yucca Mountain are *not* how well we can predict the future. The challenge for volcanism studies for the potential Yucca Mountain site is assessing risk. There is a subtle but important distinction between *prediction* of events and *assessing the risk* of future volcanic events. The prediction of future volcanic eruptions requires identifying when and where an eruption might occur and forecasting its type, or nature. The usefulness of the predictions is determined by their accuracy in time and space. In contrast, risk assessment requires estimating the likelihood and effects of future volcanism. Exact predictions of when (timing), where (location), and how large (magnitude) are not required. Instead, the risk of future volcanic events is estimated through probabilistic assessment of the likelihood and effects of the events. The important questions for forecasting volcanic risk for a 10,000-yr period become what methods can be used for assessment, what are the differences in the estimated risk using alternative methods of risk identification, and what is the uncertainty associated with the risk assessment? Ultimately, the volcanism issue will be resolved by assessing the estimation of risk, coupled with *realistic* estimations of the uncertainty of the risk assessment.

The statement that *current data* support the judgment that the Yucca Mountain site will not be disqualified because of the risk of a future volcanic eruption through the potential repository must be examined within the perspective of the uncertainty of that conclusion (DOE, 1986 1988). First, this judgment does not constitute a decision about the suitability of the potential site. The suitability of the site will be based on an assessment of the performance of the waste isolation system site. Second, the DOE will, in future program documents, make the formal decision on the qualification of the Yucca Mountain site with respect to volcanism. Third, no consensus on the issue of volcanic risk will ever exist. A judgment must be made about what constitutes a sufficient level of agreement to make a decision. Disagreement among reputable scientists is common, perhaps expected, when dealing with uncertain data and events. However, the significance of different views must be examined from a risk perspective, not on judgments of the individual merits of different data interpretations. Fourth, an indeterminate aspect of assessing volcanic risk is judging the amount and confidence needed in the information used to resolve the issue. What level of information is required for completeness? There will always be benefits from further studies, further testing of assumptions and conclusions, and further development of alternative models. These potential benefits must be weighed against the cost, the time requirements, and reasonableness of continuing studies. Part of the process of balancing these alternatives is assessing what level of uncertainty is acceptable for judging issues that could disqualify a site. These decisions will be made by the DOE in future program documents.

Finally, there is a paradox that envelops volcanism studies. There were only a few volcanic centers (seven or eight centers) formed in the YMR during the last 2 Ma (Crowe 1990). This small number of past events means the risk of future eruptions is low, but the uncertainty of calculating that risk is large. If there had been more volcanic events in the Yucca Mountain area, there would be a more robust data set to define the risk of future eruptions, but the risk of a future eruption would be *higher*. This tradeoff must, of course, be viewed positively. Again, the challenge is to define risk, bound the risk by *realistic* assessments of uncertainty, and compare the results with both the qualification and licensing requirements. While this is a difficult task, data summarized in this report provide a reasonable degree of confidence that the risk of future volcanism can be adequately assessed for geologic disposal of high-level radioactive waste.

The purpose of this volcanism status report is to bring a sense of scientific perspective to the many questions raised in this Introduction. Additionally, this report should provide a better understanding of the uncertainty associated with volcanic risk assessment. Society has entered an era of increased concern over the interactions between man and the environment, and we must somehow learn to make objective decisions balancing risk with potential benefits (Lewis 1990). This report provides a summary current to the date of publication of the results of a long history of volcanism studies (1978 to early 1994). It provides more complete arguments, with accompanying supporting data, that the Yucca Mountain site is not disqualified with respect to the risk of a future volcanic eruption through the potential repository site. The conclusion continues to be supported by site characterization studies and will continue to be assessed in future studies pending formal decisions on site suitability by the DOE.

The unique perspectives of this volcanism status report are several. First, we present the most current and comprehensive information concerning the geologic record of the YMR. Second, we assess topics related to volcanism such as the tectonic setting of past volcanic events, the petrology of the basaltic lavas, and the current scientific understanding of processes of magma dynamics. Third, we present our best estimates of the probability of magmatic disruption of a potential repository at Yucca Mountain, the controlled area surrounding a repository, and the YMR. These estimates are presented both as mean, or most likely values, and as cumulative probability distributions obtained through risk simulation. These probability estimations are used primarily to aid the DOE in assessing the possible disqualification of the Yucca Mountain site, and the data presented in the report may eventually become an important component of future studies concerned with evaluation of the performance of the waste isolation system.

The approach used to assess the risk of volcanism follows a threefold process (Crowe et al. 1992). We first identify the sequence of volcanic events and coupled effects that could affect a buried repository. Second, data are obtained to predict the controlling rates of volcanic activity and the spatial relations of this activity with respect to the location of a repository site. Third, those events are combined into a logical framework to estimate the risk of future volcanism. The framework of these volcanism studies involves a probabilistic assessment of risk, where risk is a combination of the probability of a volcanic event and the consequences of that event for an underground repository (Crowe et al. 1982; Crowe 1986; Crowe et al. 1992). This probabilistic approach provides a progressive, or iterative, method of evaluating the volcanism problem. Initial probability calculations are made using assumptions supported by the most current data for the Yucca Mountain site. These calculations are tested continuously and refined as more data are gathered.

The initial stages of probability calculations were made from 1980 to 1982. We have tested these conclusions with respect to site disqualification nearly continuously for more than a decade. It is time, therefore, to present the calculations formally and to solicit evaluations of the validity of the arguments. By making decisions now concerning the presented assessments of the risk of future volcanism, we can assess the validity of these decisions, the assumptions required for the decisions, and the quality of data supporting the decisions.

The risk of volcanism can be divided into four categories or scenarios from the perspective of the geometry of magma intersection and the mechanism of potential dispersal of waste radionuclides. These are

1. Direct intersection of a potential repository by ascending magma accompanied by eruptions (uppertwo parts of Fig. 1.1);
2. Direct intersection of the controlled area or the YMR by ascending magma accompanied by eruptions;
3. Intrusion of magma near the repository (below, into, or above) without eruptions (bottom part of Fig. 1.1); and
4. Intrusion of magma away from the repository in the controlled area or the YMR without eruptions.

These categories are established from the perspective of the mechanisms of dispersal of radioactive waste (Fig. 1.1). For the first two categories, the radioactive waste is dispersed by eruptive processes. There may be enlargement of the zone of magma/waste contact by secondary processes (thermal convection, groundwater effects) but the driving force for dispersing the waste is magmatic, and the dispersal is nearly instantaneous (compared with a 10,000-yr isolation time). The driving force for the dispersal of waste for categories three and four is secondary or coupled processes. Not only the effects of volcanism on a repository must be forecast, but also how those effects might change the ability of a repository system to isolate waste.

The categories are useful for identifying the effects on a repository of different volcanic events, but they cannot be completely separated as physical processes. Basaltic volcanic eruptions are invariably accompanied by intrusions at depth. The intrusions mark the shallow pathways of magma ascent to the surface and may range from simple vertical dikes to complex, sill-like bodies (Crowe et al. 1983b; Valentine et al. 1992; 1993a). Intrusion of basalt magma into the shallow crust (>1 km) may be unlikely without associated eruptions. All known field sites of shallow basalt intrusions in the YMR were also sites of *eruptions* (Crowe et al. 1983a; 1986; Crowe 1990; see also Chapters 2 and 7). Generally, the closer to the surface a basalt magma ascends in the crust, the more likely it is to erupt simply because of decreasing lithostatic overburden.

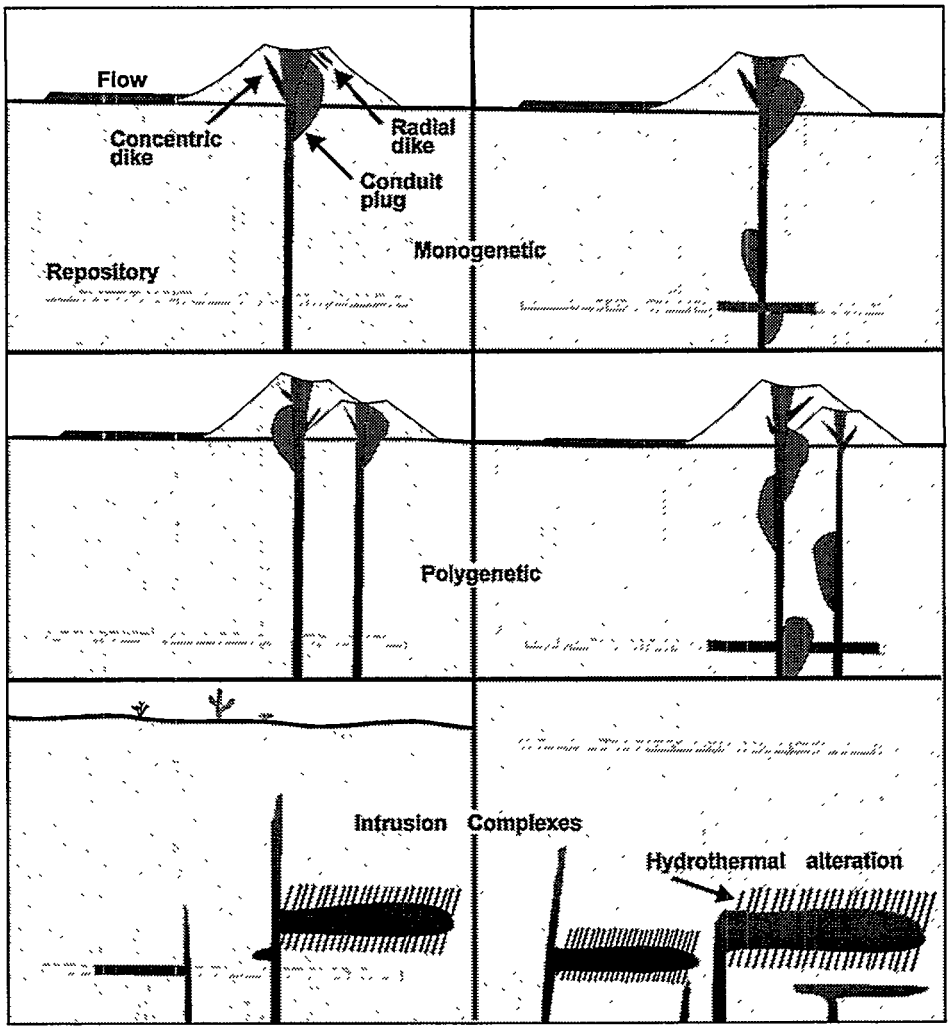


Fig. 1.1 Schematic diagrams of eruption and intrusion scenarios for potential magmatic activity in the Yucca Mountain region.

This report provides a summary of volcanism work through April 1994 and is divided into nine chapters. Chapter 1 is this introduction. Chapter 2 describes the geologic setting and history of volcanism in the YMR. Chapter 3 describes the tectonic setting of the YMR and the relationship of sites of basaltic volcanism to that setting. Chapter 4 provides a brief overview of the geochemistry of basalt magmatism and magmatic models of the evolution of basalt centers in the YMR. Chapter 5 presents an overview of magma dynamics. The evolutionary pathways of volcanism are traced from generation of magma in the mantle, through ascent and interim storage in the mantle or crust. Pertinent parts of the problem are surveyed and mathematical and physical descriptions of magma processes are emphasized. Chapter 6 is a summary, in chronological order, of the papers and conclusions developed in volcanism studies providing a complete bibliography of volcanism studies and documenting important conclusions developed from past work. Volcanism studies are summarized for work sponsored by the DOE, the NRC and their contractors, the state of Nevada, and other participants in the repository program. Many review questions and comments about volcanism studies neglect material already covered at length in published volcanism studies. We have attempted to make this work more assessable by summarizing the results of the past decade of volcanism studies. Chapter 7 of this report describes the current results of an assessment of volcanic risk for the Yucca Mountain site. The status of data is summarized current to the writing of this

report. Chapter 8 examines remaining site characterization issues. The pros and cons of different interpretations of volcanism data are examined, and the impact of these different models is evaluated for the probabilistic risk assessment. Chapter 9 summarizes conclusions of this volcanism status report.

Each chapter of this report is written purposefully to stand alone. Sufficient background discussion and reference material are presented in each chapter so it can be read separately. To facilitate access to background material, we provide a reference list at the end of each section. This organization leads to some repetition of information, but it allows the reader to focus on selected topics of interest without having to read the entire report. The most important chapters for understanding the volcanism issue are Chapters 1, 2 and 7. Chapters 3, 4, 5, and 6 provide extended background information on specific topics.

The following conclusions concerning the risk of volcanism for the Yucca Mountain site of the potential repository are presented early in order to guide the reader to relevant chapters for further information. A major goal is to encourage discussion about the completeness or validity of the conclusions in order to resolve some volcanism issues by illuminating any differences of opinion that may exist and identifying any gaps in the logic of the arguments used. We are still in the site characterization phase of studies and have continuing opportunities to collect focused data to resolve different views that affect probabilistic volcanic risk assessment. We recognize also that no attempt to synthesize data and complex arguments will be fully acceptable to all readers. By presenting the volcanism work and conclusions in a single report, we hope to facilitate identification of any parts of the work that may be unacceptable, as well as identify topics that may benefit from further study or modification.

Stated briefly, the major conclusions and perspectives of this volcanism status report are

1. *The absence of post-Miocene silicic volcanism in the YMP makes the recurrence probability so low that the risk of silicic volcanism is insignificant for the potential Yucca Mountain site.* No additional information is needed to resolve this issue other than an evaluation of the results of drilling of exploratory holes at aeromagnetic anomaly sites identified as potential buried volcanic centers or intrusions to determine if the anomaly sites are produced by Pliocene or Quaternary silicic volcanic rocks.

2. *The occurrence probability of future volcanic event's directly intersecting the repository and dispersing radioactive waste through surface eruptions is low—mean and median values are slightly greater than 10^{-8} events per yr.* This conclusion supports the judgments that the potential Yucca Mountain site is not disqualified solely because of the risk of a future volcanic eruption through the site. The logic, supporting data, and risk simulation modeling for this conclusion are presented in Chapter 7.

3. *The judgment of a low probability of magmatic disruption of the potential Yucca Mountain site is not final. It will be tested constantly and reformed, if required, through the full process of site characterization.* Alternative models will continue to be developed and tested to decide if they invalidate any conclusions or any steps leading to the conclusions. Lists and discussion of alternative models for the recurrence rate and structural controls of sites of basaltic volcanism are described in Chapters 3 and 7.

4. *The uncertainty of estimates of the probability of magmatic disruption of the repository, the controlled area, and the YMR can be constrained by considering both (1) multiple alternative chronology models and (2) multiple eruptive and structural models of basaltic volcanism. Bounds on the distribution of these data can be established through comparison with analogous basaltic*

volcanic fields. The uncertainty of this information is conveyed by presenting the data as cumulative probability distributions. The data and background information explaining the derivation of cumulative probability distributions are presented in Chapter 7.

5. *The uncertainty of the estimations of the probability of magmatic disruption is sufficiently large that no major classes of volcanic scenarios can currently be eliminated from consideration for their contribution to the cumulative releases of the waste isolation system during 10,000 yr.* All volcanic events will be considered in studies of the performance of the waste isolation system of the potential Yucca Mountain site.

6. *The conclusions presented for parts of the volcanism issue do not imply prejudgment of the information.* The basic premise of scientific research is continuous testing of models. The best approach to establishing the validity of a conclusion is through repeated attempts to disprove either the conclusion or its assumptions. By stating early judgments concerning the volcanism issue, we can extend the process of attempting to disprove. Additionally, if the site should be disqualified because of the risk of volcanism, then it is prudent to do so immediately.

7. *The conclusions of this report are presented primarily to solicit formal interactions and comments from interested parties.* It is important to determine now, if there are disagreements with the methodology and the logic of the approaches used, if there are flaws in the assumptions, or if the conclusions are incorrect or supported inadequately. The logic, the methodology, and the results of probabilistic risk assessment of volcanism are an important part of performance assessment studies that will provide the basis for judging the suitability of the site should it be submitted for a license application. The basis for estimation of the probability of magmatic disruption of the repository, the controlled area, and the region needs to be examined. Are the assumptions and conclusions of the estimations valid? Are supporting data sufficient to draw conclusions? Have data been ignored? Are alternative models omitted from the analyses? It is critical to start a questioning period immediately.

8. *A secondary goal of this report is to subject the volcanism studies and conclusions to the scrutiny of the scientific community by publishing it in the open literature.*

9. *Important topics of continuing work in volcanism studies are drilling of aeromagnetic anomalies; completion of field, geochronology, and geochemistry studies; and assessment and analog comparisons of the magmatic evolution Crater Flat volcanic zone. Revised probability calculations will incorporate the results of this work. Probability calculations will be completed for the probability of polygenetic activity at existing volcanic centers and for the formation of polygenetic volcanic clusters.* These topics are discussed in Chapters 2, 4, 7, and 8.

10. *A major emphasis of future volcanism studies will be on assessing eruptive and subsurface effects of volcanic activity.* This work is not described in this volcanism status report. It is discussed in Study Plan 8.3.1.8.1.2 (Valentine et al. 1993b).

III. References

Bolt, B. A., W. L. Horn, G. A. Macdonald, and R. F. Scott, *Geological Hazards* (Springer-Verlag, New York, 1975), 328p.

Briggs, J., and F. D. Peat, *Turbulent Mirror* (Harper and Row, New York, 1989), 222p.

Casti, J. L., *Searching for Certainty* (William Morrow and Comp., New York, 1990), 496p.

Crowe, B. M., "Volcanic Hazard Assessment for Disposal of High-Level Radioactive Waste," in *Active Tectonics: Impact on Society* (National Academy Press, Washington, DC., 1986), Chap. 16, p. 247-260.

Crowe, B. M., "Basaltic Volcanic Episodes of the Yucca Mountain Region ," in *Proceedings High-Level Radioactive Waste Management Conference, Las Vegas, Nevada,* (American Nuclear Society, La Grange Park Illinois, 1990), Vol. 1, pp. 65-73.

Crowe, B. M., and W. J. Carr, "Preliminary Assessment of the Risk of Volcanism at a Proposed Nuclear Waste Repository in the Southern Great Basin," U.S. Geological Survey Open-File Report 80-375, 15 p. (1980).

Crowe, B. M., M. E. Johnson, and R. J. Beckman, "Calculation of the Probability of Volcanic Disruption of a High-Level Radioactive Waste Repository Within Southern Nevada, U.S.A.," *Radioactive Waste Management* **3**, 167-190 (1982).

Crowe, B. M., D. T. Vaniman, and W. J. Carr, "Status of Volcanic Hazard Studies for the Nevada Nuclear Waste Storage Investigations," Los Alamos National Laboratory Report LA-9325-MS 47 p (1983a).

Crowe, B. M., S. Self, D. Vaniman, R. Amos, and F. Perry, "Aspects of Potential Magmatic Disruption Of A High-Level Radioactive Waste Repository In Southern Nevada.," *Journal Geology* **91**, 259-276 (1983b).

Crowe, B. M., R. Picard, G. Valentine, and F. V. Perry, "Recurrence Models of Volcanic Events: Applications to Volcanic Risk Assessment," in *Proceedings High-Level Radioactive Waste Management Conference, Las Vegas, Nevada, (American Nuclear Society*, La Grange Park Illinois, 1992) **2**, p. 2344-2355.

Crowe, B.M., F.V. Perry, G.A. Valentine, P.C. Wallmann and R. Kossik, "Simulation Modeling of the Probability of Magmatic Disruption of the Potential Repository Yucca Mountain Site," in *Proceedings Site Characterization and Model Validation Focus'93 Symposium Volume* (American Nuclear Society, La Grange Park, Illinois, 1993), p. 182-191.

DOE (U.S. Department of Energy), "Environmental Assessment: Yucca Mountain Site, Nevada Research and Development Area, Nevada," Office of Civilian Radioactive Waste Management report DOE/RW-0073, (1986).

DOE (U.S. Department of Energy), "Site Characterization Plan, Yucca Mountain Site, Nevada Research and Development Area, Nevada," Office of Civilian Radioactive Waste Management report DOE/RW-0199, (1988).

Dubois, J., and J. L. Cheminee, "Fractal Analysis of Eruptive Activity of Some Basaltic Volcanoes," *Journal Volcanology Geothermal Research* **45**, 197-208 (1991).

Devaney, R. L., "Chaotic Explosions in Simple Dynamical Systems," in *The Ubiquity of Chaos*, S. Krasner, Ed., (American Association Advance Science, Washington, DC. 1990), Chapter 1.

Lewis, H. W., *Technological Risk* (W. W. Norton and Company, Inc., New York, 1990), 353p.

Link, R., S. E. Logan, H. S. Ng, F. A. Rockenbach, and K. J. Hong, Parametric Studies of Radiological Consequences of Basaltic Volcanism," Sandia National Laboratories Report SAND 81-2375, 219p., (1983).

Moon, F. C., *Chaotic and Fractal Dynamics* (John Wiley & Sons, Inc., New York, 1992), 508p.

National Research Council, "Ground Water at Yucca Mountain, How High Can It Rise?," *Final Report of the Panel on Coupled Hydrologic/Tectonic/Hydrothermal Systems at Yucca Mountain* (National Academy Press, Washington, DC., 1992), 231p.

Peitgen, H.-O., H. Jurgens, and D. Saupe, *Chaos and Fractals: New Frontiers of Science* (Springer-Verlag, New York, 1992), 984p.

Perry, F. V., and B. M. Crowe, "Geochemical Evidence for Waning Magmatism and Polycyclic Volcanism at Crater Flat, Nevada," in *Proceedings High Level Radioactive Waste Management Conference, Las Vegas, Nevada,* (American Nuclear Society, La Grange Park, Illinois, 1992),Vol. 2, p. 2356-2365.

Shaw, H. R., "Uniqueness of Volcanic Systems," U.S. Geological Survey Professional Paper 1350, p. 1357-1394 (1987).

Sornette, A., J. Dubois, J. L. Cheminee, and D. Sornette, "Are Sequences of Volcanic Eruptions Deterministically Chaotic?" *Journal Geophysical Research* **96**, 11931-11945 (1991).

Stewart, I., *Does God Play Dice* (Blackwell, Cambridge, Massachusetts, 1989), 348p.

Swanson, D. A., T. J. Casadevall, D. Dzurisin, R. T. Holcomb, C. G. Newhall, S. D. Malone, and C. S. Weaver, "Forecasts and Predictions of Eruptive Activity at Mount St. Helens, 1975-1984," *Journal Geodynamics* **3**, 397-423 (1985).

Tazieff, H. and J. C. Sabroux, *Forecasting Volcanic Events* (Elsevier, Amsterdam, 1983), 635p.

Turcotte, D.L., *Fractals and Chaos in Geology and Geophysics* (Cambridge, University Press, New York, 1992), 221p.

United Nations Educational, Scientific, and Cultural Organization, *The Surveillance and Prediction of Volcanic Activity,* (UNESCO, Paris, 1971), 166p.

Valentine, G.A., B.M. Crowe, And F.V. Perry, "Physical Processes and Effects of Magmatism in the Yucca Mountain Region," in *Proceedings High Level Radioactive Waste Management Conference Las Vegas, Nevada,* (American Nuclear Society, La Grange, Illinois, 1992) Vol. 3, p. 2344-2355.

Valentine, G.A., K.M. Growes, C.W. Gable, F.V. Perry And B.M. Crowe, "Effects of Magmatic Processes on the Potential Yucca Mountain Repository: Field and Computational Studies," in *Proceedings Focus'93 Symposium Volume,* (American Nuclear Society, La Grange, Illinois, 1993a) p. 167-173.

Valentine, G.A., B. M. Crowe, and F.V. Perry, "Study Plan 8.3.1.8.1.2 Physical Processes of Magmatism and Effects on the Potential Repository," YMP-LANL-SP-8.3.1.8.1.2, Los Alamos National Laboratory (1993b).

Wallmann P.C., I. Miller, and R. Kossik, "Assessment of Volcanic and Tectonic Hazards to High Level Radioactive Waste Repositories," in *Proceedings High Level Radioactive Waste Management, Las Vegas, Nevada,* (American Nuclear Society, La Grange, Illinois, 1993), Vol. 4, p. 188-195.

Younker, J. L., W. B. Andrews, G. A. Fasano, C. C. Herrington, S. R. Mattson, R. C. Murray, L. B. Ballou, M. A. Revelli, L. E. Shephard, W. W. Dudley, D. T. Hoxie, R. J. Herbst, E. A. Patera, B. R. Judd, J. A. Docka, and L. D. Rickertsen, "Report of the early site suitability evaluation of the potential repository site at Yucca Mountain, Nevada," Science Applications International Corporation Report SAIC-91/8000 (1992).

CHAPTER 2: GEOLOGIC SETTING OF BASALTIC VOLCANISM IN THE YUCCA MOUNTAIN REGION

I. Summary

Yucca Mountain is a linear mountain range composed of Miocene ignimbrite erupted from the Timber Mountain–Oasis Valley (TM-OV) caldera complex, the major silicic complex of the southwest Nevada volcanic field. Miocene silicic volcanism in the field was succeeded by late Miocene/Quaternary basaltic volcanic activity. This basaltic activity is divided into two episodes: basalt of the Silicic episode (BSE) that occurred during the waning stage of silicic volcanism and Postcaldera basalt (9 million years [**Ma**] to Quaternary). These two major episodes of basaltic volcanism have been studied as part of the Yucca Mountain Site Characterization Project (YMP). The levels of detail of the studies vary with the age of the volcanic activity. The most detailed studies are of the Pliocene and Quaternary (4.8 to 0.1 Ma) basaltic volcanic centers, because they provide the most representative record of the nature of the most recent volcanic activity in the Yucca Mountain region (YMR) and the most important data for assessing the risk of future volcanism.

The BSE occurs in three major geographic groups: (1) basalt exposed in the moat zone of the Timber Mountain caldera, (2) basalt near and flanking the Black Mountain caldera, and (3) basalt of the YMR. The Postcaldera episode includes the Older postcaldera basalt (OPB) that occurs north and northeast of Yucca Mountain and the Younger postcaldera basalt (YPB) that crops out west, southwest, and south of Yucca Mountain (except the basalt of Buckboard Mesa). The OPB consists of the 8 Ma basalt of Rocket Wash, the basalt of Pahute Mesa (~9 Ma), the basalt of Paiute Ridge (8.0–8.7 Ma), the basalt of Scarp Canyon (8.7 Ma), the basalt of Frenchman Flat (8.6 Ma), and the basalt of Nye Canyon (6.5–7.0 Ma). Each basalt unit is a relatively small–volume basalt center (<1 km^2) formed by clusters of scoria cones with associated lava flows. The centers formed at or along basin-range faults and at the intersection of basin-range faults and ring-fracture zones of caldera complexes except for the basalt of Nye Canyon. The latter basalt unit forms a northeast-cluster of centers that does not follow local structure. Two centers of the basalt of Nye Canyon formed partly from hydrovolcanic eruptions. The basalt of Paiute Ridge consists of dissected scoria cones and flows underlain by a complex of sills, dikes, and lopolithic intrusions.

The YPB consists of seven clusters of Pliocene and Quaternary volcanism; six of the clusters occur in a narrow northwest-trending zone called the Crater Flat volcanic zone (CFVZ). The oldest and largest volume basaltic volcanic center of the YPB is the basalt of Thirsty Mesa, a newly recognized Pliocene volcanic center. It consists of three coalesced, small scoria cones surmounting a lava mesa. The age of the unit is 4.8 Ma. A negative aeromagnetic anomaly was drilled by a private company and has been shown to be a buried basalt center of 3.9 Ma. The 3.7-Ma basalt of southeast Crater Flat comprises six north-trending dissected scoria cones and associated moderate-volume lava flows. It is the largest volume Plio/Quaternary basalt in the Crater Flat alluvial basin. The unit formed largely from Hawaiian fissure eruptions accompanied by outpouring of sheet-like lobes of aa lava flows. The basalt of Buckboard Mesa (2.9 Ma) crops out in the moat zone of the Timber Mountain caldera, northeast of Yucca Mountain. Nearly 1 km^3 of lava vented from a small scoria cone and an associated northwest-trending fissure located southeast of the scoria cone. The Quaternary basalt of Crater Flat consists of an arcuate alignment of basalt centers extending along the axis of Crater Flat. Individual centers of the alignment include, from southwest to northeast, the Little Cones, the Red Cone, the Black Cone, and the Makani Cone centers. Greater than 90% of the volume of the four centers is contained in the scoria cone and lava units of the Red Cone and Black Cone centers. The Little Cones center consists of two closely spaced, small scoria cones.

Lava flows were extruded from and breached the south wall of the southwest center. The Little Cones yield K-Ar age determinations of 1.1 to 0.76 Ma. These ages are consistent with the degree of dissection, the degree of horizon development in soils, and with the magnetic polarity of the center. The Red Cone and Black Cone centers are analogous volcanic landforms with similar eruptive histories. Each consists of a main scoria cone surmounted by a crater filled with agglutinated spatter, large lava blocks, and scoria. The main scoria cones of both centers are flanked to the south by eroded scoria mounds that vented aa lava flows. Potassium-argon ages of between 0.84 and 1.55 Ma were reported for Red Cone; radiometric ages for Black Cone range between 0.8 and 1.1 Ma. Soil and geomorphic data are consistent with these ages. The Makani center is a deeply dissected remnant of a scoria cone and lava flow. Potassium-argon age determinations for this center range from 1 to 1.66 Ma. A continuing area of controversy for the Quaternary basalt of Crater Flat is the eruptive models of individual centers, and the age differences between each center. Exploratory data analyses of K-Ar and $^{40}Ar/^{39}Ar$ age determinations using standard statistical methods (with outliers removed) indicated that the mean age of all centers is 1.0 ± 0.1 Ma. Paleomagnetic data are consistent with the findings that the centers are all close in age and formed from a single pulse of magma, but they do not provide conclusive proof of this. Field, geomorphic, soil, and petrologic data suggest some of the centers could be polygenetic and might different slightly in the age. The difference in ages of the centers must be less than the detection limits of K-Ar and $^{40}Ar/^{39}Ar$ chronology methods (0.1 Ma).

The Sleeping Butte centers are located 45 km northwest of Yucca Mountain. They consist of two centers, the southwest Little Black Peak center and the northeast Hidden Cone center. Each consists of a small-volume main scoria cone flanked by blocky aa lava flows that vented from radial dikes at the base of the cone. The Little Black Peak center appears from field, geomorphic, petrologic, and paleomagnetic data to be a simple monogenetic center with a K-Ar age of about 320 to 380 thousand years (ka). The Hidden Cone center is more complex and may have formed from at least two temporally distinct eruptions. The age of the major volume of the Hidden Cone center is also about 320 to 380 Ma. The scoria-fall eruptions that mantled the main cone of the center may be as young as late Pleistocene.

The Lathrop Wells volcanic center is the youngest and most carefully studied basaltic volcanic center of the YMR. The center is located at the south end of Yucca Mountain, near the intersection of northwest- and northeast-trending fault systems; most of the vents are aligned along northwest-trending fissure systems. The basalt center formed from multiple time-distinct eruptions that comprise four chronostratigraphic units. The oldest chronostratigraphic unit (I) consists of four groups of lava flows and local pyroclastic deposits marking the vents for the lava flows. These volcanic deposits occur along multiple, northwest-trending fissures located south, beneath, north, and northeast of the main cone. The scoria and spatter deposits of chronostratigraphic unit I were modified extensively by erosion prior to formation of chronostratigraphic unit II. Chronostratigraphic unit II consists of two sets of lava and pyroclastic deposits. The largest volume lava of the center was erupted from a northwest-trending fissure that is coparallel to a northwest-trending normal fault, which displaces the Timber Mountain tuff but not the basaltic deposits. Small-volume lobes of lava were erupted from a west/northwest-trending fissure that extends from the north end of the northwest-trending fissure system. A short, northwest-trending fissure marked by scoria mounds formed at the northeast base of the main scoria cone. Widespread scoria-fall and pyroclastic-surge deposits were erupted from vents that are inferred to be concealed beneath the modern main cone. The eruptive events of chronostratigraphic unit III formed most of the main scoria cone and small-volume lobes of a blocky aa lava flow that erupted from a vent northeast of the main cone. Chronostratigraphic unit IV includes small-volume eruptions from a cluster of inferred small satellite vents south of the main cone that have been removed by commercial quarrying. The eruptive events of this

chronostratigraphic unit have been established through the identification of local tephra beds that have distinctive major- and trace-element chemistry.

The delineation of individual chronostratigraphic units has been established on the basis of detailed field, stratigraphic, geomorphic, and soils studies. The individual chronostratigraphic units can be discriminated uniquely by their major- and trace-element geochemical compositions. The chemistry of the units is inconsistent with a simple monogenetic eruption model and instead requires formation from multiple magma batches consistent with a polygenetic classification of the volcanic center (multiple, time-distinct volcanic eruptions).

The difficult problem of establishing the age of the multiple volcanic events at the Lathrop Wells volcanic center has been approached by applying multiple geochronology and age-correlated methods (K-Ar, U-Th disequilibrium, cosmogenic helium, thermoluminescence (TL), geomorphic, soils, paleomagnetic, and petrologic studies). Recent results show some convergence in the range of ages obtained using the different methods, but the data remain consistent with multiple eruptive and chronology models. Conventional whole-rock K-Ar ages of lava units of the Lathrop Wells volcanic center give a mean age of 137 ± 52 (1*s*) ka. The age is obtained by averaging age determinations from chronostratigraphic units of probable different ages. Moreover, the age determinations show a positive correlation between percentage radiogenic argon and the measured age of the sample. Published $^{40}Ar/^{39}Ar$ age determinations of the same rock samples as the conventional K-Ar data set also show a positive correlation between percentage radiogenic argon and age. The mean age of all measured $^{40}Ar/^{39}Ar$ age determinations is 162 ± 62 (1*s*) ka, and is again obtained by averaging age determinations from separate chronostratigraphic units. At best, the K-Ar and $^{40}Ar/^{39}Ar$ ages provide maximum estimates of the ages of the two oldest chronostratigraphic units (I and II). The data sets cannot be used to establish the range in age of the volcanic center or to discriminate the ages of individual chronostratigraphic units. Uranium-thorium disequilibrium age determinations have been obtained for lavas of chronostratigraphic units I and III. Mass spectrometric analyses of separated phases yielded isochrons with ages of 135 + 20 – 15 and 125 + 25 – 30 (1σ) ka, in apparent agreement with the K-Ar and $^{40}Ar/^{39}Ar$ age determinations. Problems with the results of U-Th disequilibrium measurements include 1) a small degree of U-Th fractionation in measured phases and 2) a similarity in measured ages of volcanic units that are inferred to be of probable different ages.

The ages of the chronostratigraphic units at Lathrop Wells center have also been estimated by measuring the accumulation of cosmogenic ^{3}He in 25 surface samples. The preferred ^{3}He ages of chronostratigraphic unit I range from about 80 to 90 ka, but represent minimum ages because the sampled deposits were covered by scoria-fall deposits of chronostratigraphic unit II. The ^{3}He ages of chronostratigraphic unit II range from 80 to 100 ka. Deposits of chronostratigraphic unit III show the greatest range in ^{3}He ages (30–65 ka) because many of the samples were collected from the main scoria cone, a nonresistant geomorphic feature. The age of the unit may be >65 ka if the ages are interpreted as minimum ages. This interpretation does not explain however, the wide variations (40%) in replicate ages for samples collected from the geomorphically unmodified main cone. A sample collected from the interior of a lava flow yielded an age of about 6 ka consistent with a zero age. TL age determinations give reproducible and consistent ages of 4 to 9 ka for tephra units of chronostratigraphic unit IV that are interbedded with soils showing horizon development. TL ages of about 25 ka for baked sediments beneath lava of chronostratigraphic unit II are inconsistent with the age determinations of all other chronology methods.

Geomorphic studies of the degree of dissection of deposits of the Lathrop Wells volcanic center are consistent with an age of no older than 20 ka for the youngest events (chronostratigraphic units III and IV) at the center. This is consistent with the TL ages of the youngest tephra units but is somewhat younger than the measured ^{3}He ages of the main cone. The systematic differences in degree of erosion of volcanic landforms of chronostratigraphic units I, II, and III require a time difference between each unit. Paleomagnetic data have been obtained to augment studies by Champion (1991) and Turrin et al. (1991) and now have been measured for all chronostratigraphic units at the volcanic center. The between-site dispersion of directions of the primary magnetization of units differs considerably for some sites because of a combination of difficulty in sampling intact material and lightening strikes. Paleomagnetic data obtained are not dissimilar from those reported by Turrin et al. (1991). However, the data do not support the contention that individual eruptive features have unique paleomagnetic signatures that can be confidently separated from other eruptive features. Eruptive features of the center have recorded directions of the latest Quaternary geomagnetic field that are well within the expected one-sigma range of paleosecular field variation about the spin-axis direction and have limited application to stratigraphic studies. There is no indication of a single volcanic event occurring during a period of unusual geomagnetic activity.

The field relations of the volcanic units are well constrained. The chronology of the units remains uncertain and the existing data must be used cautiously to test the field relations. Three alternative models are presented for the eruptive history of the Lathrop Wells center. These include, respectively, a four event eruption model (>130, 80–90, 65, and 4–9 ka), a three event eruption model (120–140, 65 and 4–9 ka), and two event eruption model (120–140, 4–9 ka).

II. Introduction

Yucca Mountain is a linear range located in southern Nevada, near the south end of the Great Basin physiographic province. The range extends from Highway 95 northward to Yucca Wash (Fig. 2.1). Yucca Mountain is broken into individual blocks separated by linear valleys. These physiographic features were produced by sets of north and northeast-trending faults that have displaced fault-bounded blocks down to the west accompanied by gentle (6–7°) east-directed tilting (Scott and Bonk 1984). The linear valleys mark generally the surface traces of the block-bounding faults.

Early exploration studies of the YMR consisted primarily of drilling of continuously cored boreholes for geologic studies and large diameter boreholes for hydrologic investigations (Department of Energy [DOE] 1986; 1988). The drilling was supplemented by surface mapping and geophysical studies. These combined studies lead to the identification of a central part of the range as the most structurally intact segment. A 6-km^2 area was designated as the exploratory block (Fig. 2.1). An area surrounding the exploratory block (86 km^2) was designated as the controlled area.

The volcanic rocks that formed Yucca Mountain were emplaced during eruptive cycles of the TM-OV caldera complex (Christiansen et al. 1977; Byers et al. 1976; Broxton et al. 1989; Byers et al. 1989). The Yucca Mountain site itself, including the surface rocks and the rocks extending to the depth of the potential repository horizon, comprises volcanic units of the Paintbrush Tuff, which is a major outflow ignimbrite of the Claim Canyon caldera segment of the TM-OV caldera complex (Lipman et al. 1966a).

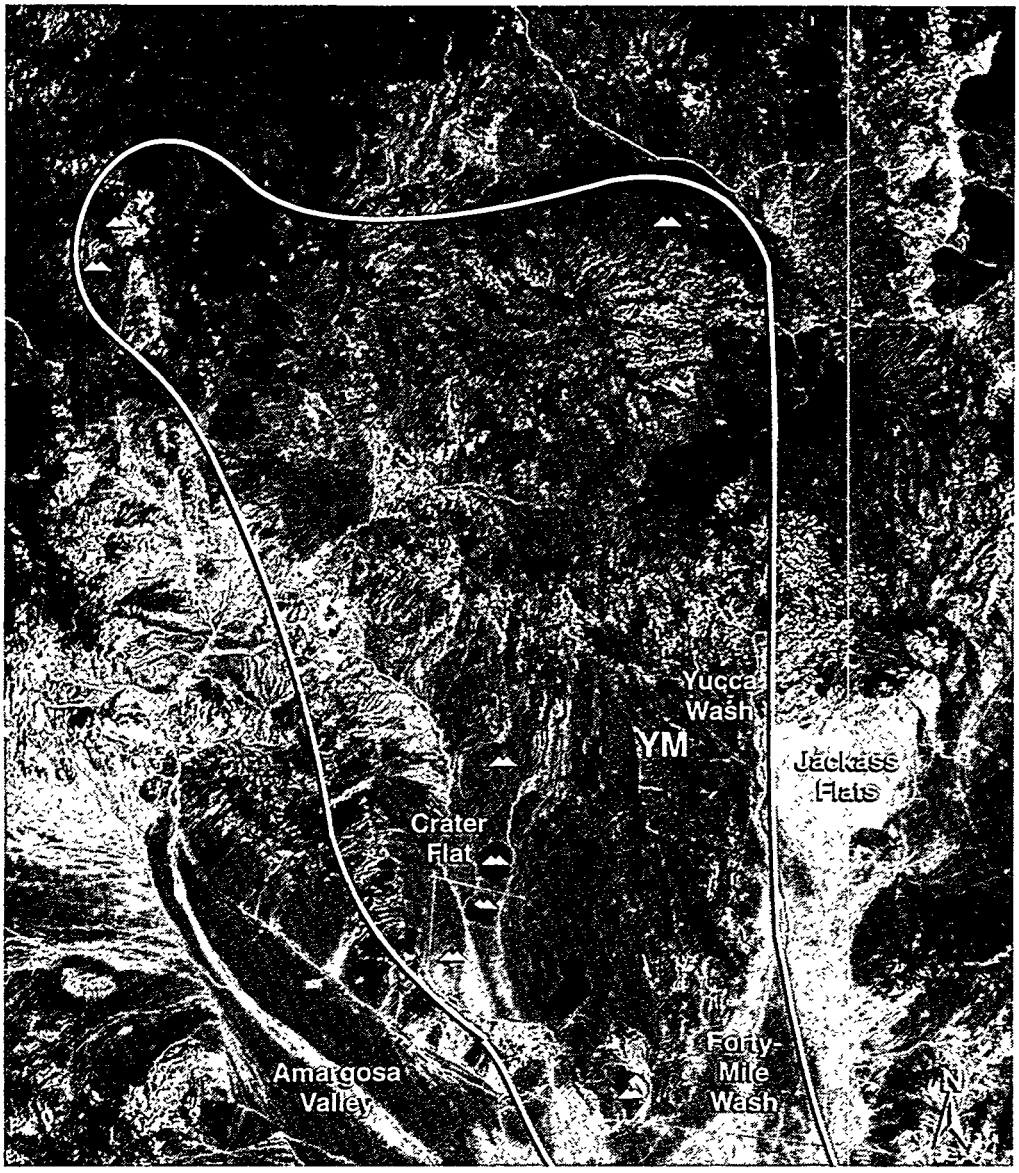


Fig. 2.1 Digital satellite image showing the location of the Yucca Mountain site and Quaternary volcanic centers in the YMR. The YMR is defined as the area of the irregular polygon that encloses the Yucca Mountain site and the Pliocene and Quaternary basaltic volcanic centers in the region. Yucca Mountain is a linear range located on the southwest edge of the Nevada Test Site, about 160 km northwest of Las Vegas, Nevada. The mountain extends from Highway 95 on the south to Yucca Wash on the north, a distance of about 25 km. The mountain is bounded on the east by Jackass Flat (the western boundary of Jackass Flat is defined by Fortymile Wash), on the west by Crater Flat, and on the south by the Amargosa Valley. An approximately 6-km^2 area in the center part of Yucca Mountain has been identified as the exploratory block (DOE 1988). It is surrounded by the controlled area, about 86 km^2. There are seven Quaternary basaltic volcanic centers in the Yucca Mountain area (<1.8 Ma). These centers are noted by the special symbol on Fig. 2.1.

The voluminous record of silicic volcanism in the YMR is part of an extensive, time-transgressive pulse of mid-Cenozoic volcanism that occurred throughout much of the southwestern United States. The Yucca Mountain range is in the south-central part of a major Cenozoic volcanic field that covered an area exceeding 11,000 km^2. The field has been named the Southwestern Nevada Volcanic Field (SNVF) (Christiansen et al. 1977; Byers et al. 1989) (Fig. 2.2).

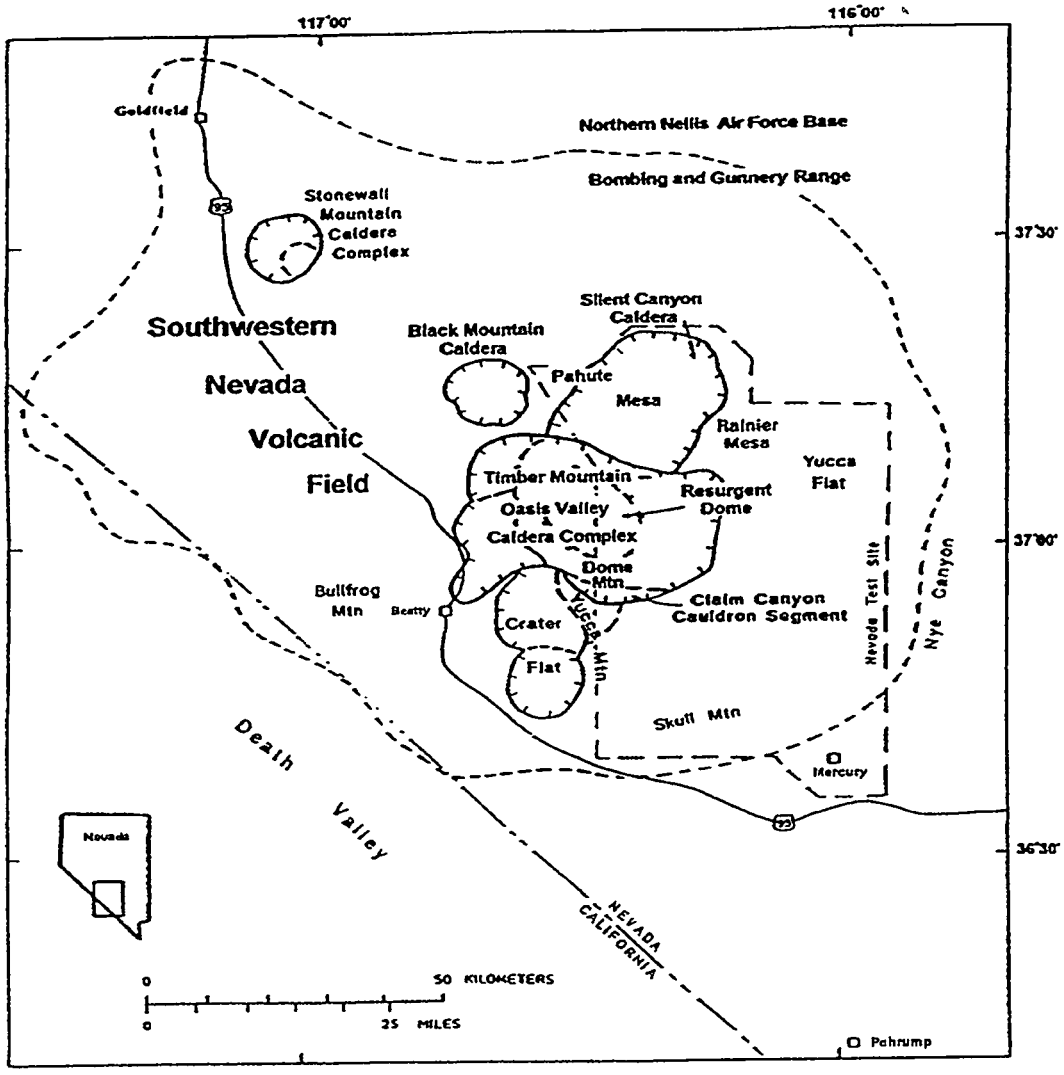


Fig. 2.2 The Southwest Nevada Volcanic Field (from Byers et al. 1989). Yucca Mountain is upheld by a thick sequence of ignimbrites derived from multiple caldera-forming, eruptive cycles of the Claim Canyon and TM-OV caldera complexes. The existence of caldera complexes at Crater Flat, which borders Yucca Mountain to the west, is regarded as controversial by some workers.

The time-space distribution of volcanic activity in the Basin and Range province has been described by many authors (Armstrong et al. 1969; McKee 1971; Lipman et al. 1971; Lipman et al. 1972; Christiansen and Lipman 1972; Snyder et al. 1976; Stewart et al. 1977; Stewart and Carlson 1978; Christiansen and McKee 1978; Cross and Pilger 1978; Smith and Luedke 1984; Luedke and Smith 1984; Axen et al. 1993). During the Mesozoic era, magmatism in the cordillera was distributed in linear belts parallel to the continental margin (Armstrong and Ward 1991). In the southwestern United States, these

belts became locally inactive or disrupted about 80 Ma and formed the Laramide magmatic gap (Armstrong 1974). Renewed silicic magmatism following the Laramide hiatus initiated about 50 Ma in the northeast part of the Great Basin. Sites of eruptive activity migrated south and southwest progressively in time and space across an area of Nevada and adjoining parts of Utah (Stewart et al. 1977; Armstrong and Ward 1991). The loci of eruptive centers during this voluminous silicic volcanism were distributed along arcuate east/west-trending volcanic fronts (Stewart et al. 1977). The leading edge of the migrating front during successive increments of time marked the area of the most intensive volcanic eruptions. There was a dramatic waning of volcanic activity in the lee, or backside, of the front (Stewart et al. 1977) and virtually no volcanic activity ahead of the front. The period of most voluminous silicic volcanic activity in the YMR occurred between 15 to 11 Ma. The YMR marks the southern limit of the spread of time-transgressive volcanic activity.

Two significant changes in the regional volcanic and tectonic patterns occurred about 13 to 10 Ma at the approximate latitude of the YMR. First, the progressive southern migration of volcanism halted. Silicic eruptive activity continued in diminished volumes and migrated predominantly to the southwest and southeast, following less systematic patterns than the migration of preceding volcanic activity. Post-Miocene volcanic activity approached present positions along the east and west margins of the Great Basin (Christiansen and McKee 1978; Smith and Luedke 1984). These changed patterns in migration of volcanism left a conspicuous amagmatic gap extending from the south edge of the Nevada Test Site south to the latitude of Las Vegas (Fig. 2.3). This gap coincides with a major increase in the regional gravity field that forms the south boundary of the gravity low of the Great Basin (Eaton 1978). This latitude (35° N)

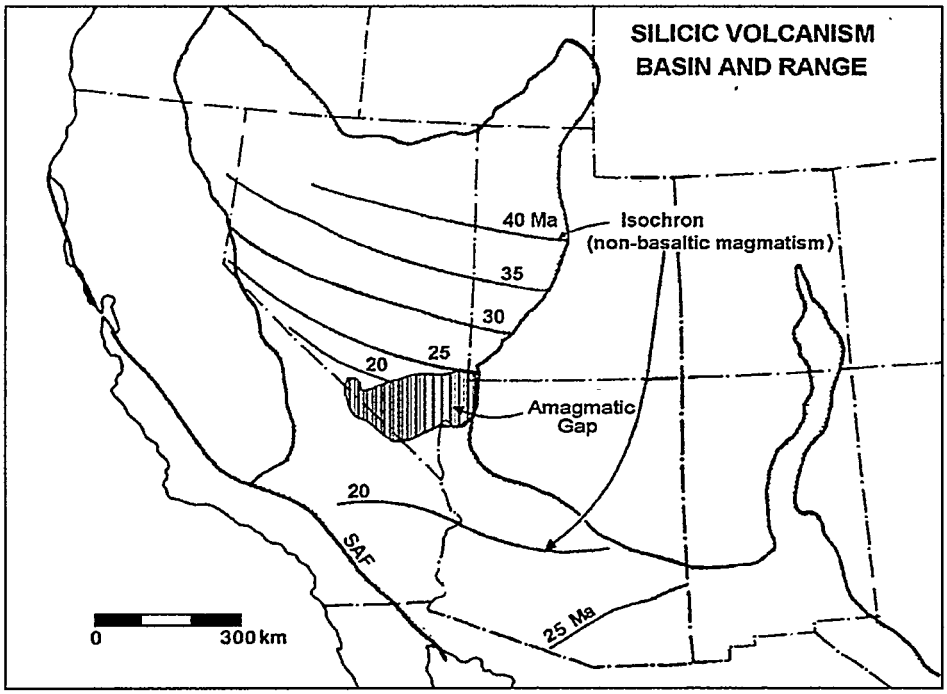


Fig. 2.3 Time-transgressive, mid-Cenozoic volcanism of the Basin and Range province (modified from Farmer et al. 1989). Numbered contour lines locate the position of arcuate, migrating fronts of silicic volcanism during increments of Cenozoic time. Yucca Mountain is located at the southern limit of the southern migration mid-Cenozoic silicic volcanism. The YMR borders the north edge of a zone in southern Nevada distinguished by its absence of Mesozoic and Cenozoic volcanism and plutonism. This zone, referred to as the amagmatic gap, includes much of the central Basin and Range subprovince of Wernicke (1992) and Jones et al. (1992).

also coincides with the approximate position at 10–20 million years ago of the boundary between the incoherent subducted slab or "slab gap" south of the Mendocino fracture zone and persisting subducted slab to the north (Severinghaus and Atwater 1990).

Second, at about 10 million years ago a transition in the composition of volcanic activity occurred. This change is consistent with a time-transgressive switch across the southwest United States from

predominantly silicic volcanism to bimodal basalt-rhyolite volcanism (fundamentally basaltic volcanic activity) (Christiansen and Lipman 1972). The exact timing of this transition in the YMR cannot be defined precisely. It may be marked by a transition from near homogeneous quartz latite and rhyolite ignimbrite (>13 Ma) to eruptions of compositionally zoned ash flows units (<12 Ma) that range from high-silica rhyolite at their base (SiO_2 > 75%) to quartz latitic caprocks (SiO_2 < 70%). This transition in the Nevada Test Site region is probably marked by the eruption of the Paintbrush Tuff (Christiansen and Lipman 1972; Christiansen et al. 1977). Alternatively, the transition may be recorded by the widespread appearance of moderately voluminous basaltic volcanism (Crowe 1990). The age of this basaltic volcanic activity is bracketed between the eruption of the Timber Mountain Tuff (11.2 Ma) and the peralkaline ash-flow sheets of the Black Mountain caldera complex (8.5 Ma) (Crowe 1990).

III. Basaltic Volcanism: Yucca Mountain Region

Field and geochronology data for the basaltic volcanic rocks of the YMR define two episodes (Crowe 1990). The first episode of bimodal basalt-rhyolite volcanism is called basalt of the Silicic episode (BSE). This episode postdates but is close in age to most of the silicic eruptions of the TM-OV complex. For this report, we describe only the basaltic units present in and around the Timber Mountain highland and the YMR. Other basaltic units, associated primarily with the Black Mountain–Stonewall Mountain calderas, are not described.

The second basaltic episode includes spatially scattered, small-volume centers marked by scoria cones and lava flows of alkali basalt. These rocks range in age from 8 Ma to Quaternary. They are divided into two cycles (Crowe 1990), the Older postcaldera basalt (OPB) and the Younger postcaldera basalt (YPB). The field relations and geochronology of the basalt cycles of the YMR are described in following sections.

The level of detail of studies of basaltic units of the YMR varies with the age of the volcanic units. Pre-Pliocene basalt units of the region (>6.5 Ma) were studied primarily in reconnaissance. The outcrop relations of the units, as depicted on published quadrangle maps of the U.S. Geological Survey, were checked in the field. Samples were collected of the basalt units. They were examined petrographically and analyzed geochemically (Crowe et al. 1986). The stratigraphic relations of the pre-6.5 Ma basaltic volcanic units were evaluated in the field and geochronology data (whole-rock K-Ar age determinations) were obtained where required to discriminate the ages of the rocks.

By contrast, the basaltic units of the YPB have been the focus of much more detailed studies. All units of this cycle have been mapped or remapped at scales of 1:12,000 to 1:4000. The eruptive sequences of individual centers were assessed largely by detailed mapping using new geochronology data (Crowe 1990; Crowe et al. 1992) aided by petrographic and geochemical analyses of the rocks. Geochronology results from conventional K-Ar age determinations have been supplemented with results from application of age-calibrated geochronology methods to cross check the ages of the youngest Quaternary volcanic centers. The increased level of detail of geologic and geochronologic data as the age of basalt centers decreases is a purposeful attempt to focus the work on assessment of the Pliocene and Quaternary volcanic history of the YMR. It is this part of the geologic record that provides the most important basis for forecasting the risk of future volcanic activity.

Much of the geochronology data for the basalt of the YMR is unpublished or collected before implementation of a fully qualified Quality Assurance program. While these data are of high scientific quality, they do not meet the recent Los Alamos YMP quality assurance requirements. Because of this

problem, we present only minor discussion of the nonqualified geochronology data, adding references to publications, if available. In contrast, the fully qualified data are presented in Table 2.1 and are discussed in the text. Again, this treatment of the nonqualified data is not a negative reflection on the scientific quality of the data. If necessary, some of these data will be evaluated with respect to current QA requirements. If the data cannot meet the new QA requirements, it will be used to guide the acquisition of new needed information should the Yucca Mountain site be considered formally as a potential repository site for high-level radioactive waste.

A. Basalt of the Silicic Episode

The BSE crops out throughout the YMR. These basaltic rocks are identified by a suite of characteristics; however, none of the features are individually unique. The first is the close association, in space and time with the eruptive activity of the calderas of the TM-OV complex. The BSE postdates closely the eruption of the Timber Mountain Tuff (11.2 Ma). Many of the basalt units of this episode underlie stratigraphically the Thirsty Canyon Tuff (8.5 Ma) (Noble et al. 1992). Second, the largest-volume centers of the BSE are located in the ring-fracture zone of the Timber Mountain caldera complex and record a waning phase of the caldera-related volcanic activity (Fig. 2.4). Third, all centers of the BSE were large volume eruptive units (>3 km^3 dense rock equivalent [DRE]). Their present surface outcrops form major topographic features (eroded shield volcanoes or lava mesas where basalt lavas cap modern topographic ridges). Third, the BSE exhibit a wide range in geochemical composition (basalt to basaltic andesite or latite). They exhibit a much larger range of compositional variation than the PCB (Crowe et al. 1986; Crowe 1990).

The BSE is divided into three major groups, based on their geographic distribution. These are (1) basalt exposed in the moat zone of the Timber Mountain caldera, (2) basalt near and flanking the Black Mountain caldera, and (3) basalt of the Yucca Mountain area (Fig. 2.4).

1. Mafic Lavas of Dome Mountain. The most important occurrence of basaltic rocks by volume is in the southeast edge of the Timber Mountain caldera (Fig. 2.4). Here, mafic lavas are interbedded with two major successions of rhyolite lava. They overlie the rhyolite of Fortymile Wash and underlie the rhyolite of Shoshone Mountain (10.3 ± 0.3 Ma) (Noble et al. 1992; Minor et al. 1993). The basalt and rhyolite define a bimodal association marking the waning postresurgence stage of the Timber Mountain caldera (Christiansen et al. 1977). The largest volume of basaltic magma is the mafic lavas of Dome Mountain. These lavas have been described by Luft (1964) and Marsh and Resmini (1992). They form an assemblage of basalt and basaltic andesite with a local thickness of >300 m. They are interbedded with volcaniclastic breccia and conglomerate in the ring-fracture zone of the Timber Mountain caldera. These sedimentary units are moat breccias deposited in the collapsed interior of the Timber Mountain caldera. The outcrops of the mafic lavas of Dome Mountain form a slightly arcuate shield volcano centered at Dome Mountain proper (Fig. 2.4). The area of surface exposure of the mafic lavas of Dome Mountain is about 50 km^2. Their minimum volume is about 10 km^3 (DRE). The feeder vents for the mafic lavas of Dome Mountain, as noted by Luft (1964), are not exposed. However, a source near Dome Mountain is required by the near symmetrical centering and increased thickness of the lava shield and individual lava flows at Dome Mountain. The likely structural control for the eruption of the mafic lavas of Dome Mountain is the ring-fracture system of the Timber Mountain caldera.

The mafic lavas of Dome Mountain can be divided into two informal units, based on their petrographic features. Porphyritic basalt (phenocrysts of olivine-clinopyroxene) crops out in east Cat Canyon. The lavas are overlain locally by the Thirsty Canyon Tuff and have been dated at 10.8 ± 0.5 Ma

(Kistler 1968). These basalts were mapped as separate units from the mafic lava of Dome Mountain (Carr and Quinlivan 1966; Byers et al. 1966). However, basalt lavas interbedded in the upper part of the mafic lavas of Dome Mountain in Fortymile Canyon are identical petrographically and chemically and are probably equivalents of the Cat Canyon lavas. Pilotaxitic to trachytic textured basaltic andesite forms the major volume of the shield lavas of Dome Mountain. Luft (1964) describes trachyandesite to latite lavas in the upper part of the section at Dome Mountain that are similar to the basaltic andesite but with somewhat higher contents of SiO_2 (56–60 weight percentage [wt%]).

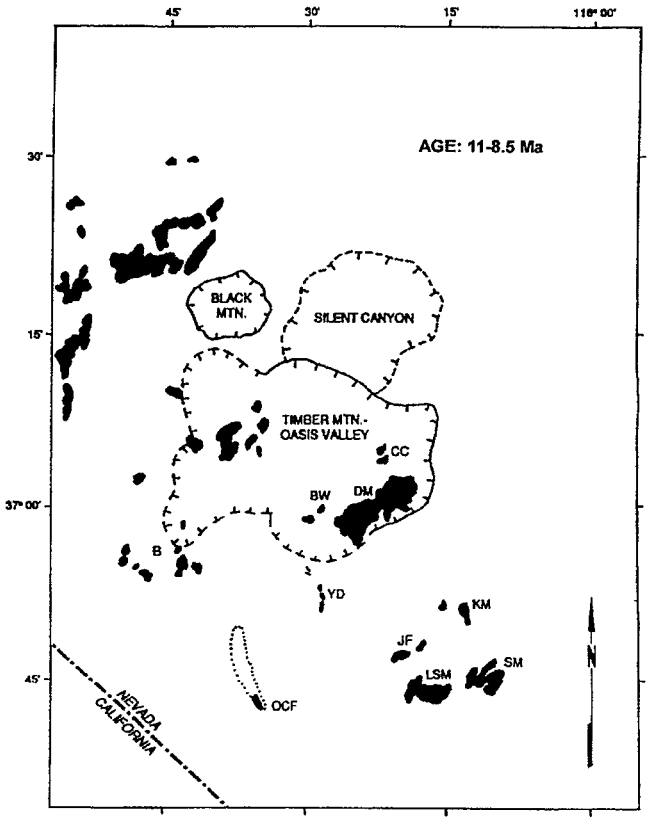


Fig. 2.4 Distribution of the BSE. CC: basalt of Cat Canyon, DM: basalt of Dome Mountain, BW: basalt of Beatty Wash, B: basalt of the Beatty area, SM: basaltic andesite of Skull Mountain, LSM: Little Skull Mountain, KM: mafic rocks of Kiwi Mesa, JF: basalt of Jackass Flat, YD: dike of Yucca Mountain, OCF: older basalt of Crater Flat (modified from Crowe, 1990).

In the northern and western part of the outcrop area of the mafic lavas of Dome Mountain, the unit is onlapped with a slight angular discordance by thin basalt flows informally called the basalt of Beatty Wash. These lavas were mapped separately from the mafic lavas of Dome Mountain (Christiansen and Lipman 1966) and extend from Dome Mountain west along Beatty Wash (Fig. 2.4).

2. Basaltic Rocks of the Black Mountain Caldera. Basaltic volcanic rocks crop out on all but the eastern flanks of the Black Mountain caldera (Fig. 2.4). These basalt units overlap in age with the peralkaline volcanic units of the caldera. They underlie, are interbedded with, and overlie ash-flow units of the Thirsty Canyon Tuff (Minor et al. 1993). Many of the outcrops of basalt are located in the Nellis Bombing and Gunnery Range. Because of restricted access, the basalts have been sampled only at scattered

localities around Black Mountain (Crowe et al. 1986). A sequence of eroded basalt vents and lava flows are exposed south of Black Mountain (Minor et al. 1993). These lavas underlie the Thirsty Canyon Tuff. Basalt lava exposed north of Black Mountain (Minor et al. 1993) underlie and locally overlie the Thirsty Canyon Tuff.

3. Basaltic Volcanic Rocks, Yucca Mountain Area. Basaltic volcanic rocks of the BSE comprise three geologic units in the eastern Yucca Mountain area and two additional units at and southwest of Yucca Mountain. Two of the eastern units were shown on published geologic maps (Ekren and Sargent 1965; Sargent and Stewart 1971; Sargent et al. 1970). These are the basaltic andesite of Skull Mountain and the basalt of Kiwi Mesa (Fig. 2.4). A third unit, the basalt of Jackass Flats, has been separated in more recent geologic reports (Crowe et al. 1986; Frizzel and Shulters 1990).

The basalt of Kiwi Mesa crops out as a small lava mesa on the east side of Jackass Flats (Fig. 2.4). The lavas overlie the Timber Mountain Tuff and are locally overlain by the rhyolite of Shoshone Mountain. The basaltic andesite of Kiwi Mesa is chemically and petrographically identical to the mafic lavas of Dome Mountain (Crowe et al. 1986).

The south and southeast perimeters of Jackass Flat are bounded by Skull and Little Skull Mountains. These small ranges are capped by a sequence of mesa-forming lava flows and flow breccia that locally exceed 60 m in thickness. This unit is the basaltic andesite of Skull Mountain. The lavas are distinguished in the field by the presence of abundant phenocrysts of bipyrimidal quartz (Crowe et al. 1986). Moreover, they are the only known lavas in the region that are subalkaline in composition (Crowe et al. 1983a, 1986). This quartz-bearing basaltic andesite of Skull Mountain overlies the lavas of the Wahmonnie-Salyer center and the Paintbrush and Timber Mountain tuffs. It has a whole-rock K-Ar age of 10.2 ± 0.5 Ma.

Several small outcrops of dissected lava are flanked by alluvium in the central part of Jackass Flats (Fig 2.4) (Frizzel and Shulters 1990). These lavas have been dated by the K-Ar method at 11.0 ± 0.4 and 11.2 ± 0.4 Ma. Correlative lavas (petrographically and geochemically) are interbedded with the upper part of the sequence of basaltic andesite of Skull Mountain at Little Skull Mountain but not at Skull Mountain (Crowe et al. 1986). Samples of the lavas at Little Skull Mountain have been dated at 8.4 ± 0.4 Ma, which is inconsistent with the age of the inferred correlative lavas of Jackass Flats.

The Solitario Canyon fault forms the western edge of the potential Yucca Mountain site (Scott and Bonk 1984). The north trace of the fault near its intersection with Drill Hole wash is intruded by a basaltic dike. The dike is exposed locally along the northwest edge of the block (Fig. 2.4) and in trench 10. Exposures of the dike in trench 10 show that the dike both intrudes the fault plane and has been offset by subsequent episodes of movement on the Solitario Canyon fault. North of trench 10, the strike of the dike swings to the northwest. It crops out discontinuously, forming en echelon dikes in the Tiva Canyon member of the Paintbrush Tuff. This change in strike coincides with an abrupt change in the trend of the topography of ridges and valleys, from north/south- to northwest-trending, and occurs at the north end of the exploratory block of Yucca Mountain. Scott and others (1984) suggest that the northwest-trending valleys are underlain by right-slip faults that are inferred to be part of the Walker Lane structural system. Alternatively, Carr (1984 1988 1990) and Carr et al. (1985 1986) suggest that the dikes follow the outer ring fracture zone of a buried caldera. The dike has been dated at 10.0 ± 0.4 Ma (Carr and Parrish 1985).

The older basalt of Crater Flat (Crowe et al. 1986) crops out along the south slope of an arcuate ridge forming the south boundary of Crater Flat (Fig. 2.4). The outcrops consist of the remnants of

oxidized vent-scoria intruded by dikes and small plugs. These units are probable eroded roots of at least one, and more likely several, scoria cones. Directly east of the scoria deposits, there is a sequence of thin lava flows and flow breccia that are petrographically similar to and probably derived from the plugs or cones. These lavas are overlain by slide blocks of Paleozoic carbonate. They have been dated by the whole-rock K-Ar method at 10.5 ± 0.1 Ma. The lavas dip to the northeast and are inferred to underlie the south and southwest parts of Crater Flat. This is suggested by several lines of evidence (Crowe et al. 1986). First, the lavas have a reversed magnetic polarity. They coincide with, and are the probable source of, an arcuate negative magnetic anomaly that borders the southwest part of Crater Flat (Kane and Bracken 1983). Second, petrographically and chemically similar lavas were cored at about 360 m beneath the surface in Drill Hole USW VH-2 located between Red Cone and Black Cone in the central part of Crater Flat (Carr et al. 1984; Crowe et al. 1986). These lavas were dated at about 11 Ma (Carr et al. 1984). The lavas in the drill hole have a reversed magnetic polarity, similar to the older basalt of Crater Flat. They are the inferred source of a large circular negative aeromagnetic anomaly located in west-central Crater Flat (Kane and Bracken 1983). This aeromagnetic anomaly extends south to the described anomaly of southwest Crater Flat. The combined field, geochronology, geochemical, and aeromagnetic data suggest that the west and southwest parts of Crater Flat are floored by an extensive basalt unit of 10.5 to 11 Ma.

B. Postcaldera Basalt of the Yucca Mountain Region

The second recognized episode of basaltic volcanism in the YMR is the Postcaldera basalt. These basalt centers occur at sites either well removed from eruptive centers of the TM-OV complex or are younger than and cannot be related in time to the silicic magmatic activity. The basalts consist of small-volume (<1 km^3) centers marked by clusters of scoria cones and lava flows (except for the basalt of Thirsty Mesa that has a volume of >3 km^3). They are divided into two groups, the Older postcaldera basalt and the Younger postcaldera basalt. This division is based on differences in their ages and geographic distribution (Fig. 2.5).

1. Older Postcaldera Basalt. The OPB occurs at five localities, all north and east of Yucca Mountain (Fig. 2.5). The OPB was erupted along either north/northwest-trending basin-range faults or at the intersection of basin-range faults with the ring-fracture zone of older calderas. Field evidence shows that some of the basalt units were erupted contemporaneously with movement on the extensional faults (Crowe et al. 1983b, 1986). The OPB ranges in age from 9 to 6.3 Ma (Fig. 2.5).

a. Basalt of Rocket Wash. A platy series of thin, basalt lava flows, informally named the basalt of Rocket Wash, overlies the Thirsty Canyon Tuff in the northwest edge of the Timber Mountain caldera (Fig. 2.5). This basalt, which was mapped by Lipman et al. (1966b), O'Connor et at. (1966), and Minor et al. (1993), erupted along a north-trending normal fault that marks the approximate edge of the ring-fracture zone of the Timber Mountain caldera. The vent for the basalt lavas was located at the northern edge of the mapped outcrops. This is indicated by two features. First, the outcrops of the flow thicken consistently northward. Second, deposits of eroded cone scoria are present at the north end of the exposed outcrops where they have been preserved beneath lava flows. The basalt of Rocket Wash overlies the Trail Ridge member of the Thirsty Canyon Tuff. The approximate volume of lavas (DRE) is about 0.2 km^3. The basalt yielded a K-Ar age of 8.0 ± 0.2 Ma.

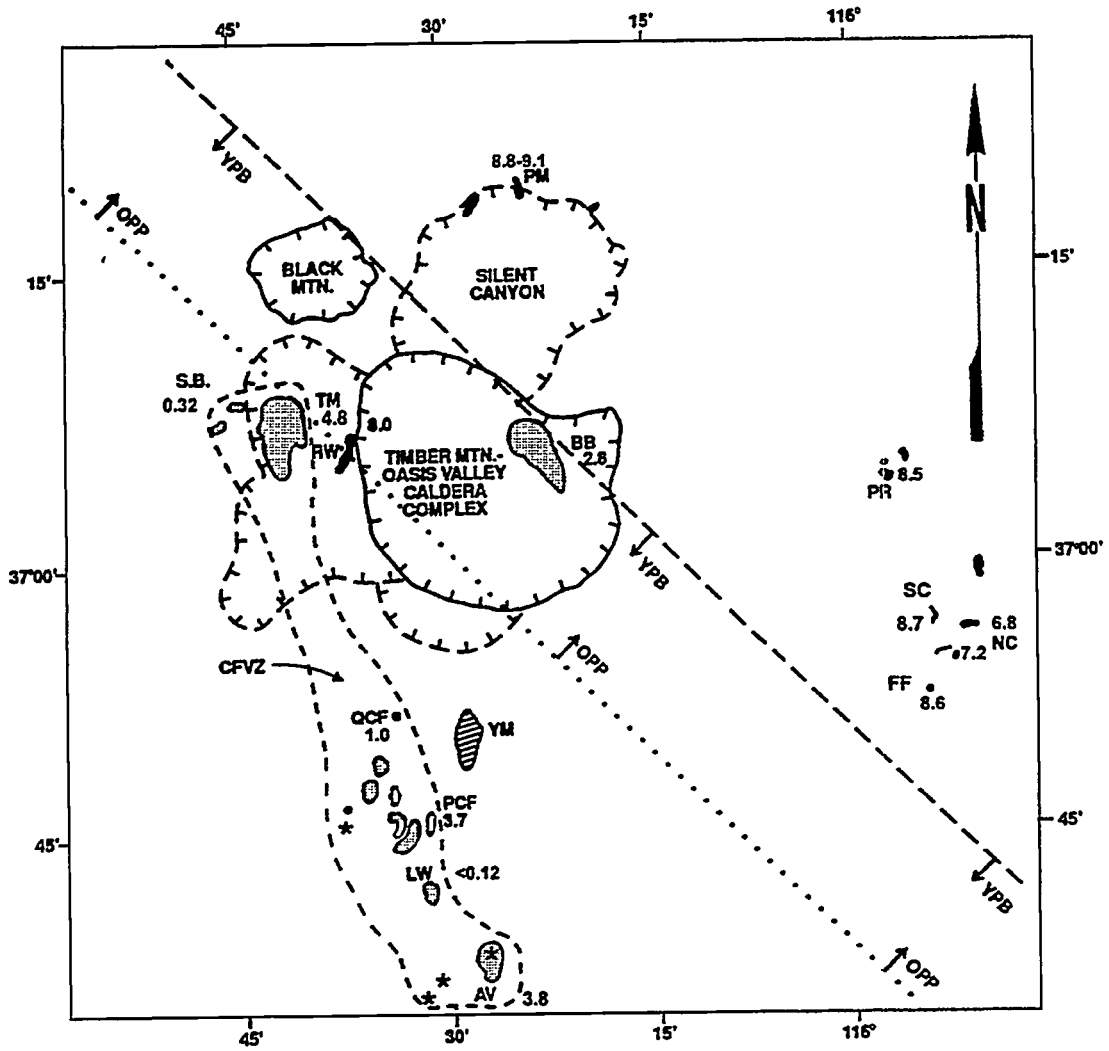


Fig. 2.5 Postcaldera Basalt of the YMR. Shaded areas are the OPB, including: RW: basalt of Rocket Wash, PM: basalt of Pahute Mesa, SC: basalt of Scarp Canyon, NC: basalt of Nye Canyon, FF: buried basalt of Frenchman Flat. Stippled areas are the YPB, including: TM: basalt of Thirsty Mesa, AV: basalt of Amargosa Valley, PCF: Pliocene basalt of southeast Crater Flat, BB: basalt of Buckboard Mesa, QCF: Quaternary basalt of Crater Flat, SB: basalt of Sleeping Butte, LW: basalt of Lathrop Wells. Asterisks mark aeromagnetic anomalies identified as potential buried basalt centers or intrusions (Kane and Bracken 1983, Crowe et al. 1986). Dashed line encloses the area of the CFVZ. Numbers associated with the symbols for the volcanic units of the OPB and YPB are the age of the volcanic centers in million of years. Modified from Crowe and Perry (1989).

b. Basalt of Pahute Mesa. Three spatially separate but related basalt units of the OPB crop out in the north part of the ring-fracture zone of the Silent Canyon caldera. These basalts, which are informally named the basalt of Pahute Mesa, are localized at the intersection of north/northeast-trending basin-range faults within the ring-fracture zone of the Silent Canyon caldera (Fig. 2.5). They are divided into three units, each separate geographically. These are a western basalt, a central basalt, and an eastern basalt.

The western basalt is distinctly porphyritic with large resorbed megacrysts of black clinopyroxene and plagioclase. The basalt overlies the Trailridge and Spearhead members of the Thirsty Canyon Tuff. Exposed outcrops are primarily dissected cone scoria with numerous intrusive dikes. A feeder dike associated with the scoria deposits can be traced to the southwest and parallels the trend of basin-range

faults. The minimum volume of the basalt center is about 0.7 km^3 (DRE). A sample collected from the feeder dike was dated at 9.1 ± 0.7 Ma.

The central basalt center consists of at least three separate but subparallel dike systems associated with probable surface scoria cones. The existence of the scoria cones is inferred from the presence of eroded scoria deposits containing aerodynamically shaped bombs. The scoria deposits overlie the Trail Ridge member of the Thirsty Canyon Tuff and feeder dikes of the center intrude the Timber Mountain Tuff and rhyolite of Quartet Dome. The lava of the middle basalt center is conspicuously less porphyritic than the western basalt; megacrysts of black clinopyroxene and plagioclase are rare. The central basalt yielded a K-Ar age of 8.8 ± 0.1 and 10.4 ± 0.4 Ma. The older age is inconsistent with the stratigraphic relations of the central basalt center (overlying the Thirsty Canyon Tuff) and is probably in error.

The eastern basalt occurs only as three small remnant outcrops of lava and dikes. Two of the lavas crop out in alluvium, the third intrudes the Trail Ridge member of the Thirsty Canyon Tuff. The outcrop patterns of each site are elongate parallel to north/northeast-trending basin-range faults and are located on the ring-fracture zone of the Silent Canyon caldera (Orkild et al. 1972). The eastern basalt is identical petrographically to the western basalt and has not been dated.

c. Basalt of Paiute Ridge. The Halfpint Range, which forms the eastern margin of Yucca Flat, exposes a complex sequence of sills, dikes, and lopolithic intrusions of basaltic composition (Byers and Barnes 1967). Dissected scoria cones and lava flows are associated with the intrusive bodies indicating surface eruptions accompanied the formation of the intrusions (Crowe et al. 1983b; Valentine et al. 1992). The sills and lopolithic bodies occur in the interior of a northwest-trending graben. Subsurface magma intruded generally upward and locally eastward from dikes that are coplanar with northwest-trending basin-range faults. Eastward intruded magma formed sills by lifting and locally intruding the overlying sequence of tuff. At several localities, primarily in the axis of the graben, the sills sagged to form lopolithic intrusions (Byers and Barnes 1967; Crowe et al. 1983b; Valentine et al. 1992). Some of the sills differentiated *in situ* to form pods of syenite (Byers and Barnes 1967).

The northwest-trending dikes locally expand or flare upward forming vertically jointed, cylindrical bodies with associated near-vertical radial dikes. These are probably roots of eroded scoria cones (Crowe et al. 1983b; Valentine et al. 1992). In the eastern and central area of the graben, irregular feeder dikes can be traced upward into surface deposits of scoria cones and lava. This complex of intrusive and extrusive basalt, which is informally called the basalt of Paiute Ridge, exposes the geometry of shallow intrusive rocks and feeder dikes and provides an ideal locality to study the effects of shallow basalt intrusions (Valentine et al. 1992).

The surface lava from the basalt of Paiute Ridge has been dated by the whole-rock K-Ar method at 8.5 ± 0.3 Ma (Crowe et al. 1983b). The geologic relations of the surface basalt outcrops and dikes and sill complexes record a complex history of basin-range faulting in the Half Pint range. Dikes of basalt intrude into and are coplanar with several northwest-trending faults. The faults and the main graben system must, therefore, predate the basalt (>8.5 Ma). Sills of basalt are offset and downfaulted outcrops of cone scoria are present in the center of the graben. Both relationships require continuing offset on the faults after eruption and intrusion of the Miocene basalt. A possible correlative basalt with the basalt of Paiute Ridge has been reported in the subsurface of southern Yucca Flat (Drill hole UE1-H; 784 ft below the surface) and has been dated at 8.1 ± 0.3 Ma.

Recent paleomagnetic investigations by Ratcliff et al. (1993) have demonstrated that emplacement of the basalt of Paiute Ridge occurred during a geomagnetic polarity transition, probably from reverse to normal polarity. All the sills, dikes, lopolithic intrusions, and lava flows give transitional paleomagnetic data and, together, define a relatively smooth "path" for the field reversal. These data are of considerable interest for the emplacement dynamics of mafic magmas in such a setting. Given our current understanding of the duration of geomagnetic polarity reversals, it is probable that the entire complex of mafic intrusions at Paiute Ridge was emplaced in less than a few hundred to few thousand years.

A separate but petrologically related basalt, the basalt of Scarp Canyon, crops out southeast of the basalt of Paiute Ridge and west of Nye Canyon. It consists of a 3 to 4-km-long, north/south-trending basalt dike that intrudes nonwelded ash-flow, ash-fall, and reworked tuff that predates the Paintbrush Tuff. The dike locally branches into vertical radial dikes of irregular strike then widens, where it crosses a northwest-trending normal fault (Henrichs and McKay 1965). The widened dike portion has funnel-shaped outer contacts marked by scoriaceous breccia mixed with country rock and forms a plug mass that is probably the eroded roots of a former surface center. The basalt of Scarp Canyon yielded a whole-rock K-Ar date of 8.7 ± 0.3 Ma.

d. Basalt of Nye Canyon. The last major unit of the OPB is the basalt of Nye Canyon (Fig. 2.5). This unit consists of at least four centers; one is buried beneath alluvial deposits of northeast Frenchman Flat (Carr, 1974). There are three surface centers of basalt that define a northeast-trending alignment of basalt centers. The basalt of Nye Canyon is the oldest basalt unit in the YMR that shows a northeast-structural trend. That is the predominant direction of dike orientation and alignment of clusters of centers in post-Pliocene basalt in the region (Crowe et al. 1983; Crowe and Perry 1989; Crowe 1990).

The northeastern center of the basalt of Nye Canyon consists of a moderately dissected scoria cone surrounded on the south and southwest by a thin lava flow, mostly buried beneath alluvial deposits. The northeastern center has been dated at 6.3 ± 0.2 Ma. The middle and southern basalt centers are eroded tuff rings (Crowe et al. 1986) formed by mixed strombolian and hydrovolcanic activity. The interiors of both tuff rings are partly to completely filled by scoria deposits and lava and record episodes of mixed strombolian and hawaiian eruptive activity that followed the hydrovolcanic eruptions. The middle basalt center is the most primitive basalt geochemically in the region (Crowe et al. 1986; Farmer et al. 1989). It contains abundant nodules of gabbro, and less commonly, wherlite. A plug from the middle center has been dated at 6.8 ± 0.2 Ma. The southern center is formed at the eastern edge of a large ring dike. The dike extends nearly continuously in a 320° arc extending westward from the southern center (Henrichs and McKay 1965). The ring dike has an approximate diameter of 1 km. It locally widens to form cylindrical plugs that probably mark the eroded roots of former scoria cones. The south center has been dated at 7.2 ± 0.2 Ma.

A fourth basalt center was intersected in a drill hole in alluvium beneath Frenchman Flat (Carr 1984). It has been dated at 8.6 Ma. This basalt may be correlative with the basalt of Nye Canyon. Alternatively, its K-Ar age suggests it may be correlative with the basalt of Scarp Canyon (Fig. 2.5).

2. Younger Postcaldera Basalt. A brief but regionally significant hiatus in volcanic activity followed eruption of the basalt of Nye Canyon. No volcanic rocks of the YMR, including both surface and subsurface rocks, have yielded age determinations in the range of 6.3 (basalt of Nye Canyon) and 4.8 Ma (basalt of Thirsty Mesa). The second cycle of the post-caldera basalt, the YPB includes all volcanic rocks younger than the basalt of Nye Canyon. In order of decreasing age, these basalts include the basalt of Thirsty Mesa, the basalt of Amargosa Valley, the basalt of southeast Crater Flat, the basaltic andesite of

Buckboard Mesa, the Quaternary basalt of Crater Flat, the basalt of Sleeping Butte, and the Lathrop Wells basalt center (Crowe 1990). These basalt centers, except the basaltic andesite of Buckboard Mesa, all occur in a narrow northwest-trending zone located west and south of the Yucca Mountain site (Fig. 2.5). This zone has been named the CFVZ (Crowe and Perry 1989). The basalt centers of the YPB, with two exceptions, consist of clusters of probably coeval, small-volume centers aligned along predominantly northeast (one north) structural trends. The exceptions are the basaltic andesite of Buckboard Mesa and the Lathrop Wells center. The basaltic andesite of Buckboard Mesa consists of a main scoria cone located on a northwest-trending fissure. The Lathrop Wells cone consists of only one center.

a. Basalt of Thirsty Mesa. The basalt of Thirsty Mesa comprises a thick accumulation of fluidal lava and local feeder vents marked by dissected scoria cones surmounting the lava mesa (Fig. 2.5). These lavas, viewed from the west, appear to form a shield volcano but the volcanic landform is actually more complex than a simple shield. The lavas were erupted onto a preexisting plateau formed by ignimbrite of the Thirsty Canyon Tuff. The flows form a convex upward-mesa surface above the plateau.

The topographic summit of the mesa is formed by eroded deposits of scoria marking subdued mounds that probably represent the main sites of extrusion of the lavas. This interpretation is supported by the gradual increase in thickness and the symmetrical distribution of the lava flows about the scoria mounds. The mounds trend north/south, probably reflecting the predominant structural control of the center. The basalt of Thirsty Mesa covers an area of about 22 km^2 with a maximum thickness of about 200 m. The approximate volume of the center was estimated at 3 km^3 (DRE; Crowe et al. 1992). However recent field work revealed that we may have over-estimated the lava thickness and the volume of the center may be less than 3 km^3. The lavas are sparsely porphyritic olivine-basalt with phenocrysts and microphenocrysts of olivine.

The lava mesa shows moderate geomorphic degradation. Lava flow margins are eroded. The lava flow surfaces have well-developed surface pavements containing soil with horizon development. There is no evidence of preserved primary flow-top topography. The scoria vents have been dissected significantly but still maintain a rounded mound-form and uphold the high-standing topography of the mesa. Minor et al. (1993) reported an $^{40}Ar/^{39}Ar$ age of 4.6 Ma for the basalt of Thirsty Mesa. We have obtained $^{40}Ar/^{39}Ar$ ages for a sample collected from the west base of the lavas of Thirsty Mesa and a dike sample collected from one of the summit scoria cones. The ages are, respectively, 4.68 ± 0.03 and 4.88 ± 0.04 (2σ) Ma (Table 2.1). These ages are in good agreement with the age reported by Minor et al. (1993), and geomorphic data (Crowe et al. 1992). The basalt of Thirsty Mesa has a reversed magnetic polarity. Adequate geochronology data have been obtained to document the age of the basalt of Thirsty Mesa.

The lava mesa, prior to 1992, was thought to underlie the Thirsty Canyon Tuff and therefore to be of Miocene age. The revised field relations and the new age determinations show that it is a newly identified Pliocene volcanic unit of the YMR. Accordingly, the basalt of Thirsty Mesa is significant for several reasons. First, the mesa is located in and provides additional evidence for the existence of the CFVZ of Crowe and Perry (1989). Second, the basalt of Thirsty Mesa is the largest volume volcanic unit of the YPB. The volume of basalt (≤ 3 km^3) equals the volume of some of the basaltic units of the BSE. Third, the basalt of Thirsty Mesa is an evolved alkali basalt , but is distinguished chemically from the basalt of Crater Flat by significantly higher potassium content (Vaniman and Crowe 1981; Vaniman et al. 1982).

Table 2.1 $^{40}Ar/^{39}Ar$ Ages of Basaltic Volcanic Centers in the YMR[1]

Sample	Geologic Unit	Description	$^{40}Ar/^{39}Ar^2$	$^{37}Ar/^{39}Ar^2$	$^{36}Ar/^{39}Ar^2$	^{39}Ar (10^{-13} mol)	$^{40}Ar^*$ % rad.	Age (Ma)	± (2σ)	Weighted Age (Ma)
NE-10-1-91-1-BMC	Thirsty Mesa	Basal lava flow, west side	19.58	1.05	0.04	7.47	40.5	4.68	0.04	4.68 ± .03
			23.1	1.06	0.05	5.69	33.9	4.68	0.05	
NE-10-1-91-2-BMC	Thirsty Mesa	Dike, summit scoria cone	19.29	0.92	0.04	5.22	41.9	4.79	0.05	4.88 ± .04
			23.1	0.93	0.05	5.73	35.7	4.96	0.05	
Well 25-1-BMC	Amargosa Valley	Cuttings, drill hole	23.22	1.48	0.06	4.11	27.8	3.88	0.07	3.85 ± .05
			24.92	1.47	0.06	3.34	25.9	3.81	0.08	
CF10FVP	SE, Crater Flat	Dike, southern vent	40.04	2.16	0.12	3.14	14.9	3.58	0.09	3.65 ± .06
			29.4	2.18	0.08	4.07	21.1	3.71	0.08	
CF12FVP	SE, Crater Flat	Lava lake, central vent	30.23	2.3	0.08	3.49	20.9	3.71	0.07	3.69 ± .05
			28.71	2.31	0.08	3.99	21.3	3.67	0.06	
CF14FVP	SE, Crater Flat	Lava flow, north exposure	19.85	2.29	0.05	4.58	32.2	3.8	0.06	3.75 ± .04
			17.74	2.32	0.04	9.15	35.0	3.73	0.04	
BC1FVP	Quat, Crater Flat	Black Cone, summit lava lake	89	1.98	0.3	3.8	1.9	1.03	0.21	1.05 ± .14
			74.21	1.94	0.25	2.89	2.4	1.07	0.18	

Table 2.1 (Cont.)

Sample	Geologic Unit	Description	$^{40}Ar/^{39}Ar^2$	$^{37}Ar/^{39}Ar^2$	$^{36}Ar/^{39}Ar^2$	^{39}Ar (10^{-13} mol)	$^{40}Ar^*$ % rad.	Age (Ma)	± (2σ)	Weighted Age (Ma)
BC3AFVP	Quat, Crater Flat	Black Cone, replicate of BC3FVP	82.31	1.89	0.27	4.55	2.0	1.01	0.21	0.96 ± 0.15
			77.27	2.00	0.26	2.48	2.0	0.91	0.21	
BC6FVP	Quat,Crater Flat	Black Cone, southern lava flow	27.29	2.05	0.09	3.75	5.9	0.96	0.07	0.94 ± .05
			29.1	2.07	0.09	3.45	5.1	0.92	0.07	
BC12FVP	Quat, Crater Flat	Black Cone, northern lava flow	33.37	1.62	0.11	4.31	5.4	1.08	0.09	1.05 ± .08
			38.14	1.75	0.12	3.94	4.2	0.99	0.12	
CF15FVP	Quat, Crater Flat	Little Cones, southern dike	58.88	1.64	0.19	3.65	3.1	1.11	0.14	1.02 ± 0.10
			56.65	1.65	0.19	4.82	2.7	0.93	0.15	
LW20FVP	Lathrop Wells	Ql1d, Old Quarry Flow	29.63	1.62	0.1	5.9	1.6	0.28	0.06	***
			29.62	1.65	0.1	5.98	1.8	0.31	0.08	
			23.75	1.63	0.08	5.13	0.7	0.09	0.06	

1 Samples were irradiated at the Ford Reactor, University of Michigan, using ANU K-Ar standard GA1550 biotite as a flux monitor and Fish Canyon biotite as a cross check. J-factor = 0.00033 ± 1.

2 Not corrected for interfering reactions. K correction ($^{40}Ar/^{39}Ar$) = 0.0467; Ca correction (36Ar/37Ar) = 0.0002279; Ca correction (39Ar/37Ar) = 0.0007.

*** Replicate ages are too variable to calculate a meaningful weighted age.

b. Basalt of Amargosa Valley. A negative aeromagnetic anomaly was identified in the Amargosa Valley, several kilometers south of the town of Amargosa Valley (Kane and Bracken 1983; Crowe et al. 1986) (Fig. 2.5). The anomaly was drilled in 1991 by a private company (Harris et al. 1992). Samples of cuttings of the basalt were obtained and submitted for K-Ar age determinations. An age of 3.85 ± 0.05 Ma was obtained for the cuttings under YMP controls (Table 2.1). Turrin (1992, p. 231) reported an $^{40}Ar/^{39}Ar$ age of a basalt sample from the exploratory drill hole of 4.4 ± 0.07 Ma. This is significantly older than the age of 3.85 Ma, and additional age determinations may be required to investigate the discrepancy in ages.

The boundaries of this newly drilled basalt unit are prominently delineated on aeromagnetic maps (Kane and Bracken 1983; Langenheim et al. 1992 1993). The main mass of the basalt is located 3 km south of the town of Amargosa Valley. The near-circular outline of the northern part of the anomaly suggests it may be the main conduit or vents for the center. A lobate aeromagnetic mass extends to the south of the main mass and may outline a lava flow derived from the center. The aeromagnetic anomaly is inferred to represent a former surface basalt center buried by alluvium deposits in a zone of higher sedimentation along the trace of the Fortymile Wash (Fig. 2.1; Fig. 2.5). The area of coverage of the aeromagnetic anomaly is about 20 km^2. If the basalt is a buried center and has dimensions typical of local lava flows and scoria cones, its volume is estimated to be about 0.2 to 0.4 km^3 (DRE). An estimate of 0.3 km^3 was obtained for the basalt based on modeling of the gravity and aeromagnetic data (V. Langenheim, personal communication, 1993). Two other aeromagnetic anomalies are present in the south central part of the Amargosa Valley and may represent buried basalt centers (Langenheim et al. 1993). These will be investigated by exploratory drilling as part of the Yucca Mountain site characterization studies.

c. Basalt of Southeast Crater Flat. The basalt of southeast Crater Flat has been described by Crowe and Carr (1980), Vaniman and Crowe (1981), Vaniman et al. (1982), Crowe (1990), and Perry and Crowe (1992). The basalt unit consists of an alignment of north-trending dissected scoria cones and associated moderate-volume lava flows (Fig. 2.5). The scoria cones extend south in an en echelon pattern from the east central part of Crater Flat. The former presence of individual centers is indicated primarily by the presence of eroded deposits of oxidized cone scoria. The scoria contains aerodynamically shaped bombs and spatter. The large size of the bombs (>0.5 m) and local agglutination of the spatter requires near-vent deposition. However, scoria outcrops are deeply eroded, discontinuous, and retain no primary constructional topography.

The geometry of vent zones can be reconstructed by detailed mapping of three surface features. First, the north and east parts of one cone (here named the Radial center) are preserved beneath a cover of thin aa flows probably derived from the center. The south side of this cone is upheld by an increased degree of induration of the scoria in proximity to a north/south-trending swarm of lenticular dikes. This combination of features provides sufficient preservation of the radial dips of scoria deposits to reconstruct the location of the former near-circular cone. Second, a series of elongate lava masses are exposed in the center parts of vents of the basalt of southeast Crater Flat. These masses are not lava flows. They are preserved remnants of lava ponded in the elongate vent of individual centers. This interpretation is suggested by the gentle inward dips of the lava (10°–20°) around the circumference of the exposures and the presence of scoria deposits beneath and buttressed against the lava ponds. These elliptical lava ponds have long axes trending north/south suggesting the lava ponds filled elongate vents (fissures), not the craters of symmetrical scoria cones. The direction of the elongation of the lava ponds is coparallel to the trend (north/south) of linear feeder dikes. Third, lenticular dikes expanded locally forming irregular plugs with vertical cooling joints. These plugs are associated with an increased thickness of indurated deposits of scoria. The dips of the scoria deposits, recognized by the presence of aerodynamically shaped bombs, are relatively steep (15°–25°) and require deposition at or near eruptive vents.

Lavas of the basalt of southeast Crater Flat are the most aerially extensive of the YPB. They form sheet-like flows that flank, to the south and east, the described vent zones. In no case, however, can the lavas be traced directly to their individual feeder sources. Cross sections of the flows show that they are relatively thin (3–5 m) aa flows with basal breccia of clinker and blocky vesicular upper surfaces. The flows are offset more than a meter (west-side down) along north/south-trending faults that may be related to exposed faults in the northwest part of Yucca Mountain (Crowe and Carr 1980; Smith et al. 1990). The lava flows are covered to the east by alluvium, and the section is probably displaced downward several tens of meters by faults concealed beneath alluvium. This displacement is suggested by several features. First, the eroded outcrop edge of the flows trends north/south and parallels local basin-range faults, suggesting that the present flow margin is fault-controlled. Second, petrologically similar lava flows are exposed in easternmost Crater Flat where they are faulted against the bedrock tuff of Yucca Mountain or overlie an erosional surface developed on the poorly consolidated deposits of the Paintbrush and Timber Mountain Tuffs. Third, aeromagnetic data show the lava flows are continuous beneath the alluvium (Kane and Bracken 1983). Vents distinguished in the field can be identified in the aeromagnetic data by north/south elongation and local near-circular patterns of magnetic contours. These patterns are not observed in the eastern outcrop areas of the basalt of southeast Crater Flat where the rocks are concealed beneath alluvium or are faulted against Miocene tuff. This suggests that there are probably no *major* eruptive centers concealed beneath the alluvial deposits.

The basalt of southeast Crater Flat was dated initially at 3.84 ± 0.13 and 3.64 ± 0.13 Ma (Vaniman et al. 1982). Sinnock and Easterling (1983) obtained ages of 4.27 ± 0.46, 3.73 ± 0.06, and 3.89 ± 0.17 Ma for replicate sets of whole-rock, K-Ar age determinations obtained from splits of the same sample collected at one site in the basalt of southeast Crater Flat. The samples were analyzed at three separate chronology laboratories (values reported as unweighted averages with 1σ standard deviations). A second sample site was collected from outcrops of the basalt of southeast Crater Flat and analyzed at the same three laboratories. This site yielded average ages of 4.22 ± 0.08, 3.69 ± 0.09, and 4.00 ± 0.13 Ma, respectively (Sinnock and Easterling 1983). The differences in age determined from the three laboratories are systematic (i.e., laboratory "B" generally reported the youngest date from any sample site) and are probably related to differences in sample preparation methods and instrumentation among the three laboratories. Unpublished K-Ar ages of about 3.91 ± 0.20 and 3.75 ± 0.12 Ma have been obtained by the U.S. Geological Survey for samples collected from a dike exposed in cone scoria and a lava, respectively. New $^{40}Ar/^{39}Ar$ ages of 3.65 ± 0.06, 3.69 ± 0.06, and 3.75 ± 0.04 (2σ) Ma have been obtained for the basalt of southeast Crater Flat (Table 2.1). The consistency of age determinations for this unit at multiple analytical laboratories suggests the chronology of this unit is well established by the existing radiometric ages. All measured samples of the basalt of southeast Crater Flat have a reversed magnetic polarity (Vaniman and Crowe 1981; Vaniman et al. 1982). The similarity in age of the basalt of Amargosa Valley and the basalt of Crater Flat suggests that the units were probably erupted about the same time but as spatially separate units.

d. Basalt of Buckboard Mesa. The basalt of Buckboard Mesa is the second largest basalt by volume of the postcaldera basalt units of the region (1 km^3 [DRE]). It comprises aphyric to sparsely porphyritic lavas erupted in the northeast part of the ring-fracture zone of the Timber Mountain caldera (Fig. 2.5). The lavas were erupted mainly from a scoria cone in the northwest part of the outcrop area (Scrugham Peak). Additional lava flows vented from a fissure that extends southwest for about 5 km from the base of Scrugham Peak. This fissure is marked both by a subdued linear ridge in the present-day topography and by the presence of scoria and agglutinated spatter exposed in craters excavated during high-explosive experiments (Lutton 1968, Fig. 1). The basalt erupted into and filled topographic valleys between the east and west branches of Fortymile canyon (Lutton 1968). Subsequent erosion lead to inverted

topography and the flows now form a mesa top. The majority of outcrops of the basalt of Buckboard Mesa around the margins of the mesa and within the explosion craters expose a single major lava flow with only local multiple flow lobes (Lutton 1968). Lutton (1968) described cores from boreholes near Scrugham Peak in which two flows could be distinguished. A second lava flow can also be discriminated in outcrops northwest of Scrugham Peak by local changes in topography and the presence of phenocrysts of kaersutite in the upper lava flow.

The major volume of the basalt of Buckboard Mesa is an aphyric to sparsely porphyritic olivine-bearing trachyandesite (mean SiO_2 content of 53.5 wt% (Lutton 1968; Crowe et al. 1986) with abundant plagioclase microphenocrysts and microlites and minor clinopyroxene. Whole-rock K-Ar ages of 2.82 ± 0.04 and 2.79 ± 0.10 Ma were obtained for cores from the basalt of Buckboard Mesa recovered from Drill holes WDH-11 and WDH-12. Unpublished whole-rock K-Ar ages of 2.93 ± 0.03 Ma for the kaersutite-bearing flow, and 3.07 ± 0.29 Ma for the main flow unit have been obtained by the U.S. Geological Survey; these ages are consistent with the positive magnetic polarity of the lavas. Additional samples of the basalt of Buckboard Mesa have been submitted for $^{40}Ar/^{39}Ar$ age determinations and these data should be available in calendar year 1995.

e. Quaternary Basalt of Crater Flat. A series of four Quaternary basalt centers form a northeast-trending, slightly arcuate cluster of basalt centers extending along the axis of Crater Flat. From southwest to northeast, these centers consist of, respectively, Little Cones, Red Cone, Black Cone, and the Makani Cone (the latter cone is named informally in this report).

(1) The Little Cones. The Little Cones consist of two separate cones of small dimensions. The southwest cone is breached on the south side probably from extrusion of a lava flow that is buried beneath alluvial deposits. Two, possibly three small mounds of eroded cone scoria are present about 0.5 km south of the southwest cone and are marked by erosional rubble of cone scoria containing aerodynamically shaped bombs; a small feeder dike is exposed in the cone rubble. Most of the samples of basalt of Little Cones that have been collected for chemistry and K-Ar age determinations have been obtained from this feeder dike. Trenching of the scoria deposits show that they are deposits of vent facies and represent eroded remnants of satellite cones. Two small lava flows partly covered by alluvium flank the northwest and southwest edges of the southeast satellite cone.

The northeast cone is a symmetrical scoria cone and is slightly smaller than the southwest cone. There is no evidence of extrusion of lava from this cone, based either on examination of surface exposures or the aeromagnetic data of Kane and Bracken (1983).

Both of the Little Cones centers are eroded significantly, and rills are conspicuously developed on the cone slopes. The cone-slope angles are less than the angle of repose and cone-slope aprons are developed at the base of the cones. Wells et al. (1990) described preliminary soils and geomorphic data for both centers. They note that the degree of soil development and geomorphic degradation of the Little Cones is comparable to stage II soils in the Cima volcanic field. A K-Ar age of about 1.1 ± 0.3 Ma was obtained for the feeder dike south of the Little Cones (Crowe et al. 1982; Vaniman et al. 1982). An unpublished K-Ar age of a sample collected at the same site was dated by the U.S. Geological Survey at 0.76 ± 0.20 Ma. A recently obtained $^{40}Ar/^{39}Ar$ age of the Little Cones feeder dike is 1.02 ± 0.10 Ma (Table 2.1). Additional samples of the Little Cones center, including volcanic bombs from the cones, have been submitted for $^{40}Ar/^{39}Ar$ age determinations. Both the Little Cone centers have reversed magnetic polarity consistent with the negative aeromagnetic anomaly associated with the centers (Kane and Bracken 1983). The reversed

magnetic polarity and the current K-Ar ages indicate the Little Cones center was probably formed in the Matayama reversed magnetic epoch.

(2) Red Cone and Black Cone Centers. The Red and Black cone centers are analogous volcanic landforms with similar eruptive histories. Each consists of a main scoria cone surmounted by a summit crater filled with agglutinated spatter, large lava blocks, and scoria (Vaniman and Crowe 1981; Smith et al. 1990; Feuerbach et al. 1990; Ho et al. 1991). The main cones are flanked by scattered scoria mounds which are erosional remnants of satellite vents. Some, or perhaps all, of the lavas of both centers were erupted from the satellite vents (Vaniman and Crowe 1981; Vaniman et al. 1982; Smith et al. 1990; Ho et al. 1991).

The Red Cone is significantly modified by erosion. The basal diameter of the cone is 440 m and the height is 55 m (measurements made using the morphometric parameters of scoria cones and colluvial aprons of Wells et al. [1990]). The cone slopes have extensive development of rills, integrated channel networks, and deep radial gullies filled with reworked scoria interbedded with soil. Erosional processes have produced a cone-slope apron extending as much as 400 m from the base of the cone slope (Wells et al. 1990). Two small dikes, which are probable offshoots from the main conduit, are exposed in the western wall of the cone (Vaniman and Crowe 1981). The vent or summit crater of the cone is filled by an accumulation of inward-dipping scoria and agglutinated spatter; aerodynamically shaped bombs in the crater-fill sequence exceed 2 m in length (Vaniman and Crowe 1981). A series of satellite cones or scoria mounds is exposed south of the main cone (Vaniman and Crowe 1981; Ho et al. 1991). These are clustered along northeast and northwest trends. Locally the mounds were the source vents of aa lava flows that flank the south part of the main cone and surround the scoria mounds (Smith et al. 1990). These lavas extend for as much as 1 km from the vents. The outcrop edges of the lavas have abrupt flow fronts with steep flow foliations indicating the present edges are close to the original flow margins; however, there has been sufficient removal of flow-top clinker and flow-margin breccia to expose the massive interior lobes of some of the aa flows.

The Black Cone center is 75 m high. The summit of Black Cone is upheld by a crater-fill sequence consisting of large blocks of strongly agglutinated spatter and small lava masses. This agglutinated sequence is much more resistant to erosion than the surrounding nonagglutinated scoria deposits and may explain partly the better geomorphic preservation of the Black Cone center, which has generally steeper cone slopes, a higher cone/height to cone/width ratio, and smaller apron development than Red Cone (Wells et al. 1990, Fig. 2).

There is limited evidence of preservation of original primary flow topography of the lava flows of both the Red Cone and Black Cone centers. The lava surfaces have been smoothed from a combination of erosion, deposition of loess, and pedogenic processes. The flow surfaces immediately north of the Black Cone center, however, retain local irregularities in the flow-top surface that are probably remnants of primary flow topography. Smith et al. (1990) noted that the northern flow abutted against topography created by the southern flows and the main cone. This prevented the north flow from flowing south of the main cone.

An initial K-Ar age determination of 1.5 ± 0.1 Ma was obtained for a lava flow directly east of the main cone of the Red Cone center (Crowe et al. 1982; Vaniman et al. 1982). Sinnock and Easterling (1983) obtained ages of, respectively, 1.53 ± 0.31, 1.12 ± 0.27, and 1.55 ± 0.15 Ma for splits of a sample collected from the same lava flow. Smith et al. (1990) reported ages of 0.98 ± 0.10, 1.01 ± 0.06, and 0.95 ± 0.08 Ma for samples from the Red Cone center. Unpublished ages by the U.S. Geological Survey for two

samples of the same lava site located east of the main cone are 0.84 ± 0.15 and 1.07 ± 0.34 Ma. There is a slightly larger spread in K-Ar ages of the Red Cone center than other centers. Additional samples have been submitted for $^{40}Ar/^{39}Ar$ age determinations from the Red Cone center to provide final documentation of the chronology of this center.

Potassium-argon ages of 1.09 ± 0.3 and 1.07 ± 0.4 Ma were obtained for the Black Cone center (Crowe et al. 1982; Vaniman et al. 1982). Unpublished K-Ar ages by the U.S. Geological Survey are 0.80 ± 0.06 for lava at the south edge of the Black Cone center and 0.83 ± 0.09 Ma for a spatter sample from the crater-fill at the summit of the cone. New $^{40}Ar/^{39}Ar$ ages of the Black Cone center are 1.05 ± 0.14, 0.96 ± 0.15, 0.94 ± 0.05 (2σ) Ma (Table 2.1).

(3) Makani Cone. The northernmost basalt center of the Quaternary basalt of Crater Flat is herein named the Makani Cone. It is the most deeply incised of the four Quaternary basalt centers. The Makani Cone consists of two small eroded remnants of aa lava flows on the west and southeast sides of the center. We originally were puzzled by the apparent degree of dissection of the Makani center (Vaniman and Crowe 1981; Crowe et al. 1992a) and speculated that it may be attributed to several causes. The center is located on a higher and steeper topographical part of the Crater Flat basin than the other centers that may have resulted in higher erosion rates. Alternatively, the center may be slightly older than the other Quaternary basalt centers of Crater Flat but new age determinations show that this is not the case. A third alternative is the Makani cone may have originally been a small center. The major volume of eruptions of the Quaternary basalt of Crater Flat is contained in the Red Cone and Black Cone centers. The volume of the Little Cones center represents, for example, only about 5% of the volume of the Black Cone and Red Cone centers. The Makani Cone may have been only a small center like the Little Cones center, and a small original size may account for its poor geomorphic preservation. New geologic mapping has shown the major part of the center is formed by a scoria/spatter cone that has been eroded to a near horizontal surface. Lava flows that flank the center probably vented from radial dikes similar to many of the other Plio-Quaternary basalt centers in the YMR (Little Cones, basalt of Sleeping Butte, and the Lathrop Wells center). The major erupted volume of the Makani cone center formed a small scoria cone, and the ratio of pyroclastic deposits/lava is low. We infer that the degree of dissection of the center is a combination of three factors including, accelerated erosion rates at higher and steeper parts of the Crater Flat basin, the relatively small erupted volume of the center, and the center was formed mostly of relatively non-resistant cone scoria/spatter. Our original estimates of the volume of lava and pyroclastic components of the center (Crowe et al. 1983b) are incorrect and will be revised.

Potassium-argon ages of 1.14 ± 0.3 and 1.07 ± 0.04 were obtained for the Makani center (Crowe et al. 1982; Vaniman et al. 1982). Unpublished ages of 1.66 ± 0.5 and 1.04 ± 0.03 Ma have been obtained for the Makani center by the U.S. Geological Survey. The older age was obtained for a sample of a basalt dike that is moderately altered. The age may be anomalously old. Additional $^{40}Ar/^{39}Ar$ age determinations will be obtained for the center to attempt to resolve the chronology data.

(4) Eruptive Models for the Quaternary Basalt of Crater Flat. One area of continuing controversy is assessing eruptive models for individual centers of the Quaternary basalt of Crater Flat. This a problem for three reasons: (1) it has been difficult to evaluate whether each center formed in a single eruption (monogenetic) or multiple time-separate eruptions (polygenetic), analogous to the Lathrop Wells center (Crowe et al. 1988; Wells et al. 1990; Crowe and Perry 1991; Crowe et al. 1990; Perry and Crowe 1992), (2) it is difficult to apply detailed methods of field, geomorphic, and soils studies because of the degree of dissection of the centers, and (3), it is difficult with the uncertainty of the chronology methods to discriminate the ages of eruptive activity between volcanic centers. Twenty-one K-Ar and $^{40}Ar/^{39}Ar$ age

determinations have been obtained for the Quaternary basalt of Crater Flat (Table 2.2),and the mean age of the centers is 1.11 ± 0.25 Ma. Exploratory statistical analyses of the K-Ar ages using the stem and leaf, box, and probability plots show that the data distribution is nonnormal, and four samples are identified as outliers. If these samples are removed, the mean age of the centers is 1.00 ± 0.11 Ma (1 *s*), and the data show a near normal distribution with no outliers. The statistically refined data set can be interpreted to indicate the centers are coeval. However, based on analog studies of the Lathrop Wells center (Crowe et al. 1992), the time between polygenetic events may be less than the 90% confidence interval of the mean ages. Thus, the precision of the chronology methods may be insufficient to test the polygenetic model. We prefer to reserve judgment on the ages and eruptive models of the basalt centers until additional $^{40}Ar/^{39}Ar$ age determinations have been obtained and geochemical studies completed.

Champion (1991) suggested all Quaternary basalt centers of Crater Flat record a single reversed polarity remanent magnetization on the basis of field and paleomagnetic analyses of samples collected from 20 sites. These paleomagnetic data were interpreted by Champion (1991) to permit the inference that the Quaternary basalt centers of Crater Flat formed contemporaneously (single magma pulse) with each center being of monogenetic origin (formed in one brief eruptive cycle). While this interpretation is consistent with the paleomagnetic data, it requires several critical underlying assumptions. First, Champion (1991, p. 63) argued that modern (Holocene) secular variation occurs at a rate of about 4° to 5° per century. He did not assess the temporal variability of the geomagnetic field during the period of eruption of the Quaternary basalt of Crater Flat. Second, the paleomagnetic data for the Quaternary centers of Crater Flat were assumed to adequately represent all volcanic events at these centers. The sample sites for collection of paleomagnetic material were not identified (Champion 1991), so this assumption cannot be evaluated. Third, and related to the second argument, is the reliability of the overall paleomagnetic data. Champion (1991) presented only site-mean directions of remanent magnetization for the Quaternary basalt of Crater Flat. Both lava and scoria were sampled for the paleomagnetic studies (Champion 1991, p. 63). The latter material may be a less reliable recorder of the ancient geomagnetic field. Without presentation of data, and in particular the demagnetization results, it is impossible to assess the variability of the field magnetization directions. The dispersion of sample directions at a site level is particularly important if the secular variation is less than the assumed 4° to 5° per century. Fourth, the four basalt centers extend in a northeast-trending arc for a distance of about 12 km, a distance longer than expected for basalt feeder dikes (except bladed dikes), and makes it unlikely that the centers were fed by a single-feeder dike system (Crowe et al. 1983b). More information is required to determine if the centers were fed from multiple dike systems and if the geochemistry of the centers is consistent with single or multiple pulses of magma. Finally, the paleomagnetic data must be considered in light of the evidence of geochemical diversity in the lavas (Vaniman et al. 1982; Perry and Crowe 1992). The assumptions associated with the paleomagnetic study must be more carefully evaluated before accepting the conclusion that each center is monogenetic and, specifically, that all centers were formed from a single magmatic event.

The recognition of time-separate events at basalt centers must be based on establishing unequivocal time gaps between eruptive events, such as the presence of soil-bounded unconformities (Crowe et al. 1992). The variable K-Ar age determinations provide permissive but not conclusive evidence of polygenetic events. Additionally, the precision of the K-Ar methods may be insufficient to test the polygenetic model.

Table 2.2 K-Ar and $^{40}Ar/^{39}Ar$ Age Determinations for the Quaternary Basalt of Crater Flat.

Volcanic Center	Age	Error (1σ)	Method	Source
Little Cones				
	1.1	0.3	Whole-rock. K-Ar	USGS (Carr)
	0.76	0.2	Whole-rock. K-Ar	USGS (Carr)
	1.02	0.1 (2σ)	$^{40}Ar/^{39}Ar$	This Report
Red Cone				
	1.5***	0.1	Whole-rock. K-Ar	USGS (Carr)
	1.53***	0.31	Whole-rock. K-Ar	USGS (Carr)
	1.12	0.27	Whole-rock. K-Ar	Sinnock
	1.55***	0.15	Whole-rock. K-Ar	Sinnock
	0.98	0.1	Mineral Separate K-Ar	State of Nevada (Smith)
	1.01	0.06	Mineral Separate K-Ar	State of Nevada (Smith)
	0.95	0.08	Mineral Separate K-Ar	State of Nevada (Smith)
Black Cone				
	1.09	0.3	Whole-rock. K-Ar	USGS (Carr)
	1.07	0.4	Whole-rock. K-Ar	USGS (Carr)
	0.8	0.06	Whole-rock. K-Ar	USGS (Turrin)
	0.83	0.09	Whole-rock. K-Ar	USGS (Turrin)
	1.05	0.14 (2σ)	$^{40}Ar/^{39}Ar$	This report
	0.96	0.15 (2σ)	$^{40}Ar/^{39}Ar$	This report
	0.94	0.05 (2σ)	$^{40}Ar/^{39}Ar$	This report
Makani Cone				
	1.14	0.3	Whole-rock. K-Ar	USGS (Carr)
	1.07	0.04	Whole-rock. K-Ar	USGS (Carr)
	1.66***	0.5	Whole-rock. K-Ar	USGS (Turrin)
	1.04	0.3	Whole-rock. K-Ar	USGS (Turrin)
Mean (all data)	***1.11***	***0.25***	***n = 21***	
Mean (outliers removed)	***1***	***0.11***	***n = 17***	

*** outlier

f. Sleeping Butte Centers. The Sleeping Butte volcanic centers are located about 20 km north of Beatty, straddling the boundary of Nellis Air Force Range (Fig. 2.5). They are 47 km northwest of the potential Yucca Mountain site. The Sleeping Butte centers consist of two spatially separate small-volume (<0.1 km3) basaltic centers. The basalt centers comprise a main scoria cone flanked by small satellite scoria cone(s). Each center erupted multiple lobes of blocky aa lava flows that extruded from the base of their main scoria cone. The southwest center, the Little Black Peak Cone, erupted through fanglomerate deposits. The northeast center, the Hidden Cone, erupted through and draped the north/northeast-facing slope of Sleeping Butte. This prominent topographic mount is upheld by resistant outcrops of moderately welded ignimbrite of Miocene age located about 1 km inward of the range front of the Pahute Mesa-Black Mountain highland. The two centers are aligned in a north/northeast direction, the preferential direction of alignment of post-Pliocene volcanic centers in the YMR (Crowe et al. 1983; Crowe and Perry 1989). The separation of the centers is 2.6 km, measured from crater center to crater center. These centers have been mapped at a scale of 1:5000 (Crowe and Perry 1991).

(1) The Little Black Peak Center. The oldest volcanic unit of the Little Black Peak volcanic center includes two mound-shaped accumulations of basalt scoria and volcanic bombs (Qs3, Fig. 2.6) located at the south margin of the main cone. These mounds are similar to the scoria mounds described at the Red Cone, Black Cone (Smith et al. 1990; Crowe 1990), and the Lathrop Wells centers (Crowe et al. 1992). There are no distinct vents or craters at the crest of the mounds. However, the abundance of large bombs (>1 m in diameter) suggests the mounds were vents for basaltic eruptions. Lenticular dikes are exposed locally in the mounds. The dikes fed short, lobate lava flows exposed west of the eastern scoria mound (Crowe and Perry 1991).

The main scoria cone (Qs1, Fig. 2.6) of the Little Black Peak center has a basal diameter of 500 m and a height of 70 m. The cone is symmetrical with a summit crater elongated slightly in a north/south direction. The upper slopes of the east side of the cone collapsed, forming an east-facing landslide scarp extending from the east edge of the crater halfway down the eastern cone flank. Exposures of scoria deposits in the scarp show that the main cone is composed predominantly of scoria-fall deposits with minor agglutinated spatter. Zones of oxidized scoria in the cone deposits were produced by oxidization of the deposits from volcanic gases emitted from the conduit or feeder dikes. The zone of oxidization is elongate in a north-northwest direction, probably reflecting the strike of the underlying feeder dike for the volcanic center. The outer slopes of the scoria cone are moderately dissected with development of radial rills. The base of the cone is encompassed by a well-developed cone-slope apron (Qs1, Fig. 2.6).

Aa lava flows were extruded from two sites on the flanks of the scoria cone. The larger, western flow vented from the northwest base of the main scoria cone. This vent site is marked by a concave indentation in the profile of the cone slope, although the vent is largely covered by deposits of the cone-slope apron. The vent location is also suggested by the thickening of the flow near the vent, and an asymmetrical extension of the zone of red oxidization of cone scoria also extends radially from the summit crater to the flank vent. The latter evidence suggests the lava flow was fed by a radial dike extending from the main conduit (Crowe and Perry 1991). Original primary flow topography of the aa flow has been infilled by eolian material, producing a largely smooth pavement surface. Remnants of the primary flow topography occur only as local areas of stepped topography in the flow top, and margins of the lava flow are eroded.

A second lava flow was extruded from the east side of the cone, and is concealed partly by the landslide deposits so the actual vent site could not be confirmed. Cross-sectional exposures of the flow

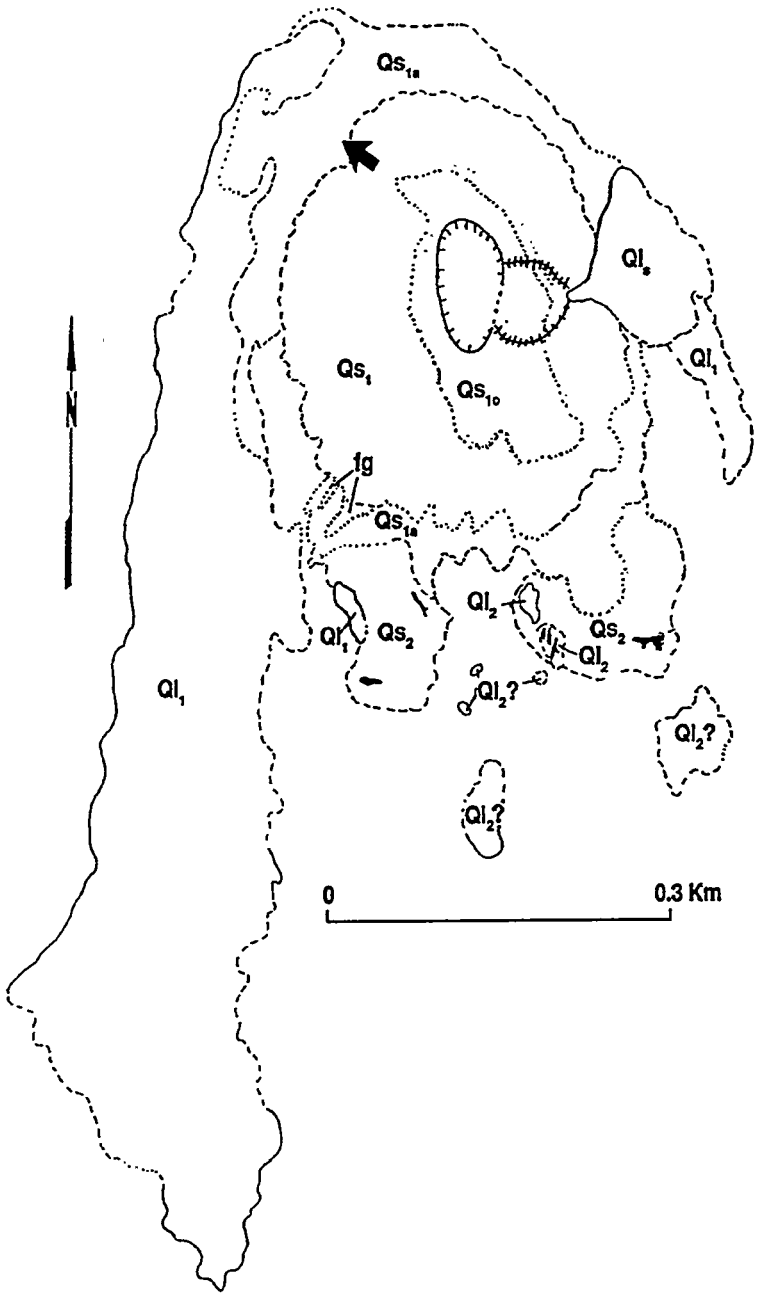


Fig. 2.6 Generalized geologic map of the Little Black Peak volcanic center of the basalt of Sleeping Butte compiled on an uncorrected aerial photograph. Lines mark contacts between geologic units and are dashed where they have been approximately located and dotted where inferred or concealed. The area outlined by dots at the summit of the main cone is the vent area and underlying feeder dikes. These features are inferred from the distribution of zones of oxidization of the cone scoria. The large arrow marks the vent for the western lava lobe. Wide, dark lines are feeder dikes in cone scoria. The line with inward facing dashes marks the crater rim of the summit cone. The line with cross-dashes is the slump scarp of the eastern crater wall. Fg: Plio-Pleistocene fanglomerate deposits, Qs3: scoria deposits of the south scoria mounds, Ql2: older lava associated with the south scoria mounds; queried where identification is uncertain, Qs1: scoria deposits of the main cone; Qs1a: cone-slope apron deposits of the main cone, Qls: slide deposits, Ql1: lava flows derived from the main cone. Figure is modified from Crowe and Perry (1991).

show that it exhibits aa morphology. This flow shows the same degree of geomorphic modification as the western flow.

Minor et al. (1993) reported a K-Ar age of about 350 ka for the Little Black Peak volcanic center.

(2) Hidden Cone Center. The Hidden cone center consists of a main scoria cone formed on the north-facing slope of Sleeping Butte (Fig. 2.7). The center was constructed in two stages: (1) a main scoria cone formed from central vent eruptions of the mildly explosive strombolian type, accompanied by extrusion of multiple lava flows at the northeast flank of the cone, and (2) a thin sequence of scoria-fall deposits was erupted during mildly explosive strombolian eruptions. These deposits mantled the eroded slopes of the previously formed main scoria cone.

The first, or oldest, event at the Hidden Cone center was the formation of most of the volume of the main scoria cone (Fig. 2.7). Scoria was deposited from strombolian eruptions and built an asymmetrical cone that draped the north-facing slope of Sleeping Butte. Because of the steeply sloped topography underlying the cone, it is highest on the north side (downslope) and lowest on the south side (upslope). The basal diameter of the cone is 0.62 km, and it is 110 m high measured from the north cone base and 25 m high measured from the south cone base. The scoria cone has an elliptical summit crater, elongate to the north. Oxidization of the cone scoria is centered on the crater but skewed slightly to the west, which suggests the eruptions that formed the center were fed by magma that moved upward along a west-dipping dike. Because of the subsequent mantling of the cone slopes by younger scoria deposits, the older scoria deposits (Qs4, Fig. 2.7) are exposed only in the summit crater and the east side of the cone (Crowe and Perry 1991). A cone-slope apron containing soils with well-developed soil horizons is exposed mostly at the north and west base of the main scoria cone (Crowe and Perry 1991).

Lava vented from two radial dike sets and from a satellite cone at the northeast flank of the main scoria cone. The major feeder vent for the flows is the northern radial dike that passes upward into a thin lava flow. The lava breached the surface above the dike about 10 m upslope from the cone base, and extended eastward and laterally down the cone slope for 1.3 km. Other lavas were fed from a second set of radial dikes and a satellite cone located east of the northeast base of the main scoria cone (Crowe and Perry 1991). All lava flows of the center show an aa flow morphology.

The lava flow units of Hidden Cone show similar degrees of erosional degradation to the lava units of the Little Black Peak center. Most of the original aa flow topography has been smoothed and the flow tops are pavement surfaces. Margins of the lava flow are erosional, not flow margins.

The youngest unit of the Hidden Cone center (Qs1, Fig. 2.7) comprises scoria-fall deposits that mantle the older cone except for the perimeter of the north and east base of the cone. The existence and inferred young age of this eruptive event are suggested by the following:

1. The outer slopes of the main cone are smooth, showing only minor degradation denoted by the formation of rills and other evidence of mass wasting on the cone slopes.

2. There is a marked contrast in the degree of degradation of the cone slopes of the Little Black Peak cone compared to the Hidden Cone despite their geographic proximity.

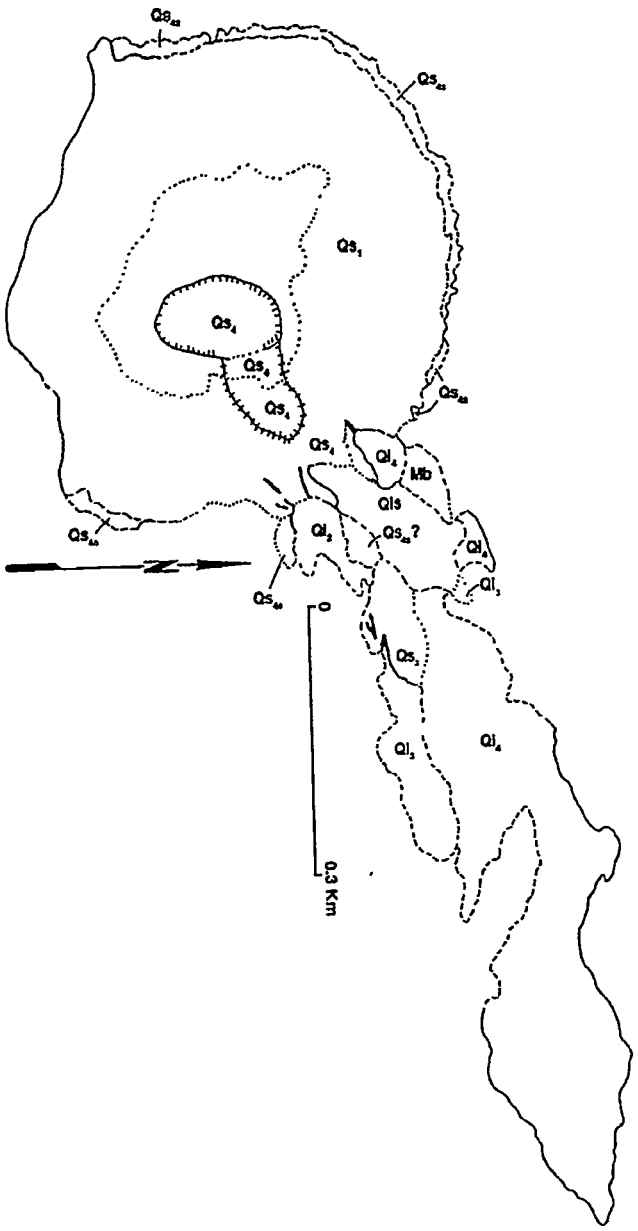


Fig. 2.7 Generalized geologic map of the Hidden Cone volcanic center of the basalt of Sleeping Butte. Map is compiled on uncorrected aerial photographs. Lines mark contacts between geologic units and are dashed where they have been approximately located and dotted where inferred or concealed. The area outlined by dots at the summit of the main cone is the vent area and underlying feeder dikes. These features are inferred from the distribution of zones of oxidization of the cone scoria. The line with inward facing dashes is the summit crater; the line with cross-dashes outlines the slump scarp of the eastern crater wall. Wide dark lines are feeder dikes. Bm: Miocene basalt, Ql4: lava flow associated with the radial feeder dike, Qs4: older scoria deposits of the main cone, Qs1a: cone-slope apron deposits of the main cone, Qls: lava flow associated with the Qs3 scoria mound, Qs3: flank scoria mound, Ql2: lava flow associated with the radial feeder dikes, Qs1: late Pleistocene or Holocene scoria-fall deposits. Figure is modified from Crowe and Perry (1991).

3. There are no apron deposits associated with the Qs1 deposits, suggesting there was an insufficient time subsequent to the youngest eruption for significant cone-slope erosion.

4. There is an erosional unconformity between the Qs4 and the Qs1 deposits exposed in the northeast section of the main cone.

5. There is significant horizon development in the soil on the Qs4 deposits and limited horizon development in the soil on the Qs1 deposits.

6. Fine-grained scoria-fall deposits are preserved on the modern alluvial surface about 0.5 km northeast of the main scoria cone.

Champion (1992, pp. 254-255) and Minor et al. (1993) noted the presence of a possible second lava flow associated with the Hidden Cone center, located northwest of the north cone base. Champion (1992) reported a K-Ar age of about 380 ka for the flow, consistent with the age of the lava flows of the Hidden Cone center. This western lava flow was identified in preliminary mapping in 1981 as being part of the Hidden Cone center. However, detailed field examination showed that the western lava flow could not be traced to the Hidden Cone. Instead it appears to be associated with deeply dissected scoria deposits that mark one of a series of basalt centers stratigraphically beneath the Thirsty Canyon Tuff. Additionally, the western lavas are overlain by a thick soil with dramatically greater horizon development than the Hidden Cone lava flows. The new K-Ar age determination provides evidence that the western flow could be associated with the Hidden Cone center. Additional field work will be conducted to verify the stratigraphic position of the western lava flow.

Whole-rock, K-Ar age determinations have been obtained for both centers of the basalt of Sleeping Butte. They are 0.29 ± 0.11, 0.32 ± 0.15, and 0.24 ± 0.22 Ma (Crowe et al. 1982). The analytical uncertainty of individual analyses generally exceeds 100 ka (Crowe and Perry 1991). Turrin (1992, p. 231) reported $^{40}Ar/^{39}Ar$ ages of about 380 ka for lavas of both Sleeping Butte centers. Minor et al. (1993) reported an age of about 350 ka for the Hidden Cone center. The degree of erosional dissection of the lavas we found is consistent with these age determinations. Also, the degree of horizon development of soil on the lavas and cone-apron deposits and the degree of dissection and development of a cone-slope are consistent with a minimum age of greater than several hundred thousand years (Crowe and Perry 1991). A U-Th disequilibrium age measurement is being processed for the western lava lobe of the Little Black cone. Cosmogenic surface exposure ages using the ^{3}He method will be obtained for surface scoria deposits of the youngest event of the Hidden cone. We will also obtain $^{40}Ar/^{39}Ar$ age determinations of multiple eruptive units of both Little Black Peak and Hidden Cone by the end of 1995.

Preliminary paleomagnetic data from a limited number of sites in the lava and scoria deposits of both basalt centers were interpreted as a single or closely grouped direction of remanent magnetization (Champion 1991). Champion (1991) inferred from these data that both centers formed in a single eruptive event and, therefore, are monogenetic volcanic centers. Such an interpretation is consistent with the geology and stratigraphy of the Little Black Peak center (Crowe and Perry 1991). Unfortunately, the monogenetic classification of the Hidden Cone center may not be verifiable using paleomagnetic data, because there are no deposits of agglutinated spatter associated with the youngest eruption of the Hidden Cone center, which would provide reliable indicators of the field direction at the time of formation of this deposit. Additional geochronology work is planned to evaluate the different models of the eruptive history of the Hidden Cone center (Crowe and Perry 1991).

IV. The Lathrop Wells Center

A. Introduction

The geology and chronology of the Lathrop Wells volcanic center was described by Crowe and Carr (1980), Vaniman and Crowe (1981), Crowe et al. (1983), Crowe (1986), Wells et al. (1990, 1991, 1992), Turrin et al. (1991, 1992), Crowe et al. (1992), and Zreda et al. 1993. The volcanic deposits of the center overlie volcanic bedrock of the Paintbrush and Timber Mountain Tuffs, and alluvial deposits. These deposits are overlain locally by younger alluvium and are mantled on the north and south sides by sand, silt, and loess of Holocene age. Active sand dunes are present on the surface of lava flows exposed in the east part of the center. The Lathrop Wells center is located near the intersection of several northwest-trending faults that extend from the west parts of Yucca Mountain and the northeast-trending Stagecoach Road fault (Fig. 2.8). The center consists of a large main scoria cone and three or four sets of fissures marked by paired or individual accumulations of spatter, bombs, and scoria. Multiple-eruptive events repeatedly reoccupied two sets of the fissure systems. The majority of vents and fissures for the center are aligned along northwest trends, parallel to the northwest-trending faults. Small-volume, blocky aa lava flows vented from numerous sites along some of the fissures. Satellite cones present on the south flank of the main cone (largely removed by quarrying) may postdate formation of the major volume of the main cone.

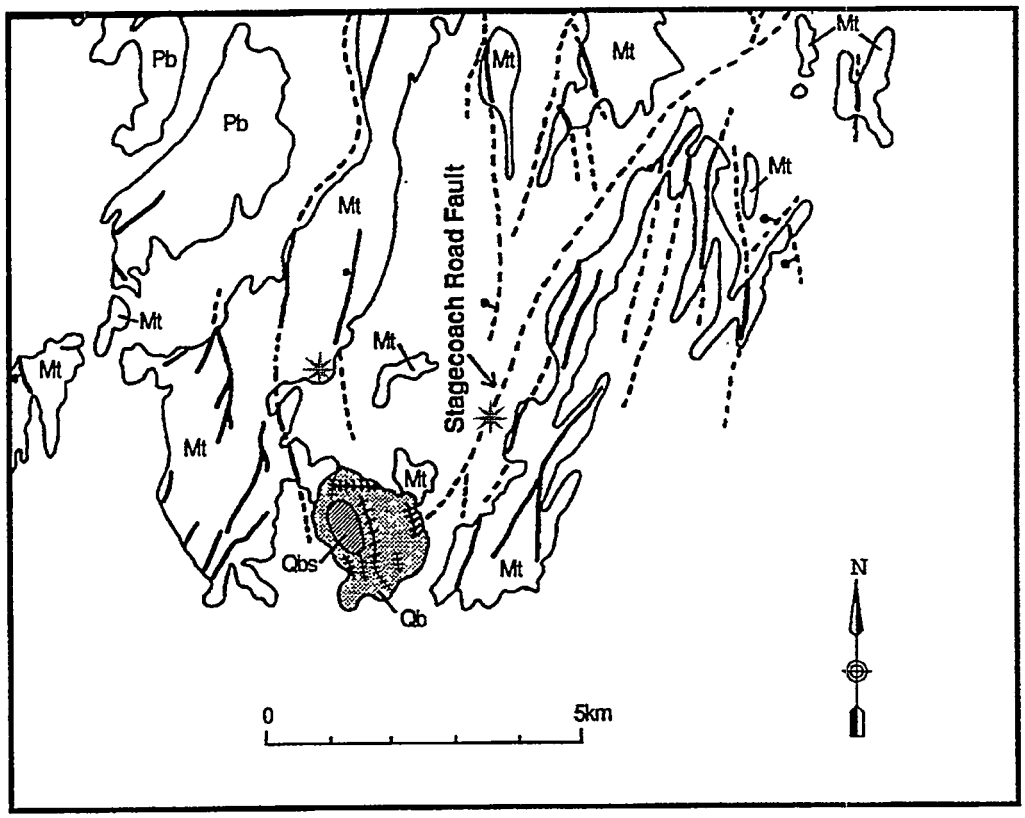


Fig. 2.8 Geologic setting of the Lathrop Wells volcanic center. The center is located at the south end of Yucca Mountain. Volcanic deposits of the center overlie Miocene tuff and alluvial deposits and are locally overlain by alluvium and eolian deposits. Mt: Miocene tuff undivided, Pb: Pliocene basalt of Crater Flat, Qb: Quaternary lava and pyroclastic deposits of the Lathrop Wells center, Qbs: Main scoria cone of the center. Cross-hatched lines are eruptive fissures and denote structural trends of eruptive vents. The star symbols mark sites where distal ash deposits from the Lathrop Wells volcanic center have been identified. Modified from Crowe et al. (1992a).

The largest scoria cone of the Lathrop Wells center, the main cone, is elongate northwest. This elongation probably was controlled in part by prevailing winds during the pyroclastic eruptions that formed the cone. Additionally, the feeder dike for the center appears to be oriented north-northwest, as indicated by two lines of evidence. First, there is a summit zone of red scoria centered about the crater and extending to the southeast and northwest. This cone feature was formed from oxidization of the scoria deposits by rising volcanic gases emitted from an inferred underlying northwest-trending dike. Second, multiple sets of northwest-trending, locally paired spatter cones and scoria mounds that demarcate eruptive fissures are present along the east base of the main cone, southeast of the main cone, and at the northeast edge of the volcanic center. An alignment of west/northwest-trending spatter cones and scoria mounds marking another fissure zone is located north-northeast of the main cone.

In the early stages of this research, the Lathrop Wells center was assumed to be a simple monogenetic volcano with an age, based on whole-rock K-Ar age determinations, of about 300 ka (Vaniman and Crowe 1981; Vaniman et al. 1982; Crowe 1986). However, two lines of evidence resulted in reevaluation of the chronology and eruptive history of the volcanic center. First, additional whole-rock, K-Ar age determinations were obtained (Sinnock and Easterling 1983). These ages ranged from about 20 to >700 ka, an unacceptably large range to have even the remotest confidence in the results of K-Ar age determinations. Second, the degree of horizon development in soils and geomorphic features of the main cone were recognized to be inconsistent with an inferred age of 300 ka. They were judged to be more consistent with an age of late Pleistocene or Holocene (Wells et al. 1988). This was a critical observation because we did not want to disregard potential evidence of recent eruptive events at the center that could result in underestimation of the risk of future volcanism for the potential Yucca Mountain site (Crowe et al. 1992). Accordingly, a new phase of field and geochronology studies was initiated starting in 1987.

The Lathrop Wells volcanic center was remapped at a scale of 1:4000, and the volcanic rocks were divided into five lithostratigraphic units (Crowe et al. 1988). More than 60 soil and tephra pits, and trenches were constructed to expose stratigraphic contacts, to assess the degree of soil development, and to facilitate collection of samples for geochronology and geochemistry studies. Five large trenches were constructed using heavy construction equipment; four were constructed on the north flanks of the center and one on the south flank. The northern trenches exposed the contacts between lava units and pyroclastic deposits, and the internal geometry and stratigraphy of scoria mounds. The south trench exposed possible late Pleistocene or Holocene tephra and soils (Wells et al. 1990; Crowe et al. 1992a). Additional geochronology studies were attempted using multiple independent isotopic methods to further constrain the age of the center (Crowe et al. 1992a). Two distinct tephra-fall units separated by alluvium were identified in surficial deposits mantling topography 3 km north of the Lathrop Wells center. These units are correlated tentatively with one or possibly two deposits of basaltic ash, separated by alluvium with soil and carbonate development, exposed in a trench along the Stagecoach fault, northeast of the Lathrop Wells center.

The wealth of new stratigraphic, geochemical, and geochronologic information provided us with increased confidence that the Lathrop Wells center was formed during four distinct eruptive episodes. Two episodes of lava extrusion occurred along flank fissures that are secondary to the site of the main cone. This eruptive activity was accompanied by deposition of scoria-fall sheets from a probable vent or vents now concealed beneath the main cone. A third eruptive episode formed the major volume of the main cone and lobes of blocky aa lava extruded from a satellite vent northeast of the main cone. The youngest eruptions of the main cone did not produce widely distributed scoria-fall deposits. The delineation of the three oldest eruptive episodes is based primarily on the recognition of erosional unconformities in the scoria-fall and vent-scoria deposits. The fourth eruptive episode is marked only by small-volume and local

fall-and-pyroclastic-surge deposits present on the south part of the center, locally separated from underlying volcanic deposits by nonconformities marked by soils with horizon development. The vents for the youngest deposits have not been identified and are inferred to have been destroyed by commercial quarrying. Recognition of these deposits has been aided, however, by their unique geochemistry, which can be discriminated from all other deposits of the center.

The complex evolution of the Lathrop Wells volcanic center requires that it is not a simple monogenetic volcano and instead must be classified as a polygenetic volcano (Crowe et al. 1988, 1989; Wells et al. 1990). Primary evidence of polygenetic events at the center is provided from field, stratigraphic, geomorphic, and soils data. Geochemical data for the volcanic center are inconsistent with a monogenetic eruptive model and are consistent with the polygenetic eruption model (see Chapter 4). Current geochronology data, while generally supporting the polygenetic model, do not definitively prove or refute the concept of multiple eruptive events. The geochronology data are inconsistent with a monogenetic model, but the model cannot be excluded solely on the basis of geochronology data. Disproving the monogenetic model requires consideration of **both** the geochronology and the field, stratigraphic, geomorphic, soil, and geochemistry data. Some workers regard the latter data as controversial (Whitney and Shroba, 1991; Turrin et al. 1991; 1992). Because of this controversy, we consider both monogenetic and polygenetic models in probabilistic volcanic risk assessment (see Chapter 7).

From oldest to youngest, the eruptive intervals of the Lathrop Wells volcanic center consist of

1. Chronostratigraphic unit I: Chronostratigraphic unit I consists of four groups of lava flows and local pyroclastic deposits that crop out along multiple, northwest-trending fissures located south, beneath, north, and northeast of the main cone. The scoria and spatter deposits mark eruptive vents of chronostratigraphic unit I and were modified extensively by erosion prior to emplacement of chronostratigraphic unit II. The age of the lava and scoria deposits of chronostratigraphic unit I are constrained to be >85 or 95 ka (minimum, cosmogenic helium and chlorine surface exposure ages), and possibly about 135 + 20 – 15 ka (U-Th disequilibrium age). *The eruptions of chronostratigraphic unit I are inferred to be the source of a carbonate-cemented, basal fall deposit interbedded with alluvial deposits several kilometers northwest, north, and northeast of the main cone.*

2. Chronostratigraphic unit II: Chronostratigraphic unit II consists of the largest-volume lava of the Lathrop Wells center, local spatter and scoria deposits that form a short, northwest-trending fissure at the northeast base of the main cone, and widespread scoria-fall and pyroclastic-surge deposits erupted from vents inferred to be concealed mostly beneath the present main cone. The lava sequence erupted from a northwest-trending fissure that parallels a northwest-trending normal fault that predates the basaltic center. The ages of deposits of chronostratigraphic unit II are presently constrained to be between about 80–90 ka (cosmogenic helium surface exposure ages) and 107 ± 33 ka ($^{40}Ar/^{39}Ar$ step-heating isochron). Existing chronology data cannot discriminate the ages of chronostratigraphic unit I from chronostratigraphic unit II. The chronostratigraphic units (I and II) are distinguished by their spatially separate eruptive vents, stratigraphic position, contrasts in their degree of geomorphic preservation and development of pedogenic carbonate, and different geochemical compositions. The scoria-fall deposits of chronostratigraphic unit II are correlated tentatively with fall and surge deposits interbedded with alluvium that overlie ash deposits of chronostratigraphic unit I several kilometers north and northeast of the main cone and are exposed in fault trenches on the west and east sides of Yucca Mountain.

3. Chronostratigraphic unit III: The eruptive events of chronostratigraphic unit III formed most of the main scoria cones of the Lathrop Wells volcanic center and small-volume lobes of blocky aa lava flows from a vent located northeast of the main cone. The scoria deposits were emplaced by intermixed strombolian and weak hydrovolcanic eruptions and did not form an extensive scoria-fall sheet. The age of this event is >40 ka, and possibly >65 ka on the basis of cosmogenic ^{3}He and ^{36}Cl ages of bombs from the main cone and cosmogenic ^{3}He ages of the lava flow. Present geochronology data indicate the main cone and lava flow are younger than the deposits of chronostratigraphic units I and II but do not conclusively rule out the possibility that the main cone could be as old as chronostratigraphic unit II. However, the marked contrast between the degree of geomorphic modification of the main cone and fall deposits of chronostratigraphic unit II indicate that chronostratigraphic unit III is significantly younger than chronostratigraphic unit II.

4. Chronostratigraphic unit IV: Small-volume eruptions formed probable small satellite vents south of the main cone that have been removed by commercial quarrying of the scoria deposits. The eruptive events of chronostratigraphic unit IV have been established from recognition of local thin beds of scoria that overlie scoria and lava flow deposits of the older chronostratigraphic units. The identification of scoria deposits of chronostratigraphic unit IV is aided by their distinctive major- and trace-element geochemistry. The age of chronostratigraphic unit IV may be bracketed by TL age determinations of silt from soil beneath (9 and 4 ka) and above (4 ka) the units.

The subdivisions of chronostratigraphic units for the Lathrop Wells volcanic center are described below, from oldest to youngest. The subdivisions used in this report are modified from Crowe et al. (1988), and Crowe et al. (1992). They are based on the most recent geologic mapping, interpretation of stratigraphic relations observed from field studies and geologic contacts exposed in trenches, and geochemical and geochronology data for all units. The unit identifications used in this report replace all previous stratigraphic subdivisions of the Lathrop Wells volcanic center. We have informally named each of the major lava sequences at the center (Fig. 2.9). These names are used in combination with the unit designations to facilitate descriptions of the eruptive events.

B. Chronostratigraphic Unit I

The oldest identified chronostratigraphic unit at the Lathrop Wells center comprises four sets of lava flow units associated with a series of overlapping, northwest-trending fissure systems that extend beneath and flank the main cone, and a second set of west/northwest-trending fissures northeast of the main cone (Fig. 2.10). Spatially associated with the lavas are eroded mound-shaped accumulations of scoria, spatter, and bombs. These pyroclastic deposits mark the vents for weakly explosive (hawaiian) pyroclastic eruptions and the eruptive sites of the lava flows. Chemically, the lavas and related pyroclastic deposits of chronostratigraphic unit I are characterized by depletions in rubidium, thorium, and the heavy rare-earth elements and by enrichments in strontium, phosphorous, the middle rare-earth elements and titanium relative to the other chronostratigraphic units (Fig. 2.11).

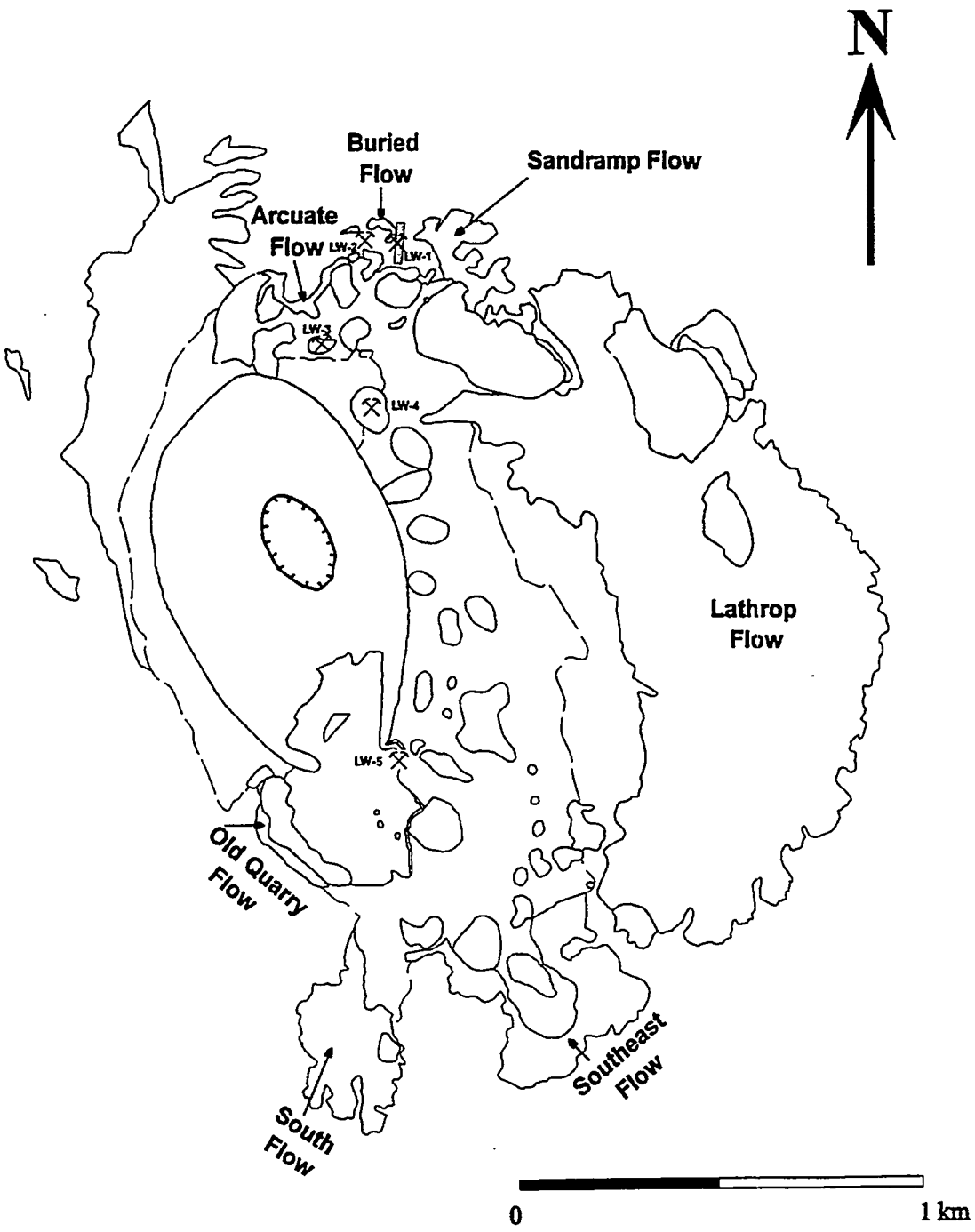


Fig. 2.9 Generalized map of the outlines of the Lathrop Wells volcanic center showing the informal names of the lava units. LW-1 through LW-5 are, respectively, the location of major trench excavations at the volcanic center

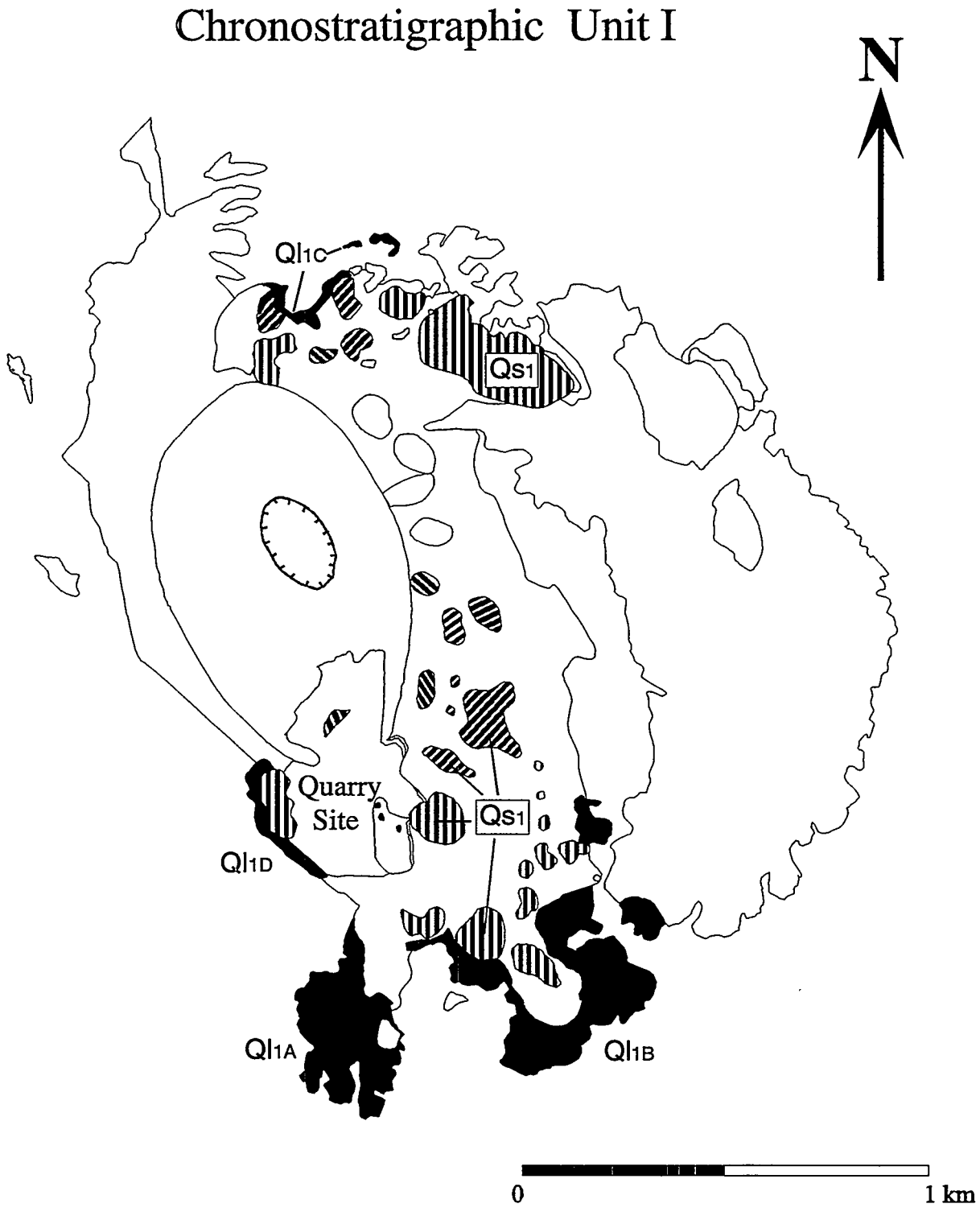


Fig. 2.10 Geologic map of the distribution of volcanic subunits of chronostratigraphic unit I of the Lathrop Wells volcanic center. The black shaded areas of the figure outline the distribution of the lava flow subunits; the cross-hatched areas outline recognizable vents (scoria and spatter mounds) for the lava subunits and fissure systems.

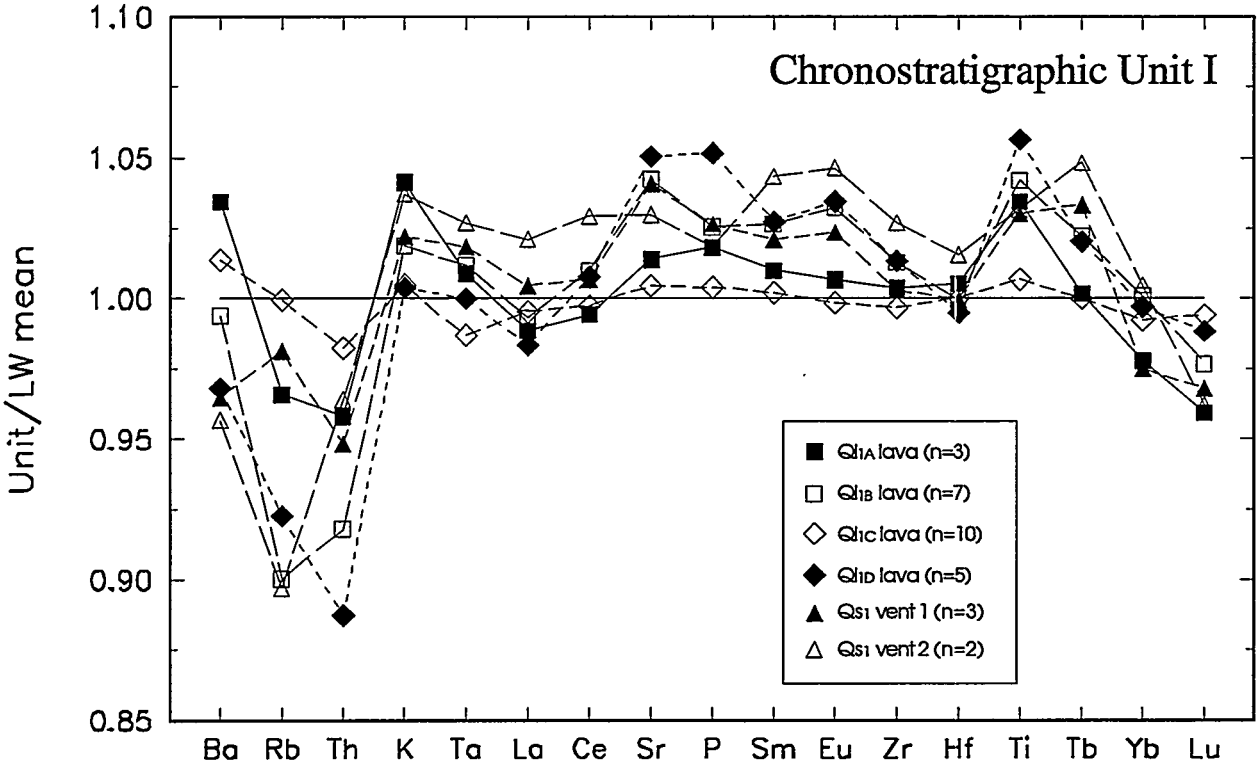


Fig. 2.11 Spidergram of elemental compositions normalized to an average composition for all analyzed samples of the volcanic units of the Lathrop Wells center ($n = 99$). Samples are designated by lava and vent deposits. Each pattern is plotted as the average of multiple analyses of specific eruptive subunits.

1. The Qs1/Ql1 Unit. The Qs1/Ql1 unit is subdivided into four subunits on the basis of the spatial distribution of their source vents and lava flows (subunit designations are indicated on Fig. 2.10; lava names on Fig. 2.9).

a. Subunit Qs1d/Ql1d: The Old Quarry Flow. Subunit Qs1d/Ql1d, informally named the Old Quarry flow because of its proximity to the original site of commercial quarrying of the scoria deposits, consists of northwest-trending, degraded mounds of scoria, local sites of agglutinated spatter, and minor, small-volume lavas. The scoria mounds, which are presumed to be the vents for the scoria deposits, have no recognizable vents or craters. They consist of conical mounds of scoria with eroded upper surfaces. However, the local thickness of scoria deposits, the coarse size of bombs (locally >1 m in long dimension), and the presence of lenticular zones of agglutinated spatter require that the deposits were erupted at the approximate site of the mounds. There has been sufficient erosional modification of the mounds to remove or obscure the primary constructional features of the vent or vents. Derivation of the scoria mounds from lava-rafting and destruction of the main cone can be eliminated by: (1) field and trench exposures that show the lava flows *overlie* the scoria deposits; (2) exposure of dikes in the scoria deposits; (3) the size of spatter and bombs in the scoria-mound deposits exceeds the size of spatter and bombs in the main cone; and (4) the chemistry of the scoria-mounds matches the chemistry of the associated lavas and is distinct from the scoria deposits of the main cone.

Blocky aa lava flows flank the scoria mounds on the north (now covered by quarry debris), west, and south sides. The lavas overlie or can be traced to the scoria mounds and were extruded from multiple sites, mostly at the base of and on the lower slopes of the scoria mounds. The flows are blocky aa lavas and

were unusually viscous for magma of basaltic composition. They form small lobate flows that extend no further than several tens of meters from their vents (Fig. 2.10). The blocky aa flows were disrupted by flowing down the slopes of their associated scoria mounds. This downslope movement (15° to 20° slopes) oversteepened the flows causing slumping and local breakup of the lava lobes. Outcrops of the flows expose steep zones of contorted flow foliation, blocky flow-top rubble, and internal zones of massive lava that mark the cores of the aa-flow interiors.

The Old Quarry flow subunit can be distinguished in outcrop by the presence of small microphenocrysts of plagioclase. It is the only unit with visible (hand lens examination) microphenocrysts of plagioclase. A scoria mound of the subunit, identified on the basis of geochemical composition and the presence of plagioclase microphenocrysts, could be traced originally beneath the main cone of the Lathrop Wells center. The exposures of this mound have now been removed by the commercial quarrying activity.

A sample of the Ql1d Old Quarry flow has been dated by the U-Th disequilibrium method at 135 + 20–15 (1σ) ka. A cosmogenic helium age (surface exposure age) of 76 ± 7 (1σ) ka has been obtained for a bomb collected from the surface of a scoria mound. This is inferred to be a minimum exposure age for two reasons. First, the sampled outcrops of the Old Quarry flow subunit are adjacent to the main cone. They were covered by scoria-fall deposits from multiple eruptive phases of the main cone and vents located beneath the main cone. Second, the modern surfaces of the Qs1 subunit are erosional; an unknown thickness of scoria has been removed from the sample site. Replicate $^{40}Ar/^{39}Ar$ ages of the Old Quarry flow are highly variable, and provide limited information on the age of the Qs1d/Ql1d unit (Table 2.1).

b. The Northern Lava Subunit. The Qs1c/Ql1c subunits comprise eroded scoria mounds exposed beneath and extending north of the main cone, scoria deposits that mark a west/northwest-trending fissure, and local lava units derived from the scoria mounds. The subunits are deeply eroded, draped by scoria-fall deposits from chronostratigraphic unit II, and locally covered by alluvium, and sand and silt of eolian origin. The distribution of the subunits, where obscured by overlying deposits, has been established through excavation of numerous small pits and two large trenches (Fig. 2.9).

A north/northeast-trending cluster of scoria mounds is exposed directly north of the main cone (Fig. 2.10). These deposits have subdued topography and diffuse boundaries between the mounds. The mounds have been eroded significantly and no longer have distinct topographic expression (primary constructional topography). Three lines of field evidence indicate considerable erosion of the scoria mounds. First, short segments of vertically dipping dikes are exposed at several locations in the scoria mounds. The dikes project 1 to 1.5 m above the scoria surface. The dikes must have been emplaced originally in scoria deposits. The projection of the dikes above the modern surface requires the removal of more than a meter of unconsolidated scoria above and flanking the dikes. Second, the crests of the mounds are marked by an anomalous concentration of large bombs. Trenching of several of the scoria mounds revealed that the abundance of large bombs is notably less in the interior of the mounds than on the crests. The accumulation of bombs on the crests of the mounds is inferred to be an effect of erosion. The coarser bomb debris was not removed during degradation of the mounds and became concentrated as a lag deposit during progressive stripping of the finer-grained scoria. Third, exposure windows through the overlying scoria-fall deposits show that the Qs1c surfaces have well developed cut-and-fill structures forming an integrated network of rills. At the north flank of the cone, these rilled surfaces can be traced beneath the geomorphically unmodified slopes of the main cone (Fig. 2.10).

An arcuate band of lava (Ql1c), informally named the arcuate flow, crops out north of and flanks the scoria mounds of Qs1c (Figs. 2.9, 2.10). This lava unit was probably derived from the flanking scoria

mounds, but the exact relations have been obscured by erosion. The lava is similar in morphology to the flanking lava flows of the other Ql1d unit described previously; and they were erupted from the base and flank scoria mounds of the Qslc scoria mound. The Ql1c lava can be traced beneath and underlies lava of the topographically higher-standing Ql2 unit. Moreover, there are local contrasts in the degree of development of carbonate coating on lava clasts in the Ql1c lava compared with the younger Ql2 lava (trenches LW-1 and LW-2). These differences may reflect different ages of the lava units, although we have not systematically examined the accumulation of carbonate in the lavas to discriminate uniquely the causes of the variations of secondary carbonate.

A second site of the Qs1c unit is present northeast of the previously described lava and scoria (Fig. 2.10). Here the scoria deposits are completely buried by pyroclastic-surge deposits of chronostratigraphic unit II and eolian sand and silt. Identification of the scoria deposits is based entirely on exposure of the units in trenches (Fig. 2.9) and the coincidence of the distribution of the scoria deposits with a sand draped, topographic mound. A lava unit of this northeast flow crops out discontinuously beneath a thick cover of eolian sand and silt and flanks the north side of the concealed Qs1c scoria deposits (Fig. 2.9). This lava was informally named the buried flow (Crowe et al. 1988; 1992a) (see Fig. 2.9, this paper). A T-shaped trench was constructed across the east edge of the buried flow. The base of the buried lava is locally greater than 10 m below the modern alluvial surface. The lava consists of a massive lobe (2 m thick) of a single flow of blocky aa lava that overlies lava clinker and thin scoria-fall deposits. The lava lobe is overlain by 5 m of autoclastic flow rubble. The flow rubble is overlain by 2 m of reworked flow rubble, in turn overlapped unconformably by eolian sands. At the south end of the trench, the buried lava underlies pyroclastic-surge deposits (Qs2fs), lava of the Ql2 subunit, and scoria of the Qs1c subunit (Fig. 2.10). Field relations here provide constraints on the interval between eruptive events of chronostratigraphic unit I and II. The flow interior of the upper part of the buried lava flow contains irregular coatings of calcite-silica on fracture surfaces. Overlying the flow is a colluvial wedge consisting of calcite-coated scoria clasts derived from colluvial deposits formed at the north base of the scoria mound of Qs1c. Both the buried flow and the colluvial deposits are overlain by the pyroclastic surge deposits of Qs2fs, which have only minor coating of pedogenic carbonate on the bottom of tephra clasts. These stratigraphic relations require a time break between chronostratigraphic units I and II of sufficient duration to allow formation of extensive secondary pedogenic carbonate in fractures of the buried lava and Qs1c scoria deposits *before* deposition and cover by the pyroclastic surge deposits.

A discontinuous, west/northwest-trending fissure is marked by elongate mounds of subunit Qs1c (Fig. 2.10). These lavas are draped by scoria-fall deposits and are partly overlapped to the east by lava flows of chronostratigraphic unit II. The mounds have been exposed by trenching at two locations and are identical in morphology and origin to the previously described scoria mounds of the Qs1d subunit. Scattered pods of lava, partly concealed by scoria-fall deposits, are present within the scoria mounds (Fig. 2.10) and probably are small flows (tens of m^3) fed from radial dikes at the flanks of the mounds of either chronostratigraphic units I or II.

No chronology data have been obtained for the Qs1c/Ql1c unit. A sample of the interior of the buried lava flow was collected for dating by the U-Th disequilibrium method and is still being processed. A sample of a Ql1c lava was dated by the cosmogenic ^{3}He method and is also being processed.

***c. Subunits Qs1a/Ql1a and Qs1b/Ql1b:* The South and Southeast Flows.** Subunits Qs1a/Ql1a and Qs1b/Ql1b are informally named the south and southeast flows because of their locations in the south part of the Lathrop Wells volcanic center (Fig. 2.10). They consist of two separate lava flows (south and southeast flows), scattered outliers of lava, and eroded scoria mounds. The south flow and vent complex

were erupted from multiple sites near the southwest base of scoria mounds exposed in the central part of the outcrop area of subunits Ql1a and Ql1b (Fig. 2.10). The flow consists of three, possibly four, lobes that partly coalesced on their distal ends but can be traced to separate sites at the inferred source vents. Scattered small outcrops of lava are present on the scoria deposits. These are partly covered by both scoria-fall deposits from chronostratigraphic unit II and eolian sands. Some of these lava outcrops can be traced laterally into their vents where they are delineated by vertical dikes. They are inferred to represent erosional remnants of small lava lobes extruded from radial dikes that extended outward from the scoria mounds. These dikes breached the surface at the flanks of some scoria mounds and erupted small volumes of lava (tens of m^3). The scoria mounds of subunit Qs1a are identical to previously described deposits. They consist of erosionally beveled deposits of vent scoria with surficial concentrations of coarse aerodynamically shaped bombs. The scoria mounds form discontinuous alignments of vents that mark fissures coparallel to and west of the Ql1d fissure. En echelon fissure systems of the Qs1a unit extend close to and probably project beneath the main cone (Fig. 2.10).

Multiple samples of the south flow (Ql1a) were dated by the cosmogenic ^{3}He method at 81 ± 7, 81 ± 9, 87 ± 6, 82 ± 5, 81 ± 7, and 85 ± 5 (all 1σ) ka. Zreda et al. (1993) obtained a cosmogenic ^{36}Cl age of 81 ± 7.3 ka for the Ql1a lava, closely agreeing with the cosmogenic ^{3}He ages. Interpretation of the ages is complicated by the presence of extensive scoria-fall deposits that originally mantled the south lava flow. Scoria-fall deposits more than 1 m thick (exposed by trenching) overlie bedrock surfaces of Paintbrush Tuff directly east of the south lava flow. These deposits locally *overlie* and must have draped the lava units of chronostratigraphic unit I; cosmogenic ages of the lava surfaces therefore must be *minimum* ages.

Turrin et al. (in press) reported a weighted mean of 157 ± 98 ka for the Ql1a lava (mean of the data set is 214 ± 86 ka) from conventional whole-rock, K-Ar age determinations. Subsequently, Turrin et al. (1991) obtained a weighted mean of 138 ± 54 ka, and a mean of 170 ± 114 ka for ^{40}Ar/^{39}Ar ages of the Ql1a lava. These inferred mean ages are somewhat older than the cosmogenic ages, but analytical uncertainty of the ages overlap. The wide range in replicate K-Ar and ^{40}Ar/^{39}Ar ages is too large to discriminate the age of the Ql1a subunit.

The southeast flow (Ql1b) erupted from multiple vents marked by eroded scoria mounds (Qs1b) distributed along coparallel, northwest-trending fissures with minor conjugate northeast-trending vents. These scoria mounds mark discontinuous fissures that extend from the south part of the center to the west/northwest-trending fissure of subunit Qs1c and flank the east side of the site of the main cone. The lava flows of the southeast flow are inferred to have vented from the southeast ends of the en echelon fissures (Fig. 2.10). The lavas of the southeast flow are blocky aa lava flows similar in morphology to the south flow. However, individual lobes of the southeast flow cannot be distinguished because of thick eolian sand cover. One lobe of the southeast flow is overlain by topographically higher-standing lavas of chronostratigraphic unit II.

Eruptive vents of the southeast flow are eroded scoria mounds with local small lava lobes and exposed feeder dikes. They are identical in morphology and occurrence to the vents of the south flow with one exception. A small cluster of northeast-trending mounds (locality A on Fig. 2.10) is capped by an asymmetrical accumulation of coarse agglutinated spatter. The morphology and shape of the spatter mounds indicate that they formed from weakly explosive spatter eruptions. The magma columns that vented to form the spatter mounds probably dipped to the southwest so that spatter erupted and accumulated preferentially to the northeast side of the vents (northeast-directed, weak-lava fountains).

A sample of flow-top clinker from the southeast flow was dated by the cosmogenic ^{3}He method at 88 ± 8 (1 σ) ka, identical to the range of cosmogenic ages obtained for the south flow. This age is also interpreted as a minimum age because the sample site must have been covered by scoria-fall deposits of chronostratigraphic unit II. A sample of aerodynamically shaped spatter was collected from the surface of a southeast spatter mound (Qs1b). It yielded a cosmogenic ^{3}He age of 61 ± 8 (1 σ) ka. This age is slightly younger than all other cosmogenic ^{3}He ages obtained for deposits of chronostratigraphic unit II. However, the spatter mound, located on the immediate flanks of the main cone, was draped by thick scoria-fall deposits of chronostratigraphic unit II. Again, the measured ^{3}He age must be a minimum exposure age.

Turrin et al. (1991) reported an age of 116 ± 13 (weighted mean) and 214 ± 86 (mean) for the samples collected from deposits of the Qs1b fissure for conventional whole-rock, K-Ar age determinations. These mean ages were obtained by *combining* the Qs1b ages with age determinations from the south flow (the Ql1a lavas of chronostratigraphic unit I). The large analytical uncertainty and poor reproducibility of replicate ages indicates that the age determinations are not useful for constraining the age of the Qs1a or the Qs1b subunits. The $^{40}Ar/^{39}Ar$ age determinations for samples that are inferred from the sample locations and descriptions of Turrin et al. (1991) to be collected from the Qs1b fissure are 149 ± 45 (weighted mean) or 129 ± 77 (mean) ka (Turrin et al. 1991). The large analytical uncertainty and poor reproducibility of these ages suggest they provide limited constraints on the age of the Qs1b subunit.

d. Scoria-Fall Deposits of chronostratigraphic unit I. An episode of cone-building pyroclastic eruptions that produced regionally dispersed scoria-fall deposits is correlated with chronostratigraphic unit I. However, because of the extensive erosion of chronostratigraphic unit I, these deposits are only partly preserved in the mappable volcanic units of the center. The recognition of this eruptive event is based on multiple lines of inferential stratigraphic and pedogenic relationships. First, carbonate cemented scoria-fall deposits have been recognized at scattered localities several kilometers north and northwest of the Lathrop Wells center. These deposits consist entirely of scoria with well-developed bubble-wall textures and no hydrovolcanic ash. Second, the basal scoria-fall deposits underlie scoria-fall and pyroclastic-surge deposits with local interbeds of alluvium between the two ashes. The upper ash is markedly less affected by pedogenic alteration than the underlying ash. Third, the upper ash is correlated with chronostratigraphic unit II on the basis of the presence of pyroclastic-surge deposits in the upper ash. The correlative pyroclastic-surge deposits at the Lathrop Wells center are interbedded with lava flows and proximal scoria-fall deposits of chronostratigraphic unit II (see discussion below). Fourth, the degree of carbonate cementation of the basal scoria-fall deposit is consistent with the degree of erosional dissection and pedogenic alteration of deposits of chronostratigraphic unit I.

Several potential inconsistencies with the correlation of the basal distal scoria-deposit to the deposits of chronostratigraphic unit I exist. Accumulations of widely dispersed scoria deposits associated with the subunits of chronostratigraphic unit I have not been identified at the Lathrop Wells center. Scoria deposits of the subunit are composed mostly of coarse spatter and agglutinate probably formed in weak hawaiian eruptions that typically do not produce widely dispersed scoria-fall deposits. These inconsistencies have several possible explanations. First, scoria deposits of chronostratigraphic unit I may have been deposited around the Lathrop Wells center but then were removed by erosion. If the time between eruptions of chronostratigraphic units I and II was of sufficient duration (several tens of thousands of years), there may have been time to erode scoria-fall deposits of chronostratigraphic unit I prior to deposition of the scoria-fall deposits of chronostratigraphic unit II. This is consistent with the erosion of vent scoria of chronostratigraphic unit I and the field relations of the distal scoria-fall deposits that are correlated tentatively with chronostratigraphic unit I. The deposits are present only where preserved in topographic lows marked by sites of accumulation of alluvium. Second, scoria deposits of subunits of

chronostratigraphic unit I (Qs1d, Qs1c, and Qs1a) can be traced beneath the main cone. Thick accumulations of scoria associated with chronostratigraphic unit I may have been present at and beneath the present site of the main cone. These deposits have been modified by erosion, by hydrovolcanic eruptions of chronostratigraphic unit II, and are concealed by deposits of chronostratigraphic unit III. These interpretations are supported in part, by the identification of bombs in deposits of chronostratigraphic unit III that are chemically identical to scoria of chronostratigraphic unit I (see following discussions). Finally, hawaiian eruptions accompanied by high-eruption fountains can sometimes produce voluminous scoria-fall deposits (Cass and Wright 1987). We are in the process of obtaining geochemical data for the distal ashes that can be used to further test unit correlations.

C. Chronostratigraphic Unit II

1. Unit Qs2/Ql2. Chronostratigraphic unit II was formed by the most voluminous pyroclastic and lava eruptions of the Lathrop Wells volcanic center. The lavas vented predominantly from a northwest-trending fissure located on the east-northeast edge of the volcanic center that coincides with the projected trace of a fault offsetting the underlying Timber Mountain Tuff (Fig. 2.12). The scoria eruptions occurred from a small, northwest-trending cluster of scoria mounds that crop out at the east base of the main cone and, inferentially, from vents beneath the main cone (Fig. 2.12). The lava and scoria subunits of chronostratigraphic unit II can be distinguished from the lava and scoria subunits of chronostratigraphic unit I by the lesser degree of erosional modification of the former. The scoria mounds of chronostratigraphic unit II are higher standing topographically than those of chronostratigraphic unit I, they have more complete conical forms, and the boundaries between individual scoria mounds can be readily identified from their topographic expression. The lava and scoria of chronostratigraphic unit II can be distinguished chemically from deposits of chronostratigraphic unit I by higher thorium concentrations and lower concentrations of strontium, phosphorus, the middle rare-earth elements, and titanium (Fig. 2.13).

a. Subunit Qs2b. A northwest-trending fissure system consisting of four paired and individual spatter mounds forms subunit Qs2b (Fig. 2.12). The fissure is coparallel with and partly overlaps the northwest-trending fissure system of the Qs1b subunit. Spatter mounds of subunit Qs2b are exposed for a distance of 0.5 km at the east base of the main cone (Fig. 2.12). The Qs2b deposits are overlain by the scoria-fall deposits of the main cone and therefore predate the eruptions of the main scoria cone (chronostratigraphic unit III). The spatter and scoria mounds of Qs2b show minor to moderate erosional modification. The summits of the conical mounds are marked by an increased concentration (erosional lag) of large volcanic bombs. Trench exposures in a large trench cut at the northwest scoria mound of the fissure show that there is a direct correlation between the dip of spatter and scoria deposits forming the mounds and the mound topography. That is, the present topography of the scoria mounds represents partially the primary volcanic topography. This is the main basis for contrasting, in the field, the scoria units of chronostratigraphic units II and I. There are two small outcrops of lava associated with the Qs2b subunit. These are exposed beneath scoria-fall deposits and eolian sand just north of the northwest scoria mound (Fig. 2.12). No age determinations have been obtained for subunit Qs2b.

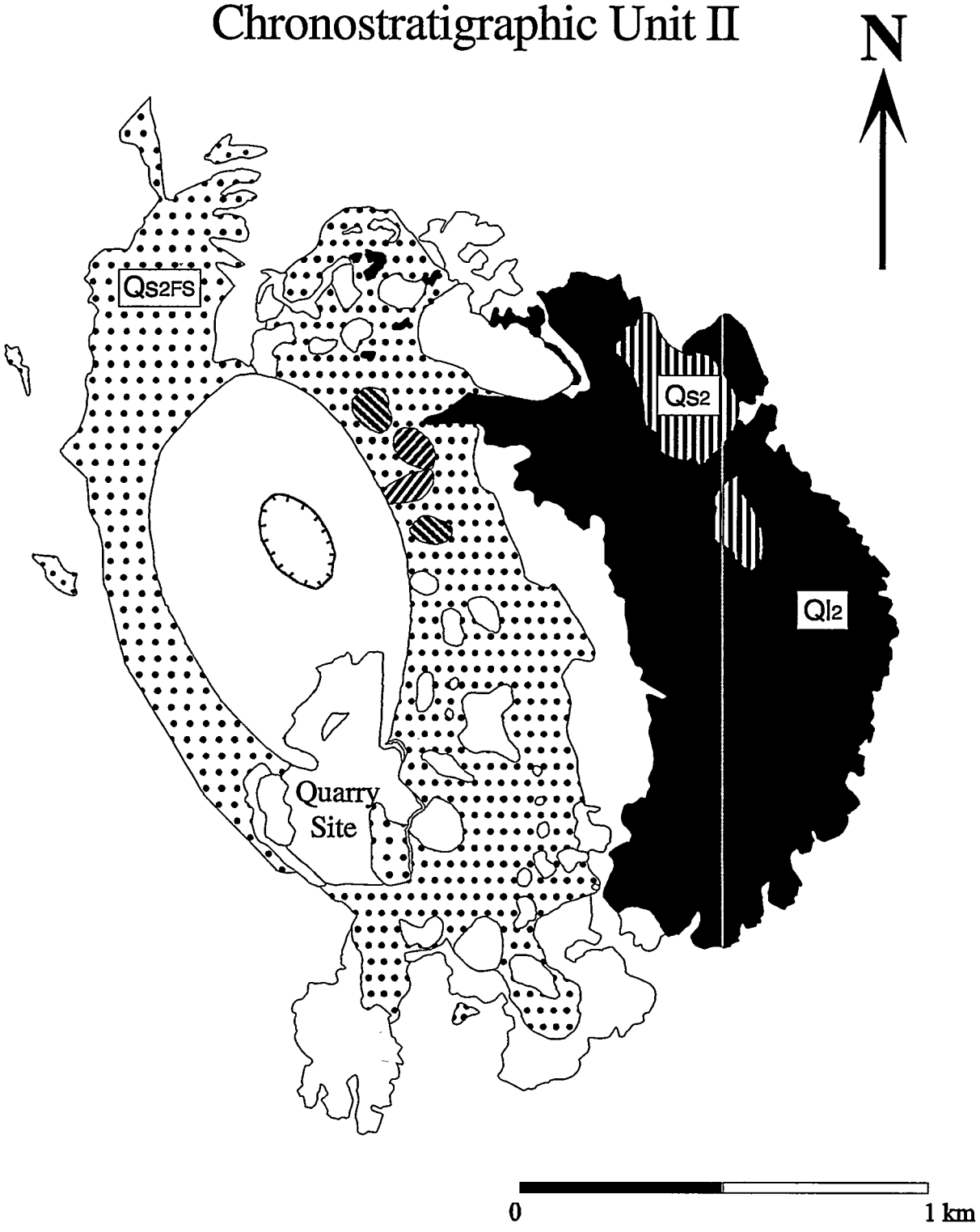


Fig. 2.12 Geologic map of the distribution of volcanic subunits of chronostratigraphic unit II of the Lathrop Wells volcanic center. The black shaded areas outline the distribution of lava flows; the cross-hatched areas denote scoria and spatter mounds; the dotted area outlines the distribution of outcrop areas of the scoria-fall sheet (with interbedded pyroclastic-surge deposits).

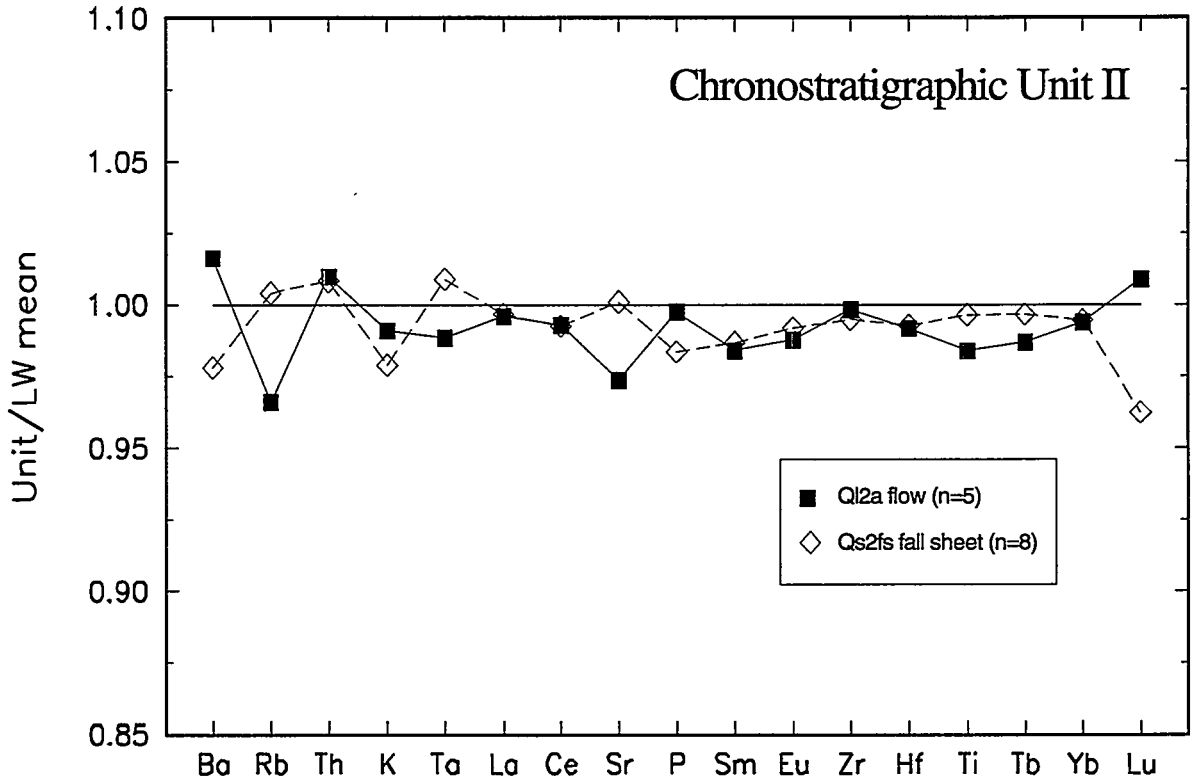


Fig. 2.13 Spidergram of elemental compositions normalized to an average composition for all analyzed samples of the volcanic units of the Lathrop Wells center ($n = 99$). Samples of chronostratigraphic unit II are designated by lava and vent deposits. Each pattern is plotted as the average of multiple analyses of specific eruptive subunits.

b. Subunit Qs2a/Ql2a. Three sites of small-volume blocky aa lavas crop out, forming a northwest-trending fissure alignment that parallels a previously formed west-northwest fissure of subunit Qs1c. These lavas mark a fissure system that did not vent notable quantities of scoria. The lavas are identical in morphology to the Ql1 subunits. They consist of oversteepened and broken lobes of lava where they extruded down the slopes of underlying scoria deposits of Qs1c. All of the lavas are small volume. They appear to have vented directly from a fissure without any significant pyroclastic eruptions.

The major lava and scoria subunit of chronostratigraphic unit II, Qs2a/Ql2a, includes a series of scoria mounds and related lavas erupted along a northwest trending fissure at the northeast edge of the volcanic center (Fig. 2.12). The fissure is coparallel to the trace of a west-down, northwest-trending fault that offsets the underlying Timber Mountain Tuff. The fault does not offset the lavas of the subunit. However, the preexisting topography associated with the fault controlled partly the distribution of the lava flows of subunit Ql2a (Fig. 2.12).

The main eruptive sites for the subunit are marked by one large and one smaller scoria mound that define the trace of the northwest-trending fissure. The fissure may extend further to the southeast, but it is covered both by its own lava flows, and eolian sand. The Ql2a lavas, informally named the Lathrop flow, form a near-continuous sheet of coalesced lobate blocky aa lava flows extending for a maximum length of 2.1 km and a maximum width of 0.9 km (Fig. 2.12). The Qs2a lavas ponded against topography upheld by

the Qs1c scoria mounds on the northwest and, therefore, postdate these deposits. West of the source fissure zone, the lavas of subunit Ql2a flowed into and coalesced within a fault-controlled topographic low. This topographic low probably coincided with a buried stream channel that followed the trace of the northwest-trending fault. The trace of the stream was diverted subsequently by emplacement of the Ql2a lavas and now follows the eastern margin of the lava flows.

East of the northwest-trending fissure, the Qs2a lavas consist of multiple flow lobes extruded from the fissure zone eastward down the dip slope formed on a shallow-dipping hogback upheld by the underlying Timber Mountain Tuff. Two lines of evidence indicate the eastern Ql2a lavas were extruded from multiple sites along the strike of the northwest-trending fissure. First, detailed field and aerial photographic examination of flow fronts and flow morphology shows that the flows form distinct flow lobes and are not a single continuous flow. A minimum of twenty individual flow lobes have been identified. There are probably more flow lobes on the southern exposure edge of the subunit but there they are obscured by a thick cover of eolian sand. Second, the flow directions of the lavas are marked by the trace of narrow (2 to 5 m width; 1 to 3 m depth) linear depressions on the flow surfaces. The features marked poorly developed aa channels that deflated below their adjoining aa flow surfaces by continued lateral flowage at the ends of the flow when lava extrusion ceased. The channels extend east and southeast of the main northwest-trending fissure indicating the lavas were extruded along the fissure length and the southeast projection of the fissure (Fig. 2.14).

Multiple age determinations using the cosmogenic ^{3}He method were obtained for samples collected at multiple sites on a Ql2a lava at the northeast exposure edge of the subunit. These are 82 ± 9, 88 ± 7, and 82 ± 4 ka. These ages are tightly clustered, suggesting an uncomplicated surface exposure history. A second sample site located on the west/northwest-trending fissure yielded the oldest cosmogenic ^{3}He age of 100 ± 9 (1 σ) ka. There is some uncertainty in the assignment of the former sample to subunit Ql2a. This will be tested by obtaining geochemical data for the sample site. The lavas of subunit Ql2a are located northeast of the main cone, outside the primary dispersal axis of scoria-fall deposits of chronostratigraphic unit II, which reach maximum thickness northwest and southeast of the main cone. Moreover, stream-cut exposures of the base of the Ql2a lava flow show that the units overlies pyroclastic surge deposits that are correlated with more extensive pyroclastic surge deposits to the west. These pyroclastic surge deposits occur in the upper third of the scoria-fall deposits and indicate the lava flows were extruded during the latter stages of formation of the scoria-fall deposits. This stratigraphic position and the location of the Ql2a lava unit indicates that only a limited thickness of scoria was deposited on unit Ql2a. The tight clustering of cosmogenic ^{3}He ages suggests the ages may approach the crystallization age of the subunit. The cosmogenic ^{3}He ages are slightly younger than but are not analytically distinguishable from the ages obtained for the Ql1a, Ql1b and Ql1c lavas; the emplacement age of the latter lavas is almost certainly older because they were covered by the scoria-fall deposits of chronostratigraphic unit II.

Conventional K-Ar whole-rock ages of the same Ql2a lavas are 188 ± 22 ka (weighted mean) and 139 ± 68 ka (arithmetic mean) for three replicate samples (Turrin et al. in press). The ^{40}Ar/^{39}Ar age determinations of splits of the same samples yielded a weighted mean of 217 ± 64 ka and a mean of 153 ± 110 ka (Turrin et al. 1991). An age of 239 ± 189 ka was obtained by the conventional K-Ar method (mean of all whole-rock age determinations of the Ql2a subunit reported in Turrin et al. [in press]). They also reported a weighted mean of the K-Ar age determinations of 137 ± 37 ka, but this number was obtained by discarding the results of one sample set of the Ql2a lava. Turrin et al. (1991) reported an age



Fig. 2.14 Digitized image of aerial photograph of the Lathrop Wells volcanic center showing the outcrop distribution of the Lathrop lava flow. The flow was emplaced in two settings. West of the northwest-trending fissure, the lavas ponded in a topographic low formed parallel to the trace of the now buried northwest-trending (down to the west) fault (ponded flows). East of the fissure, the lavas were extruded down a gentle, east-tilted hogback formed on the upthrown side of the fault. The lavas formed lobate flows with small aspect ratios (lava lobes). Aa flow channels extend along the central part of individual lava lobes channels and can be traced toward their source: the trace of the northwest-trending fissure.

of 183 ± 21 ka for the Qs2a lavas based on $^{40}Ar/^{39}Ar$ age determinations, but this age was reported as a weighted mean that included samples from both the Ql1c and Ql2a subunits. Moreover, four samples were discarded from the data set without defined rejection criteria. The mean age of the $^{40}Ar/^{39}Ar$ age determinations is 277 ± 234 ka for the combined data sets using the published values of Turrin et al. (1991, Table 1). The mean age of the sample set becomes 182 ± 97 ka if four samples are removed from the data set. These samples are identified as outliers using standard statistical tests of the data distribution and can be rejected on that basis. Turrin et al. (1992) reported an isochron age of 107 ± 33 ka from $^{40}Ar/^{39}Ar$ step-heating spectra for a sample of the Ql2a lava (see also discussion in Zreda et al. 1993). This age is in close agreement with the cosmogenic ^{3}He surface exposure ages. All of these K-Ar and $^{40}Ar/^{39}Ar$ age determinations are in agreement with the cosmogenic ^{3}He ages on the basis of the following assumptions: (1) the calibration accuracy of the ^{3}He exposure ages is ± 30%, and (2) the best representation of the K-Ar and $^{40}Ar/^{39}Ar$ ages is the mean, not the weighted mean, of replicate age determinations (see discussions in the Chronology section of the chapter).

A TL age determination on sediments exposed beneath the Ql2a lava yielded an age of 24.5 ± 2.5 ka (Crowe et al. 1992). This age is discordant with ages obtained by other chronology methods and may not reflect the emplacement age of the lava. We have been unable to explain this discordance. To further constrain the emplacement age of this unit, we are obtaining $^{40}Ar/^{39}Ar$ dating of sanidine from tuff xenoliths enclosed within the Ql2a lava.

c. Subunit Qs2fs: The Scoria-fall sheet of chronostratigraphic unit II. A subunit of chronostratigraphic subunit II is formed by widespread interbedded scoria-fall and pyroclastic-surge deposits (Qs2fs) of chronostratigraphic unit II. This unit is distributed elliptically around the main cone and was probably erupted from concealed vents beneath the cone. The deposits are correlated with chronostratigraphic unit II on the basis of multiple lines of evidence. First, the pyroclastic-surge deposits are interbedded with the scoria-fall sheet. These pyroclastic-surge deposits overlie lavas of Ql2b in trench LW-2 and underlie lavas of Ql2a in stream-cut exposures at the north outcrop area of the Lathrop lava. These interfingering stratigraphic relations require that the fall sheet is equivalent stratigraphically to the Ql2 lava sequence. Second, exposed deposits of the widespread scoria-fall sheet are reworked. Locally, the upper parts of the fall sequence have been removed by erosion even where the scoria deposits covered low-angle topography. The large continuous mantle of scoria-fall deposits northwest of the main cone that drapes a ridge upheld by exposures of the Topopah Springs tuff has well developed rills. The degree of reworking and geomorphic modification of the scoria-fall deposits contrasts markedly with the unrilled, 29° slopes of the outer surface of the main cone. Thus, the deposits that form the outer cone slopes of the main cone (chronostratigraphic unit III) must be younger than and cannot be correlated with the rilled, reworked scoria-fall sheet. Finally, the scoria-fall sheet can be distinguished chemically from scoria deposits of the main cone (chronostratigraphic unit III) by lower thorium and higher titanium concentrations (Figs. 2.13 and 2.16).

The scoria-fall deposits (Qs2fs) mantle the underlying basaltic and alluvial units and locally rest on bedrock of Miocene tuff. The fall deposits are thickest on the northwest and southeast sides of the cone, probably reflecting prevailing winds during the eruptions. We have systematically examined the scoria-fall deposits in trenches constructed around the cone except on the east side, where the mantle of sand covering the deposits is too thick to penetrate with our backhoe equipment. Three distinctive layers are present in the scoria-fall deposits. Each layer consists of multiple-fall units with reversely graded bases and fine-grained tops. The subdivisions in the fall sheet are identified on the basis of multiple fine-grained ash layers between layers and the local presence of pyroclastic-surge deposits, which form the middle layer of the scoria-fall deposits. Size data for maximum clast size and layer thickness have been measured in the fall

layers and are currently being processed. We will use the clast size data to constrain models of the location of the vents for the deposits and to reconstruct column dynamics for studies of effects of volcanism (Valentine et al. 1992, 1994).

Locally the Qs2fs fall sheet rests on scoria-fall deposits of chronostratigraphic unit I. The upper part of these underlying scoria-fall deposits are deeply weathered. There is a marked increase in the degree of pedogenic alteration of the scoria-fall deposits of chronostratigraphic unit I versus the overlying scoria deposits; the alternation contrast can be traced along a planar contact suggesting the fall-sheet deposits of chronostratigraphic unit II buried a weathered surface formed on the underlying deposits. Locally, there are stringers of carbonate cemented silt at the contact but no development of soil.

Hydrovolcanic eruptions occurred during the middle eruptive stage of chronostratigraphic unit II. The distribution of pyroclastic-surge deposits from the hydrovolcanic eruptions has been determined through systematic examination of the scoria-fall sheet in trenches. The deposits crop out extensively northwest and west of the main scoria cone (Fig. 2.12). Thick deposits of the pyroclastic surge are present in the subsurface beneath eolian sands and silt north of the main cone; they locally exceed 2 m in thickness where ponded in topographic lows. The contact between pyroclastic-surge deposits and Ql1c lavas was exposed in trenches LW-1 and LW-2. In trench LW-1, vesicular clinker marking the upper surface of the lava shows coatings of pedogenic carbonate along fractures at the edges and bottoms of lava blocks. The overlying pyroclastic-surge deposits contain very limited or no amounts of carbonate coating. This requires a time break between emplacement of the Ql1c lava flow and subsequent deposition of the pyroclastic-surge deposits, consistent with stratigraphic relations described above.

The pyroclastic-surge unit was probably derived from a vent located beneath the main cone. This conclusion is based on two observations. First, the pyroclastic-surge deposits are present in outcrops on the north and northwest circumference of the main cone. The proximity of the deposits to the cone suggest they were derived from the vicinity of the main cone. Second, the pyroclastic-surge deposits are interbedded with the scoria-fall deposits that encompass the main cone. The thickest accumulations of the pyroclastic-surge deposits occur directly north and northwest of the main cone. This locally reflects channeling of the pyroclastic surges in preeruption topographic lows. Additionally, the phreatomagmatic eruptions that produced the deposits may have been erupted preferentially to the north and northwest by the blast dynamics. The volumes of the surge deposits are sufficiently large that the eruptions should have formed a tuff ring or wide, flat-floored crater. The absence of such a volcanic landform is enigmatic. The preferred explanation for the absence of a tuff ring is that it is buried beneath deposits of subsequent strombolian eruptions of chronostratigraphic unit III. Continued commercial quarrying of the main cone may resolve this question.

Probable correlative scoria and ash deposits are present up to 4 km north and northwest of the Lathrop Wells center and in a trench exposure cut across the Stagecoach fault, 5 km northeast of the Lathrop Wells center (Fig. 2.9). At both localities, an upper ash with recognizable cross-bedded deposits characteristic of deposition by pyroclastic-surge processes overlies an alluvial deposit that in turn is underlain by fall deposits correlated with chronostratigraphic unit I. The distal ash deposits thus closely match the stratigraphic relations of the lower part of the volcanic stratigraphy of the Lathrop Wells volcanic center.

D. Chronostratigraphic Unit III

1. Unit Qs3/Ql3. Chronostratigraphic unit III of the Lathrop Wells center comprises two subunits, Qs3, the main cone deposits and Ql3, multiple lobes of small volume blocky aa lavas erupted along the trace of the west/northwest-trending fissure of chronostratigraphic unit II (Fig. 2.15). The scoria and lava units of chronostratigraphic unit III are distinguished from units I and II by thorium enrichment and titanium depletion of the former units (Fig. 2.16).

a. Subunit Qs3: The Main Cone. The scoria deposits of the main cone comprise subunit Qs3 (Fig. 2.16). These deposits were emplaced from mildly explosive strombolian eruptions with intervals of more energetic explosions of hydrovolcanic origin. The resulting landform is a composite scoria cone with dimensions slightly larger than typical scoria cones (Wood 1980; Crowe et al. 1983a). The main scoria cone is elongate northwest/southeast, has a maximum diameter of 1 km (northwest/southeast), a minimum diameter of 0.5 km (southwest/northeast), and a height of about 100 m. The cone is surmounted by a crater, elongate to the northwest, with a maximum diameter of 250 m and depth of <20 m. The cone has been excavated extensively on the southeast side. Cliff exposures reveal the internal structure and sequence of eruptive events that formed the volcanic landform. Interior parts of the cone consist of massive-to-fine-bedded scoria-fall deposits exhibiting radial dips of 15° to >22°. The interior exposures of these deposits are strongly oxidized along a northwest-trending zone; outer deposits of the cone away from the zone are formed of black tephra. The oxidization, as noted above, was probably produced by alteration of the scoria from gases emitted from an underlying feeder dike. The northwest trend of the oxidized scoria deposits is coparallel to the elongation of the cone, and also aligns with the en echelon fissures of the southern fissure systems of chronostratigraphic unit I. This northwest-trending zone controlled the eruptive sites of part of the oldest eruptive events and was reoccupied by subsequent eruptive events during formation of chronostratigraphic units II and III.

Middle cliff exposures in the main cone expose radially dipping scoria deposits, interbedded with lenticular zones of slope-reworked scoria deposits. The latter beds formed from avalanching or slumping of scoria down the cone slopes during cone growth. These types of deposits and the processes associated with their formation were described for the growth of Stromboli volcano by McGetchin and Chouet (1975). The upper parts of the cliff exposures on the southeast and southwest sides of the main cone expose distinctive plane-parallel to low-angle cross-bedded scoria. These beds are composed of mixtures of red and black scoria. The deposits were emplaced by pyroclastic surge associated with weak hydrovolcanic eruptions, based on the presence of fragmental clasts with angular faces broken across vesicular structure, the presence of sideromelane and hydrovolcanic shards in groundmass ash (Crowe et al. 1986; Wohletz 1986), local lenses of slightly palagonitized fine-grained ash in the deposits, and an abundance of cauliflower-shaped bombs (see Fisher and Schminike 1984). The red and black scoria deposits, which have a distinctive purple appearance in outcrop, are composed of varying proportions of scoria reworked from preexisting parts of scoria cone. These deposits have been observed only on the southern sides of the main cone. The upper surface of the main cone is capped by thin soils with weak horizon development (Wells et al. 1990).

The interior of the crater walls of the main cone is composed predominately of relatively fine-grained, highly vesiculated scoria with a paucity of large bombs. There is no agglutination of the scoria-fall deposits exposed through the complete section of deposits in the quarry cliffs at the south end of the cone. The cone must have been constructed from strombolian bursts that efficiently fragmented the melt. A slightly greater content of moderate-sized bombs are exposed in the summit crater compared to the interior parts of the cone.

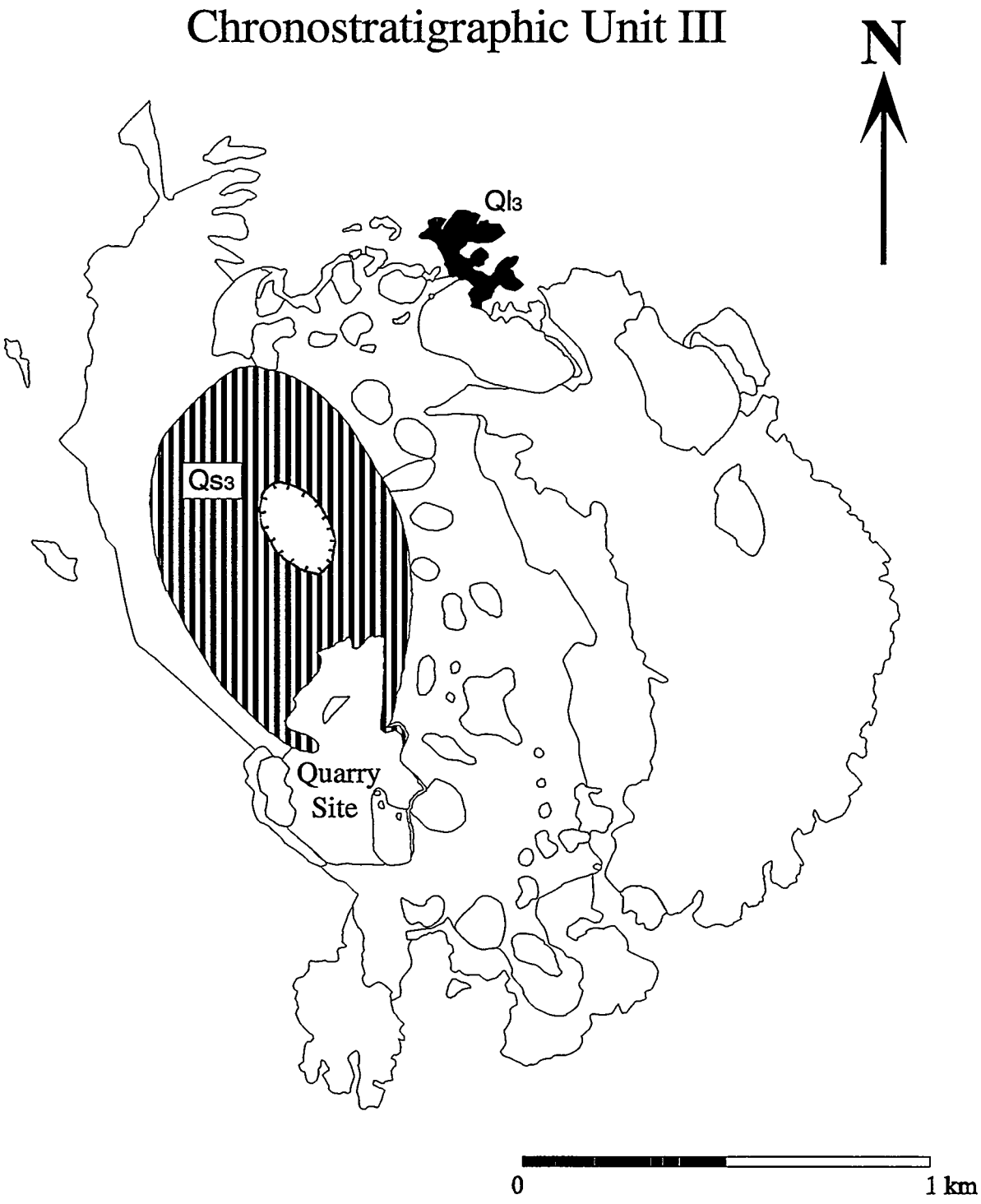


Fig. 2.15 Geologic map of the distribution of volcanic subunits of chronostratigraphic unit III of the Lathrop Wells volcanic center. The black shaded areas of the figure outline the distribution of the lava flow subunits; the dark, horizontally-hatched areas outline recognizable vents (scoria and spatter mounds) for the lava subunits and fissure systems. The scoria-fall deposits for chronostratigraphic unit III are not widely distributed and they are infiltrated by eolian sand. They cannot be mapped as a separate geologic unit.

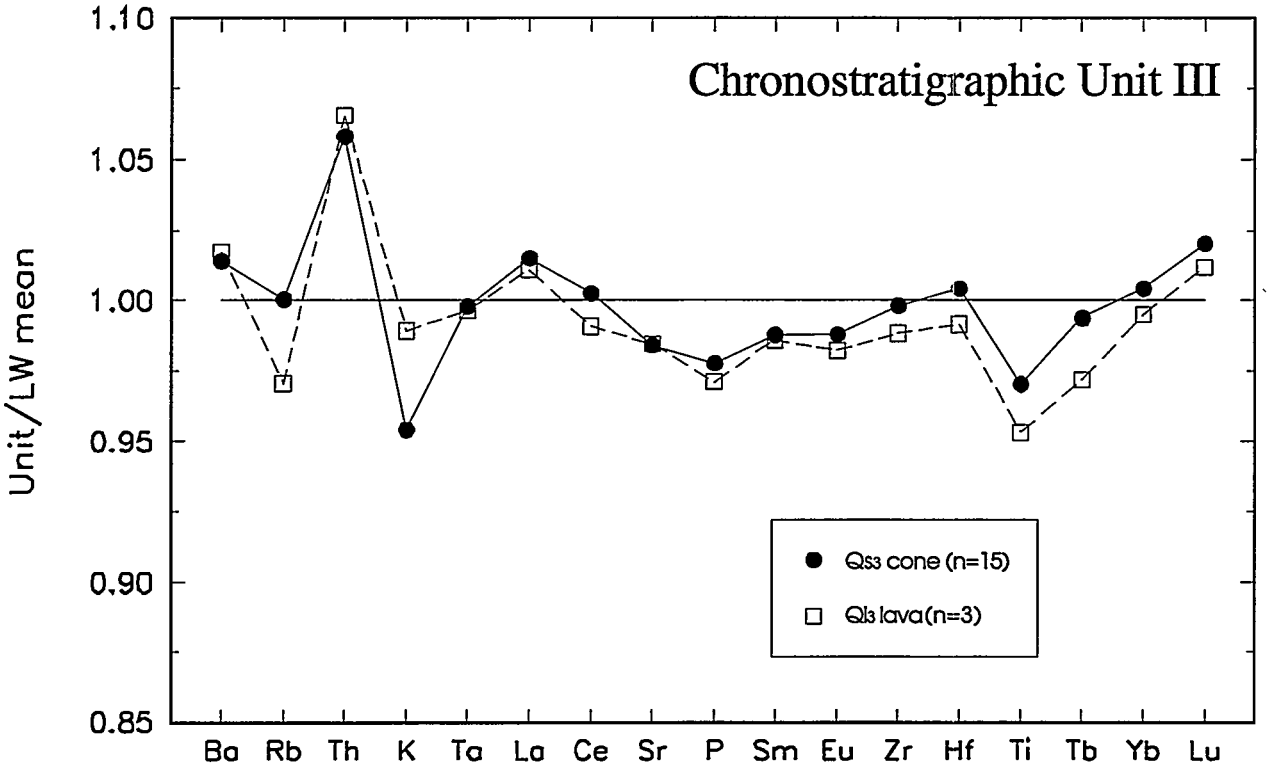


Fig. 2.16 Spidergram of elemental compositions normalized to an average composition for all analyzed samples of the volcanic units of the Lathrop Wells center ($n = 99$). Samples of chronostratigraphic unit III are designated by lava and vent deposits. Each pattern is plotted as the average of multiple analyses of specific eruptive subunits.

Accidental lithic fragments of the underlying Miocene tuff are present in the scoria deposits. They range in size from <1 mm to >0.3 m. The fragments were partly to moderately fused during contact with basalt melt; some of the fragments are banded with intermixed layers of basalt and fused tuff. The lithic fragments are conspicuous in outcrop because of their marked contrast in color with the red and black scoria. While visually striking, their abundance by volume is <0.1% (Crowe et al. 1983a).

The pyroclastic eruptions of chronostratigraphic unit III did not form a widely distributed scoria-fall sheet. There are exposures of the eroded deposits of Qs1c at the north base of the main cone. These deposits are not erosional windows through a fall sheet of chronostratigraphic unit III, but instead are areas of the older deposits that were not covered by the younger eruptions. This is indicated by two lines of evidence. First, the outer slopes of the main cone are unmodified (Wells et al. 1990). They have not been affected by down-slope wasting. Second, trenches constructed at the north base of the main cone show that there are no cone-slope apron deposits at the base of the cone. We have been unable to find identifiable scoria-fall deposits beyond the flanks of the main cone primarily because of development of a limited fall sheet associated with subunit Qs3. However, the base of the cone is covered by thick ramps of eolian sand and silt, which probably conceal scoria-fall deposits of Qs3.

The surficial exposures of the scoria-fall sheet of chronostratigraphic unit II are distinguished from cone-slope deposits of chronostratigraphic unit III by two criteria. First, the scoria-fall deposits of chronostratigraphic unit II are extensively reworked, rilled, and locally channeled. The cone slopes are

unmodified except for minor slope slumping (Wells et al. 1990). The prominent geomorphic differences between the deposits require a time break between the eruptions of chronostratigraphic units II and III (Fig. 2.15). Second, the scoria deposits of chronostratigraphic units II and III have slightly different geochemical compositions (Figs. 2.13 and 2.16).

Multiple cosmogenic ^{3}He ages have been obtained for the scoria deposits of chronostratigraphic unit III. Cone scoria scraped from the outer cone-slope surface several tens of meters below the west summit of the main cone yielded an age of 35 ± 5 ka. Multiple bombs collected from the cone summit yielded ages of 56 ± 7, 36 ± 5, and 29 ± 5 (all 1 σ) ka. The bombs were collected from a flat part of the rim crest of the main cone to minimize the effects of erosion through mass wasting down the cone slopes. A large bomb collected about 10–20 m below the crest yielded an age of about 43 ± 3 (1 σ) ka. This bomb projected 20 cm above the modern cone surface. The variability in exposure ages for the multi-sample cosmogenic ^{3}He ages indicates the samples do not share a uniform exposure history.

The traditional interpretation of the cosmogenic ages is that the best approximation of the age of the cone is >56 ± 17 ka. This is the maximum measured exposure age combined with an age calibration uncertainty of 30% (Poths and Crowe 1992). Zreda et al. (1993) reported cosmogenic ^{36}Cl ages of 83 ± 9.2 and 68 ± 5.7 ka for bombs from the summit of the main cone. The two ages are indistinguishable analytically and give a mean age of 75 ± 11 ka. The mean age is slightly older than the cosmogenic ^{3}He ages of summit bombs. However, Zreda et al. (1993) noted that the bomb sample giving the oldest cosmogenic ^{36}Cl age is altered, and the alteration component could not be separated from the rest of the rock. If this sample is suspect and should be discarded because of alteration, the remaining sample (68 ± 5.7 ka) is in reasonable agreement with the oldest cosmogenic ^{3}He age.

An alternative explanation for the spread of cosmogenic surface ages for chronostratigraphic unit III is that some of the dated bombs debris may be derived from the underlying deposits of either chronostratigraphic unit I or II. They therefore could have had cosmogenic exposure history prior to their incorporation in deposits of chronostratigraphic unit III and thus give anomalously old ages. This alternative explanation is rejected for two reasons. First, only the upper surface of older cones would have been exposed to the cosmogenic influx, and the underlying and larger volume of the deposits should have been shielded. Second, the geochemistry of summit bombs used for the cosmogenic ^{3}He age determinations matches the geochemistry of chronostratigraphic unit III.

There is a remaining unresolved inconsistency with the results of the cosmogenic ^{3}He ages. The oldest ages obtained for bombs from the summit are about 40% older than ^{3}He ages obtained for scoria and bombs on the cone slopes. The younger ages of the latter samples would require a minimum 0.5 m of erosional removal of scoria to shield the deposit and produce the resulting age differences. The pristine, unrilled cone slopes and absence of a cone-slope apron at the base of the cone are inconsistent with this interpretation.

The cosmogenic ^{3}He ages are slightly younger than the exposure ages obtained for the subunits of chronostratigraphic units I and II. The cosmogenic ^{36}Cl ages from the cone summit are younger if the altered sample is discarded. If that sample is included, the cone summit and lava ages of chronostratigraphic unit I overlap analytically (Zreda 1993). However, the cosmogenic ^{36}Cl samples were collected from the south lava flow at a locality that must have been covered by at least a meter of scoria-fall deposits. Thus, the coincidence in ages of the ^{36}Cl ages of the cone summit (chronostratigraphic unit III) and the southern lava flow is attributable to the lava flow's being shielded by the now eroded scoria-fall deposits of chronostratigraphic unit II.

Turrin and Champion (1991) show sample sites for conventional K-Ar age determinations for the main cone (samples TSV-283 and TSV-129) but do not report results. Champion (1991) and Turrin et al. (1991) have argued that the main cone and associated subunits of chronostratigraphic unit II are no more than 100 years younger than the lava flow units. This conclusion is based largely on paleomagnetic studies where the authors cite a 4.7° difference in the two grand mean magnetization directions for the main cone and associated subunits and the lavas of chronostratigraphic unit III. Regardless of the interpretation of the paleomagnetic data, the reported differences in the grand mean magnetization directions, if valid, are consistent with the contrasting degrees of erosional modification of the respective chronostratigraphic units. (Note: The cited paleomagnetic correlations may be obscured by the inclusion of data from scoria and lava deposits of Qs1a and Ql1a with the volcanic units of the main cone. We assign, in this report, Qs1a/Ql1a to the oldest chronostratigraphic unit based on field, geomorphic, and petrologic criteria.)

There are several concerns with the quality of the paleomagnetic data and the stratigraphic and chronological interpretations based on the paleomagnetic data of Champion (1991) and Turrin et al. (1991). First, samples for paleomagnetic studies of chronostratigraphic unit II were collected from both weakly agglutinated and nonagglutinated scoria deposits (Turrin et al. 1991). At best, some of the samples may be marginally suitable for reliable high-precision determinations of field directions (Holcomb et al. 1986). In addition, the sample sites should have markedly different measurement precision although there is no way of evaluating this because the data are not presented in sufficient detail. Discrimination of the chronostratigraphic units can be demonstrated only through presentation and analysis of both demagnetization data and statistical parameters for individual sites. Second, the cone summit is formed primarily of nonagglutinated spatter. There is only a small population of slightly agglutinated bombs that possibly could record satisfactorily the field magnetization directions. Third, the cone summit is the highest topographic point in the area. Samples collected from the summit for paleomagnetic studies should be highly susceptible to modification from exposure to lightning strikes. We encountered difficulties in obtaining high-precision magnetization directions for samples collected from the topographically low-standing lava flows because of high-intensity lightning effects (Crowe et al. 1992). Fourth, the summit eruptions of the main scoria cone were formed partly by hydrovolcanic eruptions. This interpretation is based on the local presence of fine-bedded, partly palagonitized ash and cauliflower bombs (Crowe et al. 1986, Wohletz 1986) in the summit deposits. These deposits, unless carefully screened to eliminate sampling of redeposited hydrovolcanic clasts, are unsuitable for paleomagnetic studies. This has been verified by the identification of bombs in the summit deposits that have been reworked from scoria deposits of chronostratigraphic unit I. Finally, it is difficult, if not impossible, to use paleomagnetic data to provide absolute differences in the ages of volcanic deposits. The measured field magnetic directions of the center are close to the mean Quaternary dipole field (spin axis) (Turrin et al. 1991, 1992; Crowe et al. 1992; Wells et al. 1992). Even if the main cone and chronostratigraphic unit III prove to be distinct, the different directions can be used only to establish a minimum age difference between the rocks (Turrin et al. 1992; Wells et al. 1992).

b. Subunit Ql3. All lava subunits were assumed in previously published field studies of the Lathrop Wells volcanic center to predate eruptions of the main cone (chronostratigraphic unit III). Newly obtained geochemical data provide evidence that one set of lavas is chemically identical to the scoria deposits of the main cone (thorium enrichment and titanium depletion) and could be assigned to chronostratigraphic unit III. These lavas comprise a group of topographically high-standing lavas (Ql3) that crop out about 0.5 km northeast of the north base of the main cone (Fig. 2.15). They are herein informally named the Sand Ramp lava flow because they were emplaced over a low-angle sand-ramp surface.

The Ql3 lava consist of three distinct lobes of blocky aa lava flows. They were erupted from the center part of the west/northwest-trending fissure of chronostratigraphic unit II. The Ql3 lava was erupted over low-angle sand-ramp surfaces. Several lines of geomorphic evidence are consistent with the assignment of the Ql3 lavas to chronostratigraphic unit III. First, the lavas are not draped by scoria-fall deposits of chronostratigraphic unit II, and they have a relatively thin covering of eolian sand. Second, they have steep, unmodified flow fronts ranging in height from 3 to 4 m with only minimum areas of exposure of massive aa flow interiors. In contrast, the aa flow interiors are commonly exposed in all other lava units from erosion of the blocky aa flow rubble. Third, the lava has the best preserved surface morphology of any lava flow in the center using comparative assessment of the morphology of lava units from aerial photographs.

Cosmogenic ^{3}He surface exposure ages were obtained for surface samples from two lava lobes of the Ql3 subunit. These ages are 67 ± 6 and 53 ± 7 ka. The surface exposure ages, which are from samples of unmodified lava flow surfaces, overlap with the oldest cosmogenic ^{3}He ages of bombs from the summit of the cone. This provides an independent collaboration that formation age of the main cone could be recorded by the oldest cosmogenic ages of the main cone. One potential inconsistency remains, however, in establishing the age of the Ql3 lava flow. A cosmogenic ^{3}He age of 100 ± 9 (1 σ) ka was obtained for a surface lava sample collected near the source of the Ql3 lava. We tentatively correlate this sample with the Ql2b lava subunit but cannot distinguish definitively the sample site from the Ql3 lava unit. We are obtaining geochemical data for this sample to assign it more definitively to either chronostratigraphic unit II or III.

A U-Th disequilibrium isochron age of the Ql3 lava is 125 + 20 – 15 (1σ) ka, a reproducible age verified by replicate analyses of mineral and phase separates collected from the same sample of the Ql3 lava. Analytically this appears to be a valid isochron age, but the age is determined from phases with only small degrees of fractionation of uranium and thorium.

The $^{40}Ar/^{39}Ar$ age determinations for the Ql3 lavas range from 66 to 311 ka with a mean age of 153 ± 110 ka (Turrin et al. 1991). These ages are too variable to constrain precisely either the age or the stratigraphic assignment of the lava.

E. Chronostratigraphic Unit IV

1. Unit Qs4. The deposits of chronostratigraphic unit IV are small-volume tephra deposits that crop out only south of the main cone (Fig. 2.17). This is in an area of commercial quarrying activity and many critical outcrops have been modified or removed; the south side of the cone continues to be an area of active commercial quarrying of cinder. The Qs4 unit consists of local fall and flow-emplaced basaltic tephra, inferred to be derived from small satellite cones (now quarried with only remnants present) south of the main cone. The tephra units of chronostratigraphic unit IV overlie deposits of chronostratigraphic units I, II and III, and are separated from tephra of chronostratigraphic unit III by soil deposits with horizon development. They thus must be separated by a time break from deposits of chronostratigraphic unit III. The tephra units of chronostratigraphic unit IV are chemically diverse and have chemical characteristics that are distinct from other chronostratigraphic units (Fig. 2.18).

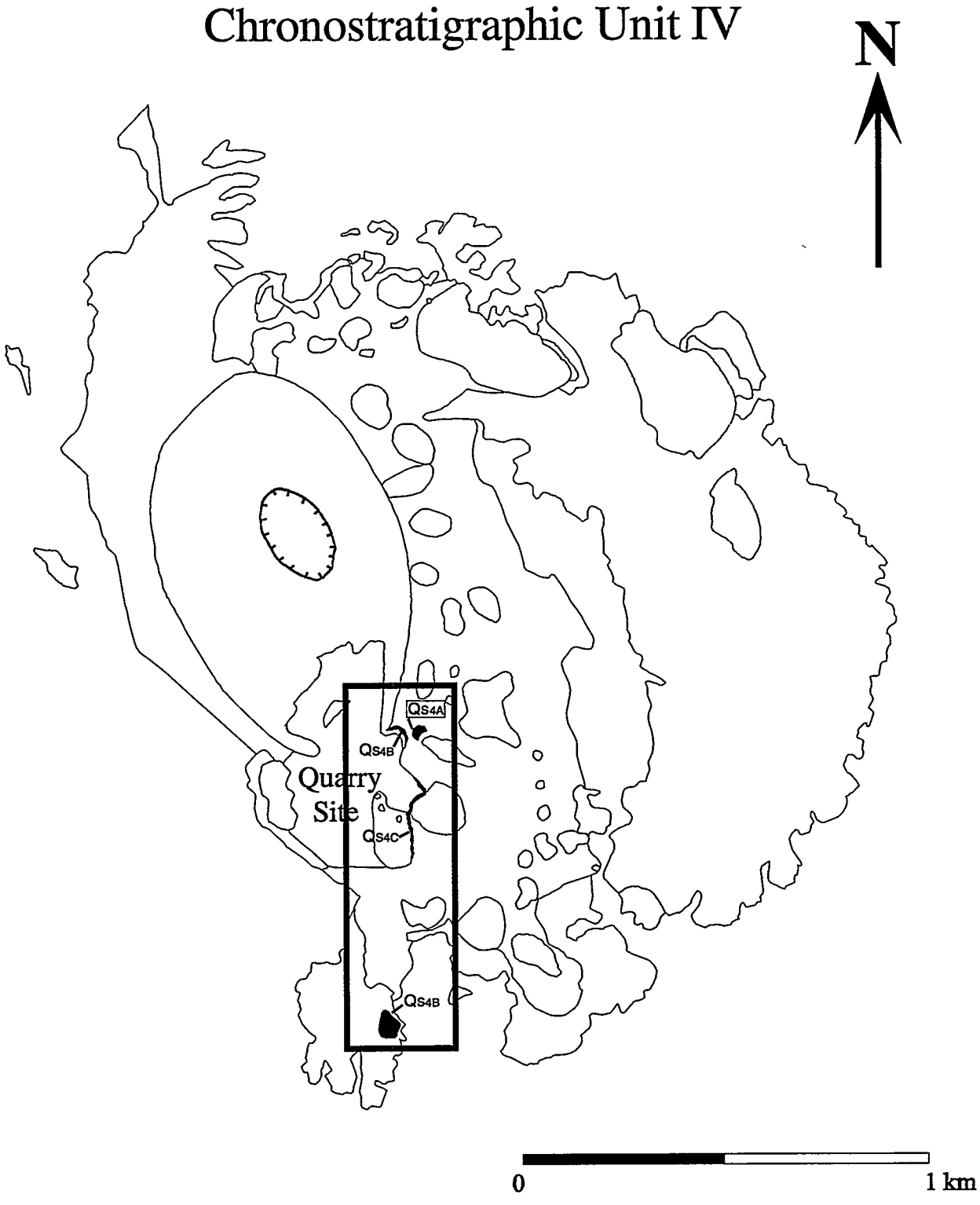


Fig. 2.17 Geologic map of the distribution of volcanic subunits of chronostratigraphic unit IV of the Lathrop Wells volcanic center. The deposits consist only of thin beds of tephra that are interbedded with soil containing horizon development. These deposits occur only on the south side of the volcanic center, mostly in the area outlined by the vertical rectangle.

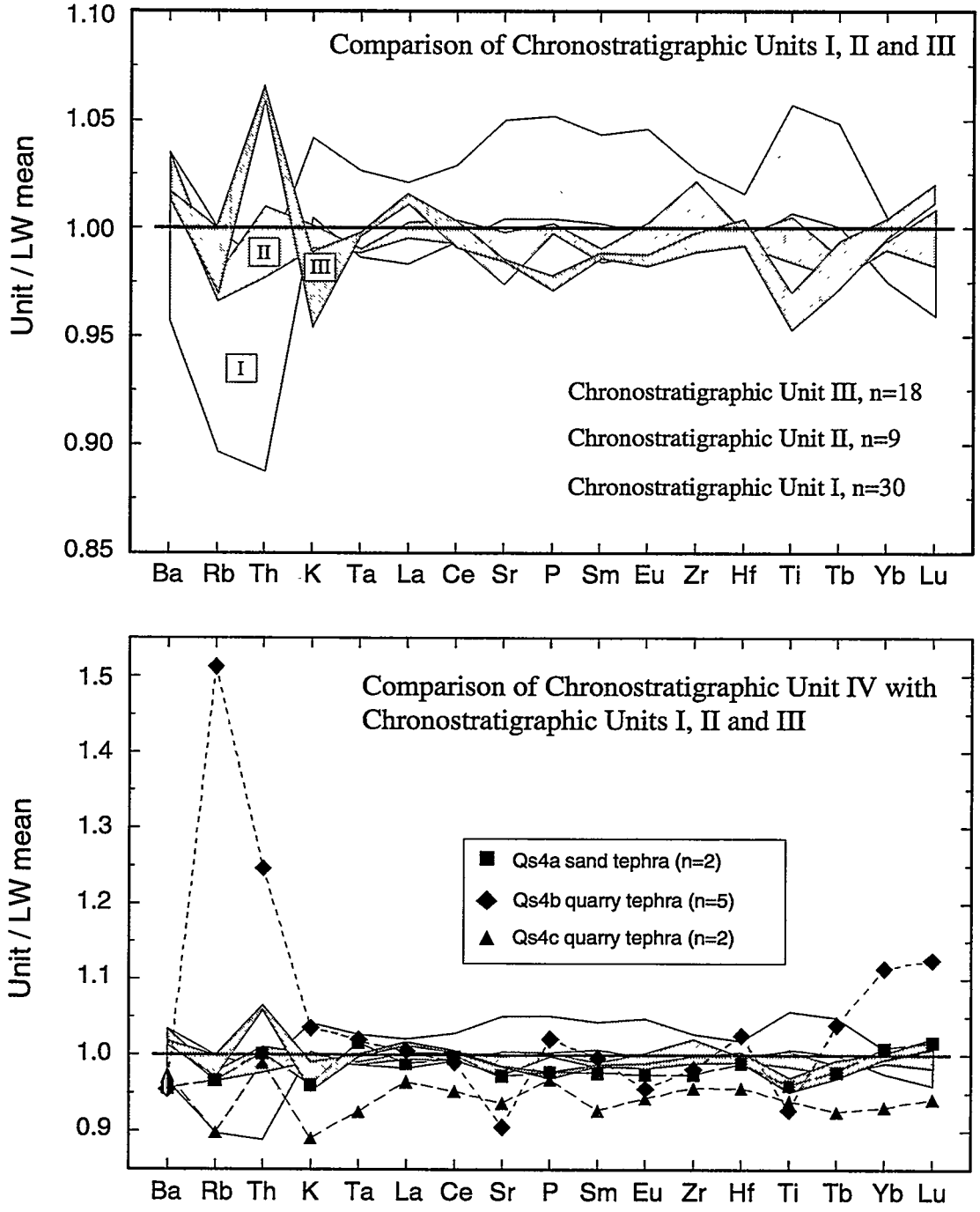


Fig. 2.18 Spidergram of elemental compositions normalized to an average composition of all analyzed samples of the volcanic units of the Lathrop Wells center (n = 99). Samples of chronostratigraphic unit IV are designated by subunit. Each pattern is plotted as the average of multiple analyses of specific eruptive subunits.

a. Qs4c. Subunit Qs4c consists of a locally prominent black tephra-fall deposit about 0.5 m thick with thin interbedded, pyroclastic-surge units. It is exposed only in quarry cuts southeast of the main cone. This deposit cannot be traced directly to local vent conduits but does overlie deposits of chronostratigraphic unit II. We therefore identify the black tephra fall as a subunit of chronostratigraphic unit IV on the basis of its stratigraphic position and distinctive chemical composition. This subunit has the highest magnesium number ([Mg/Mg + Fe2+] x 100) of any volcanic unit at the Lathrop Wells center (58 versus 54 ± 1 for all other units) indicating a less evolved magma. Lesser fractionation may account for the lower incompatible trace-element concentrations of this subunit relative to all other eruptive units at the Lathrop Wells center.

b. Subunit Qs4b. Scoria-fall and pyroclastic-surge (?) deposits probably associated with or erupted from the Qs4 vents were described originally at only one outcrop (Crowe et al. 1988, 1992a; Wells et al. 1990), a small cliff exposed by quarrying activity, several tens of meters south of the base of the main cone. Here, thin tephra beds, inferred to be primary flow deposits of hydrovolcanic origin, are separated by multiple soils with weak horizon development. These tephra units were correlated initially with a distinctive sequence of plane-parallel bedded, scoria-fall and hydrovolcanic deposits identified in the south quarry wall of the main cone (Crowe et al. 1992). However, petrologic studies have shown that the tephra units in the quarry (Qs4b) are chemically distinctive from the scoria units (Qs3) of the main cone.

The presence of the soil deposits beneath and between the Qs4b tephra units at the base of the cone requires their separation as a distinct chronostratigraphic unit. While this separation is used herein, there is controversy concerning the origin of the tephra deposits (Whitney and Shroba 1991; Turrin et al. 1992). The basis of the controversy is whether the tephra beds are primary (deposited directly from fallout from eruption columns) (Wells et al. 1991) or have been reworked from tephra deposits on the flanks of the main cone (Qs3) by surficial processes. If the deposits are of primary volcanic origin, they record a complex history of intermittent volcanic activity with periods of inactivity that must exceed several thousands of years to permit the development of horizons in the interbedded soils. Alternatively, if the deposits are reworked, they record episodes of surficial erosion and deposition and do not require multiple eruptive events.

Evidence cited in support of a reworked origin of the deposits include the presence of eolian sand or silt in the tephra deposits (Whitney and Shroba 1991) and granulometric data for the tephra beds that are inferred to be inconsistent with a primary origin of the deposits (Turrin et al. 1992). The authors of both papers suggest the deposits were formed from slope erosion of the main scoria cone of the Lathrop Wells center. The evidence supporting a primary origin of the beds includes the planar tops and bottom contacts over an outcrop distance of several tens of meters, draping or uniformity of the thickness of the deposits over basal contact irregularities, unsupported fabric of the deposits, and reverse grading reflecting eruption column dynamics (Wells et al. 1991, p. 662).

Several points provide strongly contradictory evidence for a reworked origin of the deposits. First, there is an absence of cross-bedding and bedding lenticularity. The tephra deposits show uniformity of bedding thickness and no bedding lamination except poorly developed, reverse grading. These deposits contrast markedly with a sequence of reworked deposits that overlie the section above the tephra beds (Wells et al. 1990). These reworked deposits are lenticular, and locally cross-bedded within discrete erosional channels. They contain supported clasts of basaltic debris with rotated long dimensions.

Second, proponents of the interpretation that the tephra beds are reworked suggested they are ". . . younger cone-apron deposits formed during subsequent erosion of the cinder cone" (Turrin et al. 1992, p. 556). A key and generally undisputed observation of the characteristics of the main cone of the Lathrop Wells center is the absence of cone-slope erosion and formation of a cone-slope apron (Wells et al. 1990). A further complication is that the tephra deposits are located several tens of meters from the base of the main cone. The only way the tephra beds could represent cone-slope deposits would be if the south part of the cone (which has been removed by quarrying) was, in contrast to the rest of the cone, significantly eroded. To investigate this unlikely possibility, historic photographs of the south cone exposure have been obtained. These photographs were taken in the 1930's prior to any modification of the cone by quarrying (Fig. 2.19). There is no evidence in the photograph of extensive cone-slope erosion of the south cone wall that would be required to form cone-slope apron deposits tens of meters from the base of the cone. Third, the presence of eolian silt and sand in the tephra beds is not inconsistent with a primary origin of the deposits. This material was introduced as a wind-blown constituent during soil pedogenesis. It is precisely the presence and formation of soil horizons in this material that requires time intervals between the tephra-fall units. Granulometric analyses cannot easily be used to discriminate reworked from primary tephra. Granulometric analyses of undisputed scoria-fall deposits with soil at the Lathrop Wells center and other Quaternary basalt centers in the southwest United States overlap with the grain-size distribution curves of Turrin et al. (1992). Finally, the distinctive geochemistry of the Qs4b tephra rules out derivation by reworking from either the main cone or any other eruptive unit identified at the Lathrop Wells volcanic center (Fig. 2.18). The tephra is distinguished by higher concentrations of thorium, rubidium, and the heavy rare-earth elements, indicating that it represents a primary volcanic event from a magma of different chemical composition than preceding eruptive units. Thus, multiple lines of evidence indicate it is physically impossible for the tephra deposits to be reworked, cone-slope deposits.

A surficial cover of local lenses of reworked tephra overlie the surface of the Ql1a lava flow at multiple localities 0.5 to 1.0 km south of the Qs4b quarry. Samples of the tephra were collected and analyzed for their major and trace-element composition. These data show that the tephra can be correlated geochemically and texturally with the Qs4b tephra and thus indicate the Qs4b unit represents a relatively widely dispersed tephra fall event.

c. Subunit Qs4a. Recent trenching a few tens of meters east of the original Qs4b quarry exposure revealed a 0.5 m thick section of fine-grained, slightly reworked tephra overlying sand and silt deposits that, in turn, overlie the Qs4b tephra units. This tephra is somewhat similar to the scoria of the main cone (Qs3) in concentrations of most incompatible elements (Fig. 2.17), but has slightly lower concentration of barium, thorium, and lanthanum, lower lanthanum/cesium ratio, a slightly higher magnesium number (55.2 versus 53.6), and higher cobalt (32.4 versus 30.0). Thus, for the same reasons presented for the Qs4b tephra, this tephra could not be derived from scoria reworked from the main cone. We interpret this tephra to represent the deposits of a primary volcanic event.

Local sections of thin primary and reworked(?) basaltic scoria were recently noted in field and trenching studies immediately south of the Old Quarry lava flow. A thin deposit of subunits Qs4b or Qs4a has been identified tentatively at this site about 1.0 km south of the main cone. Here unconsolidated, fine-grained tephra about 3 cm thick overlies a thick, prominent Av soil zone that caps scoria-fall deposits of chronostratigraphic unit II. Trace element analyses of this tephra will be obtained to test for correlations of these upper tephra units.

Two soil units beneath the tephra beds of chronostratigraphic unit IV in the quarry deposits have been dated by the TL method at 9.9 ± 0.7 ka and 3.7 ± 0.4 ka, and the ages are in correct stratigraphic sequence (Crowe et al. 1992, Wells et al. 1992). If these age determinations correctly record the chronology

of primary volcanic activity, two small volume eruptions have occurred at the Lathrop Wells center since ~4 ka, indicating an unusually long and complicated eruptive history, which is somewhat unexpected based on historic and geologic studies of small-volume basalt centers (Wood 1980, Wood and Kienle 1990).

No direct radiometric age determinations have been obtained for chronostratigraphic unit IV.

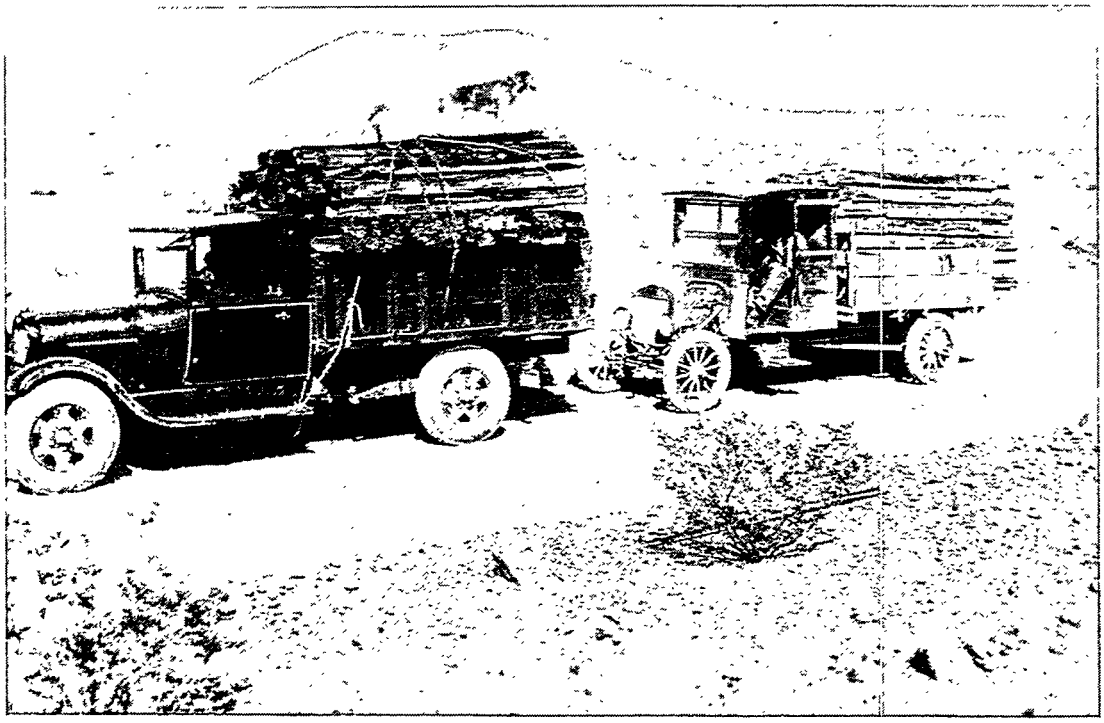


Photo courtesy of Jack Crowell, Beatty, NV

Fig. 2.19 Historic photograph of the south flank of the Lathrop Wells volcanic center. The photograph was taken before initiation of quarrying activity at the center. The south flanks of the center are unmodified by erosion indicating that tephra deposits south of the cone could not be derived from erosion of the cone slopes. The date of the photograph is estimated to be about 1930 based on identification of the approximate date of manufacture of the automobiles.

F. Application of Multiple Geochronology Methods: The Chronology of the Lathrop Wells Center

The Lathrop Wells volcanic center has been the subject of comprehensive geochronology studies. More field and geochronology data have been gathered at the Lathrop Wells center than all of the Pliocene and Quaternary volcanic centers of the YMR; it may be one of the most carefully studied small-volume Quaternary basaltic volcanic centers in the world. Establishing the chronology of the center has proven to be problematic using both conventional and developmental geochronology methods. The age of the center (<150 ka) is near the lower analytical limit for the conventional K-Ar methods, particularly for low-potassium, basaltic volcanic rocks. The ages of most of the volcanic units of the center are too old to date using the ^{14}C method, even if sources of datable carbon were present. We are applying developmental chronology methods that have limited histories of testing and development for young volcanic rocks (U-Th disequilibrium, cosmogenic ^{3}He, TL). Finally, we are attempting to resolve stratigraphic relations and the chronology of volcanic events at a level that is near the limit of the discrimination abilities of current geochronology methods and field geologic studies.

Not surprisingly, given the unprecedented level of detail of studies of the Lathrop Wells center, there have been and continue to be controversies concerning the interpretations of the data. The origins of the controversies are differences in interpretation of the age and eruptive history of the center (Turrin et al. 1991; 1992; Wells et al. 1992) and differences in opinions of what constitutes a conclusive data set (Crowe et al. 1992). We have chosen, in recognition of these controversies, to apply a variety of largely independent geochronology methods. It is important to establish the age of the Lathrop Wells volcanic center with an acceptable degree of confidence in order to apply this information to volcanic risk assessment for the potential Yucca Mountain site. Increased confidence in the results of chronology studies will be obtained if there is convergence in the age determinations using independent chronology methods.

In the following parts of Chapter 2, we assess by individual methods the results of geochronology studies for the Lathrop Wells center. We attempt to evaluate the underlying assumptions, resulting data, and the strengths and the weakness of each method recognizing that there may never be a complete consensus concerning the results and interpretations of the geochronology data.

1. K-Ar Age Determinations. A large number of conventional K-Ar age determinations of whole-rock. samples of basalt from the Lathrop Wells volcanic center have been obtained from multiple analytical laboratories (Sinnock and Easterling 1983; Turrin and Champion 1991; Turrin et al. 1991). These age determinations show a wide range in measured ages (negative ages to > 700 ka), generally large analytical errors for individual measurements, and poor reproducibility between analytical laboratories (Crowe et al. 1992). The most comprehensive summaries of the results of the whole-rock K-Ar age determinations are by Turrin and Champion (1991) and Turrin et al. (in press). They obtained replicate K-Ar ages of whole-rock, samples collected at separate sites in the Ql1, Qs3, and Ql3 units. The measured ages of their samples range from 34 to >650 ka. Turrin and Champion (1991) reported a weighted mean of 116 ± 13 ka for their Ql5 unit (a combination of Ql1a, Qs1b, and Qs3 units) and 133 ± 10 ka for their Ql3 unit (a combination of Ql2 subunits).

There are three concerns with these reported ages. First, the combination of units does not correspond to the stratigraphic subdivisions established from the field and trenching studies. Second, the analytical errors of the K-Ar ages are too large because of low radiogenic yield for the results to be used to discriminate the ages of different volcanic units. Third, the weighted mean is not an acceptable method for calculating the age of the units because the data show a nonGaussian distribution (Crowe et al. 1992; Wells

et al. 1992), and there is evidence of systematic bias in the age determinations toward older ages, probably due to the presence of excess argon.

We have attempted to evaluate the conventional K-Ar age determinations of Turrin and Champion (1991). Their measured ages are grouped by the defined volcanic stratigraphic units used in this report. The age determinations were not obtained under an approved Quality Assurance program and cannot be used for the YMP. However, the age determinations are of high quality analytically and can be used as an aid to interpreting the age of the volcanic center. Additional K-Ar or $^{40}Ar/^{39}Ar$ age determinations are being obtained under a fully qualified Quality Assurance program and will be used to verify the nonqualified K-Ar data.

Sixteen whole-rock, K-Ar age determinations were reported for chronostratigraphic units I, II, and III (3 age determinations for subunit Ql3, 9 age determinations for subunit Ql2a, and 4 age determinations for subunit Ql1a) (Turrin et al. in press). Descriptive statistics for the age determinations are listed in Table 2.3. The ages range from a minimum of 37 ± 29 ka to a maximum of 571 ± 360 ka.

Table 2.3 Descriptive Statistics for Conventional K-Ar and $^{40}Ar/^{39}Ar$ Data Sets of Turrin et al. (1991). Ages in ka.

Statistic	Convention K-Ar	Conventional K-Ar (outliers removed)	$^{40}Ar/^{39}Ar$	$^{40}Ar/^{39}Ar$ (outliers removed)
N	16	12	32	25
Min	37	37	-20	42
Max	571	211	947	311
Range	534	174	967	269
Mean	214	134	231	161
Median	154	147	170	147
Variance	22,719	2,717	40,082	4,545
Standard Deviation	150	52	200	67
Standard Error	38	15	35	13
Skewness	1.13	-0.49	2.1	0.5

The mean of the data set is 214 ± 151 ka (1 *s*). The sample variance is large (22719) and there are several indicators of a nonnormal data distribution. These include that the mean (214 ka) is greater than the median (154 ka) and the data are positively skewed (1.13). The nonnormal distribution of the data is shown in Fig. 2.20, a probability plot of the data set. The plot shows a nonlinear data distribution, with significant deviation in the upper tail (older ages). The data set was evaluated using the box, and stem and leaf diagrams. These plots show the presence of outlier data points in the data set. The outliers are samples collected from a flow lobe of subunit Ql2a. This flow is notable in the field by the presence of abundant fragments of tuff probably derived from the underlying Timber Mountain Tuff. These samples were judged to have a high possibility of being contaminated and were removed from the data set. The revised data were rerun through successive iterations using the statistical routines. All outlier points identified in successive runs were removed from the data set. Twelve K-Ar determinations remain after this screening. Descriptive

statistics for the edited sample set are listed in the second column of Table 2.3. The minimum age of the edited sample subset is 37 ± 29 ka (unchanged from the original data set), and the revised maximum age is 211 ± 340 ka. The sample mean of the screened data set is 134 ± 52 ka and its probability plot is near-linear (Fig. 2.21). The variance of the sample set is reduced by almost an order of magnitude from the original data set and the mean is close to but still slightly smaller than the median. The data set with outliers removed shows negative skewness (–0.49).

The sample mean of 134 ± 52 ka (1 *s*) can be regarded as an approximation of the age of lava units of the Lathrop Wells volcanic center with two cautions. First, the data set, even with outliers removed, shows a positive correlation between percentage radiogenic argon and measured age of the sample (Fig. 2.22). This positive correlation suggests the whole-rock age determinations are probably biased toward older ages. The real age of the dated lavas may be somewhat younger than the mean of 137 ka. Second, the mean age of the conventional K-Ar data set is valid only if the dated volcanic units are from the same volcanic unit or all the volcanic units have the same age. This is contradicted by field, stratigraphic, geomorphic, soil, and chemical data that show the dated lavas are from three distinct chronostratigraphic units with probable different ages. We conclude that the conventional K-Ar data set provides only a gross estimation of the age of the Lathrop Wells volcanic center and cannot be used to discriminate the identity or ages of individual units.

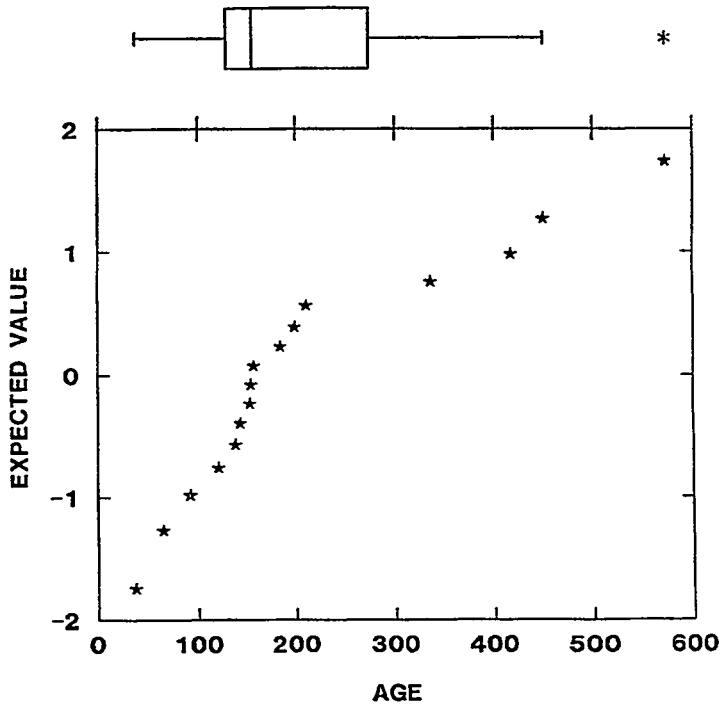


Fig. 2.20 Probability and box plots of the conventional whole-rock, K-Ar data of Turrin et al. (1991). The data are nonlinear on the probability plot indicating a nonGaussian distribution. This is verified in the box diagram, which shows nonsymmetrical hinges and the presence of outliers. The median of the box diagram is marked by the center vertical line. The median splits the data in half, and the hinges split the remaining halves in half. The whiskers, or end lines of the box diagram, bound the range of data, which falls within 1.5 Hspreads, where Hspread is the interquartile range. Values outside the whiskers are plotted with asterisks and are considered to be outliers. The scale of the box diagram is the same as the x-axis of the probability plot. Plots and statistical routines are from SYSTAT version 5.0.

2. $^{40}Ar/^{39}Ar$ Age Determinations. Turrin et al. (1991) report weighted means of 183 ± 21 ka for a combination of units Ql3 and Ql2a, 138 ± 54 ka for unit Ql1a, and 149 ± 45 ka for unit Qs1b for samples from the Lathrop Wells center that were analyzed using a whole-rock $^{40}Ar/^{39}Ar$ method, fundamentally the same method as the K-Ar method. These age determinations were not obtained under approved YMP quality assurance requirements. However, they again are judged to be good data analytically and useful potentially for constraining the age of the Lathrop Wells center. However, the same interpretative concerns exist for these samples as the conventional K-Ar age determinations. Specifically, the chronology data are combined for units that do not correspond to the chronostratigraphic units. Additionally, the data distribution is nonGaussian and there is evidence of contamination (correlation between percentage radiogenic argon and age) (Fig. 2.25) of some of the samples. However, in this case, Turrin et al. (1991) note that some of the samples are contaminated and exclude these age determinations from their data interpretations.

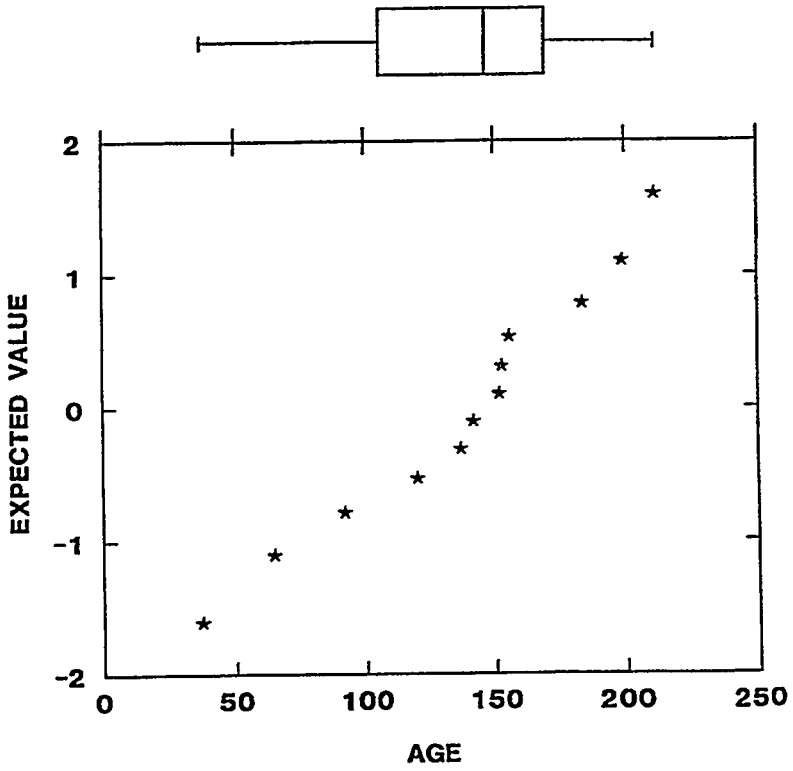


Fig. 2.21 Probability and box plots of the conventional whole-rock, K-Ar data of Turrin et al. (1991a) with outliers removed. The data show improved linearity on the probability plot and near symmetrical hinges on the box diagram. The features of the box diagram are the same as for Fig. 2.20. The scale of the box diagram is the same as that of the x-axis of the probability plot.

The $^{40}Ar/^{39}$ Ar ages of samples from chronostratigraphic units I, III, and III range from –20 ± 263 to 947 ± 24 ka. The mean age is 232 ± 200 ka (Turrin et al. 1991). Descriptive statistics for this sample set are listed in Table 2.3. The mean (232 ka) is greater than the median (170 ka). The data are strongly skewed positively (2.1), and there is large variance. The probability plot (Fig. 2.23) shows the data are nonnormal with an upper tail skewed toward older ages. The box, and stem and leaf diagrams identify, through successive iterations, four samples as outliers. These are the same four samples that were inferred to be contaminated by Turrin et al. (1991). The samples were removed from the data set and the data set rerun through the statistical routines until all identified outliers were removed. Descriptive statistics for the revised data set are listed in Table 2.3. The revised data show improved linearity on the probability plot (Fig. 2.24). However, the mean still exceeds the median and the data remain positively skewed (0.5). This strongly suggests that the variance in the data set cannot be entirely analytical. The best estimate of the

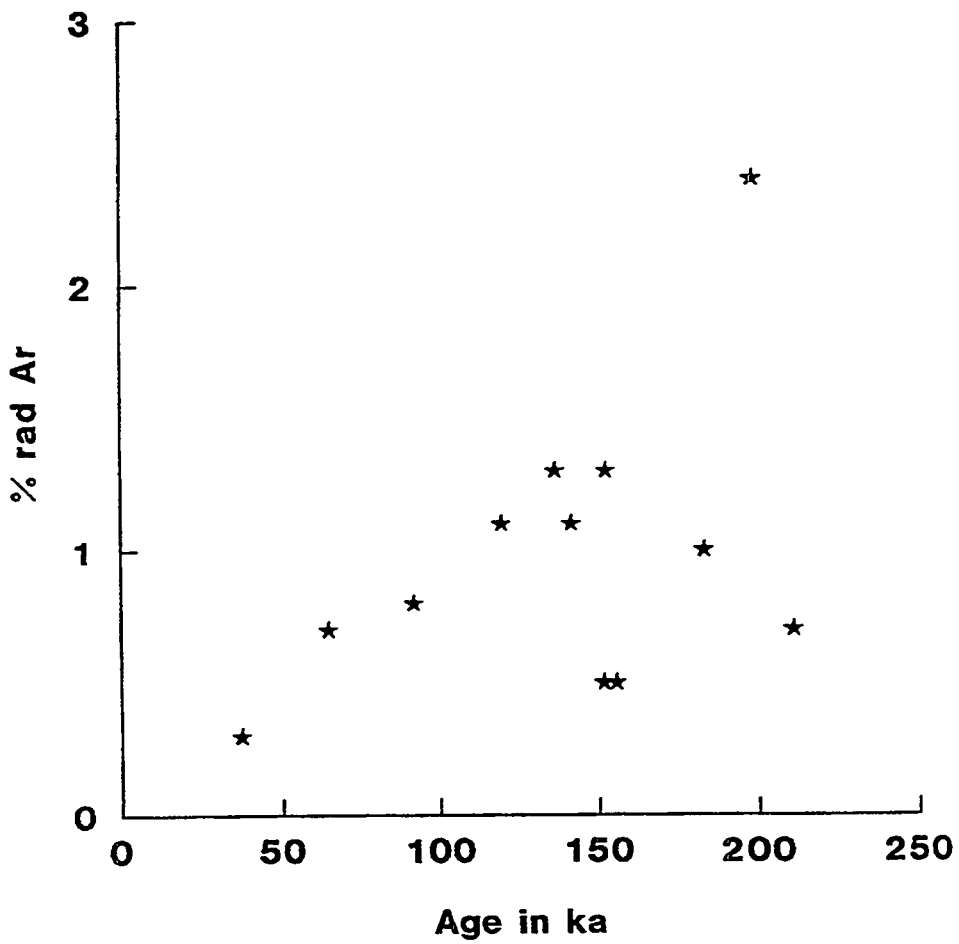


Fig. 2.22 Plot of percentage radiogenic argon versus age by the conventional K-Ar age determinations of Turrin et al. (1991a). The data show a positive correlation between age and percentage radiogenic argon, suggesting the age determinations are contaminated and biased toward older ages. The plot uses the same data set as Fig. 2.20, so the effect of outliers is removed.

age of the older three chronostratigraphic units combining all data is 162 ± 67 (1*s*) or 162 ± 134 (2*s*) ka. However, the revised data set of the $^{40}Ar/^{39}Ar$ age determinations, similar to the conventional K-Ar age determinations, shows a positive correlation between percentage radiogenic argon and age (Fig. 2.25). The $^{40}Ar/^{39}Ar$ data must, like the conventional K-Ar data set, provide only an estimated maximum age estimate for the older chronostratigraphic units.

Turrin (1992, pp. 226–235) reported preliminary results of step-heating data for selected samples of the Lathrop Wells centers. These results show increased abundance of radiogenic argon, and are less subject to bias toward older ages from the presence of excess argon or contamination. The preliminary results show promise for constraining more precisely the ages of the Lathrop Wells center. The revised ages of subunit Ql2a from the Lathrop Wells center are 104, 123, and 122 ka (Turrin et al. 1992). Insufficient information was presented to list the analytical errors associated with these measurements. However, Turrin et al. (1992) presented an isochron age of 107 ± 33 ka for unit Ql2a. These ages are younger than the conventional K-Ar and data of Turrin and Champion (1991) and Turrin et al. (1991) and support the interpretation that the latter age determinations are somewhat old because of excess argon. They overlap analytically with ages reported for the lavas of Ql2a obtained by the cosmogenic ^{3}He method.

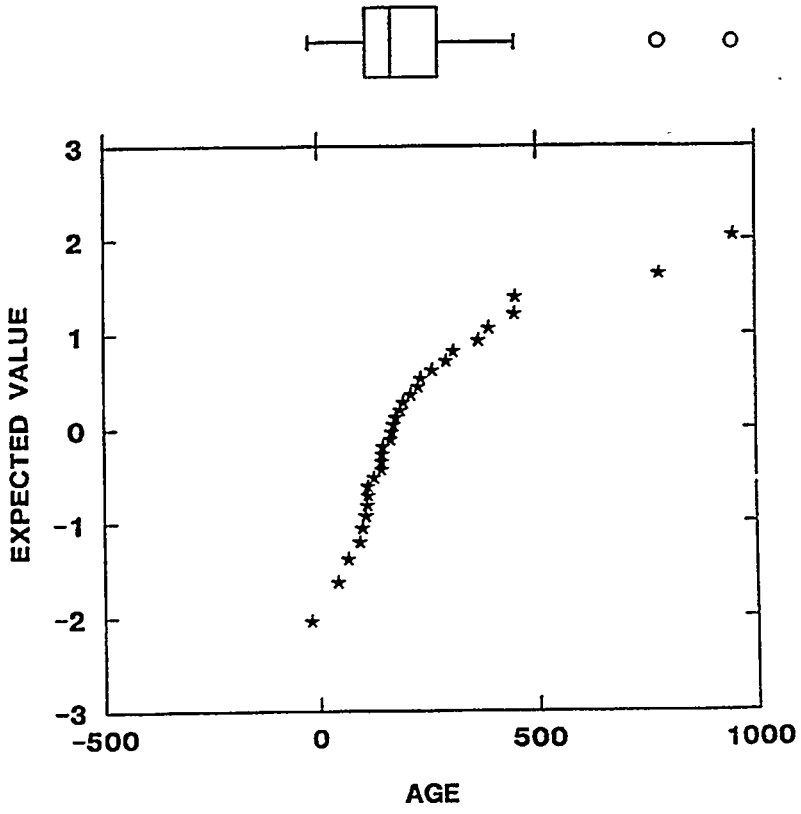


Fig. 2.23 Probability and box plots of the $^{39}Ar/^{40}Ar$ data of Turrin et al. (1991). The data show a nonlinear distribution on the probability plot indicating a nonGaussian distribution. The box diagram shows nonsymmetrical hinges and the presence of outliers and far outside outliers. The markings of the box diagram are the same as Fig. 2.20. The scale of the box diagram is the same as that of the x-axis of the probability plot.

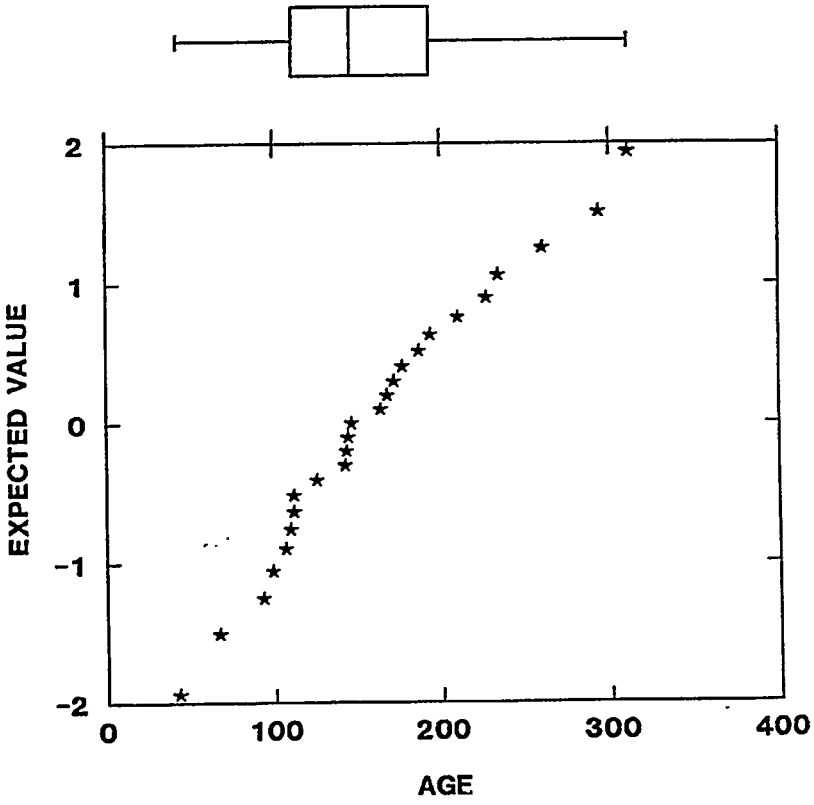


Fig. 2.24 Probability and box plots of the $^{39}Ar/^{40}Ar$ data set of Turrin et al. (1991) with outliers removed. The data show an improved distribution on both the probability and box plots but are still skewed toward older ages. The features of the box diagram are the same as Fig. 2.20. The scale of the box diagram is the same as that of the x-axis of the probability plot.

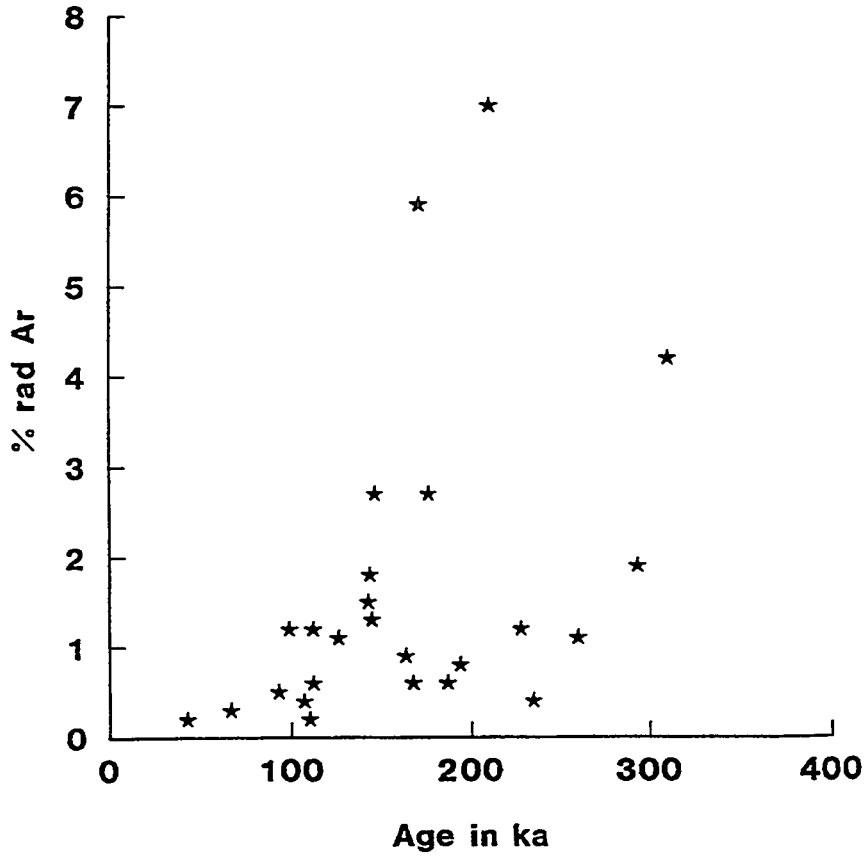


Fig. 2.25 Plot of percentage radiogenic argon versus age for the $^{40}Ar/^{39}Ar$ age determinations of Turrin et al. (1991). These data, like the conventional K-Ar age determinations, show a positive correlation between percentage radiogenic argon and age, suggesting the age determinations are biased toward older ages.

3. Summary. Conventional K-Ar and $^{40}Ar/^{39}Ar$ age determinations can be examined only for samples collected from combinations of chronostratigraphic units I, II, and III. The methods yield mean ages of about 137 ± 52 ka (1s) and 162 ± 67 ka (1s), respectively. Both methods are insufficiently precise to discriminate the ages of individual volcanic units. The presence of data outliers, the positively skewed data distribution, and the positive correlation between percentage radiogenic argon and age all suggest the age determinations are biased slightly toward older ages. The presence of excess argon in olivine phases (Poths and Crowe 1992) indicates that excess argon could be present in other phases, notably glass, which is a common groundmass constituent. An alternative source of the excess argon may be from incorporation of lithic fragments of Miocene tuff. These fragments show evidence megascopically of partial melting, and the excess argon introduced into the lava during partial melting may have had insufficient time to degas efficiently before solidification of the lavas. Concerns about the range of data and particularly the correlation between radiogenic argon and age suggest that the radiometric age determinations must be interpreted cautiously. At best they may be maximum ages. Although the age bias may not be large, it is complicated by combining radiometric ages from different chronostratigraphic units.

4. U-Th Disequilibrium Age Determinations. Mass spectrometric techniques were used to obtain ^{238}U-^{230}Th disequilibrium isochron ages for lavas from chronostratigraphic units I and III. Under appropriate conditions, this method can provide the crystallization age of the lava. A fundamental assumption of application of the U-Th disequilibrium method is a short residence time for the crystallized mineral assemblages both in storage and in ascent relative to the eruption age of the rocks. The small grain size and the absence of phenocrysts (only microphenocrysts) suggest this assumption has been met. Application of the U-Th disequilibrium method also requires measurable fractionation between the phases

that can be separated from the rock. We have been unable, despite considerable laboratory effort, to obtain phases with sufficient U-Th separation to produce high precision isochrons. The observed small degree of U-Th fractionation in measured phases appears to be a characteristic of the minerals themselves, not a reflection of poor physical separation of phases.

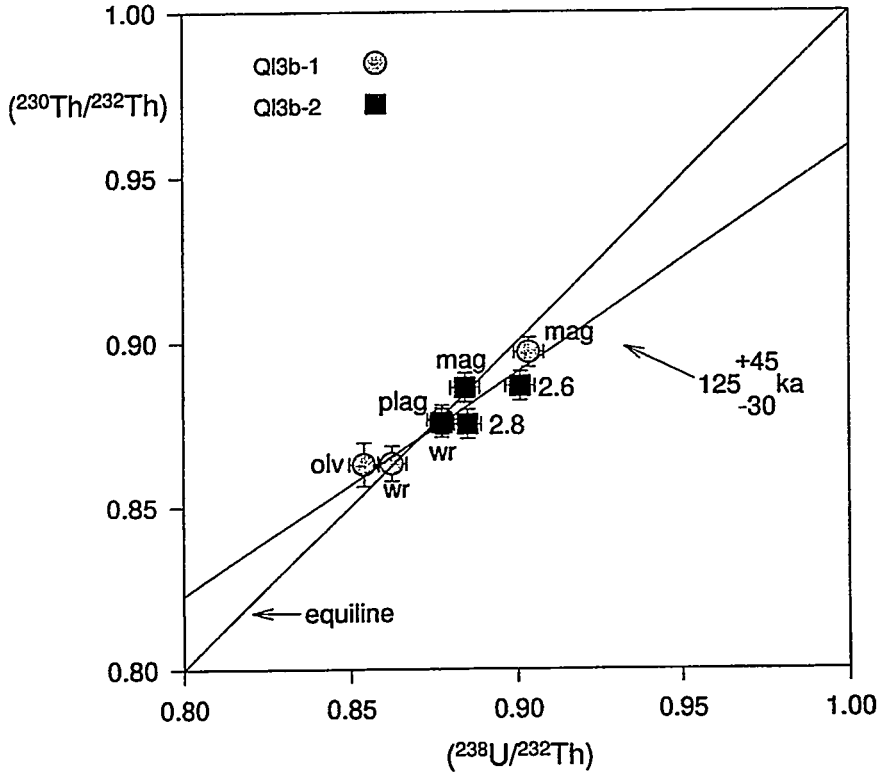


Fig. 2.26 U-Th isochron plot for the Ql3 lava.

Two attempts were made to obtain an isochron age for the Ql3 lava. The first measurement, made using solid source mass spectrometry, was 140 ± 40 (1 *s*) ka (Crowe et al. 1992). Additional attempts were made to obtain more refined separation of mineral phases using the same sample of the Ql3 lava. A second mass spectrometric measurement gave an isochron age of 125 + 45–30 (1 *s*) ka (Fig. 2.26). A larger spread in U/Th ratios was obtained for the Ql1d lava (Fig. 2.27). The isochron age of this sample is 135 + 20–15 (1 *s*) ka. The microphenocrystic olivine and plagioclase separates for the Ql1d isochron plot off the isochron in the direction of uranium enrichment (Fig. 2.27). Interactions between uranium-rich fluids and magma are commonly discussed in the literature and may provide an explanation for the points of Fig. 2.27 that plot off the isochron. However, examples similar to the plot of the Ql1d data have not been reported previously in the literature. The fine-grained phases of the sample appear to have been unaffected by the uranium enrichment and therefore may postdate the interaction with uranium-rich fluids. Electron microprobe data for the microphenocrysts and fine-grained phases of the sample may provide more information about the relationship among the analyzed phases used for the isochron of Fig. 2.27.

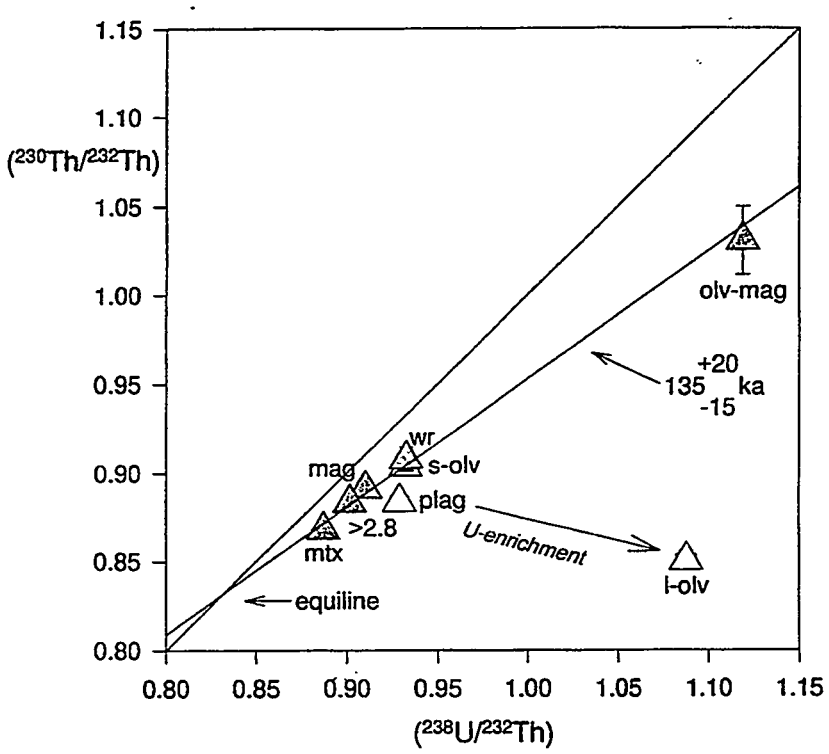


Fig. 2.27 U-Th isochron for the Ql1d lava.

Two lines of evidence support the reliability of the U-Th disequilibrium isochron ages: (1) the ages are internally consistent and reproducible for both replicate and separate samples of lava units, and (2) the ages are generally consistent with the results of the K-Ar ages of the lava units (Turrin et al. 1991; 1992). The weaknesses or inconsistencies of the isochron ages are twofold: (1) there is limited U/Th fractionation of analyzed phases in both sample sets and some evidence of complexity in the distribution of uranium in the analyzed phases of the Ql1d sample; and (2) field, stratigraphic, geomorphic, and chemical data suggest that the two lava units are from distinct volcanic events of probably different ages. This is perhaps best illustrated by the field relations of the lavas of chronostratigraphic units I and III. A Ql1c lava crops out about 0.4 km directly east of the analyzed Ql3 lava. The flow bottom is 10 m below the modern surface, and the flow top is covered by several meters of colluvial and eolian debris. The top of the Ql3 lava is 3 to 4 m above the modern surface. We conclude that there should be a measurable difference, using the U-Th disequilibrium method, in the ages of the analyzed lavas. Two explanations are possible for the similarity in measured ages. First, differences in the ages of the two lavas may be less than the analytical precision of the U-Th isochron ages (25 to 40 ka). Second, the U-Th isochron ages may be affected by other processes and may not record the eruption age of the volcanic events.

5. Cosmogenic Helium Surface Exposure Ages. We have estimated the ages of chronostratigraphic units at the Lathrop Wells volcanic center by measuring the accumulation of cosmogenic ^{3}He in samples collected from surface outcrops of subunits (Crowe et al. 1992, Poths and Crowe 1992). Multiple samples were collected from surface exposures on the Ql1a, Ql1b, Qlld, Ql2a, and Ql3 lavas. Collections of volcanic bombs were made from the summit and the flanks of the main scoria cone (Qs3), and scoria mounds of the Qs1d, Qs1b, and Qs1a subunits. The results of these measurements are reported in Table 2.4.

Lava samples were collected from primary lava flow surfaces with unrestricted exposure to the cosmic ray influx. Several tens of square meters of outcrop were inspected at each site in an attempt to identify unmodified surfaces. A variety of criteria were employed. Generally, we attempted to avoid areas of active sand accumulation. Samples were collected from aa spines that projected above the height of active sand deposition/movement to avoid samples with histories of surface cover. Primary surfaces could be identified by the presence of vesicular flow tops and irregular clinker surfaces. In some cases we were able to collect specimens with preservation of fragile surface flow textures. Areas of fractured rock were avoided where samples could spall, rotate, or change surface geometry. The degrees of rock varnish coatings were examined on the flow surfaces. Freshly exposed surfaces or surfaces with complex exposure history from processes of rock fracturing, spallation, or mechanical weathering could be identified by the contrasts in surface coatings of rock varnish. Generally, replicate samples yielded consistent ages for samples collected in small areas. Additionally, samples collected from related but spatially separate flows gave consistent results (Ql1a and Ql1b flows). The consistency in the ^{3}He ages suggests that careful collection of surface samples from lava flows can give reproducible results and the exposure history of lava samples to cosmic ray flux at these sites is not complicated. Marked differences in sample ages were noted for only one lava site and the main cone.

Samples collected from scoria cones, not unexpectedly, show more age variability than the lava samples, directly reflecting the erosional instability of the scoria surfaces. The most variable cosmogenic ^{3}He age measurements were obtained for the suite of samples collected from the main cone, the most geomorphically unstable feature in the center. The same effect was noted by Zreda et al. (1993) for ^{36}Cl ages of flow and scoria surfaces although they analyzed only a small number of replicate samples. Generally, ^{3}He ages collected from scoria deposits should be interpreted as minimum ages, and the best approximation of the emplacement age should be provided by the oldest helium exposure ages.

We collected one set of samples to test the assumptions of the cosmogenic ^{3}He surface exposure method for obtaining age determinations and to test independently the assumption of no unidentified inherited ^{3}He component. A sample was collected in the interior of the buried flow (Ql1c) exposed in trench LW-1. The flow was shielded from the surface by at least 5 m of debris. If all of the methods for obtaining surface exposure ages are correct and the sample was always shielded form cosmic rays, it should give a zero age. The measured age of the sample is 5.9 ± 2.3 ka for a lava from chronostratigraphic unit I that should be >100 ka and provides verification that the method assumptions for the cosmogenic ^{3}He method are reasonable. The non-zero age of the sample may result from penetration of the muon component of the cosmic ray flux to considerable depth.

There are two concerns with age determinations obtained by the cosmogenic ^{3}He method. The first is the possible varied surface exposure history of the dated material. Minimum ages will be obtained if there has been erosional removal of deposits originally covering the sampled surface. For example, field studies have shown that the deposits of chronostratigraphic unit I were covered by as much as 2.5 m of scoria-fall deposits. Resulting cosmogenic ^{3}He ages of these surfaces must be minimum ages. We attempt to minimize this effect by measuring samples from multiply correlated surfaces, and emphasize the oldest ages obtained from a suite of age determinations. If the ^{3}He ages are strongly biased toward younger ages, we should obtain a spread of ages for samples collected from multiple sample sites. The surfaces can be no younger than the oldest age determination. Second, the calibration of the ^{3}He surface production rates are still subject to debate and vary significantly with altitude and latitude. Most of the cited helium ages in the western United States are calibrated to one locality (Cerling 1990). The calibration of the ^{3}He production rate is undergoing refinements. Several workers have recently published calibrations in the 10–20 ka age range that are in good agreement (Cerling and Craig 1993; Laughlin et al. 1994). However, some caution is reasonable given that calibrations of production rates for rock units with ages > 20 ka are lacking in the

geologic literature. We cannot rule out the possibility that calibrations may be off as much as 30% (Poths and Crowe 1992) for rocks with ages of 100 ka.

Table 2.4. Cosmogenic ^{3}He Age Determinations for the Lathrop Wells Center.

Sample No.	Unit	Description	$^{3}He_c$	± [^{3}He]	Type	Prod Rate	Age	Error (1σ)
Chron Strat I								
Q6H-2-BMC	Qs1d	scoria mound	$1.69x10^{7}$	$1.5x10^{6}$	Bomb	221	76	7
LW89FVP1	Ql1a	Aa lava surface	$1.71x10^{7}$	$1.3x10^{6}$	Lava	215	87	7
LW89FVP2	Ql1a	Aa lava surface	$1.58x10^{7}$	$1.7x10^{6}$	Lava	215	81	9
Q5H-1BMC1	Ql1a	Aa lava surface	$1.52x10^{7}$	$1.5x10^{6}$	Lava	215	78	8
Q5H-1BMC2*	Ql1a	Aa lava surface	$1.82x10^{7}$	$1.2x10^{6}$	Lava	215	85	6
Q5H-2BMC1	Ql1a	Aa lava surface	$1.87x10^{7}$	$1.3x10^{6}$	Lava	215	87	6
Q5H-3BMC1	Ql1a	Aa lava surface	$1.77x10^{7}$	$1.0x10^{6}$	Lava	215	82	5
Q5H-4BMC1	Ql1a	Aa lava surface	$1.75x10^{7}$	$1.5x10^{6}$	Lava	215	81	7
Q5H-5BMC1	Ql1a	As lava surface	$1.83x10^{7}$	$1.1x10^{6}$	Lava	215	85	5
Q5BH-1FVP1	Ql1b	Aa lava surface	$1.90x10^{7}$	$1.7x10^{6}$	Lava	215	88	8
Q1H-1BMC	Qs1b	Mound bomb	$1.3x10^{7}$	$1.8x10^{6}$	Bomb	221	61	8
Chron Strat II								
Q3H-1FVP	Ql2a	As lava surface	$2.22x10^{7}$	$2.0x10^{6}$	Lava	222	100	9
LW4-2-91-1ABMC	Ql2a	Aa lava surface	$1.66x10^{7}$	$1.9x10^{6}$	Lava	222	82	9
LW4-2-91-3BMC1	Ql2a	Aa lava surface	$1.87x10^{7}$	$2.2x10^{6}$	Lava	222	92	11
LW4-2-91-3BMC2*	Ql2a	Aa lava surface	$1.87x10^{7}$	$1.3x10^{6}$	Lava	222	84	6
Q4H-1FVP	Ql2a	Aa lava surface	$1.83x10^{7}$	$1.0x10^{6}$	Lava	222	82	4
Chron Strat III								
QCS1-1BMC1	Qs3	Cone slope scrape	$8.4x10^{6}$	$1.1x10^{6}$	Scoria	243	35	4
LW86FVP1	Qs3	Summit bomb	$1.4x10^{7}$	$1.6x10^{6}$	Bomb	245	63	7
LW86FVPMag2*	Qs3	Summit bomb	$1.1x10^{7}$	$1.6x10^{6}$	Bomb	245	50	7
LW87FVP	Qs3	Summit bomb	$8.0x10^{6}$	$1.2x10^{6}$	Bomb	245	36	5
LW88FVP1	Qs3	Summit bomb	$6.9x10^{6}$	$1.3x10^{6}$	Bomb	245	31	6

Table 2.4 (Cont.)

Sample No.	Unit	Description	^3He_c	± [^{3}He]	Type	Prod Rate	Age	Error (1σ)
LW88FVP2*	Qs3	Summit bomb	$6.3x10^6$	$1.0x10^6$	Bomb	245	28	4
LW4-2-91-6BMC	Qs3	Cone slope bomb	$9.8x10^6$	$7.0x10^5$	Bomb	242	43	3
LW83FVP2	Ql3	As lava surface	$1.08x10^7$	$1.5x10^6$	Lava	222	54	7
LW83FVP1	Ql3	Aa lava surface	$1.36x10^7$	$1.2x10^6$	Lava	222	67	6
Shielded Samples								
LWQ1HA-FVP	Qs1u	Mound bomb	1.0x106	$7.8x10^5$	Shielded	221	4.8	3.5
Q7H-1AFVP	Ql1c	lava flow interior	1.3x106	$5.0x10^5$	Shielded	222	5.9	2.3
Summary Statistics								
Chron Strat I	Mean	81 ka	Std Dev	8	n = 10			
Chron Strat II	Mean	88 ka	Std Dev	8	n = 4			
Chron Strat III	Mean	41 ka	Std Dev	11	n = 11			

* duplicate samples

The oldest age obtained by the cosmogenic ^{3}He method provides a preferred estimate of the ^{3}He age of the chronostratigraphic units of the Lathrop Wells center. Mean values of replicate measurements are not valid estimates of the age of units. However, comparison of mean values can aid in interpreting the data. The mean value of replicate measurements is 81 ± 8 ka (chronostratigraphic unit I), 88 ± 8 ka (chronostratigraphic unit II), and 41 ± 11 ka (chronostratigraphic unit III). The most variable measurements, as expected are for the scoria units of chronostratigraphic unit III. One obvious observation from Table 2.4 is an older mean age of chronostratigraphic unit II compared to chronostratigraphic unit I. However, this difference is can be explained readily from the field relations of the volcanic units. First, large-volume scoria-fall deposits were erupted during the evolution of chronostratigraphic unit II. Scoria-fall deposits more than 2 m thick covered and shielded outcrops of chronostratigraphic unit I near the main scoria cone. Second, the Lathrop flow overlies the pyroclastic-surge deposits of chronostratigraphic unit II. It therefore was emplaced after eruption of the largest volume of the scoria-fall deposits. Third, the Lathrop flow, where the majority of samples were collected for cosmogenic ^{3}He age determinations, is located east of the northwest-trending elliptical dispersal axis of the scoria-fall deposits. These field relations strongly suggest that the similarity in cosmogenic ^{3}He ages of chronostratigraphic units I and II were produced by shielding of the surfaces of chronostratigraphic unit I by scoria-fall deposits of chronostratigraphic unit II. This is further demonstrated by Fig. 2.28, a plot of the south part of the Lathrop Wells center showing the minimum thickness of the Qs2fs deposits and the cosmogenic ^{3}He ages of lava surfaces from chronostratigraphic unit I. The measured thickness of the scoria-fall deposits is a minimum thickness, as noted above, because the upper surface of the unit is an erosional surface. Thickness measurements show that the lava flows of chronostratigraphic unit I must have been covered by more than 2 m of scoria-fall deposits. Moreover, the thickness of the fall deposits near the cone flanks probably exceeded 3 m. The measured cosmogenic ^{3}He ages for deposits of chronostratigraphic unit I decrease systematically with

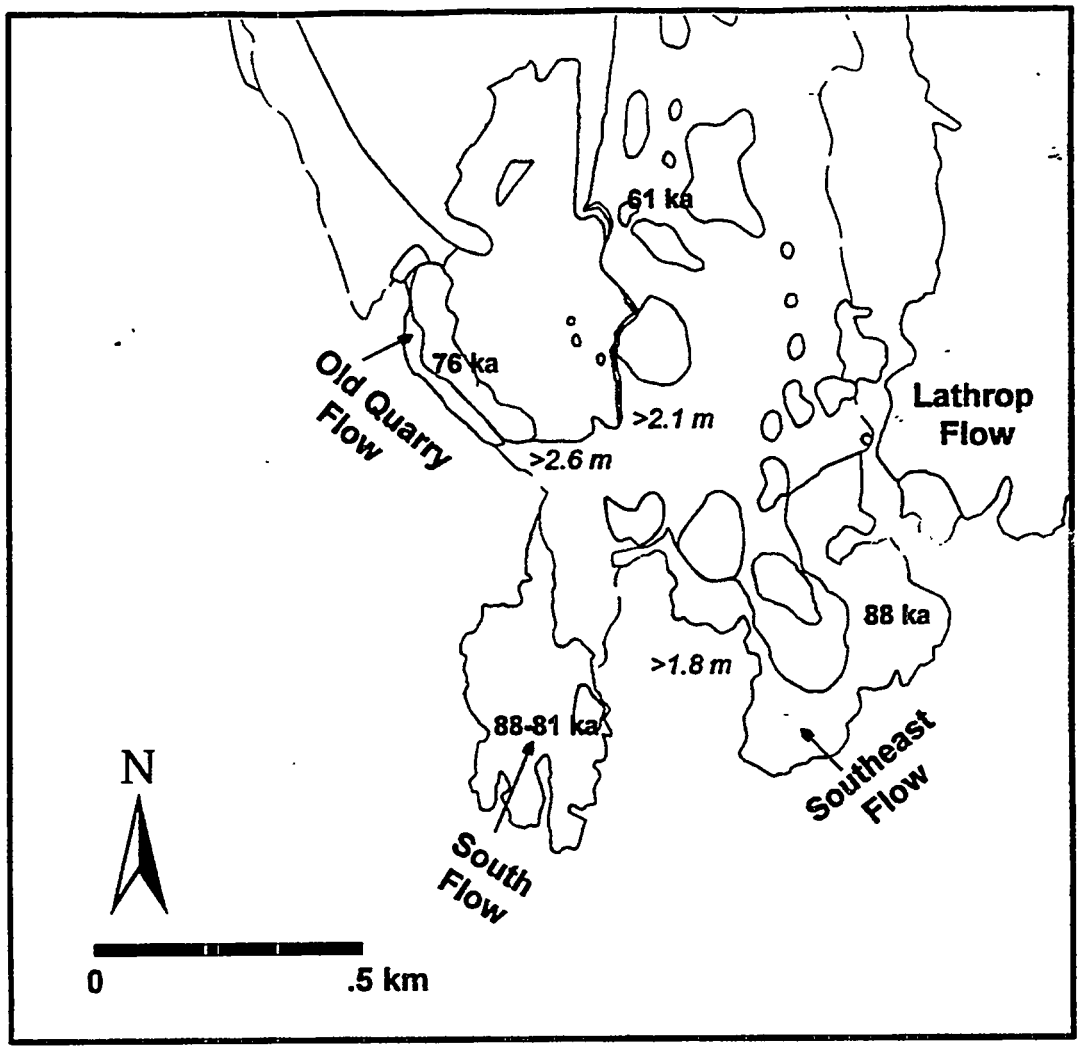


Fig. 2.28 Cosmogenic ^{3}He ages of chronostratigraphic unit I plotted with minimum estimated thickness of scoria-fall deposits of chronostratigraphic unit II. The thicknesses of scoria-fall deposits were measured in trenches cut with a 4 x 4, truck-mounted backhoe. The sites listed are localities where the base of the fall deposits could be located, and most of the section of fall-deposits are exposed. The top of the fall-deposits is moderately to deeply eroded. All thickness is therefore a minimum. Reconstruction of the preserved thickness shows that all sites where cosmogenic ^{3}He ages were measured were covered by at least 2 m of scoria-fall deposits. The effect of this cover is shown by the distribution of the surface exposure ages. They decrease in age with decreasing distance from the main cone.

decreased distance from the area of the main cone, the inferred source of the voluminous scoria-fall deposits (Fig. 2.28). This provides confirmation that the measured cosmogenic ages (^{3}He and ^{36}Cl) (Zreda et al. 1993) of chronostratigraphic unit I are minimum ages.

Corrections of the cosmogenic ^{3}He ages could possibly be estimated by calculating the cosmogenic ray shielding produced by the variable thicknesses of scoria for the individual sample localities. While this is possible in principle, the assumptions required for the estimations do not give reasonable constraints on the ages of deposits of chronostratigraphic unit I. Age corrections can be estimated according to the formula:

$Ea = Se + (Pc\ depth/Pc\ surface \times Tb)$

where *Ea* is the measured cosmogenic ^{3}He age, *Pc depth* is the ^{3}He cosmogenic production rate at depth x, where x is given in cm below the surface, *Pc surface* is the ^{3}He cosmogenic production rate at the surface, and *Tb* is the time buried at depth *x*. The ratio of *Pc depth/Pc surface* can be readily calculated assuming a bulk density of scoria deposits of 1.6 g/cm^3 and an attenuation length of 179 g/cm^2. The *Se* can be only approximated since it is a sum of two components: (1) the interval following the eruption of chronostratigraphic unit I and preceding eruption of chronostratigraphic unit II, and (2) the interval after erosional exposure of the dated lava surface. The best estimate of the first component is about 45 ka, but this presumes an estimate of the age of chronostratigraphic unit I, the information we are attempting to obtain by the corrected calculation. The *Tb* cannot be estimated because it is dependent on rates of erosion that must be climate-dependent and, therefore, varied considerably during the last 100 ka. Assuming a 2 m initial depth of burial and substituting this minimum depth in the equation shows that dated surfaces cannot be buried very long and still give the measured ages of Fig. 2.28. The scoria must have been stripped rapidly in comparison to the age of the surface. One perplexing observation, however, is the uniformity of measured ages for replicate samples collected from the south lava flow surface. These samples were collected from aa flow spines that projected variable distances (0.1 to 0.5 m) above the general flow surface. The observed uniformity of measured ages for the samples requires that the scoria was stripped both uniformly and rapidly. All assumptions concerning the measured cosmogenic ^{3}He ages of chronostratigraphic unit I, however require them to be minimum ages.

A secondary finding from studies of the noble gas components of the lavas of the Lathrop Wells center is the presence of excess ^{40}Ar released by crushing olivine (Poths and Crowe 1992). Crushing of olivine grains released an argon component with ^{40}Ar/^{36}Ar ratios of 371 ± 8 and 328 ± 7 for the olivine in the Ql3 and the Ql2a lavas. These ratios are substantially above the atmospheric ratio of 295 and indicate the presence of ^{40}Ar in excess of that produced by decay of ^{40}K. Age determinations based on the ^{40}Ar/^{39}Ar system require careful evaluation for the potential effects of excess argon.

6. Thermoluminescence Age Determinations. Seven analyses of four different samples have been obtained using the TL method. These results are judged to be analytically reliable and reproducible but must be viewed as preliminary. The TL method has not been used previously in attempts to date soil units for a volcanic center. Analytical methods used for this method are described in Crowe et al. (1992).

Three samples were collected from a buried soil separating the upper tephra deposits of the main cone in the south quarry wall and tephra of chronostratigraphic unit IV. These samples yielded TL ages of 8.9 ± 0.7, 9.9 ± 0.7, and 8.7 ± 1.0 ka (Crowe et al. 1992). Soil units within and above the scoria-fall deposits of chronostratigraphic unit IV (Wells et al. 1990) yielded ages of 3.7 ± 0.4, 3.7 ± 0.4, and 4.5 ± 0.4 ka. Important features of these TL ages are that the replicate analyses are reproducible and that the data are in correct stratigraphic sequence. They provide the only numerical age constraints on the youngest eruptions of the center. The TL ages of soil units overlying the tephra deposits constrain the age of pedogenic processes that post-date volcanic activity.

A second set of TL samples was collected from reworked, volcaniclastic deposits. These deposits were exposed several tens of centimeters from the basal contact of an overlying aa flow lobe of Ql2. These samples yielded an age of 24.5 ± 2.5 ka (Crowe et al. 1992). Resampling and analyses of a second sample yielded a preliminary age estimate of 30 ka. Thus, reproducible TL ages of the Ql2 lava unit are significantly younger than the results of other chronology methods. We currently have no reasonable explanation for the age discrepancy.

7. Geomorphic Studies. Geomorphic features of the Lathrop Wells volcanic center were described previously by Wells et al. (1990). They equated the geomorphic and pedogenic features of the Lathrop Wells center with a 15 to 20 ka cone in the Cima volcanic field. The close comparison of the centers suggested, by inference, that the youngest eruption of the Lathrop Wells center is no older than 20 ka. These constraints are based on the assumption that the rates of operation of erosion and soil formation are approximately similar between the Cima and Crater Flat volcanic fields. New cosmogenic ^{3}He and TL ages for the Black Tank center in the Cima volcanic field provide increased support for the geomorphic correlation (Crowe et al. 1992). These data support an age between 9 and 14 ka for the main cone sequences at the Black Tank center. Trenching has demonstrated that the base of the main scoria cone at Lathrop Wells is flanked by an eolian sand-ramp deposit which displays little evidence of mass wasting or colluviation from the cone slopes, supporting the inference that the cone slope is virtually unmodified by erosional processes (Wells et al. 1990).

Preliminary mapping has been completed of the surficial geology of the Lathrop Wells volcanic center and immediately surrounding areas. The purpose of the mapping is to show the geologic context of the volcanic center with respect to surficial deposits and landforms that surround, underlie, and overlie the volcanic units of the center. Three major types of surficial deposits and features have been mapped: those associated with (1) volcanic landform development (constructional volcanic features) and the modification of the landforms, (2) eolian erosion and deposition, and (3) fluvial and colluvial processes. Initial observations from the geologic mapping include the following:

1. Garland development (eruption-induced mass movement deposits) is primarily limited to the northern and western flanks of the main scoria cone. Weakly developed rills occur near the cone summit on the southwestern and eastern flanks of the main cone.

2. Large-scale eolian landforms including transverse dunes, coppice dunes, and eolian wind streaks occur primarily on the Ql2a lava flow; older lava flows are mantled by scoria-fall deposits and eolian sand mantles.

3. The scoria-fall deposits of Qs2fs have been extensively modified by erosional and depositional processes. These deposits are locally interbedded with alluvial units.

4. The volcanic units at the Lathrop Wells center appear to have the following landscape/stratigraphic relations with alluvial fan and stream deposits:
   a. all volcanic units are inset below and possibly are older than alluvial fan units.
   b. the main scoria-fall sheet is interbedded with and underlies alluvial fan deposits.
   c. younger alluvial units are inset into or overlie the youngest volcanic units.

The significance of the field and geomorphic observations can be related to the models of landscape evolution which have been developed for desert basins of the western U.S. Time-transgressive changes from Pleistocene-dominant climatic regimes to those of the Holocene yield significant changes in the vegetation and consequently the response of alluvial systems. Specifically, this transition is marked by destabilization of hill slopes with vegetation reduction, movement of sediment from hill slopes into streams, and the deposition of alluvial fan units. It is hypothesized that an alluvial unit designated as Qf1 may be late Pleistocene/early Holocene alluvial fan deposits which have been recognized so widely in this region. If so, the scoria-fall sheet and associated pyroclastic-surge deposits (Qs2fs), which are stratigraphically beneath unit Qf1, should correspond to the late Pleistocene (<30 ka) and not to the late-middle Pleistocene (>70 ka but <140 ka).

The systematic differences in degree of erosion of volcanic landforms between chronostratigraphic units I, II, and III suggest a time difference between the units. The most compelling argument for this time difference is provided by exposures located directly north of the main cone. Here the degraded surface formed on the Qs1c scoria deposits can be traced beneath the virtually unmodified cone slope of Qs3. Similarly, there is a marked contrast between the degree of erosional modification of the Qs2fs surfaces compared to the main cone slopes (Qs3). These relations appear difficult to explain without a time gap between the respective units.

Two tephra units have been recognized in outcrops located about 2–3 km north and northwest between the Lathrop Wells center. Several features of the tephra demonstrate a significant difference in age between the two deposits. There are marked differences in the amount of calcium carbonate cementation and the relations of the units to the local landscape and stratigraphy. The older, cemented scoria shows clast displacement by calcium carbonate plasma and locally is within a channel bottom that lies below an alluvial fan unit with moderately well-developed soil. The younger tephra unit is uncemented, lies stratigraphically above the cemented scoria, is concordant with the slopes of the present landscape, and is overlain by alluvial fan deposits with a weakly developed soil profile.

8. Soil Studies. Study of soils on volcanic landforms associated with the Lathrop Wells center shows that weakly developed calcic soils have formed in scoria deposits that flank the north and south side of the main cone and on the cone slope (Wells et al. 1990). The surface of the lava flows is almost completely mantled by eolian deposits or by pyroclastic deposits. These deposits have only incipient soil development in the upper several decimeters. The primary pedogenic features exhibited by the soils include weakly developed "vesicular A" horizons and weakly developed B horizons in which fine sands, silt, clay, calcium carbonate, and trace amounts of soluble salts have accumulated. The presence of substantial amounts of quartz and other pedogenic materials (calcium carbonate and sulfates or chloride salts) that are rare or absent in the basaltic tephra unequivocally demonstrates the eolian origin of most of these pedogenic materials.

The most strongly developed soils have been observed on the erosional surface cut into scoria mound deposits of Qs1c located northeast of the main cone. These soils have the thickest, most well-developed vesicular A horizons in soil observed to date, ranging from 5 to 8 cm thick and possessing strong, coarse, platy structure with subordinate subangular blocky to prismatic structure. The subjacent Bwk horizons are approximately 8 to 17 cm thick with subangular to blocky structure. These horizons do not, however, exhibit color hues or chromas substantially redder than those of the least-altered loamy sandy parent materials or the most recently accumulated materials above the vesicular A horizon. Pedogenesis in the lowest 1 m of the profile exposed in pits is characterized by the accumulation of moderately thick to thin, largely discontinuous coatings of carbonate, gypsum, and soluble salts. A small amount of pedogenic silica may also have accumulated. The content of these materials diminishes progressively with depth with the most incipient coatings being observed at depths of 1.3 to 1.5 m in the parent scoria materials. A soil observed on the steeper part of the cone slope has a similarly thick, calcareous B horizon, but lacks the well-developed vesicular A horizon.

Soil observed in the sequence of buried scoria units exposed in the quarry on the south side of the center (Wells et al. 1990) is more weakly developed. It exhibits 2 to 4 cm thick vesicular horizons and very incipient, calcareous cambic B horizons. The scoria parent materials have carbonates, salts, and perhaps silica accumulated primarily on the bottoms of scoria fragments.

In contrast, soil formed in sand ramps that flank the cone is very weakly developed. Pedogenesis is indicated primarily by slight increases in disseminated carbonate with depth and accumulation of very thin,

discontinuous coatings of carbonates and perhaps salts on the bottoms of many of the larger coarse fragments. Scoria fragments in such deposits commonly exhibit thicker and nearly continuous coatings of carbonate. However, the nonsystematic spatial location of the coatings on the fragments as a function of depth shows that only a minor volume of material has been derived from higher positions on the cone slope by gravitational forces. Soil on the cone slope, as noted previously, has Bk horizons with carbonate-coated fragments, which provide a source for most of the fragments with thick carbonate coatings observed in the sand ramp deposits and distal cone-slope sediments and soils.

The medium- and fine-grained sandy deposits of eolian origin are inferred to bury previously formed vesicular horizons of soils in the scoria deposits. These deposits range from 2 cm to over 1.3 m thick in the sand ramps. They are present below the weakly developed scoria pavement and have little or no soil development. These soil/stratigraphic relations suggest an increase in eolian activity during the late Holocene, resulting in the deposition of locally thick accumulations of sand. Subsequent to deposition of the sand, geomorphic conditions were presumably sufficiently different to enable the development of cumulic soils. These soils incorporated much finer-grained desert loess and formed accretionary cambic B and vesicular A horizons.

Soils formed in scoria deposits or in aprons that flank flows at the Cima volcanic field have also been examined (Wells et al. 1985; Renault 1989; Royek 1991). These soils are generally similar to soil on the flow surfaces. However, the soils formed in scoria deposits associated with the youngest scoria cones in the Cima volcanic field possess relatively weak development of Avk horizons. Their B horizons are not as red or thick as those typically observed in the phase 1 soils on associated lavas. This indicates that much of the eolian material entrapped on surfaces associated with scoria is readily translocated through the highly permeable, open framework scoria to depths of more than a meter by infiltrating soil water. In the lower part of the soil profiles, the initially fragile, glass-coated irregularities and edges of scoria fragments are altered by infiltrating water, as shown by the presence of reddish-brown coatings on the tops of the fragments, the destruction of vesicle edges and spines, and the chemical alteration of glass. Pedogenic accumulation of calcium carbonate, salts, and perhaps some amorphous silica primarily on the bottoms of the fragments is a major attribute of these soils. Soil development in cone aprons resembles that observed on flows. Similarly, soil development on scoria-cone aprons of older cones resembles observed phase 2 soils, demonstrating the primary role of cumulic pedogenesis on this volcanic landform.

Crowe et al. (1992) compared the development of soils on volcanic units of the Lathrop Wells volcanic center with studied centers of the Cima volcanic field (Dohrenwend et al. 1986; Wells et al. 1990). They did not propose that pedogenic processes at the Lathrop Wells center are identical to those at the Cima volcanic field. However, they did note that there are no indications that the rates or processes of soil formation are substantially different. If eolian influx had been higher at the Lathrop Wells center, thick deposits of desert loess would have mantled stable Pleistocene and Holocene landforms and soils throughout the area. This has not been observed. Equally, eolian activity in the YMR cannot be substantially lower than the Cima volcanic field because of the presence, in the former, of active sand dunes on flows and the nearby dune field (Big Dune) in the Amargosa Valley. Abundant sources of eolian materials, including desert loess, are provided by the adjacent basins, many of which contain large playas. Accordingly, we conclude that the weakly developed soils of the Lathrop Wells center closely resemble the Holocene soils in the Silver Lake area and the Cima volcanic field. We infer that the soils must have formed over a similar time span, the soil on the volcanic units of the Lathrop Wells center having formed over a period spanning the late Pleistocene and Holocene.

Soil development on chronostratigraphic unit III appeared initially to be inconsistent with K-Ar and U-Th age determinations for the lava flows of greater than 100 ka (Wells et al. 1990). Instead, the degree

of soil development is more consistent with the cosmogenic ^{3}He age determinations that indicate the lava flow sequences could be <100 ka. However, several factors may have affected the degree of soil development on the deposits of chronostratigraphic unit I. First, studies of volcanic surfaces in the Cima volcanic field show that soil development may be retarded on rubbly aa flows compared with pahoehoe flows. The fragmental nature of the aa flow surfaces and resulting high porosity enable repeated deep flushing of eolian materials to depths of several meters. This may prohibit development of an increasingly less permeable surface mantle in which well developed cumulic soils (and stone pavements) can form. Second, there are local indicators of greater soil development or pedogenesis on some of the lavas of chronostratigraphic unit I. Trench exposures show locally the development of laminated calcite zones in buried soil and carbonate-coated fractures and joint surfaces in greater thickness and continuity than expected given the weak development of surface soils. Third, intermittent surface cover by active dunes has occurred on many of the lava and scoria surfaces of the Lathrop Wells volcanic center. Deposition of a sand mantle has profoundly influenced soil development. Where the sand deposits are deep, the development of soils has been terminated. Where sand deposits are thinner, there has been an accelerated rate of development of cumulic horizons. Fourth, the scoria mounds of chronostratigraphic unit I are not stable landforms where parent materials conducive to soil formation are preserved. The evidence of erosional modification of the scoria mounds (exposed feeder dikes, nonprimary [volcanic] surface forms; lag accumulations of bombs) indicates that the summits and slopes of the mounds are not stable surfaces. Finally, there has been insufficient trenching of chronostratigraphic unit I to provide thorough documentation of the maximum development of soils. It is premature and outside the scope of completed soil studies to conclude that soil development is inconsistent with geochronology data suggestive of ages of >100 ka for some volcanic units. The major emphasis of work to date has been on the geomorphology and development of soils on the youngest units of the volcanic center (Wells et al. 1990, 1991).

The differences in the degree of soil development between chronostratigraphic units I and II and chronostratigraphic unit III are consistent with a time gap between the units. However, it is difficult and unwarranted to speculate on the extent of the time differences between the units. The unmodified geomorphic form and weak degree of horizon development in soil on the Qs3 deposits (Wells et al. 1990) are consistent with an age of <50 ka. This unit has been sufficiently well studied to conclude that the limited development of horizons in soils and unmodified geomorphic form is inconsistent with an age of the cone of >100 ka (compare with Turrin et al. 1991).

9. Paleomagnetic Studies. Considerable paleomagnetic data have been obtained for the Lathrop Wells volcanic center to test inferred age differences of different eruptive events (Fig. 2.29, Table 2.5). Turrin et al. (1991) report that the paleomagnetic data from the volcanic rocks fall into two statistically distinguishable populations. They correlated the populations with their revised definitions of units Qs5 and Ql3. Champion (1991) and Turrin et al. (1991) interpreted the angular difference between the means of the two field magnetic populations to indicate an age difference between the two events of only about 100 years. We note however, that the geologic unit Qs5 defined by Turrin et al. (1991) includes subunits of chronostratigraphic units I, II, and III as defined in this report. Specifically, our subunit Qs3 (one of the younger subunits) was included in the paleomagnetic data used to define a magnetization characteristic of their map unit Qs5. Additionally, not all volcanic subunits of the Lathrop Wells center were sampled in their paleomagnetic studies (Wells et al. 1992). The conclusions regarding the paleomagnetic data of Turrin et al. (1991) are premature, at best, because of inconsistent stratigraphic assignment of volcanic units and the incompletely reported paleomagnetic data set. We have attempted to augment the paleomagnetic data set for the Lathrop Wells volcanic center of Champion (1991) and Turrin et al. (1991) for two reasons. First, as noted above, not all units were sampled for paleomagnetic studies. Unsampled

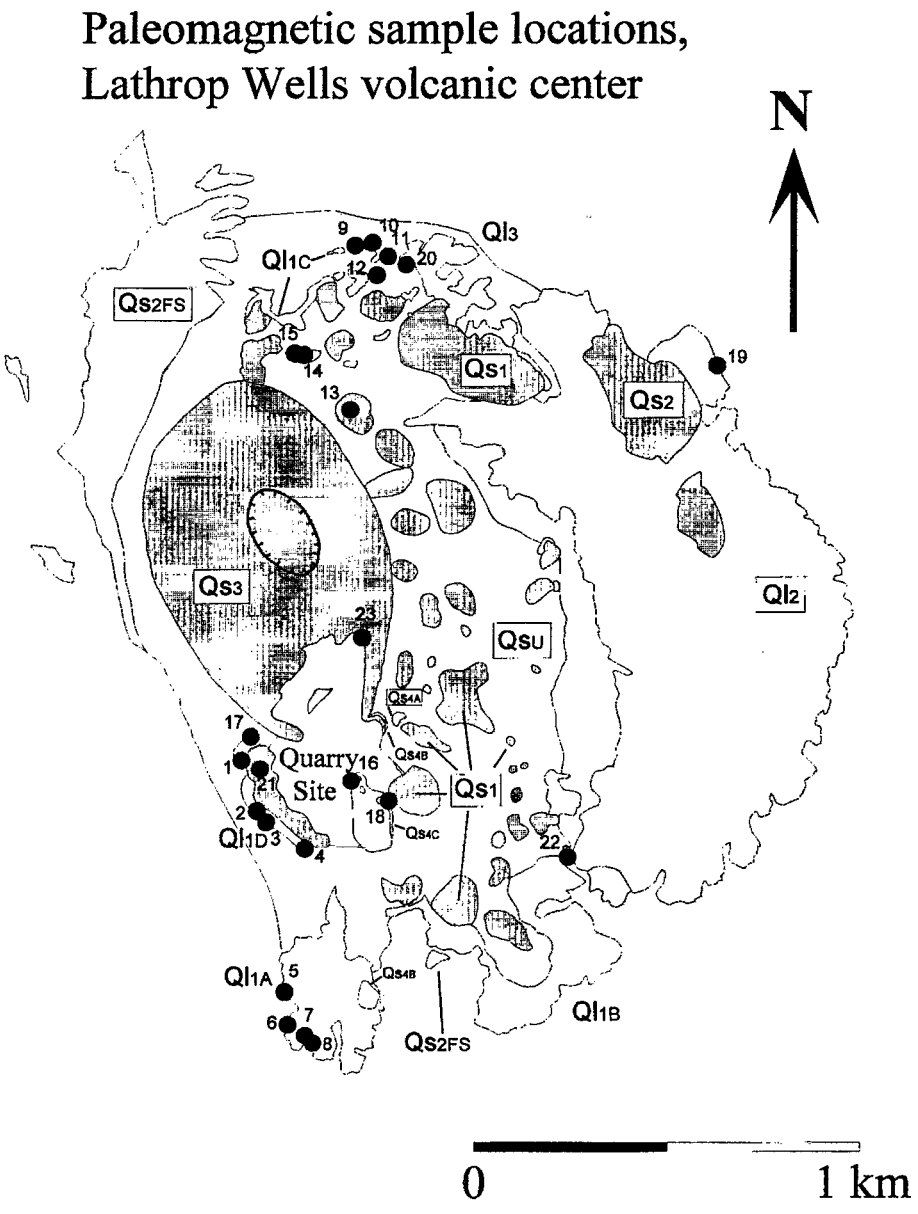


Fig. 2.29 Locations of the 23 paleomagnetic sampling sites at the Lathrop Wells volcanic center

and unstudied units from their studies include Ql1d, Qs1d, Ql1c, Qs1c, and the Qs1b/Ql1b lava flows. This omission includes the major lava subunits of the oldest volcanic units. Second, previously conducted paleomagnetic studies of the Lathrop Wells center were not completed under an approved Quality Assurance program. Although the data may be of good quality analytically, they cannot be used directly for licensing in the YMP. We have sampled and analyzed new paleomagnetic sites and have attempted to qualify, by comparison, much of the previously obtained paleomagnetic data.

Table 2.5 Paleomagnetic data for the Lathrop Wells Volcanic Center.

Site [Sample]	Rock Type, ID	n/N/No	Decl.	Incl.	α95	k	α951-3	α951-2	k1-3	k1-2	Azimuth	VGP Lat	VGP Long	Comments
LW1	Flow, Ql1d	9/9/09	2.7	53.5	5.4	93.2	2.3	6	-201.9	-31.1	81.3			
LW2	Flow, Ql1d	9/9/09	13.8	53.3	3.5	210.9	2.2	3.6	-216.4	-82.9	145.4			
LW3	Flow, Ql1d, out of place													
LW4	Flow, Ql1d, out of place													
LW5	Flow, Ql1a	8/8/11	18.5	53.6	7.1	62.3	4.4	7	-63.2	-26.1	132.8			
LW6	Flow, Ql1a, out of place													
LW7	Flow, Ql1a	10/10/12	346.3	53.8	5.3	83.8	3.6	5.4	-75.9	-34.9	179.3			
LW8	Flow, Ql1a	6/6/08	358.3	45.3	5.5	147.9	3.6	4.9	-127.9	-69	106			
LW9	Buried Flow, Ql1c	10/10/10	350.8	42.1	7.5	42.9	2.8	8.7	-131.5	-14.1	30.5			
LW10	Buried Flow, Ql1c	7/7/10	17.1	52.2	6.6	85.2	2.6	7.1	-211.4	-29	66.2			
LW11	Flow Ql1c, trench	11/11/16	11.2	46.9	2.4	359.2	1.6	2.6	-370.5	-136.4	94.4			
LW12	Flow Ql1c, trench	9/9/13	6.8	54.6	5.1	102.3	2.1	5.8	-247.5	-33.5	126.9			
LW13	Scoria Mound, Qs2u		**Spec.Decl.**	**Spec.Incl**	**MAD**	**Circle**	**Circle**	**MAD**						
A			29.1	45.6	3.8									
B			22.4	55.4	3.7									
C			6.4	61.1	1.9									
D			323.2	64.5	7.1									
E			7	54.9	6.4									
F			6.3	55.3	3.3									
G			24.3	49.9	2.8									
H			303.7	51.2	2.2									
I			352.3	56	5.3									
J			6.2	49.2	4.8									
K														
L			353.1	57.4	1.3									
M			9	61.3	8.4									
N			8	59.1	6.5									
O														
P			5.1	58.4	6									
total	Scoria Mound, Qs2u	12/12/12	2.8	57.7	6.8	34.8	2.2	8.3	-147.1	-11.2	111.6	87.8	-36.9	
LW14	Scoria Mound, Qs1u		**Spec.Decl.**	**Spec. Decl.**	**MAD**	**Circle**	**Circle**	**MAD**						
A			356.6	42.1	1.4									
B														
C			11.2	39.4	5.5									
D			353.6	46.8	2.5									
E			277.8	-6.7	11.7									plane
E			2.6	36.6	4.8									
F														
G			355.7	45.5	2.7									
H														
I														
J			5	55.1	3.3									
K			4.1	55.7	2.6									
L			9.5	49.8	4.1									
M														
N			2	52.4	1.3									
O														
P														
Q														
R			354.6	33.5	2.5									
S			10	54.4	0.8									
total		11/11/11	2	46.7	5.1	81.8	2.9	5.6	-108.4	-29.4	16.3	79.8	53.2	
LW15	Dike, Qs1u	10/10/10	2.2	52.2	3.1	364.9	2.3	2.8	-254.3	-184.6	20.7			
LW16	Plug, Ql1u	10/10/10	3.6	52.2	1.2	935	0.9	1.3	-675.8	-400.4	33.3			
LW17	Flow, Ql1d	10/10/10	355	52	3.8	128.6	2	4.4	-197.7	-43.7	61.3			

LW18	Plug, Ql1u	10/10/10	6.8	53.7	4.1	142.1	2.6	5.8	-239	-48.5	117.4			
LW19	Flow, Ql2	10/10/10	6.3	52.5	2.9	307.7	1.7	3.1	-372.8	-114.4	65.8			
LW20	Flow, Ql3	10/10/10	352.9	53.6	5.2	215.5	2	5	-474.9	-79.8	103.8			
LW21	Ql1d, Rubble		**Spec. Decl**	**Spec. Incl.**	**MAD**	**Circle**	**Circle**	**MAD**						
A			343.6	39.5	4.2									
B			74	34.9	3.8	326.6	20.7	14.9						
C			95.5	61.5	4.6									
D			87.5	57.9	2.3									
E			75	54.8	4.1									
F			95.2	59.2	3.1									
G			101.2	59.4	5.6									
H			204	30	4.4									
I														
J			112	25.4	4.8									
K														
L			121	27.7	7.5	220.7	19.3	7.4						
M			77.1	35.2	8.5									
N														
O			103	60	10.2									
P			92.9	60.1	8.2									
total		10/10/14	93.9	48.9	11.4	18.9	8.3	11.3	-16.2	-9.1	143	15	-53.3	Combined I/p: 95.0,52.6, 8.5,10.6
LW22	Plug, Ql1u	10/10/10	2.8	53.6	1.8	937.9	1	1.9	-1192.3	-349	173.2			
LW23	Main Cone, Qs3		**Spec. Decl**	**Spec. Incl.**	**MAD**	**Circle**	**Circle**	**MAD**						
A			342.8	53.2	6.78	134.5	-66.7	15.3						
B			128.1	-23.5	3.4	193.3	39.9	19.3						
C			15.1	13.2	4.7	94.1	-30.1	21.2						
D			113.7	-16.9	2.7									
E														
F			120.1	4.9	2.1	208	-20.5	14.6						
G			384.4	1.9	2.5									
H			204.3	-45.2	2.3	350	-33.5	8.7						
I			7.7	-56.7	7.2	64.6	-14.8	3.1						
J						169.4	76.6	18						
K			223	23.6	4.3									
L														
M			194	-5	4.1									
N														
O			19	59.2	1.1	173.2	-9.5	9						
P			16.4	-47.2	3.8	284.6	-2.8	1.8						
Q			92.3	12.3		16.3	-48.9	3.8						
R														
S														
T			348.4	51.8	4.6	348.8	-48.6	15.4						
U														
V														
W			192.5	55.7	4.4	316	18.8	12.5						
X														
Y			179.1	14	4.1	89.6	-12.1	4.3						
Z			16.4	63.9	8.5									
AA			13.7	19.6	4.9	125.8	48.3	13.2						
BB														
CC														
DD			9.5	50.8	3.8	146.6	29	8						
total			26.1	58.2	36.9	1.6	19.9	20.8	-2.6	-2.4	131.7	78.7	57.1	Combined I/p: 10.5, 49.9

Ten paleomagnetic sites were sampled for paleomagnetic studies at the Lathrop Wells center in 1991. Each sampling site consisted of eight to twelve independently oriented samples, collected as cylinders using a portable drilling apparatus. Individual sample sites were collected over an area of several cubic meters. Four sites were located in the Ql1d lavas, four in the Ql1a lavas, and two in the Ql1c lava on the north flank of the main cone (Fig. 2.29). At least one specimen per site has been subjected to progressive alternating field demagnetization, the technique most commonly used to assess the direction and relative intensity of all components of magnetization in magnetite-bearing rocks. In most cases a well-defined, univectoral decay of the magnetization to the origin of the demagnetization diagram is identified (Fig. 2.30). This magnetization is interpreted to be the primary thermoremanent magnetization acquired in the initial cooling of each lava flow. The directions of primary magnetizations have been calculated after visual inspection of demagnetization diagrams three-dimensional least-squares fit. The observed between-site dispersion of the directions of the primary magnetization differs considerably (Fig. 2.31). This is interpreted to reflect one of two problems associated with sampling surface exposures of young basaltic lavas. The first is the difficulty in sampling intact material. Samples in one or a series of adjacent and rotated blocks may give directions of magnetization that are internally consistent yet discrepant in comparison to those from samples collected from the same part of the site (Fig. 2.31).

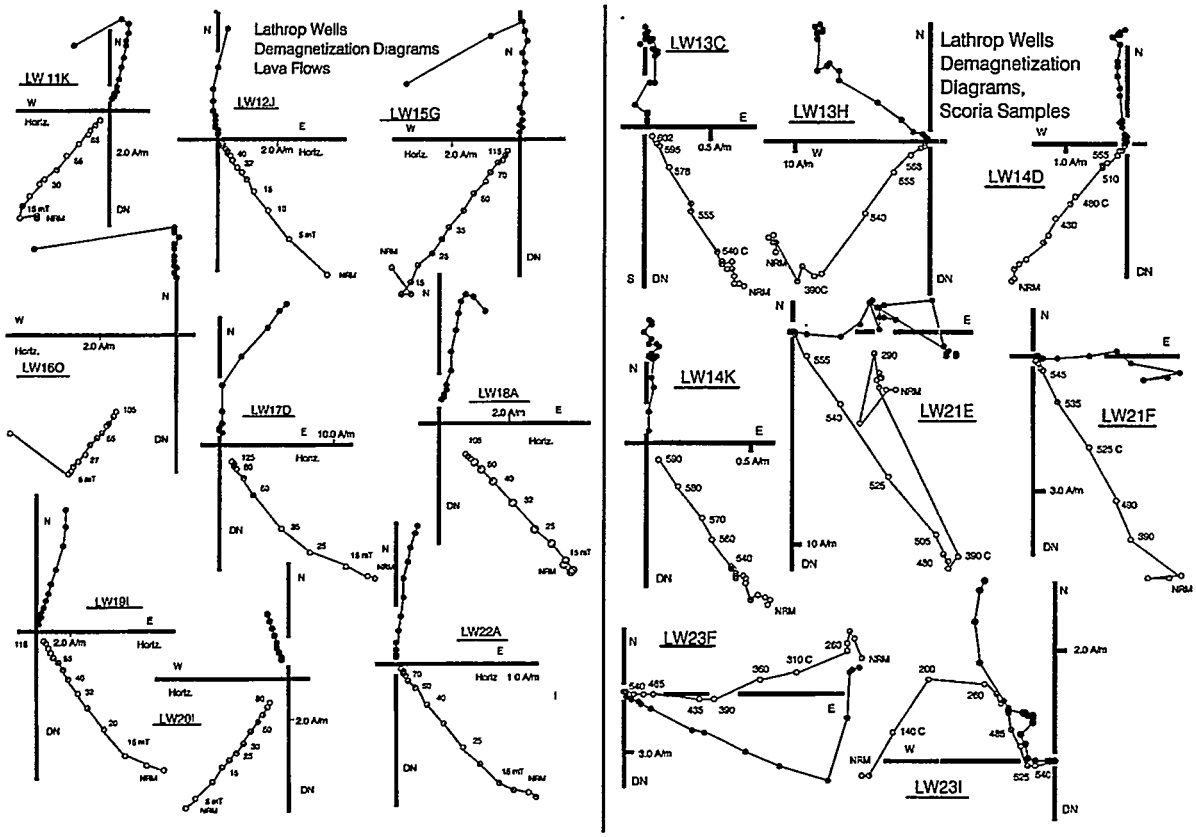


Fig. 2.30 Representative modified orthogonal demagnetization diagrams showing the endpoint of the magnetization vector projected onto the horizontal (EW, NS) plane (filled circles) and the true vertical (horizontal, U/D) plane (open circles) for samples from lava flows (Fig. 2.30a) and scoria mounds (Fig. 2.30b) from the Lathrop Wells volcanic center. Each projection shows the complete demagnetization sequence, using either alternating magnetic field (peak fields given beside vertical projections, in MilliTesla) or thermal (temperatures beside vertical projections) demagnetization. For most of the examples shown, the direction of the magnetization vector trending toward the origin of the diagram and isolated over a broad range of peak fields or laboratory unblocking temperatures is determined with a high degree of confidence.

The second problem is lightning strikes. Here, an artificial, generally randomly dispersed magnetization is superimposed on a primary, well-grouped magnetization. In some cases this artificial magnetization can be fully removed in alternating field demagnetization; in others it cannot be removed and results at best in a site-mean direction defined with poor precision.

Several sites give well-grouped, interpretable paleomagnetic data. Two sites in Ql1d give site mean directions of magnetization (Declination = 2.7, Inclination = 53.5, n = 8 samples, site LW1; Declination = 13.8, Inclination = 53.3, n = 9 samples site LW2) (Fig. 2.31). These directions are statistically indistinguishable, at a 95 % level of confidence, from the directions reported by Turrin et al. (1991) for their unit Ql3. Two other sites in Ql1d give dispersed paleomagnetic data. Finding intact material in the Ql1a subunit has proven more difficult. Three sites in the Ql1a subunit yield well-grouped site-mean directions of magnetization (Declination = 18.5, Inclination = 53.6, n = 8 samples, LW5; Declination = 346.3, Inclination = 53.8, n = 10 samples, site LW7; and Declination = 358.3, Inclination = 45.3, n = 6 samples site LW8) (Fig. 2.29). Again, these directions are similar to the two group mean directions reported by Turrin et al. (1991) for their unit Ql3. Two sites sampled in subunit Ql1c (LW9, LW10) yielded magnetizations that vary in dispersion (Fig. 2.31). Because of the poor surface exposures of this flow, it is unlikely that a well-grouped direction of magnetization will be obtained for these deposits.

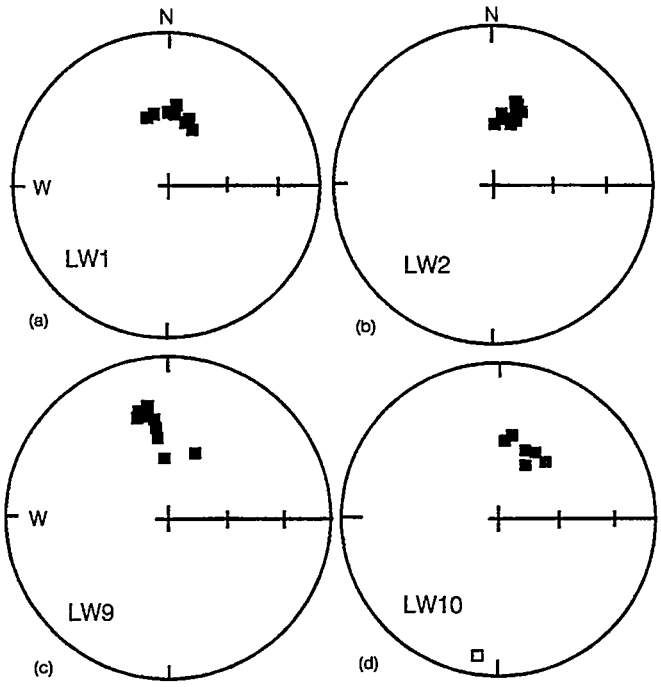


Fig. 2.31 Examples of site-level dispersion of paleomagnetic data from lava flows at the Lathrop Wells volcanic center. Equal area projections of sample magnetization directions determined from progressive demagnetization for the following sites: LW1 and LW2 from the Ql1d lava; LW9 and LW10 from the Ql1c lava. For all projections, lower hemisphere projections are indicated in solid symbols and upper hemisphere projections in open symbols.

New and probably final sets of samples for paleomagnetic study were collected in the fall of 1992. Sample sites (LW11 to LW23) were chosen in an attempt to provide optimum determinations of field magnetization directions for the volcanic subunits. The buried lava flow of subunit Ql1c was excavated to expose the massive interior of the blocky aa flow at two localities, and the two sites give well-grouped magnetizations (Declination = 11.2, Inclination = 46.9, n = 11 samples, site LW11; and Declination = 6.8, Inclination = 54.6, n = 9 samples, site LW12). Scoria mounds dissected by backhoe, of subunits Qs1c and Qs2a (sites LW13, LW14), were studied by collecting oriented scoria clasts from intact sequences of vent scoria buried originally beneath several meters of vent scoria. The clasts were sampled using a relatively unorthodox technique that is explained herein in sufficient detail to preclude confusion. Selected clasts were fixed with glass cover slips using auto-seal cement. The cement dried in less than an hour providing a firm, flat surface for orientation that was permanently fixed to the sample. A strike and dip orientation was made on the cover slip using both magnetic and, when possible, solar, compass and clinometer. The scoria clast

was then easily removed from the dissected unconsolidated scoria deposits. Clasts were prepared into specimens for paleomagnetic measurement by drilling cylinders perpendicular to the oriented cover slip face. The sampling technique proved effective, and the only difficulty encountered was with labeling of final specimens because of the high vesicularity of the scoria clasts. All specimens were demagnetized using progressive thermal methods because of their potentially complex thermal history over the temperature range of magnetization blocking and because of the possibility that much of the geologically significant remanence was carried in hematite. The results from the two backhoe-dissected scoria mounds were most acceptable (Declination = 2.8, Inclination = 57.7, n = 12 independent clasts, site LW13; and Declination = 2.0, Inclination = 46.7, n = 11 independent clasts, site LW14) and consistent with the sampled lava flows. We interpret the paleomagnetic data to indicate that these deposits remained at elevated temperatures (i.e. at least 500°C) throughout the time of formation (aerial ejection and accumulation). Further, the magnetization in the clasts represents a post-emplacement thermally acquired remanence. Demagnetization behavior and overall intensities of magnetization of these clasts give no indication that the mounds were affected by lightning strikes.

We also used this technique to collect scoria clasts from a newly constructed roadcut in subunit Qs1d (site LW21) and from a quarry exposure of the main cone (site LW23). Scoria clasts from site LW21 yield a magnetization direction that is well-grouped at the site level (Declination = 93.8, Inclination = 43.9, n = 10 independent clasts) but unusual with respect to the late Quaternary time- averaged geomagnetic field for the Lathrop Wells locality and, of course, all of the other paleomagnetic data obtained from the volcanic center. The results could be interpreted in several ways. One possibility is that the site records a short-lived, high-amplitude excursion of the geomagnetic field. A second is that the magnetization characteristic of the site/deposit is an artifact of post-emplacement mechanical disruption of at least the sampled part of the deposit. At present, we find the first interpretation unrealistic or difficult to assess. None of the other features of the Lathrop Wells volcanic center yield magnetization indicative of high-amplitude field excursions. Moreover, we have limited faith in the paleomagnetic results because of the nature of the sampled deposits. The second alternative is preferred but remains untested. Individual scoria clasts from site LW23 generally give well-defined magnetization in progressive demagnetization (Fig. 2.30). The directions isolated from the clasts are highly dispersed at the site level, and no interpretable magnetization could be obtained from the sampled site in the main cone. Unlike the small and relatively oxidized scoria mounds at sites LW13 and LW14, it appears that scoria clasts comprising at least part of the main cone have been mechanically disrupted at moderate temperatures after the majority of the magnetization in the clasts was thermally blocked. This is consistent with the morphology and inferred eruptive mechanisms of the respective deposits. Sites LW13 and LW14 were collected from small scoria mounds probably formed by weak, poorly dispersed hawaiian spatter eruptions. The well-grouped magnetizations are consistent with limited cooling of the samples before deposition. In contrast, the eruptions of the main cone (Qs3) produced highly fragmented and dispersed scoria that must have cooled before deposition. This is consistent with an absence of a well-grouped, interpretable magnetization from the main cone sample sites.

Outcrops of strongly agglutinated scoria were drilled, and oriented cores were collected from two vent zones (sites LW16 and LW18) in unit Qs1 located southwest of the main cone. These features yield exceptionally well-grouped magnetizations that are statistically indistinguishable (at >95% confidence) from results reported by Turrin et al. (1991) for their unit Ql3 (Declination = 3.6, Inclination = 52.2, n = 10 samples, site LW18). For purposes of comparison, one site was established in the Ql2a lava (site LW19) on the southeast margin of the volcanic center. This site gave a well-defined site-mean direction (Declination = 6.3, Inclination = 52.5, n = 10 samples) consistent with the findings of Turrin et al. (1991) for this eruptive unit. One additional site was established in subunit Ql1d (site LW17), which gave a site-mean magnetization (Declination = 355.0, Inclination = 52.0, n = 10 samples) that is statistically indistinguishable from the results from site LW1, the site we place most faith in defining the magnetization

characteristic of the volcanic feature. We occupied a site in Ql3 along the northeast margin of the volcanic center (site LW20) that yielded a site-mean direction of magnetization (Declination = 352.9, Inclination = 53.6, n = 10 samples) slightly west of the majority of the Lathrop Wells results but of similar inclination. Finally, site LW22 was in the Qs1 scoria and yielded an exceptionally well-defined site-mean direction (Declination = 2.8, Inclination = 53.6, n = 10 samples) that is indistinguishable from the two unit mean directions reported by Turrin et al. (1991).

Paleomagnetic investigations at the Lathrop Wells volcanic center were designed to extend and not duplicate completely the voluminous work by Champion (1991). Rather, the investigations principally involved gathering paleomagnetic data for newly identified eruptive units as well as testing the suitability of different types of basaltic volcanic rocks (pyroclastic deposits versus lava) for recording high-quality paleomagnetic information. The paleomagnetic data obtained from the two phases of sampling at the Lathrop Wells volcanic center are not dissimilar from those reported by Turrin et al. (1991). Except for the results from site LW21, which are difficult to interpret at present, the data obtained in this study do not reveal any evidence for relatively high-amplitude field phenomena recorded by the Lathrop Wells volcanic deposits. In addition, the data do not support the contention that individual eruptive features have unique paleomagnetic signatures that can be confidently separated from other eruptive features. This conclusion must be placed into perspective. It is difficult to compare thoroughly the results of the present study with previous efforts (Champion 1991; Turin et al. 1991). An insufficient amount of information has been published in their studies to document the manner in which mean magnetizations and, thus, associated statistics were established for their unit Ql5 (which includes deposits from both chronostratigraphic units I and III). An even more fundamental concern is the lack of adequate discussion or documentation of raw demagnetization data and the compilation of results (for example, acceptance criteria and ratios), including pertinent statistical parameters, at the site level.

Champion (1991) and Turrin et al. (1991) argue that deposits of their unit Ql5 yield a magnetization direction that differs by 4.7° from what we interpret to be a grand mean magnetization direction (obtained from several site means) primarily from our chronostratigraphic unit II. This difference, if real, provides support for the subdivisions between chronostratigraphic units I and III and between units II and III. Acceptance of their interpretation requires two sets of information. First, their information needs to be separated and evaluated independently for each of the four chronostratigraphic units. Second, acceptance of their interpretation requires more information on the integrity of the demagnetization data for individual samples as well as the statistical parameters associated with site- and overall unit-mean determinations. In principle, the quality of the determination of a "grand" mean for a particular eruptive unit (for example, multiple lobes of a single lava flow or aligned sets of scoria mounds where several site means have been obtained), must consider the dispersion of results at the site level. Methods for evaluating this problem have been discussed by Cox (1970). A "grand" mean may be associated with a high concentration of site means (and thus a very small value of alpha 95), but each of the site means may in fact be very poorly determined. Other concerns include: (1) the ability of nonagglutinated scoria deposits that include a hydrovolcanic component to record and preserve the primary magnetic signature with high fidelity, (2) much of the information for the Ql5 unit of Turrin et al. (1991) was obtained from non-agglutinated volcanic bombs from the summit of the main cone that is especially susceptible to lightning strikes, and (3) essentially all of the paleomagnetic data for the Lathrop Wells center fall near the time-averaged (spin axis), late Quaternary field direction (Declination = 0.0, Inclination = +57) (Fig. 2.32). We elaborate below on the third point.

The secular variation record of the paleomagnetic field has been studied and modeled by numerous investigators over the past two decades using the highest quality paleomagnetic data available (for example, sequences of lava flows from relatively undisturbed areas). The paleosecular variation is described in terms of the scatter or dispersion about the spin axis of Virtual Geomagnetic Poles (VGPs) obtained from the raw paleomagnetic data. Most models for the scatter of the results are based on several possible contributors to paleosecular variation. One is simple dipole wobble. The result of virtually all the models proposed is that the VGP scatter (angular standard deviation) is quite large. For example, using Model G (McFadden et al. 1991), the VGP scatter at the latitude of the Lathrop Wells center is about 15° ± 1°. The angular standard deviation of field directions, randomly sampled over a period of time of constant polarity (groups of 10^4 yr

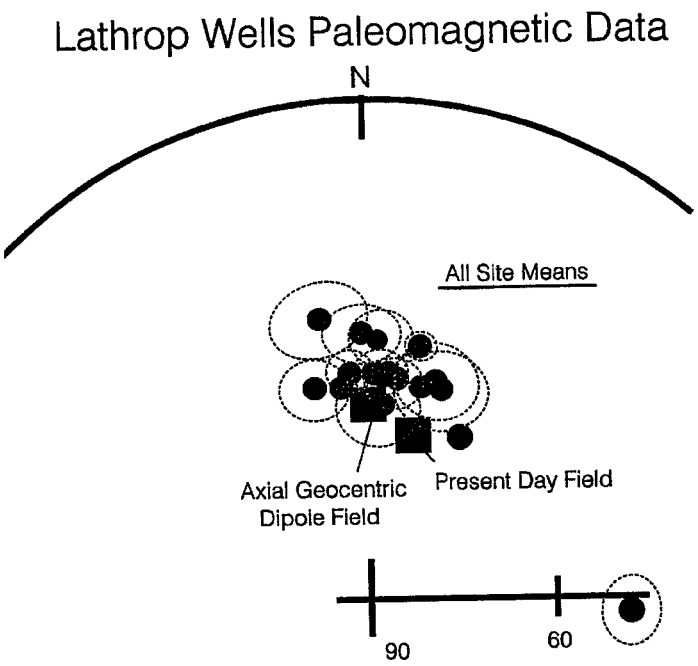


Fig. 2.32 Summary of paleomagnetic data from the Lathrop Wells volcanic center. Equal area projection of *in situ* mean paleomagnetic directions for the total number of accepted and/or interpretable paleomagnetic sites. Large squares are the Quaternary time-averaged (spin axis) axial geocentric dipole field and the present-day (1985) field. Projected cones of 95% confidence are shown for each site mean. There is a 95% level of confidence that the true mean direction for the site, determined from an infinite number of independent samples, lies within the cone of 95% confidence

or more) would be slightly less than the VGP scatter, but nonetheless greater than 10°. Essentially all the eruptive features of the Lathrop Wells center have recorded directions of the latest Quaternary geomagnetic field that are well within the expected one-sigma range of paleosecular field variation about the spin-axis direction (Fig. 2.32). These data provide at best only a very limited opportunity to identify time-distinctive eruptive events. There is no indication of a single volcanic event occurring during a period of unusual geomagnetic activity.

G. Alternative Models of the Eruptive History of the Lathrop Wells Volcanic Center

We have reached an important stage in field, stratigraphic, geochronologic, and geochemical studies of the Lathrop Wells volcanic center. Nearly all planned field, stratigraphic, and trenching studies have been completed. The field and stratigraphic studies appear well integrated, and many diverse observations have converged into a coherent understanding of the eruptive history of the volcanic center. A particularly gratifying aspect of the work is the strong agreement obtained between the established stratigraphic units and geochemical data. Four major eruptive intervals have been identified and described

as chronostratigraphic units (time-distinctive eruptive intervals) and each unit has a distinctive geochemical composition. What remains elusive, however, is the establishment of a consistent chronologic framework for the chronostratigraphic units (Table 2.6). There are two philosophies or approaches that can be applied generally to the integration of field and geochronology data. One approach emphasizes the observable field relations over the results of chronology methods. When apparent conflicts develop between data sets, the field relations are given precedence over the results of chronology measurements. The second approach takes the opposite perspective. Proponents of this approach tend to emphasize the results of one chronology method over another, sometimes but not always with good justification. We prefer the first approach and place a higher level of confidence on the fundamental field relationships of stratigraphic units over discordant chronology data.

The following field observations and interpretations appear firm for the Lathrop Wells volcanic center. They provide the fundamental foundation for the development of three evolutionary models of the eruptive history of the Lathrop Wells volcanic center.

1. The vent deposits of chronostratigraphic unit I are deeply dissected and generally have poorly preserved primary constructional volcanic landforms. The erosional surface developed on these deposits can be traced beneath the unmodified slopes of the main cone. Deeply dissected scoria vents of chronostratigraphic unit I underlie and are juxtaposed with topographically higher standing scoria vents and lavas of chronostratigraphic unit II. The deposits of chronostratigraphic unit I must be significantly older than chronostratigraphic unit III and may be somewhat older than deposits of chronostratigraphic unit II.

2. The scoria-fall deposits of chronostratigraphic unit II can be uniquely correlated with the lava events of the unit by the interfingering stratigraphic relations of their associated pyroclastic-surge deposits.

3. The degree of erosional dissection of the scoria-fall sheet of chronostratigraphic unit II contrasts markedly with the unmodified slopes of the main cone (formed by the eruptions of chronostratigraphic unit III). The outer slopes of the main cone are as steep as 29°. The topographic slopes of the scoria-fall sheet are subhorizontal to <15°. It appears physically impossible for the units to be of similar age and have the observed different degrees of erosional dissection. This provides strong evidence that deposits of chronostratigraphic unit II *must* be older than deposits of chronostratigraphic unit III.

4. Scoria deposits of chronostratigraphic unit IV are separated from scoria deposits of chronostratigraphic unit III by multiple occurrences of soil with horizon development. The fundamental debate concerning the deposits of chronostratigraphic unit IV is whether they are primary or secondary (reworked) in origin. The field characteristics and unique chemical composition of the deposits of chronostratigraphic unit IV in comparison to deposits of all other chronostratigraphic units requires that they were formed by a unique volcanic event–they *cannot* be reworked from a preexisting deposit.

5. The removal of the inferred eruptive vents for chronostratigraphic unit IV by commercial quarrying activity may make it impossible to achieve a scientific consensus on the recognition of this unit.

6. Multiple lines of stratigraphic, geomorphic, soil, geochemical, and geochronology data suggest The Lathrop Wells volcanic center formed during multiple, time-distinct eruptive events and is not a simple monogenetic volcanic center.

Table 2.6 Summary Table of All Geochronology Data for the Lathrop Wells Volcanic Center.

	Subunit	Age	Error	Method	Comment	Site
Chrono I	Qs1d	76	7	^{3}He	Scoria Covered	Old Quarry Scoria
	Ql1d	135	20-15	U-Th	U-alteration	Old Quarry Flow
	Qs1b	61	8	^{3}He	Scoria Covered	Scoria Unit Mound
	Qs1b	214	86	K-Ar	Invalid	Combined Unit
	Qs1b	129	77	$^{40}Ar/^{39}Ar$		
	Ql1b	88	8	^{3}He	Scoria Covered	Southeast Flow
	Ql1a	81	7	^{3}He	Scoria Covered	South Flow
	Ql1a	87	6	^{3}He	Scoria Covered	South Flow
	Ql1a	82	5	^{3}He	Scoria Covered	South Flow
	Ql1a	81	7	^{3}He	Scoria Covered	South Flow
	Ql1a	85	5	^{3}He	Scoria Covered	South Flow
	Ql1a	214	86	K-Ar	Invalid	South Flow
	Ql1a	170	114	$^{40}Ar/^{39}Ar$		South Flow
	Ql1a	79	3.4	^{36}Cl	Scoria Covered	South Flow
	Ql1a	96	4.5	^{36}Cl	Scoria Covered	South Flow
	Ql1a	85	4.6	^{36}Cl	Scoria Covered	South Flow
	Ql1a	78	4.6	^{36}Cl	Scoria Covered	South Flow
	Ql1c	100	9	^{3}He	Uncertain Unit	Flow vent
Chrono II	Ql2a	82	9	^{3}He	Minimum	Lathrop Flow
	Ql2a	88	8	^{3}He	Minimum	Lathrop Flow
	Ql2a	82	4	^{3}He	Minimum	Lathrop Flow
	Ql2a	139	68	K-Ar		Lathrop Flow
	Ql2a	153	110	$^{40}Ar/^{39}Ar$		Lathrop Flow

	Subunit	Age	Error	Method	Comment	Site
	Ql2a	107	33	Step Heating		Lathrop Flow
	Ql2a	24.5	2.5	TL	Invalid	Lathrop Flow
Chrono III	Qs3	35	5	^{3}He	Minimum	Main Cone
	Qs3	56	7	^{3}He	Minimum	Main Cone
	Qs3	35	5	^{3}He	Minimum	Main Cone
	Qs3	29	5	^{3}He	Minimum	Main Cone
	Qs3	43	3	^{3}He	Minimum	Main Cone
	Qs3	83	9.2	^{36}Cl	Altered/Minimum	Main Cone
	Qs3	68	5.7	^{36}Cl	Minimum	Main Cone
	Ql3	67	6	^{3}He	Minimum	Sandramp Flow
	Ql3	53	7	^{3}He	Minimum	Sandramp Flow
	Ql3	125	+35-30	U-Th		Sandramp Flow
Chrono IV	Qs4	8.9	0.7	TL		Lowest Soil
	Qs4	9.9	0.7	TL		Lowest Soil
	Qs4	8.7	1	TL		Lowest Soil
	Qs4	3.7	0.4	TL		Soil 2
	Qs4	3.7	0.4	TL		Soil 4
	Qs4	4.5	0.4	TL		Soil 4

Fig. 2.33 is a geologic map of the Lathrop Wells volcanic center showing the combined distribution of rock units for the four chronostratigraphic units. The chronology data for the Lathrop Wells center are not definitive with respect to the ages of the four chronostratigraphic units. We have been unable to obtain definitive chronology data using the applied range of geochronology methods. New step heating $^{40}Ar/^{39}Ar$ data are being obtained for suites of fragments of partly fused tuff collected from lava and scoria units of the Lathrop Wells center. Preliminary data from these studies will be available in early calendar year 1995. We will make further revisions to the chronology models of the center using these new results, but anticipate that the data may not be definitive. Table 2.6 summarizes all chronology data available for the Lathrop Wells volcanic center where there are acceptable constraints on the stratigraphic relations of the analyzed samples. The only data that do not meet the acceptance criteria are U-series data for

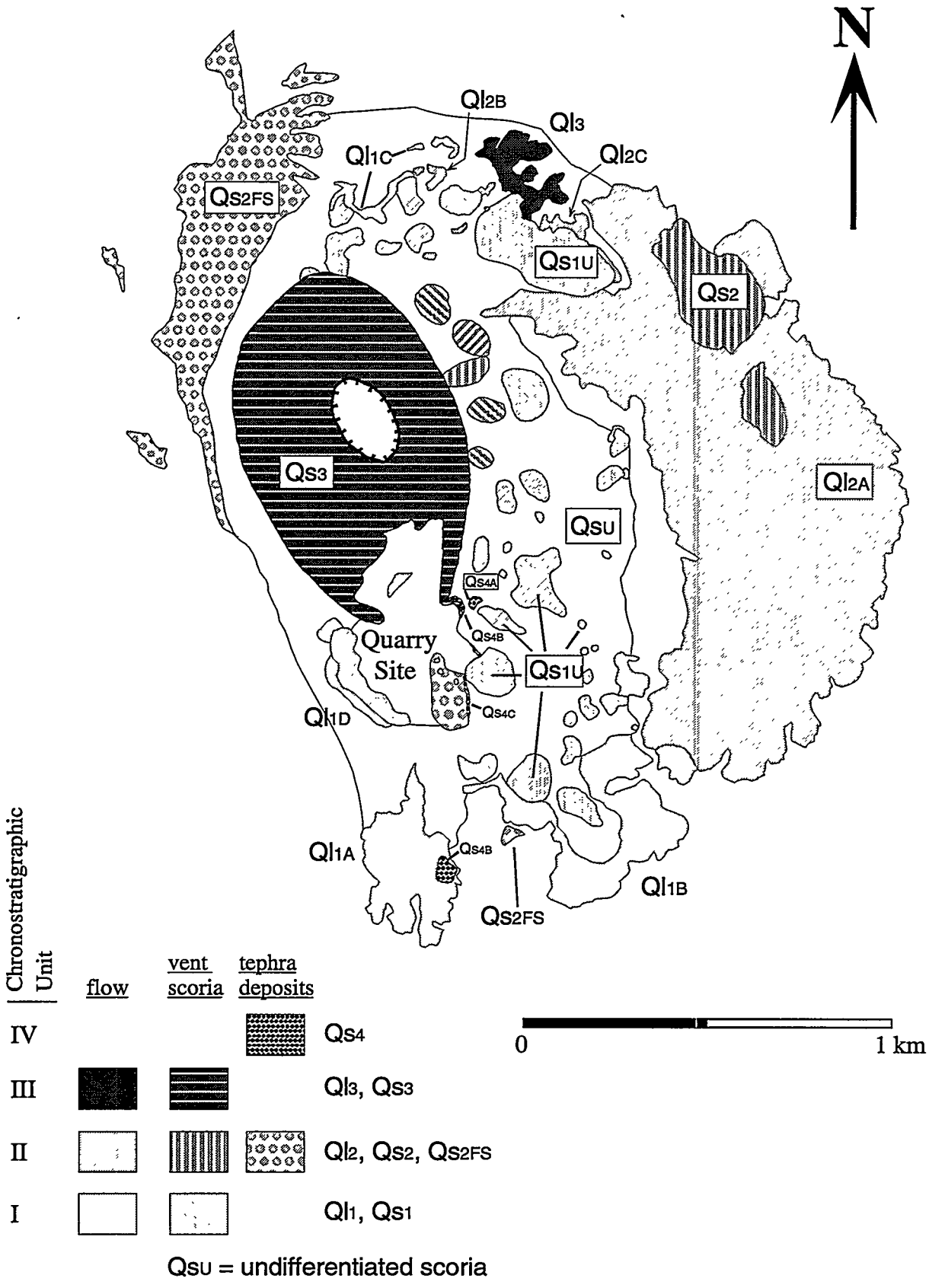


Fig. 2.33 Geologic map of the Lathrop Wells volcanic center showing the distribution of all chronostratigraphic units of the center

soil carbonate and one set of cosmogenic ^{36}Cl analyses. The data from Table 2.6 are used to develop three alternative models for the evolution of the Lathrop Wells volcanic center. The first model (Model A) is a four-fold division of the volcanic deposits of the Lathrop Wells volcanic center emphasizing constraints from the field and stratigraphic data. We attempt to assign approximate or best estimates of ages to the four chronostratigraphic units using primarily insights from field data supplemented by the chronology data from Table 2.6. Where emphasize the field data for Model A where there are inconsistencies in the geochronology data. Models B and C assign increased importance to the results of chronology data for the four chronostratigraphic units. These models may be preferred by workers choosing to emphasize the results of individual geochronology methods over field and stratigraphic relations.

1. Model A. Model A is a four-event polygenetic model. The age of the lava and scoria sequences of chronostratigraphic unit I are presumed to be at least 120 to 130 ka based on (in decreasing order of acceptability) the U-Th disequilibrium age of the Old Quarry flow lava, the minimum cosmogenic ^{3}He ages of multiple units, and the mean ages of multiple K-Ar and $^{40}Ar/^{39}Ar$ age determinations. The discordance in erosion between chronostratigraphic units I and II is assumed to have significance in age assignments. The age of chronostratigraphic unit II is assumed to be between 85 and 95 ka (oldest cosmogenic ^{3}He age determinations). The age of chronostratigraphic unit III is inferred to be best estimated at about 55 to 65 ka on the basis of the oldest cosmogenic ages (^{3}He, ^{36}Cl) of the main cone and the Ql3 lava flow (Sandramp lava). The erosional unconformity between the scoria-fall deposits of chronostratigraphic unit I and the cone-slope deposits of the main cone is assumed to be significant. The age of eruptive events of chronostratigraphic unit IV is less than 4 and 9 ka on the basis of TL ages of soil beneath tephra-fall units. The two tephra units observed in distal sections and fault trenches are correlated with chronostratigraphic unit II.

2. Model B. Model B is a three-event polygenetic model. It is identical to Model A, except that chronostratigraphic unit II is not inferred to be distinctively younger than chronostratigraphic unit I. This model assumes that the difference in erosion and burial of the different units is not significant and represents differences in the erosional resistance of vent scoria versus lava flows. The U-Th disequilibrium age of the Old Quarry lava and the mean K-Ar and $^{40}Ar/^{39}Ar$ ages of other lavas are assumed to be the best estimate of the age of chronostratigraphic units I and II. All cosmogenic ^{3}He and ^{36}Cl ages for the units are assumed to be minimum ages because of shielding of primary surfaces by scoria-fall deposits of chronostratigraphic unit II and local cover by eolian sand. The ages of chronostratigraphic unit III and IV are assumed to be the same as in Model A. The tephra units observed in distal sections are correlated with the oldest chronostratigraphic units (>120 to 130 ka) and chronostratigraphic unit III (55 to 65 ka).

3. Model C. Model C is a two-event polygenetic model. The age of the three oldest volcanic units at the Lathrop Wells center is assumed to be about 125 to 140 ka on the basis of the results of the U-Th disequilibrium ages and the mean K-Ar and $^{40}Ar/^{39}Ar$ ages. The results of all other age determinations are assumed to be invalid. The results would, in this model, represent a combination of poorly developed and/or calibrated methods and shielding of samples used for cosmogenic age determinations from scoria-fall and eolian deposits. The age of chronostratigraphic unit IV is less than 4 and 9 ka. The multiple ash horizons observed in distal outcrops and trenches are assumed to be stratigraphic complications of erosional reworking of surficial ash.

V. REFERENCES

Armstrong, R. L., "Magmatism, Orogenic Timing, and Orogenic Diachronism in the Cordillera from Mexico to Canada," *Nature* **247**, 348-351 (1974).

Armstrong, R. L., E. B. Ekren, E. H. Mckee, and D. C. Noble, "Spacetime Relations of Cenozoic Silicic Volcanism in the Great Basin of the Western United States," *America Journal of Science* **267**, 478-490 (1969).

Armstrong R. L., and P. Ward, "Evolving Geographic Patterns of Cenozoic Magmatism in the North American Cordillera: the Temporal and Spatial Association of Magmatism and Metamorphic Core Complex," *Journal Geophysical Research* **96**, 13, 201-13, 224 (1991).

Atwater, T., "Implications of Plate Tectonics for the Cenozoic Tectonic Evolution of Western North America," *Geological Society America* **81**, 3513-3536 (1970).

Axen, G. J., W. J. Taylor, and J. M. Bartley, "Space-Time Patterns and Tectonic Controls of Tertiary Extension and Magmatism in the Great Basin of the Western United States," *Geological Society America* **105**, 56-76 (1993).

Baksi, A. K., K. A. Hoffman, and E. Farrar, "An $^{40}Ar/^{39}Ar$ Age for the Termination of Chron 5; A New Calibration Point for the Miocene Section of the Gpts," *American Geophysical Union* **73** (43), 630 (1992).

Brown, W. J., S. G. Wells, Y. Enzel, R. Y. Anderson, and L. D. McFadden, "Later Quaternary History of Pluvial Lake Mojave, Silver Lake, and Soda Lake Basins, Southern California," *Quaternary Research* (in Press).

Broxton, D. E., R. G. Warren, F. M. Byers, Jr., and R. B. Scott, "Chemical and Mineralogic Trends Within the Timber Mountain Oasis Valley Caldera Complex, Nevada: Evidence for Multiple Cycles of Chemical Evolution in a Long-Lived Silicic Magma System," *Journal Geophysical Research* **94**, 5961-5985 (1989).

Byers, F. M., Jr., C. L. Rogers, W. J. Carr, and S. J. Luft, "Geologic Map of the Buckboard Mesa Quadrangle, Nye County, Nevada," U.S. Geological Survey Map GQ-552 (1966).

Byers, F. M., Jr., and H. Barnes, "Geologic Map of the Paiute Ridge Quadrangle, Nye and Lincoln Counties, Nevada," U.S. Geological Survey Quadrangle Map GQ-577 (1967).

Byers, F. M., Jr., W. J. Carr, P. P. Orkild, W. D. Quinlivan, and K. A. Sargent, "Volcanic Suites and Related Cauldrons of Timber Mountain-Oasis Valley Caldera Complex, Southern Nevada," U.S. Geological Survey Professional Paper 919, 70 pp. (1976).

Byers, F. M., Jr., W. J. Carr, and P. P. Orkild, "Volcanic Centers of Southwestern Nevada: Evolution of Understanding," 1960-1988, *Journal Geophysical Research* **94**, 5908-5924 (1989).

Carr, W. J., and W. D. Quinlivan, "Geologic Map of the Timber Mountain Quadrangle, Nye County, Nevada," U.S. Geological Survey Map GQ-503 (1966).

Carr, W. J., "Regional Structural Setting of Yucca Mountain, Southwestern Nevada, and Late Cenozoic Rates of Tectonic Activity in Part of the Southwestern Great Basin, Nevada and California," U.S. Geological Survey Open-File Report 84-854, 109 pp. (1984).

Carr, W. J., and L. D. Parrish, "Geology of Drill Hole USW VH-2, and Structure of Crater Flat, Southwestern Nevada," U.S. Geological Survey Open-File Report 85-475, 41 pp. (1985).

Carr, W. J., F. M. Byers, Jr., and P. P. Orkild, "Stratigraphic and Volcano-Tectonic Relations of Crater Flat Tuff, and Some Older Volcanic Units, Nye County, Nevada," U.S. Geological Survey Professional Paper 1323, 28 pp. (1986).

Carr, W. J., "Volcanic-Tectonic Setting of Yucca Mountain and Crater Flat, Southwestern Nevada," in *U.S. Geological Survey 1790: U.S. Geologic and Hydrologic Investigations of a Potential Nuclear Waste Disposal Site at Yucca Mountain, Southern Nevada*, M. D. Carr and J. C. Yount, Eds., (Department of Interior, U.S. Geological Survey, Reston, Virginia, 1988), pp. 35-49

Carr, W. J., "Styles of Extension in the Nevada Test Site Region, Southern Walker Lane Belt; an Integration of Volcano-Tectonic and Detachment Fault Models," *in Geological Society America Memoir 176: Basin and Range Extensional Tectonics Near the Latitude of Las Vegas, Nevada*, B. P. Wernicke, Ed., (Geological Society America, Boulder, Colorado, 199), pp. 283-303.

Cerling, T. E., and H. Craig, "Cosmogenic ^{3}He Production Rates from 39° N to 46° N Latitude, Western USA and France," *Geochemica Cosmochemica Acta* **58**, 249-255 (1994).

Cerling, T., "Dating Geomorphologic Surfaces Using Cosmogenic ^{3}He," *Quaternary Research* **33**, 148-156 (1990).

Champion, D. E., "Volcanic Episodes Near Yucca Mountain as Determined by Paleomagnetic Studies at Lathrop Wells, Crater Flat, and Sleeping Butte, Nevada," *in Proceedings High Level Radioactive Waste Management Conference, Las Vegas, Nevada, (*America Nuclear Society, La Grange Park, Illinois) **61-67** (1991).

Champion, D. E., Oral Presentation to the United States Nuclear Waste Technical Review Board, Panel On Structural Geology and Geoengineering, Meeting on Volcanism, Las Vegas, Nevada (September 14, 1992).

Christiansen, R. L., and P. W. Lipman, "Geologic Map of Topopah Spring NW Quadrangle, Nye County, Nevada," U.S. Geological Survey Quadrangle Map GQ-444 (1965).

Christiansen, R. L., and P. W. Lipman, "Cenozoic Volcanism and Plate Tectonic Evolution of the Western United States, II, Late Cenozoic," *Philosophical Transactions Royal Society London Series A*, **271**, 249-284 (1972).

Christiansen, R. L., P. W. Lipman, W. J. Carr, F. M. Byers, Jr., P. P. Orkild, and K. A. Sargent, "The Timber Mountain-Oasis Caldera Complex of Southern Nevada," *Geological Society America* **88**, 943-959 (1977).

Christiansen, T. L., and E. H. McKee, "Late Cenozoic Volcanic and Tectonic Evolution of the Great Basin and Columbia Intermontane Regions," in *Cenozoic Tectonics and Regional Geophysics of the Western Cordillera*, R. B. Smith and G. P. Eaton, Eds., Geological Society America Memoir 152, 283-311 (1978).

Coleman, S. M., K. L. Pierce, and P. W. Birkeland, "Suggested Terminology for Quaternary Dating Methods," *Quaternary Research* **28**, 314-319 (1987).

Coney, P. J., "Mesozoic-Cenozoic Cordilleran Plate Tectonics," in *Cenozoic Tectonics and Regional Geophysics of the Western Cordillera*, Smith, R. B, and G. P. Eaton, Eds., Geological Society America Memoir 152, pp. 33-49 (1978).

Coney, P. J., "The Regional Tectonic Setting and Possible Causes of Cenozoic Extension in the North American Cordillera," *in Continental Extensional Tectonics*, M. P. Coward, J. F. Dewey, and P. L. Hanock, Eds., Geol. Soc. Spec. Publ. London **28**, 177-186 (1987).

Cox, A., "Latitude Dependence of Angular Dispersion of the Geomagnetic Field", *Geophysical Journal Royal Astron. Society*, **20**, 253-292 (1970).

Cross, T. A., and R. H. Pilger, "Constraints On Absolute Motion and Plate interaction inferred from Cenozoic Igneous Activity in the Western United States," *America Journal of Science* **278**, 865-902 (1978).

Crowe, B. M., "Volcanic Hazard Assessment for Disposal of High-Level Radioactive Waste," *in Active Tectonics: Impact On Society* (National Academy Press, Washington, DC., 1986), Chap. 16, 247-260

Crowe, B. M., "Basaltic Volcanic Episodes of the Yucca Mountain region," *Proceedings High-Level Radioactive Waste Management Conference, Las Vegas, Nevada(*American Nuclear Society, La Grange Park Illinois 1990), pp. 65-73.

Crowe, B. M., and W. J. Carr, "Preliminary Assessment of the Risk of Volcanism at a Proposed Nuclear Waste Repository in the Southern Great Basin," U. S. Geological Survey Open-File Report 80-375, pp. 15 (1980).

Crowe, B. M., M. E. Johnson, and R. J. Beckman, "Calculation of the Probability of Volcanic Disruption of a High-Level Radioactive Waste Repository Within Southern Nevada, USA," *Radioactive Waste Management* **3**, 167-190 (1982).

Crowe B. M., D. T. Vaniman, and W. J. Carr, "Status of Volcanic Hazard Studies for the Nevada Nuclear Waste Storage Investigations," Los Alamos National Laboratory report LA-9325-MS 47 p. (1983a).

Crowe, B. M., S. Self, D. Vaniman, R. Amos, and F. Perry, "Aspects of Potential Magmatic Disruption of a High-Level Radioactive Waste Repository in Southern Nevada," *Journal of Geology* **91**, 259-276 (1983b).

Crowe, B. M., K. H. Wohletz, D. T. Vaniman, E. Gladney, and N. Bower, "Status of Volcanic Hazard Studies for the Nevada Nuclear Waste Storage Investigations," Los Alamos National Laboratory Report LA-9325-MS, Vol. II 101 p. (1986).

Crowe, B., C. Harrington, L. McFadden, F. Perry, S. Wells, B. Turrin, and D. Champion, "Preliminary Geologic Map of the Lathrop Wells Volcanic Center," Los Alamos National Laboratory Report LA-UR-88-4155 (1988).

Crowe, B. M., and F. V. Perry, "Volcanic Probability Calculations for the Yucca Mountain Site: Estimation of Volcanic Rates," *Proceedings Nuclear Waste Isolation in the Unsaturated Zone, Focus '89, Symposium*, America Nuclear Society, 326-334 (1989).

Crowe, B. M., and F. V. Perry, "Preliminary Geologic Map of the Sleeping Butte Volcanic Centers," Los Alamos National Laboratory Report LA-12101-MS, 11 pp. (1991).

Crowe, B., R. Morley, S. Wells, J. Geissman, E. McDonald, L. McFadden, F. Perry, M. Murrell, J. Poths, and S. Forman, "The Lathrop Wells Volcanic Center: Status of Field and Geochronology Studies," *Proceedings High-Level Radioactive Waste Management Conference, Las Vegas, Nevada* (American Nuclear Society, La Grange Park, Illinois 1992) pp. 1997-2013.

DOE (U.S. Department of Energy), "Environmental Assessment: Yucca Mountain Site, Nevada Research and Development Area, Nevada," Office of Civilian Radioactive Waste Management Report DOE/RW-0073, (1986).

DOE (U.S. Department of Energy), "Site Characterization Plan, Yucca Mountain Site, Nevada Research and Development Area, Nevada,", Office of Civilian Radioactive Waste Management Report DOE/RW-0199, (1988).

Dohrenwend, J. C., S. G. Wells, and B. D. Turrin, "Degradation of Quaternary Cinder Cones in the Cima Volcanic Field, Mojave Desert, California," *Geological Society America* **97**, 421-427 (1986).

Eaton, G. P., R. R. Wahl, H. J. Prostka, D. R. Mabey, and M. D. Kleinkopf, "Regional Gravity and Tectonic Patterns: their Relation to Late Cenozoic Epirogeny and Lateral Spreading in the Western Cordillera," in *Cenozoic Tectonics and Regional Geophysics of the Western Cordillera*, R. B. Smith, R. B., and G. P. Eaton, Eds., Geological Society America Memoir 152, 51-91 (1978).

Ekren, E. B., and K. A. Sargent, "Geologic Map of the Skull Mountain Quadrangle, Nye County, Nevada," U.S. Geological Survey Quadrangle Map GQ-387 (1965).

Farmer, G. L., F. V. Perry, S. Semken, B. Crowe, D. Curtis, and D. J. DePaolo, "Isotopic Evidence On the Structure and Origin of Subcontinental Lithospheric Mantle in Southern Nevada," *Journal Geophysical Research* **94**, 7885-7898 (1989).

Feuerbach, D. L., E. I. Smith, and M. Shafiqullah, "Structural Control of Pleistocene Volcanism in Crater Flat, Nevada," *Geological Society America Abstracts with Programs* **22**, p. A134 (1990).

Fisher, R. V., and H. U. Schminike, *Pyroclastic Rocks*, (Springer-Verlag, Berlin, 1984) 472 p.

Frizzel, V. A., and J. Shulters, "Geologic Map of the Nevada Test Site," U.S. Geological Survey, Misc. Invest. Series, Map I-2046 (1990).

Harris, A. G., J. E. Repetski, J. L. Clayton, J. A. Grow, M. D. Carr, and T. A. Davis, "Results from 1991 Wildcat Wells Near Yucca Mountain, Nevada," *Geological Society America Abstracts with Programs* **24**, 17 (1992).

Henrichs, E. N., and E. J. Mckay, Geologic Map of the Plutonium Valley Quadrangle, Nye and Lincoln Counties Nevada: U.S. Geological Survey Geologic Quadrangle Map GQ-384, Scale 1:24,000 (1965).

Ho, C. H., "Time Trend Analysis of Basaltic Volcanism for the Yucca Mountain Site," *Journal Volcanology Geothermal Research* **46**, 61-72 (1991).

Ho, C. H., E. I. Smith, D. L. Feuerbach, T. R. Nauman, "Eruptive Probability Calculation for the Yucca Mountain Site, USA: Statistical Estimation of Recurrence Rates," *Bulletin Volcanology* **54**, 50-56 (1991).

Holcomb, R., D. E. Champion, and M. L. McWilliams, "Dating Recent Hawaiian Lava Flows Using Paleomagnetic Spectral Variation," *Geological Society America* **97**, 829-839 (1986).

Kane, M. F., and R. E. Bracken, "Aeromagnetic Map of Yucca Mountain and Surrounding Regions, Southwest Nevada," U.S. Geological Survey, Open-File Report 83-616, 19 pp. (1983).

Kistler, R. W., "Potassium-Argon Ages of Volcanic Rocks in Nye and Esmeralda Counties, Nevada, Studies of Geology and Hydrology, Nevada Test Site," *Geological Society America Memoir* **110**, 252-262 (1968).

Langenheim, V. E., S. F. Carle, D. A. Ponce, and J. D. Philips, "Revision of An Aeromagnetic Survey of the Lathrop Wells Area, Nevada," U.S. Geological Survey, Open-File Report 91-46, 17 pp. (1991).

Langenheim, V.E., K.S. Kirchoff-Stein, and H.W. Oliver, "Geophysical Investigations of Buried Volcanic Centers Near Yucca Mountain, Southwest Nevada", in *Proceedings High Level Radioactive Waste Management Conference, Las Vegas, Nevada*, (American Nuclear Society, La Grange Park, Illinois 1993), pp. 1840-1846.

Laughlin, A. W., J. Poths, H. A. Healey, S. Reneau, and G. Woldegabriel, "Dating of Quaternary Basalts Using the Cosmogenic ^{3}He and ^{14}C Methods With Implications for Excess ^{40}Ar," *Geology* **22**, 135-138 (1994).

Lipman, P. W., R. L. Christiansen, and J. T. O'Connor, "A Compositionally Zoned Ash-Flow Sheet in Southern Nevada," U.S. Geological Survey Professional Paper 524, 47 pp. (1966a).

Lipman, P. W., W. D. Quinlivan, W. J. Carr, and R. E. Anderson, "Geologic Map of the Thirsty Canyon Se Quadrangle, Nye County, Nevada," U.S. Geological Survey Quadrangle Map, GQ-489 (1966b).
Lipman, P. W., H. J. Prostka, and R. L. Christiansen, "Evolving Subduction Zones in the Western United States, As Interpreted from Igneous Rocks," *Science* **174**, 821-825 (1971).

Lipman, P. W., H. J. Prostka, and R. L. Christiansen, *in* "Cenozoic Volcanism and Plate Tectonic Evolution of the Western United States, I: Early and Middle Cenozoic," *Philosophical Transaction Royal Society London, Series* A **271**, 217-248 (1972).

Luedke, R. G., and R. L. Smith, "Map Showing Distribution, Composition, and Age of Late Cenozoic Volcanic Centers in the Western Conterminous United States," U.S. Geological Survey, Misc. Inv. Series, Maps I-1523 (1984).

Luft, S. J., "Mafic Lavas of Dome Mountain, Timber Mountain Caldera, Southern Nevada," U.S. Geological Survey Professional Paper 501d, 14-21 (1964).

Lutton, R. J., "Internal Structure of the Buckboard Mesa Basalt," *Bulletin Volcanology* 579-593 (1968).

Marsh, B. D, and R. G. Resmini, "Longevity of Magma in the Near Surface: A Study Using Crystal Sizes in Lavas," in *Proceedings High Level Radioactive Waste Management Conference, Las Vegas, Nevada,* (American Nuclear Society, La Grange Park, Illinois 1992) pp. 2025-2032.

McFadden, L. D., S. G. Wells, and J. C. Dohrenwend, "Influences of Quaternary Climatic Changes on Processes of Soil Development on Desert Loess Deposits of the Cima Volcanic Field," Catena **13**, 361-389 (1986).

McFadden, P.L., R.T. Merril, M.W. Mcelhinny, and S. Lee "Reversals of the Earthís Magnetic Field and Temporal Variations of the Dynamo Families," *Journal Geophysical Research*, **96**, 3923-3933 (1991).

McKee, E. H., "Tertiary Igneous Chronology of the Great Basin of Western United States Implications for Tectonic Models," *Geological Society America* **82**, 3497-3502 (1971).

Minor, S.A., D.A. Sawyer, R.R. Wahl, V.A. Frizzell, Jr., S.P. Schilling, R.G. Warren, P.P. Orkild, J.A. Coe, M.R. Hudson, R.J. Fleck, M.A. Lanphere, W.C. Swadley, and J.C. Cole, "Preliminary Geologic Map of the Pahute Mesa 30' X 60' Quadrangle, Nevada," U.S. Geological Survey, Open-File Report 93-229, (1993).

Noble, D. C., R. D. Krushensky, E. J. McKay, and J. R. Ege, "Geologic Map of the Deadhorse Flat Quadrangle, Nye County, Nevada," Map GQ-614, U.S. Geological Survey, Washington, D.C. (1967).

Noble D. C., S. I. Weiss, and E. H. McKee, "Magmatic and Hydrothermal Activity, Caldera Geology, and Regional Extension in the Western Part of the Southwestern Nevada Volcanic Field" (1992).

O'Connor, J. T., R. E. Anderson, and P. W. Lipman, "Geologic Map of the Thirsty Canyon Quadrangle, Nye County, Nevada," U.S. Geological Survey Quadrangle Map, GQ-524 (1966).

Orkild, P. P., K. A. Sargent, and R. P. Snyder, "Geologic Map of Pahute Mesa, Nevada Test Site, and Vicinity, Nye County, Nevada," Map I-567, U.S. Geological Survey, Washington, D.C., (1972).

Poths, J., and B. M. Crowe, "Surface Exposure Ages and Noble Gas Components of Volcanic Units at Lathrop Wells Volcanic Center, Nevada," American Geophysical Union **73**, 610 (1992).

Perry, F. V., and B. M. Crowe, "Geochemical Evidence for Waning Magmatism and Polycyclic Volcanism at Crater Flat, Nevada," *in Proceedings High Level Radioactive Waste Management: Conference Las Vegas, Nevada,* (American Nuclear Society, La Grange Park, Illinois 1992), pp. 2356-2365.

Reheis, M. C., J. W. Harden, and R. R. Shroba, "Morphology and Rate of Development of Late Quaternary Soils, Silver Lake, California," *Soil Science Society of America* **53**, 1127-1139 (1989).

Renault, C. E., "Hillslope Processes On Late Quaternary Cinder Cones of the Cima Volcanic Field, Eastern Mojave Desert, California," M.S. Thesis, University of New Mexico, Albuquerque, New Mexico, 121 pp. (1989).

Royek, T. M., "Soil Stratigraphic and Soil Geomorphic Studies in Eolian Deposits Mantling Late Pleistocene Basalt Flows, Cima Volcanic Field, Mojave Desert," California, M.S. Thesis, University of New Mexico Albuquerque, New Mexico, 109 pp. (1991).

Sargent, K. A., and J. H. Stewart, "Geologic Map of the Specter Range NW Quadrangle, Nye County, Nevada," U.S. Geological Survey Geologic Quadrangle Map GQ-884, Scale 1:24,000 (1971).

Sargent, K. A., E. J. McKay, and B. C. Burchfiel, "Geologic Map of the Striped Hills," Quadrangle Map GQ-882, Scale 1:24,000 (1970).

Scott, R. B., and J. Bonk, "Preliminary Geologic Map of Yucca Mountain, Nye County, Nevada," U.S. Geological Survey Open-File Report 84-494, Scale 1:12,000 (1984).

Scott, R. B., G. D. Bath, V. J. Flanigan, D. B. Hoover, J. G. Rosenbaum, and R. W. Spengler, "Geological and Geophysical Evidence of Structures in Northwest-Trending Washes, Yucca Mountain, Southern Nevada, and their Possible Significance to a Nuclear Waste Repository in the Unsaturated Zone," U.S. Geological Survey Open-File Report 84-567, 23 pp. (1984).

Severinghaus, J., and T. Atwater, "Cenozoic Geometry and Thermal State of the Subducting Slabs Beneath Western North America," *in Basin and Range Extensional Tectonics Near the Latitude of Las Vegas, Nevada*, B. P. Wernicke, Ed., Geological Society America **176**, 1-22 (1990).

Sinnock, S., and R. G. Easterling, "Empirically Determined Uncertainty in Potassium-Argon Ages for Plio-Pleistocene Basalts from Crater Flat, Nye County, Nevada," Sandia National Laboratories, Albuquerque, New Mexico, Sand82-2441, 17 p. (1983).

Smith, E. I., D. L. Feuerbach, T. R. Nauman, and J. E. Faulds, "The Area of Most Recent Volcanism Near Yucca Mountain, Nevada: Implications for Volcanic Risk Assessment," *in Proceedings, High-Level Radioactive Waste Management Conference, Las Vegas, Nevada*, (American Nuclear Society, La Grange Park, Illinois 1990) pp. 81-90.

Smith, R. L., and R. G. Luedke, "Potentially Active Volcanic Lineaments and Loci in Western Conterminous United States," *in Explosive Volcanism: Inception, Evolution and Hazards, Geophysics Study Committee, National Research Council*, (National Academy Press, Washington, D.C., 1984) p. 47-66.

Snyder, W. S., W. R. Dickenson, and M. L. Silberman, "Tectonic Implications of Space-Time Patterns of Cenozoic Magmatism in the Western United States," *Earth Planetary Science Letters* **32**, 91-106 (1976).

Stewart, J. H., W. J. Moore, and I. Zietz, "East-West Patterns of Cenozoic Igneous Rocks, Aeromagnetic Anomalies, and Mineral Deposits, Nevada and Utah," *Geological Society America* **88**, 67-77 (1977).

Stewart, J. H., and J. E. Carlson, "Generalized Maps Showing Distribution, Lithology, and Age of Cenozoic Igneous Rocks in the Western United States," *Geological Society America* **152**, 263-264 (1978).

Turrin, B. D., J. C. Dohrenwend, R. E. Drake, and G. H. Curtis, "K-Ar Ages from Cima Volcanic Field, Eastern Mojave Desert, California," *Isochron/West* **44**, 9-16 (1985).

Turrin, B. D., and D. E. Champion, "$^{40}Ar/^{39}Ar$ Laser Fusion and K-Ar Ages from Lathrop Wells Nevada, and Cima, California: The Age of the Latest Volcanic Activity in the Yucca Mountain Area," *in Proceedings High Level Radioactive Waste Management Conference, Las Vegas Nevada*, (American Nuclear Society, La Grange Park, Illinois, 1991) pp. 68-75.

Turrin, B. D., D. Champion, and R. J. Fleck, "$^{40}Ar/^{39}Ar$ Age of the Lathrop Wells Volcanic Center, Yucca Mountain, Nevada," *Science* **253**, 654-657 (1991).

Turrin, B. D., D. E. Champion, and R. J. Fleck, "Measuring the Age of the Lathrop Wells Volcanic Center at Yucca Mountain," *Science* **257**, 556-558 (1992).

Turrin, B. D. Oral Presentation to the United States Nuclear Waste Technical Review Board, Panel on Structural Geology and Geoengineering, Meeting on Volcanism, Las Vegas, Nevada (September 15, 1992, pp. 222-273).

Turrin, B. D., D. E. Champion, R. J. Fleck, G. H. Curtis, and R. E. Drake, "K-Ar Ages and Paleomagnetic Directions from the Lathrop Wells Volcanic Center, Southwestern Nevada: Evidence for Polycyclic Volcanism" (in Press).

Vaniman, D. T., and B. M. Crowe, "Geology and Petrology of the Basalts of Crater Flat: Applications to Volcanic Risk Assessment for the Nevada Nuclear Waste Storage Investigations," Los Alamos National Laboratory Report LA-8845-MS, 67 pp. (1981).

Vaniman, D. T., B. M. Crowe, and E. S. Gladney, "Petrology and Geochemistry of Hawaiite Lavas from Crater Flat, Nevada," *Contributions Mineralogy Petrology* **80**, 341-357 (1982).

Wells, S. G., J. C. Dohrenwend, L. D. McFadden, B. D. Turrin, and K. D. Mahrer, "Late Cenozoic Landscape Evolution on Flow Surfaces of the Cima Volcanic Field, Mojave Desert, California," *Geological Society America* **96**, 1518-1529 (1985).

Wells, S. G., L. D. McFadden, C. E. Renault, B. D. Turrin, and B. M. Crowe, "A Geomorphic Assessment of Quaternary Volcanism in the Yucca Mountain Area, Nevada Test Site, Southern Nevada," *Geological Society America Abstracts With Programs* **20**, 242 (1988).

Wells, S. G., L. D. McFadden, C. E. Renault, and B. M. Crowe, "Geomorphic Assessment of Late Quaternary Volcanism in the Yucca Mountain Area, Southern Nevada: Implications for the Proposed High-Level Radioactive Waste Repository," *Geology* **18**, 549-553 (1990).

Wells, S. G., L. D. McFadden, C. E. Renault, and B. M. Crowe, "Reply On Geomorphic Assessment of Late Quaternary Volcanism in the Yucca Mountain Area, Southern Nevada: Implications for the Proposed High-Level Radioactive Waste Repository," *Geology* **19**, 661-662 (1991).

Wells, S. G., B. M. Crowe, and L. D. McFadden, "Measuring the Age of the Lathrop Wells Volcanic Center at Yucca Mountain," *Science* **257**, 555-558 (1992).

Wernicke, B. P., R. L. Christiansen, P. C. England, and L. J. Sonder, "Tectonomagmatic Evolution of Cenozoic Extension in the North American Cordillera," in *Continental Extensional Tectonics*, M. P. Coward, J. F. Dewey, and P. L. Hancock, Eds. (Geological Society Special Publication, London, 1987) pp. 203-221.

Wohletz, K. H., "Explosive Magma-Water Interactions: Thermodynamics Explosion Mechanisms, and Field Studies," *Bulletin Volcanology* **48**, 245-264 (1986).

Whitney, J. W., and R.R. Shroba, "Reply On Geomorphic Assessment of Late Quaternary Volcanism in the Yucca Mountain Area, Southern Nevada: Implications for the Proposed High-Level Radioactive Waste Repository" *Geology*, **19**, 661, (1991).

Williams, W. J., J. Poths, E. Anthony, C. T. Olinger, M. Whitelaw, and J. Geissman, "Magmatic $^{3}He/^{4}He$ Signatures, ^{3}He Surface Exposure Dating and Paleomagnetism of Quaternary Volcanoes in the Rio Grande Rift, New Mexico," America Geophysical Union **73**, 610 (1992).

Wood, C. A., "Morphometric Analysis of Cinder Cone Degradation" *Journal Volcanology Geothermal Research* **8**, 137-160 (1980).

Wood, C. A., and J. Kienle, *Volcanoes of North America*, (Cambridge University Press, Cambridge, 1990) 354 p.

Zreda, M. G., F. M. Phillips, P. W. Kubik, P. Sharma, and D. Elmore "Cosmogenic ^{36}Cl Dates for a Young Basaltic Eruption Complex, Lathrop Wells, Nevada," *Geology* **21**, (1993).

CHAPTER 3: TECTONIC SETTING OF THE YUCCA MOUNTAIN REGION: RELATIONSHIP TO EPISODES OF BASALTIC VOLCANISM

I. Summary

Yucca Mountain is located in the south part of the Great Basin physiographic province. The mountain developed as a physiographic feature through a combination of eruption and deposition of large-volume ignimbrites from the Timber Mountain–Claim Canyon caldera complexes and subsequent uplift and offset by extensional faulting. The site lies between the alluvial basins of Crater Flat and Jackass Flat. Basin-range faults that cut the rocks of Yucca Mountain trend north and northeast. The Yucca Mountain site is located at the north edge of a conspicuously amagmatic zone that exhibited no Cenozoic volcanism during episodes of Cenozoic extension. The peak of a major episode of extensional faulting that formed the physiography of the region is dated at about 12 million years (Ma). Earlier phases of strike-slip faulting associated with the Walker Lane structural zone may have affected the site but the effected rocks are largely concealed by the widespread Miocene volcanic rocks of the southwest Nevada volcanic field (SWNVF). One tectonic interpretation of the regional structural setting is that episodes of detachment faulting may have been important in developing the mid-Miocene structural framework of the Yucca Mountain site. However, there is a consensus that the active faulting at Yucca Mountain, if related to detachment faulting, represents only the final stages of movement. The Crater Flat basin bounding Yucca Mountain to the west has been interpreted by some workers as a caldera complex formed by the collapse of two nested calderas associated with eruption of the Crater Flat Tuff. An expansion of the caldera tectonic model, states that the Yucca Mountain area is in a north/northeast-trending, volcano-tectonic rift: the Kawich-Greenwater rift. The rift may be a pull-apart or right-stepped zone of rifting in the Walker Lane structural system. Faults that offset the Miocene ignimbrites at Yucca Mountain are inferred by this model to be related to rifting processes and are not detachment faults. The Amargosa Desert rift zone is a variant of the Kawich-Greenwater rift zone. It is inferred to extend from the Pahrump Valley–Death Valley basins across the Amargosa Valley to the southern part of Yucca Mountain. The rift is marked by multiple pull-apart basins bounded by strike-slip faults. Individual basins may or may not be associated with volcanic activity. Another structural model of the Crater Flat basin states that it is the site of a major, northwest-trending strike-slip fault. This system has a proposed cumulative offset of about 26 km. Several variants of a pull-apart basin origin have been proposed for the Crater Flat basin. The models assume the basin was formed by combined east-west extension and right-slip on northwest-trending faults forming a half-rhombochasm.

Basalt of the silicic episode (BSE) exhibits spatial association with Miocene caldera complexes and is distributed in a broad, northwest-trending band parallel to the Walker Lane structural system. The basalt centers of the older basalt of the Postcaldera basalt episode (PCB) occur mostly along basin-range faults and at the intersections of basin-range faults with ring-fracture zones of older caldera complexes. These units all occur north and east of the Yucca Mountain site. The distribution centroid of the Older postcaldera basalt (OPB) is located in the northeast part of the Timber Mountain caldera. In contrast, the Younger postcaldera basalt (YPB) occurs mostly in a northwest-trending zone called the Crater Flat volcanic zone (CFVZ) that is located mostly west and southwest of Yucca Mountain. One center of the YPB, the basalt of Buckboard Mesa, is located in the ring-fracture zone of the Timber Mountain caldera outside the CFVZ and northeast of Yucca Mountain. The distribution centroid of the Younger postcaldera basalt (YPB) is located in the Crater Flat basin and the distribution of the episode is distinct spatially and temporally from the distribution of the basalt centers of the OPB. These differences are consistent with a southwest migration of sites of volcanic activity through time. The locations of the vents of basalt centers of the CFVZ form a northwest alignment. The vent locations are highly correlated spatially on the basis of least

squares and distance-weighted least squares regression fits of multiple combinations of Quaternary and Pliocene and Quaternary basalt centers of the CFVZ. The best-fit curve from the regression analysis passes through the Lathrop Wells cone on the southeast, between Red Cone and Black Cone and between the Little Black Cone and Hidden Cones on the northwest. This best-fit line coincides with the axis of a three-dimensional surface fitted by distance weighted least squares regression of cone location and eruption volume. These data support the inference that repeated pulses of basalt magma ascended along a northwest-trending structure and diverted at shallow levels to form northeast-trending dikes. These dikes probably followed magma-generated fractures because the trend of clustered centers is parallel to the maximum compressive stress direction.

A wide-range of geophysical data have been obtained for the Yucca Mountain region (YMR). Seismological studies employing a local network have been underway since 1979. Earthquakes in the region are distributed in an east/west zone and display strike-slip and dip-slip offsets consistent with a northwest-trending orientation of the least principal stress axis. Earthquake clusters are difficult to relate to surface faults. Yucca Mountain is located in an earthquake-free zone (historic record), a reflection of either low stress accumulation or prehistoric seismic release. There is no correlation between seismicity and the distribution of Quaternary basalt. In fact, there may be a negative correlation between basalt sites and historic seismicity. Strain-field modeling of fault behavior in a uniform strain field shows that off-fault locations of seismicity are expected. The seismic gap in the Yucca Mountain area is coincident with a region of modeled lowest shear strain. Gravity models of the YMR show a gravity high associated with Bare Mountain and a gravity low centered in Crater Flat. These data are permissive with multiple alternative tectonic models of the basin. Comprehensive aeromagnetic and local ground magnetic data have been obtained for the YMR. These data reveal the presence of multiple anomaly sites that correlate with the surface and subsurface distribution of Cenozoic basaltic volcanic rocks. Ground magnetic data show the presence of a small intrusive body associated with the Solitario fault. The close association between aeromagnetic anomalies and the location of Pliocene and Quaternary basalt centers gives some confidence that all sites of significant basaltic volcanism have been identified. Aeromagnetic and ground magnetic experiments are planned to evaluate further the size of basaltic volcanic bodies that can be detected by magnetic methods. Geoelectric, seismic reflection and refraction data have been obtained for parts of Yucca Mountain. A bright spot on a seismic reflection profile in the Amargosa Valley is interpreted to represent a focusing of energy reflected from the midcrust by low-velocity basin fill lying about the bright spot. Teleseismic data reveal the presence of a low-velocity anomaly in Crater Flat and the Amargosa Valley. One interpretation of the velocity anomaly is that it is formed by magma located at the base of the crust extending into the upper mantle. However, other interpretations are possible and the magmatic interpretation appears inconsistent with geologic, seismic, heat flow, and magnetic data.

Quaternary basalt sites cannot be related consistently to and may not follow prevailing shallow structural features. The most consistent spatial correlations between the distribution of basalt centers and structure are with deep-seated structural features such as strike-slip faults and ring-fracture zones of caldera complexes. These structures are inferred to be passive features promoting the passage of basaltic magma. Ascent of magma along these structures may permit passage of basalt upwards through a relative stable crust in a waning tectonic setting. There is a general tendency for basalt centers to occur preferentially in alluvial basins instead of range interiors.

II. Introduction

The purpose of this chapter of the volcanism status report is to relate the record of Cenozoic basaltic volcanism of the Yucca Mountain region (YMR) to the tectonic setting of the southwest Nevada volcanic field (SWNVF). This is difficult for two reasons. First, there is a limited record of Pliocene and Quaternary

volcanic events in the YMR. The number of events is too small to prove or disprove definitively alternative tectonic models. Second, the Yucca Mountain site is in a complex geologic and tectonic setting. Yucca Mountain was formed by a thick accumulation of Cenozoic volcanic rocks that overlie concealed Paleozoic rocks. These Paleozoic rocks were faulted and folded during multiple episodes of pre-Cenozoic deformation. These rocks are exposed to the northeast and west of Yucca Mountain but not within the mountain itself. Their structural configuration beneath Yucca Mountain is only partly known.

Yucca Mountain developed as a physiographic feature through a combination of volcanic and tectonic events. Multiple large-volume, silicic pyroclastic eruptions led to the formation of the Timber Mountain–Oasis Valley caldera complex (TM-OV), the largest caldera complex of the SWNVF (see Chapter 2). The closely spaced eruption of large volumes of silicic pyroclastic rocks about 15 to 11 Ma deposited thick sheets of welded and nonwelded ignimbrites and formed plateau highlands surrounding the TM-OV complex (Byers et al 1976; Christiansen et al 1977). These ignimbrite plateaus were extended and broken by normal faulting associated with Basin and Range tectonism. South of the TM-OV complex, extensional faulting (west-side down) along north and north/northeast-trending faults was accompanied by eastward tilting of the ash-flow units. These tectonic events defined Yucca Mountain as an elongate mountain range. Multiple east-tilted, block-faulted ridge segments developed after deposition of the 12.7 Ma Paintbrush Tuff and before eruption of the 11.5 Ma Timber Mountain Tuff. This ridge and valley physiography persists today.

Before emplacement of the Paintbrush Tuff, there may have been earlier episodes of deformation in the Yucca Mountain area involving extensional, strike-slip, and detachment faulting. Yucca Mountain is located on the south flanks of the SWNVF (see Chapter 2) in a possible north/northeast-trending structural trough or rift zone that extends from Death Valley through the Amargosa basin and Yucca Mountain (Healey and Miller 1965; Wright 1987; W. Carr 1990; Brocher et al. 1993). The formation of the alluvial basins of Crater and Jackass Flats bounding Yucca Mountain to the east and west occurred mostly after deposition of the Paintbrush Tuff. However, there may have been earlier episodes of basin formation associated with the development of pull-apart basins, possibly preceding, associated with, and postdating caldera activity (Fridrich et al 1994). The eruption of over 10,000 km^3 of Miocene volcanic rocks formed a thick volcanic cover that blankets the pre-Miocene rocks of the YMR making it difficult to reconstruct the detailed history of early Cenozoic tectonic events.

Basaltic volcanism accompanied but mostly post-dates the major tectonic activity that shaped the geologic setting of the YMR. Miocene basaltic volcanism shows strong spatial associations with preexisting structural features (basin-range faults and ring-fracture zones of caldera complexes). Many sites of basaltic volcanism formed contemporaneously with phases of extensional faulting. In contrast, the Pliocene and Quaternary basaltic activity postdates the major tectonic events. The post-Miocene basaltic volcanic centers are located mostly in and flanking the alluvial basins. Some centers appear to follow or are located on basin projections of existing structure features. Other centers cannot be related easily to the distribution of known surface or subsurface structural features in the area.

A second purpose of this report is to summarize current understanding of the geologic and tectonic features of the region, progressing in scale from the southern Great Basin region to the Yucca Mountain area. Such a progression places the geologic setting of Yucca Mountain into a regional tectonic perspective. This evaluation is aided necessarily by regional geophysical data that provide important insights into possible interrelationships between regional, local, and subsurface structures. The geophysical data can also be combined with petrologic studies of basaltic volcanism (described in Chapter 4) to provide constraints on the fundamental causes and processes of basaltic volcanism. This composite view gives a

perspective for evaluating not only the structural controls of volcanic activity but also the operation of magmatic processes that produced the past record of volcanism and may control future volcanic events.

Any attempt to describe the relationship between tectonism and basaltic volcanism must be recognized as an evolutionary process linked to the present state of understanding of the geological processes. Concepts concerning, for example, the origin and tectonic development of the Basin and Range province have changed dramatically during the last few decades. During the 50's and 60's, the province was recognized as a site of structural extension. The mountains and valleys were viewed as rigid horsts and grabens, structurally bounded by steeply dipping, planar faults. Important advances during the latter part of the 60's and early 70's strongly reshaped thinking about the origin of the Basin and Range province. The unifying concepts of plate tectonics were developed. These concepts presented a largely new perspective for evaluating the driving mechanisms for development of a major extensional province in a continental setting. The Basin and Range province, based on plate tectonic concepts, attracted comparison to oceanic and continental rift zones behind active arc systems. The widespread application of radiometric dating methods to the volcanic and plutonic rocks of the province revealed the time-space patterns of the igneous rock sequences. The plutonic and volcanic records of activity in the Basin and Range province are now recognized to be part of widespread and continuing magmatic events that occurred along the western length of the North American continent since at least the Eocene. Subduction of oceanic crust associated inland by overlapping belts of continental magmatism provides a conceptual framework for explaining many, but not all, of the complex time-space associations of tectonism and volcanism in the Basin and Range province of the southwest United States.

During the 70's and 80's, perplexing sites of low-angle faulting with large sections of rock displaced or missing were recognized throughout the province. The timing of movement along many of these low-angle fault systems is now sufficiently well established to relate the tectonic events to Cenozoic extension. The identification of low-angle faults of Cenozoic age was paralleled by the recognition of the importance of exposures of complexes of metamorphic and igneous rocks throughout the Basin and Range province. The depth of formation of the these rocks, and their mid-Cenozoic uplift ages necessitated the removal of many kilometers of crust, presumably associated with the Cenozoic extension. The Basin and Range province is recognized as a region of time-transgressive extension accompanied by spatially varying mantle upwelling, volcanism, and lateral flow of the mantle and crust.

There undoubtedly will be continued progress in the reconstruction of geologic events that will lead to further understanding of the processes of tectonism and volcanism in a complex, continental rift setting. Future advances in thinking will produce new ideas, force rethinking, or even invalidate currently accepted concepts. Discussion of the tectonic setting of Yucca Mountain and the patterns of basaltic volcanism must be viewed only as a time-slice of the present state of knowledge.

Three perspectives overshadow the process of identifying the tectonic models for the occurrence of Pliocene and Quaternary basaltic volcanism in the YMR. First, it is important to evaluate and incorporate a comprehensive set of all reasonable tectonic-volcanic models for basaltic volcanism. Because of the small number of basaltic centers, multiple tectonic models can be developed, and the limited data mean that models may be neither proved nor disproved. It is more important to assess complete ranges of alternative models than it is to make judgments about which set or sets of tectonic models are more or even most correct. Second, a key product of evaluating different tectonic models is an identification of the *effects* of the different models on assessing the risk of future volcanism for the Yucca Mountain site. Third, while the task of developing tectonic models for volcanism is difficult, it must be placed into the perspective of the goals of isolation of high-level radioactive waste. A required 10,000-yr isolation period of high-level radioactive waste is long relative to societal perspectives. It is a relatively short period compared to the

millions of years required to initiate, evolve, and change the fundamental tectonic processes that have shaped and will continue to shape the Yucca Mountain area. The geologic record of tectonism and volcanism in the YMR provide consistent evidence that the processes of extension and volcanism peaked in the Miocene and waned in the Pliocene and Quaternary. It is very unlikely, barring unexpected discoveries in site characterization studies, that the fundamental tectonic setting of Yucca Mountain will change significantly during the next 10,000 years.

III. Southern Great Basin

The Yucca Mountain site is located in the southern part of the Great Basin, a subpart of the Basin and Range physiographic province of the southwestern United States. The term "Basin and Range province" as used herein refers to the broad area of the western United States dominated by fault-bounded mountain ranges separated by alluvial valleys (Stewart 1978). The province was subdivided originally on physiographic criteria (Fenneman 1931). However, many geological and geophysical properties of the province extend beyond the strict physiographic boundaries. Eaton (1982) argued that the Basin and Range province can be defined as a tectonophysical region that includes parts of ten western states and more than 10% of the area of the United States. The generally accepted boundaries of the Basin and Range province using standard geomorphic (physiographic) criteria are shown in Figure 3.1. A much larger area of the Basin and Range province can be demarcated simply from the distribution of late Cenozoic faults (Fig. 3.2). This area is close to the size of the Basin and Range province as defined by the thermophysical criteria of Eaton (1982).

There is an important distinction between the Great Basin portion of the Basin and Range province and the southern Basin and Range (Fig. 3.3). The Great Basin has been shaped generally by the recent operation of active extensional processes. It is higher standing topographically and contrasts geophysically with the southern Basin and Range province (Eaton 1982; Jones et al. 1992). The boundary between these subprovinces coincides generally with the eastward projection, between the latitudes of 36° and 37° N, of the Garlock fault, from California across Nevada and continuing to the Colorado Plateau in Arizona (Fig. 3.3) (see also Suppe et al.1975; Eaton 1982). This boundary forms the north edge of an area with no Cenozoic or Mesozoic magmatism or plutonism (Farmer et al. 1989). It marks the approximate location of a gradient in the Bouguer gravity field of almost 100 mGal (increasing to the south; Eaton et al. 1978; Hildenbrand et al. 1988). This gravity step is a significant feature of the Bouguer gravity anomaly map of North America (Hanna et al. 1989). The boundary is less prominent but recognizable on the map of historical seismicity of North America (Hildenbrand et al. 1988, their Fig. 2.3; Engdahl and Rinehart 1988). Wernicke (1992) and Jones et al. (1992) divide the Basin and Range into three tectonic provinces, the northern Basin and Range, the southern

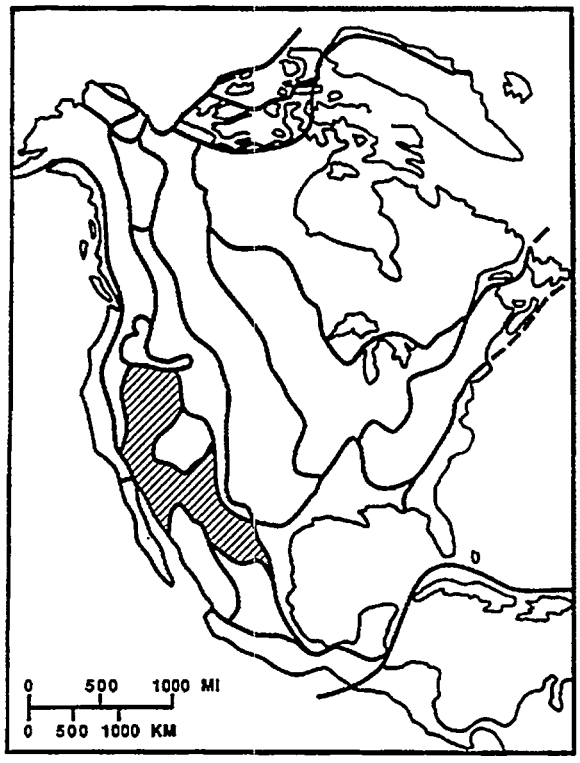


Fig. 3.1 Physiographic subdivisions of North America (modified from Bally et al. 1989). The Basin and Range province, defined on geomorphic criteria, occupies a broad area of the west and southwest United States and adjoining areas of northern Mexico (cross-hatched area).

Basin and Range, and the central Basin and Range. Their central Basin and Range province encompasses most of the area surrounding the YMR.

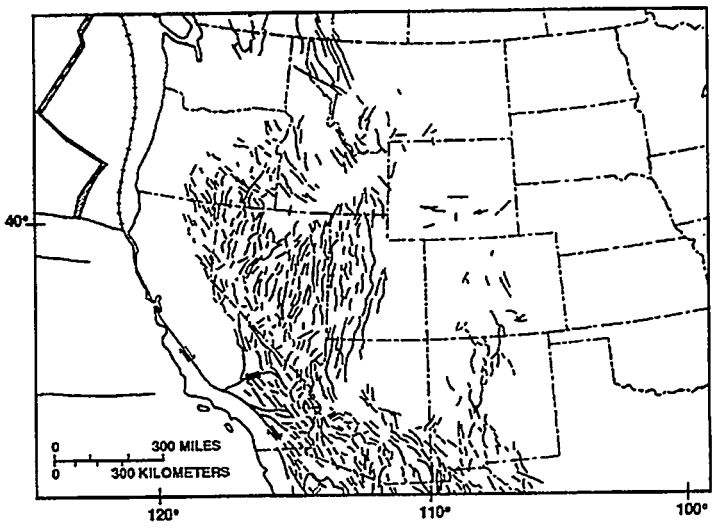


Fig. 3.2 Distribution of late Cenozoic faults in the western United States (modified from Stewart 1978). The area outlined by faults in Figure 3.2 denotes the broader Basin and Range province as defined by the thermophysical criteria of Eaton (1982) and is equal to more than 10% of the landmass of the United States.

The Yucca Mountain site has been shaped structurally by extensional faulting and by voluminous silicic volcanism predominantly in the period of 15 to 9 Ma. The site is located north of a zone that exhibited no magmatic activity during Cenozoic extension (amagmatic gap) (Farmer et al. 1989; Jones et al. 1992). Small-volume basaltic volcanism postdates the silicic volcanism and has persisted in the Pliocene and Quaternary. Episodic basaltic volcanism is likely to continue in the future. Extensional faulting occurred along generally west-dipping faults that vary in trend from about N 30° E and N 30° W. Modern studies have focused increasing attention on detachment faulting as a mechanism for accommodating extension. Many workers separate episodes of faulting into an earlier period of predominantly low-angle or detachment faulting followed by a younger period of high-angle normal faulting. There is, however, no consensus on the exact structural divisions and the timing of these subdivisions. The YMR lies in the Walker Lane structural belt, a complex zone of right-slip and subordinate left slip faults that parallels the northwestern parts of the Great Basin (Fig 3.3).

There are many published reviews of the geology and geophysical characteristics of the Basin and Range province. The following section provides an overview of the voluminous literature. Aspects of the geologic and geophysical characteristics of the Great Basin that provide an important framework for tectonic models of the YMR are emphasized. Noteworthy papers that describe important properties of the Basin and Range province with emphasis on the central Basin and Range subprovince include Nolan (1943), Shawe (1965), Hamilton and Myers (1966), Atwater (1970), Anderson (1971), Scholz et al. (1971), Stewart (1971), Lipman et al. (1972), Christiansen and Lipman (1972), Noble (1972), Kistler and Peterman, (1973), Best and Brimhall (1974), Thompson (1974), Smith and Sbar (1974), Wright et al. (1974), Snyder et al. (1976), Wright (1976), Proffett (1977), Stewart et al. (1977), Best and Hamblin (1978), Christiansen and McKee (1978), Eaton et al. (1978), Lachenbruch and Sass (1978), Smith (1978), Stewart (1978), Zoback and Thompson (1978), Eaton (1979), Eaton (1980), Lipman (1980), Stewart (1980), Guth (1981), Wernicke (1981), Zoback et al. (1981), Armstrong (1982), Eaton (1982), Hill (1982), Glazner and Supplee (1982), Vaniman et al. (1982), Wernicke and Burchfiel (1982), Coney and Harms (1984), Farmer and DePaolo (1983; 1984), Smith and Luedke (1984), Hudson and Geissman (1987), Hamilton (1988), Snoke and Miller (1988), Wernicke et al. (1988), Farmer et al. (1989), Gans et al. (1989), Oldow et al. (1989), Carr (1990), Hodges and Walker (1990), McKenna and Hodges (1990), Scott (1990), Severinghaus and Atwater (1990), Walker and Colman (1991), Jones et al. (1992), Wernicke (1992), and Axen et al. (1993).

The most striking feature of the Great Basin, relative to adjacent regions of the western United States, is the contrasting topography. The region has been broken by complex, spatially and temporally heterogeneous extensional faulting into broad basins separated by narrow, high-standing ranges (Stewart and Carlson 1974; Eaton 1982; Hildenbrand et al. 1988; Wernicke et al. 1988; Jones et al. 1992). This extension occurred primarily in the Cenozoic but the detailed timing and spatial variability of the faulting remains controversial. Many workers restrict the development of the so-called classical Basin and Range tectonism to episodes of extensional faulting that are younger than 17 Ma (post-middle Miocene; see Stewart 1978; Christiansen and McKee 1978). There is evidence of early Cenozoic faulting that preceded and was synchronous with subduction and arc magmatism (Axen et al. 1993). However, this faulting may not be related directly to the later faulting that shaped much of the modern topography (Coney 1978; 1989; Mayer 1986; Okaya and Thompson 1986; Best and Christiansen 1991). Other workers have emphasized the time-transgressive nature and spatial complexity of extensional faulting. The onset of the extensional deformation is emphasized rather than the age of continued faulting. In many areas of the Basin and Range province, extensional faulting may have begun in the Oligocene (Proffett 1977; Crowe 1978; Crowe et al. 1979; Rehrig 1986; Snoke and Miller 1988; Gans et al. 1989; Axen et al. 1993).

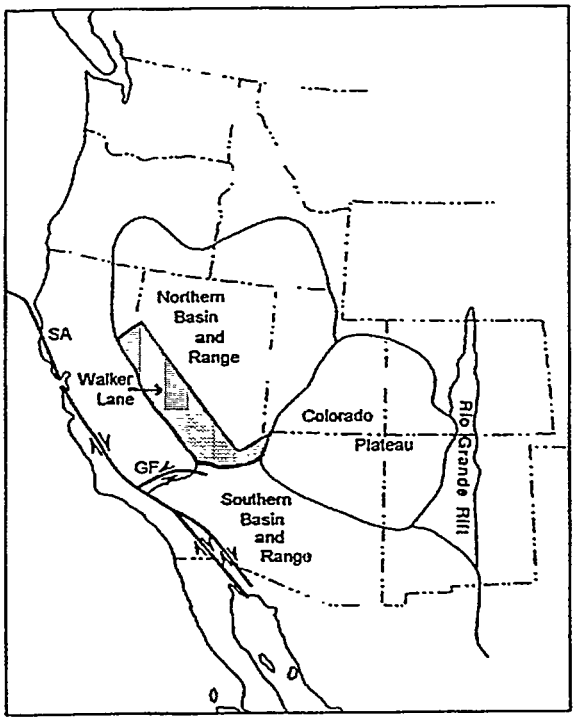


Fig. 3.3 Subdivisions of the Basin and Range province. The province is divided into the northern Basin and Range, commonly called the Great Basin, and the southern Basin and Range, commonly called the Sonoran Desert. The YMR is located near the southern end of the Great Basin north of a transition zone between the provinces that coincides with the approximate extension eastward of the Garlock fault. This transition zone has been called the central Basin and Range (Wernicke 1992; Jones et al. 1992). The cross-hatched area of the southwest Great Basin outlines the boundary of the Walker Lane structural zone. SA: San Andreas fault; GF: Garlock fault; CBR: Central Basin and Range; WL: Walker Lane structural zone.

Some workers have suggested that extensional faulting locally may be associated with the development of metamorphic core complexes (Crittendon et al. 1980). However, it has proven difficult to directly link extension, either spatially or temporally, with the development of the metamorphic complexes. An alternative interpretation is the metamorphic complexes are relics of earlier deformation (Mesozoic). They were reactivated during the period of subduction of the Farallon plate (40 to 20 Ma) and uplifted and exposed by later high-angle faulting. Many authors link the time-transgressive magmatism of the Basin and Range province with tectonism suggesting the tectonic activity, by inference, was time-transgressive (see Chapter 2). The time-transgressive nature of Basin and Range tectonism may be reflected in the modern distribution of faulting and volcanic activity. The most active areas of volcanism and tectonism in the Great Basin are along its western and eastern margins. The present eastern margin of the Great Basin, for example, appears to be expanding outward into largely unextended terrain of the Colorado Plateau (Suppe et al. 1975; Best and Hamblin 1978; Tanaka et al. 1986).

Coney (1978) divided tectonic and magmatic activity in the Basin and Range province into a period of vast ignimbrite eruptions (ignimbrite flare-up of the late Eocene to early Miocene) followed by a period

of widespread basalt eruptions, block faulting, and collapse of the Basin and Range province (post–20 Ma). He suggested the first period was controlled by subduction of the Farallon plate and the latter period by cessation of subduction and growth of the San Andreas transform system. Severinghaus and Atwater (1990) provided a refined plate tectonic perspective for the controls of basin-range faulting and volcanism. They examined the geometry and thermal state of subducting slabs beneath North America through time by reconstructing the magnetic patterns of the preserved ocean floor. Severinghaus and Atwater (1990) suggested subducting slabs became aseismic through time and ceased to strongly affect continental tectonism. The period required for reduction of the tectonic activity associated with subduction is dependent not only on the age of termination of subduction but also on the age of the subducted oceanic crust. The latter factor became important in the Miocene as segments of the oceanic rise approached the Americas plate (Severinghaus and Atwater 1990) resulting in subduction of *young*, buoyant oceanic crust.

The tectonic evolution of western North America can be constrained partly by the timing of formation and expansion of an aseismic slab gap associated with the termination of subduction. A slab gap developed as early as 35 Ma in southeast Arizona and southwestern New Mexico and extended generally northwest in time across the Basin and Range province, paralleling the development of the San Andreas transform system (Severinghaus and Atwater 1990; Figs. 8–14). While the correlations between plate locations and continental tectonic events have spatial uncertainty, they provide a mechanism from plate tectonic interactions to explain the time-transgressive magmatic and tectonic patterns of the southern Basin and Range province. There are three important constraints for the Yucca Mountain area provided by the plate tectonic reconstruction of Severinghaus and Atwater (1990). First, subduction continued in the Great Basin after development of an aseismic gap in the southern Basin and Range. This is consistent with the evidence of younger extension in the Great Basin. Second a slab-free zone inland of the Mendicino and Pioneer fracture zones formed beneath the Yucca Mountain area at about the time of cessation of silicic volcanism and during a major and possibly peak phase of extensional faulting (11 Ma). Third, the timing of the termination of the south spread of volcanism, the development of the amagmatic gap, and the east/west-trending boundary between the Great Basin and southern Basin and Range provinces can be explained by the plate-tectonic reconstruction of Severinghaus and Atwater (1990).

Late Cenozoic basin-range faults in the eastern Great Basin trend predominantly north and northeast. The consistencies of fault trends are interrupted on the southwest side of the Great Basin. Here, there may be multiple sets of normal faults with variable strikes. The range trends are more diverse, typical of the Walker Lane structural zone. Evidence of the Walker Lane structural features in the southwest Great Basin include northwest alignment of silicic volcanic centers (Carr 1974, 1990; Carr et al. 1984), northwest alignment of large-volume basalt centers (Crowe 1990), zones of oroclinal bending of mountain ranges (Shawe 1965; Guth 1981; Scott 1990), segmented and largely inactive zones of northwest-trending probable right-slip faults (Guth 1981; Scott et al. 1984; Carr 1974, 1990), and northeast-trending left-slip faults (Carr 1984). Blakely (1988) noted that magnetic anomalies in the Walker Lane structural zone of Nevada have arcuate, northwest trends but the width of the zone of aeromagnetic anomalies is wider than the boundaries of the Walker Lane. He suggests the magnetic anomalies may be shaped by an underlying tectonic fabric that predates the modern topography–perhaps related to the Precambrian breakup of North America.

Blackwell (1978) and Lachenbruch and Sass (1978) described high values of observed heat flow in the Great Basin. This evidence is consistent with the distribution of Quaternary volcanic rocks and the abundance of thermal springs in the region. Lachenbruch and Sass (1978) suggested that much of the anomalous heat is transferred from the asthenosphere by convection accommodated by pervasive flow of the crust and/or intrusion of magma. They developed thermomechanical models of these processes and demonstrated a relationship between heat flow, asthenosphere flux, lithosphere thickness, extension rate,

and the rate of production of basalt magma in the mantle. Extension, based on their heat-flow models, was facilitated through brittle fracturing and penetration of the crust by basalt dikes or by warming and thinning of the crust through underplating by basalt. The YMR is located in a region of lower heat flow called the Eureka Low. The lower heat flow of this zone may, however, be an effect of reduction of the background heat flow by groundwater flow (Sass et al. 1987). Suppe et al. (1975), Eaton et al. (1978), and Eaton (1982) noted the high average elevation of the Great Basin (>1.4 km), and the general coincidence of this area of high topography with areas of high heat flow. Eaton (1982) concluded that the high topography of the region is best explained by isostatically driven, vertical expansion of the lithosphere as a result of heating from below.

An additional major feature of the Great Basin is its position in a regional gravity low (Eaton et al. 1978; Eaton 1980, 1982; Hildenbrand et al. 1988; Hanna et al. 1989). Eaton et al. (1978) described the collection of associated features that provide constraints on the gravity field and tectonic setting of the Great Basin. These features are the low Bouguer gravity field with a bilateral distribution of long-wavelength anomalies, the thin crust, the high heat flow, the past record of widespread magmatic activity, the concentration of Quaternary volcanic rocks at the east and west margins, and widespread extensional faults.

Jones et al. (1992) examined the geological, geochemical, and geophysical data for the central part of the Basin and Range province. They note that there is significant heterogeneity in the record of the response of the mantle and crust to Cenozoic extension. Jones et al. (1992) suggest that the limited topographic differences between strongly extended and largely unextended regions of the central Basin and Range requires lateral flow of crustal material into the extended areas. They summarized geochemical data supporting movement of crustal material. Specifically, these interpretations are based on isotopic data for basaltic rocks that show ancient lithospheric mantle is preserved beneath the central Basin and Range (Vaniman et al. 1982; Farmer et al. 1989; Jones et al. 1992) while to the north and west, asthenospheric mantle lies beneath the crust. The most buoyant and by inference warmest mantle lies under the Sierra Nevada range and not under the strongly thinned crustal sections of Death Valley and Lake Mead (Jones et al. 1992).

Aeromagnetic data for the state of Nevada and the southern Great Basin were compiled by Hildenbrand and Kucks (1988) and Hildenbrand et al. (1988). Blakely (1988) used a two-step process to calculate apparent magnetization contrasts for these data. He first analyzed the distribution of the Curie temperature isotherm and assessed the tectonic implications of regional features from an analysis of the aeromagnetic data. One of the most prominent features of the region is the presence of a magnetic "quiet zone"–a zone on the aeromagnetic map of Nevada showing a lack of magnetization contrasts. This feature has commonly been interpreted as the product of a relatively shallow depth to the Curie temperature isotherm (Zeitz et al. 1970; Christiansen and McKee 1978). However, Blakely (1988) showed that the absence of short-wavelength anomalies in the quiet zone cannot be explained by a shallow Curie temperature isotherm. He noted that deep magnetic sources influence the long-wavelength anomalies but not the short-wavelength attributes. Blakely (1988) examined alternative causes and suggested the quiet zone may be caused by intense hydrothermal alteration that could diminish the magnetic properties of the magnetic rocks (see Eaton et al. 1978).

Blakely (1988) described the northern Nevada rift, a north/northwest-trending zone of aeromagnetic anomalies that is best developed in north central Nevada. This rift zone is inferred to be underlain by mafic extrusive and intrusive rocks that formed in response to mid-Miocene extension (Zoback and Thompson 1978). The rift zone ends in central Nevada but gravity data indicate the rift could extend further south

(Blakely 1988). The gravity anomalies to the south are probably produced by upper crustal sources (Simpson et al. 1986) and may coincide with thick low-density fill of caldera complexes (Carr 1990).

Blakely (1988) applied a Fourier domain technique to the Nevada aeromagnetic data, noting carefully the assumptions and cautions required to apply this method. He used these data to estimate basal depths of magnetic sources. Two regional features persist in his analysis that correlate with recognized heat-flow anomalies. These are the Battle Mountain high and the Eureka low. The Battle Mountain high is an area of shallow depth to the Curie temperature isotherm and coincides with an area of exceptionally high heat flow (Lachenbrach and Sass 1978). The Eureka low has an unusually deep basal depth to the Curie temperature isotherm (> 25 km; see Blakely 1988). This correlation is not expected if the Eureka low is caused by a near-surface hydrologic phenomena (contrast with Sass et al. 1987). It must be associated with deep seated features. Especially notable, again, is the coincidence of this area with the amagmatic gap and an area of probable preservation of lithospheric mantle (Farmer et al. 1989; Jones et al. 1992).

Patterns of historic seismicity broadly outline the borders of the Great Basin with diffuse but significant seismicity in the interior parts (Smith and Sbar 1974; Smith 1978; Engdahl and Rinehart 1988; Hildenbrand et al. 1988) (see Fig. 3.4 this paper). Distinct zones of seismicity extend along the western margin of the province (east edge of the Sierra Nevada range, Owens Valley–Long Valley region). A secondary belt of seismicity extends from this zone into central Nevada. The eastern margin of the Great Basin is defined by the southern seismic belt (Smith 1978). A somewhat diffuse zone of east/west seismicity extends across the southern Great Basin through the YMR (Smith and Sbar 1974). The record of seismicity in the latter area has been complicated, however, by underground explosions from testing of nuclear weapons in the Nevada Test Site. A somewhat diffuse but distinctive zone of seismicity extends around the borders of the Colorado plateau (Smith 1978; Engdahl and Rinehart 1988). There is an approximate although imperfect correlation between zones of seismicity in the Great Basin and sites of Quaternary faulting (Naturka et al. 1982; Hill 1982; Carr et al. 1988). However, diffuse seismicity commonly does not coincide with surface faults, and seismic slip at depth may be discordant with fault patterns (Arabasz and Julander 1986, Gomberg 1991a,b). Focal depths tend to be shallow and rarely exceed 20 km (Smith 1978; Eaton 1982).

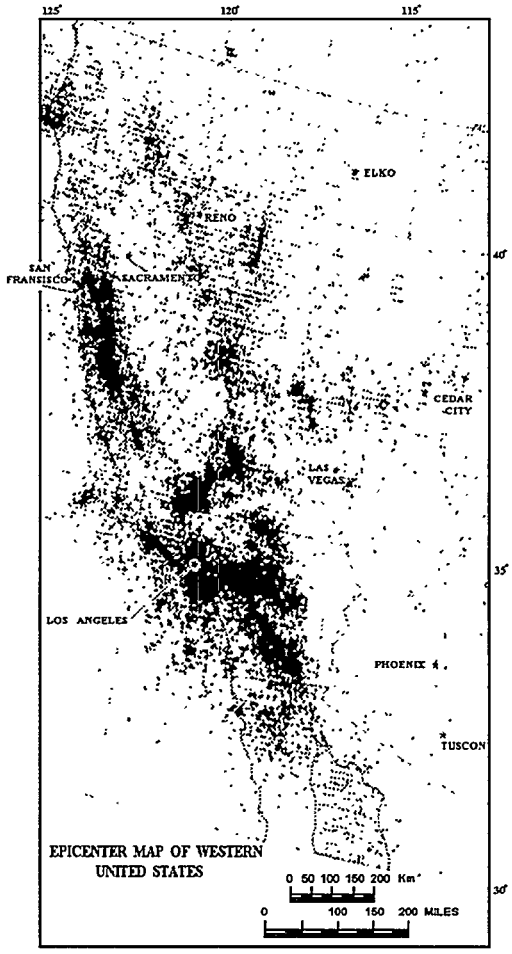


Fig. 3.4 Seismicity map of the western United States (after Smith 1978).

The Great Basin is characterized, from seismic studies, by a relatively thin crust (<30 to 35 km) (Mooney and Braile 1989; Benz et al. 1990; Jones et al. 1992). Mooney and Braile (1989) noted slightly lower crustal seismic velocities of the Basin and

Range province (6.2 km·sec^{-1}) and the local presence of a high-velocity basal crustal layer (7.3 to 7.5 km·sec^{-1}). The latter may be consistent with intrusion of mantle melts into the lower crust (Lachenbrach and Sass 1978; Okaya and Thompson 1986). An important feature of this region is the anomalously low-velocity, low-density upper mantle with P-wave velocities of 7.6 and 7.9 km·sec^{-1} (Priestley et al. 1982; Benz et al. 1990; Holbrook 1990). Jones et al. (1992) emphasized that there is not a close correlation between buoyancy of the crustal column and degree of crustal extension. They suggest that the style of lithospheric extension must vary both along and across the strike of the Great Basin.

IV. Tectonic Setting: Yucca Mountain Region

We examine, in this section, the tectonic setting of the YMR, focusing on the structure of Yucca Mountain and the adjacent Crater Flat basin. The Crater Flat basin contains most of the sites of Pliocene and Quaternary basaltic volcanism in the YMR. The most recent descriptions of the tectonic setting of the area (Hamilton 1988; Carr and Monsen 1988; Wright 1987; Scott 1990; Carr 1990; Fridrich and Price 1992; Fridrich et al. 1994) are emphasized because these discussions include data acquired through the site characterization studies for the Yucca Mountain site.

Yucca Mountain, as noted in the Chapter 2 of this report, forms part of the south flank of the TM-OV caldera complex (Byers et al. 1976, 1989; Christiansen et al. 1977;). This caldera complex, a Miocene volcanic feature, is still expressed physiographically. Many of the constructional features formed during volcanic eruptions (caldera depression, resurgent dome) are still partly preserved topographically. The caldera depression is outlined by a circular valley. The resurgent dome of the caldera, Timber Mountain, is a topographic high. It trends northwest, parallel to the Walker Lane structural zone. The TM-OV caldera complex is flanked on the north, northwest, and south by plateau highlands constructed and upheld by voluminous ignimbrites. These plateau highlands have been subsequently offset by normal faults. The TM-OV caldera complex is bordered to the east by high topography upheld by a north/northwest-trending zone of structurally high standing, Paleozoic rocks (predominantly carbonate and argillite lithologies). Farther east, Yucca Flat is a deep, fault-controlled, north-trending basin. A younger sequence of ignimbrites, the Thirsty Canyon Tuff, was erupted from the Black Mountain caldera located northwest of the TM-OV complex (Noble and Christiansen 1974; Noble et al. 1984). Ash-flow sheets of these units overlie outflow facies of the Timber Mountain Tuff and extend into the caldera depression of the TM-OV complex. The west side of the TM-OV includes the topographically lower-standing caldera segments.

Ekren et al. (1968) documented two sets of basin-range faults in the Nevada Test Site and Nellis Air Force Range. They noted that early basin-range faults trend northwest and northeast. These faults locally predate the Belted Range Tuff (14 Ma) and may have formed as early as about 26 Ma (Ekren et al. 1968). A second set of north-trending faults is constrained by stratigraphic relations to be younger than about 18 Ma. These faults had well developed, probable fault-controlled topography before the eruption of the Thirsty Canyon Tuff (Ekren et al. 1968). Extensional faulting in the Yucca Mountain vicinity is largely contemporaneous with volcanic activity at about 11–13 Ma. There are suggestions of a poorly documented phase of tectonism, possibly Basin and Range tectonism, that predates the Paintbrush Tuff (Snyder and Carr 1984; Fox and Spengler 1989; Wright 1987; Carr 1990). Snyder and Carr (1984) presented evidence of possible pre-Paintbrush normal faulting including a greater degree of displacement of Paleozoic rocks compared to the overlying section of ignimbrites, and evidence of a possible fault-controlled Paleozoic surface extending beneath Yucca Mountain near Busted Butte. Evidence is persuasive that an episode of range-bounding faulting postdates eruption of the Paintbrush Tuff (12.8 Ma) and partly predates but locally involves the Timber Mountain Tuff (11.5 Ma) (see Scott 1990; Carr 1990).

Considerable work for the site characterization studies is continuing to assess the risk of future seismic activity for the Yucca Mountain site. A key concern is defining the state of recent tectonic activity. A number of authors have presented arguments (see W. Carr 1984; M. Carr et al. 1988; Scott 1990) that strain rates have decreased markedly from a maximum in the Miocene but still show a low degree of activity in the Quaternary. The youngest tectonic activity may reflect a renewed episode of faulting and volcanism starting in the Pliocene and continuing in the Quaternary (Fox and Carr 1989). However a major difficulty in testing this conclusion is the time gap in the geologic record between the eruption of the Timber Mountain Tuff (11.5 Ma) and the oldest basin-fill deposits of the alluvial valleys. Very limited geologic data are available to constrain rates of tectonism during this gap in the geologic record.

Scott (1990) provided the most complete description of the shallow structure of Yucca Mountain, based on detailed geologic mapping at a scale of 1:12,000 (Scott and Bonk 1984). He argued that Yucca Mountain has been modified by structures associated with extended terranes of the Basin and Range province and sites of oroclinal bending typical of the Walker Lane structural system. Scott (1990) described the mountain as a series of east-tilted, fault-controlled ridges that bifurcate southward. The southern part of the mountain shows an increase in the number of faults, an increase in the offset along the faults, a decrease or shallowing of the west dip of the faults, and an increase in the amount of east-tilt of the volcanic section. Paleomagnetic data from the Tiva Canyon member of the Paintbrush Tuff suggest progressive north to south (25° km) clockwise rotation of the range about a vertical axis (Scott 1990; Rosenbaum et al. 1991).

Scott (1990) summarized three types of evidence that the major normal faults of Yucca Mountain are listric (flattening downward). First, he cited a 12° decrease in the dip of a fault cutting the west slope of Busted Butte. Second, he noted, from drilling data, a decrease in dip of about 21° km^{-1} for the Ghost Dance fault. The third line of evidence is an increase in stratal dips on the east side of tilted fault blocks (compared with the west side). Scott (1990) inferred the presence of a low-angle normal fault as an accommodation structure beneath Yucca Mountain. Such an interpretation requires the faults of Yucca Mountain to form a low-angle stack of normal faults above a basal detachment fault. The east bounding breakaway zone for a detachment system could be the Paintbrush Canyon fault (Fox and Carr 1989) or a structural zone bounding the east side of Yucca Mountain (Brocher et al. 1993). An alternative explanation, however, is that the observed flattening of faults is a near-surface phenomenon and the major extensional faults are near vertical.

Hamilton (1988) described detachment faulting in the Death Valley region of California and Nevada. He suggested that detachment faults exposed in Bare Mountain, the Bullfrog Hills, and the Funeral Mountains may be domiform exposures of a single west/northwest-dipping fault surface that was eroded as the upper plate of the Grapevine Mountains slid westward. Key points of the Hamilton model (1988) are twofold. First, the detachment faults may be major, initially west-dipping faults that were raised and rotated as they were unroofed progressively by tectonic denudation. Second, the detachment systems decrease in age to the west. The youngest activity on these systems is in the Death Valley region. Hamilton (1988) agrees with the model of Scott (1990) that the middle Miocene faulting of Yucca Mountain represents a headwall complex that allowed slip on the Bare Mountain detachment fault to reach the surface. However, Hamilton (1988) argues that the Quaternary displacement of these faults only applies to the final "gasps" of detachment slip. Thus, most of the detachment deformation predated the episodes of extensional faulting that displaced the ignimbrite sheets of Yucca Mountain.

Another perspective for the regional models of detachment systems is provided by M. Carr and Monsen (1988). They accept the continuous detachment model of Hamilton (1988) but argue that the faults of Yucca Mountain have a different movement history than the extensional terrain of Bare Mountain and

the Bullfrog Hills. Fox and Carr (1989) endorse the detachment models but argue that the listric nature of normal faults at Yucca Mountain can be neither confirmed nor refuted with current data.

Nearly all proponents of the presence of regional detachment systems relate the extensional faulting of the YMR to either late-stage episodes of regional detachment faulting or to subsequent and possibly unrelated uplift. These differences have important implications on the timing of past faulting, the degree of modern tectonic activity, and the seismic risk for Yucca Mountain. However, the important perspective for understanding the distribution of basaltic volcanism is the possible role of detachment faults in providing crustal pathways for ascent of basalt magma. The differences between the detachment models are less important than the issue of whether detachment system(s) are present in the YMR and could, in the modern tectonic setting, provide ascent pathways for basaltic magma.

A largely different tectonic model for the Yucca Mountain setting has been proposed by W. J. Carr and associated co-authors (W. Carr 1984; Snyder and Carr 1984; Carr and Parrish 1985; Carr et al. 1986; W. Carr 1988). They suggest Yucca Mountain is bordered to the west by a caldera complex, the Crater Flat–Prospector Pass caldera. The collapse of two inferred nested calderas was followed by infilling of the caldera depression by ignimbrites of the Paintbrush and Timber Mountain Tuffs and alluvial sediments (Fig. 3.5). These volcanic and sedimentation events are inferred to have formed the Crater Flat basin. Carr et al. (1986) and W. Carr (1988) suggested the caldera is divided into two parts. The northern part of the caldera, the Prospector Pass caldera segment, is believed to be the source of the Tram member of the Crater Flat Tuff. The larger Crater Flat caldera is believed to be the source of the Bullfrog and Prow Pass members of the Crater Flat Tuff. Evidence for the caldera complex includes: (1) the semicircular shape of the southern part of Crater Flat; (2) the large compound gravity low of Crater Flat (nearly 50 mGal) which is inferred to be produced by an infilled compound caldera depression; (3) the distribution and thickness of the individual members of the Crater Flat Tuff; (4) the presence of local Miocene dike systems in Bare and Yucca Mountains that may represent ring dikes of the caldera complex; (5) the presence of a thick local wedge of monolithologic breccia, resembling collapse breccia, in the upper part of the Bullfrog member near the south edge of Crater Flat; and (6) the truncation in Crater Flat of a persistent east/west aeromagnetic anomaly.

M. Carr and Monsen (1988), Hamilton (1988), Scott (1990), and Fridrich and Price (1992) summarized arguments against an origin of the Crater Flat depression as a caldera complex. The primary arguments are several. First, the facies variations of the Crater Flat Tuff do not appear consistent with a caldera source in Crater Flat. Second, the stratigraphic sequence noted in VH-1 and VH-2, particularly the absence of a break between the Prow and Bullfrog members of the Crater Flat Tuff, are inconsistent with the presence of a caldera in southern Crater Flat. Third, the gravity data indicate the Crater Flat basin extends in the subsurface southward beyond the southern physiographic margin of the Crater Flat and thus is not uniquely associated with the proposed caldera structure. Fourth, intrusive dikes inferred to follow the ring-fracture zone and mark the margin of the calderas may simply follow local basin-range structure.

W. J. Carr extended his concepts of the tectonic setting of the YMR and attempted to accommodate his caldera models with models of detachment faulting (Carr 1990). He suggested the YMR is split by a north-trending volcano-tectonic rift that encompasses several coalesced caldera complexes. The proposed rift represents a pull-apart or a right-stepped zone of rifting in the larger Walker Lane structural system. Carr (1990) suggests the rift became a breakaway zone for detachment faulting to the west. To the east, the normal faults are probably not associated with a recognized major detachment system. The importance of this proposed rift, the Kawich-Greenwater rift (Carr 1990), is its structural trend.

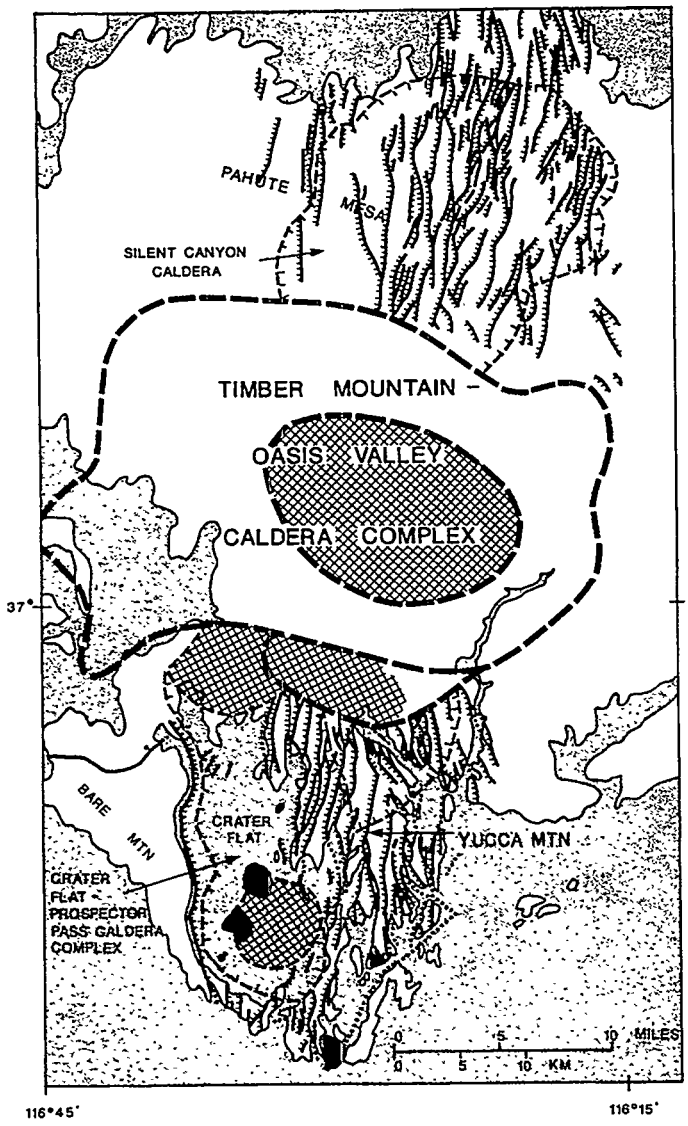


Fig. 3.5 Proposed caldera complexes and the distribution of Quaternary basaltic volcanic rocks of the Crater Flat area (modified from Carr 1990). Snyder and Carr (1984), Carr and Parrish (1985), Carr et al (1986) and Carr (1982, 1984, 1988, 1990) propose that the southern part of Crater Flat is underlain by the Crater Flat caldera and the northern half of the Crater Flat basin is a segment of the larger Prospector Pass caldera. The Pliocene and Quaternary volcanic rocks of Crater Flat occur in the moat zone and across the resurgent dome of the proposed Crater Flat caldera. One center is located in the Prospector Pass caldera segment. The cross-hatured areas are the inferred resurgent parts of the caldera complexes (after Carr, 1990) and the black areas are Quaternary basalt centers (see Chapter 2 for identification of individual Quaternary basalt centers).

The rift, or structural trough, trends north/south from the Greenwater Range, on the east flank of southern Death Valley, through the Yucca Mountain area to Kawich Valley (Carr 1990) (Fig. 3.6). This proposed rift zone obliquely spans part of the Walker Lane structural zone in the southern Great Basin and encompasses the Yucca Mountain site. The rift could provide a controlling structure for the location of the past and possibly future occurrences of basaltic volcanic rocks in the YMR.

The important characteristics of the Kawich-Greenwater rift include (all from Carr 1990):

1. It is identified structurally on the north and south by aligned caldera complexes and by closely spaced sets of north-to-northeast-trending faults that offset the ignimbrite sheets. These fault systems may be distinguished by their close surface spacing and the geometry and distribution of offset of the Timber Mountain Tuff. Part of the fault system is exposed in a northeast zone extending across Pahute Mesa. An inferred related fault zone extends through Yucca Mountain (Carr 1990, his Fig. 6).
2. The west side of the rift is structurally more abrupt than the east, forming an asymmetrical graben structure.

3. The axis of the rift, particularly on the south side, may be marked by a diffuse gravity low in the regional Bouguer gravity map.
4. Volcanism occurred along the length of the rift, primarily during the Miocene. Large-volume eruptions associated with caldera centers in the YMR concluded with the eruption of the Timber Mountain Tuff and associated units about 11.5 Ma. Tectonic activity in the area diminished markedly since the termination of silicic eruptions. The southern part of the rift was active about the same time as the northern rift, but silicic eruptions continued in the latter until about 5 Ma.
5. The Kawich-Greenwater rift lies near and parallel to a regional volcano-tectonic feature called the Death Valley–Pancake Range basalt belt (Carr 1984), a zone marked by basaltic volcanism of primarily Pliocene and Quaternary age.
6. Faults of the Yucca Mountain area are inferred not to be detachment faults but are related instead to gravity sliding into a topographic low formed by a graben structure in Crater Flat.
7. The presence of Pliocene and Quaternary basalt in the Crater Flat area indicates the ". . . process of rifting may be continuing but at a very much reduced rate and probably under a different stress regime than in the Miocene" (Carr 1990, p. 290). These basalts are inferred to have followed ring-fracture zones of calderas at depth and diverted to northeast-striking tension fractures as they neared the surface.

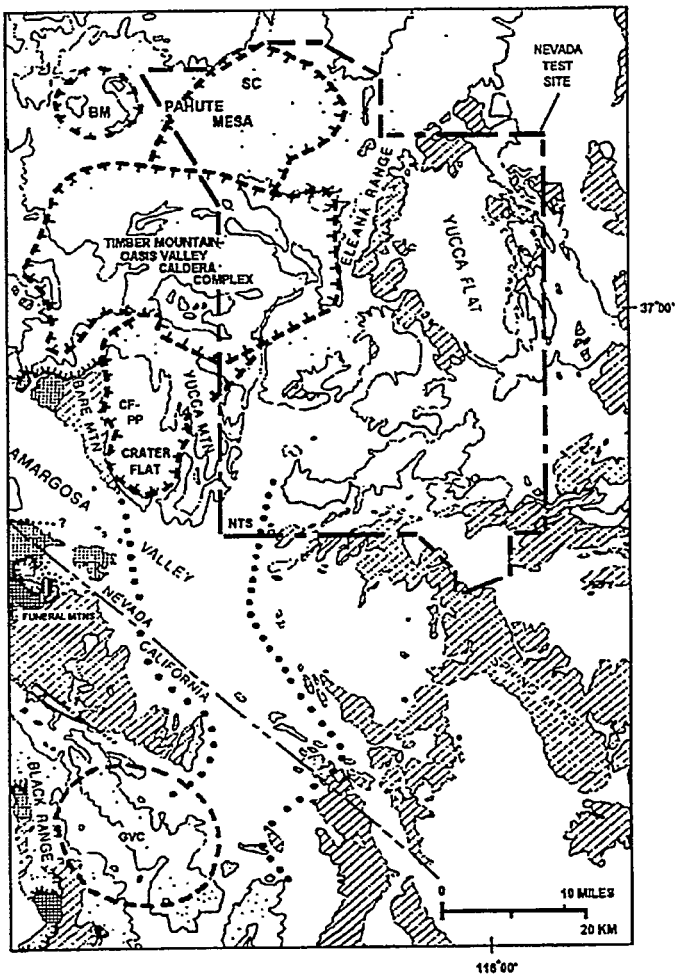


Fig. 3.6 Kawich-Greenwater rift zone (after Carr 1990). The zone is marked by an alignment of coalesced caldera complexes of the TM-OV caldera complex. It extends south across the Amargosa Valley into the Death Valley area of California.

An additional and alternative model of the tectonic setting of Yucca Mountain involves episodes of older strike-slip faulting. Wright (1987) argues that detachment systems typical of the Death Valley area are not regional features. He suggests instead that they are unconnected systems that were bounded originally by strike-slip faults. The timing and style of development of low-angle detachment faults by this model are dependent on the history of faulting of individual basins; the detachments are not of regional extent.

Wright (1987) infers that the Crater Flat basin may be the north part of a zone of pull-apart basins called the Amargosa Desert Rift Zone (ADRZ). This structure encompasses a series of structural blocks bounded by segments of strike-slip faults connected by en echelon, obliquely oriented normal faults (Fig. 3.7). The primary evidence in support of this rift is threefold. First, a series of gravity lows is inferred to define pull-apart basins extending to the south and southeast of Crater Flat (Wright 1987). Second, pull-apart basins associated with extensional and strike-slip faulting have been documented in other adjoining

areas of the Basin and Range (Death Valley, Emigrant Valley). Third, northwest-trending faults of the Pahrump Valley area may be still active strands of basin-bounding, strike-slip faults.

Pull-apart activity based on the Wright model (1987) may have begun in the YMR as early as 14 to 16 Ma. This activity was replaced in time by predominantly normal faulting. The Crater Flat basin, with associated sites of volcanic activity, could represent a northern segment of the ADRZ. A strike-slip component of the late Miocene (<12.4 Ma) basin development is suggested by the rotation of the Tiva Canyon member, as inferred from paleomagnetic data (Rosebaum et al. 1991). The Wright (1987) model shares some common features with the Kawich-Greenwater rift model of Carr (1990). A key difference is that the Wright model attributes basin formation primarily to tectonic processes; volcanic activity may be only subsidiary to tectonic activity. The Carr model relates development of the northern part of the Kawich-Greenwater rift zone to volcanic process with tectonic activity secondary. The models overlap and are in agreement largely for the south part of the proposed rifts. Both models emphasize development of tectonic rifts or pull-apart zones south of Crater Flat extending to Death Valley (Wright 1987; Carr 1990). Wright (1987) suggests that the ADRZ may not connect with the southern Death Valley volcanic field but instead with a pull-apart basin formed in Pahrump Valley. Carr (1990) extends the Kawich-Greenwater rift into the volcanic and pull-apart basins of southern Death Valley. The most marked differences in the rift models are for the origin of the Crater Flat basin. Carr (1990) maintains that the creation of the Crater Flat depression is from caldera collapse associated with cycles of ash-flow eruption. He notes, however, that the caldera collapse may have been contemporaneous with or modified by rifting and graben formation.

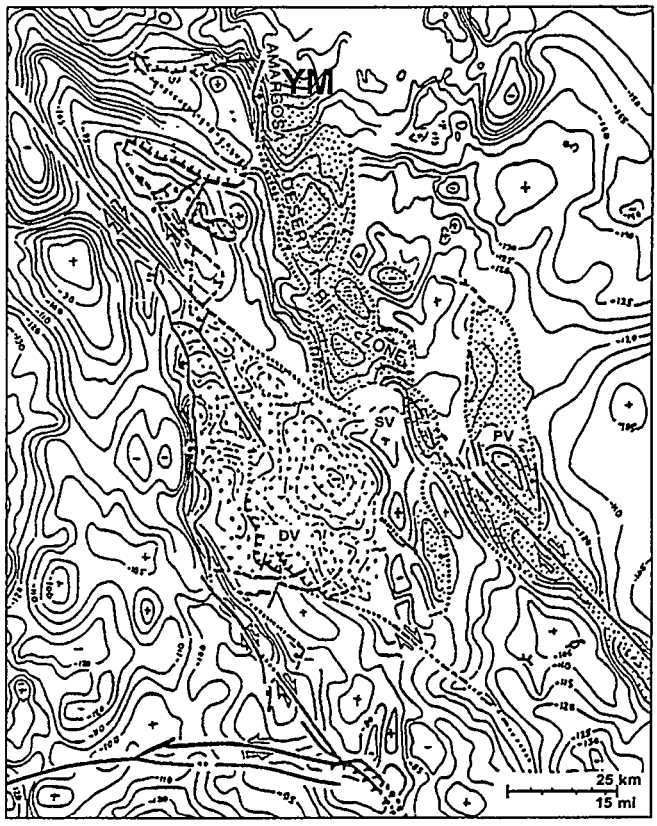


Fig. 3.7 ADRZ superimposed on the Bouguer gravity map (modified from Wright 1987). The rift zone extends from Crater Flat on the north, south-southwest across the Amargosa Valley, and bifurcates into the Stewart Valley (SV) and Pahrump Valley (PV) basins, and the central Death Valley plutonic-volcanic field (DV). The YM is the location of the exploratory block of Yucca Mountain.

The absence of distinctive magnetic anomalies in or beneath the alluvial fill of the Amargosa Valley suggests the proposed pull-apart basins of the valley were not accompanied by eruption of voluminous volcanic rocks (Kane and Bracken 1983; Wright 1987). Wright suggests the timing of development of the basins of the Amargosa Valley is pre-Paintbrush (>13 Ma). His arguments are based on the geologic relations of the Crater Flat–Prospector Pass caldera and a K-Ar age of 13.2 Ma for an ash found in sedimentary fill near Ash Meadows.

A related but slightly different origin for the Crater Flat basin was inferred by Schweickert (1989). He proposed the presence of a buried right-slip fault that transects the southern Amargosa Valley and Crater Flat basin. A cumulative offset of about 26 km was inferred along the fault zone from an inferred offset of a distinctive overturned fold-thrust system of Mesozoic age. The lack of surface expression of the fault lead Schweickert (1989) to suggest that activity on the fault predates the Paintbrush Tuff. He argues,

however, that the clockwise rotation of the Tiva Canyon member may indicate continued shear strain along the fault. Schweickert (1989) notes further that the strong northwest-trending alignment of the Quaternary volcanic centers (CFVZ) may mark the surface projection of the fault trace. This model is largely compatible with a pull-apart origin of Crater Flat. However, the strike-slip model of Schweickert (1989) requires only a single strike-slip fault. The rift model of Wright (1987) requires that the basins of the rifts formed by movement on a combination of en echelon northwest-trending faults. The latter interpretation is more consistent with the gravity data of southern Crater Flat and the Amargosa Valley. Both areas show distinct zones of northwest-trending gravity lows outlining en echelon basins (Wright 1987).

A modification of the pull-apart models was presented by Fox and Carr (1989). They suggested that the resumption of basaltic magma in Crater Flat about 3.7 Ma marked a renewed episode of extensional tectonism in the Yucca Mountain area. The eruption sites of the basalts were inferred to coincide with an axis of extension and crustal pull-apart between east-dipping faults of Bare Mountain and west-dipping faults of Yucca Mountain. O'Neill et al. (1991) described evidence of strike-slip faulting and oroclinal bending of Yucca Mountain. They suggested, on the basis of fault geometry, fault offsets, and paleomagnetic data, that formation of strike-slip, pull-apart basins on scales of meters to kilometers may be an ongoing process. Both the Fox and Carr (1989) and the O'Neill et al. (1991) models require extension and pull-apart formation to be an active process, albeit much reduced from an earlier episode of Miocene extension. Fridrich and Price (1992) and Fridrich et al. (1994) provided expanded data on the origin of Crater Flat based on new surface mapping. They note that the basin is bounded on the south by a northwest-trending, right-slip fault and possibly to the northeast by an inferred right-slip fault beneath Yucca Wash. Fridrich and Price (1992) note increased faulting and tilting of the volcanic sections bordering Crater Flat and suggest the basin formed from intermittent tectonism from about 15 to < 1 Ma. They suggest the Crater Flat basin formed by synchronous east/west extension and north/west right-slip forming a half-rhombochasm. New geologic mapping and geophysical data have strengthened evidence of the pull-apart model of Fridrich and Price (1992). This work is in progress and only preliminary results were available during the final editing of this volcanism status report. This new work relates the alignment of Pliocene and Quaternary basalt centers and sites of Miocene basaltic volcanism with a zone of distributed dextral shear that accommodated the differential extension along a half graben formed during the opening of Crater Flat.

Multiple tectonic models have been proposed and will continue to be proposed for the Yucca Mountain site and the basins flanking the Yucca Mountain site. Individual models have different implications for the distribution of basaltic volcanism in the region. No attempt is made to discriminate the most likely or most favored tectonic model for the structural setting. Instead every model is evaluated for its effect on probabilistic volcanic risk assessment. The tectonic models described in Chapter 3 are used directly in assessments of spatial and structural models of E2, the probability of a future volcanic event (intrusive or eruptive) intersecting a potential repository or the repository system (see Chapter 7). The development and assessment of tectonic models will continue through multiple iterations of probabilistic volcanic risk assessment through the full process of site characterization studies.

V. Tectonic Setting: Time-space Patterns of the Distribution of Basaltic Volcanism

This section of Chapter 5 examines the distribution of basaltic volcanic rocks in the region by defined basaltic episodes (Crowe 1990; see also Chapter 2, this report) and attempts to relate the time-space patterns of volcanism to the described tectonic models of the YMR.

A. Silicic Episode

The distribution of the oldest sites of basaltic volcanism, the BSE is shown in Fig. 3.8. Two major distribution patterns are exhibited by this basalt episode: (1) spatial associations with caldera complexes, and (2) distribution parallel to the Walker Lane structural zone.

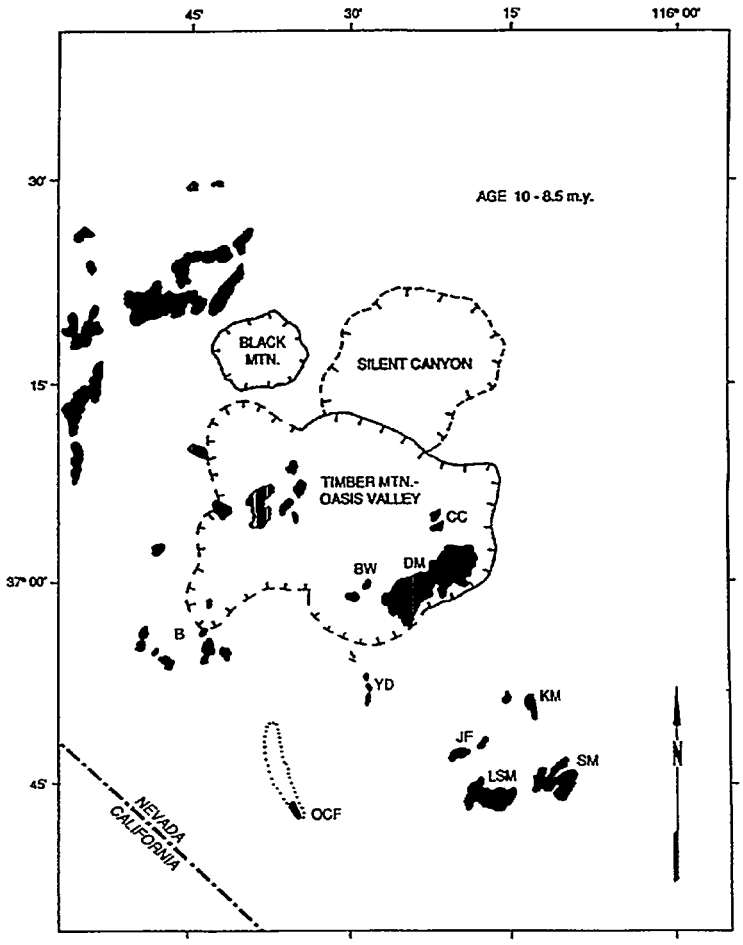


Fig. 3.8 Distribution of the BSE. CC: basalt of Cat Canyon, DM: basalt of Dome Mountain, BW: basalt of Beatty Wash, B: basalt of the Beatty area, SM: basaltic andesite of Skull Mountain, LSM: Little Skull Mountain, KM: mafic rocks of Kiwi Mesa, JF: basalt of Jackass Flat, YD: dike of Yucca Mountain, OCF: older basalt of Crater Flat (modified from Crowe 1990).

Many of the basalt units of the BSE occur in or on the flanks of the large caldera complexes of the TM-OV caldera complexes (Fig. 3.8). The basalt of Dome Mountain was erupted in the moat zone of the Timber Mountain caldera and basaltic volcanic rocks crop out along the western caldera segments of the TM-OV (Fig. 3.8; see also Chapter 2). Basaltic volcanic rocks are present on both the north and south flanks of the Black Mountain caldera. These rocks underlie and overlie the Thirsty Canyon Tuff. An extensive sequence of basaltic volcanic rocks is present in the subsurface along the west, south, and southeast margins of Crater Flat (Kane and Bracken 1983; Crowe et al. 1986). These basaltic rocks were penetrated in VH-2 (Carr and Parrish 1985). The basalt lavas may have erupted along the ring-fracture zone of the proposed Crater Flat–Prospector Pass caldera (Carr 1990). Alternatively, the basaltic rocks may have erupted in a strike-slip bounded, pull-apart basin. The presence of the basaltic volcanic rocks is permissive with either model. However, the age difference between the inferred caldera-related ignimbrite (Crater Flat Tuff; 14 Ma) and the basalt units (11 to 11.5 Ma) is more consistent with a pull-apart model of the Crater Flat basin. North/south-trending basalt dikes dated at 10 Ma (Scott 1990; Carr 1990) are exposed along the Solitario Canyon fault at the northwest edge of the Yucca Mountain site (Fig. 3.10). The dikes are inferred by Carr (1984) to follow the eastern edge of the Crater Flat–Prospector Pass caldera. Alternatively, as noted by Scott (1990), the dikes may follow basin-range faults.

The basaltic volcanic rocks of Little Skull and Skull Mountains (10 Ma) (Crowe et al. 1983a) exhibit no obvious relationships to caldera complexes. They occur on the south and southwest flanks of the 15 Ma Wamonie-Salyer volcanic center. However, the age difference between the volcanic groups (10 Ma versus 14 Ma) suggests they are unrelated. Scattered volcanic rocks thought to correlate with the BSE have

been reported in drill holes in the Amargosa Valley (Brocher et al. 1993). The relatively subdued aeromagnetic signature of the Amargosa Valley suggests these basaltic rocks are not associated with major accumulations of volcanic rocks.

The BSE is inferred to represent the ending phase of a major pulse of silicic volcanism associated with the TM-OV. The close association in space and time between silicic and basaltic magmatism strongly suggests the magmatic events are related. Incursion of basaltic magma into the interior parts of the TM-OV suggests the underlying silicic magma was sufficiently solidified to allow propagation of basalt magma through the chamber. A waning phase of basaltic volcanism has been recognized at the terminal stages of volcanism at many silicic centers in the southwest United States (for example, Bailey et al. 1976; Crowe et al. 1979).

B. Postcaldera Basalt

The distribution of the Postcaldera basalt (PCB) is more restricted spatially compared to the distribution of the BSE. The latter basalt units (BSE) occur in a broadly distributed, slightly northwest-elongate band extending across a large part of the YMR (Fig. 3.8). In contrast, the PCB occurs at spatially scattered localities including two northwest-trending bands, the CFVZ and a northwest-trending zone east of Frenchman and Yucca Flats (Fig. 3.9). The contrasting distribution of the basalt episodes is consistent with the close association in time between the BSE and the waning stage of silicic volcanism. Basalt magma of moderate volume was erupted around the flanks of and locally in the caldera complexes in response to the waning thermal pulse that produced the large-volume silicic volcanism. In contrast, basalt units of the PCB are markedly smaller in volume and more restricted spatially. The volume decrease and lack of temporal or spatial association with the caldera complexes are consistent with the PCB representing a phase of basaltic volcanic activity that is unrelated to Miocene volcanism of the SWNVF (Crowe 1990). Volcanic rocks of the OPB occur north and northeast of the Yucca Mountain site (Fig. 3.9). In contrast, all basalt centers of the YPB, except one unit, the basalt of Buckboard Mesa, occur west, south, and northwest of the Yucca Mountain site (Figs. 3.9, 3.10).

Boundaries between the two basalt cycles of the PCB can be drawn differently using different approaches. The most direct and simple approach is to draw a boundary by visual inspection to delineate the distribution areas of the two cycles. This boundary (Fig. 3.10) is a curving line that trends approximately west/northwest and separates geographically the PBC. A second approach assumes structural control of the distribution of the basaltic volcanic centers. Northwest-trending boundaries between the basalt cycles are drawn in Fig. 3.9. These boundaries assume the distribution of the units is controlled by structural features of the Walker Lane zone (Crowe and Perry 1989). The boundaries between the cycles, as drawn, delineate northeast and southwest zones that overlap in the area of the Timber Mountain caldera (Fig. 3.9). These spatially separate zones are consistent with a southwest migration or more correctly, a southwestward stepping, through time of the areas of basaltic activity (late Miocene to Quaternary; Crowe and Perry 1989; Crowe 1990). Note that the northwest-trending boundaries are not drawn solely from the distribution of basaltic volcanic rocks. Instead the *orientation* of the lines is defined from inferred northwest-trending structural features of the Walker Lane structural zone and the distribution of Cenozoic volcanic rocks in the SWNVF (Carr 1984; Crowe 1990). The *location* of the lines is however, constrained from the distribution of the volcanic centers of the PCB.

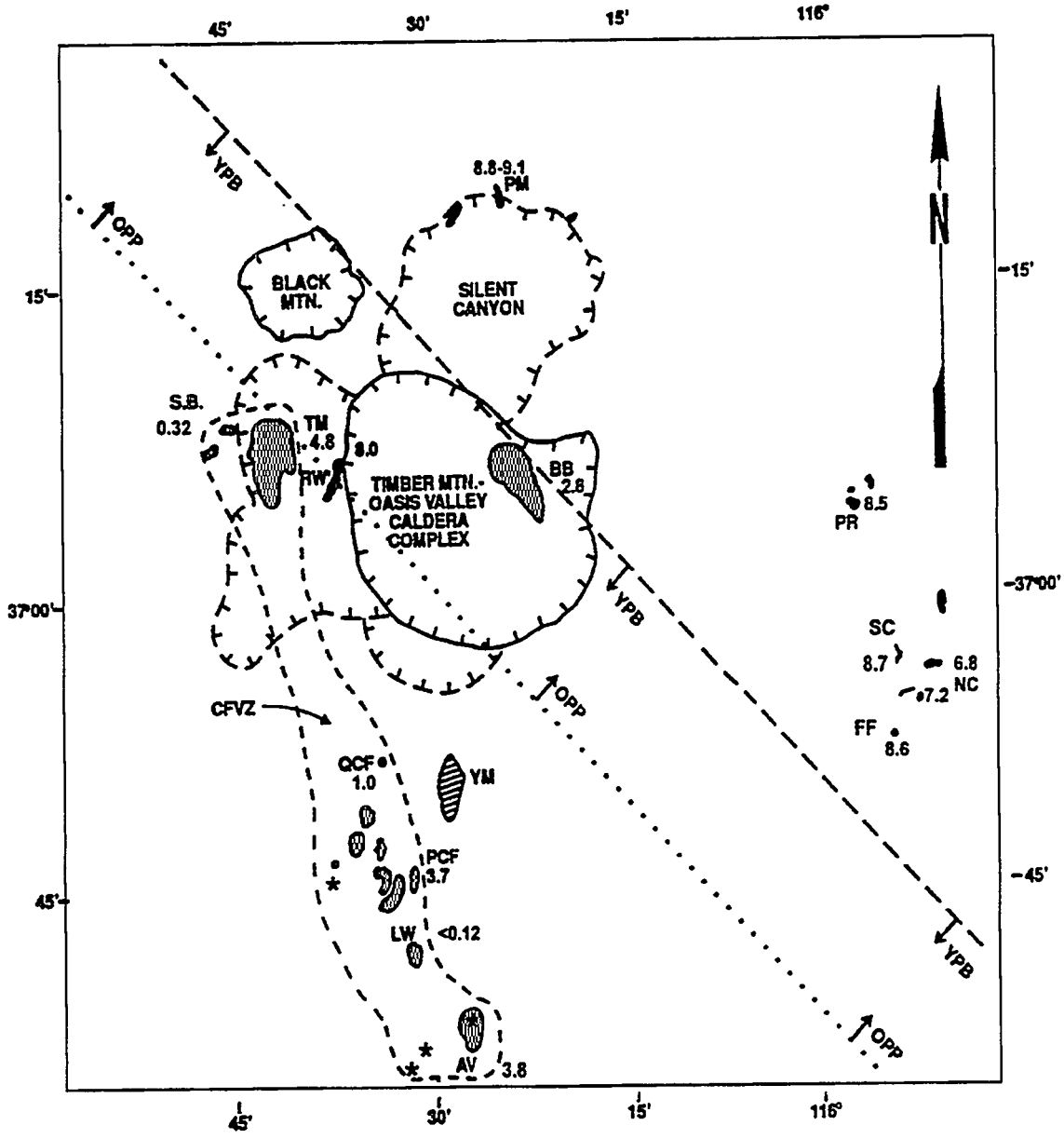


Fig. 3.9 PCB of the YMR. Black-filled areas are the volcanic units of the OPB and YPB including: RW: basalt of Rocket Wash, PM: basalt of Pahute Mesa, SC: basalt of Scarp Canyon, NC: basalt of Nye Canyon, TM: basalt of Thirsty Mesa, AV: basalt of Amargosa Valley, PCF: Pliocene basalt of southeast Crater Flat, BB: basalt of Buckboard Mesa, QCF: Quaternary basalt of Crater Flat, SB: basalt of Sleeping Butte, LW: basalt of Lathrop Wells. Asterisks mark aeromagnetic anomalies identified as potential buried basalt centers or intrusions (Kane and Bracken 1983; Crowe et al. 1986). Dashed line encloses the area of the CFVZ. Numbers associated with the symbols for the OPB and YPB are the age of the volcanic centers in million years. The northwest-trending lines subdivide the OPB and the YBP into southwest and northeast fields with the boundaries following structural features of the Walker Lane structural system. Modified from Crowe and Perry (1989).

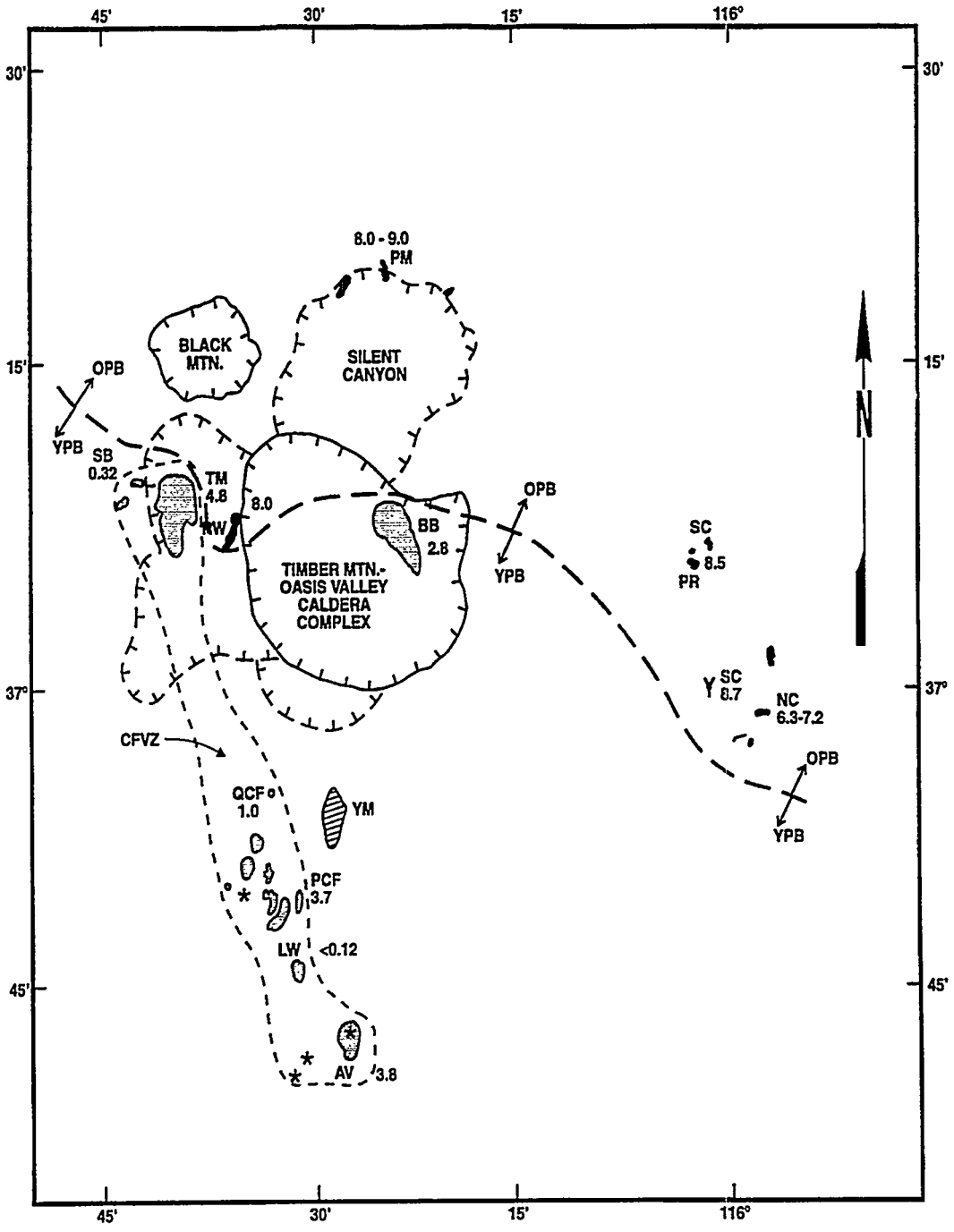


Fig. 3.10 Alternative geographic subdivisions of the PCB episode of the YMR. Symbols and numbers are the same as in Figure. 3.9. The thick dashed line is a line drawn visually that separates the OPB and the YPB. The OPB occur entirely north and east of the Yucca Mountain site. The YPB, except for the basalt of Buckboard Mesa (BB), is located south, west, and northwest of the Yucca Mountain site.

A third approach, which is independent of underlying assumptions, is to use statistical tests to examine different models of the time-space distribution of basaltic volcanic centers of the PCB. If there are no temporal or spatial differences in the cycles, the statistical descriptors of the PCB should be nondiscriminatory. If there has been time and/or spatial migration, the distributions should be distinctive. Figure. 3.11 is a histogram plot of the ages of the volcanic events of the PCB. The ages of volcanic units of the PCB were established from existing age determinations (see Chapter 2). The number of assigned ages for each unit corresponds to the number of volcanic events for each cycle, where an event is a discrete volcanic center (see Chapter 7). This approach uniformly weights volcanic centers and is a more suitable approach than examining the distribution of individual K-Ar age determinations. The histogram shows the distribution of estimated ages for the PCB is bimodal with peaks in event ages at about 8–9 and 3–4 Ma. A two-sample t-test rejects the null hypothesis that the means are similar for the basalt cycles with a p-value of <0.0005.

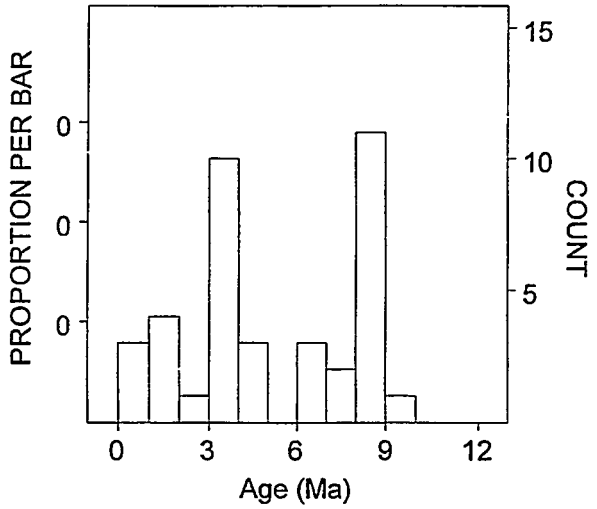


Fig. 3.11 Histogram of ages for the PCB of the YMR. The number of ages assigned to the PCB is equated to the number of volcanic centers, not individual K-Ar age determinations. The histogram shows a bimodal distribution with peaks at 3–4 and 8–9 Ma. A two-sample t-test rejects the null hypothesis that the means are similar for the basalt cycles with a p-value of <0.0005.

Figure 3.12 is a plot of the locations by latitude and longitude of the volcanic centers of the PCB, separated by basalt cycles. The centroid of each distribution is calculated at the 90% confidence limit using a Gaussian ellipsoid approximation for the distributions. The plot shows that the distribution centroids of the basalt cycles are distinct spatially. A west/northwest-trending ellipse is calculated for the centroid of the OPB. It is located in the northeast edge of the Timber Mountain caldera (Fig. 3.12). A spatially separate centroid is drawn at the 90% confidence limit for the basalt units of the YPB (Figure 3.12). This ellipse is centered in Crater Flat. For comparison, the calculated centroid of all basalt vents of the PCB is also drawn on Fig. 3.12. This centroid is located in the south-central part of the Timber Mountain caldera. It bears no spatial relationship to the distribution of the basalt centers. The location of the centroids of the basalt distributions are based on the variance in the X and Y coordinates of the vents assuming a Gaussian spatial distribution. This distribution assumption is probably not correct but the uncertainty introduced by the assumption is small and would not lead to rejection of the conclusion that the distributions of volcanic centers for the basalt cycles of the PCB are distinctively different.

C. Older Postcaldera Basalt

Basalt centers of the OPB show close spatial and temporal associations with sites of extensional faulting. The vents for the basalt of Rocket Wash are located on a north/south-trending basin-range fault that follows the approximate location of the ring-fracture zone of the Timber Mountain caldera (Lipman et al. 1966; O'Connor et al. 1966). The three spatially separate eruptive centers of the basalt of Silent Canyon all occur on the Silent Canyon ring-fracture zone where it is intersected by northeast-trending basin-range faults (Orkild et al. 1969). Erosion has cut into these centers exposing feeder dikes. These dikes all trend northeast, paralleling the basin-range faults. These field relations are consistent with the shallow rise of magma along or coparallel to the basin and range faults (Orkild et al. 1969).

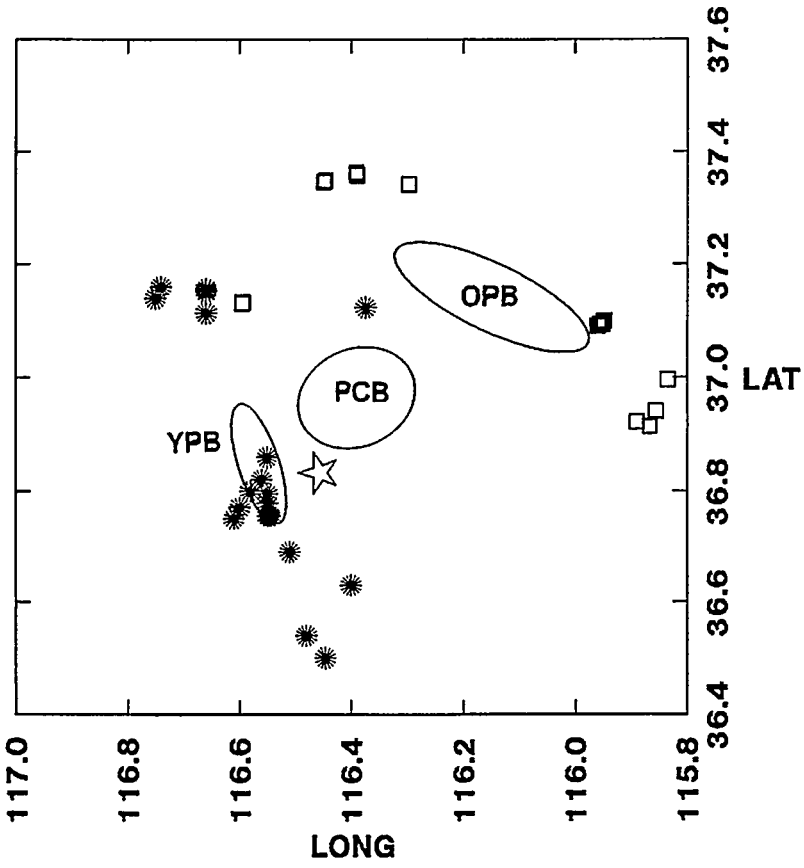


Fig. 3.12 Location of the distribution centroid by basalt cycle for the PCB. The centroid for each basalt cycle was calculated using the bivariate ellipse module of SYSTAT. The OPB label identifies the centroid for the OPB located near the intersection of the northeast part of the Timber Mountain and southwest part of the Silent Canyon calderas. The YBP label identifies the centroid for the YPB located in Crater Flat. The centroid labeled PCB is the composite centroid for the two basalt cycles and is located in the southeast part of the TM-OV complex. It is a meaningless centroid because of the difference in ages and spatial distribution of the basalt cycles. Square symbols are the locations of vents of the OPB; asterisks mark the vents of the YPB. The large star is the location of the Yucca Mountain site.

The basalt of Paiute Ridge occurs as a complex of basalt dikes, sills, and discordant intrusions with local preservation of surface lava flows and scoria cones (Byers and Barnes 1967; Crowe et al. 1983a; Valentine et al. 1992). Multiple sets of dikes locally fed intrusions that follow northwest-trending basin-range faults. At several localities, the dikes are offset by the northwest-trending faults. These relations require that the basaltic magmatism closely accompanied extensional faulting (Crowe et al. 1983a).

The basalt of Scarp Canyon consists of 3–4 km, generally north/south-trending basalt dikes that locally follow northwest-trending extensional faults (Hinrichs and McKay 1965). The dikes expand into probable conduit plugs near the intersection of northwest- and north-trending faults.

The basalt of Nye Canyon, the youngest basalt cluster of the PCB, does not appear to follow existing bedrock structure. It comprises an aligned set of four northeast-trending basalt centers. These centers are parallel to the maximum compressive stress direction, the most likely direction of dike propagation in the modern stress field (Crowe et al. 1983a, Zoback 1989). This represents the first occurrence of a change in the structural-parallel patterns of the basalt centers of the OPB, a change that has persisted for the YPB. Thus, the basalt of Nye Canyon is significant for two reasons. First, it is the oldest basalt cluster that exhibits a northeast trend of age-correlated, aligned basalt centers. Second, it is the only basalt unit of the OPB that crosscuts and appears to have formed independently of the prevailing shallow bedrock structure.

D. Younger Postcaldera Basalt

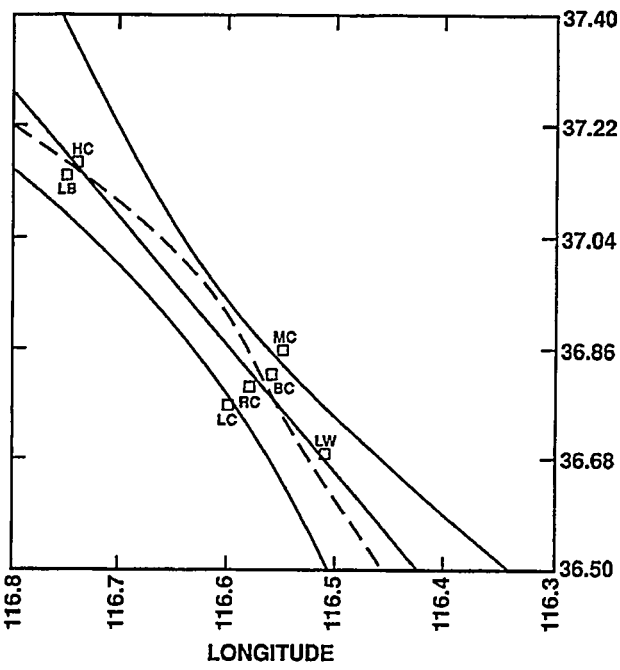
Crowe and Perry (1989) described the patterns of distribution of volcanic centers of the PCB. They noted several spatial trends. First, basalt centers of the OPB and the YPB tend to form in northwest-trending zones parallel to structures of the Spotted Range–Mine Mountain section of the Walker Lane structural belt (Carr 1984). The northwest-trending alignments of centers is best expressed by the distribution of basalt centers for the YPB. All centers of this cycle, except the basalt of Buckboard Mesa, occur in a narrow northwest-trending zone that was named the CFVZ (Fig. 3.9). Second, the time-space distribution of the PCB is consistent with a southwest-directed stepping of sites of basaltic volcanic activity through time. Third, basaltic activity of the PCB tends to occur as clusters of volcanic centers where the centers form distinct aligned clusters and appear to be of similar ages. Finally, Crowe and Perry (1989) and Crowe et al. 1993 noted that there were no systematic time-space patterns to the distribution of volcanic events *within* the CFVZ.

There has been an increased effort in recent years to develop more quantitative methods for assessing patterns of alignment of volcanic vents or centers in volcanic fields (for example, Hasenaka and Carmichael 1985; Lutz 1986; Wadge and Cross 1988). Connor (1990) and Connor et al. (1992) have summarized applications using a range of bivariate methods to assess patterns in the distribution of vents in volcanic fields with high vent densities. The advantages of these methods are twofold. First, they provide quantitative and testable methods for identifying spatial patterns. Second, the methods can often distinguish random alignments from those produced by underlying structural or mechanistic controls (Wadge and Cross 1988; Connor et al. 1992). Connor (1990) used cluster analysis to search for natural groupings in the spatial distribution of over 1000 scoria cones in the TransMexican volcanic belt. He demonstrated that there is significant structure in cone distribution and used multiple methods for assessing vent alignments to reveal vent orientations within clusters.

A major difficulty with applying existing methods of evaluating distribution patterns of volcanic centers in the YMR is the limited number of centers. Additionally, and partly because of the limited number of volcanic centers, there is an increased amount of data available for each volcanic center in the YMR (location, age, volume, composition). Thus, evaluation of spatial patterns of volcanic centers can be extended to multivariate space, where the limited data become even more restrictive. We use the term cluster to describe the distribution of volcanic centers in the YMR differently than Connor (1990). Volcanic clusters in the YMR are identified as spatially aligned groups of volcanic centers with *similar ages* (see Chapter 2). The clusters are identified as events where an event is the formation of a spatially and temporally distinctive volcanic center or clusters of centers of similar ages. The orientations of the age-grouped clusters are north to northeast, parallel to the maximum compressive stress direction in the region. This strongly suggests that the stress field controls the elongation of the clusters, and individual centers of the clusters are fed by dikes that *parallel* the maximum compressive stress direction. An important feature of the distribution of basalt centers in the YMR is a northwest alignment of the distribution of volcanic centers (Crowe and Perry 1989). This alignment cannot be tested with approaches using the two-point azimuth (Lutz 1986) or the Hough transform methods (Wadge and Cross 1988) because of the small number of data points. However, linear regression can be used to test the degree of linearity in the distribution of the centers recognizing that the alignment could be fortuitous. Figure 3.13 shows a calculated best-fit line using least-squares linear regression of the locations of major eruptive vents (main scoria cone of volcanic centers) for the Quaternary basalt centers of the YPB. The vents are plotted by their latitude and longitude coordinates. The distribution of basalt centers of the YPB (excluding the basalt of Buckboard Mesa) fit closely a linear model. The linear regression line passes through the Lathrop Wells center. It bisects the cluster length of the Quaternary basalt of Crater Flat, passing between the Red Cone and Black Cone centers and the Little Black Peak and Hidden Cone centers (Fig. 3.13). The hyperbolic

bands around the regression fit line are the confidence intervals for the linear regression. They are the intervals shown at a 90% confidence limit for the *location* of the regression line. Also shown on Figure 3.13 (dashed curve) is the distance weighted least squares fit of the data set. The curve was fitted to the data using a weighted quadratic multiple regression fit that flexes for each data point and provides a simple visual test of the suitability of a linear model. Note that the distance weighted least squares deviates only slightly from the linear regression fit (Fig. 3.13). Figure 3.14 is a linear regression fit that includes the locations of all Pliocene and Quaternary basalt centers of the CFVZ. The aeromagnetic anomaly south of the town of Amargosa Valley is shown on Figure 3.14, but not the aeromagnetic anomalies in the central Amargosa Valley, which have not been drilled. The linear regression fit is similar to the line of Figure 3.13, except the northwest part of the line is offset to the northeast from the addition of the data points for the basalt of Thirsty Mesa. The hyperbolic bands are as noted in Figure 3.13, the 90% confidence bands for the location of the linear regression curve. The bands are narrower than the regression calculation using only the Quaternary centers. The dashed curve of Figure 3.14 is the distance-weighted least squares regression fit of the data set. The curve becomes nonlinear on the southeast end where its geometry is affected by the buried basalt center located south of the town of Amargosa Valley.

An additional striking feature of the CFVZ is noted by combining magma volume (dense rock equivalent) as a third variable with the location coordinates of the Quaternary and Pliocene basaltic centers. Figure 3.15 is a three-dimensional plot of these attributes for the Quaternary basalt centers of the CFVZ. The linear regression line of Figure 3.13 coincides spatially with a northwest-trending zone marking the location of the largest-volume volcanic centers. Stated differently, the volcanic centers with the largest



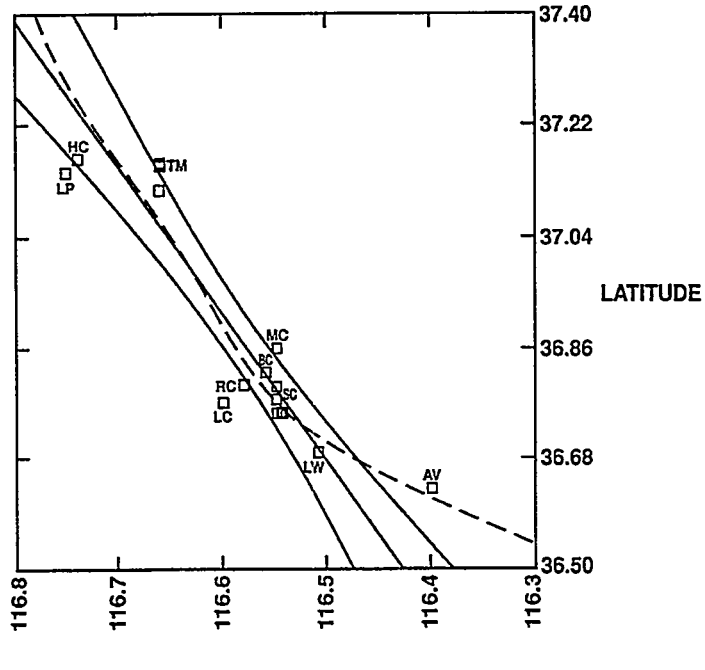


Fig. 3.13 Least squares linear regression fit of the distribution of Quaternary basalt vents of the CFVZ. The straight line is the best fit regression line; the parabolic curves enclosing the regression line are the 90% confidence intervals for the location of the regression line. The dashed line is a distance weighted least squares line. LW: Lathrop Wells center; LC: Little Cones center, RC: Red Cone center, BC: Black Cone center, MC: Makani Cone center, LP: Little Black Peak center, HC: Hidden Cone center.

Fig. 3.14 Least squares linear regression fit of the distribution of Pliocene and Quaternary basalt centers of the CFVZ. Lines and symbols are the same as in Figure 3.13 with several additions including: AV: aeromagnetic anomaly south of the town of Amargosa Valley, SE: 3.7 Ma basalt of southeast Crater Flat, TM: Pliocene basalt of Thirsty Mesa.

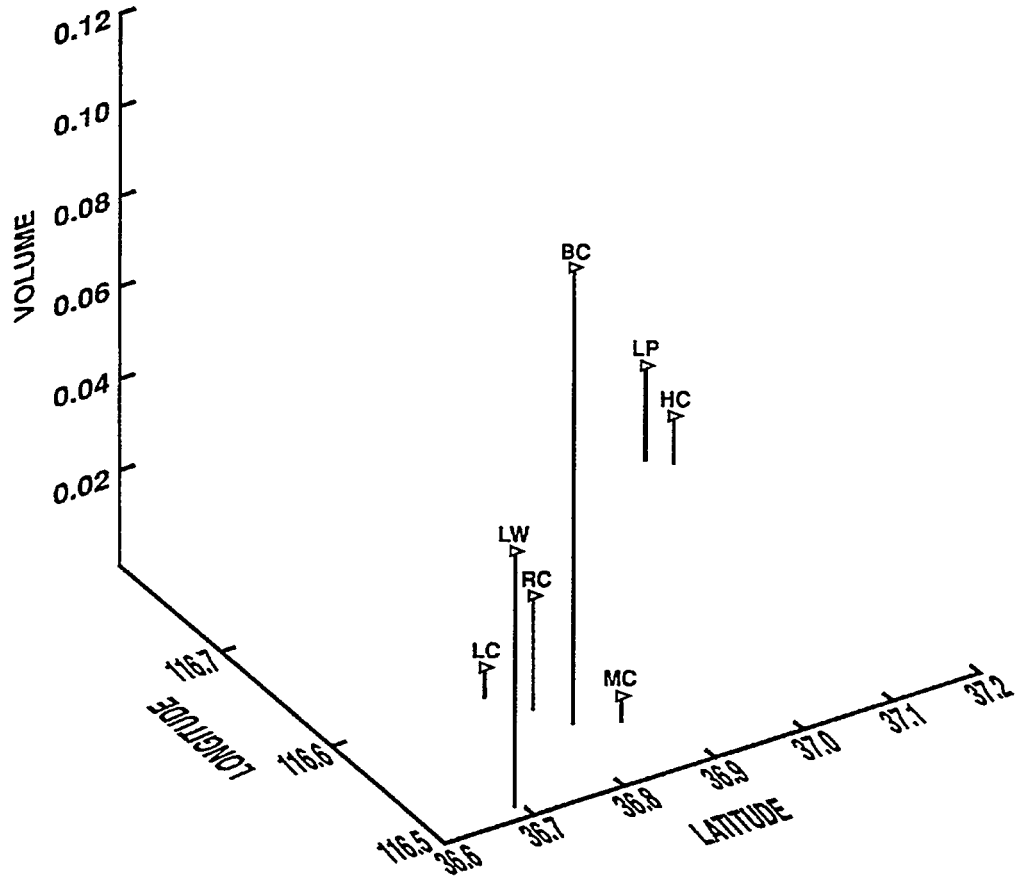


Fig. 3.15 Three-dimensional plot of magma volume versus location of the Quaternary basalt centers of the CFVZ. Symbols are the same as in Figure 3.13. The triangles denote the volume of the vent locations and the spikes connect the data points to the latitude/longitude plane.

eruptive volumes tend to occur on or adjacent to the regression line; volcanic centers located away from the regression line tend to have decreased eruptive volumes. This observation supports the inference that the location of basalt centers is controlled by a northwest-trending structure. The observed volume/location relationship of the volcanic centers remains consistent even with the addition of Pliocene volcanic centers to the data set of Figure 3.15. Figure 3.16 is a three-dimensional plot of the volume and location coordinates of the Quaternary and Pliocene basalt centers of the CFVZ. There are two differences between this plot and Figure 3.15. First, the volume of basalt centers follows an exponential distribution; the data are best displayed by plotting the log of the magma volume. Second, closely spaced basalt centers are plotted as single data points because it is impossible to identify the magma volume components of individual vents. This applies to the basalt of Thirsty Mesa and the 3.7 Ma basalt of southeast Crater Flat. The volume/space relationship of Figure 3.16 can be viewed more readily by plotting the data as a surface. Figure 3.17 is the fit of a surface to the volume/location data using distance weighted least squares where the stiffness parameter for the fit is the inverse of the number of cases ($1/n$). The surface defines a northwest-trending ridge that coincides with the location of the linear regression and distance weighted least squares fits of the location data. These data support permissively the inference that the subsurface rise of magma was guided by an existing northwest-trending structural feature. However, these conclusions are limited by the small number of data points, and the data are more restrictive for the volume axis of the surface fit than the latitude and longitude axes.

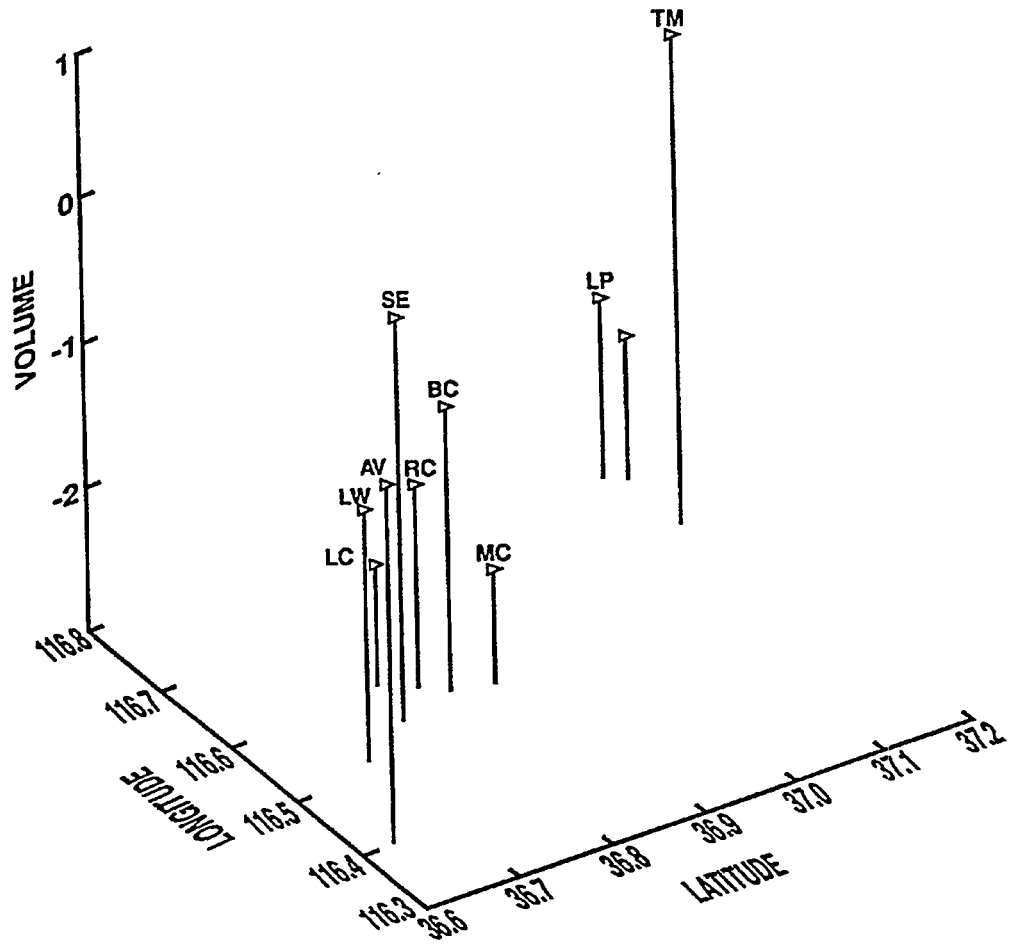


Fig. 3.16 Three-dimensional plot of the log of the magma volume versus the location of Pliocene and Quaternary basalt centers of the CFVZ. Symbols are the same as in Figure 3.14; construction of the plot is the same as in Figure 3.16. The addition of the location and magma volumes of the Pliocene volcanic centers maintains the same volume/distribution relationship noted in Figure 3.15.

An important implication of these speculations is that magma rising as dikes may reorient at shallow depths below Crater Flat. The northwest elongation of the CFVZ (Crowe and Perry 1989) suggests that rising magma probably followed northwest-trending faults or fault. However, at shallow depths the dikes must have diverged from the faults and followed the maximum compressive stress direction. This is required by the secondary north-northeast elongation of individual basalt clusters. This requires a 90° reorientation (northwest to northeast) of the feeder dikes at depth. The most logical site for this structural reorientation is probably at the density interface beneath Crater Flat between the Paleozoic rocks and the Cenozoic volcanic rocks and/or alluvial fill of the basin.

The final important structural property of the basalt centers of the YPB is their relationship to shallow faults in the Yucca Mountain area. The 3.7 Ma basalt centers of Crater Flat and the basalt of Thirsty Mesa are aligned north/south. These trends parallel the trend of local faults displacing the lava flows of the basalt of Thirsty Mesa. The eruptive fissure and scoria cone of the basalt of Buckboard Mesa are oriented northwest. The fissure system may parallel approximately the ring-fracture zone of Timber Mountain, or it may follow unexposed structures of the Walker Lane structural zone (Crowe 1990). The scoria cone of the basalt of Buckboard Mesa is also located at the intersection of an en echelon set of north-

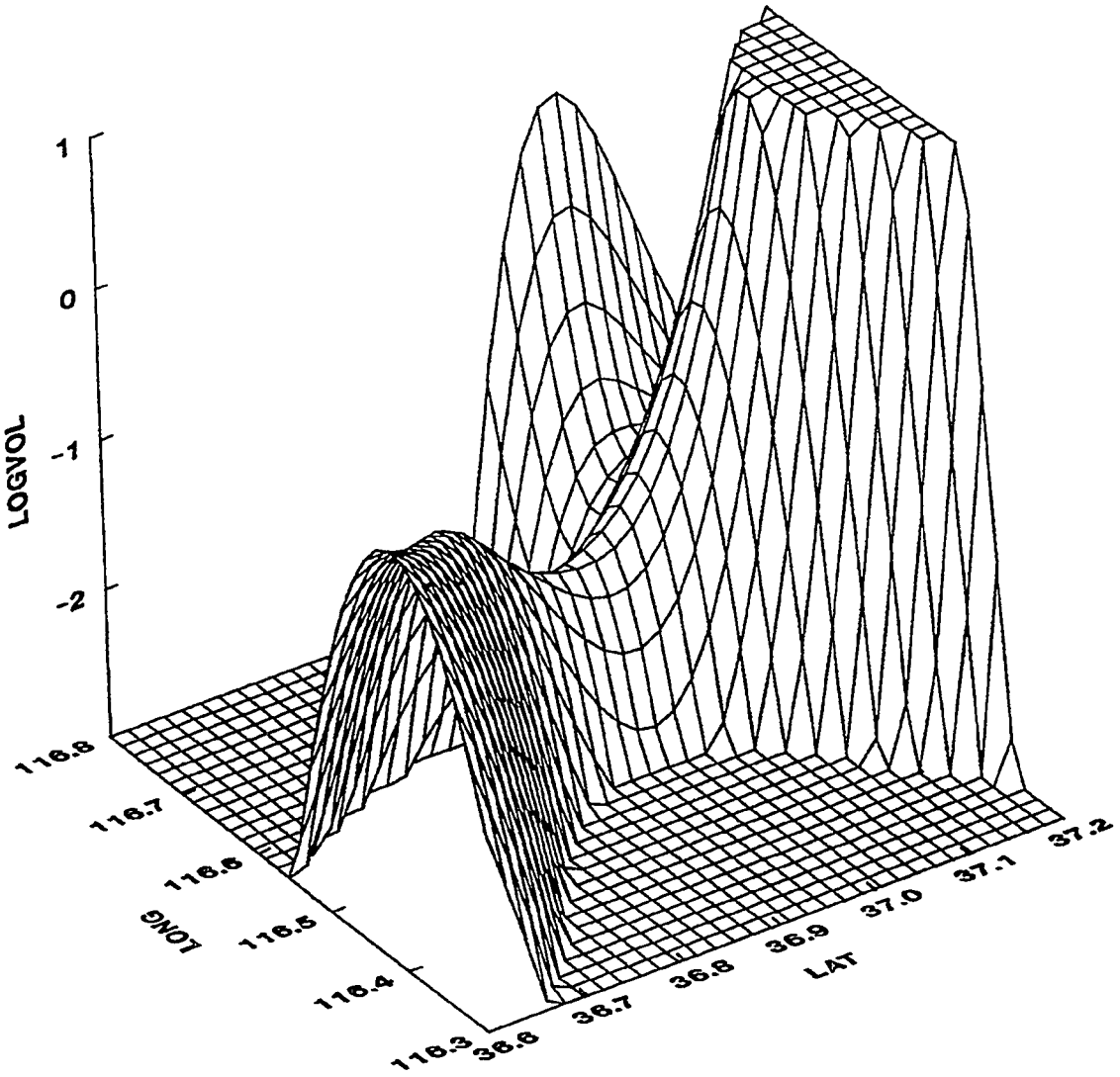


Fig. 3.17 Distance-weighted least squares surface fit of the volume/location data of the Pliocene and Quaternary basalt centers of the CFVZ. This plot provides a more easily visible illustration of the northwest trend of the volume location surface for the basalt centers. This surface parallels the trend of the linear regression fit for the location of the basalt centers. This surface bifurcates at its northwest end because of the spatial separation of the Sleeping Butte and Thirsty Mesa basalt centers. The flex of the surface is controlled by a tension parameter of $1/n$ where n is the number of volcanic centers. The surface was constructed with the hide option of the surface fitting routine and conceals parts of the surfaces which should not be visible.

northeast trending normal faults that displace the lava flows of the center. The location of the vents may have also been influenced by the presence of these structures.

By contrast, the Quaternary basalt centers show no systematic or consistent relationship to bedrock faults. The Quaternary basalt cluster of Crater Flat trends northeast across the basin. Smith et al. (1990) argue that these trends follow bedrock faults of Yucca Mountain because of the subparallel trend of aligned basalt centers with the trend of faults. However, none of the basalt centers occur along mapped traces of faults. Moreover, there is a surprising lack of a spatial association between the Quaternary basalt clusters of Crater Flat and the Bare Mountain fault, one of the major faults in the region. The basalt of Sleeping Butte forms a northeast-trending alignment that does not follow any obvious bedrock structural control (Crowe and Perry 1991). The Lathrop Wells volcanic center occurs at the approximate intersection of the

northeast-trending Stagecoach Road fault and northwest-trending faults that may correlate with the Windy Wash fault (Crowe et al. 1992b). These trends are paralleled by the trend of fissure vents in the center.

VI. Geophysical Studies: Yucca Mountain Region

A wide range of geophysical data have been obtained for the YMR; more studies are in progress (Oliver et al. 1992). In the next section we discuss aspects of the geophysical data and the constraints these data place on models of the distribution of basaltic volcanism in the YMR. The geophysical data for the YMR compliment the abundant regional geophysical data for the Great Basin subprovince of the Basin and Range province.

A. Seismic Studies

Seismic studies have constituted a major part of the site characterization studies since the earliest stages of investigations. A 47-station vertical-component seismic network was installed within a 160-km radius of Yucca Mountain in 1979 (Rogers et al. 1987). A six station supplemental mini-net was deployed on Yucca Mountain in 1981. This net lowered the detection threshold and improved the accuracy of the location of earthquakes near the Yucca Mountain site (Rogers et al. 1987). Horizontal component instruments were deployed at selected stations in 1984. This network, called the southern Great Basin seismograph network (SGBSN) (Rogers et al. 1981, 1983, 1987; Mermonte and Rogers 1987; Gomberg 1991a, 1991b; Harmsen and Bufe 1992), was designed to locate and study properties of earthquakes for a region containing tectonic features of possible significance to seismic risk assessment for the YMR. Tectonic features of regional interest (not all of which are significant for seismic risk assessment for Yucca Mountain) were reviewed by Carr (1984). They include the Death Valley–Furnace Creek fault zone and extension along the Fish Lake Valley fault zone, the east/west seismic zone (Smith and Sbar 1974; Smith 1978), the Nevada-California seismic zone, and the Nevada Test Site Paleoseismic belt that now would be called the Kawich-Greenwater rift (Carr 1990).

Rogers et al. (1987) summarized earthquake hypocenters, selected focal mechanisms, and other inferred seismicity characteristics through 1987. Conclusions from this report are:

1. Earthquakes are distributed in an east/west zone generally coincident with the east/west seismic zone.
2. Earthquakes display strike/slip and normal/slip over a depth range from near-surface to 10-15 km consistent with seismic patterns of much of the Great Basin. There is an apparent preference for right/slip on north-trending faults. Left/slip is also observed on north-northeast striking faults.
3. Earthquakes are consistent with a northwest-trending orientation of the least principal stress axis, which is rotated clockwise relative to surrounding regions (Carr 1974; Zoback 1989).
4. Earthquake clusters are difficult commonly to associate with specific faults although epicenter alignments and earthquake nodal planes are frequently subparallel to fault trends (Hildenbrand et al. 1988, Fig. 2.3).
5. A seismicity minimum may be observed between depths of 3.5 to 4.0 km.
6. Earthquake energy release per unit area is lower in the immediate Yucca Mountain area compared to regional levels. This may be attributed to low stress from tectonic uncoupling or significant prehistoric seismic energy release. Alternatively, the area could be a seismic gap with high stresses and locked faults. Rogers et al. (1987) summarized several lines of evidence supporting seismic uncoupling but noted that other interpretations are possible.

There is no evidence of a positive correlation between recorded seismicity and the distribution of Quaternary basaltic centers in the Yucca Mountain area. In fact, there may be evidence of a negative correlation of seismicity with sites of Quaternary volcanism in Crater Flat (see discussion below). Increased seismicity has occurred in the Pahranagat Shear Zone (Rogers et al. 1987) near an area of basaltic volcanism (Ekren et al. 1977). However these lavas are of Miocene age and the correlation is not significant for probabilistic risk assessment for the Yucca Mountain site. Two cautions must accompany any discussion of historic seismicity and the spatial distribution of basaltic volcanism. First, the period of recording of earthquake locations is very short relative to the recurrence rate of basaltic volcanic events. The latter is on the order of several hundred thousands of years (Crowe et al. 1992a). Second, patterns of historic seismicity may not be good predictors or indicators of future sites of Quaternary basaltic volcanism. Basalt magma probably ascends rapidly through the crust. While the ascent may be facilitated or guided by fractured rock, these pathways need not necessarily be correlated with areas of historic seismicity.

Gomberg (1991a) reviewed the seismicity patterns and the detection and location threshold of the SGBSN. She derived a spatially varying model of the detection/location capabilities of the network based on empirical relations and statistics. She used several validation tests for the model and showed that the threshold map accurately predicts the observed distribution of epicenters for all magnitude bins. This approach permits use of most of the earthquake catalog and allows evaluation of the completeness level of each subroutine. Gomberg (1991a) used the threshold model to develop a series of magnitude independent masks that were overlaid on patterns of seismicity and Quaternary faults. She identified several areas as active because they exhibit the greatest number of events at all magnitudes. These are the north end of the Furnace Creek fault, the Paranagat Shear Zone, and the north and southeast parts of the Nevada Test Site. Gomberg noted that there is an absence of seismicity at Yucca Mountain. She discussed the same causes of low seismicity as Rogers et al. (1987) but noted that seismic models predict a minimum in shear strain at Yucca Mountain. Additionally, she drew attention to relatively low levels of seismicity west of the Death Valley–Furnace Creek faults despite an abundance of young fault scarps indicative of recent tectonic activity.

In a companion paper, Gomberg (1991b) evaluated seismicity and shear strain in the southern Great Basin focusing on identifying information that can be obtained from the distribution of earthquakes in an area with long intervals between large earthquakes. She developed strain-field models assuming the long-term behavior of faults perturbs an otherwise uniform strain field. An important conclusion developed from the models is that a complex distribution of seismicity with off-fault locations is expected. These traits match the seismicity recorded by the SGBSN (Rogers et al. 1987; Gomberg 1991a). Gomberg (1991b) developed a boundary element representation of faults with historic or Holocene displacement that she used as input to the shear strain field. Modeled faults in the Yucca Mountain area were the Bare Mountain fault, the Rock Valley fault system, and the Yucca Flat fault. She assumed a maximum extension direction of N 52° W and regional displacement vector orientation of N 34°W. Results show that the highest shear strain areas, south and east of Yucca Mountain, are regions of observed high seismicity. The model showed a lack of shear strain in the north part of the Nevada Test Site. The high seismicity of this area may be induced by underground explosions from testing of nuclear weapons (Gomberg 1991b, pp. 16, 392). The seismic gap in the Yucca Mountain area is coincident with a region of modeled lowest shear strain. Parsons and Thompson (1991) suggested this feature could result from volume release associated with active magmatism (see models of Shaw 1980). Gomberg (1991b) suggests that the best explanation of the low seismicity in the Yucca Mountain area is that it is not an area of significant seismic hazard. The simple shear model also showed a rotational component of the regional deformation field, possibly compatible with paleomagnetic studies (Hudson and Geissman 1991; Rosenbaum et al. 1991). Additional iterations of the

shear model were used with slip distributions assigned to fault systems (Gomberg 1991b; Figure 11). Results were not dissimilar to the simple shear model.

The most recent update to the SGBSN studies were by Harmsen and Bufe (1992), who summarized seismic data through 1989. They noted the development of a concentration of earthquakes in the Reveille Range. They also discussed the difficulties of obtaining accurate data for earthquake hypocenters and the ambiguity this creates for focal mechanism solutions.

To summarize, seismicity studies of the YMR offer limited potential for evaluating patterns of future basaltic volcanic activity, an unsurprising result given the long recurrence time of basaltic volcanic events. One interpretation of the seismic gap noted for the Yucca Mountain area is stress release associated with Quaternary basaltic volcanism (Parsons and Thompson 1991). Alternatively, the shear models of Gomberg (1991b) suggest the gap may simply represent an area of low shear strain accumulation. Both models are compatible with the seismic record of the region.

B. Gravity Investigations

Gravity investigations were begun in the Yucca Mountain area as early as 1978. About 33,000 gravity measurements have been made. All have been adjusted to a common gravity datum and recompiled (Oliver et al. 1992). Complete Bouguer gravity maps have been published of the Nevada Test Site (Healey et al. 1987), Death Valley (Healey et al. 1980a), Goldfield (Healey et al. 1980b), Caliente (Healey et al. 1981), and Las Vegas (Kane 1979) sheets. A residual gravity map of Yucca Mountain and vicinity has been produced by Snyder and Carr (1982). The free-air, Bouguer, regional, residual and isostatic residual gravity maps have been compiled for the YMR (Hilldenbrand et al. 1988). A 1:100,000-scale isostatic gravity map of the Nevada Test Site that covers an area northeast of Yucca Mountain was published in 1990 (Oliver and Fox 1993).

Snyder and Carr (1982, 1984) summarized the volcano-tectonic setting of the YMR based largely on gravity data. They summarized interpretations of more than 2500 gravity measurements on an approximately 2-km, irregular grid. In their original work, Snyder and Carr (1982), analyzed the complete Bouguer gravity anomalies using a crustal density of 2.67 $g \cdot cm^{-3}$. They reduced the data a second time at a density of 2.0 gcm^{-3} to compensate for gravity stations within lower-density volcanic terrain. They applied an isostatic correction assuming Airy-type isotasy to remove effects of density variations deeper than 5 km. Density control was provided by density measurements of core samples and surface samples. These data were augmented by gamma-gamma and borehole gravity measurements in several drill holes (Snyder and Carr 1984). Further, they used a two-dimensional model from an east/west cross section, and a three-dimensional multiple-polygon gravity model.

The most distinctive feature of the regional gravity field is a gravity high associated with Bare Mountain that is connected with a larger gravity high over the Funeral Mountains. This high probably delineates the Funeral Mountain–Bullfrog Hills–Bare Mountain detachment complex (Hamilton 1988; M. Carr and Monsen 1988; Oliver and Fox 1993). It is interrupted only by a gravity saddle across the area of the Amargosa River, a probable result of thick accumulation of clastic sediments of the Amargosa Valley (Snyder and Carr 1984). A second gravity high, the Calico Hills gravity anomaly, coincides with the area of the Calico Hills and probably extends to the southwest beneath Busted Butte. Snyder and Carr (1984) interpret this gravity high as the product of a shallower depth to Paleozoic rocks, possibly augmented by a fault zone of pre-Paintbrush age near Busted Butte.

An additional major feature is a large gravity low, defined by the 8-mGal residual gravity contour (Snyder and Carr, Fig. 4c). This low is centered in Crater Flat but also extends east partly under Yucca Mountain and south into the Amargosa Valley. Snyder and Carr (1984) interpret this low as a combination of sector grabens and caldera collapse associated with the eruption of the Crater Flat Tuff. A permissive alternative explanation of these data is the gravity low is the result of a thick accumulation of clastic alluvial fill deposits in a series of pull-apart basins marking Crater Flat and extending to the south. Neither model can be discriminated solely on the basis of the gravity data. Moreover, it is possible the Crater Flat basin could be a composite volcano-tectonic depression. The base of the caldera or alluvial section in Crater Flat is estimated to be about 4 ± 2 km from gravity modeling or between 2 and 4 km based on seismic refraction (Snyder and Carr 1984, pp. 10, 204).

A narrow band of gravity highs separates the negative gravity anomalies of Crater Flat and the Claim Canyon and Timber Mountain caldera segments to the north (Snyder and Carr 1984). These highs are bounded to the north by a large gravity low associated with the Timber Mountain and Silent Canyon calderas (Snyder and Carr 1984).

Gravity models confirm that Crater Flat is a large topographic and structural basin. It is bounded on the west by the fault-controlled, steep escarpment of Bare Mountain and the basin extends to the east under at least part of Yucca Mountain. The gravity data have been interpreted as supporting a caldera model for Crater Flat. One alternative model, that Crater Flat is a structural depression formed at the intersection of the Bare Mountain fault and an inferred west-dipping, low-angle detachment fault or faults beneath Yucca Mountain, has also been shown to be consistent with gravity data (Oliver and Fox 1993). The combination of the depth of the structural basin and the small volume of Pliocene and Quaternary basaltic rock, makes gravity models of limited use in delineating the structural controls of the basalt units. However, the prominent gravity low of Crater Flat suggests the basaltic rocks may have followed or been influenced by structures associated with this basin. If Crater Flat is a caldera complex, it is somewhat surprising that the basaltic rocks erupted across the caldera floor. By comparison, the basalt centers of Silent Canyon and the basalt of Buckboard Mesa occur on the ring-fracture zone of, respectively, the Silent Canyon and Timber Mountain caldera complexes. An important corollary of the caldera hypothesis is that basalt centers might be expected to follow the ring-fracture zone of the suspected calderas. The observation that multiple episodes of Pliocene and Quaternary basaltic volcanic activity do not occur on the inferred ring-fracture zones is a departure from the expected patterns if Crater Flat is a caldera depression. Equally, if Crater Flat formed as a result of combined detachment faulting and movement on the Bare Mountain fault, neither structure shows strong correlations with and do not appear to have controlled the distribution of Pliocene and Quaternary basalt centers.

C. Magnetic Investigations

A wide variety of aeromagnetic and ground magnetic data have been obtained for the YMR (Oliver et al. 1992). Draped aeromagnetic profiles were flown with spacing of 0.4 and 0.8 km for a large area surrounding Yucca Mountain extending from Pahute Mesa, south to southern Death Valley, west to beyond Bare Mountain, and east into Frenchman and Yucca Flat (Oliver et al. 1992, Fig. 2.2-1). This area covers most of the terrain of interest for tectonic and volcanic studies in the YMR. Compiled maps of these areas were presented by Hildenbrand et al. (1988). Kane and Bracken (1983) described aeromagnetic anomalies in the Yucca Mountain area and surrounding region. Surface basaltic volcanic rocks have strong magnetic contrasts with surrounding rocks, particularly the alluvial fill of the valley basins. They can be correlated with a high degree of confidence with positive or negative anomalies on the aeromagnetic map, dependent on the polarity of the surface rocks (Kane and Bracken 1983). Langenheim et al. (1991; 1993) presented

aeromagnetic data for part of the Amargosa Valley. They described gravity and ground magnetic data collected for studies of the aeromagnetic anomalies in the valley.

Crowe et al. (1986) described aeromagnetic anomalies in Crater Flat and the Amargosa Valley that may represent buried volcanic centers or intrusive rocks. Exploratory drilling at two sites has penetrated buried basalt lavas which correlate with recognized surface anomalies (Crowe et al. 1986; Crowe et al. 1992b); a third basalt site was penetrated in an exploratory hole by a private company (see Chapter 2). Two, possibly three, aeromagnetic anomalies remain to be drilled as part of the site characterization program. Langenheim et al. (1991; 1993) summarized geophysical data for an anomaly site about 25 km south-southeast of the Yucca Mountain site. They constructed alternative two-dimensional magnetic models to fit the anomaly. They suggested the maximum depth of the top of a magnetic body was less than 150 m below the alluvial surface and presented evidence that the anomaly is most likely a basalt center overlying and buried in alluvium. These conclusions were verified through exploratory drilling (see Chapter 2).

Magnetic anomalies near the potential repository site have been described by Bath and Jahren (1984). These investigations were conducted primarily to evaluate buried geologic units or structures beneath the potential site area. A tabular mass of sedimentary rock was noted beneath thick deposits of the volcanic units. Major faults of the site were outlined from their displacement of the magnetized volcanic rock. The Topopah Springs member of the Paintbrush Tuff was identified as the primary source of anomalies from faulted sequences of volcanic rock. An east/west pattern of anomalies was identified. However, the amplitudes of these anomalies were reduced significantly when effects of the deeply buried argillite unit were removed. More detailed drape aeromagnetic data were obtained for parts of the Yucca Mountain site (Bath and Jahen 1985). These studies detected a prominent magnetic anomaly of 290 nanotesla located about 1 km northwest of USW H-3. Ground magnetic traverses were run to delineate the identified anomaly. Three contributing sources were assessed (Bath and Jahren 1985). First, elevated topography across the Solitario Canyon declivity gives a terrain effect. Second, ground anomalies south of the drape air anomaly indicate either an increase in magnetization or the presence of a small intrusive body. Third, there is an increase in magnetic influence from the adjacent Solitario Canyon fault. One possible interpretation of this anomaly is that it may be related to a 10-Ma basalt dike that intrudes the Solitario Canyon fault (Crowe et al. 1983a); Scott 1990; Carr 1990). In fact, the anomaly may represent a small intrusive body of basalt composition (dike or sill) emplaced off the main trace of the fault (Bath and Jahren 1985, p. 15). This body should be investigated as part of site characterization studies.

There is a sufficient amount of magnetic and aeromagnetic data to place a relatively high degree of confidence in the judgment that all significant sites of Quaternary volcanic activity have been identified in the YMR. All known Quaternary volcanic centers in the YMR are exposed conspicuously as topographic features. Two identified aeromagnetic anomalies remain to be drilled. One is located in southern Crater Flat, the second is located in the Amargosa Valley. Because basalt scoria cones and lava flows as old as 3.7 Ma are prominently exposed at the surface in Crater Flat, it is unlikely that the remaining anomalies are buried parts of former surface basalt centers of Quaternary age. Additional aeromagnetic and ground magnetic studies are planned to evaluate the scale of detectability of basalt bodies in alluvium and Cenozoic tuff. The results of past magnetic and aeromagnetic studies suggest that the presence of *undetected* basalt intrusions in alluvial fill or in Paleozoic rocks are unlikely. The latter rocks tend to nonmagnetic and basalt intrusions should be distinguished easily from aeromagnetic data. The studies of core from drill hole VH-1 show that basalt lavas in alluvium at depths of over 300 m were recognized readily from drape aeromagnetic data (Kane and Bracken 1983). Ground magnetic data will be combined with existing aeromagnetic data to examine the magnetic signature of basalt dikes exposed in the Tiva Canyon member along the Solitario Canyon fault. Aeromagnetic data will be obtained for the Miocene basalt centers of Paiute Ridge, Scarp Canyon and Nye Canyon (see Chapter 2). These data will be modeled

and the magnetic signature projected to different elevations above the ground surface to examine the detectability by magnetic methods of basaltic intrusion bodies that range from complex intrusive forms to linear dikes with small conduit plugs.

D. Geoelectric Surveys

Geoelectric surveys have been used at the Yucca Mountain site. Much of the work was completed in the early stages of site characterization. The locations of these surveys are discussed by Oliver et al. (1992). Over 130 Schlumberger soundings have been obtained in an area labeled F on Figure 2.3-1 in Oliver et al. (1992). This area covers the south part of Crater Flat and parts of the Amargosa Valley. These data may prove useful for delineating the structure of Crater Flat and provide independent tests for evidence of subsurface magma. Deep magnetotelluric data show a regional crustal anisotropy aligned with trends of the Walker Lane structural system as well as an apparent midcrustal conductor at approximately 20 km or less (Oliver et al. 1992). This zone could represent pore fluids, elevated temperatures and/or the transition to crustal ductility below the seismogenic zone (Oliver et al. 1992). Additional work will be required to assess the potential application of geoelectric surveys to understanding the structure of Crater Flat and to test for the presence of subsurface magma.

E. Seismic Investigations

Seismic investigations have included both seismic refraction and seismic reflection surveys (Oliver et al. 1992). The most useful application from these investigations is for investigations of upper crustal structure and investigations of the middle, lower crust and upper mantle.

1. Seismic Refraction Surveys. Relevant seismic refraction surveys have included studies utilizing high-explosive (HE) and underground nuclear explosions (UNE) as sources (Hoffman and Mooney 1983). Additionally, high resolution upper-crustal profiles have been conducted in the Yucca Mountain area (Ackermann et al. 1988). Locations of the profiles are shown in Figure 2.4-2 of Oliver et al. (1992).

Refraction studies using UNE and HE sources were conducted with up to 100 portable seismographs arrayed along lines across Yucca Mountain and Jackass Flats, the Amargosa Desert through Crater Flat, and from Yucca Mountain south to southern Death Valley (Hoffman and Mooney 1983). The upper crustal structure in the Yucca Mountain area was inferred from both the seismic P-wave delays and an unreversed refraction profile. Interpretations relied heavily on existing site models, particularly the gravity models of Snyder and Carr (1982). Major points of the seismic refraction surveys are that observed delay times clearly confirm a greater depth to the prevolcanic rocks beneath Crater Flat and Yucca Mountain. Discrepancies were noted between observed and calculated delay times for Crater Flat where the observed delays exceed predicted delays. Hoffman and Mooney (1983) attribute this discrepancy to local thickness variations in the low-velocity tuff rather than a deepening of the pre-volcanic layer. The velocity models show a distinct 2.5-km-wide bench, probably representing a down-dropped block, at a depth of 1.6 km, east of Bare Mountain. Depth to basement was estimated at about 3.2 km below Crater Flat and 1.1 km below Jackass Flat. Shot point 3 recorded a crust-mantle and two intra-crustal reflections (Hoffman and Mooney 1983). These correlate with a reflection from velocity boundaries at 24 km and 30 km depth. The crust-mantle depth was fitted with a reflection from 35 km depth. Significantly, no evidence was noted of reflections from an inferred magma body below the approximate area of the Amargosa Valley (Evans and Smith 1992).

Three additional profiles were acquired in 1985. These include an east/west profile from the northern Amargosa Valley across Yucca Mountain to Jackass Flat, a north-south profile along Fortymile Wash, and an east/west profile across the Amargosa Valley south of Yucca Mountain (Oliver et al. 1992). Summaries of these surveys and data are presented in Sutton (1984, 1985). Final interpretations of the lines have not been completed. The Amargosa line crosses part of the teleseismic anomaly of Evans and Smith (1992) and extends to depths of about 30 km.

2. Seismic Reflection. Seismic reflection studies have been used primarily to examine shallow structure in the Yucca Mountain area. Recently acquired test lines that provide data on the deeper structure (up to 15 seconds) have been run in the Amargosa Valley (Oliver et al. 1992). Brocher et al. (1990, 1993) described the results of a 27-km seismic reflection profile across the Amargosa Valley. The line crossed three Cenozoic alluvial basins. Interpretations of the line were concerned primarily with extensional structures. A laterally continuous, near-flat-lying reflector at 100 to 200 m was interpreted as a basalt flow, a flow that probably is part of the BSE. Brocher et al. (1993) reported a large-amplitude reflection or midcrustal bright spot on the seismic reflection profile. While the reflection could be interpreted as a midcrustal magma body, Brocher et al. (1993) argue that the Amargosa Valley and a similar anomaly in Death Valley are caused by focusing of energy reflected from the midcrust by low-velocity basin fill lying above the bright spot (see also Hamilton 1988).

The seismic reflection profile across the Amargosa Valley demonstrated the feasibility of seismic reflection profiling for the YMR. Plans for seismic reflection profiling across Crater Flat and Yucca Mountain have been described by Hunter et al. (1993). The profiling was shot and data acquired in December of 1994.

F. Teleseismic Studies

Teleseismic topography has been used to explore the three-dimensional seismic properties of the YMR (Iyer 1988; Montfort and Evans 1982). The recent report by Evans and Smith (1992) has the most application to evaluations of volcanic risk for the Yucca Mountain site. While the results of teleseismic tomography can be ambiguous, the method has been the most successful of geophysical techniques used for delineating magma in the crust or mantle (Iyer 1988).

Evans and Smith (1992) described the results of analyzing analog teleseismic data from 1979 to 1980 and digital data collected in 1982. They noted two large velocity anomalies. The first is centered beneath the Silent Canyon caldera and the northern part of the Timber Mountain caldera. The body is present near the depth of the Moho downward to about 200 km. This high-velocity body has been noted in many previous studies (Spence 1974; Montfort and Evans 1982; Taylor 1983). It has been interpreted as the crystallized roots beneath silicic calderas and the depleted "paleo-magma pathway" of the lower crust and mantle below the coalesced calderas. The second anomaly is a velocity low. It is centered south and southeast of Yucca Mountain and Crater Flat (Evans and Smith 1992, Fig. 3). Evans and Smith (1992) suggest this body trends east/west to northeast/southwest. They argue the body may extend to an area of Pliocene and Quaternary basaltic volcanism near St. George, Utah (Dueker and Humphreys 1990). However the connection with that area is not obvious from the data of Evans and Smith (1992, Fig. 3). Humphreys and Dueker (1994a) note that the seismic velocity of the upper mantle of the western U.S. is considerably slower than the upper mantle beneath the North American craton. In a companion paper, Humphreys and Dueker (1994b) infer from *P* wave imaging that upper mantle beneath the continental interior of the western U.S. trends northeast, discordant to tectonic structure but consistent with the distribution of young volcanic activity. They suggest the mantle trends are a consequence of partial melt variations enhanced by compositional variations.

A third significant observation based on the teleseismic tomography is the presence of low-velocity material beneath and east of the Solitario Canyon area (Evans and Smith 1992), probably at midcrustal depths. They argue that this feature is most likely related to an inferred caldera or volcano-tectonic depression in Crater Flat following the model of Carr (1988).

Evans and Smith (1992) suggest the large low-velocity anomaly may be partial melt and represent the source of the basaltic magma that formed the volcanic centers in Crater Flat. They suggest further, that the location of the Crater Flat field is controlled by the intersection of the Walker Lane structural zone and the Spotted Range–Mine Mountain subzone. They infer, again because of the correlation with the data of Dueker and Humphreys (1990), that the low-velocity anomaly forms a track subparallel to the hot-spot vector of the North America plate with volcanic activity at both ends. This track corresponds to the St. George Volcanic Trend (SGVT) of Humphreys and Dueker (1994a,b).

The interpretations of Evans and Smith (1992) are important to an assessment of volcanic risk for the Yucca Mountain site. The low velocity anomaly, if produced by magma, is very large–on a scale approaching the size of continental or oceanic hotspots. It could represent a large heat source possibly capable of generating significant future volumes of presumably basaltic magma. The east/west to north/northeast trend of the proposed anomaly is parallel to volcanic features of the southwest United States that have been interpreted to track motion of the North American plate (Smith and Luedke 1984; Spence and Gross 1990; Humphreys and Dueker 1994a,b). The presence of sites of Quaternary basaltic activity at the ends of the anomaly are analogous to the patterns of magmatism in the Great Basin, which are concentrated at the east and west margins (Best and Brimhall 1974). The tectonic setting of Crater Flat, near the intersection of possible buried northwest-trending strike-slip faults and the zone of northeast-trending left-slip faults may be conducive to the transmittal of magma through the upper crust.

However, when examined in detail, the proposed low-velocity anomaly has inconsistencies with the geologic and geophysical record of the region. Not all of the inconsistencies were considered by Evans and Smith (1992). Multiple lines of evidence are *inconsistent* with a long-lived magma body. The center of the anomaly is south of the Nevada Test Site region where there is no Pliocene or Quaternary basaltic volcanism. This location coincides with the area of the amagmatic gap of the southern Great Basin, an anomalous area that exhibited no Cenozoic volcanism during intense episodes of extension (Guth 1981; Wernicke et al. 1988). Much of the anomaly is located beneath the Las Vegas Shear Zone, a structure proposed by Evans and Smith (1992) to have influenced the shallow rise of basaltic magma. Yet no record of basaltic magma is present anywhere along the length of the Las Vegas Shear Zone. The proposed anomaly overlaps in location with the major step in the regional gravity field, the trend of which partly parallels the low velocity anomaly. Further, this area was probably positioned above a zone of incoherent slab or a slab gap during the period of extension and silicic volcanism to the north (Severinghaus and Atwater 1990). Both the steep gradient in the gravity field and the anomalous subduction history need to be considered in any interpretation of the low velocity anomaly.

Continuing, the shape of the anomaly and its extension to the east and northeast do not appear obvious from the data of Evans and Smith (1992, Fig. 3). The low velocity zone appears to extend more definitively into adjoining areas of Death Valley and southern and southeast Nevada then east into Utah. These former areas, except for southern Death Valley, lack Quaternary volcanism. The volume of surface volcanism associated with the low-velocity anomaly is extremely small. In fact, the total volume of basalt magma erupted in Crater Flat is about 1 km^3 (Crowe et al. 1983b). This is about equal in volume to the basalt of Buckboard Mesa, a 2.9 Ma center formed near the interior of the high-velocity anomaly inferred to be the cooled residuum from magma production and ascent associated with caldera eruptions. These

volumes of magma are trivial to virtually insignificant compared to the volcanic record of other hotspot traces. Detailed time-volume and petrologic studies of the basalt cycles of Crater Flat suggest a history of waning volcanism that appears inconsistent with a large body of partial melt in the lower crust and upper mantle.

There is no recognized surface expression of the low-velocity zone either in the topography or structure of rocks of southern Nevada. If there is truly a large mass of partially molten rock in southern Nevada comparable to a hotspot trace, it could have only formed recently and not modified the shallow crust. Yet there is no modern recognized plate tectonic process inferred to be affecting the southern Great Basin that would logically lead to formation of such a body. It would have to be formed by a secondary upwelling of mantle material long post-dating the time of most intense volcanic and tectonic activity. Isotopic data for the southern Great Basin show it to be an area of preserved lithospheric mantle with no evidence of a significant asthenospheric component (Farmer et al. 1989; Jones et al. 1992).

It is unclear what the effects of the shallow crustal structure of the region have on interpretations of the teleseismic data. The position of the anomaly is within the lower crust and mantle. However, the low-velocity fill beneath Crater Flat and Yucca Mountain must affect the teleseismic data particularly because of the limited resolution at shallow depths. An unexplained inconsistency in the teleseismic data is the absence of a high-velocity zone beneath Crater Flat if the area is underlain by a caldera complex.

Seismic refraction and reflection lines in the Amargosa Valley overlap the north part of the teleseismic low-velocity anomaly. No evidence from these seismic profiles (Brocher et al. 1993) imaged the inferred magma body of Evans and Smith (1992). Finally, perhaps the most compelling argument against the magmatic model of Evans and Smith (1992) is the unusually great depth to the basal horizon of magnetic sources calculated by Blakely (1988). This regional anomaly contrasts markedly with the Battle Mountain high, an area of high heat flow, young volcanism, recent faulting, and shallow basal depth of magnetic sources.

The postulated magma bodies of Evans and Smith (1992) are important but the data are not sufficiently compelling to require priority attention in volcanism studies or major changes in the strategy of conducting volcanism studies. There are several reasons for this conclusion. First, a magmatic origin of the *P*-wave low-velocity zones is not unique–other interpretations are possible. The existence and significance of the presence of low-velocity zones should be cross-checked by other geophysical studies. Second, the presence of low-velocity teleseismic *P* wave travel time residuals in the upper mantle is not unique to the Yucca Mountain setting–these types of anomalies are common throughout the Basin and Range province. The more important issue is whether the development of the teleseismic anomalies are a relatively recent (Quaternary) phenomena and their existence reflects the operation of magmatic processes that are not recorded in the geologic and volcanic record of the YMR. The presence of multiple zones of northeast-trending imaged mantle structure suggest the anomalies developed from regional processes (Humphreys and Dueker 1994a,b). The chronology of volcanic activity in well studied northeast-trending structural zones (Snake River Plains, Jemez Volcanic Zone) show that these zones have been active during a significant part of the Cenozoic; there is no evidence to suggest the zones have developed exclusively in the late Cenozoic. To the contrary, the most compelling segment of the volcanic record that may be consistent with the formation and expression of a major zone of partial melt in the mantle is the Miocene pulse of silicic volcanic activity that formed the SWNVF. There appears to be no compelling reason to suspect that the mantle anomalies in the YMR have developed exclusively in Late Cenozoic time. Thus no firm evidence has emerged why the presence of low-velocity teleseismic zones should invalidate forecasts of future volcanic activity through assessment of the Pliocene and Quaternary volcanic record. Finally, two additional sources of information will be acquired as part of continuing site characterization studies that

will further test models of magma bodies in the YMR. The first is the seismic reflection/refraction line across Crater Flat. The second is a planned upgrade of the seismic network that will provide increased quality of acquired teleseismic data. If any data are obtained supporting the alternative interpretations of the significance of partial melt in the mantle beneath the YMR, further geophysical experiments will be conducted and exploration will be focused on the alternative models.

VII. Tectonic Models of Basaltic Volcanism in the Yucca Mountain Region

This part of Chapter 3 examines and identifies tectonic models of the distribution of basaltic volcanism in the YMR that could be used in assessment of volcanic risk. The models are selected using the background information presented on the tectonic setting of basaltic volcanism in the YMR. We emphasize the evaluation and consideration of multiple alternative models, and do not focus on a single or even a set of preferred models. Tectonic models that can credibly be used to describe the distribution of basaltic volcanism in the YMR are compiled and described briefly. Application of the models to volcanic risk assessment is described in Chapter 7 of this report.

Crowe and Carr (1980) summarized the probable structural controls of sites of basaltic volcanism in the southern Great Basin. They noted the tendency for sites of past basaltic volcanic activity to occur along three features. These are:

1. Basin and range faults,
2. Intersections of basin and range faults with ring-fracture zones of caldera complexes, and
3. Areas of intersection of northwest-trending, right-slip faults and northeast-trending, left-slip faults.

Crowe et al. (1983a) compiled a table of the structural setting of all known sites of Pliocene and Quaternary basalt centers in the southern Great Basin. They described the same patterns of structural controls of basalt centers summarized earlier by Crowe and Carr (1980). Crowe et al. (1983a) suggested there is no consistent and predictable association between sites of basaltic volcanic activity and structural or tectonic features. Rather, they suggest the structural and tectonic features provide the structural pathways for the ascent of basalt magma from depth.

Several points require emphasis before summarizing the volcanic-tectonic models of the region. The Basin and Range province has unquestionably been a site of significant extensional faulting and associated volcanism during Cenozoic time. The region constitutes a major active tectonic province of the North American continent. However, tectonic activity has not continued at uniform levels in all parts of the province. Cenozoic extensional faulting and volcanism of the Basin and Range province exhibit time-transgressive patterns of activity. There is agreement that the major tectonic activity in the YMR occurred in the Miocene and peaked between 12.7 and 11.5 Ma. This latter interval coincides with the time of maximum basaltic volcanic activity. The volume of basaltic magma erupted in the YMR during the Miocene exceeded 10 km^3. The volume of basaltic magma erupted during the Pliocene is estimated at 4.2 km^3. The volume of erupted basaltic magma during the Quaternary in the YMR is <0.5 km^3. The volume of Pliocene and Quaternary basaltic magma erupted in the YMR is extremely small compared with the volume of basaltic magma erupted in the active eastern and western boundaries of the Great Basin. Thus, while the tectonic evolution of Yucca Mountain is important, the peak of tectonic activity that shaped the region has long passed.

What is important to determine for volcanic risk assessment is the controls of the location of sites of volcanism during the waning phases of basaltic volcanism and tectonism. There is widespread evidence of a low-velocity upper mantle underlying most of the Basin and Range province. The most compelling

explanation for the low seismic velocities is the presence of a small component of interstitial partial melt. Thus much if not all of the area of the Basin and Range province appears to have the potential for producing basaltic magma. The abundance of Quaternary basalt and rhyolite volcanic centers in the active margins of the province strongly suggests that active tectonism plays a key role in promoting ascent of magma through the crust. Likewise, the minor eruptive volumes but ubiquitous distribution of basalt centers in the less active interiors of the Basin and Range province suggest that cooled and largely inactive crust prohibits the rise of magma. We suggest accordingly that the controls of the occurrence of basalt in the YMR are probably provided by the distribution of structures that promote ascent of magma.

Two major generalizations can be made about the distribution of Quaternary volcanism in the YMR. First, Quaternary basalt sites, in marked contrast to basalt of Pliocene and Miocene age, do not appear to be controlled by or follow prevailing surface structural features. Second, structures that penetrate the deepest into the crust appear to show the strongest correlations with sites of Pliocene and Quaternary basalt volcanic centers. These structures are strike-slip faults (both northwest-trending right-slip faults and northeast-trending left-slip faults) and ring-fracture zones of caldera complexes. Additionally, pull-apart basins, particularly active basins associated with strike-slip faults, may be important structural elements promoting ascent of basalt magma. Third, there is not a direct relationship between structural features and sites of basaltic volcanic activity. Some structures may be preferential sites for ascent of basalt magma but there is not a causative relationship between structure and volcanism. That is, the structural features of the YMR which are associated with basalt sites appear simply to be passive features promoting the passage of but not causing basaltic magmatism. In fact, the presence of favorable structures may be required to promote ascent of basalt through the relatively inactive crust of the region. Finally, there is a common but not universal restriction of sites of Quaternary basaltic volcanic centers to alluvial basins of the Basin and Range province. This relationship seems best established for the less tectonically active interior parts of the province than the active exteriors. All Quaternary basalt centers of the southern Great Basin, except the Hidden Cone center, occur within or at the margins of alluvial basins. The Lunar Crater volcanic field and the basalt of Buckboard Mesa have been cited in the geologic literature as Quaternary basalt centers or fields developed inside of ranges (for example, Smith et al. 1990). However this is simply a difference of opinion concerning the definition of basins. Both examples include basalt centers developed in the basin interior of caldera complexes. Two causative processes may control the tendency for basalt centers to form in or at the margins of basins. The alluvial basins may simply be the shortest pathways to the surface for ascending magma. The likely control in this case is lithostatic load. Alternatively, the alluvial basins may be located at the sites of active tectonism in an overall pattern of waning tectonic activity.

A. Detachment Systems

A wealth of geologic information suggests detachment systems are present in the YMR. Debate will undoubtedly continue concerning the location, age, geometry, and regional relationships of these detachment systems. The existence of at least local detachment systems seems well established. An important remaining debate is whether the Quaternary faulting at Yucca Mountain is related to waning activity on a detachment system (Scott 1990) or is a phase of extensional faulting that is unrelated to older detachment faulting (M. Carr and Monsen 1988).

The potential role of low-angle or detachment fault systems as pathways for magma for the upward movement of basalt major is a much debated question. Several authors (deVoogd et al. 1986; Serpa et al. 1988) suggest a midcrustal bright spot below southern Death Valley is associated with the Split Cone, a Quaternary basalt center formed along and offset by the southern Death Valley fault. They suggest low-angle faults provided migration pathways for the basalt magma. However, theoretical studies of the dynamics of ascent of basaltic magma (see Chapter 5) suggest basalt magma ascends by a mechanism of

self-generated hydraulic fractures forming predominately vertical fractures. Low-angle faults probably do not represent a potential or favorable pathway for basalt magma. By inference, high-angle faults above detachment systems may have no deep links to magma pathways through the crust. This may explain the absence of any notable spatial relationship between detachment structures and sites of Pliocene or Quaternary basaltic magma. *Detachment systems, while potentially important aspects of tectonic, faulting, or seismic studies, are not judged to be important elements for understanding the structural controls of basaltic volcanism in the Yucca Mountain area.*

B. Caldera Models

Ring-fracture zones of caldera complexes appear to represent potential structural pathways for basalt magma. This has long been recognized in geologic studies of the region (Crowe and Carr 1980; Carr 1984). Debate continues concerning the presence or absence of caldera complexes in Crater Flat and beneath the western edge of Yucca Mountain. The presence of Pliocene and Quaternary basalt centers in the interior of Crater Flat appears inconsistent with caldera models. However, present stratigraphic, structural and geophysical data do not conclusively prove or disprove the existence of caldera complexes. *Caldera models, pending acquisition of new drill hole and geophysical data that may provide more definitive tests of the caldera interpretations, must be considered in tectonic studies of the structural controls of basaltic volcanic activity.*

C. North/Northeast-Trending Rifts

The Kawich-Greenwater rift of Carr (1990) is a proposed north/northeast-trending structural zone that extends through Yucca Mountain. The rift itself is not closely associated with Pliocene or Quaternary sites of basaltic volcanism. Some sites of basaltic volcanism occur within the rift, others occur outside of the rift. The rift model forms a subset of the northeast-trending, Death Valley–Pancake Range volcanic zone (Crowe et al. 1986; Carr 1990). The structural model of Smith et al. (1990) can be viewed as a subset of the Kawich-Greenwater rift and the Death Valley-Pancake Range zone. None of these models provide explanations for the occurrence or location of individual sites of basaltic volcanism. They appear instead to be broad zones marked by a suite of structural features within which there occurs preferential occurrences of Pliocene and Quaternary basaltic volcanic centers compared to areas outside the zones. *Tectonic models of northeast-trending rifts or zones extending through the YMR are of limited use for understanding the tectonic controls of basaltic volcanism. However, these models will be used in assessing regional structural controls of basaltic volcanism.*

D. Pull-Apart Basins

Increased attention has been given in the recent geologic literature to structural models involving strike-slip bounded, pull-apart genesis of basins in the southern Great Basin (Wright 1987; O'Neill et al. 1991; Fridrich and Price 1992). Sites of basaltic volcanism may show strong spatial associations with the pull-apart basins. Basaltic volcanism may be associated with individual basins (Fridrich and Price 1992) or with aligned basins forming tectonic zones (Wright 1987). Basaltic volcanism in southern Crater Flat may be associated spatially with a half-rhombocasm (Fridrich and Price 1992). *Tectonic models relating sites of basaltic volcanism to post-middle Miocene basin formation in strike-slip bounded, pull-apart basins will be used for the YMR.*

E. Crater Flat Volcanic Zone

Pliocene and Quaternary basaltic volcanism in the YMR occurs in a narrow, northwest-trending zone located west and southwest of Yucca Mountain named the CFVZ (Crowe and Perry 1989). The delineation of the zone is based on the distribution of Pliocene and Quaternary volcanic centers. There are a variety of permissive explanations of the zone, a direct outgrowth of the fact that the zone does not follow a continuous surface structure. The zone may represent a buried structural feature of the Walker Lane structural zone. Schweickert (1989) suggested the basalt centers may mark the traced of a concealed, northwest-trending strike-slip fault exhibiting tens of kilometers of offset of Paleozoic rocks. The zone may be associated with a strike-slip bounded basin in Crater Flat (O'Neill et al. 1991; Fridrich and Price 1992) or it may cross multiple pull-apart basins. The CFVZ does not intersect the potential repository site at Yucca Mountain. Nonetheless, structural models have been developed for relating the volcanic zone to risk assessment (Crowe et al. 1988; Department of Energy [DOE] 1991). *The CFVZ will be used in the application of tectonic models to determinations of the structural controls of basaltic volcanism in the YMR.*

F. North-Northeast-trending Structures

A submodel of the CFVZ is the presence of north/northeast-elongated clusters of basalt centers, secondary to the northwest-trending volcanic zone. These northeast-trending zones probably represent control by the shallow stress field of the direction of injection of basalt dikes. These dikes may be offshoots of basin-bounding strike-slip faults (DOE 1990; Fridrich and Price 1992), concealed strike-slip faults (Schweickert 1989), or concealed structural features of the Walker Lane structural zone (Crowe and Perry 1989; Crowe 1990). Smith et al. (1990) has suggested the northeast-trending clusters are following normal faults exposed in the bedrock west of the Yucca Mountain site. *Tectonic models incorporating possible structural controls of north/northeast-trending structures will be used in assessments of volcanic risk for the Yucca Mountain site.*

G. Alluvial Basins

Structural models associating sites of basaltic volcanism with alluvial basins will be used in assessing tectonic models for the Yucca Mountain site.

VIII. References

Ackermann, H. D., W. D. Mooney, D. B. Snyder, and V. D. Sutton, "Preliminary interpretation of Seismic Refraction and Gravity Studies West of Yucca Mountain, Nevada and California," in *U. S. Geological Survey Bulletin 1790: Short Contributions to the Geology and Hydrology of a Potential Nuclear Waste Site at Yucca Mountain, Southern Nevada*, M. D. Carr and J. C. Yount, Eds. (Department of Interior, U. S. Geological Survey, Reston, Virginia, 1988), pp. 23-33.

Anderson, R. E., "Thin Skin Distension in Tertiary Rocks of Southeastern Nevada," *Geological Society America* **82**, 43-58 (1971).

Arabasz, W. J., and D. R. Julander, "Geometry of Seismically Active Faults and Crustal Deformation Within the Basin and Range-Colorado Plateau Transition in Utah," *Geological Society America Special Paper 208: Extensional Tectonics of the Southwestern United States: A Perspective on Processes and Kinematics*, L. Mayer Ed. (Geological Society America, Boulder, Colorado, 1986), pp. 43-74.

Armstrong, R. L. "Cordilleran Metamorphic Core Complex -- From Arizona to Southern California," *Annual Review Earth Planetary Sciences* **10**, 129-154 (1982).

Atwater, T., "Implications of Plate Tectonics for the Cenozoic Tectonic Evolution of Western North America," *Geological Society America* **81**, 3513-3536 (1970).

Axen, G. J., W. J. Taylor, and J. M. Bartley, "Space-Time Patterns and Tectonic Controls of Tertiary Extension and Magmatism in the Great Basin of the Western United States," *Geological Society America* **105**, 56-76 (1993).

Bailey R. A., G. B. Dalrymple, and M. A. Lanphere, "Volcanism, Structure, and Geochronology of Long Valley Caldera, Mono County, California," *Journal Geophysical Research* **81**, 725-744 (1976).

Bath, G. D., and C. E. Jahren, "Interpretations of Magnetic Anomalies at a Potential Repository Site Located in the Yucca Mountain Area, Nevada Test Site," U. S. Geological Survey Open-File Report 84-120, 40 pp. (1984).

Bath, G. D., and C. E. Jahren, "Investigation of an Aeomagnetic Anomaly On West Side of Yucca Mountain, Nye County, Nevada," U. S. Geological Survey Open-File Report 85-459, 24 pp. (1985).

Benz, H. M., R. B. Smith, and W. D. Mooney, "Crustal Structure of the Northwestern Basin and Range Province from the 1986 Program for Array Seismic Experiment," *Journal Geophysical Research* **95**, 21823-21842 (1990).

Best, M. G., and W. H. Brimhall, "Late Cenozoic Alkalic Basaltic Magmas in the Western Colorado Plateaus and the Basin and Range Transition Zone, USA, and their Bearing on Mantle Dynamics," *Geological SocietyAmerica* **85,** 1677-1690 (1974).

Best, M. G., and E. H. Christiansen, "Limited Extension During Peak Tertiary Volcanism Great Basin of Nevada and Utah," *Journal Geophysical Research* **96**, 13,509-13,528 (1991).

Best, M. G., and W. K. Hamblin, "Origin of the Northern Basin and Range Province: Implications from the Geology of its Eastern Boundary," in *Geological Society America Memoir 152: Cenozoic Tectonics and Regional Geophysics of the Western Cordillera*, R. B. Smith, and G. P. Eaton, Eds. (Geological Society America, Boulder, Colorado, 1978), pp. 313-340.

Blackwell, D. D., "Heat Flow and Energy Loss in the Western United States," in *Geological Society America Memoir 152: Cenozoic Tectonics and Regional Geophysics of the Western Cordillera*, R. B. Smith, and G. P. Eaton, Eds. (Geological Society America, Boulder, Colorado, 1978), pp. 175-208.

Blakely, R. J., "Curie Temperature Isotherm Analysis and Tectonic Implications of Aeromagnetic Data from Nevada," *Journal Geophysical Research* **93**, 11,817-11832 (1988).

Brocher, T. M., P. E. Hart and S. F. Carle, "Feasibility Study of the Seismic Reflection Method in Amargosa Desert, Nye County, Nevada," U. S. Geological Survey Open-File Report 89-133, 150 pp. (1990).

Brocher, T. M., M. D. Carr, K. F. Fox Jr., and P. E. Hart, "Seismic Reflection Profiling Across Tertiary Extensional Structures in the Eastern Amargosa Desert, Southern Nevada, Basin and Range Province," *Geological Society America* **105**, 30-46 (1993).

Byers, F. M., Jr., and H. Barnes, "Geologic Map of the Paiute Ridge Quadrangle, Nye and Lincoln Counties, Nevada," U. S. Geological Survey Quadrangle Map GQ-577 (1967).

Byers, F. M., Jr., W. J. Carr, P. P. Orkild, W. D. Quinlivan, and K. A. Sargent, "Volcanic Suites and Related Cauldrons of Timber Mountain-Oasis Valley Caldera Complex, Southern Nevada," U. S. Geological Survey Professional Paper 919, 70 pp. (1976).

Carr, W. J., "Summary of Tectonic and Structural Evidence for Stress Orientation at the Nevada Test Site," U. S. Geological Survey Open-File Rep. 74-176, 83 pp. (1974).

Carr, W. J., "Volcano-Tectonic History of Crater Flat, Southwestern Nevada, as Suggested by New Evidence from Drill Hole Usw-Vh-1 and Vicinity," U. S. Geological Survey Open-File Report 82-457, 58 pp. (1982).

Carr, W. J., "Regional Structural Setting of Yucca Mountain, Southwestern Nevada, and Late Cenozoic Rates of Tectonic Activity in Part of the Southwestern Great Basin, Nevada and California," U. S. Geological Survey Open-File Report 84-854, 109 pp. (1984).

Carr, W. J., "Volcanic-Tectonic Setting of Yucca Mountain and Crater Flat, Southwestern Nevada," in *U. S. Geological Survey Bulletin 1790: U. S. Geologic and Hydrologic Investigations of a Potential Nuclear Waste Disposal Site at Yucca Mountain, Southern Nevada*, M. D. Carr and J. C. Yount, Eds., 35-49 (Department of Interior, U. S. Geological Survey, Reston, Virginia, 1988), pp. 35-49.

Carr, W. J., "Styles of Extension in the Nevada Test Site Region, Southern Walker Lane Belt; An Integration of Volcano-Tectonic and Detachment Fault Models," in *Geological Society America Memoir 176: Basin and Range Extensional Tectonics Near the Latitude of Las Vegas, Nevada*, B. P. Wernicke, Ed. (Geological Society America, Boulder, Colorado, 1990), pp. 283-303.

Carr, W. J., F. M. Byers Jr., and P. P. Orkild, "Stratigraphic and Volcano-Tectonic Relations of Crater Flat Tuff and Some Older Volcanic Units Nye County, Nevada," U. S. Geological Survey Open-File Report 84-114, 42 pp. (1984).

Carr, W. J., and L. D. Parrish, "Geology of Drill Hole USW VH-2, and Structure of Crater Flat, Southwestern Nevada," U. S. Geological Survey Open-File Report 85-475, 41 pp. (1985).

Carr, W. J., F. M. Byers, Jr., and P. P. Orkild, "Stratigraphic and Volcano-Tectonic Relations of Crater Flat Tuff, and Some Older Volcanic Units, Nye County, Nevada," U. S. Geological Survey Professional Paper 1323, 28 pp. (1986).

Carr, M., S. J. Waddell, G. S. Vick, J. M. Stock, S. A. Manson, A. G. Harris, B. W. Cork, and F. M. Byers, "Geology of Drill Hole UE25P#1; A Test Hole into Pre-Tertiary Rocks Near Yucca Mountain, Southern Nevada," U. S. Geological Survey Open-File Report 86-175, 87 pp. (1986).

Carr, M. D., and S. A. Monsen, "A Field Trip Guide to the Geology of Bare Mountain," in *This Extended Land Geological Society America Cordilleran Section Meeting, Field Trip Guidebook: 1988,* D. L. Weide, and M. L. Faber, Eds. (University of Nevada at Las Vegas Geoscience Department Special Publication 2, 1988), pp. 50-57.

Christiansen, R. L., and P. W. Lipman, "Cenozoic Volcanism and Plate Tectonic Evolution of the Western United States, II, Late Cenozoic," *Philosophical Transactions Royal Society London Series A* **271,** 249-284 (1972).

Christiansen, R. L., P. W. Lipman, W. J. Carr, F. M. Byers, Jr., P. P. Orkild, and K. A. Sargent, "The Timber Mountain-Oasis Caldera Complex of Southern Nevada," *Geological Society America* **88,** 943-959 (1977).

Christiansen, T. L., and E. H. Mckee, "Late Cenozoic Volcanic and Tectonic Evolution of the Great Basin and Columbia Intermontane Regions," in *Geological Society America Memoir 152: Cenozoic Tectonics and Regional Geophysics of the Western Cordillera*, R. B. Smith, and G. P. Eaton, Eds. (Geological Society America, Boulder, Colorado, 1978), pp. 283-311.

Coney, P. J., "Mesozoic-Cenozoic Cordilleran Plate Tectonics," in *Geological Society America Memoir 152: Cenozoic Tectonics and Regional Geophysics of the Western Cordillera: Cenozoic Tectonics and Regional*

Geophysics of The Western Cordillera, R. B. Smith and G. P. Eaton, Eds. (Geological Society America, Boulder, Colorado, 1978), pp. 33-49.

Coney, P. J., and Harms, T. A., "Cordilleran Metamorphic Core Complexes: Cenozoic Extensional Relics of Mesozoic Compression," *Geology* **12**, 550-554 (1984).

Connor, C. B., "Cinder Cone Clustering in the Transmexican Volcanic Belt: Implications for Structural and Petrologic Models," *Journal Geophysical Research* **95**, 19,395-19,405 (1990).

Connor, C. B., C. D. Condit, L. S. Crumpler, and J. C. Aubele, "Evidence of Regional Structural Controls on Vent Distribution: Springerville Volcanic Field, Arizona," *Journal Geophysical Research* **97**, 12,349-12,359 (1992).

Crittendon, M. D., Jr., P. J. Coney, and G. H. Davis, Eds., *Geological Society America Memoir 153: Cordilleran Metamorphic Core Complexes* (Geological Society America, Boulder, Colorado, 1980), 490 pp.

Crowe, B. M., "Cenozoic Volcanic Geology and Probable Age of Inception of Basin-Range Faulting in the Southeasternmost Chocolate Mountains, California," *Geological Society America* **89**, 251-264 (1978).

Crowe, B. M., J. C. Crowell, and D. Krummenacher, "Regional Stratigraphy and K-Ar ages of Cenozoic Volcanic Rocks, Southeastern California," *American Journal Science* **279**, 186-216 (1979).

Crowe, B. M., "Basaltic Volcanic Episodes of the Yucca Mountain Region," in *Proceedings High Level Radioactive Waste Management Conference, Las Vegas, Nevada* (American Nuclear Society, La Grange Park, Illinois 1990), pp. 65-73.

Crowe, B. M., and W. J. Carr, "Preliminary Assessment of the Risk of Volcanism at a Proposed Nuclear Waste Repository in the Southern Great Basin," U. S. Geological Survey Open-File Report 80-375 (1980).

Crowe B. M., D. T. Vaniman, and W. J. Carr, "Status of Volcanic Hazard Studies for the Nevada Nuclear Waste Storage Investigations," Los Alamos National Laboratory Report LA-9325-MS (1983a).

Crowe, B. M., S. Self, D. Vaniman, R. Amos, and F. Perry, "Aspects of Potential Magmatic Disruption of a High-Level Radioactive Waste Repository in Southern Nevada.," *Journal Geology* **91**, 259-276 (1983b).

Crowe, B. M., K. H. Wohletz, D. T. Vaniman, E. Gladney, and N. Bower, "Status of Volcanic Hazard Studies for the Nevada Nuclear Waste Storage Investigations," Los Alamos National Laboratory Report LA-9325-MS, Vol. II (1986).

Crowe, B., C. Harrington, L. McFadden, F. Perry, S. Wells, B. Turrin, and D. Champion, "Preliminary Geologic Map of the Lathrop Wells Volcanic Center," Los Alamos National Laboratory Report LA-UR-88-4155 (1988).

Crowe, B. M. and F. V. Perry, "Volcanic Probability Calculations for the Yucca Mountain Site: Estimation of Volcanic Rates," in *Proceedings Nuclear Waste Isolation in the Unsaturated Zone Focus '89, Symposium Volume* (American Nuclear Society, La Grange Park, Illinois, 1989), pp. 326-334.

Crowe, B. M., and F. V. Perry, "Preliminary Geologic Map of the Sleeping Butte Volcanic Centers," Los Alamos National Laboratory Report LA-12101-MS (1991).

Crowe, B. M., R. Picard, G. Valentine, and F. V. Perry, "Recurrence Models of Volcanic Events: applications to Volcanic Risk assessment," in *Proceedings High Level Radioactive Waste Management Conference Las Vegas, Nevada* (American Nuclear Society, La Grange Park, Illinois, 1992a), pp. 2344-2355.

Crowe, B., R. Morley, S. Wells, J. Geissman, E. Mcdonald, L. Mcfadden, F. Perry, M. Murrell, J. Poths, and S. Forman, "The Lathrop Wells Volcanic Center: Status of Field and Geochronology Studies," in *Proceedings High Level Radioactive Waste Management Conference Las Vegas, Nevada* (American Nuclear Society, La Grange Park, Illinois, 1992b), pp. 1997-2013.

DeVoogd, B., L. Serpa, L. Brown, E. Hauser, S. Kaufman, J. Oliver, B. W. Troxel, J. Willemin, and L. A. Wright, "Death Valley Bright Spot: a Mid-Crustal Magma Body in the Southern Great Basin, California," *Journal Geology* **12**, 64-67 (1986).

DOE (U. S. Department of Energy), "Site Characterization Plan, Yucca Mountain Site, Nevada Research and Development Area, Nevada,", Office of Civilian Radioactive Waste Management Report DOE/RW-0199, (1988).

DOE (U. S. Department of Energy), "Study Plan 8.3.1.8.5.1 Probability of Magmatic Disruption of the Repository," By Crowe, B., Ed., Prepared By Los Alamos National Laboratory for the Department of Energy, 52 pp. (1990).

Dueker, K. and E. Humphreys, "Upper-Mantle Velocity Structure of the Great Basin," *Geophysical Research Letter* **17**, 1327-1330 (1990).

Eaton, G. P., "A Plate-Tectonic Model for Late Cenozoic Crustal Spreading in the Western United States" in *Rio Grande Rift: Tectonics And Land Magmatism*, R. E. Riecker, Ed. (American Geophysical Union, Washington D.C, 1979), pp. 7-32.

Eaton, G. P., "Geophysical and Geological Characteristics of the Crust of the Basin and Range Province," in *Continental Tectonics, Studies in Geophysics* (National Academy of Sciences, Washington, D.C., 1980), pp. 96-113.

Eaton, G. P., "The Basin and Range Province; Origin and Tectonic Significance:," *Annual Reviews Earth Planetary Science* **10**, 409-440 (1982).

Eaton, G. P., R. R. Wahl, H. J. Prostka, D. R. Mabey, and M. D. Kleinkopf, "Regional Gravity and Tectonic Patterns: their Relation to Late Cenozoic Epirogeny and Lateral Spreading in the Western Cordillera," in *Geological Society America Memoir 152: Cenozoic Tectonics And Regional Geophysics Of The Western Cordillera*, R. B. Smith, and G. P. Eaton, Eds. (Geological Society America Boulder, Colorado, 1978), pp. 51-91.

Ekren, E. B., C. L. Rogers, R. E. Anderson, and P. P. Orkild, "Age of Basin and Range Normal Faults in Nevada Test Site and Nellis Air Force Range, Nevada," in *Geological Society America Memoir 110: Nevada Test Site*, E. B. Eckel, Ed. (Geological Society America, Boulder, Colorado, 1968), pp. 247-250.

Ekren, E. B., P. P. Orkild, K. A. Sargent, and G. L. Dixon, "Geologic Map of Tertiary Rocks, Lincoln County, Nevada," U. S. Geological Survey Quadrangle Map I-1041 (1977).

Engdahl, E. R., and W. A. Rinehart, "Seismicity Map of North America," Geological Society America Continent-Scale Map-004 (1988).

Evans, J. R., and M. Smith III, "Teleseismic Tomography of the Yucca Mountain Region: Volcanism and Tectonism," in *Proceedings High Level Radioactive Waste Management Conference, Las Vegas, Nevada* (American Nuclear Society, La Grange Park, Illinois, 1992), pp. 2371-2380.

Farmer, G. L., and D. J. Depaolo, "Origin of Mesozoic and Tertiary Granite in the Western United States and Implications for Pre-Mesozoic Crustal Structure: 1. Nd and Sr Isotopic Studies in the Geosyncline of the Northern Great Basin," *Journal Geophysical Research* **88**, 3379-3401 (1983).

Farmer, G. L., and D. J. Depaolo, "Origin of Mesozoic and Tertiary Granite in the Western United States and Implications for Pre-Mesozoic Crustal Structure: 2. Nd and Sr Isotopic Studies of Unmineralized and Cu- and Mo-Mineralized Granite in the Precambrian Craton," *Journal Geophysical Research* **89**, 10141-10160 (1984).

Farmer, G. L., F. V. Perry, S. Semken, B. Crowe, D. Curtis, and D. J. Depaolo, "Isotopic Evidence on the Structure and Origin of Subcontinental Lithospheric Mantle in Southern Nevada," *Journal Geophysical Research* **94**, 7885-7898 (1989).

Fenneman, N. M., *Physiography of Western United States* (Mcgraw-Hill Book Co. Inc., New York, 1931), 534 pp.

Fox, K. F., Jr., and M. D. Carr, "Neotectonics and Volcanism at Yucca Mountain and Vicinity, Nevada," in *Radioactive Waste Management* **13**, 37-50 (1989).

Fridrich, C. and J. Price, "Tectonic Framework of Crater Flat Basin, Adjacent to Yucca Mountain Nevada: A Preliminary Report," *Abstract Geological Society America* **23**, A189 (1992).

Fridrich C. J., B. M. Crowe, M. R. Hudson, V. E. Langenheim, and G. A. Thompson, "Structural Control of Basaltic Volcanism in a Region of Oblique Extension, Southwest Nevada Volcanic Field," *EOS Transactions, American Geophysical Union 1994 Fall Meeting* **75** (44), 603 (1994).

Gans, P. B., G. Mahood, and E. Schermer, "Synextensional Magmatism in the Basin and Range Province: A Case Study Eastern Great Basin," *Geological Society America Special Paper 233*(Geological Society America, Boulder, Colorado, 1989).

Glazner, A. F., and J. A. Supplee, "Migration of Tertiary Volcanism in the Southwestern United States and Subduction of the Mendocino Fracture Zone," *Earth Planetary Sciences Letters* **60**, 429-436 (1982).

Gomberg, J., "Seismicity and Shear Strain in the Southern Great Basin of Nevada and California," *Journal Geophysical Research* **96**, 16,383-16,399 (1991a).

Gomberg, J., "Seismicity and Detection/Location Threshold in the Southern Great Basin Seismic Network," *Journal Geophysical Research* **96**, 16401-16414 (1991b).

Guth, P. L., "Tertiary Extension North of the Las Vegas Valley Shear Zone Sheep and Desert Ranges, Clark County, Nevada," *Geological Society America* **92**, 763-771 (1981).

Hamilton, W., "Detachment Faulting in the Death Valley Region, California and Nevada" in *U. S. Geological Survey Bulletin 1790: Short Contributions to the Geology and Hydrology of a Potential Nuclear Waste Site at Yucca Mountain, Southern Nevada*, M. D. Carr and J. C. Yount, Eds. (Department of Interior, U. S. Geological Survey, Reston, Virginia, 1988), pp. 23-33.

Hamilton, W., and W. B. Myers, "Cenozoic Tectonics of the Western United States," *Reviews of Geophysics* **4**, 509-549 (1966).

Hanna, W. F., R. E. Sweeney, T. G. Hildenbrand, J. G. Tanner, R. K. Mc Connell, R. H. Godson, "The Gravity Anomaly Map of North America," in *The Geology of North America: An Overview,* W. Bally and A. R. Palmer, Eds. (Geological Society America, Boulder, Colorado, 1989).

Harmsen, S. C. and C. G. Bufe, "Seismicity and Focal Mechanism for the Southern Great Basin of Nevada and California: 1987 Through 1989," U. S. Geological Survey Open-File Report 91-572, 208 pp. (1992).

Healey, D. L., and C. H. Miller, "Gravity Survey of the Amargosa Desert Area of Nevada and California," U. S. Geological Survey Technical Letter NTS-99, 32 pp. (1965).

Healey, D. L., R. R. Wahl, and H. W. Oliver, "Death Valley Sheet of Complete Bouguer Gravity Map of Nevada," Nevada Bureau of Mines and Geology Map 68 (1980a).

Healey, D. L., R. R. Wahl, and H. W. Oliver, "Bouguer Gravity Map of Nevada, Death Valley Sheet," Nevada Bureau of Mines and Geology Map 69 (1980b).

Healey, D. L., D. B. Snyder, R. R. Wahl, and F. E. Currey, "Bouguer Gravity Map of Nevada; Caliente Sheet," Nevada Bureau of Mines Map M70 (1981).

Healey, D. L., R. H. Harris, D. A. Ponce, and H. W. Oliver, "Complete Bouguer Gravity Map of the Nevada Test Site and Vicinity, Nevada," U. S. Geological Survey Open-File Report 87-506 (1987).

Hildenbrand, T. G., A. M. Rogers, H. W. Oliver, S. C. Harmsen, J. K. Nakata, D. S. Aitken, R. N. Harris, and M. D. Carr, "Regional Geologic and Geophysical Maps of the Southern Great Basin," in *U. S. Geological Survey Bulletin 1790: Geologic and Hydrologic Investigations of a Potential Nuclear Waste Disposal Site at Yucca Mountain, Southern Nevada* M. D. Carr, and Yount, J. C., Eds. (Department of Interior, U. S. Geological Survey, Reston, Virginia, 1988), pp. 3-21.

Hildenbrand, T. G., and R. P. Kucks, "Total intensity Magnetic Anomaly Map of Nevada," Nevada Bureau of Mines and Geology Map 93a (1988).

Hill, D. P., "Contemporary Block Tectonics; California and Nevada," *Journal Geophysical Research* **87**, 5433-5450 (1982).

Hodges, K. V., and J. D. Walker, "Petrologic Constraints on the Unroofing History of the Funeral Mountain Metamorphic Core Complex, California," *Journal Geophysical Research* **95**, 8437-8445 (1990).

Hoffman, L. R., and W. D. Mooney, "A Seismic Study of Yucca Mountain and Vicinity, Southern Nevada: Data Report and Preliminary Results," U. S. Geological Survey Open-File Report 83-588, 50 pp. (1983).

Holbrook, W. S., "The Crustal Structure of the Northwesten Basin and Range Province, Nevada, from Wide-angle Seismic Data," *Journal Geophysical Research* **95**, 21,843-21,869 (1990).

Hudson, M. R., and J. W. Geissman, "Paleomagnetic and Structural Evidence for the Middle Tertiary Counterclockwise Block Rotation in the Dixie Valley Region, West-Central Nevada," *Journal Geology* **15**, 638-642 (1987).

Hudson, M. R., and J. W. Geissman, "Paleomagnetic Evidence for the Age and Extent of Middle Tertiary Counterclockwise Rotation Dixie Valley Region, West Central Nevada," *Journal Geophysical Research* **96**, 3979-4006 (1991).

Humphreys, E. D., and K. G. Dueker,"Western U. S. Upper Mantle Structure," *Journal Geophysical Research* **99**, 9615-9634 (1994a).

Humphreys, E. D., and K. G. Dueker, "Physical State of the Western U. S. Upper Mantle," *Journal Geophysical Research* **99**, 9635-9650 (1994b).

Hunter, W. C., R. W. Spengler, and T. M. Brocher, "Seismic Reflection Profiling: Essential Geophysical Data for Yucca Mountain, Nevada," in *Proceedings High Level Radioactive Waste Management Conference Las Vegas, Nevada* (American Nuclear Society, La Grange Park, Illinois, 1993), pp. 1835-1839.

Jones, J. H., B. P. Wernicke, G. L. Farmer, J. D. Walker, D. S. Colman, L. W. Mckenna, and F. V. Perry, "Variations Across and Along a Major Continental Rift: An Interdisciplinary Study of the Basin and Range Province, Western USA," *Tectonophysics* **213**, 57-96 (1992).

Kane, M. F., and Bracken, R. E., "Aeromagnetic Map of Yucca Mountain and Surrounding Regions, Southwest Nevada," U. S. Geological Survey Open-File Report 83-616 (1983).

Kistler, R. W. and Z. E. Peterman, "Variations in Sr, Rb, K, Na, and initial $^{87}Sr/^{86}Sr$ in Mesozoic Granitic Rocks and intruded Wall Rocks in Central California," *Geological Society America* **84**, 3489-3512 (1973).

Lachenbruch, A. H., and J. H. Sass, "Models of an Extending Lithosphere and Heat Flow in the Basin and Range Province," in *Geological Society America Memoir 152: Cenozoic Tectonics and Regional Geophysics of the Western Cordillera*, R. B. Smith, and G. P. Eaton, Eds. (Geological Society America, Boulder, Colorado, 1978), pp. 209-250.

Langenheim, V.E., S.F. Carle, D.A. Ponce, and J.D. Philips, "Revision of an Aeromagnetic Survey of the Lathrop Wells Area, Nevada," U.S. Geological Survey, Open-File Report 91-46, 17pp. (1991).

Langenheim, V. E., K. S. Kirchoff-Stein, and H. W. Oliver, "Geophysical Investigations of Buried Volcanic Centers Near Yucca Mountain, Southwest Nevada," in *Proceedings High Level Radioactive Waste Management Conference, Las Vegas, Nevada* (American Nuclear Society, La Grange Park, Illinois 1993), pp. 1840-1846.

Lipman, P. W., W. D. Quinlivan, W. J. Carr, and R. E. Anderson, "Geologic Map of the Thirsty Canyon SE Quadrangle, Nye County, Nevada," U. S. Geological Survey Quadrangle Map, GQ-489 (1966).

Lipman, P. W., H. J. Prostka, and R. L. Christiansen, "Cenozoic Volcanism and Plate Tectonic Evolution of the Western United States, I, Early and Middle Cenozoic," *Philosophical Transactions of the Royal Society of London Series A* **271,** 217-248 (1972).

Lipman, P. W., "Cenozoic Volcanism in the Western United States: Implications for Continental Tectonics," in *Continental Tectonics* (National Academy of Sciences, Washington, D.C., 1980), pp. 161-174.

Lutz, T. M., "An analysis of Orientations of Large-Scale Crustal Structures: A Statistical approach Based on Area Distributions of Pointlike Features," *Journal Geophysical Research* **91,** 421-434 (1986).

Mayer, L., "Topographic Constraints on Models of Lithospheric Stretching of the Basin and Range Province, Western United States," in *Geological Society America Special Paper 208: Extensional Tectonics of the Southwestern United States: A Perspective on Processes and Kinematics*, L. Mayer Ed. (Geological Society America, Boulder, Colorado, 1986), pp. 1-14.

Mckenna, L. W. and K. V. Hodges, "Constraints on the Kinematics and Timing of Late Miocene-Recent Extension Between the Panamint and Black Mountains, Southeastern California," in *Geological Society America Memoir 176: Basin and Range Extensional Tectonics Near the Latitude of Las Vegas, Nevada*, B. P. Wernicke, Ed. (Geological Society America, Boulder, Colorado, 1990), pp. 363-376.

Mermonte, M. W. and A. M. Rogers, "Historical Catalog of Southern Great Basin Valleys, West-Central Nevada," M. S. thesis, University of Nevada, Reno (1987).

Montfort, M. E., and J. R. Evans, "Teleseismic Studies of the Earth's Crust and Upper Mantle in Southern Nevada," *EOS Transactions American Geophysical Union* **63,** 1099 (1982).

Mooney, W. D., and L. W. Braile, "The Seismic Structure of the Continental Crust and Upper Mantle of North America," in *The Geology of North American Overview*, W. Bally and A. R. Palmer, Eds. (Geological Society America, Boulder, Coloado, 1989), pp. 39-52.

Noble, D. C., "Some Observations On the Cenozoic Volcano-Tectonic Evolution of the Great Basin, Western United States," *Earth and Planetary Science Letters* **17**, 142-150 (1972).

Noble, D. C., and R. L. Christiansen, "Black Mountain Volcanic Center, in Guidebook to the Geology of Four Tertiary Volcanic Centers in Central Nevada," *Nevada Bureau of Mines Geology Report* **19**, 22-26 (1974).

Noble, C. C., T. A. Vogel, S. I. Weiss, J. W. Erwin, E. H. Mckee, and L. W. Younker, "Stratigraphic Relations and Source Area of Ash-Flow Sheets of the Black Mountain and Stonewall Mountain Volcanic Centers," *Journal Geophysical Research* **89,** 8593-8602 (1984).

Nolan, T. B., "The Basin and Range Province in Utah, Nevada, and California," U. S. Geological Survey Professional Paper 197-D, 141-193 (1943).

O'Connor, J. T., R. E. Anderson, and P. W. Lipman, "Geologic Map of the Thirsty Canyon Quadrangle, Nye County, Nevada," U. S. Geological Survey Quadrangle Map, GQ-524 (1966).

O'Neill, J. M., "Strike-Slip Faulting and Oroclinal Bending at Yucca Mountain, Nevada: Evidence from Photogeologic and Kinematic Analysis," *Geological Society America Abstracts With Programs* **25**, A119 (1991).

O'Neill, J. M., Whitney, J. W. and M. R. Hudson, "Photogeologic and Kinematic Analysis of Lineaments at Yucca Mountain, Nevada: Implication for Strike-Slip Faulting and Oroclinal Bending," U. S. Geological Survey Open-File Report 91-623, 24 pp. (1992).

Okaya, D. A. and G. A. Thompson, "Involvement of Deep Crust in Extension of Basin and Range Province," in *Geological Society America Special Paper 208: Extensional Tectonics of the Southwestern United States: A Perspective on Processes and Kinematics*, L. Mayer Ed. (Geological Society America, Boulder, Colorado, 1986), pp. 15-22.

Oldow, J. S., A. W. Bally, H. G. Avé Lallemant, and W. P. Leeman, "Phaneraozoic Evolution of the North American Cordillera United States and Canada," A. W. Bally, and A. R. Palmer Eds. in *The Geology of North America: an Overview*, W. Bally and A. R. Palmer, Eds. (Geological Society America, Boulder, Colorado, 1989), pp. 139-232.

Oliver, E. L. Hardin, and P. H. Nelson, "Status of Data, Major Results, and Plans for Geophysical activities, Yucca Mountain Project," Prepared for DOE by the USGS and SAIC, (1992).

Oliver, H. W., and K. F. Fox, "Structure of Crater Flat and Yucca Mountain, Southeastern Nevada, as Inferred from Gravity Data," in *Proceedings High Level Radioactive Waste Management Conference, Las Vegas, Nevada* (American Nuclear Society, La Grange Park, Illinois 1993), pp. 1812-1817.

Orkild, P. P., K. a. Sargent, and R. P. Snyder, "Geologic Map of Pahute Mesa, Nevada Test Site and Vicinity, Nye County, Nevada," U. S. Geological Survey Miscellaneous Investigations Map I-567 (1969).

Parsons, T., G. A. Thompson, "The Role of Magma Overpressure in Suppressing Earthquakes and Topography: Worldwide Examples," *Science* **253,** 1399-1402 (1991).

Priestley, K. F., A. S. Ryall, and G. S. Fezie, "Crust and Upper Mantle Structure in the Northwest Basin and Range Province," *Seismology Society American* **72,** 911-923 (1982).

Proffett, J. M., Jr., "Cenozoic Geology of the Yerington District, Nevada and Implications for the Nature and Origin of Basin and Range Faulting," *Geological Society American* **88,** 247-266 (1977).

Rehig, W. A., "Processes of Regional Tertiary Extension in the Western Cordillera: Insights From the Metamorphic Core Complexes," in *Geological Society America Special Paper 208: Extensional Tectonics of the Southwestern United States: A Perspective on Processes and Kinematics*, L. Mayer Ed. (Geological Society America, Boulder, Colorado, 1986), pp. 97-122.

Rogers, a. M., S. C. Harmsen, and W. J. Carr, "Southern Great Basin Seismological Data Report for 1981 and Preliminary Data analysis," U. S. Geological Survey Open-File Report 81-1086, 148 pp. (1981).

Rogers, A. M., S. C. Harmsen, W. J. Carr, and W. J. Spence, "Southern Great Basin Seismological Data Report for 1981, and Preliminary Data Analysis," U. S. Geological Survey Open-File Report 83-669, 240 pp. (1983).

Rogers, A. M., S. C. Harmsen, and M. E. Meremonte, "Evaluation of the Seismicity of the Southern Great Basin and its Relationship to the Tectonic Framework of the Region," U. S. Geological Survey Open-File Report 87-408, pp. 196 (1987).

Rosenbaum, J. G., M. R. Hudson, and R. B. Scott, "Paleomagnetic Constraints On the Geometry and Timing of Deformation at Yucca Mountain, Nevada," *Journal Geophysical Research* **96,** 1963-1980 (1991).

Sass, J. H., A. H. Lachenbrunch, W. W. Dudley, Jr., S. S. Priest, and R. J. Munroe, "Temperature, Thermal Conductivity, and Heat Flow Near Yucca Mountain, Nevada, Some Tectonic and Hydrologic Implications," U. S. Geological Survey Open-File Report 87-649, 118 pp. (1988).

Scholz, C. H., M. Barazangi, and M. L. Sbar, "Late Cenozoic Evolution of the Great Basin, Western United States, as an Ensialic Interarc Basin," *Geological Society America* **82,** 2979-2990, (1971).

Schweickert, R. A., "Evidence for a Concealed Dextral Strike-Slip Fault Beneath Crater Flat, Nevada," *Abstract Geological Society America* **20,** A115 (1989).

Scott, R. B., and J. Bonk, "Preliminary Geologic Map of Yucca Mountain Nye County, Nevada, With Geologic Sections," U. S. Geological Survey Open-File Report 84-494, (1984).

Scott, R. B., "Tectonic Setting of Yucca Mountain, Southwest Nevada," in *Geological Society America Memoir 176: Basin and Range Extensional Tectonics Near the Latitude of Las Vegas, Nevada*, B. P. Wernicke, Ed. (Geological Society America, Boulder, Colorado, 1990), pp. 251-282.

Scott, R. B., G. D. Bath, V. J. Flanigan, D. B. Hoover, J. G. Rosenbaum, and R. W. Spengler, "Geological and Geophysical Evidence of Structures in Northwest-Trending Washes, Yucca Mountain, Southern Nevada, and their Possible Significance to a Nuclear Waste Repository in the Unsaturated Zone," U. S. Geological Survey Open-File Report 84-567, 23 pp. (1984).

Serpa, L., B. De Voogd, L. Wright, J. Willemin, J. Oliver, E. Hauser, and B. Troxel, "Structure of the Central Death Valley Pull-apart Basin and Vicinity From Cocorp Profiles in the Southern Great Basin," *Geological Society America* **100,** 1437-1450 (1988).

Severinghaus, J., and T. Atwater, "Cenozoic Geometry and Thermal State of the Subducting Slabs Beneath Western North Amer.," in *Geological Society America Memoir 176: Basin and Range Extensional Tectonics Near the Latitude of Las Vegas, Nevada*, B. P. Wernicke, Ed. (Geological Society America, Boulder, Colorado, 1990), pp. 1-22.

Shaw, H.R., "The Fracture Mechanisms of Magma Transport From the Mantle to the Surface," in *Physics of Magmatic Processes,* R. B. Hargraves, Ed. (Princeton University Press, Princeton, New Jersey, 1980), pp. 201-264.

Shawe, D. R., "Strike-Slip Control of Basin-Range Structure Indicated by Historical Faults in Western Nevada," *Geological Society America* **76,** 1360-1378 (1965).

Simpson, R. W., R. C. Jachens, R. J. Blakely, and R. W. Saltus, "A New Isostatic Residual Gravity Map of the Conterminous United States with a Discussion of the Significance of Isostatic Residual Anamolies," *Journal Geophysical Research* **91,** 8348-8372 (1986).

Smith, R. B., "Seismicity, Crustal Structure and Intraplate Tectonics of the Interior of the Western Cordillera," in *Geological Society America Memoir 152: Cenozoic Tectonics and Regional Geophysics of the Western Cordillera,* R. B. Smith, and G. P. Eaton, Eds. (Geological Society America, Boulder, Colorado, 1978), pp. 111-144.

Smith, R. B., and M. L. Sbar, "Contemporary Tectonics and Seismicity of the Western United States With Emphasis on the Intermountain Seismic Belt," *Geological Society America* **85,** 1205-1218 (1974).

Smith, R. L., and R. G. Luedke, "Potentially Active Volcanic Lineaments and Loci in Western Conterminous United States," in *Explosive Volcanism: Inception, Evolution And Hazards* (National Academy Press, Washington, D.C., 1984), pp. 47-66.

Smith, E. I., D. L. Feuerbach, T. R. Naumann, and J. E. Faulds, "The Area of Most Recent Volcanism Near Yucca Mountain, Nevada: Implications for Volcanic Risk Assessment," in *Proceedings High-Level Radioactive Waste Management Conference, Las Vegas, Nevada* (American Nuclear Society, La Grange Park, Illinois, 1990), pp. 81-90.

Snoke, A. W., and D. M. Miller, "Metamorphic and Tectonic History of the Northeastern Great Basin," in *Metamorphic and Crustal Evolution of the Western United States,* G. W. Ernst, Ed. (Prentice-Hall, Englewood Cliffs, New Jersey, 1988), pp. 606-648.

Snyder, W. S., W. R. Dickenson, and M. L. Silberman, "Tectonic Implications of Space-Time Patterns of Cenozoic Magmatism in the Western United States," *Earth Planetary Science Letters* **32,** 91-106 (1976).

Snyder, D. B., and W. J. Carr, "Preliminary Results of Gravity Investigations at Yucca Mountain and Vicinity, Southern Nye County, Nevada," U. S. Geological Survey Open-File Report 87-701, pp. 35 (1982).

Snyder, D. B., and W. J. Carr, "Interpretation of Gravity Data in a Complex Volcano-Tectonic Setting, Southwestern Nevada," *Journal Geophysical Research* **89,** 10,193-10,206 (1984).

Spence, W. J., "P-Wave Residual Differences and Inferences on an Upper Mantle Source for the Silent Canyon Volcanic Center, Southern Great Basin, Nevada," *Journal Geophysical Research* **38,** 505-524 (1974).

Spengler, R. W., and K. F. Fox, Jr., "Stratigraphic and Structural Framework of Yucca Mountain, Nevada," in *Radioactive Waste Management* **13,** 21-36 (1989).

Spence, W. and R. S. Gross, "A Tomographic Glimpse of the Upper Mantle Source of Magmas of the Jemez Lineament, New Mexico," *Journal Geophysical Research* **95,** 10,829-10,849 (1990).

Stewart, J. H., "Basin and Range Structure: A System of Horsts and Grabens Produced by Deep-Seated Extension," *Geological Society America* **82,** 1019-1044 (1971).

Stewart, J. H., "Basin-Range Structure in Western North America," in *Geological Society America Memoir 152: Cenozoic Tectonics and Regional Geophysics of the Western Cordillera*, R. B. Smith, and G. P. Eaton, Eds. (Geological Society America, Boulder, Colorado, 1978), pp. 1-31.

Stewart, J. H., "Regional Tilt Patterns of Late Cenozoic Basin-Range Fault Blocks, Western United States," *Geological Society America* **91,** 460-464 (1980).

Stewart, J. H., and J. E. Carlson, "Preliminary Geologic Map of Nevada," U. S. Geological Survey Misc. Field Studies Map MF-609 (1974).

Stewart, J. H., W. J. Moore, and I. Zietz, "East-West Patterns of Cenozoic Igneous Rocks, Aeromagnetic Anomalies, and Mineral Deposits, Nevada and Utah," *Geological Society America* **88,** 67-77 (1977).

Suppe, J., C. Powell, and R. Berry, "Regional Topography, Seismicity, Quaternary Volcanism and the Present-Day Tectonics of the Western United States," *American Journal Science* **274-A,** 397-436 (1975).

Sutton, V. D., "Data Report for the 1983 Seismic Refraction Experiment at Yucca Mountain, Beatty, and Vicinity, Southwestern Nevada," U. S. Geological Survey Open-File Report 84-661, 66 P., 11 Plates (1984).

Sutton, V. D., "Data Report for the 1985 Seismic Refraction Experiment at Yucca Mountain, Beatty, and Vicinity, Southwestern Nevada," U. S. Geological Survey Open-File Report 85-591, 96 pp., 17 Plates (1985).

Tanaka, K. L., E. M. Shoemaker, G. E. Ulrich, and E. W. Wolfe, "Migration of Volcanism in the San Francisco Volcanic Field, Arizona," *Geological Society America* **97**, 129-141 (1986).

Taylor, S. R., "Three-Dimensional Crust and Upper Mantle Structure at the Nevada Test Site," *Journal Geophysical Research* **88**, 2220-2232 (1983).

Thompson, G. A. and D. B. Burke, "Regional Geophysics of the Basin and Range Province," *Annual Review Earth Planetary Sciences* **2,** 213-238 (1974).

Valentine, G. A., B. M. Crowe, and F. V. Perry, "Physical Processes and Effects of Magmatism in the Yucca Mountain Region," in *Proceedings High Level Radioactive Waste Management Conference, Las Vegas, Nevada* (American Nuclear Society, La Grange Park, Illinois, 1992), pp. 2344-2355.

Vaniman, D. T. , B. M. Crowe, and E. S. Gladney, "Petrology and Geochemistry of Hawaiite Lavas From Crater Flat, Nevada," *Contributions MineralogyPetrology* **80**, 341-357 (1982).

Wadge, G., and A. Cross, "Quantitative Methods for Detecting Aligned Points: an Application to the Volcanic Vents of the Michoacan-Guanajuato Volcanic Field, Mexico," *Journal Geology* **16**, 815-818 (1988).

Walker, J. D. and D. S. Coleman, "Geochemical Constraints On Mode of Extension in the Death Valley Region," *Geology* **19,** 971-974 (1991).

Wernicke, B., "Low-angle Faults in the Basin and Range Province," *Nature* **291,** 645-648 (1981).

Wernicke, B., "Cenozoic Extensional Tectonics of the U. S. Cordillera," in *The Cordilleran Orogeny: Conterminous U. S.,* B. C. Burchfiel, M. L. Zoback, and P. W. Lipman, Eds. (Geological Society America, Boulder, Colorado, 1992), pp. 553-582.

Wernicke, B., and B. C. Burchfiel, "Modes of Extensional Tectonics," *Journal Structural Geology* **4,** 105-115 (1982).

Wernicke, B., G. J. Axen, and J. K. Snow, "Basin and Range Extensional Tectonics at the Latitude of Las Vegas, Nevada," *Geological SocietyAmerica* **100**, 1738-1757 (1988).

Wright, L. A., "Late Cenozoic Fault Patterns and Stress Fields in the Great Basin and Westward Displacement of the Sierra Nevada Block," *Journal Geology* **4,** 489-494 (1976).

Wright, L.A., "Overview of the Role of Strike-Slip and Normal Faulting in the Neogene History of the Region Northeast of Death Valley, California-Nevada," Nevada Bureau of Mines and Geology Open-File 89-1, pp. 1-11, (1987).

Wright, L. A., J. K. Otton, and B. W. Troxel, "Turtleback Surfaces of Death Valley Viewed as Phenomena of Extension," *Journal Geology* **2,** 53-54 (1974).

Zeitz, I., G. E. Andreasen, and J. C. Cain, "Magnetic Anomalies from Satellite Magnetometer," *Journal Geophysical Research* **75,** 4007-4015 (1970).

Zoback, M. L., "State of Stress and Modern Deformation of the Northern Basin and Range Province," *Journal Geophysical Research* **4,** 71056-7128 (1989).

Zoback, M. L., and G. A. Thompson, "Basin and Range Rifting in Northern Nevada: Clues From a Mid-Miocene Rift and its Subsequent Offsets," *Geology* **6,** 111-116 (1978).

Zoback, M. L., R. E. Anderson, and G. A. Thompson, "Cainozoic Evolution of the State of Stress and Style of Tectonism of the Basin and Range Province of the Western United States," *Philosophical Transactions Royal Society London Series* **300,** 407-434 (1981).

CHAPTER 4: PETROLOGIC AND GEOCHEMICAL CONSTRAINTS ON BASALTIC VOLCANISM IN THE GREAT BASIN

I. Summary

Basaltic volcanism has been the predominant form of volcanism in the Great Basin over the last 5–10 million years (Ma). Great Basin basalts are primarily alkalic in composition indicating small degrees of partial melting of relatively deep mantle sources. The compositions of basalt have become more undersaturated with time, both in the Basin and Range province as a whole and within individual volcanic fields, suggesting that the intensity of melting in the mantle has declined with time on a regional scale. The volume of basalt flux into the crust has also declined in a broad sense throughout the middle and late Cenozoic, considering that the enormous volumes of ash-flow tuff erupted in the mid-Cenozoic were fueled by a comparable or greater volume of basaltic magma. The transition from the eruption of evolved magmas to basalt in the late Cenozoic can be attributed to changes in plate tectonic processes and crustal properties with time. Isotopic and trace-element studies of basalt have documented the role of both asthenospheric mantle and lithospheric mantle in the generation of basaltic magma in the western United States. The regional distribution of these sources correlates with tectonic setting and history and may control the volume and compositional distribution of basalt relative to major physiographic boundaries.

Basalt eruptions within the Crater Flat volcanic zone (CFVZ) follow many of the same patterns seen in other basalt fields of the western United States. Eruptive volumes decrease and the depths of magma chambers possibly increase with time, suggesting an overall decrease in basalt flux from the mantle with time. An unusual aspect of several of the CFVZ basalt centers is that they erupted during multiple eruptive episodes spanning several tens of thousands of years (*polygenetic volcanism*). Geochemical data show that eruptive episodes at individual volcanic centers are geochemically distinct and cannot be related by the evolution of a single magma. Instead, the geochemical data indicate that several separate magma batches, each representing an independent episode of dike intrusion, were involved in the formation of individual polygenetic centers. The pattern of repeated dike intrusions at single volcanic centers within the Yucca Mountain region (YMR) provides spatial constraints on where magma will ascend during the lifetime of a polygenetic volcanic center.

II. Introduction

The Great Basin (encompassing most of the northern Basin and Range province; see Chapter 3 of this report) is a region that was affected during the middle and late Cenozoic by extensional tectonism and magmatism. As a result, it is characterized by thinned lithosphere, high heat flow, active faulting, high seismicity, abundant thermal springs, and the widespread distribution of Tertiary volcanic rocks (for example, Eaton 1982; see Chapter 3 of this report). Small-volume basaltic volcanism has been the characteristic form of volcanism in the Great Basin since 5–10 Ma.

Basaltic magma is generated in the upper part of the earth's mantle by partial melting of mantle peridotite. Differences in the pressure and chemistry of the source region, and in the proportion of source rock melted, create a continuous spectrum of basaltic compositions that erupt at the surface. In a simple way, basalt can be divided into two compositional categories, alkalic and tholeiitic. Alkalic basalts have high total alkalis ($Na_2O + K_2O$) and are generated at relatively great depth by small degrees of partial melting. Tholeiitic basalts have lower total alkalis and are generated at shallower depths (35–45 km) by relatively larger degrees of partial melting (Jaques and Green 1980). Experimental data (Takahashi 1980;

Takahashi and Kushiro 1983) indicate that alkalic basalts compositionally similar to those of the Basin and Range province equilibrated at pressures of 14–20 kilobars (kb), equivalent to a depth of 45–65 km. Nearly all of the basalts erupted within the Great Basin since the late Miocene are alkalic (Leeman and Rogers 1970; Best and Brimhall 1974; Farmer et al. 1989; Fitton et al. 1991).

Cenozoic intermediate to silicic calc-alkaline volcanism began in the northern Great Basin during the late Eocene and gradually swept south, ending in southern Nevada by the late Miocene (see Chapter 2 of this report). This southward sweep is thought to be related to declining plate convergence rates and steepening of the dip of the subducted slab, resulting in activation of the asthenospheric mantle wedge and generation of basaltic magma to fuel crustal magmatic systems (Cross and Pilger 1978; Lipman 1980; Best and Christiansen 1991). Eruption of calc-alkaline ash-flow tuffs reached a peak in the Great Basin between 30–20 Ma (the "ignimbrite flare-up") when >50,000 km^3 of tuff was erupted (Best and Christiansen 1991). Isotopic studies of zoned ignimbrite systems suggest that an equal or greater volume of basaltic magma was required to generate these ash-flow tuffs (Johnson 1991). Large-magnitude extension also migrated southward during the Cenozoic (see Chapter 3 of this report), although less systematically than silicic volcanism. The timing of extension and volcanism may not be well correlated in any particular area; extension locally may predate, be contemporaneous with, or postdate silicic volcanism (Axen et al. 1993).

The initiation of true basaltic volcanism in the Great Basin began in the early to middle Miocene (<17 Ma) and generally postdates major silicic volcanism and some of the major phases of extension in any particular region. For example, silicic volcanism of the Timber Mountain complex and peak extension rates in the southern Great Basin occurred simultaneously at 15–10 Ma (Wernicke et al. 1988; Scott 1990; Carr 1990). The commencement of basaltic volcanism occurred during the latter part of this period, and small-volume basaltic volcanism has continued into the Quaternary (see Chapter 2 of this report). Citing several similar examples, Glazner and Ussler (1989) argued that the transition to eruption of basalt in the western United States was not due to increased rates of extension, since basaltic volcanism in any region usually begins *after* extension rates have declined. They proposed instead that the transition was due to increases in mean crustal density resulting from extensional thinning of low-density upper crust and intrusion of mafic magma into the lower crust. Denser crust would enhance buoyant ascent and eruption of basaltic magma (see Chapter 5 of this report). This mechanism would, however, be limited to areas that had undergone high-magnitude extension or focused mafic intrusion.

The "ignimbrite flare-up" was fueled by a large flux of basaltic magma into the crust (Johnson 1991; Best and Christiansen 1991), probably as a result of reactivation of the mantle wedge above a steepening subducted slab following the slowing of subduction rates after the Laramide (Coney and Reynolds 1977; Cross and Pilger 1978; Lipman 1980). Basaltic intrusion, convection in the underlying mantle wedge, and thick crust inherited from the Laramide created an unusually hot crust by the end of the Oligocene. Thermally weakened crust may have been a prerequisite for large-magnitude "ductile" extension in the Basin and Range province in the late Oligocene to early Miocene (Morgan et al. 1986). The extensional collapse of over-thickened and thermally weakened crust followed the slowing of subduction and easing of compressional forces at the continental margin (Coney 1987). Coupled with decreased basalt flux into the crust beginning in the late Oligocene (from breakdown of the mantle wedge), conductive cooling of the thinned crust would be favored.

Overall cooling of the Cordilleran crust in the late Cenozoic is consistent with changes in extensional style and the transition to the eruption of basalt. Two overlapping phases of extensional deformation are recognized during the Cenozoic: (1) an early, mid-Tertiary phase characterized by high strain rates, a shallow brittle-ductile transition, shallow fault penetration, and eruption of voluminous intermediate to silicic volcanic rocks, and (2) a late, Miocene-Pleistocene phase ("Basin and Range event")

characterized by lower strain rates, deeply penetrating faults, the establishment of modern basin and range topography, and bimodal eruptions of basalt and high-silica rhyolite (Christiansen and Lipman 1972; Zoback et al. 1981; Eaton 1982; Morgan et al. 1986; Coney 1987; Keller et al. 1990; Armstrong and Ward 1991). The high strain rates characteristic of Oligocene extension probably in part required a hot and thermally weakened crust, while lower strain rates associated with deep, high-angle faulting are consistent with a cooler, more brittle, and mechanically stronger crust (Morgan et al. 1986). Cooling of the crust may have favored the eruption of basalt because (1) cooling of the crust increases crustal density on a regional scale (enhancing buoyant ascent of basaltic magma), (2) contamination or mixing with more silicic crustal magmas would be inhibited, and (3) basaltic magmas intruded into brittle crust would have access to deeper crustal fractures that would favor rapid ascent without differentiation (Perry et al. 1993).

III. Time-Space Trends in the Location, Composition, and Volume of Basaltic Volcanism

Basaltic volcanism in the Great Basin and adjoining regions has exhibited systematic trends in location, composition, and eruption volume through time. These trends can be related to both tectonic processes in the crust and melt generation processes in the underlying mantle.

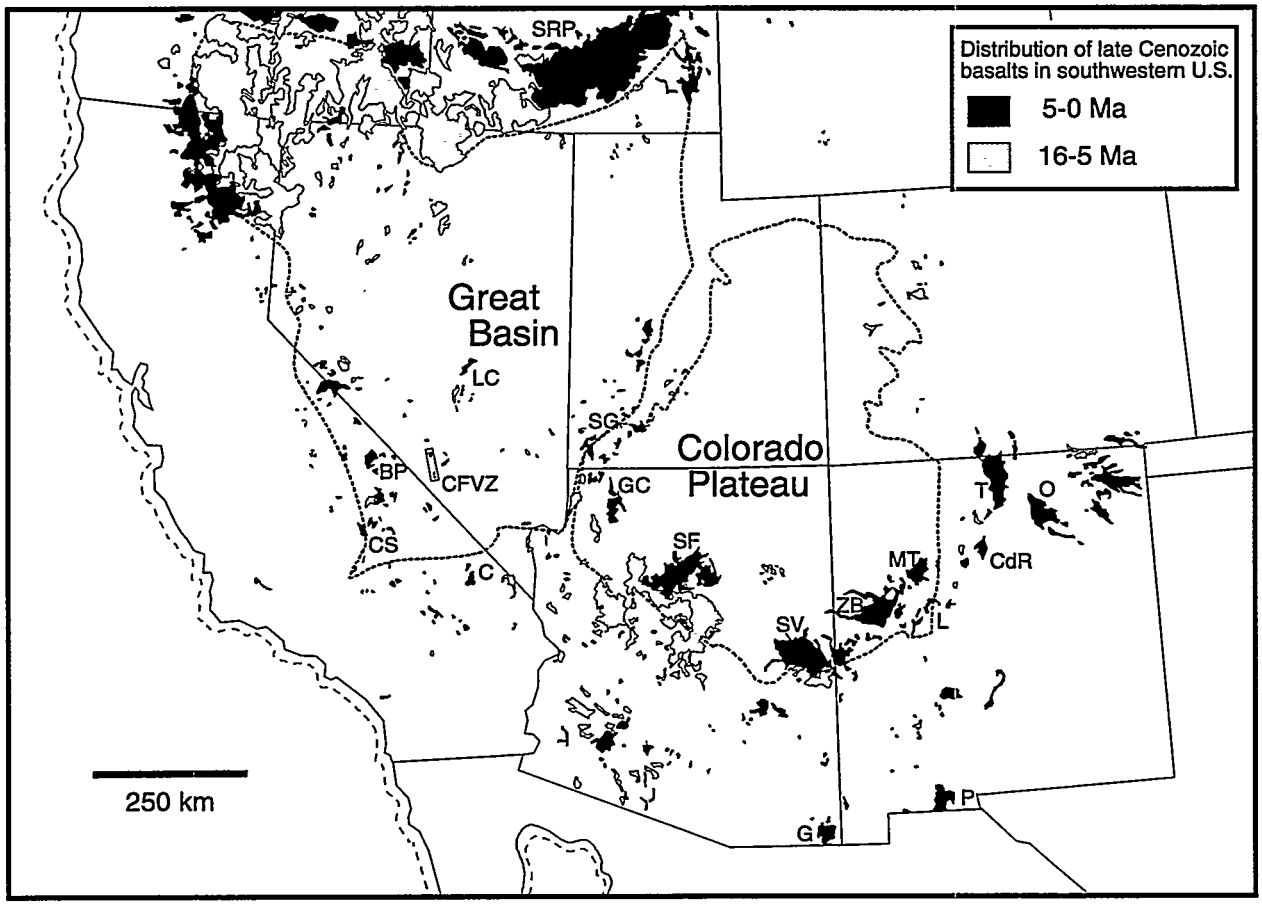


Fig. 4.1 Map of the western United States showing the distribution of basalt erupted during the past 16–5 and 5–0 Ma (after Fitton et al. 1991). Labeled volcanic fields are: BP: Big Pine, C: Cima, CdR: Cerros del Rio, CFVZ: Crater Flat volcanic zone; CS: Coso; G: Geronimo; GC: Grand Canyon; L: Lucero; LC: Lunar Crater; MT: Mount Taylor; O: Ocate; P: Potrillo; SF: San Francisco; SG: St. George; SRP: Snake River Plain; SV: Springerville; T: Taos; ZB: Zuni-Bandera.

Figure 4.1 summarizes the distribution of basaltic rocks in the western United States (excluding the Columbia Plateau) during two time periods: (1) 16–5 Ma, from near the inception of basaltic volcanism to the end of the Miocene, and (2) 5–0 Ma, from the end of the Miocene to the present. Basaltic volcanism was concentrated increasingly along major physiographic margins with time, in particular along the margins of the Great Basin and the Colorado Plateau. Post-Miocene eruption of basalt within the Great Basin interior has been sparse, with the notable exception of a band of post-Miocene basalt that extend from Death Valley to Lunar Crater in central Nevada, including the basalts of Crater Flat (Crowe et al. 1983a). The migration of basaltic volcanism to the margins of the Great Basin correlates with increased extension and seismicity in these areas, indicating that the stress regime exerts a broad control on the location of basaltic eruptions. (Christiansen and McKee 1978).

In the southwestern United States, basaltic volcanic fields that erupted the largest volumes and had the highest eruption rates are associated with the Colorado Plateau margin (Taos, Cerros del Rio, San Francisco, Springerville, Zuni-Bandera, Mount Taylor; Fig. 4.2). Many of these basalt fields erupted tholeiitic basalt in addition to alkalic basalt, indicating higher degrees of partial melting at shallower mantle depths compared to the Great Basin/Basin and Range interior. Basalt fields in the interior of the Basin and Range have volumes that seldom exceed a few tens of cubic kilometers, while several fields along the Colorado Plateau boundary have volumes of 100–300 km^3 (San Francisco, Springerville, Zuni-Bandera, Taos). Long-term eruption rates for several volcanic fields on the Colorado Plateau margin exceed 50 km^3/Ma, while rates within the Basin and Range are <20 km^3/Ma (Fig. 4.2). The volume and eruption rates of basalt fields of the Colorado Plateau margin suggest higher production rates of basaltic magma in the

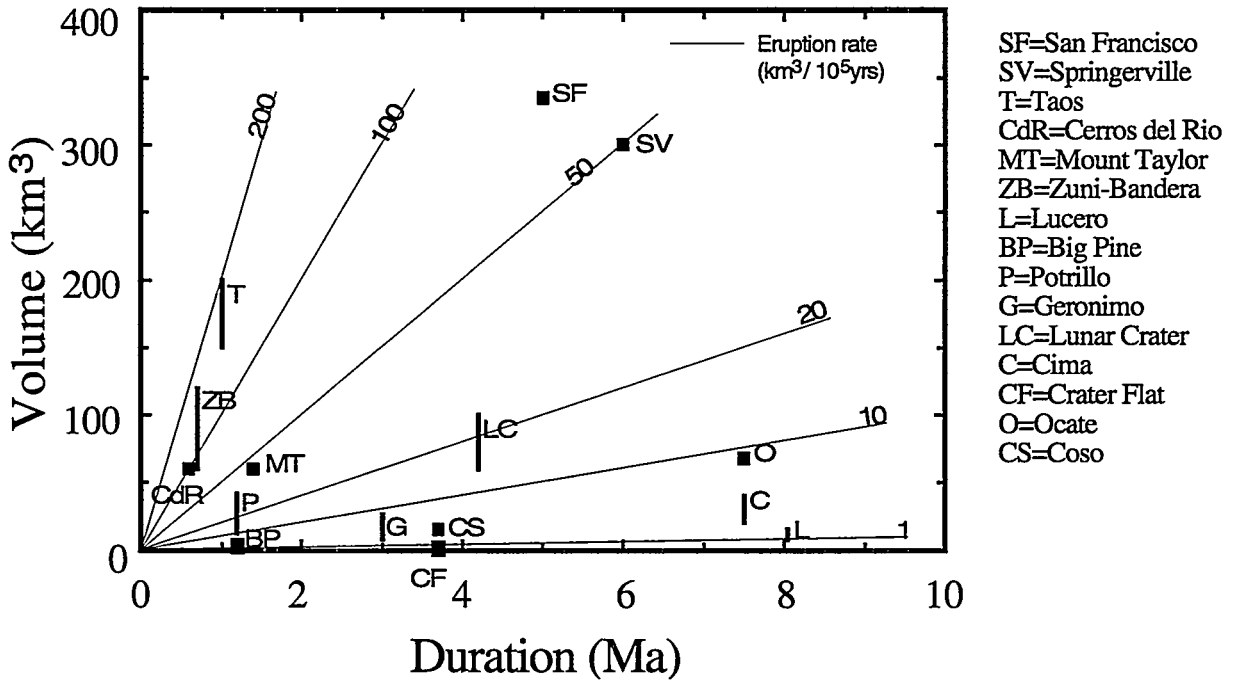


Fig. 4.2 Estimated volume versus eruption duration for late Cenozoic basaltic volcanic fields in the southwestern United States

mantle beneath these areas, compared with mantle beneath the Basin and Range interior.

The composition of basalt erupted within the Great Basin/Basin and Range has also changed systematically through time (Fitton et al. 1991). Basalt erupted since 5 Ma are as a group more silica-undersaturated (more nepheline normative) than basalt erupted before 5 Ma and also have a higher average MgO content, indicating less fractionation en route to the surface (Fig. 4.3). These data suggest that the younger group of basalt represent smaller degrees of partial melting at greater depths in the

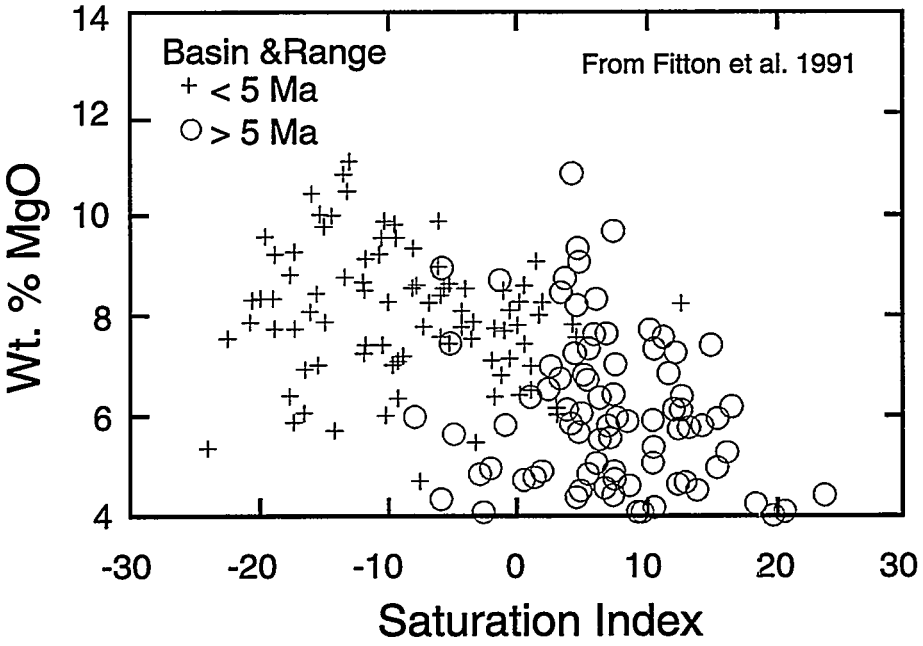


Fig. 4.3 MgO versus saturation index for basalts of the Basin and Range province, after Fitton et al. (1991). Basalts with saturation index <0 are nepheline normative, basalts with saturation index >0 are hypersthene normative.

mantle (e.g., Jaques and Green 1980). Similar changes in composition through time are seen in a number of individual volcanic fields within the Basin and Range, as discussed in a later section of this chapter. The more primitive nature of the younger basalt indicates rapid ascent from the mantle with minimal crustal residence time, possibly because of higher volatile concentrations resulting from smaller degrees of partial melting (Fitton et al. 1991). A trend to smaller degrees of partial melting through time in the Basin and Range is consistent with a decrease in volume erupted through time for a number of individual fields in the Basin and Range. The more volatile-enriched nature of these basalts, however, may result in more frequent eruptions (cf. Smith and Luedke 1984) since these magmas are more likely to ascend rapidly through the crust without achieving buoyancy stagnation (Spera 1984).

IV. The Role of the Mantle in Basaltic Volcanism

Numerous isotopic and trace-element studies of basalt have demonstrated that basalt in the western United States is derived from either asthenospheric mantle (equivalent to oceanic mantle) or ancient lithospheric mantle that has been isolated from asthenospheric convection for periods of greater than a billion years (Menzies et al. 1983; Hart 1985; Perry et al. 1987, 1988; Farmer et al. 1989; Lum et al. 1989; Menzies 1989; Cooper and Hart 1990; Kempton et al. 1991; Fitton et al. 1991; Daley and DePaolo 1992). Perry et al. (1987, 1988) proposed that the source of basalt in the western United States depends on

the timing and intensity of lithospheric extension relative to the timing of basalt eruption. In regions that have undergone little or only recent lithospheric extension, basalts are derived from lithospheric mantle, because asthenospheric upwelling has been limited and has not replaced the preexisting lithospheric mantle. In regions of more pronounced or prolonged extension, asthenospheric mantle eventually replaces lithospheric mantle and becomes the source for basalt. Isotopic evidence indicates that asthenospheric sources are present beneath the southern Basin and Range of New Mexico, Arizona, and southeastern California, as well as the central Great Basin of Nevada. These areas generally underwent the earliest and most intense extension within the Basin and Range province. Lithospheric mantle is still preserved beneath the stable regions of the Colorado Plateau, Rocky Mountains, and Great Plains. Mixed asthenosphere/lithosphere sources are present beneath most of the Colorado Plateau/Basin and Range transition zone, suggesting that these transitional areas are undergoing active conversion of lithospheric sources to asthenospheric sources (Perry et al. 1987).

Farmer et al. (1989) presented isotopic and trace-element data which suggest that basalts of the southern Great Basin have been derived from lithospheric mantle over the last 10 Ma, despite erupting in a region that has undergone active extension for the past 15–10 Ma. This region coincides with the amagmatic gap of Eaton (1982) and was the last portion of the Basin and Range province to begin extending (15–10 Ma). The relative lack of magmatism in this region may have left the lithosphere "cold" and difficult to extend (Wernicke et al. 1987). Both the thermal state and the late initiation of extension of this lithosphere may have combined to preserve lithospheric mantle beneath this region (Farmer et al. 1989).

The presence of lithospheric mantle beneath the southern Great Basin is not wholly compatible with the generation of basaltic magma beneath this region, since lithospheric mantle is generally considered too cold to partially melt. Daley (1992) proposed that if lithospheric mantle beneath the southern Great Basin is hydrous, it can generate basaltic magma at small rates of lithospheric extension, since a small amount of water in the mantle will substantially depress the peridotite solidus. A hydrous mantle source for the basalts of Crater Flat is consistent with their low rubidium contents relative to other incompatible trace elements, which suggests that phlogopite may have played a role in the partial melting process (Vaniman et al. 1982). Daley (1992) calculates that for a 100-km-thick lithosphere and no extension, 1–2 km^3 of basalt could be erupted per 100 km^2 of surface, assuming that 10% of the mantle lithosphere is hydrous, 90% of the melt generated separates from the residue, and 10% of that melt is erupted.

Melting of hydrous lithospheric mantle may also have played a role in the concentration and volume of basaltic volcanism along the Colorado Plateau margin. Best and Brimhall (1974) and Tanaka et al. (1986) suggest that volcanism within the Colorado Plateau transition zone may be caused by viscous heating as asthenospheric flow encountered the thicker lithospheric "edge" beneath the Colorado Plateau. Secondary convection in the asthenosphere, caused by lateral temperature variations (juxtaposition of hot asthenosphere and colder Colorado Plateau mantle lithosphere) may have locally enhanced asthenospheric flow, facilitating heat transport into the adjacent lithosphere (Perry et al. 1987). The combination of hydrous lithospheric mantle and enhanced heat transport from the asthenosphere may have favored the generation and eruption of voluminous alkalic and, in some cases, tholeiitic basalt. In the Great Basin/Basin and Range interior, hydrous lithospheric mantle may have been substantially removed by lithospheric extension and asthenospheric upwelling by the end of the Miocene. The absence of easily fusible lithospheric mantle, and of lateral mantle discontinuities found at physiographic margins, may combine to restrict melting to relatively small amounts at greater depths within the dry and relatively less fusible asthenosphere.

Low mantle seismic velocities beneath much of the Basin and Range province suggest that the upper mantle contains a small percentage of partial melt at all times. Ascent of this melt through the crust to produce basaltic volcanism may depend partly on where local stress regimes are conducive to magma ascent (Smith and Luedke 1984). Against the general background of small melt fractions in the Basin and Range mantle, three northeast-trending zones of enhanced partial melting have been proposed based on identification of low-velocity mantle anomalies (Spence and Gross 1990; Dueker and Humphreys 1990; Humphreys et al. 1992). The northernmost and southernmost of these zones correspond to zones of pronounced magmatism: the Snake River Plain–Yellowstone zone and the Jemez zone of the southeastern Colorado Plateau margin (Fig. 4.1). The middle zone extends from central Utah to southern Nevada and corresponds with surface volcanism at the St. George area of Utah (Dueker and Humphreys 1990) and the Crater Flat area of southern Nevada (Evans and Smith 1992). The volume of basaltic volcanism associated with the St. George zone is far less than the zones to the north and south. At Crater Flat, in particular, 4 Ma of basaltic volcanism has produced only about 1 km^3 of basalt. If the low-velocity anomaly beneath Crater Flat does represent an unusual degree of partial melting relative to the rest of the Basin and Range, it suggests that the local stress regime does not strongly favor magma ascent and eruption.

V. Evolution of Basaltic Volcanic Fields

Many long-lived (>2–3 Ma) basaltic volcanic fields in the southwestern United States display a characteristic evolution in terms of eruption volume and chemistry that can be related to changes in the intensity and depth of partial melting in the mantle. Perhaps the best documented example of systematic volume and chemical relationships through time is the Springerville volcanic field on the southern Colorado Plateau margin of Arizona (Condit et al. 1989). At Springerville, the earliest and most voluminous basalt is tholeiitic (large degree of partial melting), which erupted between 6.5 and 1.75 Ma (Condit et al. 1989; Cooper et al. 1990). After 2 Ma, volcanism shifted to less voluminous eruptions of alkalic basalt, representing smaller degrees of partial melting at greater depth in the mantle. A similar relationship is seen in the Zuni-Bandera volcanic field on the Colorado Plateau margin of western New Mexico (Laughlin et al. 1993). Tholeiite was erupted exclusively in the earliest two episodes (700–600 thousand years (ka) and 200–100 ka), while the youngest episode (<100 ka) erupted both tholeiitic and alkalic basalts. The relationships at Springerville and Zuni-Bandera are consistent with gradual waning of the intensity of mantle melting through time and the eventual extinction of the volcanic field.

Less voluminous basalt fields in the Basin and Range interior show similar patterns of evolution, although the intensity of mantle melting associated with these volcanic fields was apparently never great enough to produce tholeiitic basalt. Examples are the Cima volcanic field of southeastern California and the Lunar Crater volcanic field of central Nevada (Crowe et al. 1986; Wilshire et al. 1991; Foland and Bergman 1992). In these volcanic fields, Pliocene eruptions of alkali basalt form relatively voluminous, sheet-like flows, while Quaternary eruptions were less voluminous and compositionally more undersaturated, again indicating a progression to less intense and deeper mantle melting.

Basaltic volcanism at Crater Flat occurred in three episodes at approximately 3.7, 1, and <0.2 Ma. All of the basalt erupted at Crater Flat are alkalic (Vaniman et al. 1982), indicating relatively small degrees of partial melting in the mantle throughout the lifetime of the field. The volume of alkali basalt erupted through time has decreased, from a minimum of 1 km^3 in the oldest cycle to <0.1 km^3 at the youngest center (Lathrop Wells). The relatively long lifetime of the Crater Flat field, combined with the small volume of erupted material, results in one of the lowest eruptive rates of any basaltic volcanic field in the southwestern United States (Fig. 4.2).

Although declining volumes through time indicate a waning magmatic system, the normative compositions of basalt from different episodes (Vaniman et al. 1982) do not clearly indicate a shift to more undersaturated compositions (and hence, smaller degrees of partial melting) through time. Differences in normative composition appear to be related more to fractionation history (e.g., amphibole removal) than differences in degree of partial melting (Vaniman et al. 1982).

Another factor bearing on the evolution of the Crater Flat field is changes in the fractionation depth of magmas through time which is probably related to changes in magma chamber depth (Perry and Crowe 1992). Lavas of the oldest episode contain plagioclase, olivine, and clinopyroxene phenocrysts, while lavas of the younger episodes contain only olivine. Experimental studies of alkali basalt (Knutson and Green 1975; Mahood and Baker 1986) indicate that clinopyroxene will crystallize early in the crystallization sequence relative to plagioclase at pressures exceeding 8 kb. The lack of plagioclase in lavas of the younger episodes indicates fractionation at high pressure, within the lower crust or upper mantle. The high strontium (which partitions into plagioclase) of the younger episodes also indicates that plagioclase was not an important fractionating phase in the younger episodes. Scandium (which partitions into clinopyroxene) is lower in the youngest episodes relative to the oldest episode, indicating fractionation of clinopyroxene at high pressure. In contrast, lava of the oldest episode contains plagioclase phenocrysts, relatively low strontium, and relatively high scandium (Vaniman et al. 1982), indicating fractionation at low pressure where plagioclase and olivine dominate fractionation. These relationships indicate that magma chambers were relatively shallow (middle to upper crust) at 3.7 Ma but were deep (lower crust or upper mantle) during the younger two episodes (Perry and Crowe 1992).

Frey et al. (1990) suggest that the depth at which magma chambers were established at Mauna Kea is controlled by magma flux into the crust, with older, higher level chambers being sustained by higher magma flux, and younger, lower crustal chambers being established after magma flux declines. Younger lavas at Mauna Kea are more differentiated, suggesting that lavas derived from lower crustal chambers ascend only after magma density is lowered by fractionation of olivine + clinopyroxene. The changes in phenocryst assemblage, trace-element content, and degree of evolution of lavas erupted during the waning of Mauna Kea volcanism almost exactly mirror the changes seen at Crater Flat, suggesting that the evolution to deeper magma chambers at Crater Flat may also reflect a waning magma flux. The Mauna Kea model must be applied cautiously to Crater Flat because (1) the eruption rate at Mauna Kea is orders of magnitude higher, raising questions about whether vastly different magma fluxes can lead to similar ascent dynamics, and (2) Mauna Kea is a single volcano, with an integrated plumbing system, whereas eruptive activity at Crater Flat is spread over several distinct eruptive centers with separate plumbing systems.

Studies of the evolution of the CFVZ as a whole are still at a preliminary stage and will continue in the future. It has recently been established that Thirsty Mesa, at the northwest end of the zone, is about 4.8 Ma old and should be considered as part of the CFVZ. Thirsty Mesa is the most voluminous eruptive center in the CFVZ and evaluation of its geochemistry is important for understanding how the CFVZ has evolved over the past 5 Ma. Studies of the evolution of the CFVZ will be used to evaluate whether volcanism is waxing or waning in the Yucca Mountain region.

VI. Geochemical Evidence for Polygenetic Volcanism in the Crater Flat Volcanic Zone

A controversial aspect of the Lathrop Wells volcanic center, the youngest center in the CFVZ, is whether it is monogenetic, erupted during a single eruptive episode, or polygenetic, formed by multiple eruptive episodes spanning a period of several tens of thousands of years (Wells et al. 1990; Turrin et al. 1991; Wells et al. 1992; Turrin et al. 1992). A monogenetic volcano is formed by the ascent and eruption

of a single batch of magma, generally within a period of months to years (Wood 1980). A small-volume polygenetic volcano, if formed over a period of thousands to tens of thousands of years, would probably involve the eruption of multiple magma batches, since small-volume magmas have limited lifetimes within the lithosphere (except possibly in the case where magma recharge is involved, as discussed below). Geochemical data can generally distinguish whether lavas erupted from a volcanic center are derived from single or multiple magma batches. To test the possibility that multiple magmas were involved in the formation of the Lathrop Wells center, extensive sampling of eruptive units identified by geologic field studies was begun in 1987. To date, over 120 samples have been collected and analyzed for major, trace-element, and isotopic geochemistry to constrain the petrologic evolution of the eruptive center (Fig. 4.4). As discussed below, these data convincingly rule out the possibility that a single magma batch was involved in the formation of the Lathrop Wells center, as is commonly assumed for the formation of a monogenetic center. Combined with field observations, the geochemical data support the conclusion that the Lathrop Wells center was formed during four main eruptive episodes, involving a minimum of 6–8 separate and geochemically distinct magmas.

As discussed in Chapter 2 of this report, the presence of erosional unconformities and soil development between eruptive units indicate that the Lathrop Wells center formed during four main eruptive episodes separated by long periods ($>10^4$ years) of inactivity (Fig. 4.5). Each of the four eruptive episodes is geochemically distinct, showing characteristic depletion and enrichment patterns relative to the average Lathrop Wells composition. (Fig. 4.6). An observation of fundamental importance in interpreting the geochemical variations observed at the Lathrop Wells volcanic center is that magnesium numbers ($[Mg/(Mg+Fe^{2+})] \times 100$) of the basalts (121 samples) cluster tightly around a value of about 54 (Fig. 4.7). Magnesium numbers are a sensitive indicator of the evolution of a magma undergoing fractional crystallization, particularly of a basaltic magma where ferromagnesium minerals (olivine and clinopyroxene) are important components of the fractionating mineral assemblage. A primary basaltic magma formed in equilibrium with normal mantle peridotite will have a magnesium number of approximately 68–72. During subsequent fractional crystallization of olivine and clinopyroxene, this value will decrease. Assuming an initial magnesium number of 70, and purely olivine fractionation, about 20% removal of olivine is required for a magma to evolve to a magnesium number of 54. For a 1/1 mixture of olivine and clinopyroxene in the fractionating assemblage, about 35% removal of crystals is required. This assumes perfect fractional crystallization and Fe/Mg partition values of 0.32 and 0.25 for olivine and clinopyroxene, respectively (Furman et al. 1991). During the evolution of a magma, trace-element concentrations in the magma will change as a function of the partitioning of a particular element between the melt and crystallizing phases, and, if assimilation of crustal material or recharge by new magma occurs, the concentration of trace elements in any new material added to the evolving magma. Any model to account for the trace-element variations between eruptive units at Lathrop Wells (Fig. 4.6) must also satisfy the observation that magnesium numbers of eruptive units are almost invariably the same.

Except for lavas of chronostratigraphic unit I (which contain plagioclase and olivine phenocrysts), olivine is the only phenocryst present in Lathrop Wells eruptive units. Lower scandium contents in Lathrop Wells eruptive units compared to older eruptive centers in the CFVZ (Vaniman et al. 1982) suggest that clinopyroxene *may* have crystallized from Lathrop Wells magmas and been removed during high-pressure crystallization, as is relatively common for alkali basalt magmas (e.g., Mahood and Baker 1986). High strontium contents (>1400 ppm) relative to "normal" alkali basalts (600–800 ppm) and the lack of plagioclase phenocrysts indicate that plagioclase did not crystallize to any significant degree and that strontium has behaved as an incompatible element during the evolution of Lathrop Wells magmas. For these reasons, we consider only olivine and clinopyroxene as potentially significant fractionating phases when modeling the evolution of the Lathrop Wells magmas.

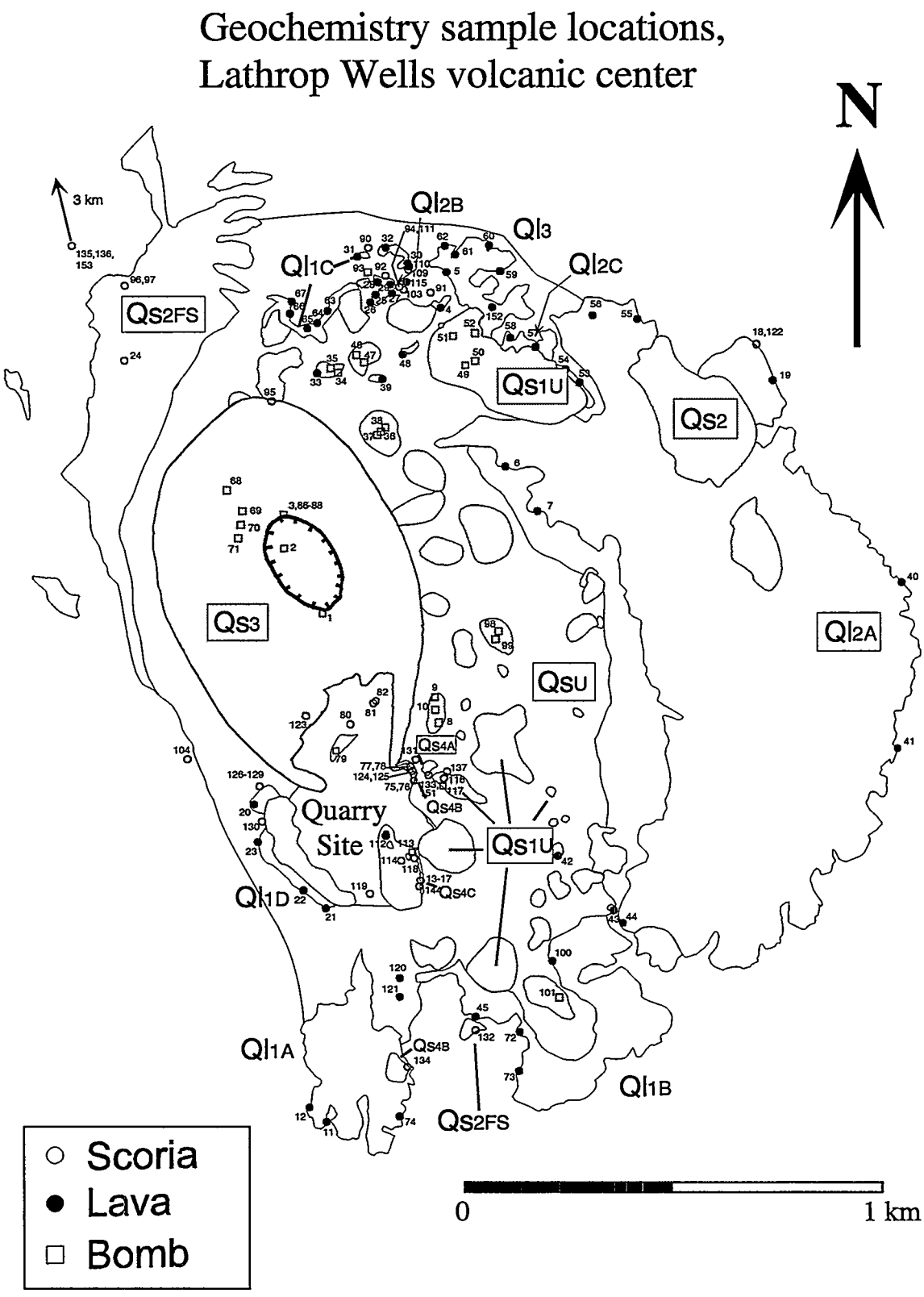


Fig. 4.4 Location of samples collected for geochemistry studies at the Lathrop Wells volcanic center.

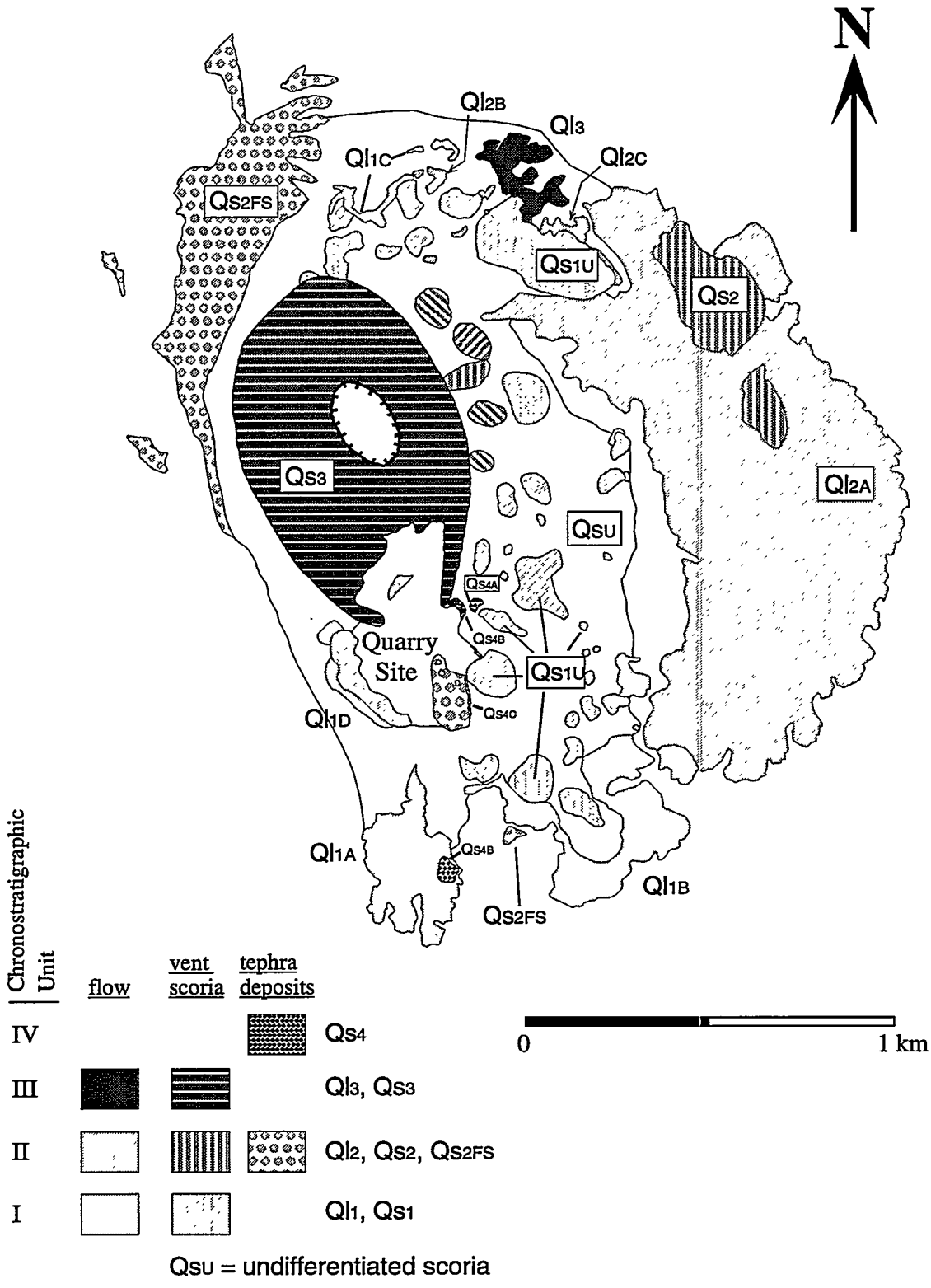


Fig. 4.5 Geologic map of the Lathrop Wells volcanic center. "Ql" refers to Quaternary lava, "Qs" to Quaternary scoria, "Qsfs" to Quaternary scoria/ash fall sheet.

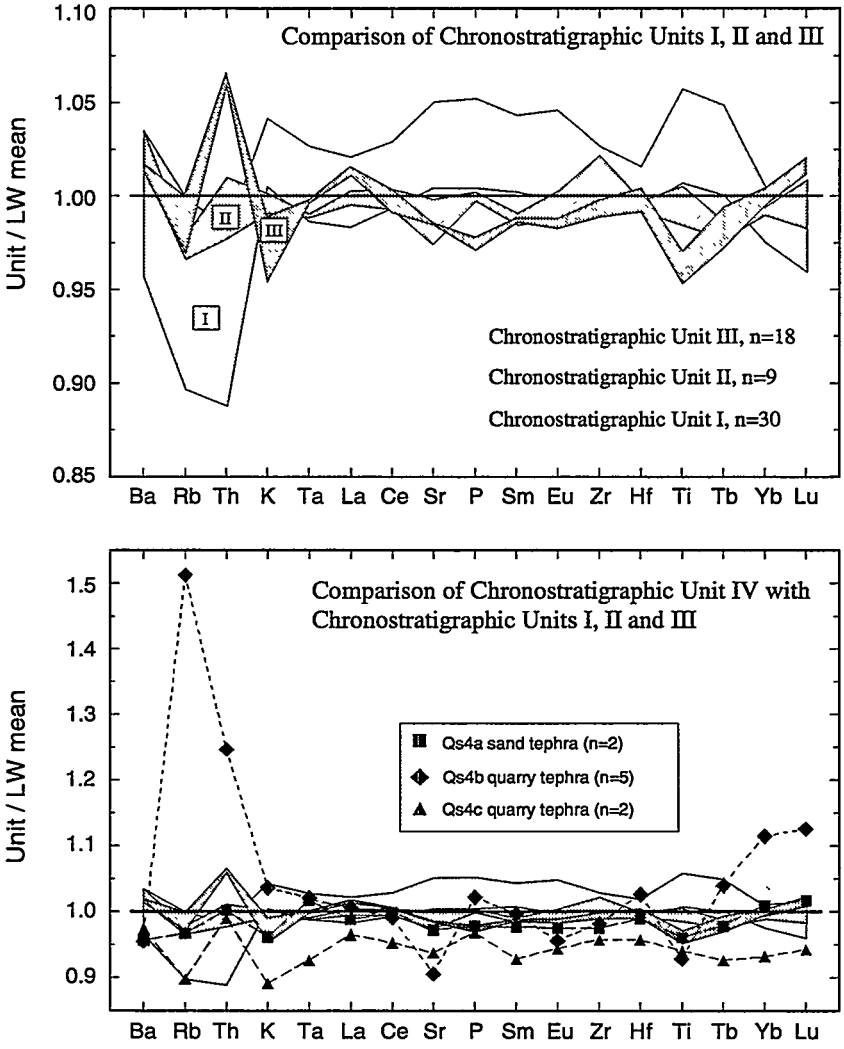


Fig. 4.6 Summary spidergram plot comparing compositions of four major eruptive episodes of the Lathrop Wells volcanic center. Spidergrams are normalized to the average Lathrop Wells composition ($n = 99$).

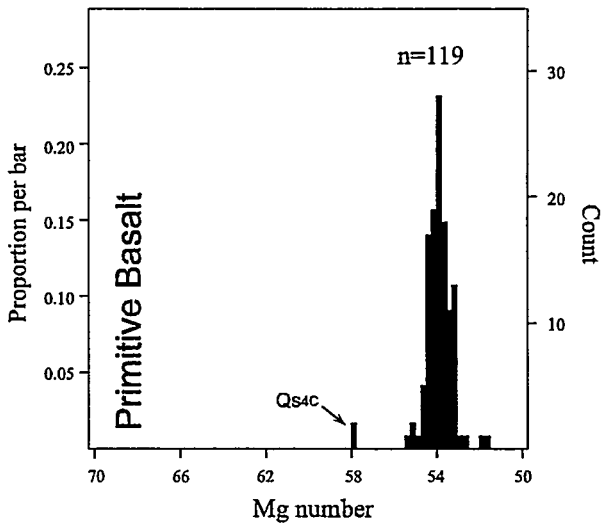


Fig 4.7 Histogram of magnesium (Mg) numbers of samples from the Lathrop Wells volcanic center.

Assuming the identity of fractionating phases is known, elements that are incompatible during fractionation can be used to test whether variations of incompatible elements are the result of simple fractional crystallization. The La/Sm and Th/K of different eruptive units show significant variations when plotted against magnesium numbers (Figs. 4.8 and 4.9). Variation of these ratios with no change in magnesium number is impossible during fractionation of olivine and clinopyroxene from a magma because fractionation of these phases will invariably decrease the magnesium number of the magma. In addition, La/Sm cannot be changed by fractionation of olivine alone and Th/K cannot be changed by fractionation of either olivine or clinopyroxene. The La/Sm ratio can only be changed by fractionation of clinopyroxene, a process that would also decrease the magnesium number of the magma. The relationships between La/Sm, Th/K, and magnesium number thus preclude magmas erupted during separate eruptive episodes from being related by fractionation of a single magma. The same argument applies to variations of neodymium and lead, both incompatible elements during olivine and clinopyroxene fractionation, which show a range of Nd/Pb ratios (Fig. 4.10). The two older eruptive units have higher Nd/Pb compared to the two younger eruptive units, a relationship that is incompatible with fractional crystallization of a single magma.

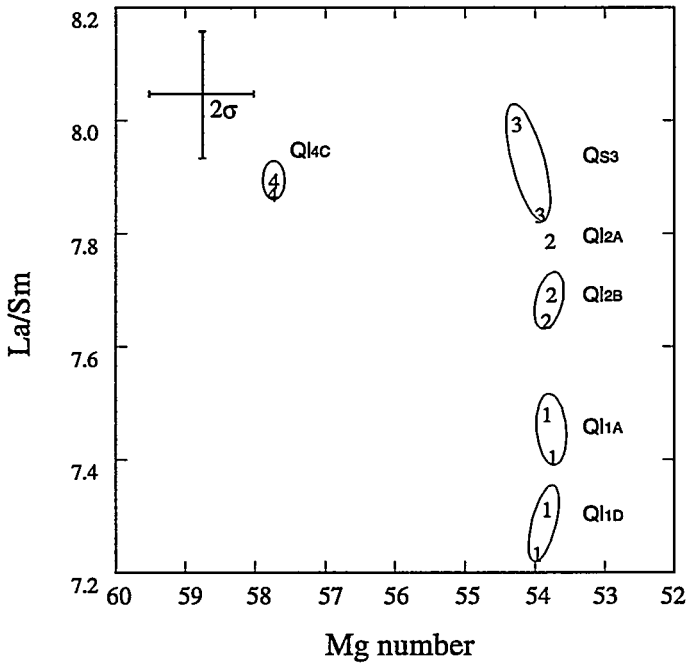


Fig. 4.8 Lanthanum (INAA determination)/samarium (isotope dilution determination) ratio versus magnesium number for eruptive units of the Lathrop Wells volcanic center.

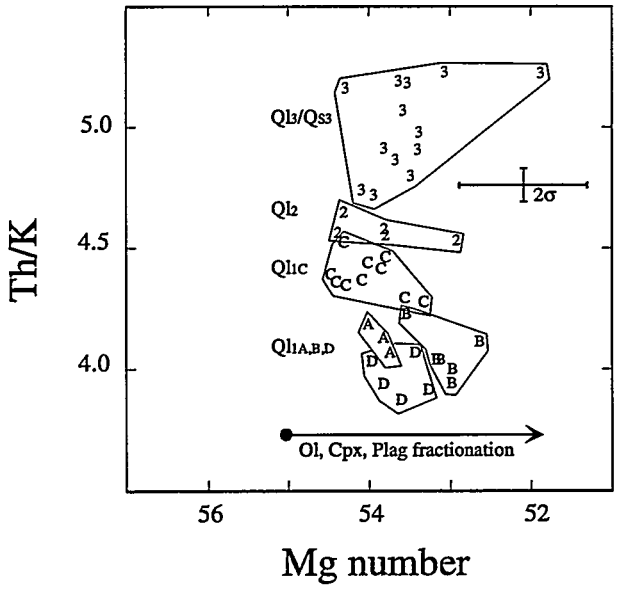


Fig. 4.9 Thorium (INAA determination)/potassium (XRF determination) ratio versus magnesium number for major lava flows and main cinder cone (Qs3) of the Lathrop Wells volcanic center. Vector represents change in magnesium number and Th/K expected for a magma undergoing fractional crystallization.

When the trace-element variations are considered in detail, a minimum of 6–8 separate magma batches can be distinguished that were involved in the formation of the Lathrop Wells center:

Magmas 1–3, Ql1a, Ql1c, Ql1d. Ql1c, the northern flow of chronostratigraphic unit I, is distinguished from the southern flows, Ql1a and Ql1d, by higher Th/K (Fig. 4.9). Units Ql1a and Ql1d can be distinguished by different La/Sm and Nd/Pb (Figs. 4.8 and 4.10) and by the presence of plagioclase microphenocrysts in unit Ql1d.

Magmas 4–5, Ql2 and Qs3/Ql3. Ql2 and Qs3/Ql3 are distinguished from each other and from other eruptive units by different La/Sm, Th/K, and Nd/Pb (Figs. 4.8–4.10).

Magmas 6–8, Qs4a, Qs4b, and Qs4c. Qs4b is distinguished from all other eruptive units at Lathrop Wells by high concentrations of rubidium, thorium, and the heavy-rare-earth elements (Fig. 4.6). Higher concentrations of rubidium and thorium could possibly be due to crustal contamination but it is unlikely that this is the cause of high heavy-rare-earth concentrations (Thompson et al. 1982). The higher concentrations of heavy-rare-earth elements at the same magnesium number of other eruptive units indicate that this is a unique magma. Qs4a and Qs4c are distinguished from other Lathrop Wells eruptive units mainly by higher magnesium numbers and lower concentrations of incompatible elements (Fig. 4.6). These relationships *may* indicate that they represent separate magmas, but more testing is required before this can be firmly established.

If the Lathrop Wells center formed during four separate eruptive episodes, the question remains why magmas supplying different eruptive episodes had almost the same magnesium numbers but different ratios and concentrations of trace elements. At least two mechanisms are possible, one involving multiple magma batches, the other involving a single magma system maintained for the lifetime of the Lathrop Wells center by a continuous or nearly continuous supply of new magma:

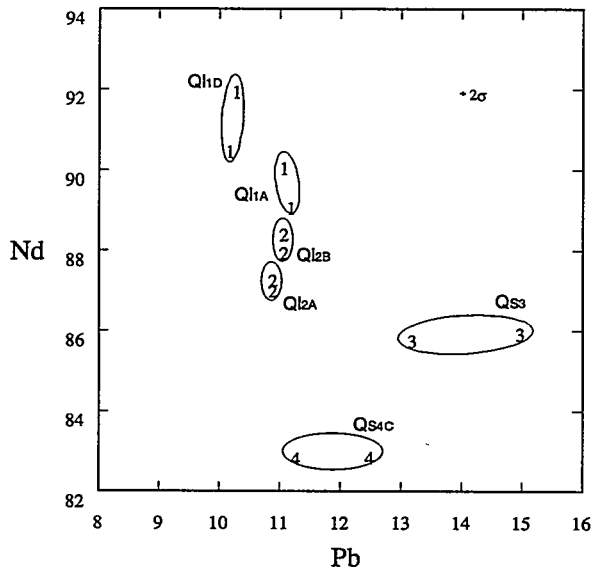


Fig. 4.10 Neodymium versus lead (isotope dilution determinations) for eruptive units of the Lathrop Wells volcanic center.

1. It is possible that the eruption mechanics of magmas were controlled by physical properties of the magmas, such as density or volatile content. Changes in the density and volatile content of a magma are controlled to a large extent by the amount and type of fractionating phases, factors which also largely control the evolution of the magnesium number of a magma (e.g., Stolper and Walker 1980) For this case, we would hypothesize that all magmas evolved along similar paths to a critical density or volatile content (and hence magnesium number) before erupting. To date, we have not explicitly attempted to quantitatively model how the density of a Lathrop Wells magma would change during fractional crystallization of olivine and pyroxene, although it is clear that it would monotonically decrease, since both phases are denser than the melt phase.

2. Another possibility is that a single magma system was active throughout the history of the Lathrop Wells center, with replenishment by new magma from depth supplying enough thermal energy to maintain the system for an extended period of time. In this scenario, the magnesium number of a single evolving magma was maintained at a steady state during recharge by more primitive magma, while trace-element concentrations and ratios continued to evolve as fractionation (and possibly crustal assimilation) proceeded.

To test the second possibility, we have developed a computer spreadsheet model which simultaneously tracks the magnesium number and trace-element composition of a magma undergoing continuous fractionation, eruption, assimilation, and recharge. Trace-element and isotopic compositions of CFVZ basalts indicate that crustal assimilation was not significant during the evolution of CFVZ magmas (e.g. Vaniman et al. 1982; Farmer et al. 1989). Preliminary modeling has therefore emphasized the effects of recharge on the evolution of a hypothetical Lathrop Wells magma system. To be successful, this model must account for incompatible-element ratio differences at the same magnesium number (e.g., Figs. 4.8 and 4.9). Preliminary modeling results indicate that (1) the magnesium number of a fractionating magma can reach a steady state at a particular value if the recharge/fractionation ratio is sufficiently high, and (2) an incompatible-element ratio can significantly change during recharge if the difference between the partition coefficients of the two elements is sufficiently large and the partition coefficient of the more compatible element is also moderately large(>0.1). This could be the case for the La/Sm ratio (Fig. 4.8), *if* clinopyroxene is the dominant fractionating phase. Olivine fractionation cannot change the La/Sm ratio because both lanthanum and samarium are highly incompatible in olivine (partition coefficients $<<0.1$). Recharge probably cannot explain differences in the Th/K ratio at constant magnesium numbers (Fig. 4.9) because both thorium and potassium are highly incompatible during olivine and clinopyroxene fractionation and therefore cannot be fractionated significantly from each other. Models of magma generation and evolution at Lathrop Wells must also account for the observation that the geochemical composition of the four major eruptive units vary systematically with time. For example, La/Sm, Th/K, and thorium generally increase with time, while TiO_2 concentrations decrease with each eruptive episode (Fig. 4.11). We have not yet begun to model these variations, but they may be related to the evolution of a lithospheric mantle source as melt generation and removal depletes certain elements in the source rock, or by a systematic decrease in the degree of mantle melting through time giving rise to a series of magma batches with successively greater concentrations of incompatible elements.

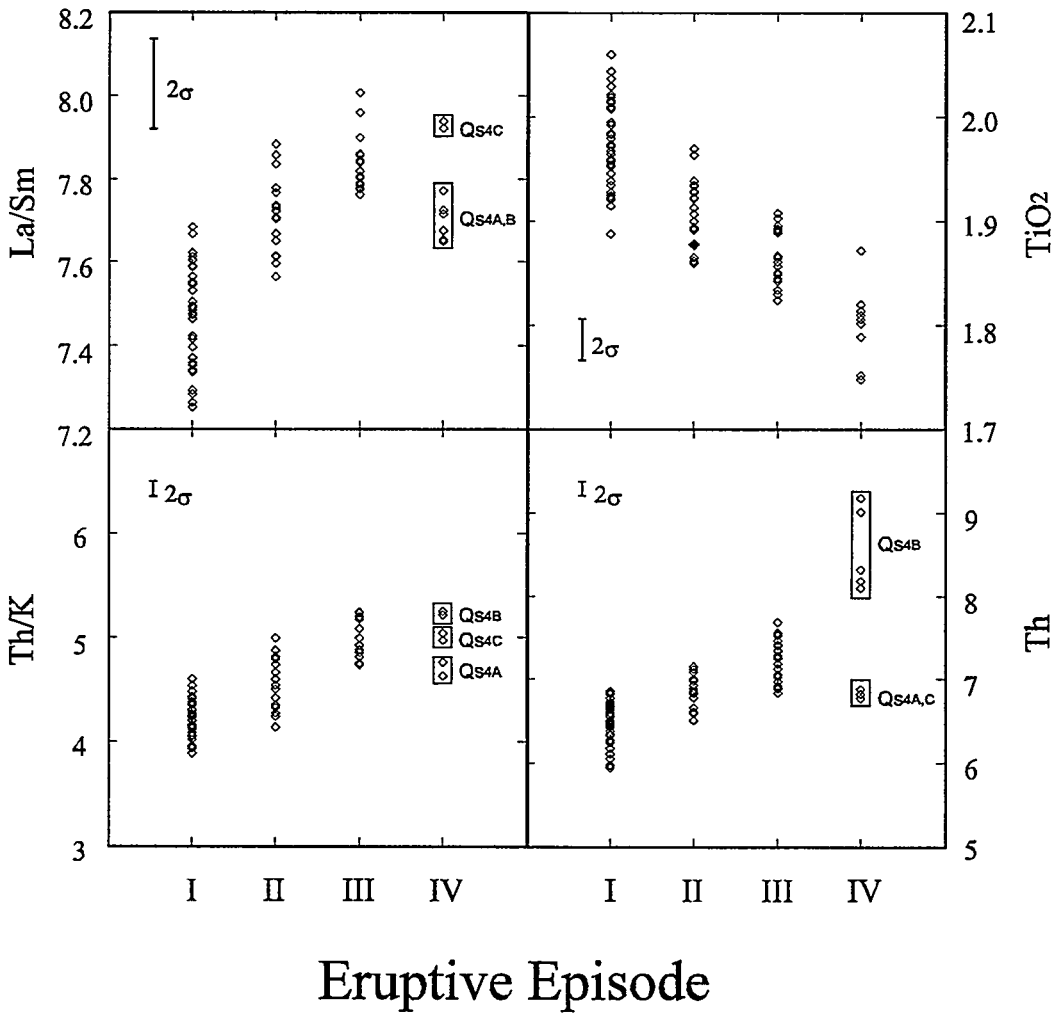


Fig. 4.11 La/Sm, Th/K, thorium and TiO_2 versus eruptive episode for the Lathrop Wells volcanic center.

To date, we have focused geochemical modeling towards testing whether a single or multiple magmas were involved in the formation of the Lathrop Wells center, mainly by testing models of simple fractional crystallization. We will continue to test more complex models of magma evolution to test whether geochemical variations observed at Lathrop Wells can be accounted for by evolution of a single magma system. Based on preliminary modeling, however, we prefer a model of separate, unrelated magma batches to account for geochemical variations observed at Lathrop Wells.

In addition to the petrologic and geochemical evidence for separate magmas at Lathrop Wells, trace-element data from lava flows at Black Cone, in Crater Flat, also indicate that different eruptive units represent distinct and unrelated magma batches. For example, a negative slope relates rubidium and lanthanum values from two different lava flows at Black Cone (Fig. 4.12). However, since both of these elements are incompatible during fractionation of either olivine or clinopyroxene, fractional crystallization will result in a positive slope (increase in both rubidium and lanthanum) and cannot explain the rubidium and lanthanum concentrations of different lava flows at Black Cone. At Paricutin, a calc-alkaline monogenetic volcano in Mexico that erupted over a 9-yr period from a chemically zoned magma chamber,

variations of rubidium and lanthanium display a positive slope (Fig. 4.13), the expected result when a single magma undergoes fractional crystallization and assimilation of crustal wallrock (McBirney et al. 1987). In contrast, the geochemical relationships at Black Cone indicate that, like Lathrop Wells, the center was formed by the eruption of multiple magma batches during polygenetic volcanism.

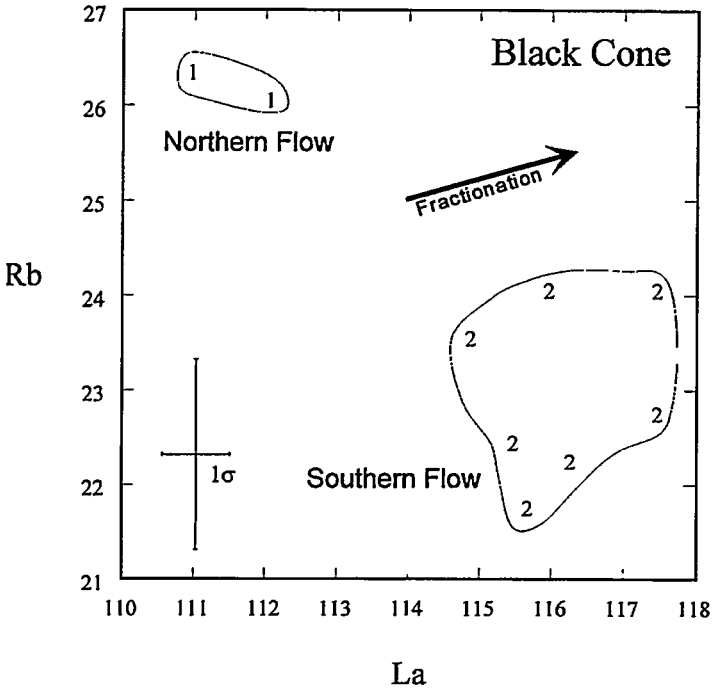


Fig. 4.12 Lanthanum versus rubidium for basalts of the Black Cone volcanic center. Vector represents the shift in rubidium and Ce concentrations expected for a magma undergoing fractional crystallization.

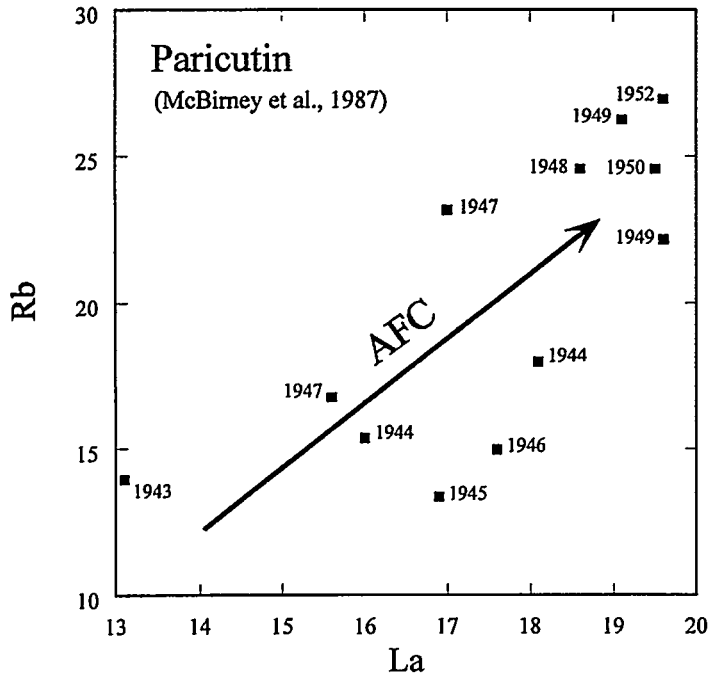


Fig. 4.13 Lanthanum versus rubidium for samples encompassing the 9-yr eruptive history of Paricutin. Numbers by each symbol indicate the year of eruption. Arrow labeled "AFC" indicates the qualitative change in Rb and La concentrations expected for a magma undergoing simultaneous assimilation/fractional crystallization.

The eruption of multiple magmas at individual eruptive centers in the YMR has important implications for volcanic risk assessment. It suggests that once a new volcanic center is established there is a tendency for subsequent magmas to ascend at the same location for a protracted period of time (~10^5 years?), possibly as a result of structural control (Chapter 3 of this of this report). Field, geochemical, and geochronologic evidence indicate that the Lathrop Wells center was formed by the eruption of multiple magma batches during four main eruptive episodes, extending from >100 ka to <4 ka ago. This extended eruptive history indicates that the most likely eruptive event in the YMR during the short term (10^4 years) is another eruption at the Lathrop Wells center, which decreases the probability that magma will directly penetrate the potential Yucca Mountain repository.

VII. References

Armstrong, R. L., and P. Ward, "Evolving Geographic Patterns of Cenozoic Magmatism in the North American Cordillera: the Temporal and Spatial Association of Magmatism and Metamorphic Core Complexes," *Journal Geophysical Research* **96**, 13,201-13,224 (1991).

Axen, G. J., W. J. Taylor, and J. M. Bartley, "Space-Time Patterns and Tectonic Controls of Tertiary Extension and Magmatism in the Great Basin of the Western United States," *Geological Society America Bulletin* **105**, 56-76 (1993).

Best, M. G., and W. H. Brimhall, "Late Cenozoic Alkali Basaltic Magmas in the Western Colorado Plateaus and the Basin and Range Transition Zone, U.S.A., and their Bearing on Mantle Dynamics," *Geological Society America Bulletin* **85**, 1677-1690 (1974).

Best, M. G., and E. H. Christiansen, "Limited Extension During Peak Tertiary Volcanism, Great Basin of Nevada and Utah," *Journal Geophysical Research* **96**, 13,509-13,528 (1991).

Carr, W. J., "Styles of Extension in the Nevada Test Site Region, Southern Walker Lane Belt; an Integration of Volcano-Tectonic and Detachment Fault Models," in *Geological Society America Memoir 176: Basin and Range Extensional Tectonics Near the Latitude of Las Vegas, Nevada*, B. P. Wernicke, Ed. (Geological Society of America, Boulder, Colorado, 1990), pp. 283-303.

Christiansen, R. L., and P. W. Lipman, "Cenozoic Volcanism and Plate Tectonic Evolution of the Western United States, II, Late Cenozoic," *Philosophical Transactions Royal Society London, Series A.*, **271**, 249-284 (1972).

Christiansen, T. L., and E. H. Mckee, "Late Cenozoic Volcanic and Tectonic Evolution of the Great Basin and Columbia Intermontane Regions," in *Geological Society America Memoir 152: Cenozoic Tectonics and Regional Geophysics of the Western Cordillera,* R. B. Smith and G. P. Eaton, Eds. (Geological Society of America, Boulder, Colorado, 1978), pp. 283-311.

Condit, C. D., L. S. Crumpler, J. C. Aubele, and W. E. Elston, "Patterns of Volcanism Along the Southern Margin of the Colorado Plateau: the Springerville Field," *Journal Geophysical Research* **94**, 7975-7986 (1989).

Coney, P. J., "The Regional Tectonic Setting and Possible Causes of Cenozoic Extension in the North American Cordillera," in *Continental Extensional Tectonics*, M. P. Coward, J. F. Dewey, and P. L. Hanock, Eds. (Geological Society Special Publication 28, 1987), pp. 177-186.

Coney, P. J, and S. J. Reynolds, "Cordilleran Benioff Zones," *Nature* **270**, 403-406 (1977).

Cooper, J. L., J. L. Aronson, C. D. Condit, and W. K. Hart, "New K-Ar Ages of Lavas from the Colorado Plateau-Basin and Range Transition Zone, East-Central Arizona," *Isochron/West* **55**, 28-31 (1990).

Cooper, J. L., and W. K. Hart, "Mantle Sources in the Arizona Transition Zone and Global Mantle Heterogeneity," *Geology* **18**, 1146-1149 (1990).

Cross, T. A., and R. H. Pilger, "Constraints on Absolute Motion and Plate interaction inferred from Cenozoic Igneous Activity in the Western United States," *American Journal Science* **278**, 865-902 (1978).

Crowe B. M., D. T. Vaniman, and W. J. Carr, "Status of Volcanic Hazard Studies for the Nevada Nuclear Waste Storage investigations," Los Alamos National Laboratory Report LA-9325-MS (1983a).

Crowe, B. M., K. H. Wohletz, D. T. Vaniman, E. Gladney, and N. Bower, "Status of Volcanic Hazard Studies for the Nevada Nuclear Waste Storage investigations," Los Alamos National Laboratory Report LA-9325-MS, Vol. II (1986).

Daley, E. E., "Temporal and Spatial Variations in Compositions of Young Mafic Volcanic Rocks of the Southwestern Basin and Range: Isotopic Constraints on the Relationship Between Thinning in the Lithosphere and Extensional Deformation of the Upper Crust," Ph.D. Dissertation, University of California, Berkeley, 205 pp. (1992).

Daley, E. E., and D. J. Depaolo, "Isotopic Evidence for Lithospheric Thinning During Extension: Southeastern Great Basin," *Geology* **20**, 104-108 (1992).

Dueker, K. and E. Humphreys, "Upper-Mantle Velocity Structure of the Great Basin," *Geophysical Research Letters* **17**, 1327-1330 (1990).

Eaton, G. P., "The Basin and Range Province: Origin and Tectonic Significance," *Annual Reviews Earth Planetary Science* **10**, 409-440 (1982).

Evans, J. R., and Smith, M., "Teleseismic Tomography of the Yucca Mountain Region: Volcanism and Tectonism," *Proceedings High-Level Radioactive Waste Management Conference, Las Vegas, Nevada* (American Nuclear Society, La Grange Park, Illinois, 1992), pp. 2371-2380.

Farmer, G. L., F. V. Perry, S. Semken, B. Crowe, D. Curtis, and D. J. Depaolo, "Isotopic Evidence on the Structure and Origin of Subcontinental Lithospheric Mantle in Southern Nevada," *Journal Geophysical Research* **94**, 7885-7898 (1989).

Fitton, J. G., D. James, and W. P. Leeman, "Basic Magmatism Associated With Late Cenozoic Extension in the Western United States: Compositional Variations in Space and Time," *Journal Geophysical Research* **96**, 13693-13711 (1991).

Foland, K. A., and S. C. Bergman, "Temporal and Spatial Distribution of Basaltic Volcanism in the Pancake and Reveille Ranges North of Yucca Mountain," *Proceedings High-Level Radioactive Waste Management Conference, Las Vegas, Nevada* (American Nuclear Society, La Grange Park, Illinois, 1992), pp. 2366-2371.

Frey, F. A., W. S. Wise, M. O. Garcia, H. West, S. T. Kwon, and A. Kennedy, "Evolution of Mauna Kea, Hawaii: Petrologic and Geochemical Constraints on Postshield Volcanism," *Journal Geophysical Research* **95**, 1271-1300 (1990).

Furman, T., F. A. Frey, and K. Park, "Chemical Constraints on the Petrogenesis of Mildly Alkaline Lavas from Vestmannaeyjar, Iceland: the Eldfell (1973) and Surtsey (1963-1967) Eruptions," *Contributions Mineralogy Petrology* **109**, 19-37 (1991).

Glazner, A. F., and W. Ussler III, "Crustal Extension, Crustal Density, and the Evolution of Cenozoic Magmatism in the Basin and Range of the Western United States," *Journal Geophysical Research* **94**, 7952-7960 (1989).

Hart, W. K., "Chemical and Isotopic Evidence for Mixing Between Depleted and Enriched Mantle, Northwestern U.S.A.," *Geochemica Cosmochemica Acta* **49**, 131-144 (1985).

Humphreys, E. D., Dueker, K. G., and G. Biasi, Western U.S. Tectonic and Volcanic Activity: the Role of the Mantle, *Geological Society America Abstracts with Programs* **24**, (5) 34 (1992).

Jaques, A. L., and D. H. Green, "Anhydrous Melting of Peridotite at 0-15 Kb Pressure and the Genesis of Tholeiitic Basalts," *Contributions Mineralogy Petrology* **73**, 287-310 (1980).

Johnson, C. M., "Large-Scale Crust Formation and Lithosphere Modification Beneath Middle to Late Cenozoic Calderas and Volcanic Fields, Western North America," *Journal Geophysical Research* **96**, 13,485-13,507 (1991).

Keller, G. R., P. Morgan, and W. R. Seager, "Crustal Structure, Gravity anomalies and Heat Flow in the Southern Rio Grande Rift and their Relationship to Extensional Tectonics," *Tectonophysics* **174**, 21-37 (1990).

Kempton, P. D., J. G. Fitton, C. J. Hawksworth, and D. S. Ormerod, "Isotopic and Trace Element Constraints on the Composition and Evolution of the Lithosphere Beneath the Southwestern United States," *Journal Geophysical Research* **96**, 13,713-13,735 (1991).

Knutson, J., and T. H. Green, "Experimental Duplication of A High-Pressure Megacryst/Cumulate Assemblage in A Near-Saturated Hawaiite," *Contributions Mineralogy Petrology* **52**, 121-132 (1975).

Laughlin, A. W., F. Perry, P. Damon, M. Shafiqullah, G. Woldegabriel, W. Mcintosh, C. Harrington, S. G. Wells, and P. Drake, "Geochronology of the Mount Taylor, Cebollita Mesa and Zuni-Bandera Volcanic Fields," Cibola County, New Mexico, *New Mexico Geology* **15**, 81-92 (1993).

Leeman, W. P., and J. W. Rogers, "Late Cenozoic Alkali-Basalts of the Basin-Range Province, USA," *Contributions Mineralogy Petrology* **25**, 1-24 (1970).

Lipman, P. W., "Cenozoic Volcanism in the Western United States: Implications for Continental Tectonics," in *Continental Tectonics* (National Academy of Science, Washington, D. C., 1980), pp. 161-174.

Lum, C. L., W. P. Leeman, K. A. Foland, J. A. Kargel, and J. G. Fitton, "Isotopic Variations in Continental Basaltic Lavas as indicators of Mantle Heterogeneity: Examples Form the Western U.S. Cordillera," *Journal Geophysical Research* **94**, 7871-7884 (1989).

Mahood, G. A., and D. R. Baker, "Experimental Constraints on Depths of Fractionation of Mildly Alkalic Basalts and Associated Felsic Rocks: Pantelleria, Strait of Sicily," *Contributions Mineralogy Petrology* **93**, 251-264 (1986).

McBirney, A. R., H. P. Taylor, and R. L. Armstrong, "Paricutin Re-Examined: a Classic Example of Crustal Assimilation in Calc-Alkalic Magma," *Contributions Mineralogy Petrology* **95**, 4-20 (1987).

Menzies, M. A., W. P. Leeman, and C. J. Hawksworth, "Isotope Geochemistry of Cenozoic Volcanic Rocks Reveals Mantle Heterogeneity Below Western USA," *Nature* **303**, 205-209 (1983).

Menzies, M. A., "Cratonic Circumcratonic and Oceanic Mantle Domains Beneath the Western United States," *Journal Geophysical Research* **94**, 7899-7915 (1989).

Morgan, P., W. R. Seager, and M. Golombek, "Cenozoic Thermal, Mechanical and Tectonic Evolution of the Rio Grande Rift," *Journal Geophysical Research* **91**, 6263-6276 (1986).

Perry, F., W. S. Baldridge, and D. J. Depaolo, "Role of Asthenosphere and Lithosphere in the Genesis of Late Cenozoic Basaltic Rocks from the Rio Grande Rift and Adjacent Regions of the Southwestern United States," *Journal Geophysical Research* **92**, 9193-9213 (1987).

Perry, F., W. S. Baldridge, and D. J. Depaolo, "Chemical and Isotopic Evidence for Lithospheric Thinning Beneath the Rio Grande Rift," *Nature* **332**, 432-434 (1988).

Perry, F. V., and B. M. Crowe, "Geochemical Evidence for Waning Magmatism and Polycyclic Volcanism at Crater Flat, Nevada," *Proceedings High-Level Radioactive Waste Management Conference, Las Vegas, Nevada* (American Nuclear Society, La Grange Park, Illinois, 1992), pp. 2356-2365.

Perry, F. V., D. J. Depaolo, and W. S. Baldridge, "Neodymium Isotopic Evidence for Decreasing Crustal Contributions to Cenozoic Ignimbrites of the Western United States: Implications for the thermal Evolution of the Cordilleran Crust," *Geological Society America Bulletin* **105**, 872-882 (1993).

Scott, R. B., "Tectonic Setting of Yucca Mountain, Southwest Nevada," *Geological Society America Memoir 176: Basin and Range Extension near the Latitude of Las Vegas Nevada*, B. P. Wernicke, Ed. (Geological Society of America, Boulder, Colorado, 1990), pp. 251-282.

Smith, R. L., and R. G. Luedke, Potentially Active Volcanic Lineaments and Loci in Western Conterminous United States, in *Explosive Volcanism: Inception, Evolution, and Hazards* (National Academy Press, Washington, D. C., 1984), pp. 47-66.

Spence, W., and R. S. Gross, "A Tomographic Glimpse of the Upper Mantle Source of Magmas of the Jemez Lineament, New Mexico," *Journal Geophysical Research* **95**, 10,829-10,849 (1990).

Spera, F. J., "Carbon Dioxide in Petrogenesis III: Role of Volatiles in the Ascent of Alkaline Magma With Special Reference of Xenolith-Bearing Lavas," *Contributions Mineralogy Petrology* **88,** 217-232 (1984).

Stolper, E., and D. Walker, "Melt Density and the Average Composition of Basalt," *Contributions Mineralogy Petrology* **74,** 7-12 (1980).

Takahashi, E., "Melting Relations of an Alkali-Olivine Basalt to 30 Kbar, and their Bearing on the Origin of Alkali Basalt Magmas," *Carnegie Institution Washington Year Book 79*, 271-276, 1980.

Takahashi, E., and I. Kushiro, "Melting of Dry Peridotite at High Pressures and Basalt Magma Genesis," *American Mineralogist* **68,** 859-879 (1983).

Tanaka, K. L., E. M. Shoemaker, G. E. Ulrich, and E. W. Wolfe, "Migration of Volcanism in the San Francisco Volcanic Field," *Geological Society America Bulletin* **97,** 129-141 (1986).

Thompson, R. N., A. P. Dicken, I. L. Gibson, and M. A. Morrison, "Elemental Fingerprints of Isotopic Contamination of Hebridean Palaeocene Mantle-Derived Magmas By Archaean Sial," *Contributions Mineralogy Petrology* **79,** 159-168 (1982).

Turrin, B. D., D. Champion, and R. J. Fleck, "$^{40}Ar/^{39}Ar$ Age of the Lathrop Wells Volcanic Center, Yucca Mountain, Nevada," *Science* **253,** 654-657 (1991).

Turrin, B. D., D. E. Champion, and R. J. Fleck, "Measuring the Age of the Lathrop Wells Volcanic Center at Yucca Mountain," *Science* **257,** 555-558 (1992).

Vaniman, D. T., B. M. Crowe, and E. S. Gladney, "Petrology and Geochemistry of Hawaiite Lavas from Crater Flat, Nevada," *Contributions Mineralogy Petrology* **80,** 341-357 (1982).

Wells, S. G., L. D. McFadden, C. E. Renault, and B. M. Crowe, "Geomorphic Assessment of Late Quaternary Volcanism in the Yucca Mountain Area, Southern Nevada: Implications for the Proposed High-Level Waste Repository," *Geology* **18,** 549-553 (1990).

Wells, S. G., B. M. Crowe, and L. D. McFadden, "Measuring the Age of the Lathrop Wells Volcanic Center at Yucca Mountain," *Science* **257,** 555-558 (1992).

Wernicke, B. P., R. L. Christiansen, P. C. England, and L. J. Sonder, "Tectonomagmatic Evolution of Cenozoic Extension in the North American Cordillera," in *Continental Extensional Tectonics,* M. P. Coward, J. F. Dewey, and P. L. Hancock, Eds. (Geological Society Special Publication 28, 1987), pp. 203-221.

Wernicke, B., G. J. Axen, J. K. Snow, "Basin and Range Extensional Tectonics at the Latitude of Las Vegas, Nevada," *Geological Society America Bulletin* **100,** 1738-1757 (1988).

Wilshire, H. G., A. V. Mcguire, J. S. Noller, and B. D. Turrin, "Petrology of Lower Crustal and Upper Mantle Xenoliths from the Cima Volcanic Field, California," *Journal Petrology* **32,** 169-200 (1991).

Wood, C. A., "Morphometric Analysis of Cinder Cone Degradation," *Journal Volcanology Geothermal Research* **8,** 137-160 (1980).

Zoback, M. L., R. E. Anderson, and G. A. Thompson, "Cainozoic Evolution of the State of Stress and Style of Tectonism of the Basin and Range Province of the Western United States," *Philosophical Transactions Royal Society London* **300,** 407-434 (1981).

CHAPTER 5: SEGREGATION, TRANSPORT, AND LOCAL STORAGE OF BASALTIC MAGMA

I. Summary

Basaltic magma of the Yucca Mountain region (YMR) originates in the upper mantle probably by processes of decompression melting. Once a melt is formed, it segregates from its solid mantle residue through a process of two-phase flow involving buoyant rise of the melt accompanied by deformation and compaction of the matrix. The mechanics of melt segregation are controlled by the equations of conservation of mass and momentum. The form of melt-matrix equations has been determined but not for all assumptions of boundary conditions. A controversial aspect of computer modeling of the melt segregation equations is the existence of solitons. Some workers argue that the formation of solitons may lead to spatial and temporal episodicity of melt segregation. Alternatively, the features may be short-lived and incapable of affecting surface volcanic patterns. Small-volume basaltic magmatism in the YMR is probably a product of relict mantle instability from athenospheric upwelling in the Miocene and/or continuing low rates of extensional deformation. There is nearly complete agreement that basalt magma ascends via fluid-assisted fracture propagation as dikes. The formation and form of magma transport in dikes have been described by many authors using different assumptions dependent on whether the shapes of magma-formed fractures are controlled by the rock properties or the dynamics of flowing magma. The latter view requires assessment of elastic deformation of the country rock and fracture, flow, and gas-properties at the dike tip. Field evidence shows that dikes can be modeled as planar cracks formed in brittle solids by pressurization and dilation associated with magma injection. Magma in dikes will rise until it erupts, solidifies, or reaches the level of neutral buoyancy (LNB). The position of the LNB in the Yucca Mountain area may be influenced by the density interface between low-density basin fill, and the Paleozoic rocks. Other processes such as crack-rate propagation, wall-rock permeability, magma-gas content, or mechanisms of volatile concentration in a dike tip could negate the controls of the LNB. One additional issue is the control of dike orientations by preexisting fractures. Field observations show that dikes can both fill fractures or fault planes or propagate by magma-induced fracture in directions controlled by the stress field. The structural controls of basaltic centers in the YMR suggest that feeder dikes may follow northwest-trending structure at depth but divert at shallow levels to north-northeast strikes following the maximum compressive stress direction.

II. Introduction

This section provides a brief overview of the processes of accumulation and ascent of basalt magma in a continental extensional setting and emphasizes the mechanisms of melt segregation and transport of magma via magma-driven fracture through the mantle and crust. Consideration is given as well to storage of basalt in the mantle and crust and at its LNB, where magma may propagate laterally. There has been substantial progress, particularly in the 1980's, in mathematically describing the processes of segregation, migration, and eruption of magma. We review the relevant aspects of these processes, focusing primarily on the constraints that can be developed for the physical dimensions of magma systems, the mechanical interactions of magma and country rock, and the rates of operation of magmatic processes. These constraints are applied where possible in attempting to understand the time-space patterns of basaltic volcanism in the YMR.

III. Melt Generation And Segregation

We assume, first, that partial melt of basaltic composition originates in the upper mantle at depths of 45 to 60 km. There is a wealth of petrologic information on the geochemical processes of melt formation constrained mostly by the major, trace-element and isotopic composition of erupted basalt (see Chapter 4). The processes controlling the formation of the magma are perhaps best known for the generation of mid-ocean ridge basalt (MORB). Melting of oceanic mantle almost certainly occurs because of adiabatic upwelling beneath mid-ocean ridge spreading centers. Here, oceanic lithosphere is upheld on a reservoir of convecting asthenospheric mantle of probable uniform composition. Recent reviews of processes controlling melting in the upper mantle are provided by Kinzler and Grove (1992), Eggins (1992), and Cordery and Morgan (1993). They note that decompression melting results when mantle rises faster than it can exchange heat with the surrounding rocks (adiabatically). Excess heat is lost through melt production, and that loss is controlled by the latent heat of fusion of mantle peridotite, the heat capacity, the ambient mantle temperature, and the pressure and compositional fields of the mantle solidus (Kinzler and Grove 1992). The degree of melting generally increases with continuing decompression. Melting continues until either conductive cooling from above lowers the temperature below the solidus or a basaltic component is extracted. The extracted melt may migrate through the matrix or move preferentially in channels but most probably moves by porous flow (D'Arcy flow). Melt velocities are assumed to be much higher than the velocity of upwelling mantle (Cordery and Morgan 1993). Percolation allows the melt to maintain equilibrium with the matrix; channel segregation isolates the melt from the matrix (Eggins 1992). The two processes have different effects on the resulting melt geochemistry.

Melt production in the mantle below the YMR is constrained by the unique upper mantle of the southern Great Basin. First, the area is located on the north edge of the amagmatic gap (see Chapter 3; Farmer et al. 1989; Jones et al. 1992). The region south of Yucca Mountain exhibited no magmatism during the Mesozoic and Cenozoic despite major plutonic episodes in the late Mesozoic (Farmer and DePaolo 1983), and profound mid-Cenozoic extension (Jones et al. 1992). Second, the isotopic composition of strontium and neodymium in basalt in the YMR shows that it is underlain by preserved lithospheric mantle (Farmer et al. 1989). The isotopic characteristics of basalt generated in the lithospheric mantle have remained uniform for basalt melts from about 10 Ma to about 100 ka, the age of the youngest basaltic volcanic center in the Yucca Mountain region (YMR) (Farmer et al. 1989). The presence of thick and cold lithospheric mantle reduces significantly the ability of athenospheric upwelling to penetrate the crust and generate magma that feeds surface volcanism (Nicolas 1990). Finally, while initiation of a melting anomaly probably occurs in the athenospheric mantle, the isotopic composition of the basalt of the YMR requires that the erupted melt component was derived from or equilibrated with the lithospheric mantle (Farmer et al. 1989).

Once a melt is formed by decompression melting, it must be segregated from its solid residue and ascend before solidification to erupt eventually at the surface. Sleep (1974) noted melt can move as a two-phase flow involving the solid rock and the melt that exists in the matrix at grain intersections. The melt-filled grain intersections form a porous three-dimensional network in the rock. The basic dynamic process is that when melt is formed, it will tend to rise and segregate driven by buoyancy. A relatively new aspect of understanding of buoyant magma transport is that movement of melt in a porous rock matrix needs to account for the effects of compaction of the solid matrix. The equations for a two-phase flow system rising through the buoyancy of the melt phase accompanied by deformation and compaction of the matrix have been described by many workers (for example, Scott and Stevenson 1984; McKenzie 1984; Fowler 1984; Scott and Stevenson 1986, 1989).

Ribe (1987), Scott and Stevenson (1989), Fowler (1990a), and Cordery and Morgan (1993) provided the most recent reviews of the basic equations of melt segregation and compaction. They noted that the mechanics of melt segregation are controlled by conservation of mass and momentum. Summarizing and using the form of the compaction-migration equations of Fowler (1990a), conservation of mass for the melt requires:

$$\chi_t + \nabla \cdot [\chi u^l] = S$$

where χ is the liquid mass fraction, u^l is the liquid velocity, and S is the melting rate. Darcy's law for the melt velocity is:

$$u^l - u^s = -k\chi \nabla [p_l + \rho_l g y]$$

where u^s is the solid velocity, k is the permeability coefficient, p_l is the liquid pressure, ρ_l is the liquid density, g is gravity, and y is the vertical coordinate. The viscous compaction relation requires:

$$p_s - p_l = -\left(\frac{\eta_m}{\chi}\right) \left[\frac{\tau_m}{p_s - p_l}\right]^{n-1} \nabla \cdot u^s$$

where p_s is the solid pressure, η_m is the mantle viscosity scale, and τ_m is the mantle deviatoric stress scale. Conservation of energy requires:

$$\rho_s L S + \rho_s c_p \frac{dT}{dt} - \beta T \left[\frac{\rho_s}{\rho_l} \chi \left(\frac{\partial p_l}{\partial t} + u^l \cdot \nabla p_l\right) + \right.$$

$$\left. \left(\frac{1-\chi}{1+r_\chi}\right) \left(\frac{\partial p_s}{\partial t} + u^s \cdot \nabla p_s\right)\right) = k \nabla^2 T$$

where L is the latent heat, c_p is the specific heat at constant pressure, T is the temperature, β is the thermal expansion coefficient, d/dt is the material derivative, r is the shrinkage ratio, and k is the thermal conductivity. Finally, the Clapeyron relation requires:

$$T = T_0 + \Gamma p_l$$

where T_0 is a reference temperature and Γ is the slope of the Clapeyron curve.

The equations for matrix flow include conservation of mass:

$$\nabla \cdot u^s = -\nabla \cdot [\chi (u^l - u^s)]$$

conservation of momentum:

$$-\nabla p_s+\nabla\cdot\tau+\nabla[(\rho_s/\rho_l)\chi(p_s-p_l)]+\rho g=0$$

and the stress/strain rate relation:

$$\tau_{ij}=\eta\left(\frac{\partial u_s^i}{\partial x_j}+\frac{\partial u_s^i}{\partial x_i}\right)$$

Fowler (1990a) notes that there is general agreement on the form of the matrix and melt flow equations but there are widely varying assumptions concerning the boundary conditions of the modeled processes. There are two areas of concern. First, a common assumption is that all the segregated magma ascends through the lithosphere via dike propagation. An alternative view is that some component of the partial melt solidifies during segregation and ascent. Second, the dynamics of melting are often neglected by assuming the melting rate **S** to be zero and ignoring the energy equation. A proposed alternative (Fowler 1990a) is to establish the boundary conditions by applying mass conservation, force balance, surface energy balance, and the continuity of temperature and free energy. Cordery and Morgan (1993) assume that the percentage of melt present is small (less than a few percent), and melt is extracted as a steady state process.

A number of workers (Scott and Stevenson 1984, 1986, 1989; Richter and McKenzie 1984; Scott et al. 1986; Scott 1988) have examined, through computer modeling and laboratory experiments, flow through compacting media using modified forms of these equations. Their results reveal the somewhat surprising existence of solitary wave solutions called solitons or magmons (Scott and Stevenson 1984, 1986). Solitons are waves that propagate through the compacting media as a porosity pulse responding to pressure gradients. Assignment of reasonable permeability and rheological properties to these features gives wavelengths of kilometers and velocities of centimeters per year. The volume of liquid within a magmon of this size is about 1 km^3 (Scott and Stevenson 1986). Most authors have been cautious about applying concepts of solitary waves to surface volcanic patterns but this phenomenon could lead to spatial and temporal episodicity of melt segregation if the patterns are not removed or obscured by processes of crustal transport. Coredery and Morgan (1993), for example, note that an assumption of steady state extraction eliminates the existence of magmons.

Fowler (1990b) examined applications of a compaction model for melt transport. He argued that solitary waves can propagate primarily under conditions of zero melting ($\mathbf{S} = 0$). Under conditions when $\mathbf{S} \neq 0$, solitary waves move at a nonconstant speed of $2z^{1/2}/\zeta$, where z is the vertical coordinate ($z = 0$ at the base of the melt zone) and ζ is the compaction height. The amplitude of the solitary waves decays according to $1/z^{1/2}$ and may exhibit nonlinearity and diffusion, leading to degrading. Fowler (1990b, his Appendix B) also obtained nonlinear equations for solitary waves by adding other melting variables and argued that the waves are only short-term features. He verified the concept of compaction length but argued that other complications such as bulk viscosity, melt refreezing, and fracturing need to be considered. Scott and Stevenson (1989) agree that solitary waves are probably not important under conditions of high melt production (fast-spreading). They suggest. however, that solitary waves could provide a mechanism for explaining oscillating magmatic rates at slow spreading

ridges. This suggests the wave phenomenon could be important for areas of low melt production associated with small-volume continental basaltic volcanism typical of the YMR. The exceptionally small volume of Pliocene and Quaternary basaltic volcanism of the YMR may be especially appropriate. However, this requires that the episodic nature of solitary wave phenomena be preserved through the processes of ascent and eruption of magma. An interesting but highly speculative concept is that the episodic nature of polygenetic eruptive models may originate or be influenced by oscillatory solitary waves. Scott and Stevenson (1989) point out that the existence of solitary waves has only been indicated from one- and two-dimensional modeling; it has not been explored yet for three-dimensional modeling. The issue of three-dimensional modeling of melt migration has been addressed by Spiegelman and Wiggins (1993). They suggest the form of melt migration in three dimensions is in spherical waves of melt fraction. These waves form from perturbations to steady-state flow, and can link to form a channel network aiding melt propagation. Spiegelman and Wiggins (1993) note that solitary waves may contribute to episodicity of magmatism derived from the mantle.

Nicolas (1986, 1990) considered constraints on the depth of melting and melt extraction of basaltic magma. While most of the considerations are for MORB, they can be applied by inference to continental settings. First, the melting process is thought to occur primarily in the athenosphere, which corresponds to the convecting mantle where heat is transferred by convective flow and the system is adiabatic (Nicolas 1990). Second, in general, a diapir initiated in the athenosphere will rise accompanied by melting until it reaches the lithosphere. Here it may keep rising but melting ceases (McKenzie 1984; Nicolas 1990). If the asthenosphere diapir has a slow ascent rate, it will barely penetrate the lithosphere. Again, we note the presence of the thick, largely unmodified and presumably cool lithospheric mantle beneath the YMR (Farmer et al. 1989). This cold upper mantle should inhibit the development of large zones of upwelling in the region. The diapirs under these conditions are probably less energetic with low upward velocities, low degree of extracted melt (<7%), and limited penetration of the lithosphere (Nicolas et al. 1987; Nicolas 1990).

A pertinent question to consider is the mechanisms responsible for the generation of the volcanic rocks in the YMR. The setting of the Yucca Mountain site in the Basin and Range province, the tectonic association with intense episodes of Miocene extensional faulting, and the exceptionally large volume of Miocene volcanism in the Southwest Nevada Volcanic Field almost certainly requires a genetic link between volcanism and large-scale athenospheric upwelling (for example, Eaton et al. 1978; Christiansen and McKee 1978; Lachenbruch and Sass 1978; Eaton 1982; Jones et al. 1992). The peak of upwelling must have coincided with the peak of tectonism and volcanism (12 Ma) (see Chapter 3), and may have significantly eroded and induced melting in the lower lithospheric mantle. The dramatic decrease in the volume of volcanism in the late Miocene in the YMR must have been in response to a decrease in the rate of athenospheric upwelling. The small-volume episode of postcaldera basaltic volcanism that has continued from the Miocene to the Quaternary clearly must not be associated with earlier large-scale athenospheric upwelling. Instead the basalts may be be formed by two alternative processes (or a combination of processes): (1) discontinous melting of hydrous heterogeneities in what is presently the lower lithospheric mantle, and (2) continuing, but at diminished rates, extensional deformation in the Basin and Range province. Tectonism, as recorded in rates of extensional faulting, has waned dramatically in the YMR since the Miocene but continues to the active (see Chapter 3). The modern low rates of extensional faulting are compatible with the generation of only small volumes of basaltic magma (<0.5 km^3 in the Quaternary). Generation and eruption of larger volumes of basaltic magma in the YMR is probably inhibited by the presence of cool lithospheric mantle (Farmer et al. 1989) and waning tectonism.

IV. Magma Ascent

Once basaltic melt is segregated, it must move to the surface rapidly to avoid solidification with decreasing temperature. There is nearly complete agreement that transport occurs through fluid-assisted fracture propagation. This conclusion is based on the global observation of basalt dikes in a range of tectonic settings in both oceanic and continental crust. Fissure eruptions at many volcanoes prove that magma is fed from linear dikes. Dikes are exposed commonly in the vent facies of dissected volcanoes. Dikes are exposed in country rock beneath and adjacent to deeply dissected volcanoes. Dike swarms are commonly observed crosscutting cratonic and ultramafic rocks. Flow of basaltic magma through fractures provides the most compelling mechanism for transmitting magma through cool country rock without temperature loss resulting in solidification (Lister and Kerr 1991).

Extraction of magma into conduits opened by melt-fracture requires that the melt pressure exceed the yield pressure of mantle peridotite. The depth of this process can be constrained best by the depth of earthquakes and deep harmonic tremor; this information is known only for oceanic island basalt. Aki and Koyanagi (1981) examined the depth distribution of harmonic tremor below Kilauea Volcano, Hawaii. They distinguished tremor from earthquakes by the duration and period of the former. The amplitude of tremor is sustained longer than earthquakes, and distant stations show the same period as close stations. Deep tremor is separated from shallow tremor by a uniform distribution of amplitude over distance for the latter. Aki and Koyanagi (1981) found seismic evidence of deep tremor to a depth of about 55 km that may mark the depth of onset of magma transport by magma-fracture. They also noted that the reduced displacement of tremor (directly proportional to the rate of magma flow) is an order of magnitude smaller than estimates of magma supply for Kilauea (Swanson 1972; Shaw 1980, 1987). Aki and Koyanagi (1981) suggested, based on this discrepancy, that a significant component of magma is transported through dikes that may propagate aseismically. Ryan (1988) showed that the seismicity patterns below Kilauea Volcano reveal the presence of a primary magma conduit that is concentrically zoned to 34 km. He interprets the zonal structure to be a central region of higher permeability surrounded by a region of numerous dikes.

The formation and form of magma transport in dikes have been described by many authors. Pollard (1976, 1987), Pollard and Muller (1976), and Delaney and Pollard (1981) described theoretical studies of dikes and calculated solutions for the equilibrium shapes of magma-formed fractures largely from a prospective of rock mechanics. Lister and Kerr (1991) note that these analyses are valid only if the intrusion shapes are determined after the magma stops flowing but has not solidified. Moreover, they suggest the dynamics of magma fracture must incorporate properties of the flowing magma, including elastic and inelastic deformation (Rubin 1993) of the country rock and fracture at the dike tip.

Spence et al. (1987) derived equations governing the steady, vertical propagation of a two-dimensional dike driven by buoyancy from a linear source. Lister (1990) extended their analysis and showed that elastic deformation and country rock strength are important primarily at the dike tip. The most recent review of fracture propagation and magma transport in dikes is by Lister and Kerr (1991). We draw heavily from their work in the following summary.

Field observations of dikes show that country rock around intrusions moved apart; there has been little sliding or offset parallel to the dike margins (Pollard 1987, p. 14). This suggests that dike intrusions can be modeled as planar cracks formed in brittle solids by pressurization and dilation associated with injection of magma (Lister and Kerr 1991). This treatment requires consideration of

elastic pressures, stresses at the fracture tip, density-driven buoyancy, viscous pressure drop associated with flowage of magma, deviatoric tectonic stress normal to the dike, and the overpressure of the magma (Lister and Kerr 1991).

The response of mantle and crustal rocks to fracture is dependent on the stresses applied and the time scale of rock response. Observed and inferred propagation velocities of magma in dikes (tens of cm to m sec^{-1}) suggest a short time scale of rock response. The strain imparted to the rock by dike emplacement is measured by the ratio of dike thickness to length (Pollard 1987); it is typically $< 10^{-3}$ to 10^{-4}. These conditions suggest rock response can be modeled as an elastic response (Lister and Kerr 1991). Rubin (1993) noted the zones of inelastic deformation are produced at the tips of propagating dikes.

Elastic response in rocks is measured by the shear modulus u and the Poisson's ratio v; typical values are 25-35 GPa and 0.22-0.28 for basalt, respectively (Lister and Kerr 1991). Dike geometry can rarely be established from field relations but can be approximated as a two-dimensional, blade-shaped crack or a three-dimensional penny-shaped crack (Maaloe 1987; Pollard 1987). Representative lengths of dikes are about 2 km long and a meter wide (Maaloe 1987).

Fractures propagate primarily by extension of preexisting microcracks governed by the stress field and bond strength near the crack tip (Lister and Kerr 1991). The stress field near the tip of a crack has the form (Lister and Kerr 1991):

$$\sigma_{ij} = K f_{ij}(\theta) / (2r)^{1/2}$$

where r and θ are plane polar coordinates centered on the crack tip, f_{ij} are a function of θ, and K is a coefficient known as the stress intensity factor. Crack propagation is governed by a critical stress intensity factor called the fracture toughness K_c (Pollard 1987).

Magma will tend to rise by buoyancy if its density is less than the density of the surrounding rock. The LNB is the level of neutral buoyancy where magma is neither positively nor negatively buoyant. The position of this zone in the crust will determine whether, and at what depth, magma may form lateral intrusions or magma chambers (Walker 1989). The difference in gravitation force on a magma body is equivalent to a hydrostatic pressure gradient on the magma given by (Lister and Kerr 1991):

$$\frac{dP_h}{dz} = (\rho_r - \rho_m)\, g$$

where $\rho_m(z)$ and $\rho_r(z)$ are the densities of magma and rock at a depth z below the surface. If the density difference is assigned a general value of $\Delta\rho$, during ascent of magma, then the total hydrostatic pressure is $\Delta P_h \approx \Delta\rho g h$ where h is the height of rise. Generally, magma is less dense than the mantle and the lower crust. The LNB in Hawaii is on the order of 3 to 6 km below the surface (Walker 1989).

The mean velocity of magma averaged across a dike width (w) depends on ∇p, the spatial gradient in the fluid pressure. For laminar flow the velocity u is:

$$u = -\frac{w^2}{3\eta}\nabla p$$

where η is the magma viscosity. Conservation of fluid volume shows that the thickness of a dike-induced fracture varies with (Lister and Kerr 1991):

$$\frac{\partial w}{\partial t} = \nabla \cdot (uw)$$

An approximation of the flow velocity u in a fracture is

$$u \sim \frac{l}{t}$$

where l is the length of the fracture and t is the time since initiation of the fracture (see Lister and Kerr [1991], Fig. 1 for the definition of h, l, and w for fractures of different geometry). A typical pressure drop in laminar flow along a fracture of length l may be estimated from combining the preceeding two equations:

$$\Delta P_v \sim \frac{\eta l^2}{w^2 t}$$

The crust of the earth is in a complex state of stress and the regional lithospheric stress deviates from the lithostatic value dependent on location. If the tectonic stress perpendicular to a dike is σ then the shape of a dike depends on σ by an effective normal stress $\sigma - \Delta P_i$. For most cases the effective overpressure $\Delta P_o = \Delta P_i - \sigma$ (where ΔP_i is the internal pressure). Lister and Kerr (1991) argue that σ does not vary significantly with depth; ΔP_o can be assumed to be constant.

Lister and Kerr (1991) evaluated the balance between ΔP_e, ΔP_f, ΔP_h, ΔP_v, and ΔP_o. The ΔP_e is approximately equal to mw/l where m is the shear modulus divided by 1 - Poisson's ratio, w is fracture thickness, and l is shorter than the other two dimensions. The ΔP_f is the internal pressure required to propagate a magma fracture, ΔP_h is hydrostatic pressure, and ΔP_v is the pressure drop by laminar flow along the length of a fracture. They used the following equations from Weertman (1971) and Pollard and Muller (1976) assuming a constant Δp:

$$p(z) = \Delta P_o + \Delta \rho g z$$

where $p(z)$ is the magmatic pressure and

$$w(z) = \frac{h}{m}(\Delta P_o + \frac{1}{2}\Delta\rho g z)\ (1-\frac{z^2}{h^2})^{1/2}$$

where $w(z)$ is the dike width and K the stress intensity at the dike tips is

$$K(\pm h) = h^{1/2}(\Delta P_o \pm \frac{1}{2}\Delta\rho g h)$$

Lister and Kerr (1991) examined the relations among the last three equations to evaluate the closure of ends of dikesandtheconditions of dike propagation. They note that a dike must exceed a vertical extent of 100 m and a width of 2 mm to propagate upwards by buoyancy (p. 10,055). Further, as h increases ΔP_h increases and ΔP_f decreases. This requires that as h gets large $\Delta P_f << \Delta P_h$ and demonstrates that rock toughness or resistance to fracture is much less important than the hydrostatic pressures (however, see Rubin 1993 for alternative views based on field observations). A dike will propagate until it reaches the LNB or solidifies. The relation between ΔP_f and ΔP_h suggests there is limited advantage gained by magma ascending along preexisting fractures (Lister and Kerr 1991), a conclusion that is not always consistent with field observations (Delaney et al. 1986; Pollard 1987; Rubin 1993)). An exception to this conclusion would be if the dike tip is deflected by existing fractures or joints and therefore preferentially follows fractures or if inelastic deformation depends upon the near-tip stress field. Lister and Kerr (1991) argue that the rate of propagation of magma is controlled primarily by viscous resistance of the flow of magma into the dike tip and that a dike is unable to close from the bottom upwards because it is difficult to expel viscous magma from a closing crack.

Lister and Kerr (1991) note that $\Delta P_h \approx \Delta P_e$ when:

$$\frac{h^2}{w} \sim \frac{m}{\Delta\rho g}$$

Since dikes are generally only one or two meters wide, $h^2/w >> m/\Delta\rho g$, and therefore $\Delta P_h >> \Delta P_e$. They conclude that the transport of magma in feeder dikes is dominated by the balance between buoyancy forces and viscous drag. They also argue that the local hydrostatic pressure gradient does not need to be positive throughout ascent. It needs to be positive only when averaged over the length of the conduit. Other considerations are that a dike is held open against elastic stresses ΔP_e by a small fluid overpressure ΔP_o. The latter is determined by the supply rate of magma from below, a variable that has not been well defined in magma transport models. The elastic pressures are large at the dike tip. Overall, propagation and transport of a feeder dike are controlled by the balance between $dP_h/dz \approx dP_f/dz$ (Lister and Kerr 1991). This allows the derivation (Lister and Kerr 1991; see also Spence and Turcotte 1990, their equation [1]):

$$\frac{\partial w}{\partial t} + \frac{\partial}{\partial z}(\frac{\rho_r - \rho_m g w^3}{3\eta}) = 0$$

V. Eruption or Intrusion of Basaltic Magma

The preceding equation shows that (neglecting temperature effects) magma will rise through the crust to be erupted at the surface or will stagnate and can spread laterally at the LNB. Ryan and Blevins (1987) and Walker (1989) discussed the importance of the LNB, particularly for the Hawaiian volcanoes. Important problems related to these concepts are the degree of overshoot of ascending magma beyond the LNB and the lateral spread of magma at the LNB. Both could lead to eruption, the former if the LNB is located at a shallow level in the crust, the latter if the combination of lateral propagation of dikes and topographic irregularity lead to breaching of the surface. The controls of lateral movement of magma at the LNB forming blade-like dikes have been discussed extensively for Kilauea Volcano, Hawaii and Krafla Volcano, Iceland by Rubin and Pollard (1987).

Buoyancy-driven magma ascent following the concepts of Lister and Kerr (1991) has several important applications to the YMR. The shallow structure of the region is characterized by low-density (basin-fill) deposits in Crater Flat and possibly beneath Yucca Mountain. The density interface between these deposits and underlying higher density deposits (Paleozoic rocks) may be about 2 to 4 km below the Yucca Mountain area based on interpretations of gravity and seismic refraction data (Snyder and Carr 1984). This density interface could control the depth of the LNB. In this case, the depth of the density interface suggests the LNB may be deep beneath the region, perhaps considerably below the depth of the potential repository. However, an unknown variable is the degree of magma overshoot through and above the LNB. Additionally, if the LNB was a completely effective barrier to ascent of magma, the basaltic rocks of the Crater Flat area would not be present. Either the LNB is not an effective barrier or other processes such as crack-propagation rate, wall-rock permeability, or initial gas content of magma may locally or temporally be more important. If the LNB is an important barrier to magma ascent, the depth of the density interface suggests that magma should not propagate to the surface but instead spread laterally at the LNB. Consideration of the significance of this phenomenon may be important mostly for evaluating the effect of intrusions on the waste isolation system of the YMR.

The concept of an LNB could provide a means of explaining the length of propagation of the longest cluster of basalt centers in the YMR, the Quaternary basalt of central Crater Flat. The length of this aligned chain is 12 km, significantly longer than typical dike lengths (Crowe et al. 1983b; Maaloe 1987; Pollard 1987; Rubin and Pollard 1987). An alternative interpretation is that the chain represents magma that upwelled beneath the Red Cone and Black Cone centers and propagated laterally as a bladed dike, at a shallow level. Note however, that topography in the Crater Flat basin would not favor the formation of bladed dikes. However, if dike propagation did occur, it would follow the direction of the maximum compressive stress direction. Makani Cone and the Little Cone centers may represent eruptive centers formed at the ends of a propagated dike system. This would require the length of dike propagation to be only 6 km (1/2 the cone cluster length). Additionally, it could explain the small volume of the end centers (Little and Makani Cones) compared to the Red Cone and the Black Cone centers. This interpretation may be tested by examination of petrology data and modeling of aeromagnetic data for Crater Flat. The basalt magma of the centers is distinctly more magnetic than the alluvial fill of Crater Flat (Kane and Bracken 1983) and it may be possible to model the aeromagnetic data, enhanced with ground magnetic data, to test for the presence and geometry of lateral feeder systems beneath the centers.

The presence of sills and lopolithic centers at the Paiute Ridge area is possibly consistent with trapping of magma at the LNB. These intrusions formed just above the interface between the Paleozoic carbonates and the primary and reworked pyroclastics of the Paintbrush Tuff (distal facies of the units exposed at Yucca Mountain), a potential density contrast and possible zone of weakness (Crowe et al. 1983b). Support for this interpretation is provided by the lopolithic structure of some intrusions (Byers and Barnes 1967; Crowe et al. 1983b). Sagging of the floor of some intrusions may have been caused by emplacement of magma with a density greater than the density of the underlying country rock. Alternative interpretations other than the LNB control of the intrusions of the Paiute Ridge area are possible. Perhaps the most convincing evidence against LNB control of intrusion depth is that many intrusions were fed by dikes that propagated to the surface. If the LNB had been an effective barrier, the magma would not have reached the surface. In some cases, the intrusions formed locally above the carbonate-pyroclastic interface and not *at* the density interface (Valentine et al. 1992). The local formation of intrusions may be controlled by asperities along fault planes that the dikes occupy (Valentine et al. 1993). The sagging of the floor of intrusions to form lopoliths may be associated with locally intense welding of the country rock, and the attendant porosity reduction, not density sagging.

An additional mechanism that may be important for the transport of magma in dikes is the possibility of exsolution of volatiles at the tips of the dikes. Lister and Kerr (1991) note that the width w of a dike approaches 0 at the crack tip. This requires the mean velocity to be very small or the pressure gradient very large. Extension of a fluid-filled crack requires low fluid pressure in the tip promoting exsolution of volatiles. Lister (1990) has, using assumptions of thermodynamic equilibrium, evaluated numerically the effects of volatiles on the dike tip. He uses the equation for the solubility of water in a basalt melt from Wilson and Head (1981), and notes that magmas are saturated in volatiles at pressures corresponding to a lithostatic overburden of at most a few km and probably not more than a few hundred meters. When p_{vol} is large under a lithostatic overburden exceeding the volatile saturation pressure, volatiles should occupy only a small region of the tip. The length of this volatile-filled region extends as the dike propagates toward the level of $p_{vol} = 0$ and the magma is saturated in volatiles (Lister and Kerr 1991). At this volatile saturation level, the rate of bubble nucleation from the magma will be too large to maintain thermodynamic equilibrium between the volatiles in the dike tip and the magma. Volatile exsolution will extend throughout the melt and the system would have to be modeled as a two-phase compressible flow. This mechanism would decrease the density and propagate dikes above the LNB of a volatile undersaturated melt (Lister and Kerr 1991; p. 10,070). Lister (1990) approximated the length of the volatile-filled region and noted that it can become surprising large below the depth of volatile saturation (Lister and Kerr 1991; their fig.18). This again, may be a critically important mechanism to promote overshooting of the LNB and eruption of magma at the surface.

The viscosity of basalt magma is strongly temperature dependent (Ryan and Blevins 1987). A small drop in temperature caused by heat loss to the country rock promotes a viscosity increase, and an increase in viscous pressure. Delaney and Pollard (1982) note that a magma traveling more than a few kilometers from an upper crustal source at typical propagation velocities will solidify in a few hours (assuming a 2 meter dike thickness). The time for complete solidification of a dike can be approximated by (Lister and Kerr 1991):

where λ is a numerical coefficient dependent on the solidification temperature and thermal properties of the magma and solidification layer and k is the thermal diffusivity of the magma. This calculation

$$t_s = \frac{w^2}{\lambda k}$$

neglects the advective supply of heat caused by the flow of the magma and overestimates the likelihood of dike solidification. Bruce and Huppert (1990) emphasized the importance of latent heat of solidification and the effect of thermal advection of magma on the temperature profile of a dike. They used two-dimensional modeling to show that for dike widths of greater than about 1 m, flow blockage from solidification will be reversed by continued supply of heat through magma flow. This reversal can exceed heat loss into the country rock, and result in melting and expansion of dike widths. Bruce and Huppert (1990) also described preliminary three-dimensional modeling of a range of other effects, the most important being the well-described localization of fissure eruptions in distinct conduits through the duration of a fissure eruption. An unconsidered implication of the Bruce-Huppert model, however, is the effect of melting on magma composition. Geochemical and isotopic studies of basalt magmas in a range of setting show that it is rare for basalt to be contaminated with country rock, particularly shallow country rock. If the advective supply of heat is significant over a depth range, country-rock contaminated basalt should be observed more commonly.

Lister and Kerr (1991) conclude that a dike cannot propagate further than a critical length approximated by:

$$l_s \sim P_e w$$

where *Pe* is the Peclet number. They suggest that while models are not yet capable of incorporating the mechanics of dike propagation and effects of solidification, several important conclusions can be drawn. First, solidification rates are significant for narrow dikes (tens of cms) over distances of a few kilometers. Narrow dike regions freeze and become narrower, and wide regions tend to melt and become wider. Second, loss of heat from the narrow dike tip will cool the magma and increase viscosity increasing the need for source pressure to maintain flow into the dike tip. This can lead to inflation of a dike behind a blocked dike tip. It may provide a mechanism for observed large dike widths in frozen magma conduits beneath eruptive centers. Third, the earlier discussions of the unimportance of elastic stresses associated with dike propagation suggest the growth of a chilled layer may be easily overcome by dike expansion.

A final problem for this section is the issue of whether a dike path follows a preexisting fracture or fracture system or the dike propagation direction is determined by the stress field. To examine this question, basic data have to be gathered on the geometry of dike systems, their relation to local fractures, and the relationship to other features such as magma reservoirs. Pollard (1987) has noted that many dikes display minor irregularities called cusps, steps, buds and segments. He notes that these irregularities have a length scale that is much less than the dike length, and are not important unless they are near the dike tip. Pollard (1987; his Fig. 9) showed that the principal direction of dike propagation is parallel to the long dimension of these features.

The geometry of a dike is determined at least in part by the path established by the dike tip. A long recognized feature of dikes is that they are emplaced commonly perpendicular to the least compressive stress direction (Pollard 1987). Delaney et al. (1986) described mafic dikes that intruded

sedimentary rocks on the Colorado Plateau. These dikes are associated with joint sets in country rock that are closely spaced near the dikes but increase in spacing away from the dikes. They suggest that the joints are formed by fracturing of the host rock by tensile stress generated by magmatic pressure beyond the tips of propagating dikes. The joints become juxtaposed with the dike body with continued propagation. Delaney et al. (1986) contrast dikes with self-generated fractures propagated perpendicular to the least compressive stress direction with dikes that parallel regional joint sets. They suggest that magma can invade older or existing joints if the magmatic pressure exceeds the horizontal stress acting across the joint plane. This may be optimized by two situations. First, it may occur if the horizontal principal stress difference is small compared to the magmatic driving pressure. Second, it may also occur if joints are nearly perpendicular to the direction of least compressive stress.

Delaney et al. (1986; their appendix A) developed criteria for identifying dikes intruded along older joints. These include field evidence for slip that is substantial in comparison to dilation and formation of crack splays if the dike propagates beyond the ends of the joint. In the latter case, magma must create its own fracture, and would turn or splay toward the direction of maximum principal stress.

Pollard (1987) recognized three fracture modes for the orientation of dikes. The first is a planar dike that follows a fracture produced by the least compressive stress acting perpendicular to the dike plan. The second is a curved dike. This is produced by a spatial rotation of the least compressive stress about an axis parallel to the dike periphery. The third is a segmented dike produced by a spatial rotation of the least compressive stress about an axis parallel to the propagation direction. Pollard (1987) presented criteria needed to verify control of dike paths by preexisting fractures that are not parallel to the least compressive stress direction. These are that the fractures must be older than the dikes, and have comparable planar dimensions. Second, shear displacements must be found along the dike indicating that dilations were accompanied by slip induced by the resolved shear stress across the dike.

Baer and Reches (1991) examined dike propagation mechanisms for a dike swarm crossing different rock units. They noted that intrusion mechanisms were different for each rock unit indicating host rock properties played a role in controlling dike propagation mechanisms, directions, and detailed geometry. Dikes in a stratified sequence formed segments contained within distinct stratified layers. Dikes in massive sandstones formed smaller segments, and had associated dike fingers with intermittent smooth portions and patches with slickensides. The dike propagation through the massive sandstones was inferred to form through alternating stages of fluidization, viscous flow and brittle deformation. These dike systems were emplaced horizontally, along dike-generated fractures. Baer (1991) suggest the dikes propagated at the LNB and were driven by the density difference between the magma and host rock.

We have limited information about the geometry and relationship of feeder dikes for Pliocene and Quaternary basalt centers in the YMR because of the minor degree of erosional modification of the centers. The primary exposure of dikes is in cone scoria where the dikes exhibit highly irregular geometry that is unrelated to the regional stress field (Crowe et al. 1983b).

Several inferences can be offered on the probable form of subsurface dikes in the area. First, the regional alignment of major vents for all Pliocene and Quaternary basalt centers of Crater Flat are northwest (see Chapter 3). This alignment is inferred to be controlled by structural features at depth, and may not be controlled by the shallow stress field. This inference is based on the repeated

appearance of basalt centers ranging in age from 4.8 to < 0.1 Ma along a preferential northwest trend. The recurrence of temporally distinct events (contrasted with coeval cone clusters) on the same directional trends, suggests the presence of a long-lived subsurface structural control of the ascent of magma. Additionally, as shown in Chapter 3, the direction of alignment of Pliocene and Quaternary volcanic centers coincides with the surface of maximum magma eruption volumes. The strong correlation between center alignment and eruption volumes provides significant support for the rise of magma at depth along northwest-trending structures. This conclusion is in strong contrast with Lister and Kerr (1991) who, as noted earlier, conclude that rock is weak, and preexisting fractures are not important in dike propogation. Rubin (1993) presented arguments that the mechanical properties of country rock are important. The most compelling argument is the apparent discrepancy between laboratory measurements of fracture energy compared with field observations of country rock effects from dike propagation. Field evidence demonstrates that inelastic deformation at dike tips can be much larger than those produced at the tips of tensil cracks in laboratory experiments. Moreover, deformation of country rock is observable adjacent to dikes for a range of rock types.

An alignment of clusters of scoria cones of probable similar age provide probably the best indicator of the local trend of shallow feeder dikes (for example, Nakamura 1977). These alignments, in the YMR, include the north-south cluster of the 3.7 Ma centers, the north-northeast cluster of the Quaternary basalt of Crater Flat, and the north-northeast cluster of the basalt of Sleeping Butte. These directions are perpendicular or near-perpendicular to the least compressive stress direction (Stock et al. 1985). The Lathrop Wells volcanic center consists of only one scoria cone, and no structural trend can be assigned to a single cone. However, the predominant direction of fissure systems in the center are northwest. The two distinct structural settings of basalt centers in Crater Flat (northwest-trending localization of vents of different ages; northeast-trending, coeval cone clusters) probably requires reorientation of dikes at a shallow depth.

A preferred model for dike emplacement in the Yucca Mountain area is ascent of pulses of basalt magma at depth along northwest-trending structures followed by a shallow north-northeast reorientation of dikes (90 degrees) parallel to the maximum compressive stress direction. This is consistent with the lengths of the different structures. The northwest-trending Crater Flat volcanic field (Crowe and Perry 1989), extends for over 50 kilometers. This exceeds the maximum length of known dikes except bladed dikes, propagating laterally from a shallow magma reservoir. Northeast trending cone alignments range from 2.6 to 12 km, consistent with formation from individual feeder dikes. The dike model may be tested with geophysical data, particularly aeromagnetic data. It may be possible to use geophysical methods to determine if there is a change in dike orientation from north-northwest to northwest with depth. If this reorientation is recognized, the depth of the reorientation compared with the depth of the potential repository at Yucca Mountain may provide key information on the likely depth of occurrence of basalt intrusions. This dike reorientation could coincide with a reduction in confining pressure for two regimes of dike propagation (Rubin 1993): northwest following structure at higher confining pressure, and northeast associated with magma-induced fractures at lower confining pressures.

Finally, it is difficult to establish a relation between vent alignments, and local structure for individual basalt centers in the YMR. Alignments of fissures, vents, scoria mounds and scoria cones define conjugate northwest and north-northeast trends (Crowe and Carr 1980; Vaniman et al. 1982; Crowe et al. 1983; Crowe 1990, Smith et al. 1990; Ho et al. 1991). These directions parallel the expected directions of dike and structural trends. But the data sets are inconsistent (see Chapter 3). Some basalt centers are located along structures or intersections of multiple structures; others appear

independent of structure. Exposure of dikes in country rock associated with the Pliocene and Quaternary basalt centers is insufficient to identify structurally controlled or stress-controlled dike features using the criteria of Delaney et al. (1986) and Pollard (1987). If these features could be identified, northwest-trending dikes would be expected to be structurally controlled (fracture controlled), and north-northeast trending dikes would be stress-controlled.

VI. Future Work

Future expanded work on processes of magma dynamics is planned as part of Study Plan 8.3.1.8.1.2, *Physical Processes of Magmatism and Effects on the Potential Repository.* Our intent is to use the foundation of surveyed literature from Section V as a starting point for further examination of the physical controls of magma generation, evolution, ascent, and eruption in the YMR. The purpose of this work is to provide an independent cross-check on probabilistic studies. Rates of volcanic activity for probabilistic volcanic risk assessment are established primarily from the volcanic record of the YMR (see Chapter 7). The magma dynamics studies will examine physical processes of magmatism in the YMR using geophysical and petrologic data to constrain rates of magma production. The purpose of the work will be to ensure that magmatic processes as represented in probabilistic estimates are compatible with physical and geochemical data for the YMR. A schematic overview of this work is provided by Fig. 5.1, a cross-section of the crust-mantle in the YMR. Generation of basalt melt in the region may have occurred in either the convecting asthenosphere or in the lithospheric mantle. Isotopic studies of basalts of the YMR show that they must be derived from or have equilibrated with lithospheric mantle to obtain their distinctive Sr and Nd isotopic compositions. This provides two important constraints on models of basalt genesis. First, if melt initiation is assumed to occur in the asthenosphere, then extracted melt must move through the lithospheric mantle through matrix percolation and not channel segregation. The latter process would isolate the melt from the matrix. Second, there must be substantial vertical continuity of preserved lithospheric mantle in the YMR. The Younger postcaldera basalt has decreased systematically in volume and exhibited geochemical trends from the Pliocene to the Quaternary that are consistent with decreasing degrees of partial melting or deepening of the depth of melting. Yet the isotopic composition of Sr and Nd have remained uniform.

The issue of formation of solitary waves associated with melt migration remains controversial. Such waves if preserved through magma ascent, are most likely to occur for areas of low magma flux when melt extraction is non-steady state. Both conditions may be appropriate for the waning tectonic setting of the YMR. The velocity and volume of melt (1 km^3 extracted; < 0.1 km^3 erupted) associated with solitary waves could contribute to the episodic nature of polygenetic volcanism at some basalt centers. The dynamics of these processes will be examined to determine if their time constraints and volumes are consistent with observed patters of volcanism in the YMR.

The evolved compositions and scarcity of phenocryst phases in the lavas of the Younger postcaldera basalt (particularly the Quaternary lavas) requires that they fractionated extensively prior to ascent and eruption, and the fractionating phases were removed (see Chapter 4). The most logical place for that fractionation and crystal removal to take place is at the mantle-crust density face, below the plagioclase stability field. We will examine the dynamics of processes of mantle fractionation and density controlled buoyant ascent to compare them with the observed temporal patterns of eruptive events for both polygenetic events and for the formation of new volcanic centers.

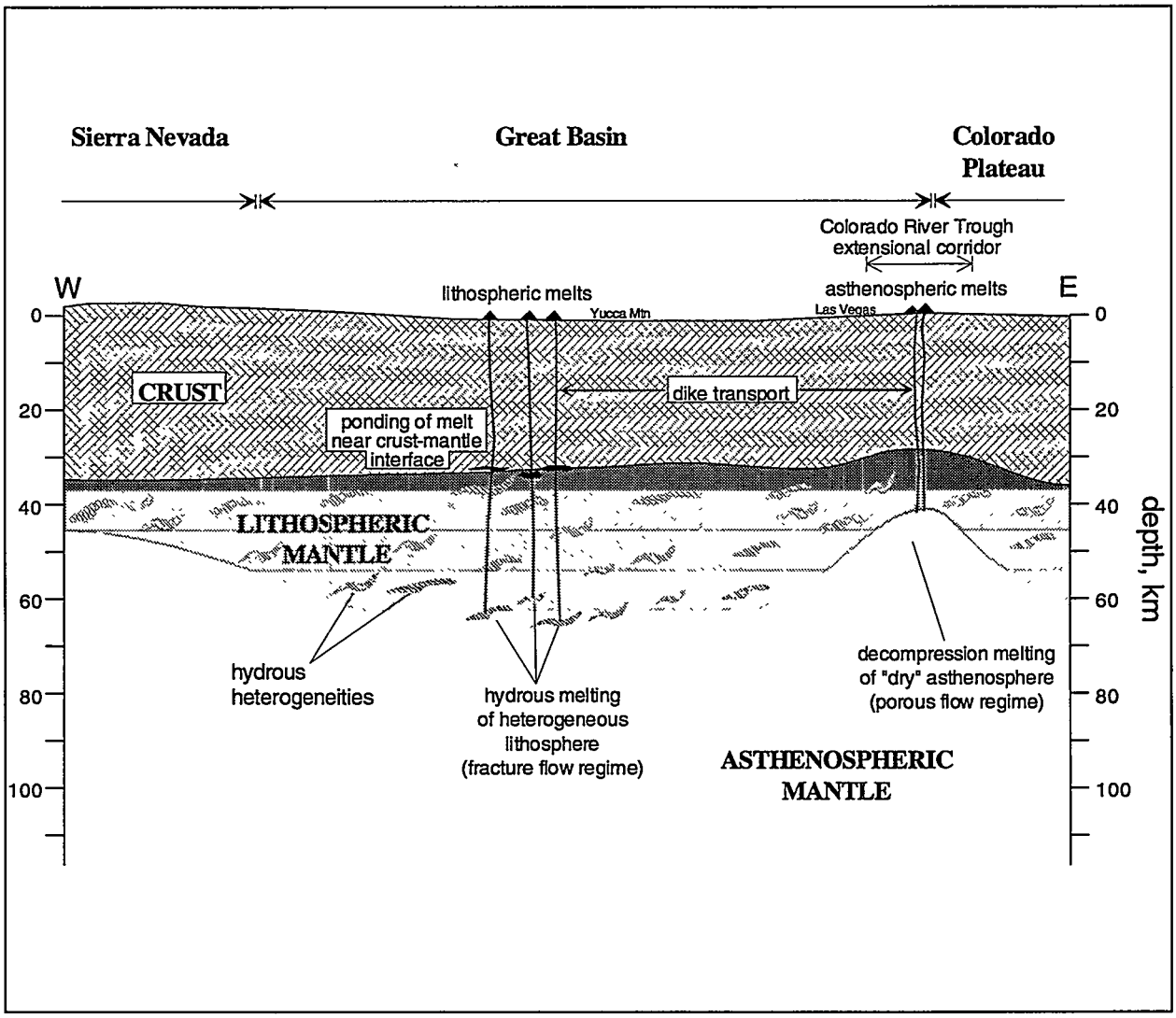


Fig. 5.1 Schematic cross-section of the southern Great Basin showing the distribution of the crust, lithospheric mantle, and athenospheric mantle. Two end members processes for generation of basaltic melts are possible. The first is decompressive melting of the asthenosphere. Basalt derived from this source is inferred to migrate by channel segregation through the thinned lithospheric mantle without equibrating, therefore maintaining its asthenospheric mantle compositions for Sr and Nd. The second end member, which is more appropriate to the YMR, is generation of basaltic magma by hydrous melting of heterogeneous lithosphere. An alternative hybrid source for basaltic magmas of the YMR is decompressive melting of the asthenosphere followed by matrix percolation of melt through the lithospheric mantle allowing equilibration with the lithospheric mantle. Both the hydrous melting end member and the hybrid athenospheric-lithospheric equilibrated melts must be trapped and fractionate at the crust-mantle density interface, followed by rapid ascent through the crust.

Finally, the ascent of basalt magma below the YMR almost certainly occurs rapidly in the form of basalt dikes. We will examine the volume constraints on the minimum volumes required to initiate an ascent pulse of magma, and the ratio between the volume of magma resident in ascent versus eruption. Unique aspects of Quaternary basaltic volcanism in the YMR are their small volumes and episodicity. Average event recurrence times for the formation of new volcanic centers are about 200 to 300 ka; event recurrence times for polygenetic events are on the order of 10 to 100 ka. We will compare these temporal constraints with dynamic processes of magma ascent. Magma ascent in the shallow crust may be controlled at a depth of 2-10 km by the presence of deep-seated structural features; shallow propagation of dikes may occur as swarms following the local stress field (maximum compressive stress direction). Assessment of the importance of the LNB, crack-tip fracture interaction, and the local stress field may be important in identifying high probability sites for future eruption of basalt magma.

VII. REFERENCES

Aki, K., and R. Koyanagi, "Deep Volcanic Tremor and Magma Ascent Mechanism under Kilauea, Hawaii," *Journal Geophysical Research* **86**, 7095-7109 (1981).

Baer, G. "Mechanisms of Dike Propagation in Layered Rocks and Massive, Porous Sedimentary Rocks," *Journal Geophysical Research* **96**, 11,911-11,929 (1991).

Baer, G., and Z. Reches, "Mechanics of Emplacement and Tectonic Implications of the Ramon Dike Systems, Israel," *Journal Geophysical Research* **96**, 11,895-11,910 (1991).

Bruce, P. M., and H. E. Huppert, "Solidification and Melting along Dykes by the Laminar Flow of Basaltic Magma", in *Magma Transport and Storage*, M. P. Ryan, Ed. (John Wiley& Sons, New York, New York, 1990), pp. 87-101.

Byers, F. M., Jr., and H. Barnes, "Geologic map of the Paiute Ridge Quadrangle, Nye and Lincoln Counties, Nevada," U.S. Geological Survey Quadrangle Map GQ-577 (1967).

Christiansen, T. L., and E. H. Mckee, "Late Cenozoic Volcanic and Tectonic Evolution of the Great Basin and Columbia Intermontane Regions," in *Geological Society America Memoir 152: Cenozoic Tectonics and Regional Geophysics of the Western Cordillera*, R. B. Smith, and G. P. Eaton, Eds. (Geological Society America, Boulder, Colorado, 1978), pp. 283-311.

Cordery, M. J., and J. P. Morgan, "Convection and Melting at Mid-Ocean Ridges," *Journal Geophysical Research* **98**, 19,477-19,503.

Crowe, B. M., "Basaltic Volcanic Episodes of the Yucca Mountain region ," in *Proceedings High-Level Radioactive Waste Management Conference, Las Vegas, Nevada (*American Nuclear Society, La Grange Park Illinois, 1990), Vol. 1, pp. 65-73.

Crowe, B. M., and W. J. Carr, "Preliminary Assessment of the Risk of Volcanism at a Proposed Nuclear Waste Repository in the Southern Great Basin," U.S. Geological Survey Open-File Report 80-375, 15 pp. (1980).

Crowe, B. M. and F. V. Perry, "Volcanic Probability Calculations for the Yucca Mountain Site: Estimation of Volcanic Rates," in *Proceedings Nuclear Waste Isolation in the Unsaturated Zone, Focus '89* (American Nuclear Society, La Grange Park, Illinois, 1989) pp. 326-334.

Crowe, B. M., D. T. Vaniman, and W. J. Carr, "Status of Volcanic Hazard Studies for the Nevada Nuclear Waste Storage Investigations," Los Alamos National Laboratory report LA-9325-MS 47 pp. (1983a).

Crowe, B. M., S. Self, D. Vaniman, R. Amos, and F. Perry, "Aspects of Potential Magmatic Disruption Of A High-Level Radioactive Waste Repository In Southern Nevada.," *Journal Geology* **91**, 259-276 (1983b).

Delaney, P. T., and D. D. Pollard, "Solidifaction of Basaltic Magma During Flow in a Dike," *American Journal Science* **282**, 856-885 (1982).

Delaney, P. T., and D. D. Pollard, "Deformation of Host Rocks and Flow of Magma During Growth of Minette Dykes and Breccia-Bearing Intrusions near Ship Rock New Mexico, U.S. Geological Survey Professional Paper 1202, 61 pp. (1981).

Delaney, P. T., D. D. Pollard, J. I. Ziony, and E. H. McKee, "Field Relations Between Dikes and Joints: Emplacement Processes and Paleostress Analysis," *Journal Geophysical Research* **91**, 4920-4938 (1986).

Eaton, G. P., R. R. Wahl, H. J. Prostka, D. R. Mabey, and M. D. Kleinkopf, "Regional Gravity and Tectonic Patterns: their Relation to Late Cenozoic Epirogeny and Lateral Spreading in the Western Cordillera," in *Geological Society America Memoir 152: Cenozoic Tectonics And Regional Geophysics Of The Western Cordillera*, R. B. Smith, and G. P. Eaton, Eds. (Geological Society America Boulder, Colorado, 1978), pp. 51-91.

Eaton, G. P., "The Basin and Range Province; Origin and Tectonic Significance:," *Annual Reviews Earth Planetary Science* **10**, 409-440 (1982).

Eggins, S. M., "Petrogenesis of Hawaiian Tholerites: II, Aspects of Dynamic Melt Segregation," *Contributations Mineralogy Petrology* **110**, 398-410 (1992).

Farmer, G. L., and D. J. Depaolo, "Origin of Mesozoic and Tertiary Granite in the Western United States and Implications for Pre-Mesozoic Crustal Structure, 1, Nd and Sr Isotopic Studies in the Geocline of the Northern Great Basin," *Journal Geophysical Research* **88**, 3379-3401 (1983).

Farmer, G. L., Perry, F. V., Semken, S., Crowe, B., Curtis, D. and DePaolo, D. J., "Isotopic Evidence on the Structure and Origin of Subcontinental Lithospheric Mantle in Southern Nevada," *Journal Geophysical Research* **94**, 7885-7898 (1989).

Fowler, A. C., "A Compaction Model for Melt Transport in the Earth's Asthenosphere. Part I: The Basic Model," in *Magma Transport and Storage*, M. P. Ryan, Ed.,(John Wiley & Sons, England, 1990a) pp. 3-14.

Fowler, A. C., "A Compaction Model for Melt Transport in the Earth's Asthenosphere. Part II: Applications," in *Magma Transport and Storage*, M. P. Ryan, Ed. (John Wiley & Sons, Chichester) Chapter 1, pp. 15-32 (1990b).

Fowler, A. C., "Mantle and Magma Dynamic", in *Dynamic Differentiation, Notes of the GFD Summer Program, Woods Hole Oceanographic Institution*, W. Malkus, Ed., (Woods Hole MA, WHOI 84-44), 74-77 (1984).

Ho, C. H., E. I. Smith, and D. L. Feuerbach, and T. R. Naumann, "Eruptive Probability Calculations for the Yucca Mountain Site, USA: Statistical Estimation of Recurrence Rates," *Bulletin Volcanology* **54**, 50-56 (1991).

Jones, J.H., B.P. Wernicke, G.L. Farmer, J.D. Walker, D.S. Colman, L.W. McKenna, and F.V. Perry, "Variations Across and Along a Major Continental Rift: an Interdisciplinary Study of the Basin and Range Province,

Western USA," *Tectonophysics*, **213**, p. 57-96 (1992).

Kane, M. F., and R. E. Bracken, "Aeromagnetic Map of Yucca Mountain and Surrounding Regions, Southwest Nevada," U.S. Geological Survey, Open-File Report 83-616, 19 pp. (1983).

Kinzler, R. and T. L. Grove, "Primary Magmas of Mid-ocean Ridge Basalts 2. Applications," *Journal Geophysical Research* **97**, 6907-6926 (1992).

Lachenbruch, A. H., and J. H. Sass, "Models of an Extending Lithosphere and Heat Flow in the Basin and Range Province," in *Geological Society America Memoir 152: Cenozoic Tectonics and Regional Geophysics of the Western Cordillera*, R. B. Smith, and G. P. Eaton, Eds. (Geological Society America, Boulder, Colorado, 1978), pp. 209-250.

Lister, J. R., and R. C. Kerr, "Fluid-Mechanical Models of Crack Propagation and their Application to Magma Transport in Dykes," *Journal Geophysical Research* **96**, 10,049-10,077 (1991).

Lister, J. R., "Buoyancy-driven Fluid Fracture: Similarity Solutions for the Horizontal and Vertical Propagation of Fluid-filled Cracks," *Journal Fluid Mechanics* **217**, 213-239 (1990).

Maaloe, S. "The Generation and Shape of Feeder Dykes from Mantle Sources," *Contributions Mineralogy Petrology* **96**, 47-55 (1987).

McKenzie, D.P., "The Generation and Compaction of Partial Melts," *Journal Petrology* **25**, 713-765 (1984).

Nakamura, K. "Volcanoes as Possible Indicators of Tectonic Stress Orientation: Principle and Proposal," *Journal Volcanology Geothermal Research* **2**, 1-16 (1977).

Nicolas, A., "Melt Extraction from Mantle Peridotites: Hydrofracturing and Porous Flow, with Consequences for Oceanic Ridge," in *Magma Transport and Storage*, M. P. Ryan, Ed. (John Wiley & Sons, Chichester, 1990) Chapter 10, pp. 159- 174.

Nicolas, A., "A Melt Extraction Model Based on Structural Studies in Mantle Peridotites," *Journal Petrology* **27**, 999-1022 (1986).

Nicolas, A., G., F. Lucazeau, and R. Bayer, "Peridotite Xenoliths in Massif Central Basalts, France: Textural and Geophysical Evidence for Asthenospheric Diapirism," in *Mantle Xenoliths*, P. Nixon, Ed. (John Wiley, & Sons, Chichester, 1987), p. 844.

Pollard, D. D., "Elementary Fracture Mechanic Applied to the Structural Interpretation of Dykes, *Geological Association Canada Special Paper* **34**, 5-24 (1987).

Pollard, D. D., "On the Form and Stability of Open Hydraulic Fractures in the Earths's Crust," *Geophysical Research Letter* **3**, 513-516 (1976).

Pollard, D. D., and O. H. Muller, "The Effects of Gradients in Regional Stress and Magma Pressure on the Form of Sheet Intrusions in Cross Section," *Journal Geophysical Research* **81**, 975-984 (1976).

Richter, F. M., and D. P. McKenzie, "Dynamical Models for Melt Segregation from a Deformable Matrix," *Journal Geology* **92**, 729-240 (1984).

Ribe, N. M., "Theory of Melt Segregation - a Review," *Journal Volcanology Geothermal Research* **33**, 241-253

(1987).

Rubin, A. M., and D. D. Pollard, "Origins of Blade-like Dikes in Volcanic Rift Zones," U.S. Geological Survey Professional Paper 1350, 1449-1470 (1987).

Rubin, A. M., "Tensile Fracture of Rock at High Confining Pressure: Implications for Dike Propagation", *Journal Geophysical Research* **96**, 15,919-15,935 (1993).

Ryan, M. P., "The Mechanics and Three-dimensional Internal Structure of Active Magmatic Systems: Kilauea Volcano, Hawaii," *Journal Geophysical Research* **93**, 4213-4248 (1988).

Ryan, M. P., and J. Y. K. Blevins, "Viscosity of Synthetic and Natural Silicate Melts and Glasses at High Temperatures and 1 Bar (10^5 Pascals) Pressure and at High Pressures," U.S. Geological Survey Bulletin 1764, pp. 1-563 (1987).

Scott, D. R., "The Competition between Percolation and Circulation in a Deformable Porous Medium," *Journal Geophysical Research* **93**, 6451-6462 (1988).

Scott, D. R., and D. J. Stevenson, "Magma Solitons," *Geophysical Research Letter* **11**, 1161-1164 (1984).

Scott, D. R., and D. J. Stevenson, "Magma Ascent by Porous Flow," *Journal Geophysical Research* **91**, 9283-9296 (1986).

Scott, D. R., and D. J. Stevenson, "A Self-consistent Model of Melting, Magma Migration and Buoyancy-driven Circulation Beneath Mid-ocean Ridges," *Journal Geophysical Research* **94**, 2973-2988 (1989).

Scott, D. R., D. J. Stevenson, and J. A. Whitehead, "Observations of Solitary Waves in a Viscously Deformable Pipe," *Nature* **319**, 759-761 (1986).

Shaw, H. R., "Uniqueness of Volcanic Systems," in *Volcanism in Hawaii*, R. W. Decker, T. L. Wright, and P. H. Stauffer, Eds., U.S. Geological Survey Professional Paper 1350, **2**, 1357-1394 (1987).

Shaw, H. R., "The Fracture Mechanisms of Magma Transport from the Mantle to the Surface, in *Physics of Magmatic Processes*, R. B. Hargraves, Ed. (Princeton University Press, Princeton, New Jersey1980) pp. 201-264

Sleep, N. H., "Segregation of Magma from a Mostly Crystalline Mush," *Geological Society America Bulletin* **85**, 1225-1232 (1974).

Smith, E. I., D. L. Feuerbach, T. R. Naumann, and J. E. Faulds, "The Area of Most Recent Volcanism Near Yucca Mountain, Nevada: Implications for Volcanic Risk Assessment," in *Proceedings High-Level Radioactive Waste Management Conference, Las Vegas, Nevada* (American Nuclear Society, La Grange Park Illinois, 1990), 1, 81-90 (1990).

Snyder D. B. and W. J. Carr, "Interpretation of Gravity Data in a Complex Volcanotectonic Setting, Southwestern Nevada," *Journal Geophysical Research*, **89**, 10,193-10,206 (1984).

Spence, D. A., and D. L. Turcotte, "Buoyancy-driven Magma Fracture: a Mechanism for Ascent through the Lithosphere and the Emplacement of Diamonds," *Journal Geophysical Research* **95**, 5133-5139 (1990).

Spence, D. A., P. W. Sharp, and E. L. Turcotte, "Buoyancy-driven Crack Propagation: A Mechanism for Magma

Migration," *Journal Fluid Mechanics* **174**, 135-153 (1987).

Spiegelman, M., and C. Wiggings, "Great Balls of Fire: Magma Migration and Magma Solitary Waves in 3-D", *EOS*, Transactions American Geophysical Union **74**, 684 (1993).

Stock, J. M., Healy, J. H., Hickman, S. H., and Zoback, M. D., "Hydraulic Fracturing Stress Measurements at Yucca Mountain, Nevada, and Relationship to the Regional Stress Field," *Journal Geophysical Research* **90**, 8691-8708 (1985).

Swanson, D. A., "Magma Supply Rate at Kilauea Volcano, 1952-1971," *Science* **1975**, 169-170 (1972).

Valentine, G.A., B.M. Crowe, And F.V. Perry, "Physical Processes and Effects of Magmatism in the Yucca Mountain Region," in *Proceedings High Level Radioactive Waste Management Conference Las Vegas, Nevada* (American Nuclear Society, La Grange, Illinois, 1992) Vol. 3, pp. 2344-2355.

Valentine, G.A., K.M. Growes, C.W. Gable, F.V. Perry And B.M. Crowe, "Effects of Magmatic Processes on the Potential Yucca Mountain Repository: Field and Computational Studies," in *Proceedings Focus93 Symposium Volume* (American Nuclear Society, La Grange, Illinois, 1993) pp. 167-173.

Vaniman, D. T., and B. M. Crowe, "Geology and Petrology of the Basalts of Crater Flat: Applications to Volcanic Risk Assessment for the Nevada Nuclear Waste Storage Investigations," Los Alamos National Laboratory Report LA-8845-MS, 67 pp. (1981).

Vaniman, D. T., B. M. Crowe, and E. S. Gladney, "Petrology and Geochemistry of Hawaiite Lavas from Crater Flat, Nevada," *Contributions Mineralology Petrology* **80**, 341-357 (1982).

Walker, G. P. L., "Gravitational (Density) Controls on Volcanism, Magma Chambers and Intrusions," U.S. Geological Survey Professional Paper 1350, 1449-1470 (1989).

Weertman, J., "Theory of Fluid-filled Crevasses in Glaciers Applied to Vertical Magma Transport Beneath Ridges," *Journal Geophysical Research* **76**, 1171-1183 (1971).

Wilson, L. and J. W. Head "Ascent and Eruption of Basaltic Magma on the Earth and Moon," *Journal Geophysical Research* **86**, 2971-3001 (1981).

Zoback, M. I., R. E. Anderson, and B. A. Thompson, "Cainozoic Evolution of the State of Stress and Style of Tectonism of the Basin and Range Province of the Western United States," *Philosophical Transactions Royal Society London Series A* **300**, 407-434 (1981).

CHAPTER 6: HISTORY OF VOLCANISM STUDIES

I. Summary

Volcanism studies for the Yucca Mountain Site Characterization Project (YMP) began in 1979 with an assessment of silicic volcanism. The geochemistry of volcanic rocks from the Black Mountain and Silent Canyon caldera complexes were compared and judged to be from separate magma systems. Evidence was summarized for the inference that the Black Mountain magma system is extinct. The risk of future silicic volcanism was judged not to be a significant issue for the Yucca Mountain site.

In 1980, the methods for assessing the risk of future basaltic volcanism were formalized. Preliminary bounds on the probability of magmatic disruption and the consequences of such an event were assessed. Regional patterns of volcanism were evaluated and structural controls of sites of basaltic volcanism were described.

The first studies of the geologic, petrologic, and geochemical features of basaltic volcanism in Crater Flat were presented in 1981. Major-and trace-element variations of the basalt cycles were assessed along with the major-element analyses of mineral phases. A systematic decrease through time in the volume of magma erupted in the Crater Flat area was described.

In 1982, trace-element enriched, Pliocene and Quaternary lava of Crater Flat were classified as straddle-type alkali basalt with noteworthy volumes of hawaiite similar in composition to Pliocene and Quaternary basaltic volcanic rocks in the eastern Great Basin. Revised calculations of the probability of magmatic disruption of a potential repository were completed. The probability of disruption of a potential repository site was *bounded* between 4.7×10^{-8} and 3.3×10^{-10} yr^{-1}. The first volcanism drill hole (V-series holes) was completed in Crater Flat in 1982. A large positive aeromagnetic anomaly in central Crater Flat was shown not to be produced by Pliocene or Quaternary volcanic rocks. Additionally in 1982, the first indications of what would become a long-lived controversy concerning the interpretation of whole-rock, K-Ar age determinations of basaltic volcanic rocks became evident. Replicate splits of samples of basalt lava from the Lathrop Wells volcanic center were analyzed at three independent laboratories. The resulting ages ranged from negative ages to >700 thousand years (ka), an unacceptably wide range of replicate age determinations.

Three major studies of basaltic volcanism were completed in 1983. The first of a series of status reports on volcanism studies was published. The regional geology of basaltic volcanic fields extending from southern Death Valley, California to the Pancake Range of central Nevada was described. The regional characteristics and patterns of the petrology and geochemistry of basaltic volcanism in the southern Great Basin were described. The status and uncertainty of risk assessment studies for future volcanism were summarized. The second major study comprised development and descriptions of volcanic scenarios for future volcanic events using the record of volcanic activity in the Yucca Mountain region (YMR). Small-volume eruptions of hawaiite magma forming scoria cones and lava flows were identified as the most likely future volcanic event to effect the Yucca Mountain site. Magma of basaltic composition was inferred to ascend as dike-like pulses with velocities of 1 to tens of cm sec^{-1}. The composition and petrology of aphyric to sparsely porphyritic hawaiite magmas were recognized to require a multistage ascent history. Data on the dimensions and forms of basalt feeder dikes were described from analog basalt sites in the YMR. Linear dikes were recognized as the most likely form of basalt intrusions but sill-like intrusions were described at one locality (Paiute Ridge in the Half Pint range). The dispersal of radioactive waste in basalt eruptions was bounded by analogy to the distribution of lithic fragments in basaltic volcanic deposits.

Hydrovolcanic explosions were judged not to be important for future eruptions in the hydrological setting of the immediate Yucca Mountain site. Third, the first calculations of radiological releases associated with a scenario of basalt magma penetrating a repository and erupting were assessed. Radiological releases were examined for waste entrained in basalt eruption components (scoria cone, lava flow, scoria-fall sheet, and regional dispersal with fine-grained ash).

In 1984, a summary paper on the structural and tectonic setting of the YMR was competed.

Exploratory drilling and examination of core from the second volcanism drill hole was completed in 1985. A large negative aeromagnetic anomaly in west-central Crater Flat was shown to be produced by a sequence of buried lava flows (360 m depth). The lava flows were identified to be reversely polarized and were dated at 11.3 ± 0.4 million years (Ma).

A generalized overview of volcanism studies was published as a chapter in a book in 1986. The paper summarized all aspects of volcanism studies and presented new information on the possibility of hydrovolcanic eruptions at the Yucca Mountain site. Basaltic volcanic centers in the YMR were inferred to be simple monogenetic volcanoes, an interpretation that would be modified in future work. The second volcanism status report was also completed in 1986. The report summarized the progress for volcanism studies for topics identified as areas of uncertainty from previous studies. Appendices were compiled with sample descriptions and lists of major- (140 samples) and trace-element (68 samples) analyses of basaltic rocks in the YMR. The environmental assessment (EA) for the Yucca Mountain site was completed in 1986. Volcanism was identified as a potentially adverse condition for the Yucca Mountain site and judged to require additional investigations.

The formal strategy of volcanism studies was described in the Site Characterization Plan published in 1988. A three-part strategy for volcanism studies was presented in three separate study plans. These included: Study 8.3.1.8.1.1, Probability of Magmatic Disruption of the Repository; Study 8.3.1.8.1.2, Physical Processes of Magmatism and Effects on a Potential Repository; and Study 8.3.1.8.5.1, Characterization of Volcanic Features. The chronology of the Lathrop Wells volcanic center was reassessed in 1988 from the perspective of new geomorphic and soil studies and continuing concerns with the results of conventional whole-rock, K-Ar age determinations. The center was recognized to have possibly formed during multiple, time-separate volcanic events. The age of the youngest event at the center, the formation of the main scoria cone, was estimated to be late Pleistocene or possibly as young as Holocene. A revised geologic map (scale 1:4000) of the Lathrop Wells center was completed in 1988.

In 1989, a paper was published on the significance of new developments in understanding of alternative models of eruption of basaltic volcanism at small volcanic centers and these alternative models were assessed for their applications to volcanic risk assessment. The complex evolution of the Lathrop Wells center was described, and new K-Ar age determinations were presented for the lava flows of the center. The concept of polygenetic volcanism at small volume centers was defined and revised assessments of volcanic risk for the potential repository were presented incorporating new information.

Attempts to begin to bring aspects of volcanism studies to closure were initiated in 1989. A paper was published on the recurrence rate of volcanic events. The Crater Flat Volcanic Zone (CFVZ) was identified and described. An alternative method of calculating λ, the recurrence rate of volcanic events, through assessing cumulative magma volume versus time, was presented. A third publication in 1989 summarized studies of the isotopic composition of strontium, neodymium, and lead for basalt centers of the YMR.

An overview paper was presented in 1990 on the time-space patterns of late Cenozoic basaltic volcanism in the YMR. Alternative chronology models were presented for the Lathrop Wells volcanic center. These models attempted to accommodate the different opinions on the age and eruptive history of the center. Study Plan 8.3.1.8.5.1, Characterization of Volcanic Features, was released in 1990. This Study Plan provided a detailed description of the activities and methods for gathering the fundamental data that would be used for volcanism studies. Five activities were described: 8.3.1.8.5.1.1, Volcanism Drill Holes; 8.3.1.8.5.1.2, Geochronology Studies; 8.3.1.8.5.1.3, Field Geologic Studies; 8.3.1.8.5.1.4, Geochemistry of Scoria Sequences; and 8.3.1.8.5.1.5, Evolutionary Patterns of Basaltic Volcanic Fields. The year 1990 saw the publication of the first technical overview studies by the state of Nevada. They described the regional patterns of basaltic volcanism in the southern Great Basin and adjacent areas of Arizona, and suggested that high-angle normal faults control the location of volcanic centers in the vicinity of Yucca Mountain. They applied and discussed a traditional hazard-zone concept where past sites of basaltic volcanism are identified as high risk zones for future volcanic events.

In 1991, several papers describing alternative views of the chronology and eruptive models of basaltic centers in the YMR were presented by the U.S. Geological Survey. Paleomagnetic data were inferred to demonstrate that the Lathrop Wells and other Pliocene and Quaternary basalt centers were all formed by monogenetic eruptions. While two eruptive events were recognized at the Lathrop Wells center, the difference in ages of the events was inferred to be no more than a century. A second paper presented preliminary results of $^{40}Ar/^{39}Ar$ ages combined with conventional K-Ar age determinations for the Lathrop Wells volcanic center. The age of the center was inferred to be bracketed between 119 and 141 ka. The same data were published in a third paper which concluded that the Lathrop Wells center formed in two eruptive events dated at 136 ± 8 and 141 ± 9 ka. A geologic map of the Sleeping Butte centers was also completed in 1991. Both centers were inferred to be formed by mildly explosive strombolian eruptions that lead to the formation of a main scoria cone flanked by satellite vents and aa lava flows. The Little Black Peak center was judged to be a monogenetic center, and the Hidden Cone center was inferred to have possibly formed in two time-distinct volcanic events. Several papers were published by the state of Nevada on volcanic probability studies of the YMR in 1991. Alternative distribution models of the recurrence of basaltic events were presented. Arguments were made that the existing data base of basaltic events was inadequate to define recurrence intervals of volcanic events. The paper concluded that past probabilistic studies underestimated recurrence rates. Study Plan 8.3.1.8.1.1, Probability of Magmatic Disruption of the Repository, was completed in 1991. This Study Plan was divided into four activities. These include: Activity 8.3.1.8.1.1.1, Location and Timing of Volcanic Events; 8.3.1.8.1.1.2, Evaluation of the Structural Controls of Basaltic Volcanic Activity; 8.3.1.8.1.1.3, Presence of Magma Bodies in the Vicinity of the Site; and 8.3.1.8.1.1.4, Revised Probability Calculations and Assessments.

The year 1992 saw a large number of papers completed on volcanism studies related to the Yucca Mountain project. The long-awaited resumption of surface-disturbing activities allowed construction of soil pits at the Lathrop Wells volcanic center. A summary paper was completed on the status of field and geochronology studies for the center. The center was divided into three chronostratigraphic units. The results of K-Ar, U-Th, cosmogenic helium, thermoluminescence (TL), soil, geomorphic, and paleomagnetism studies of the center were described. A paper was published on recurrence models of volcanic events. Arguments were presented, in a separate paper, in favor of application of a homogeneous Poisson model for calculating the recurrence of volcanic events. Summary and revised calculations of the recurrence rate were published and the rate was bounded by comparison to other large-volume basaltic volcanic fields of the Basin and Range province. A separate paper described application of Monte Carlo techniques for estimating the disruption ratio of the conditional probability of repository disruption. Simulations were used to constrain the ratio using the geometry and physical constraints of dike dimensions. Models of northwest- and northeast-trending dikes and a renewal model of volcanic activity at

the Lathrop Wells center were used in the simulations. A paper interpreting teleseismic tomographic data for the YMR was published in 1992. A large low-velocity anomaly was described south and southeast of the Yucca Mountain site. This anomaly was attributed to the presence of bodies of basalt magma in a broad zone that extends northeast, parallel to the trace of hot-spot vectors of the North America plate. The patterns of temporal and geochemical variation of basaltic magma in the Crater Flat area were described in another 1992 paper. Systematic differences in mineral assemblages and trace-element and isotopic geochemistry indicate that magma chambers of the youngest cycles of basaltic activity have deepened through time consistent with waning volcanic activity. Trace-element and isotopic data for the Lathrop Wells volcanic center show that it did not form as a simple monogenetic center. Instead, the data support formation from temporally or spatially discrete magma batches. Revised assessments of the consequences of magmatic disruption of the potential repository were described in 1992. Two processes of volcanic activity that could effect a potential repository were recognized. First, magma could ascend through a repository and erupt. Second, subsurface effects of hydrothermal processes could alter the hydrologic conditions of a waste isolation system from intrusion of basalt magma through or near a repository. Analog studies of shallow intrusions in the Paiute Ridge area were described. The results of two-dimensional modeling of emplacement of a basalt sill in country rock were evaluated. The preliminary results of two-phase flow modeling of pyroclastic eruptions were presented. A review paper of progress in volcanism studies was published in 1992. New information was presented on the structural controls of volcanic activity. A summary table of all calculated disruption ratios for the YMR was compiled. Another review of probability studies was published by the state of Nevada. Investigators from the state used a nonhomogeneous Poisson process (NHPP) to estimate the instantaneous recurrence rate and a homogeneous Poisson process (HPP) to estimate future events. The 90% confidence intervals were assigned to the recurrence rate to assess uncertainty. A worst case disruption ratio of volcanic events was determined by applying a variant of the volcanic chain structural model. This value, combined with the confidence intervals for the recurrence rate, was used to estimate a probability of magmatic disruption of 1 x 10^{-6} to 6.7 x 10^{-7} yr^{-1}. A comment and response to interpretations by the U.S. Geological Survey on the age of the Lathrop Wells center were published in *Science* in 1992.

In 1993, a paper was published on the cosmogenic ^{36}Cl ages of the Lathrop Wells volcanic center. Samples were obtained from three sites and yielded an average age of 81 ± 7.9 ka. This age was inferred to be inconsistent with but did not exclude the possibility of multiple, time-separate eruptions at the Lathrop Wells center. A paper was published on geophysical investigation of buried volcanic centers in the Amargosa Valley and emphasized the results of geophysical modeling of an aeromagnetic anomaly south of the town of Amargosa Valley. Three different two-dimensional magnetic models were fitted to the observed magnetic field. Golder Associates Inc. used the Repository Integration Program (RIP) to assess classes of disruptive events for the Yucca Mountain site. Their simulations showed that the disruption of the potential site by volcanism does not result in significant releases of radioactive waste.

Four papers were completed in late 1993, all concerned with the probability and effects of magmatic disruption of the potential repository site. Alternative probabilities were estimated using nonhomogeneous models for the spatial distribution of volcanic events. The resulting estimates (0.8 to 3.4 x 10^{-8} events yr^{-1}) were in agreement with previously published and current probability estimates. A paper was published using alternative methods for stochastic modeling of the probability of dikes intersecting a repository. Three sets of alternative structural models were used for the distribution of volcanic events in the YMR. These results were combined with E1 (recurrence interval) to estimate the probability of magmatic disruption of the repository. These estimates were recalculated to correct estimates of E1 for specific structural models of E2 (intersection probability) and yielded estimates similar to other published probability estimates. Preliminary results of studies of lithic fragments in basaltic deposits were completed and three models presented for the incorporation of lithic fragments in magma. The formation of shallow

sills was inferred not to be controlled by the level of neutral buoyancy and instead was related to reorientation of the stress field at asperities in fault planes. Simulation modeling was used to bound the probability of magmatic disruption of the repository using multiple alternative models of E1 and E2. The RIP computer code was used to assess the sensitivity of volcanic disruption scenarios on the performance of the waste isolation system.

II. Introduction

The purpose of Chapter 6 of this volcanism status report is to trace the history of development of studies that led to the present understanding of the assessment of risk of volcanism for the Yucca Mountain site. We summarize the important literature on volcanic studies for the YMP starting from 1979. The improvements in data collection and progressive interpretations from field and laboratory studies are highlighted for each described paper. Conclusions developed from the data are described along with their implications for an evaluation of volcanic risk. We divide this section into two parts. The first part covers work completed before the Site Characterization Plan (SCP) (Department of Energy [DOE] 1988). The second part includes information obtained since publication of the SCP. Discussions are labeled by the year of the publication and descriptive titles of the studies are provided. We have attempted to describe and preserve the original content of the publications. However, we have also provided editorial comments where new information has changed interpretations, where data may be used incorrectly, or where assumptions for data that are critical to interpretations were not clearly presented. Additionally, some editorial comments are presented to highlight information from the hindsight of current understanding of volcanism data for the YMR. The comments have been italicized to alert the reader that the comments could be viewed as subjective. A primary purpose of this chapter is to aid the reader in acquiring an overview perspective of volcanism studies. Additional detailed information on individual topics can be found in the cited references and in other sections of this report.

The potential risk of future volcanic activity relative to underground isolation of high-level radioactive waste was recognized as an important concern in the earliest stage of studies of the Yucca Mountain site. A peer review panel was convened in July 1979 to evaluate concerns of tectonics, seismicity, and volcanism (Crowe et al. 1983a). Two statements were issued from this panel. First, the risk of future silicic volcanism was judged to be negligible. Second, the risk of basaltic volcanism was judged not to be a disqualifying issue for location of a repository for storage of high-level radioactive waste. The issue was recognized, however, to require additional study.

III. Progress Before The Site Characterization Plan

A. Publications in 1979

1. Silicic Volcanism. Crowe and Sargent (1979) described the geology and geochemistry of the Black Mountain and Silent Canyon volcanic centers. The volcanic rocks of both centers comprise a subalkaline-peralkaline geochemical association. The Silent Canyon volcanic center is a buried caldera complex of late Miocene age located on the north part of the Nevada Test Site (NTS). The Black Mountain volcanic center forms a slightly elliptical caldera of late Miocene age. It is the youngest major silicic volcanic center in the YMR. Both calderas formed from the eruption of voluminous ignimbrites and lavas. The Belted Range Tuff was erupted from the Silent Canyon center, the Thirsty Canyon Tuff from the Black Mountain center. Major-element geochemical data were compared with geologic data for the two centers to determine if the centers share a common magmatic origin. The resulting data show that the Black Mountain and Silent Canyon centers are distinctly separate in time, space, and composition. They both exhibit peralkaline geochemical affinities but evolved from unrelated magma systems. Volcanic activity

associated with the formation of the Black Mountain center represents a separate and renewed phase of volcanism following a relatively brief magmatic hiatus. Several lines of evidence suggest the magmatic cycle of Black Mountain has ended. First, the youngest volcanic rocks of the center are >8 Ma. Cooling times for large silicic bodies, even assuming heat loss solely by conduction, are insufficient to maintain molten magma without replenishment by new magma injected at depth. Second, the volume of magma erupted during successive cycles of activity declined progressively during the evolution of the Black Mountain center consistent with a waning system. There remains a finite but numerically incalculable probability of recurrence of Black Mountain–type volcanism in the YMR. That possibility was judged not to be a significant issue for isolation of high-level radioactive waste in the YMR. *There have been two new developments in regional studies of silicic volcanism. First, regional studies of silicic volcanism not associated with the YMP (McKee et al. 1989) revealed the presence of a Pliocene silicic center, the Mount Jackson dome complex, located west of Stonewall Mountain. This center is 105 km northwest of Yucca Mountain. It is too distant to be significant, but it is now recognized to be the youngest silicic volcanic center in the region. Second, three sites of aeromagnetic anomalies that could represent silicic intrusive rocks have been investigated by exploratory drilling. None of the drilled anomalies are produced by silicic volcanic rocks. The judgment that the risk of future silicic volcanism is not significant for the YMP continues to be valid but complete closure of the issue remains dependent on completion of drilling of aeromagnetic anomalies.*

B. Publications in 1980

1. Development of Methods of Risk Assessment for Future Basaltic Volcanism. The first published evaluation of the hazards of basaltic volcanism for the Yucca Mountain site was by Crowe and Carr (1980). They established a two-fold approach to volcanism hazards. The first involved characterizing the geology, chronology, occurrence, and tectonic setting of Pliocene and Quaternary volcanism in the YMR. The second included using the gathered data for assessment of the consequences and probability of repository disruption. The second approach used a procedure for volcanic hazard assessment developed by Crowe (1980).

Crowe and Carr (1980) described the volcanic record of Crater Flat. They divided the volcanic centers into three age groups using geomorphology. These divisions correspond to the southeast basalt of Crater Flat, the Quaternary basalt centers of central Crater Flat, and the Lathrop Wells volcanic center. *These subdivisions continue to be used in volcanism studies.* Crowe and Carr (1980) recognized the presence of aeromagnetic anomalies near the Red, Black, and the Little Cones centers that were inferred to be buried volcanic centers. They summarized the results of preliminary K-Ar whole-rock ages for the centers and assigned the three units to magnetic epochs using the magnetic polarity of the rock units and the results of K-Ar age determinations.

Crowe and Carr (1980) assessed the risk of volcanism as a conditional probability defined as the product of a rate of volcanism and an area ratio. Rate calculations were estimated by examining the number of events per time using different combinations of volcanic centers and time periods. They established the area ratio by noting first, that basalt centers are fed from narrow dikes with small disruption zones and second, by assuming that there are three feeder dikes for each center. Because the combined area of the multi-dike disruption zone was small (0.36 km^2) compared to the area of the repository, the area ratio was defined as the area of the repository divided by the area of a 25-km circle centered at the Yucca Mountain site. The sensitivities of these calculations were examined by using different combinations of centers within circles of 25-km and 50-km radii. Calculated values of the conditional probability ranged from 10^{-8} to 10^{-9} yr^{-1}. *These were the first volcanic probability estimations for the Yucca Mountain site. The probability calculations were defined as a linear combination of variables instead of as an*

exponential equation. This did not introduce significant errors in the calculations because the exponential equation is linear for the duration of the waste isolation period (length of time of the probability estimations).

Preliminary consequence analyses were evaluated for disruption of a potential repository. Crowe and Carr (1980) listed the following constraining variables for assessing the potential for radionuclide releases from an underground repository:

1. depth of burial of waste below the surface,
2. geometry of magma-waste interaction,
3. nature or style of volcanism, and
4. lag time prior to magmatic disruption.

Important constraints for these variables are that future volcanism is likely to consist of strombolian or phreatomagmatic eruptions of basaltic magma. Deep burial of waste reduces the potential for disruption and dispersal of waste if basalt centers are fed by linear dikes. The longer the interval between emplacement of waste and potential volcanic disruption, the lesser the consequences of dispersal because of radioactive decay of radionuclides.

Crowe and Carr (1980) summarized the regional patterns of volcanism in the Great Basin. They described time-space migration of silicic volcanism and the restriction of basaltic activity largely to the east and west margins of the Great Basin region. They identified four areas of Quaternary volcanism in the interior of the Great Basin. These include southern Death Valley, Crater Flat, an area north of Beatty (Sleeping Butte centers), and the Lunar Crater field. Crowe and Carr (1980) suggested that there are three typical tectonic settings for Pliocene and Quaternary basalt sites in the southern Great Basin. These include:

1. small northeast-trending rift zones or areas of relatively young extension,
2. caldera ring fracture zones, and
3. right-stepped offsets in northwest-trending, right-slip shear zones or intersections of northeast-trending, left-slip faults with these zones.

C. Publications in 1981

1. Geology, Petrology, and Geochemical Studies of Basaltic Volcanism in Crater Flat. The field geology, petrology, and geochemistry of the basalt of Crater Flat were described by Vaniman and Crowe (1981). They subdivided the basaltic rocks of Crater Flat into three distinct cycles (3.7, 1.1, and 0.3 Ma) using geologic mapping, K-Ar age determinations, and measurements of the magnetic polarity of the rocks. These subdivisions follow the three basalt cycles established by Crowe and Carr (1980). Each cycle of basaltic volcanic activity consists of multiple scoria or spatter cones and associated lava flows. The volcanic landforms are progressively more eroded and modified with increased age. Preliminary geologic maps (scale 1:12,000) were compiled for parts or all of the units of each volcanic cycle. The petrography, major- and trace-element whole-rock geochemistry, and mineral chemistry of the basalt units were described. The rocks are sparsely porphyritic with phenocrysts of olivine, minor plagioclase, and rare amphibole. Geochemically, they are mildly nepheline to hypersthene normative and are classified as hawaiite in composition. Seven K-Ar whole-rock age determinations for the basalt cycles were published. Vaniman and Crowe (1981) provided the first estimates of magma volumes of the associated centers. They were the first to recognize a systematic decrease in the volume of erupted magma and a possible increase in eruptive frequency through time. They suggested the systematic decreases in magma volume provided

possible evidence of waning of magmatic activity during the last 4 Ma. *The volume decrease in erupted basalt of Crater Flat remains a valid observation, even with refined volume calculations using more recent geologic mapping.*

D. Publications in 1982

1. Origin of Trace Element Enriched, Hawaiite Lava of Crater Flat. Vaniman et al. (1982) described further the petrology and geochemistry of the three cycles of hawaiite lava of the Crater Flat area. They noted that the cycles considered together form a straddle-type association as defined by Miyashiro (1978). Less-evolved basalt plot near the normative olivine-diopside divide on the basalt tetrahedron and the more-evolved basalt project into the hypersthene or nepheline fields. They modeled possible fractionation trends for the rocks, noting that removal of olivine, clinopyroxene, and amphibole could produce the lavas of more evolved composition. Varied parentage is more evident between cycles although the cycles are consistently of hawaiite composition. Basalts, particularly from the youngest two cycles are enriched in incompatible trace elements, but depleted in rubidium. The Rb/Sr ratios of the rocks are far too low to generate the $^{87}Sr/^{86}Sr$ ratios typical of basalt of the southern Great Basin. The low Rb/Sr ratios limit processes that could produce the trace-element enrichment. Possible processes of magma formation and evolution include cyclic recharge of an evolving magma chamber or decreased degrees of partial melting with phlogopite as a residual phase in a metasomatically enriched mantle source.

2. Revised Probability Calculations; Probability Bounds. Crowe et al. (1982) refined the volcanic risk assessment for the Yucca Mountain site. They developed a mathematical model for the volcanic disruption probability assuming that eruptive events occur independently, they are exponentially distributed, and the number of events in time intervals of length t is Poisson distributed with mean λt where λ is the recurrence rate. They estimated recurrence rates by counting volcanic events per time and by evaluating the cumulative volume of erupted magma versus time. Crowe et al. (1982) developed a refined method for calculating the disruption ratio (area ratio of Crowe and Carr 1980). They recognized that disruption ratios using circles of different radii are arbitrary and do not assess spatial trends in the distribution of volcanic centers. Crowe et al. (1982) developed a computer program to find the minimum area circle containing the volcanic centers of interest and the potential repository site. They evaluated all combinations of recognized volcanic centers in the region and developed systematic calculations of the disruption ratio.

Crowe et al. (1982) assembled all probability calculations into tables, emphasizing the importance of the range of values rather than individual calculations. They established a lower or minimum annual probability bound of repository disruption from a future volcanic event of 3.3×10^{-10} yr^{-1} from the probability tables. This was based on a Quaternary rate of magma production and a disruption ratio established by the minimum area ellipse for all volcanic centers of Quaternary age in the YMR. The upper or maximum probability bound of 4.7×10^{-8} yr^{-1} was established by including all volcanic centers of the Pancake Range-Death Valley volcanic zone (see chapter 3, this paper) and the minimum area ellipse for that zone. These values have been used subsequently in many reports assessing the suitability of the Yucca Mountain site with respect to the risk of volcanism.

3. Results of the First Volcanism Drill Hole. The exploratory hole USW-VH-1 was drilled in central Crater Flat in December 1980 (Carr 1982). The hole was sited to explore a positive aeromagnetic anomaly in central Crater Flat to determine if it was produced by late Cenozoic volcanic rocks. Additionally, the anomaly was drilled to investigate a possible source of a silicic pumice dated at 6.3 ± 0.8 Ma by the fission-track method on zircon. The source of the pumice was not located in VH-1 nor were new

basalt units noted in the section penetrated by the drill hole (Carr 1982). The source of the positive aeromagnetic anomaly was inferred to be a thickened section of the Bullfrog member of the Crater Flat tuff. *The source of the positive aeromagnetic anomaly in Crater Flat remains undetermined.*

4. K-Ar Age Determinations: The First Glimpse of a long-lived Controversy. Sinnock and Easterling (1982) analyzed the reproducibility of the K-Ar dating method for young basalt. They submitted controlled samples of basalt from the Lathrop Wells center, the Red Cone center, and the 3.7 Ma centers to three separate analytical laboratories. None of the laboratories were informed of the identity of the samples. Variance in the analytical results increased with decreasing age of the basalt units. There was good agreement in K-Ar ages for the 3.7 Ma basalt, moderate agreement for the Red Cone center, and poor agreement for the Lathrop Wells center. The K-Ar ages for the Lathrop Wells samples ranged from negative ages to >700 ka. Mean ages were 80 to >700 ka (Sinnock and Easterling 1982). *This paper provided the first indication of potential problems with whole-rock, K-Ar age determinations of young (<500 ka) basalt, a problem that continues.*

E. Publications in 1983

1. Volcanism Status Report, Death Valley–Pancake Range Volcanic Zone, Basaltic Volcanic Fields of the southern Great Basin, Tectonic Setting, Uncertainty of Volcanism Risk Assessment. Crowe et al. (1983a) summarized the status of volcanism studies for the YMR. They described the geology of basalt fields extending from southern Death Valley, California through the Pancake Range of central Nevada. The regional distribution of Pliocene and Quaternary basaltic volcanic rocks was established to place the volcanic patterns of the Yucca Mountain area in a regional perspective. Crowe et al. (1983a) noted that there are two types of volcanic fields in the region. These are major fields (Type I) with large magma volumes and a high cone density (number of cones per km^2 examples include the Lunar Crater, Reveille and Greenwater fields) and small fields (Type II) with low magma volumes and a low cone density (examples include Crater Flat and the Quaternary record of the southern Death Valley field). The Yucca Mountain site is adjacent to a Type II volcanic field. Crowe et al. (1983a) defined the Death Valley–Pancake Range volcanic zone (DV-PR) (Crowe et al. 1983a, Plate I; see also Carr 1984) and summarized the geologic, petrologic features and tectonic setting of volcanic fields in this zone (Crowe et al. 1983a, Table I). Crowe et al. (1983a) calculated basalt volumes for basalt centers of the YMR. The petrology and geochemistry of basaltic volcanism in the southern Great Basin were summarized with emphasis on trends through time. The status of volcanic risk assessment for the YMR was summarized. They presented and discussed three major questions important to an understanding of volcanic risk assessment. These are (Crowe et al. 1983a, p. 36):

1. Can the processes of basaltic volcanism be understood with a sufficient degree of confidence to define the potential hazards of future volcanism?
2. What are the areas of uncertainty in volcanic hazard assessment?
3. What are the procedures to resolve the issue of potential volcanic hazards for geologic disposal of radioactive waste within the YMR area?

Crowe et al. (1983a) noted that there are uncertainties in understanding processes of basaltic volcanism used to assess volcanic risk. The uncertainties are dominated by the reliability of predictions using the past geologic record, which is controlled by how well the geologic record is interpreted and magmatic processes can be quantified for forecasting future volcanic events. These uncertainties will remain but can be accommodated by *bounding* the risk of volcanism using multiple approaches. Crowe et al. (1983a) summarized evidence why the risk of volcanism for potential disposal of high-level radioactive waste in the Yucca Mountain area is low. The primary evidence is the low rates of volcanic activity in the

region since the Pliocene, the low probability of future volcanism disrupting an underground repository, and the limited consequences of repository disruption by magmatic activity. They listed studies in progress that may provide further information to assess volcanic risk. These studies are: (1) the mechanism and frequency of formation of shallow intrusions, (2) the compositional changes in volcanic fields through time, (3) the possibility of future bimodal volcanism (contemporaneous basalt-rhyolite eruptions), and (4) the origin of incompatible-element enriched Pliocene and Quaternary basalt. Crowe et al. (1983a) identified predictive geology as nothing more elaborate than *estimations* of future events. They noted that there is time-uncertainty in probability calculations and additional uncertainty in assumptions required for consequence analysis. Finally, Crowe et al. (1983a) recognized the need for presenting information on volcanic risk for a potential repository at Yucca Mountain in scientific and public forums and attempting to establish acceptable levels of risk from scientific and public perspectives. *An uncertainty that continues in assessments of volcanic risk is the absence of clearly defined regulatory standards of acceptable or nonacceptable risks. While the risk of volcanism for the Yucca Mountain site has been bounded through scientific studies, the interpretation of the significance of that risk continues to be difficult to interpret because of the subjectivity of the regulatory standards.*

2. Scenario Development for Consequence Analysis. Crowe et al. (1983b) traced the processes of magma generation, ascent, eruption, and dispersal of basalt magma with respect to potential magmatic disruption of a repository at Yucca Mountain. They reiterated the conclusions of Vaniman and Crowe (1981) and Vaniman et al. (1982) that the composition of Pliocene and Quaternary basalt in the region is hawaiite, and follows the Straddle-A classification of Miyashiro (1978). Basalt magma was assumed to ascend in narrow dikes with velocities ranging from 1 cm sec^{-1} to 1 m sec^{-1}. The composition and mineralogy of erupted basalt were recognized to require interrupted ascent; the magmas were inferred to be stored at the crust-mantle interface where they fractionated and decreased the density of the melt, promoting continued ascent through increased buoyancy.

Crowe et al. (1983b) summarized data on the dimensions and forms of basalt feeder systems. The most important feeder systems were inferred to be linear dikes that were recognized at several of the dissected centers of Miocene age. However, shallow intrusions consisting of dikes and sills were recognized at one locality. Evidence was summarized suggesting linear dikes are the most common forms of feeder systems for basalt centers like the basalt of Crater Flat. The dispersal of waste material in erupting basalt magma was constrained by analogy to the distribution of country rock fragments (lithic fragments) in basalt deposits. The primary mechanism of dispersal was inferred to be by strombolian eruptions. The exclusion of hydrovolcanic activity was based on the considerable depth of the water table beneath Yucca Mountain and the low moisture content of most rocks above the water table. Both factors suppress the occurrence of hydrovolcanic eruptions.

Size parameters of basalt centers in the YMR were compiled, including height, width, cone volume, flow volume, and total magmatic volume converted to dense rock equivalents. A noteworthy feature of the basalt centers of the region is a high ratio of cone volume (pyroclastic component) to flow volume (lava).

Crowe et al. (1983b) evaluated the dispersal pathways of waste radionuclides should a potential repository be disrupted by ascending magma which erupted at the surface. Waste pathways were inferred to primarily follow the pyroclastic component of a strombolian eruption. Major depositional sites were the scoria cone, the scoria-fall sheet, and a fine-grained component carried by prevailing winds. The most important pathway of waste material by volume using this analogy is in the scoria-fall sheet.

Subsequent studies have largely verified the studies of Crowe et al. (1983b) but with two important modifications. First, the issue of the subsurface geometry of basalt feeder systems remains an

area of concern. While the general model of scoria cones fed by linear feeder dikes at depth is valid, it is difficult to establish statistics on the relative abundance of simple feeder dikes versus more complicated basalt intrusions. The concept that rising magma seeks a position of neutral buoyancy at shallow crustal levels (see Chapter 3) has received increased attention in the last few years. Also magma reservoirs formed at shallow crustal levels may be capable of propagating dikes horizontally for long distances (Rubin and Pollard 1987; Walker 1989; Baer and Reches 1991). While shallow crustal magma chambers are not recognized, the new observations are important for considering maximum dike lengths. Second, the occurrence of future hydrovolcanic activity in the Yucca Mountain setting, while unlikely using field criteria, may not be ruled out conclusively from theoretical models of water-magma interaction.

3. Completion of Consequence Analysis for Basaltic Volcanism: The First Radiological Release Calculations for Magmatic Disruption of the Repository. Link et al. (1983) used the data foundation from Crowe et al. (1983b) to calculate radiological releases from magmatic disruption of a hypothetical repository located at Yucca Mountain. These studies, which generally fall under the title of consequence analysis (*performance assessment using current program terminology*), involve identification of volcanic processes that could lead to failure of a waste isolation system and calculation of the results of failure expressed as radiological levels of released waste elements. Link et al. (1983) calculated the radiological releases associated with magmatic disruption for two possible hypothetical repositories located at Yucca Mountain (spent fuel and reprocessed waste). The calculations assumed a repository capacity of half the estimated volume of spent fuel or reprocessed waste generated by commercial reactors through the year 2000. A range of geometric arguments was used to determine the number of canisters intersected by magma rising along a linear dike. Assuming a random orientation of the dike geometry relative to the repository tunnel complex, magma would intersect about seven canisters of spent fuel and one canister of reprocessed waste. All waste contacted by magma was assumed to be erupted preferentially with the pyroclastic component of a strombolian eruption. Radiological releases were examined from waste entrained in the basalt eruption column and from exposure to waste-bearing scoria deposits, resuspended particles, and radionuclides entering the food chain. The worse case for an airborne dose resulted in a cumulative total of 25 health effects in 10^6 yr. A second worse case was calculated for dose effects from scoria deposits (scoria cone, scoria fall-sheet) including effects of erosion and transport during a period of 10^6 yr. This yielded 2800 health effects. Link et al. (1983) calculated the total activity that would be transported to the surface normalized to 10^3 MTHM. The total expected release for 10^4 yr is 1.8 Ci or 0.038 Ci/10^3 MTHM for spent fuel and 1.3 Ci or 0.034 Ci/10^3 MTHM for reprocessed waste (Link et al. 1983, p. 163.)

Several assumptions used in this study will require modification for revised release calculations. First, more recent data on repository design, tunnel geometry, and nature of the waste inventory should be used. The geometry of waste-magma intersection in a repository should be evaluated assuming the most probable direction of dike propagation. This direction is north-northeast, perpendicular to the least compressive stress direction. Additionally, the assumption that all waste encountered by magma rising in a dike would be carried to the surface is undoubtedly too conservative. Finally, field observations show that lithic fragments are present in lava as well as the pyroclastic component of strombolian and hawaiian eruptions.

F. Publications in 1984

1. Structural and Tectonic Setting of the YMR. Carr (1984) described the structural setting of the YMR. He provided expanded discussion of the DV-PR zone and suggested that some of the Pliocene-Pleistocene basalt centers of the YMR occur along northeast-trending, rift-like structures.

G. Publications in 1985

1. Second Volcanism Drill Hole. Drill hole USW-VH-2 was drilled and cored to a depth of over 1200 m in 1983. The hole was located on the flanks of a negative aeromagnetic anomaly centered west of Red and Black Cones. The purposes of the drill hole were to evaluate evidence of the post-Pliocene evolution of volcanism in Crater Flat, to determine the cause of an aeromagnetic gradient between the drill hole site and drill hole USW-VH-1 (Carr 1982), to evaluate the origin of a large negative aeromagnetic anomaly in east-central Crater Flat, and to evaluate the late Cenozoic structural history of Crater Flat (Carr and Parrish 1985). Buried basalt was intersected in the drill hole at a depth of 360 m. It consisted of lava of reversed magnetic polarity that was dated at 11.3 ± 0.4 Ma (Carr and Parrish 1985). The basalt lava was judged to be the source of the prominent aeromagnetic low. The basalt was correlated with an exposed basalt at the south end of Crater Flat dated at 10.5 ± 0.1 Ma (Carr and Parrish 1985).

H. Publications in 1986

1. Volcanism Summary Report in a Book Published by the National Research Council Entitled Active Tectonics: Impact on Society. Crowe (1986) completed a review of volcanic hazard assessment for disposal of high-level radioactive waste focusing on studies of the YMR through 1985. The purpose of the paper was to publish the methods of assessing volcanic risk in a forum that could be read by a wide audience of the geologic community. Crowe (1986) summarized data presented in past publications. New information was presented on the possibility of hydrovolcanic eruptions. A relative-frequency diagram of crater depth for hydrovolcanic craters was presented. The average depth to the potential repository horizon at Yucca Mountain is greater by more than four standard deviations than the mean depth of hydrovolcanic craters. Crowe (1986) discussed the reliability of geologic data used for risk assessment. He noted that the data must be judged against research standards established in the current geologic literature. Further, the results of risk assessment have been published in the geologic literature to provide wide exposure to the geologic community. Crowe (1986) discussed the possibility of bias in volcanic hazard studies. He suggested the best method to overcome bias was to present both positive and negative findings of scientific studies. Finally, he noted that there is an element of uncertainty in all probabilistic studies in geology. *An important assumption of the behavior of small-volume basaltic volcanic centers described in this paper is that they are monogenetic (formed in short-duration eruptions–weeks, months, or at most years). This assumption leads to the inference that a volcanic event represented by ascent of magma through a repository and feeding an eruption is a single transient event. Subsequent work has raised the possibility that some of the basalt centers of the YMR were formed by multiple, temporally distinct volcanic events. This possibility requires reevaluation particularly for the consequences of repository disruption by volcanic events that could be more spatially and temporally complicated than monogenetic volcanic events.*

2. Second Volcanism Status Report; Discussion of the Issues of the Mechanism of Emplacement of Shallow Intrusions, the Possibility of Future Bimodal Volcanism, the Origin of Trace-Element Enriched Basalt, and the Likelihood of Hydrovolcanic Activity. Crowe et al. (1986) published a second status report on volcanism for the Yucca Mountain Project. The 1986 report discussed areas of uncertainty identified in the previous volcanism status report. A series of appendices in the report compiled major-element data (original analyses normalized to 100%) for over 140 analyses, trace-element data for 68 analyses, sample descriptions for all analyzed rocks, and grain-size data for tephra from the Lathrop Wells volcanic center.

The first area of identified uncertainty was the mechanism of emplacement of shallow intrusions. Crowe et al. (1986) noted that the most common feeder structure exposed in dissected basalt centers is

linear dikes. Exceptions were described at three areas, the Paiute Ridge area east of Yucca Flat, the Funeral Mountains west of Amargosa Valley, and the middle and southern tuff rings of Nye Canyon, northeast of Frenchman Flat. Crowe et al. (1986) summarized arguments for and against the formation of sills and irregular intrusions beneath Yucca Mountain. They concluded that shallow intrusions may be possible in the tectonic setting of Yucca Mountain. This topic represents an area of uncertainty in consequence analysis for volcanic risk assessment.

The second area of uncertainty was the time-space patterns of basaltic volcanic fields of the Great Basin. Crowe et al. (1986) discussed the possibility that the Crater Flat volcanic field might evolve in the future to form a large-volume, high-cone density volcanic field. They examined the volcanic patterns of the YMR and contrasted them with long-lived, high-cone density volcanic fields of the DV-PR volcanic zone. These fields include the Lunar Crater volcanic field and the Death Valley volcanic field. No evidence was noted in the patterns of the three fields to support the interpretation that the Crater Flat volcanic field would evolve toward a more active field. Crowe et al. (1986) listed two cautions with this conclusion. First, only three volcanic fields were examined for the evaluation of the volcanic patterns. These data may be too limited for confidence in predicting future volcanic patterns. Second, volcanism and tectonism are closely coupled in time and space. Volcanism models must be integrated with tectonic models of the YMR to assess future patterns of activity.

Crowe et al. (1986) examined the possibility of future bimodal volcanism in the YMR (coexisting basalt-rhyolite magmas). They noted that the subsurface feeder systems of silicic centers are much larger and there is an increased potential for regional dispersal of tephra in explosive eruptions of silicic composition. Both factors could increase the consequences of repository disruption. They summarized the data of Kane and Bracken (1983) concerning aeromagnetic data and identified anomalies in the YMR and noted that the size of some of the anomalies indicates they could be produced by buried silicic centers. Crowe et al. (1986) described the results of two drill holes: VH-1 in east-central Crater Flat and VH-2 located between Red Cone and Black Cone. Neither drill hole intersected silicic intrusive rocks. A third aeromagnetic anomaly that could be a silicic center was identified in the Amargosa Valley, a few kilometers south of the town of Lathrop Wells. They suggested this anomaly must be penetrated by exploratory drilling to resolve concerns of the potential for future silicic volcanism. *The aeromagnetic anomaly in the Amargosa Valley was drilled in exploration studies by a private company. Samples of cuttings recovered from the drill hole show that the aeromagnetic anomaly is caused by a buried basalt of Pliocene age.*

The origin of trace-element enriched basalt of the YMR was evaluated. Crowe et al. (1986) concluded that the causative process(es) for generation of trace-element enriched basalt could not be either crustal contamination or a young (late Cenozoic) metasomatic volcanic event. They noted that the origin of trace-element enriched basalt remains a much debated topic of volcanic petrology. *More recent studies have attributed the isotopically anomalous and trace-element enriched basaltic volcanic rocks of the Yucca Mountain area to generation of the magmas from ancient lithospheric mantle (Farmer et al. 1989).*

Crowe et al. (1986) gathered additional data on the possible importance of future hydrovolcanic eruptions at Yucca Mountain. They completed revised geologic mapping of the southern and middle basalt centers of Nye Canyon, noting that both are tuff rings, and were formed from hydrovolcanic explosions and infilled subsequently by lava lakes with interbedded scoria deposits. Tephra studies were completed for the Lathrop Wells volcanic center. These studies showed that the tephra sequences were formed by two distinct fragmentation mechanisms. These include fragmentation from both strombolian eruptions and hydrovolcanic eruptive mechanisms. They noted that hydrovolcanic eruptions occurred both early and late in the evolution of the main cone of the Lathrop Wells center. Crowe et al. (1986) summarized

experimental data from fuel-coolant interactions that could be applied to hydrovolcanic explosions. These data are consistent with a spontaneous nucleation-pressure suppression model but less so with a thermal detonation model. They concluded that theoretical models of magma-water interaction show that hydrovolcanic explosions are possible at the Yucca Mountain setting. However, geologic evidence indicates hydrovolcanic explosions are unlikely to exhume a repository. They suggested consequence studies of radioactive releases should be revised to incorporate an opening phase of hydrovolcanic activity followed by strombolian eruptions.

Finally, Crowe et al. (1986) noted that more complete models of the tectonic framework of the YMR are needed. These models should be integrated with observed patterns of past volcanic activity.

3. Environmental Assessment. The probability estimates of magmatic disruption of a repository of Crowe et al. (1982) were used in the EA for Yucca Mountain (DOE 1986). The conditional probability of magmatic intrusion of the repository was evaluated for the favorable condition of 10 CFR Part 960.4-2-7 b. A mean value of 1.3×10^{-4} events yr^{-1} with a standard deviation (one *s)* of 1.33×10^{-4} events yr^{-1} for 10,000 years was calculated for the volcanic disruption probability using the data tables of Crowe et al. (1982, Tables IV and V). The conclusion of the EA (DOE 1986, pp. 6–262) was that additional investigations were needed to more accurately constrain the probability of volcanic disruption. *The mid-range value of the probability of volcanic eruptions may not be well represented by a calculation using a conventional mean derived from the data tables of Crowe et al. (1982). The data tables were constructed to establish the bounds of the probability of repository disruption. No attempt was made to establish a representative probability range or to examine the statistical properties of the distribution of probability values.*

I. Publications in 1988

1. Site Characterization Report. The risk of basaltic volcanism for the Yucca Mountain site was summarized in Sections 1.5.1.2 and 1.5.1.3 of the SCP (DOE 1988). The conclusion of the EA (DOE 1986) was reiterated with respect to the favorable condition of 10 CFR Part 960.4-2-7 b: additional work was recognized to be required to resolve the volcanism issue. The plans for this additional work were summarized in Chapter 8.3 of the SCP (DOE 1988). These included Study 8.3.1.8.1.1 Probability of Magmatic Disruption of the Repository; Study 8.3.1.8.1.2, Physical Processes of Magmatism and Effects on a Potential Repository; and Study 8.3.1.8.5.1, Characterization of Volcanic Features.

A three-part strategy was presented in the SCP for volcanism studies. First, the probability of magmatic disruption of a repository would be calculated to determine if the site would or would not be disqualified solely from the direct effects of volcanism. The basis for this decision would be a determination of whether the probability of magmatic disruption of the repository is less than 1 in 10,000 in 10,000 years. If the answer to that question is yes, studies of the eruptive effects of volcanism would be ended. If the answer to that question is no, the second part of the strategy would be started. Studies would evaluate the probability of magmatic disruption of a repository *and* the probability of eruptive releases of radionuclides to the accessible environment. This work would be based on evaluation of natural analogues (eroded volcanic centers) to quantify or bound the percentage of a repository inventory that would be released at the surface in an eruption. If the probability of releases exceeding the regulatory criteria are less than 1 in 10,000 in 10,000 years, studies of the eruptive releases of volcanism would be terminated. If the probability is less than the cutoff value, performance assessment studies would be required to assess the possibility of disqualification of the Yucca Mountain site. The third part of the study will evaluate the potential radiological releases from eruptive and intrusion (coupled) effects of magmatic disruption of the controlled area and the repository. The thrust of these studies is to provide data for evaluating the

contribution of potential releases from eruptive and intrusion scenarios for the performance of the total waste isolation system.

IV. Progress Since The Site Characterization Report

A. Publications in 1988

1. Reassessment of the Chronology of the Lathrop Wells Volcanic Center; New Geomorphic and Soils Studies. In 1988, there was a major reevaluation of the chronology of the Lathrop Wells volcanic center using comparative soils and geomorphic studies of the volcanic landforms (Wells et al. 1988, 1990; Crowe et al. 1988). Geomorphic and pedologic data from selected volcanic landforms in the Cima volcanic field were compared with data from the Crater Flat volcanic field. These results, coupled with newly obtained K–Ar age determinations and revised geologic mapping, lead to reevaluation of the chronology and stratigraphic data. Wells et al. (1990) concluded that the K-Ar age determinations for the Lathrop Wells center may have overestimated the age of the center. They suggested the youngest activity from the center could be as recent as late Pleistocene or Holocene. Further, the center could be polygenetic: formed from multiple, time-discrete eruptive events. Wells et al. (1990) compared morphometric, pedogenic, and stratigraphic data for volcanic centers from basaltic volcanic fields in California and Nevada. . They showed that a sequence of tephra deposits exposed near the south cone base contained interbedded soils with significant horizon development. The presence of the soils provided the primary basis for the interpretation of polygenetic volcanic activity. *The recognition of the potentially young age of the main cone of the Lathrop Wells center was significant for two reasons. First, it provided evidence that the most recent volcanic event in the region is younger than originally estimated. Second, the possibility that the center could have formed by multiple (polygenetic) events required reevaluation of scenarios used for determining the consequences of volcanic events. There has been continued controversy whether the main cone of the Lathrop Wells center is as young as late Pleistocene or Holocene and formed during multiple, temporally separate events that are significantly younger than the lava eruptive events. This controversy may never be resolved to the satisfaction of all research scientists. Nonetheless, the possibility and implications of polygenetic volcanic events have been considered in probabilistic assessments to ensure the consequences or effects of volcanic disruption of a potential repository are not underestimated.*

2. Revised Geologic Map of the Lathrop Wells Volcanic Center. Crowe et al. (1988) completed a revised geologic map of the Lathrop Wells volcanic center. The center was remapped at a scale of 1:4000 on color aerial photographs. The eruptive history of the center was reconstructed using a combination of field mapping, geomorphic studies, geochronology studies, and preliminary results of paleomagnetic studies of volcanic units. The center was inferred to have formed from multiple volcanic events separated by intervals of no eruptive activity (polygenetic activity). The duration between events was estimated to be several thousand to several tens of thousands of years. The age of the volcanic center was estimated to be less than 100 ka and probably less than 50 ka. *Recent studies provide compelling evidence that the oldest lava flow sequences(chronostratigraphic unit I) of the Lathrop Wells center are >100 ka. The age of the main cone is still not well constrained but multiple lines of evidence suggest it is probably <50 ka.*

B. Publications in 1989

1. New Developments in Concepts of Basaltic Volcanism, Evidence of Complex Evolution of the Lathrop Wells Center, New K-Ar Age Determinations, Definition of Polygenetic Volcanism, Revised Volcanic Risk Assessment Using Multiple Volcanic-Eruption Scenarios. Crowe et al. (1989) summarized new developments in volcanism studies for the Yucca Mountain Project. They noted that small

volume basalt centers have traditionally been inferred to form during short duration events (months or years; see Wood 1980). However, the recent studies of the Lathrop Wells center show that it may be substantially younger than initial age estimates of 270 ka that were based on whole rock K-Ar age determinations. They summarized evidence that the scoria cone could be substantially younger than the K-Ar age determinations and the center may have a more complex history of volcanism than the typical monogenetic centers. First, revised field mapping showed that there could be at least four time-distinct, eruptive events. Second, geomorphic features of the cone were inferred to be consistent with an age that was possibly as young as late Pleistocene or Holocene. Third, stratigraphic sections exposed in quarry cliffs south of the cone revealed a sequence of buried soils, primary and reworked tephra, and eolian deposits. The presence of soils with development of horizons between tephra units requires a hiatus between eruptive events. Different field magnetic directions were recorded from paleomagnetic studies of volcanic units.

New K-Ar age determinations were obtained from five sample sites in the lava flow units of the center. The data were judged to be of good quality analytically, but difficult to interpret. The resulting ages were clearly younger than previously reported K-Ar ages for the center. They may or may not separate into two groups. The lava flow groups were not statistically different in age (F test) unless one sample site was discarded. This sample site appeared anomalous and yielded a K-Ar age of 480 ka. It plotted as an outlier on a probability plot of percentage radiogenic argon versus age.

Crowe et al. (1989) defined and contrasted polygenetic versus polycyclic volcanism. *(Here we retain the term polyclic to reflect the content of the summarized paper).* They noted that polygenetic volcanoes are characterized by intermittent eruptions over time spans of 10^{-5} to 10^{-6} yr. Volume of eruptions may exceed 10 km^{-3}. They commonly are associated with a subvolcanic reservoir. Fedotov (1981) argued that a high magma supply rate, $>10^{-7}$ m^{-3} yr^{-1}, is required to maintain intermittent or continuous basaltic volcanism in a continental setting. The term polycyclic volcanism was used (Crowe et al. 1989) to refer to small-volume (<1 km^3) volcanic centers that exhibit intermittent volcanic activity where the time between events exceeds the cooling time for basalt magma in the shallow crust (several tens of years).

Crowe et al. (1989) assessed the impact of the revised chronology studies and polygenetic activity on volcanic risk assessment for the Yucca Mountain site. They completed revised regression calculations with time as the independent variable and magma volume as the dependent variable. The slope of the curve, which is the magma output rate, did not change significantly from previous calculations (Crowe et al. 1982). Revised calculations of O_p, the magma-output rate, declined from 130 m^3 yr^{-1} to 66 m^3 yr^{-1} during the approximately 4 Ma history of volcanism in the Crater Flat area.

Two scenarios were developed for future volcanic activity in the Yucca Mountain area (Crowe et al. 1989). These are the recurrence of a small-volume scoria eruption at either the Lathrop Wells or the Hidden Cone centers and the formation of a new center of basaltic volcanism. The former event was judged to be insignificant because of the distance of the centers from the Yucca Mountain site. Identified concerns include seismic activity, which would typically be swarm-type activity of generally small magnitude and centered more than 20 km from Yucca Mountain. The magnitude of this seismic activity would likely be much smaller than the design earthquake for the potential repository. No mechanism could be identified for small-volume eruptions at these centers to affect the groundwater system at Yucca Mountain.

The second scenario, formation of a new volcanic center, has been the focus of studies for volcanic risk assessment. It is the identified volcanic event that has a finite probability of disrupting the repository. *The possible recurrence of another eruptive event at the Lathrop Wells or Hidden Cone center is not*

used to justify a low risk of volcanic activity for the Yucca Mountain site. It may be the most likely future event in the YMR but because it is a probable low consequence event it is inferred to be less important from a risk perspective than the formation of a new volcanic center.

2. Recurrence Rate of Volcanic Events; Cumulative Magma Volume Versus Time, Recognition of the Crater Flat Volcanic Zone. Crowe and Perry (1989) described methods for estimating volcanic recurrence rates for probability calculations. This was the first of a series of papers that attempted to bring to closure parts of the studies of volcanism risk assessment. They described the distribution of volcanic centers, emphasizing a southwest stepping of volcanism between 6.5 and 3.7 Ma. They described a recurrence pattern of basaltic events where new eruptive sites are marked by probable coeval clusters of centers. These clusters appear to be of similar age within the analytical limits of K-Ar age determinations. Crowe and Perry (1989) noted that all basalt centers of the youngest episode of volcanism, except the basalt of Buckboard Mesa, occur in a narrow northwest trending zone. They named this zone the CFVZ.

Crowe and Perry (1989) summarized methods to calculate λ, the recurrence rate of volcanic events. These include evaluation of intervals of volcanic activity for evidence of periodicity, event counts for set periods of geologic time (Quaternary period, 3.7 Ma basalt cycle), and calculation of magma output rates. They noted first that the number of volcanic events is insufficient to establish recurrence intervals. Second, they discussed limitations of event counts. This method is based on an assumed Poisson distribution of events in time. However, vent or cone counts record only the recognition of a volcanic event. They do not account for the magnitude of events. Additionally, vent counts are insensitive to variations in rates through time. Therefore, the λ can be biased toward higher or lower values by varying the observation period t of the rate estimations.

Crowe and Perry (1989) suggested a preferred alternative for calculating λ, which is used repeatedly in published studies of active volcanic fields. This method is based on constructing a curve of cumulative magma volume versus time. They provided background information on the use of this plot and cited examples of usage from the volcanological literature. The most significant feature of a plot of cumulative magma volume versus time is it provides a method of assessing the time variability of magma-output rates. They suggested that the magma-output rate represents a composite response to the initiation, growth, and decline of thermal or magma-generating events in the mantle. In this model, the lithosphere acts as a moderating influence (event filter) on volcanic activity. Crowe and Perry (1989) presented a plot of cumulative magma volume versus time for the Springerville volcanic field using data from Condit et al. (1989). This field exhibits classic stages of time-volume-evolution of a volcanic field, including a short waxing period during the birth of the field, a long interval of steady-state activity, and waning activity during the last 100 ka (Crowe and Perry 1989, Fig. 2).

Several important assumptions are required to use a magma-output rate for extrapolating future volcanic events. First, the volcanic record must reflect the operation of a coherent period of tectonic activity. They argued that the youngest episode of volcanic activity in the region (4.0 Ma and younger) provides that perspective. Second, the magma output rates are assumed to be regulated by the tectonic setting of the site. Magma is generated in the mantle. It ascends through or is trapped in the crust in response to the dynamics of the tectonic setting. Third, the record of basaltic volcanism must be considered carefully with respect to the temporal and spatial variability of volcanic events in establishing a magma-output rate.

The magma-output rate for the YMR decreases with decreasing age. If the basalt of Buckboard Mesa (2.9 Ma center in the moat zone of Timber Mountain) is added to the cumulative volume curve, the flattening of the curve through time is more pronounced.

There are several key questions or areas of uncertainty for establishing the magma output rate for the YMR. Are steady-state rates valid for an area of intermittent volcanism over a period of the last 3.7 Ma? What is the significance of the variability in calculated magma-output rates? Crowe and Perry (1989) noted in particular that a sensitive assumption for calculating the magma output rate is the inferred volume of the scoria-fall sheets of each center, particularly in the case of the four Quaternary basalt centers of Crater Flat (greater uncertainty in extrapolating the volume of eroded scoria-fall sheets because several centers are involved).

Evaluating estimates of λ obtained from magma-output rates requires a careful identification of the physical meaning of the rate. It is a long-term rate associated with the intermittent formation of basalt centers. More correctly, it is a rate that applies to formation of clusters of volcanic events since each plotted point is a summation of the volume of multiple centers. Crowe and Perry (1989) presented several methods for estimating the volume of an initiating volcanic event. Their recommended approach was to use the volume of the smallest volcanic cluster, the basalt of Sleeping Butte. *An alternative model that is being studied is to calculate the minimum volume of magma required to initiate a dike ascent event which propagates through the crust without freezing because of solidification. Spence and Turcotte (1985) estimated the minimum magma volume of a dike initiation event to be 10^8 m^3 using assumed values of crustal thickness, dike thickness, and dike cooling rates. This approach is however, almost impossible to apply to the volcanic record of the YMR because it would require evaluating the erupted volume and the volume of intrusive rocks associated with a volcanic event.*

3. Isotopic Composition of Strontium, Neodymium, and Lead for Basalt of the YMR, Preservation of Ancient Lithospheric Mantle. Farmer et al. (1989) presented new trace element and neodymium, strontium, and lead isotopic data for late Cenozoic basalt of southern Nevada and adjacent parts of California. They noted that ε_{Nd} values range from +10.1 to –10.4 and vary regularly with geographic position. The ε_{Nd} values for basalt are progressively more negative for an area extending south from central Nevada to the YMR (+4.7 at the Lunar Crater volcanic field; –10.4 in the YMR). Farmer et al. (1989) showed that most basalt in the YMR has ε_{Nd} values of less than –7 and this distinctive isotopic signature is independent of age or degree of trace-element enrichment. The $^{87}Sr/^{86}Sr$ values of the basalt of southern Nevada covary with the neodymium isotopic compositions. Basalt of the YMR has strontium isotopic ratios of 0.7070 to 0.7075. Lead isotopic data for the basalt of the YMR plot within a narrow range of $^{206}Pb/^{204}Pb$, $^{207}Pb/^{204}Pb$, and $^{208}Pb/^{204}Pb$ (Farmer et al. 1989). The values plot to the right of the geochron and above the northern hemisphere reference line.

Farmer et al. (1989) argued that basalt of the YMR comprises a spatially distinct isotopic population that can be separated isotopically from basalt inferred to be derived from upwelled asthenospheric mantle. One possible explanation for the isotopic characteristics of the basalt of the YMR is that they have undergone a greater degree of crustal contamination than other basalts of the Basin and Range province. However, a critical observation for the basalt of the YMR is that they show uniform neodymium, strontium, and lead isotopic compositions for sites ranging in age from Quaternary to about 10 Ma. This would not be expected if the basalt represented mixtures of mantle-derived magma and bulk or selectively assimilated crust (Farmer et al. 1989). A preferred alternative is that the basalt was derived from lithospheric mantle that has been preserved beneath this region despite late Cenozoic extension, an observation consistent with the amagmatic history of the area south of YMR throughout the Phanerozoic.

Thus the mantle beneath the YMR may have been relatively cold and difficult to extend. The preservation of mantle lithosphere in southern Nevada may therefore, be largely controlled by the preextension thermal gradient within the lithosphere itself (Farmer et al. 1989). This is consistent with the mantle lithosphere representing ancient continental mantle formed during formation of Precambrian continental crust. The data and interpretations support the hypothesis that preextension lithospheric mantle currently exists beneath southern Nevada and eastern California. The preservation of lithospheric mantle appears to be unique relative to the other parts of the Basin and Range province (Farmer et al. 1989).

C. Publications in 1990

1. Volcanic Patterns of the YMR; Time-Space Migration of Volcanism, Multiple Chronology Models for the Lathrop Wells Volcanic Center. Crowe (1990) described basaltic volcanic episodes of the YMR located in the south-central part of the southwest Nevada volcanic field. He presented evidence of two distinct episodes of basaltic volcanism in the last 10–12 Ma. These include large-volume basalt associated with the waning phase of the Timber Mountain–Oasis Valley caldera complex and small-volume, Postcaldera basalt. The latter was divided into two cycles. These include: (1) an older cycle of activity (9 to 6.3 Ma), all units of which occur north and east of Yucca Mountain (Older postcaldera basalt [OPB]), and (2) a younger episode of activity, the Younger postcaldera basalt (YPB) (3.7 Ma to late Pleistocene). All basalt of the YPB, except the basalt of Buckboard Mesa, occur within a narrow northwest-trending zone west and southwest of Yucca Mountain (CFVZ of Crowe and Perry 1989). Crowe (1990) showed that there are two distinct patterns through time for the volcanic activity of the episodes. The first is a dramatic decrease in the volume of eruptive units. Eruptive volumes of individual events of the basalt of the silicic episode exceed several cubic kilometers. Eruptive volumes of centers of the YPB are less than 1.0 km^3 and average about 0.1 km^3. *(This does not include the newly recognized Pliocene basalt of Thirsty Mesa).* Small-volume basalt eruptions have occurred repeatedly in the YMR since about 8.5 Ma. *(The only exceptions to this generalization are the larger volume basalt of Thirsty Mesa and the basalt of Buckboard Mesa).* Second, the time-space patterns of volcanic activity of the YPB are consistent with a southwest stepping of volcanic activity between eruption of centers of the OPB and YPB. This pattern mimics the migration patterns of older silicic volcanic activity.

Crowe (1990) described the geology of each center of the Postcaldera basalt, providing more detailed data for the Pliocene and Quaternary volcanic centers. He described the controversy concerning the age of volcanic units of the Lathrop Wells volcanic center. Because the chronology data are incomplete, three permissive models for the age and eruptive sequence of the center were summarized. Inferences concerning the nature of the most likely future volcanic activity in the YMR are:

1. The most likely composition of future volcanism is alkali basalt (hawaiite).
2. Future eruptions will probably be strombolian with a potential for hydrovolcanic activity at sites where the water table is shallow.
3. The highest probability of a recent event is a recurrence of a small-volume eruption at either the Lathrop Wells or the Sleeping Butte volcanic centers. These eruptions would probably be analogous to the last eruptions at the centers. This prediction assumes validity of the polygenetic model of basalt eruptions, a concept still being investigated.
4. The primary event of concern for siting of a potential repository at Yucca Mountain is the formation of a new volcanic center or cluster of centers. This event has a finite probability of occurring at and disrupting the Yucca Mountain site. The most likely site of formation of a new volcanic center is in the CFVZ.

2. Study Plan 8.3.1.8.5.1 Characterization of Volcanic Features; Data Gathering Activities for Volcanism Studies. Study Plan 8.3.1.8.5.1, Characterization of Volcanic Features, was completed and submitted to the Nuclear Regulatory Commission in 1990. This Study Plan describes planned research for five activities that are the major data gathering activities for volcanism studies for the YMP. The first activity is 8.3.1.8.5.1.1, Volcanism Drill Holes. The purpose of this activity is to evaluate, using exploratory drilling, the origin of aeromagnetic anomalies that could represent buried basaltic volcanic centers or shallow intrusive rocks of basaltic or silicic composition. The second activity is 8.3.1.8.5.1.2, Geochronology Studies. The purpose of this activity is to refine the geochronology data for volcanic events in the YMR with an emphasis on basaltic volcanic rocks of Quaternary age. Multiple age measurements using a variety of isotopic, radiometric, and age-correlated methods will be used. These studies attempt to increase confidence in the accuracy of geochronology results by seeking convergence among different geochronology methods. The geochronology methods are crosschecked by field, stratigraphic, soil, geomorphic, and petrology data. The third activity is 8.3.1.8.5.1.3, Field Geologic Studies. The purpose of this activity is to collect and provide geologic control on the stratigraphic relations of samples used for the geochronology studies. Additionally, field studies will establish the field geologic relations, the volume of erupted volcanic material, and the eruptive history of Pliocene and Quaternary basaltic volcanic centers in the YMR. A third part of this activity will be an evaluation of the distribution and the significance of Pliocene and Quaternary silicic volcanic centers in the Great Basin. The fourth activity is 8.3.1.8.5.1.4, Geochemistry of Eruptive Sequences. The purpose of this activity is to sample and analyze the composition of volcanic units recognized from the field geologic studies of Quaternary basaltic volcanic centers in the YMR. Eruptive units established from field and geochronology studies will be analyzed for whole-rock, major- and selected trace-elements. Mineral compositions will be determined for phenocryst, microphenocryst, and groundmass phases. These data will be used to evaluate the magmatic evolution and geochemical processes for each center. Strontium and neodymium (and possibly lead and oxygen) isotopic analyses will be obtained for selected eruptive units. These data will be used to evaluate geochemical processes of magma formation and to test plausible models that may lead to understanding the genesis of the magmas that formed the Quaternary centers. Additionally, polygenetic and monogenetic models for the centers will be tested through examination of the geochemical and isotopic data. The fifth activity is 8.3.1.8.5.1.5, Evolutionary Cycles of Basaltic Volcanic Fields. The purpose of this activity is to study the evolutionary patterns (time, space, magma effusion rates, volume, geochemistry) of continental basaltic volcanic fields in the southwest United States. We will attempt to determine if there are systematic patterns to the initiation, evolution, and cessation of activity in basaltic volcanic fields. Additionally, we will attempt to determine if these patterns can be used to identify the stage of activity of the basaltic volcanic field of Crater Flat, which in turn would be used to predict and constrain the nature of future volcanic activity.

3. First Publication of Technical Overview of Volcanism Studies by the State of Nevada. Smith et al. (1990) described the area of most recent volcanism near Yucca Mountain and examined the implications of that information for an assessment of volcanic risk. This work was sponsored by the state of Nevada in their role of providing technical overview of the Yucca Mountain Project. Smith et al. (1990) examined the spatial and temporal patterns of post–6 Ma volcanism in the southern Great Basin. They suggested that volcanism in the Yucca Mountain area should be viewed as part of the volcanic record of the southern Great Basin. They argued that local patterns of migration of volcanic activity in the Yucca Mountain area (summarized in Crowe and Perry 1989; Crowe 1990) lack regional significance. Smith et al. (1990) suggested that basalt centers occur commonly along range margins but also in range interiors. They cited supporting evidence for the latter observation using the setting of the basalt of Buckboard Mesa and the basalt centers of western Arizona, adjacent to Lake Mead. Finally, they suggested that high-angle normal faults control the location of volcanic centers in the Yucca Mountain area.

Smith et al. (1990) defined the area of most recent volcanism (AMRV) as an area enclosing all known post–6 Ma volcanic centers in the region. *This area of Plio-Quaternary volcanism is identical to Case 1a of the random structural model of Crowe et al. (1982) and is nearly identical to the YMR as defined in Chapters 2 and 3.*

Smith et al. (1990) described the geology of the Red and Black Cone centers of Crater Flat and presented a preliminary geologic map of Red Cone. They infer that the arc of Quaternary volcanic centers in Crater Flat follows the same fault set that offsets the Paintbrush Tuff west of the Yucca Mountain site. They suggested further that the faults controlling vent locations experienced clockwise rotation similar to the rotation of Yucca Mountain (Rosenbaum et al. 1991). Smith et al. (1990) noted that the Lathrop Wells volcanic center formed along a splay of the Solitario Canyon fault.

The geology of the Fortification Hill and Reveille Range volcanic fields were described and cited as possible analogues to the volcanic centers of the Yucca Mountain area. The Fortification Hill volcanic field is composed of alkali basalt centers and associated lava that erupted between 5.9 and 4.7 Ma (Smith et al. 1990). The Reveille Range volcanic field is located in central Nevada, 80 km east of Tonopah. Basaltic volcanism in the field ranges from 6 to 3 Ma. Dikes exposed in the Fortification Hill field have aspect ratios of 10^{-2} to 10^{-3} and widths of 0.5 to 2 m (Smith et al. 1990). *A significant difference between the basalt centers of the Fortification Hill and Reveille Range fields and the basalt of Yucca Mountain is the volume of eruptive units. Basalt centers of the former fields exhibit volumes in excess of 1 km^3. In contrast, the basalt centers of Crater Flat have eruptive volumes of <0.1 km^3.*

Smith et al. (1990) defined volcanic chains as aligned groups of related volcanic centers that are controlled by a single structure or a set of related structures. They suggest the Fortification Hill–Lava Cascade group forms a chain 25 km long with a width of 3 km or possibly 15 km. They suggest chain dimensions for the Reveille Range are comparable to those of the Fortification Hill volcanic field.

The analog data from the Fortification Hill and Reveille Range fields were used to define high-risk zones for volcanism in the AMRV (Smith et al. 1990). These risk zones are centered on the Quaternary volcanic centers of the YMR and have assigned dimensions from the analog studies. *This usage of risk does not follow standard definitions of risk which is a product of probability and consequences. Rather, the risk zones of Smith et al. (1990) are based on the assumption that future volcanic activity will occur in the same zones or site as past activity. This assumption has merit and follows traditional methods used to assess volcanic hazards of active volcanic centers and fields. However, the defined zones are structural or effect zones identified from past sites of volcanic activity. The assumption is made that past sites and their associated structural zones will be sites of future volcanic activity. An observation that is inconsistent with this approach, however, is that none of the past zones overlap, even using unrealistically long chain lengths from other volcanic fields. Thus if the geologic record of volcanism is examined as a test case of the risk zone model, there is a low success rate using older sites of volcanic activity (Pliocene) to predict the location of younger volcanic center sites (Quaternary).*

D. Publications in 1991

1. Alternative Views by the U.S. Geological Survey; Monogenetic versus Polygenetic Eruption Models. Champion (1991) summarized paleomagnetic data for the Pliocene and Quaternary basalt centers of the YMR. He noted that the 3.7 Ma volcanic centers of Crater Flat exhibit tightly grouped mean magnetic directions suggesting contemporaneous or nearly contemporaneous eruptive events. Similar conclusions were reached for the four aligned, 1.2 Ma basalt centers of Crater Flat. Champion (1991) also examined the Sleeping Butte centers northwest of Yucca Mountain. Here two directions of remanent

magnetization were described for the lava flows and cone scoria of the two centers. However, the directions are separated by an angular difference of only 3°. Champion (1991) suggests the cones and associated flows probably formed during an approximately 100-yr interval. Finally, Champion (1991) presented results of paleomagnetic studies of the Lathrop Wells center. Two directions of remanent magnetization were obtained from the two units of the Lathrop Wells center. The cited angular difference between the directions is 4.7° which he suggested indicates an age difference of only a century. Champion (1991) argues, using paleomagnetic data, that all of the centers of the YMR are monogenetic. *Three significant assumptions and limitations of the data of Champion (1991) were not discussed. First, Champion (1991) did not present demagnetization or measurement data for individual sites of collected samples; only mean site data were presented. The presented data are inadequate to test or verify his conclusions. Second, he assumed secular variation during the time of eruption of the different volcanic cycles was analogous to modern secular variation. Third, paleomagnetic data cannot be used to constraint the* ***maximum*** *difference in the age of volcanic units, particularly for volcanic events that have magnetization directions close to the time-average (spin-axis) Quaternary magnetic direction.*

2. Alternative Views by the U.S. Geological Survey; Age of the Lathrop Wells Volcanic Center. Turrin and Champion (1991) summarized the results of $^{40}Ar/^{39}Ar$ and conventional whole rock, K-Ar ages of the Lathrop Wells volcanic center. They suggested that the age of the center is bracketed between 119 ± 11 and 141 ± 10 ka. This age estimate is based on calculation of a variance weighted mean of replicate K-Ar whole and $^{40}Ar/^{39}Ar$ laser fusion age determinations. They suggest the age determinations are consistent with age constraints for surficial deposits in the YMR. Turrin and Champion (1991) combined the results of K-Ar and paleomagnetic studies and concluded that while there were two distinct volcanic events at the Lathrop Wells center, the events are closely spaced in time and should be treated as a single event for assessments of volcanic risk. *The K-Ar ages published by Turrin and Champion (1991) are accepted as potentially valid measurements of the ages of volcanic units of the Lathrop Wells center. In question, however, is the use of a variance weighted mean for measurements that are nonGaussian with large variance that cannot be attributable solely to analytical error. Additionally, the measured K-Ar ages are for lava units of the center and may not constrain the age of the main cone.*

3. Geologic Map of the Sleeping Butte Volcanic Centers; Possible Polygenetic Eruptions of the Hidden Cone Center. Crowe and Perry (1991) completed a preliminary geologic map and report on the basalt of Sleeping Butte. This unit includes two spatially separate, small-volume basalt centers. The centers are estimated to be between 200 and 400 ka using whole-rock, K-Ar age determinations with large analytical uncertainty. The southern center, the Little Black Peak center, consists of a main scoria cone, two small satellite scoria mounds, and associated small lava flows. The northern center, Hidden Cone, formed in two eruptive episodes. The first included formation of the main scoria cone and was accompanied by intrusion of multiple lobes of aa lava erupted from radial dikes. The second episode consisted of formation of a scoria-fall event that draped the older cone and deposited thin tephra northeast of the cone. The latter event may, using multiple lines of evidence, be of late Pleistocene or Holocene age. *Recent work by the U.S. Geological Survey shows that a second northwestern lava flow may have erupted from the Hidden Cone center. This interpretation is being evaluated through further field studies at the center.*

4. Alternative Views by the US Geological Survey; The Lathrop Wells Volcanic Center. Turrin et al. (1991) estimated the age of the Lathrop Wells volcanic center using paleomagnetic and new $^{40}Ar/^{39}Ar$ age determinations. They argue that there have been only two eruptive events at the center and that ages of those events are indistinguishable analytically. The preferred ages of these events are, using a variance weighted mean, 136 ± 8 and 141 ± 9. Turrin and Champion (1991) suggest that the two identified units at the center have mean field magnetic directions that differ at the P = 0.0002 significance level. They note that the time interval between two directions of magnetization cannot be established from field magnetic

data. However, they argue by analogy to paleomagnetic studies for Sunset Crater, Arizona, that the age difference between the two eruptive events is about 100 yr. Turrin and Champion (1991) correlate primary and reworked cinders located 3 to 4 km northwest of Lathrop Wells to the volcanic center. They argue that uranium trend ages on Quaternary stratigraphic units indicate the cinders were deposited between 240 and 145 ka. Finally, Turrin and Champion (1991) argue that the age constraints of Wells et al. (1990) using geomorphic and soil criteria are miscalibrated. *The same constraints described above apply to the radiometric age determinations and the paleomagnetic data. Additionally, the stratigraphic relations and age of the Quaternary alluvial units associated with the basaltic ash have not been sufficiently well established to constrain the ages of the volcanic events of the Lathrop Wells center.*

5. Volcanism Probability Studies; State of Nevada. Ho (1990, 1991) examined the applicability of the simple Poisson model for eruption forecasting. He argued that the Poisson model may not be applicable to all volcanoes and proposed two alternative distribution models. The first is a negative binomial distribution where the Poisson process is expanded to include a gamma-mixing distribution on λ. The second is for an NHPP with a Weibull intensity. An advantage of this model is it can accommodate nonsteady-state eruptive activity. Ho examined published eruption data for a range of volcanoes using his suggested nonhomogeneous Poisson models.

Ho (1991) undertook time-trend analysis of past patterns of basaltic volcanism in the YMR. He argued that a simple Poisson model may not be applicable to volcanism in the region if there has been variability in activity through time (waning or waxing). Further, he argued that a simple Poisson model is hard to justify for the limited data set (small number of Pliocene and Quaternary volcanic events) in the YMR.

Ho (1991) estimated the instantaneous recurrence rate of volcanic events using an NHPP with Weibull intensity. He based the time-trend analysis on a combination of basalt episodes and age cycles. The observational intervals ranged from 12 to 1.6 Ma and he varied assumptions of the nature and chronology of volcanic events. Ho estimated midpoints of the time interval for the next eruption which ranged from 4.2 to 0.6 Ma. For all but one estimation, he noted a slight developing trend (β values of 1.09 to 2.55). Ho concluded on this basis that a simple Poisson model could underestimate the risk of volcanism for the Yucca Mountain site. *The midpoint intervals of Ho (1991) yielded values that are consistent or smaller (lower probability) than the recurrence rate calculations of Crowe et al. (1982). There is not a significant difference in the calculations. The β values of >1 were obtained by assuming polygenetic volcanic activity at all the centers of Crater Flat, an unverified assumption, and by discarding the 3.7 Ma volcanic events (see Chapter 7). This usage is inconsistent with the definition of volcanic events used in Chapter 7. Polygenetic activity is based on the argument that once an event occurs at a volcanic center there is an increased probability that another event will occur at the same center. So defined, these events are not independent and are used incorrectly in the distribution model of Ho (1991). An alternative and more physically meaningful way to structure the probability model is to define the formation of a volcanic center as an individual event and treat polygenetic events as a geometric complexity of a repository disrupting event.*

Ho (1991) suggested that volcanic risk for the Yucca Mountain site should be expressed as a percentage of the required isolation time of high-level radioactive waste. On the basis of this recommendation, he estimated a *risk* of volcanism to be about 5% for the specified 10^4-yr isolation period. *Volcanic risk can be expressed as an annual or interval-specified value; either usage is correct and widely used in the risk assessment literature. Ho (1991) did not calculate volcanic risk. He calculated a 5% chance of a future volcanic eruption in an unspecified area of the YMR during the next 10,000 yr. Stated simply, he calculated the probability of recurrence, only one variable in the conditional*

probability model of future disruption of the Yucca Mountain site. Estimating the risk of volcanism requires calculation of the recurrence probability, the probability of repository disruption, and the probability of releases exceeding the regulatory requirements for disposal of high-level radioactive waste.

Ho et al. (1991) examined the probability of disruption of the Yucca Mountain site by future volcanic eruptions. They noted the probability procedure outlined in Crowe et al. (1982) was a more formal approach to probability modeling than attempted previously. However, they argued that the existing data base (for the YMR) is inadequate to constrain the recurrence rate of volcanic events.

Ho et al. (1991) reviewed past methods used by Crowe et al. (1982) to calculate λ, the recurrence rate of volcanic events. They argued that none of the methods are satisfactory and proposed alternative methods for estimation. They used maximum likelihood estimates and let X denote the number of volcanic events from an assumed Poisson process. They estimated the successive number of eruptions from consecutive intervals of length constrained to the Quaternary period. The estimator became simply the total number of eruptions divided by the observation period (Ho et al. 1991). They adopted the definition of repose time used by Klein (1982) which measures events from repose time to the onset of the next eruption. Ho et al. (1991) noted that the repose time is difficult to define and redefined this variable to represent the time between the onset of eruptions for a specified observation period. Ho et al. (1991) argued that past volcanic probability are invalid because the volume of eroded volcanic deposits was not calculated. *The volume of eroded deposits was considered in estimations of magma volumes used in past probability estimations*

Ho et al. (1991) argued that estimation of E the number of volcanic events, has not been properly determined. *They defined E to include polygenetic events, not the formation of a new volcanic center (see Chapter 7). Their definition does not maintain the event independence required for the conditional probability model. Moreover, E can be determined if it is defined as the rate of formation of volcanic events where a volcanic event is the formation of a new volcanic center.*

Ho et al. (1991) described the geology of Black Cone and argued that the complexity of the center invalidates previous models of the total number of eruptions. *The main basis of this statement is a semantics disagreement in the definition of a volcanic event. Ho et al. (1991) treated each vent in a scoria-complex as an event.* Ho et al. (1991) made the valid observation that it is difficult to distinguish ages of volcanic events using the K-Ar method for cones within clusters of centers. They conclude by calculating recurrence rates using their equations (2) and (4) and suggest that Crowe et al. (1982) underestimate the risk of volcanism. *Their estimated values of the recurrence rate are included in the probability bounds established by Crowe et al. (1982).*

6. Study Plan 8.3.1.8.1.1 Probability of Magmatic Disruption of the Repository. The study plan was completed and submitted to the Nuclear Regulatory Commission in 1991. This Study Plan is divided into four activities. The first activity, 8.3.1.8.1.1.1, is the Location and Timing of Volcanic Events. This activity involves collating geologic maps of the location of volcanic centers, with accompanying tables listing and referencing information on the geochronology of volcanic events, the eruptive history of the center, and the volume of major volcanic deposits. The second activity is 8.3.1.8.1.1.2, Evaluation of the Structural Controls of Basaltic Volcanic Activity. This activity attempts to establish the probability that, given a future volcanic event, the event would disrupt the repository, the controlled area, or the YMR. The locations of sites of volcanic activity are controlled generally by existing structure or the local stress field. This activity seeks to identify those controls and determine how the controls would affect the disruption parameter of the probability calculation. The third activity is 8.3.1.8.1.1.3, Presence of Magma Bodies in

the Vicinity of the Site. This involves an assessment of whether there is evidence of recent changes in processes controlling volcanism that could modify future patterns of volcanic activity. The major concern is with the possible existence of magma in the crust beneath the YMR. The final activity is 8.3.1.8.1.1.4, Revised Probability Calculations and Assessment. This activity will attempt to establish numerically the probability of future magmatic disruption of the repository, the controlled area, and the YMR. It is concerned primarily with the determination of whether the Yucca Mountain site could be disqualified solely on the basis of the likelihood of future magmatic activity. *Study Plan 8.3.1.8.1.1, Probability of Magmatic Disruption of the Repository, was revised using review comments by the Nuclear Regulatory Commission. They correctly pointed out that the Study Plan only considers the probability of eruptive events and should be expanded to include discussion of the probability of both the eruption and intrusion events on a potential repository. These changes were made to the Study Plan and have been incorporated in this volcanism status report.*

E. Publications in 1992

1. Resumption of Surface Disturbing Activities for Site Characterization Studies; Status of Field and Geochronology Studies of the Lathrop Wells Volcanic Center. Crowe et al. (1992a) described the status of field and geochronology studies of the Lathrop Wells volcanic center current to December of 1991. They summarized the past controversies concerning the age and eruptive sequence of the center. They emphasized the importance of increasing the confidence in interpretations of chronology data by using combined isotopic, radiogenic, and age-correlated methods. They noted that the assumptions, strengths, and weaknesses of each chronology method need to be assessed to facilitate an impartial evaluation of geochronology results. The stratigraphy of the Lathrop Wells volcanic center was revised using the results of exposure of stratigraphic contracts through trenching. This trenching was initialed in 1991 following several years of no surface disturbing activity because the state of Nevada did not issue required permits to the DOE.

The volcanic units of the Lathrop Wells center were divided into three chronostratigraphic units (Crowe et al. 1992a). These chronostratigraphic units are separated by soil-bounded unconformities. The degree of horizon development in the soils requires the time between eruptions to far exceed the inferred duration of basaltic eruptive events and the longevity of basalt magma in the shallow crust. This is the basis for the classification of the volcano as a polygenetic center.

The oldest unit of the Lathrop Wells center, chronostratigraphic unit I, consists of three lavas, with minor cone scoria exposed discontinuously beneath younger deposits. These include a buried lava and scoria deposits on the north side of the cone as well as three sets of lava flows and cone scoria exposed on the south and southwest edge of the center. Trenching of a buried lava flow northeast of the main cone revealed that it underlies primary and reworked surge and scoria-fall deposits that contain a soil with distinct horizon development. This sequence in turn underlies younger lava flows. *Subsequent trenching studies completed after publication of this report showed that the buried flow is not separated from the overlying lava flow by a buried soil. The described soil infiltrates but does not underlie the youngest lava flow of this flow sequence. The unit contact is marked by an unconformity with different degrees of pedogenic alteration deposits above and below the contact.*

Chronostratigraphic unit II consists of the major volume of the deposits of the volcanic center including the main cone, a northwest-trending fissure formed at the base of the cone, two sequences of blocky aa lavas north and northeast of the main cone, and two fissure systems associated with the lava flows.

Chronostratigraphic unit III consists of tephra-fall deposits with interbedded soil with horizon development exposed in quarry walls at the south flank of the main cone. This includes the deposits described by Wells et al. (1990). *There is continuing controversy concerning the origin of the tephra-fall deposits. A number of workers maintain the tephra deposits are of reworked origin and do not record multiple volcanic events. New geochemistry studies described in Chapter 2 have demonstrated with increased confidence that the tephra deposits cannot be reworked. The same chronostratigraphic units with minor modifications are used in this volcanism status report. However, the chronostratigraphic unit descriptors (I, II, III, and IV) are reversed (I oldest; IV youngest) to be consistent with established conventions in Quaternary geologic studies.*

A range of geochronology methods has been used to attempt to establish the age of the Lathrop Wells volcanic center (Crowe et al. 1992a). The methods include the conventional K-Ar and $^{40}Ar/^{39}Ar$ methods, the U-Th disequilibrium method using solid source mass spectrometry, surface exposure ages using cosmogenic ^{3}He, and TL. Additional age determinations for the center have been reported by other workers using the ^{36}Cl method.

The results of K-Ar and $^{40}Ar/^{39}Ar$ methods have been described by Turrin and Champion (1991) and Turrin et al. (1991). They summarized previously published K-Ar and $^{40}Ar/^{39}Ar$ age determinations. The strengths of these results are that they represent the best established and most carefully tested chronology methods used a the Lathrop Wells volcanic center. Additionally, the reported ages are consistent with the preliminary results obtained using the U-Th disequilibrium method. The weaknesses of the methods are several. First, both whole rock and laser fusion ages extract potassium and argon from an assemblage of minerals. This requires the assumption that the distribution of potassium and argon is uniform in the mineral and glass phases. Second, the spread in reported ages is too large to be explained as analytical error. There are differences in the age distributions of the K-Ar and $^{40}Ar/^{39}Ar$ data sets. Averaging of the data sets may not be appropriate. Finally, and perhaps most important, the distribution of the age determinations is nonGaussian. The data are skewed toward older ages.

The results of uranium-series dating of samples of the Lathrop Wells volcanic center were described by Crowe et al. (1992a). They obtained an isochron age of 150 ± 40 ka for a lava unit of chronostratigraphic unit II. The precision of the isochron is limited by the small degree of Th/U fractionation for the separated phases. There is no reason to discount the age, but it is regarded as preliminary and more age determinations are in progress. *(A revised U-Th disequilibrium age using new mineral separates with a greater spread in the U/Th ratio are 50 ka).*

The surface exposure ages of chronostratigraphic units of the Lathrop Wells center have been estimated by measuring the accumulation of cosmogenic ^{3}He (Crowe et al. 1992a). Ages of 23 to 48 ka have been obtained for chronostratigraphic unit III. The variability in the ages of this unit may result from differences in the surface exposure history of the samples, particularly for samples collected from the summit of the main cone. A cosmogenic exposure age of 64 ± 6 ka was obtained for chronostratigraphic unit III. Concerns with the cosmogenic ^{3}He method are the uncertainty of the surface exposure history of samples and the calibration of ^{3}He production rates.

TL age estimates have been obtained for the chronostratigraphic units of the center (Crowe et al. 1992a). Samples from soil units interbedded with tephra units of chronostratigraphic unit I yielded TL ages of about 4 to 9 ka. A sample was collected from sediments below a lava flow lobe of chronostratigraphic unit II. It yielded a TL age of 24.5 ± 2.5 ka. *This age remains inconsistent with the cosmogenic helium and K-Ar age determinations.*

Soil and geomorphic studies of the Lathrop Wells center have been aided by trenching of stratigraphic contacts allowing observation of horizon development in soils. Weakly developed horizons in soils of the center most closely resemble late Pleistocene and Holocene soils in the Silver Lake and Cima areas of California (Crowe et al. 1992a). The studied soils on many of the volcanic units of the Lathrop Wells center probably cannot be older than 20 ka and almost certainly cannot be older than 50 ka. The primary uncertainty in these assignments is the variability in rates of development of pedogenic processes at the correlated sites. *An important observation made from the trenching studies is that basaltic scoria deposits form geomorphically unstable surfaces under most conditions. Surfaces developed on scoria are too transitory to preserve soils that provide a complete record of pedogenic processes. The degree of soil development on scoria deposits can only be used for constraints on the minimum age of the deposits.*

New paleomagnetic data have been obtained for previously unstudied volcanic units of the center (Crowe et al. 1992a). These data yield results that are generally consistent with the averaged field magnetic directions reported by Champion (1991) and Turrin et al. (1991). However, several cautions accompany the interpretation of the paleomagnetic data. First, the field magnetic directions coincide with the average Quaternary field direction. This reduces the utility of discriminating eruptive events using field magnetization directions. Second, the angular difference between paleomagnetic data sets can at best constrain the ***minimum*** age difference between the sampled rocks, not the ***maximum*** difference. Third, the reproducibility of our studies of field magnetic directions are more variable than the results reported by Champion (1991) because of a combination of lightning-induced isothermal remanent magnetization and the quality of the preserved outcrops.

2. Recurrence Models of Volcanic Events; Definition of the Tripartite Probability, Application of a Simple Poisson Model, Revised Values of the Recurrence of Volcanic Events. Crowe et al. (1992b) defined the conditional probability used to evaluate the risk of volcanism and the geologic assumptions required for a probabilistic model of magmatic disruption of a potential repository at Yucca Mountain. This probability combined with the likelihood of release of radionuclides to the accessible environment during the 10,000-yr isolation period (Pr_{dr}) is modeled as:

$$Pr_{dr} = Pr(E3 \text{ given } E2,E1)Pr(E2 \text{ given } E1)Pr(E1)$$

where E1 denotes the recurrence rate of volcanic events in the YMR, E2 denotes the probability that a future magmatic event intersects the repository, and E3 denotes the probability that magmatic disruption of the repository leads to eruptive releases of radionuclides to the accessible environment. A volcanic event is defined as a spatially and temporally distinct episode of surface basaltic volcanism. There may be multiple sites or eruptive vents on the surface but the event is defined from the perspective of a buried repository. It represents an incursion of magma into the repository followed or not followed by surface eruption. *An item of continuing confusion in the published literature on probabilistic risk assessment for the Yucca Mountain site is the definition of a volcanic event. The preferred usage of a volcanic event is the formation of new volcanic center. This event has a finite probability of intersecting the potential repository site. Separate vents at a volcanic center are not necessarily recognized as separate volcanic events, nor are polygenetic events. This is discussed in Chapter 7).*

The assumptions required to estimate Pr(E1) include (Crowe et al. 1992b):

1. The past record of basaltic volcanic activity in the region is judged to provide the most reliable indicator of the recurrence rate of future volcanic events.

2. Interpretations of the geologic record are judged to be reliable in forecasting future events. If there are discrepancies or differences of opinion over the geologic record, these can be resolved by developing alternative models of the recurrence rate.
3. There have not been recent (last few hundred thousand years) changes in the rate of operation of processes which control the generation, ascent, and eruption of basalt magma in the YMR.

There is a clear and nonreducible element of uncertainty introduced in application of a probabilistic approach using the limited data set of past volcanic events in the YMR. The current level or anticipated level of knowledge of the operation of magmatic processes precludes development of a fully deterministic approach to predicting volcanic events. In fact, the new science of chaos requires scientists to rethink fundamental ideas about the inherent predictability of physical processes. Rather than debate this issue, however, Crowe et al. (1992b) evaluated three questions concerning recurrence of volcanic events. What are reasonable time-distribution models? Can the models be structured to not underestimate volcanic risk? Can the uncertainty of a small data set be bounded by comparison with analog studies of other volcanic fields?

Crowe et al. (1992b) reviewed time-distribution models for volcanism ranging from simple Poisson, nonhomogeneous Poisson, to deterministic chaotic. They concluded that a simple Poisson model represents the most direct approach to probabilistic assessments using a small data set. It does not introduce unsupported complexity that may not be meaningful physically and it can be tested against physical models of volcanic processes (waning, waxing, steady state). The types of errors associated with a Poisson model can be assessed and bounded. *Ho (1991) argued that a Poisson model is not appropriate for a limited data set. A corollary of that argument, however, is that any distribution model is hard to justify using a limited data set. The absence of data precludes evaluating the data set using standard tests for goodness of fit. Ho (1991) also rejected arguments by Crowe and Perry (1989) showing that a plot of cumulative magma volume versus time provides a method for testing time trends in volcanic activity. Ho argued correctly that evaluation of magma volume versus time is simply a modified form (similar to a sequenced or triggered process) of a simple Poisson process. He did not recognize, however, that an assessment of erupted volumes of magma through time provides a means of testing assumptions of steady-state eruptive behavior.*

Calculations of the recurrence rate of volcanic events (E1) using a simple Poisson model were listed by Crowe et al. (1992b). They summarized assumptions and listed Pliocene and Quaternary volcanic events in the YMR. A potentially new Pliocene event was identified from unpublished work by the U.S. Geological Survey and verified from our field observations. The event is the basalt of Thirsty Mesa, a relatively large volume basaltic center east of the Sleeping Butte volcanic centers. This lava mesa was estimated to be of Pliocene age and it was included in subsets of the recurrence calculations. Recurrence rate estimations range from 10^{-5} to 10^{-7} events yr^{-1}. The geometric mean of the recurrence rates is about 4 x 10^{-6} events yr^{-1} or equivalent to the formation of a new volcanic center every 250 ka. Simple evaluation of the physical plausibility of recurrence rates allows rejection of unrealistic high or low rates. The recurrence rates after screening cluster in the range of 1 to 6 x 10^{-6} events yr^{-1} (Crowe et al. 1992b). After over a decade of study, there have been no significant changes in the recurrence rate calculations of Crowe et al. (1982). Moreover, calculations by other workers using different approaches (Ho 1991; Ho et al. 1991) yielded results that fall within this range.

The uncertainty in the recurrence models of volcanic events can be bounded by applying simple Poisson models to the Quaternary record of volcanism in the Cima and Lunar Crater volcanic fields. By analogy, a recurrence rate of 10^{-5} yr^{-1} (an event recurrence time of 100 ka) can be regarded as a firm ***upper*** bound to rates of volcanic activity for the YMR.

3. Monte Carlo Technique for Estimation of the Probability of Disruption of a Repository by Propagation of Volcanic Dikes. Sheridan (1992) developed a method for determining a probability function for different spatial models of the structural controls of volcanic activity in the Yucca Mountain area. He used Monte Carlo simulation to plot the trace of volcanic dikes. Input parameters for the simulation are the geometry of the volcanic field and the geometry of the dikes. He developed a computer program that counts the number of intersections of the repository during simulations. The geometry of the volcanic field is constrained by alternative hypothesis of the structural controls of the volcanic field and the distribution of vents in the field. Three models were used. The first is based on the record of basaltic volcanism in the region. The volcanic field is oriented northwest; dikes within the field are oriented northeast. The second model assumes the volcanic field and the dikes are controlled by the shallow stress field and both are oriented northeast. Model three assumes that a center of renewed volcanism will be located at Lathrop Wells; it was modeled with a narrow aspect ratio and was oriented toward the Yucca Mountain site. Sheridan rated model three as the least likely, model two as more likely than model three, and model one as the most likely.

Results of the simulation modeling show that the frequency of repository intersection is controlled by the field geometry and the standard deviation of the field size. The frequency increases as a linear function for low values of the standard deviation of the field size but reaches a peak and declines slightly. This is because the spacing between dikes increases at a faster rate than the increases in the size of the field (Sheridan 1992). The position of the slope change in the frequency varies somewhat with the different field models. Maximum probability values for models one through three are, respectively, 6×10^{-3}, 1.4×10^{-2}, and 1.7×10^{-2}. If the distribution of volcanic centers in Crater Flat is used to define the standard deviation, the modeled frequency of intersections is 1.1×10^{-3}, 1.0×10^{-2}, and 5.3×10^{-3} for models one, two, and three, respectively.

4. Teleseismic Tomography of the YMR; Applications to Volcanism Studies. Evans and Smith (1992) presented the results of application of teleseismic tomographic studies of compressional phases to delineate subsurface magma chambers. They observed an upper-mantle, high-velocity anomaly beneath the Miocene Silent Canyon caldera that is inferred to represent the residuum of voluminous Miocene silicic volcanism. A second observed feature is a large low-velocity anomaly south and east of Yucca Mountain and centered southeast of Yucca Mountain. Evans and Smith (1992) suggest that the low-velocity anomaly may be the source of Quaternary basalt in the Crater Flat area, and the anomaly may extend northeast to the area of St. George, Utah, parallel to the trace of hot-spot vectors of the North America plate. They infer, because of the association with young basaltic volcanism, that the anomaly is produced by partial-melt but acknowledge that other interpretations are possible. Dueker and Humphreys (1991) suggest the anomaly may record the remnants of the poorly absorbed slab of the Farallon plate. Evans and Smith (1992) suggest the partial-melt model can be tested by additional experiments using shear-wave velocity and compressional-wave attenuation teleseismic tomography. *One inconsistency with the Evans and Smith (1992) interpretation of the teleseismic data is that the location of the center of anomaly in an area that has been amagmatic throughout the Mesozoic and Cenozoic (Farmer et al. 1989; Jones et al. 1992).*

5. Geochemical Evidence of Waning Magmatism; Polygenetic Volcanism. Perry and Crowe (1992) described the temporal and geochemical evolution of basaltic magmatism in the Crater Flat area. Additionally, they examined geochemical and isotopic variation among the basalt units of the Lathrop Wells volcanic center to test models of volcanic activity (monogenetic versus polygenetic). Systematic differences in phenocryst assemblages, trace-element concentrations and isotopic compositions of strontium and neodymium indicate that magma chambers of the youngest two episodes of basaltic magmatism in Crater Flat were at deeper crustal levels than the oldest episode. The primary evidence for this conclusion is

the absence of plagioclase as a near-liquidus phase in the younger basalt episode requiring crystallization below 8 kb (Perry and Crowe 1992). This interpretation is consistent with the strontium and scandium contents of the basalt units, reliable indicators of the importance of fractionation of plagioclase and clinopyroxene.

The evolution of the postshield alkali basalt of Mauna Kea, Hawaii, shows striking similarities to the patterns of evolution of the basalt of Crater Flat. In both cases, declining eruptive volumes through time were accompanied by a change from more primitive porphyritic basalt to evolved, aphyric basalt (hawaiite). Again, in both cases, lower scandium contents and higher strontium contents in the younger basalt provide a distinctive signature of the progression to deeper crustal magma chambers. Frey et al. (1990) attributed the changes at Mauna Kea to a waning magma flux that could no longer maintain shallow magma chambers. Perry and Crowe (1992) apply the comparisons to the Mauna Kea system cautiously because of the vastly higher magma fluxes for the Hawaiian system. Moreover, the changes in the Crater Flat field are recorded at spatially isolated centers, not a single shield complex, as is the case for the Mauna Kea volcano.

Geochemical data for eruptive units of the Lathrop Wells volcanic center can provide important tests of the monogenetic versus polygenetic models of volcanism. A monogenetic origin of the center requires the units to be related by fractionation process to a single magma batch. The polygenetic model suggests the center was formed from temporally discrete magma batches.

Trace-element variations of the Lathrop Wells center show that the eruptive units identified from detailed field studies are distinct geochemically (Perry and Crowe 1992). They used process identification diagrams to test the origin of the trace-element variations. A plot of lanthanum versus La/Sm shows that eruptive units at Lathrop Wells have a range of La/Sm ratios, even at similar lanthanum contents. An increase in La/Sm with increasing lanthanum content could be produced by fractionation of clinopyroxene. This would require unit Ql1d, part of the oldest chronostratigraphic unit at the center to represent the least evolved magma. However, a plot of strontium versus scandium, shows that unit Ql1d is the most evolved magma (with respect to fractionation of clinopyroxene). This inconsistency rules out derivation of the eruptive units from a single magma that fractionated at shallow levels. Sequential variation in units from the oldest to the youngest at the Lathrop Wells center in La/Sm contents is consistent with decreasing degrees of partial melting. This is consistent with a waning of processes of melt production with time through the evolution of the center.

Neodymium and strontium isotopic data indicate that unit Ql1d is distinct from the rest of the analyzed eruptive units. While the isotopic variations could be produced in a single magma batch undergoing a complex evolution, the trace-element variations make it more likely that the isotopic differences record evolutionary paths of distinct magma batches.

More work is needed to assess the geochemical variations of the Lathrop Wells center. Current data, however, appear to discriminate consistently against a simple monogenetic origin of the volcanic center (see Chapter 4) .

6. Revised Assessments of the Consequences of Magmatic Disruption of the Potential Repository, Perspectives from Modeling of Intrusion and Eruption Processes. Valentine et al. (1992) examined the physical processes and effects of magmatism in the YMR. Volcanic activity can affect the isolation system of a repository by two potential processes. First, disruption of a repository could occur by ascending magma followed by surface dispersal of a portion of the radioactive inventory from subsequent eruptions. Second, subsurface effects of hydrothermal processes and altered hydrology can be induced by

intrusion of magma through or near a repository. The subsurface effects do not necessarily need to be coupled with surface eruptions. Initial calculations of the volume of waste that might be erupted during a basalt eruption indicate the regulatory release limits might be exceeded. However, these calculations are based on the conservative assumption that all waste that comes into contact with magma is carried to the surface and dispersed.

Valentine et al. (1992) summarized continuing field studies of the characteristics of shallow intrusions in the Paiute Ridge area, an analog site for shallow volcanic intrusions. These studies are concerned with identifying the potential for dispersal of waste by basalt intrusions and their effects on a waste isolation system. Observations at the Paiute Ridge area show that intrusive sills occurred only on the floor of a graben. Dikes locally intrude the horst blocks. Most dikes are coplanar with normal faults. Small radial dikes are present in country rock associated with probable conduit plugs. Some dikes locally fed sills that differentiated to form concentrically-zoned pods with syenite interiors.

The host rocks (primary and reworked Paintbrush Tuff) in the Paiute Ridge area were welded at the contact with the basalt intrusions (Valentine et al. 1992). Welding effects decrease to zero at a distance of 1 to 5 m from the dike margins. Welding effects can be used to constrain modeling of the thermal and hydrothermal processes that may affect a repository intruded by basalt magma. Moreover, welding alters the hydrologic properties of rock so that groundwater flow would be altered from a preintrusion state. The hydrologic properties of the dike itself may produce changes in groundwater flow, although those changes would be most pronounced in the saturated zone, not the unsaturated zone.

Valentine et al. (1992) presented preliminary results of two-dimensional modeling of emplacement of a basalt sill in country rock. The sill chamber is formed of two parts, a stable bottom half (cooler, denser on the bottom) and an unstable upper part (cooler, denser on top). The magma cools along a thermal boundary layer. As the boundary layer thickens, the roof and sidewalls become unstable and form downwelling plumes. The bottom layer grows by simple thermal diffusion. The plumes can carry cool fluid downward until they reach the lower bottom boundary layer.

Valentine et al. (1992) also carried out two-phase flow modeling of basaltic pyroclastic eruptions. They are developing quantitative methods for mapping pyroclastic facies of small basaltic centers and used these data in combination with two-phase hydrodynamic simulations to estimate eruption conditions of ancient volcanic centers.

7. Structural Controls of Volcanic Activity. Crowe et al. (1992c) reviewed progress in volcanism studies during 1990 and 1991. They summarized information presented in Crowe and Perry (1991), Crowe et al. (1992a,b), Perry and Crowe (1992), and Valentine et al. (1992). New information was developed on the structural controls of volcanic activity. They noted that the major limitation of this calculation (Pr[E2]) is the same as the limitation for the estimations of volcanic recurrence models; there is only a small number of basalt centers in the region. This makes it virtually impossible to prove or disprove structural models. They emphasized attempting to define or bound the range of values using multiple alternative approaches in estimating Pr(E2).

Crowe et al. (1992c) summarized the different models for the structural controls of volcanic activity. These include the random models of Crowe et al. (1982), the CFVZ model of Crowe and Perry (1989), the AMRV model of Smith et al. (1990), the volcanic chain model of Smith et al. (1990), and the northeast-trending structural zone of Naumann et al. (1991). A table of estimated values of E1 was developed. The values range from 1.3×10^{-3} (dimensionless ratio) to 3.9×10^{-3} for the northeast-trending structural zone. An estimated median value for E2 using the compiled data table is 2.8×10^{-3}.

8. Estimations of Volcanic Disruption, Continued Probability Studies by the State of Nevada. Ho (1992) published another review of probability studies for the Yucca Mountain site. He summarized background information on the national policy for disposal of high-level waste and the importance of estimating the potential risk of volcanism for the Yucca Mountain site. He described the volcanic history of the YMR, mostly referencing work by Crowe and Perry (1989), Crowe (1990), and Smith et al. (1990). Ho (1992) discussed the probability model of volcanism used by Crowe et al. (1982) and described the assumptions of the simple Poisson model. He reiterated the point made in a previous article (Ho et al. 1991) that a Poisson model does not allow for waning or waxing trends in volcanism through time. He criticized the ". . . statistical work of Crowe et al. (1982), and Crowe and Perry (1989) as seriously flawed. Specifically, the probabilistic results are based on idealized model assumptions, a premature database, and inadequate estimates of the required parameters, which lead to questionable conclusions about (the) volcanic stability of the proposed Yucca Mountain repository." (p. 351)

Ho (1992) argued that an HPP or simple Poisson process, is based on the assumption that λ is independent in time t and the repose times between eruptions are independent exponential variables with mean $= 1/\lambda$. He proposed using a nonhomogeneous Poisson process (NHPP) where the constant λ is a function of $(\lambda)t$ and is called the nonhomogeneous intensity function. Ho (1992) suggested using the rate function, μt, in a form that follows a Weibull distribution *WEI,* where

$$\mu t = t/\theta^{\beta}$$

The parameter μ increases as a function of t if β is >1 and decreases with t if β is <1. For the case of $\beta =$ 1, the form of the distribution is the same as the exponential expression of the HPP. Ho (1992) recognized that volcanic eruptions may be caused by a range of physical processes resulting in random effects on the time-distribution of eruptive events. He suggested estimating the instantaneous recurrence rate ($\lambda[t\,]$) at time t using a NHPP with Weibull intensity but using a HPP to estimate future eruptions, treating future events as a stochastic process. *This form of the probability distribution means that the approach used by Ho (1992) differs from the simple Poisson model only if* $\beta \neq 1$.

Ho (1992) examined the recurrence rate for basaltic volcanic events in the YMR. He assigned one volcanic event to each major volcanic center and assumed for lack of contradictory data that each center is about the same age. Ho (1992) identified four volcanic events at 3.7 Ma, one at 2.8 Ma, five at 1.2 Ma, two at .28 Ma, and one at 0.01 Ma. *The number of volcanic events and age assignments for the vents are in agreement generally with other probability studies with two significant differences. Ho (1992) chose the youngest possible age for the Lathrop Wells volcanic center, an age of 10 ka (p. 348). A more realistic age assignment would be between 45 and 120 ka since only a very small volume of the center could be as young as 10 ka. Further, his assigned ages for the Sleeping Butte center are probably too young using the geochronology results described in Chapter 2.*

Ho (1992) calculated an instantaneous recurrence rate of 5.0×10^{-6} yr^{-1} for the Pliocene and Quaternary volcanic events (6 Ma period) with $\beta = 2.29$ and an instantaneous recurrence rate of 5.5×10^{-6} yr^{-1} and $\beta = 1.09$ for Quaternary volcanism. *The calculated rates are roughly similar to rates calculated by other workers. They are equivalent, assuming an exponential distribution model, to 30 eruptive events in the Pliocene (there were 14 to 17 events) and 8.8 events in the Quaternary (there were 7 events). Why the discrepancy for the Pliocene events? The answer is in how the problem was constructed. The Pliocene calculation was for a 6-Ma period. There were no volcanic events during the first 2.3 Ma of this period. The length of the interval of inactivity forces the majority of the volcanic events into the latter*

half of the period and produces a calculation of $\beta = 2.29$ *(see discussion of nonhomogeneous Poisson models in Chapter 7). A more realistic calculation would be to chose an observation period that is equal to the duration of the activity of the YPB episode. This difference in probability estimates illustrates two things. First, probability estimations must be constructed carefully to be physically meaningful, particularly if an instantaneous rate is calculated (Crowe and Perry 1989). Second, the* $\beta = 1.09$ *for the Quaternary period is close to an exponential fit and suggests that the simple Poisson model would provide an adequate fit to the data.*

Ho (1992) argues that the estimated recurrence rates are point estimates and do not assess uncertainty. He calculated 90% confidence intervals for the Quaternary calculation that give interval bounds of 1.85×10^{-6} yr^{-1} to 1.26×10^{-5} yr^{-1}. He uses these interval bounds in his calculations of the probability of volcanic disruption of the Yucca Mountain site.

Ho (1992) examined the probability that any single volcanic event is disruptive, or intersects the potential repository. He let **p** represent the probability that an eruptive event is disruptive. Assuming the event follows a HPP, the number of disruptive events Xt_o in $[0,t_O]$ has a constant rate of $f\mathbf{p}t_O$ (p.356). He argued that the probability of at least one disruptive event represents "risk". *In reality, Ho (1992) examined the probability of repository disruption, not* ***risk*** *which requires an assessment of both the probability and consequences of repository disruption. However, he carefully defined his use of the term risk so there is no confusion. He calculated the probability of repository disruption.*

Ho (1992) defined risk as

$$\text{Risk} = 1 - \exp\{ - \lambda t \, \mathbf{p} t_O\}$$

This is a modified form of the same equation used by Crowe et al. (1982). Ho (1992) used a Bayesian approach that allows a prior distribution of **p** and assumes the instantaneous recurrence rate is constant. His "risk" model becomes

$$\text{Risk} = 1 - \int_p \exp\{ -\lambda t \, pto\} \pi p \; dp$$

Ho (1992) discussed at length the determination of the prior distribution for **p**. He attempted to choose the prior distribution using structural models of volcanic centers in the YMR. Ho (1992) uses the structural models of Smith et al. (1990) where the high-risk zones of volcanism are identified by assigning northeast-trending structural zones to the location of past volcanic centers. *The concerns with this structural model were described in the discussion of the work by Smith et al. (1990).* Ho (1992) uses the half-length of the chain model for the Lathrop Wells center to obtain $p = a/A = 8/75 = 0.11$, where a is the area of the repository and A is the half-length area of the chain for the Lathrop Wells center. He chose this value as the upper limit for **p**. He applied the 90% confidence bounds to the instantaneous rate and calculated the probability of repository disruption as 1.0×10^{-7} to 6.7×10^{-7} yr^{-1}.

These are the first published values for the probability of repository disruption that exceed the bounds published in Crowe et al. (1982). It is instructive to try to understand why the values differ and the physical meaning of the calculations of Ho (1992). First, a major paradox of volcanism studies is provided by the number of volcanic events. There are only a small number of volcanic events that have affected the YMR in the Quaternary (7–8 volcanic events dependent on whether the Little Cones center is counted as two events). The small number of events means there have been few past events and by inference are likely to be few future events. However, a corollary of the inference is that while the risk

(used as a relative term) is small the uncertainty of calculating the risk is relatively large (by virtue of the small sample size that prohibits statistical robustness of calculations). Reversing the logic of this argument, if there were a larger sample size (more volcanic events) the uncertainty of the calculations would decrease but ***the risk would increase.*** *There are probably few people who would argue that increased risk would be preferred to increased uncertainty.*

We are faced, therefore, with assessing the question of the risk of future volcanism knowing that the uncertainty of the answer will be by definition large. Crowe et al. (1992b) constructed arguments, using observations of the physical processes of volcanism, that there are bounds to the recurrence rate that can be assigned to volcanic events in the YMR. Those bounds are provided by the number or recurrence rates of volcanic events in large, very active volcanic fields of the Basin and Range province. Ho (1992), using straightforward statistical arguments, assigned upper or bounding intervals to λ*, the recurrence rate, using 90% confidence limits. However, he applied these confidence limits to* ***worse case bounds not midpoint estimates.*** *As a result, the values he used exceed recurrence rates for the most active basaltic fields in the Basin and Range province.*

Second, Ho (1992) held the recurrence rate fixed and assigned it to an area of 75 km^2 *to determine the probability of repository disruption. This means that the value he determined for* λ *was estimated for an area exceeding 2000* km^2 *but assigned without modification to an area of only 75* km^2*. This would be realistic if there was some reasonable geologic explanation why the next volcanic eruption will occur* ***only*** *within the confines of the small 75-*km^2 *rectangle. As noted above, the model of Smith et al. (1990) has a very low success rate at predicting the sites of future eruptions using the location of past eruptions. The significance of the calculations of Ho (1992) can be placed in perspective by comparing his calculations to recurrence rates of very active volcanic fields. Basaltic volcanic fields have vent densities (number of vents or cones per square kilometer) that range from 0 .2 to approaching 0.4 events* km^{-2} *(Crowe et al. 1992b). Extrapolating the upper rate interval of Ho (1992) to the 75-*km^2 *area for the length of the Quaternary period gives a vent density of about 0.3. Thus Ho's (1992) calculation establishes an upper bound that states that the probability of disrupting a repository at the Yucca Mountain site is about equivalent to placing a repository in the middle of the Lunar Crater or Cima volcanic fields. Clearly, that is not a physically realistic calculation and illustrates the pitfalls of making probability estimations without examining their physical meaning.*

9. Comment and Response to the Article Published in *Science* on the Age of the Lathrop Wells Volcanic Center. Wells et al. (1992) listed several concerns with the paper by Turrin et al. (1991) on the age of Lathrop Wells volcanic center. First, the paper by Turrin et al. (1991) ignored published information on the stratigraphy and presence of soil-bounded unconformities in the volcanic units of the Lathrop Wells center. These unconformities suggest a hiatus in eruptive activity. They noted that several sources of data supporting a younger age of the center were ignored, including TL ages of soil and cosmogenic helium ages. The K-Ar and $^{40}Ar/^{39}Ar$ age determinations were critiqued not based on the analytical results but on the method of averaging the data. Specific concerns were that the determinations have a mean larger than the median, outliers are present and unrecognized in their data set, four age determinations were discarded without criteria, there are influential cases in the regression plots, there were no discussions of possible sources of data error other than analytical, and there was no discussion of potential problems of recoil of ^{39}Ar. Wells et al. (1992) concluded that the weighted mean is unsupported at best and may be invalid if all sources of variance in the data set are not analytical. Second, they noted that paleomagnetic data can only be used at best to infer a minimum age difference between volcanic units. Moreover, they discussed inconsistencies in the presentation of the paleomagnetic data and concerns with the measurement of magnetization directions for samples collected from the summit of the main scoria cone. Finally, Wells et

al. (1992) noted that the simplified volcanic history proposed for the volcanic center by Turrin et al. (1991) was inconsistent with geochemical and isotopic data. These data support a polygenetic model for the center formed from magma batches that were both physically and/or temporally distinct.

Turrin et al. (1992) rebutted the comments presented by Wells et al. (1992). They noted that the evidence of soil-bounded unconformities is based on the presence of sand, silt, and lapilli-size tephra in deposits near the south flank of the cone. They argue that the deposits are simply reworked parts of the cone and are irrelevant to the age of volcanic activity at the center. They presented granulometry data for the deposits they interpret as indicating the tephra deposits are not "volcanogenic" in origin and dismiss on this basis the TL age determinations. Turrin et al. (1992) argue that cosmogenic helium ages for the Lathrop Wells center represent results of developmental methods and are minimum ages. They cite a U-Th disequilibrium age for one of the lavas that is consistent with their K-Ar and $^{40}Ar/^{39}Ar$ results. Turrin et al. (1992) argue that samples were discarded from their data set using either $^{37}Ar/^{39}Ar$ ratios, or recognition of analytically distinct ages, or both. They suggest the data set is normally distributed with the contaminated samples removed. They argue that there are not influential data points in their regression calculations and they used a regression method that does not permit influential data points. Turrin et al. (1992) argue that ^{39}Ar recoil is not a problem with the Lathrop Wells volcanic samples. They presented new $^{40}Ar/^{39}Ar$ step-heating spectra that give an isochron age of 107 ± 33 ka. Turrin et al. (1992) agreed with the comments by Wells et al. (1991) that the angular difference between two field magnetization directions by itself only suggest a minimum age difference between volcanic units. They argue, however, that the paleomagnetic data used in combination with other geologic information can be used to estimate "absolute" age differences. They note that problems with the paleomagnetic data at the summit of the main cone are attributable to samples that were rotated by a slope-dependent slumping process. Finally, Turrin et al. (1992) argue that the geochemical and isotopic data for the Lathrop Wells center provide no constraints on the duration and number of events. They suggest the slight variations in the chemical data are consistent with monogenetic volcanism.

The differences in opinion concerning the age and eruptive history of the Lathrop Wells volcanic center are long-standing and probably not resolvable to the mutual satisfaction of all researchers involved in the work. The important point of the controversies is not the existence of the differences of opinion. In fact, different points of view for problems like volcanism are a clear indication that multiple opinions are being considered by the YMP. What is important is how the different opinions affect assessment of the volcanic risk for the Yucca Mountain site.

The differences in opinion concerning the age of the Lathrop Wells center have narrowed to an age range that has no significance in assessment of volcanic risk for the Yucca Mountain site. The age of the lava-flow sequences appear well bracketed between 70 and 140 ka. Further resolution of their ages may be beyond the capability of the present geochronology methods. A remaining concern is the age of the main cone of the Lathrop Wells center. An important point of recent agreement is that the cone is probably >45 ka. This is sufficiently old that the event is not significant using volume-predictable probability models. Finally, the issue of the monogenetic versus polygenetic eruptive history of the Lathrop Wells center remains unresolved. It can be accommodated reasonably by using both polygenetic and monogenetic models in assessments of the consequences of potential repository disruption. This is the approach that has been used in all recent assessments of volcanic risk for the Yucca Mountain site.

F. Publications in 1993

1. Alternative Age Determinations of the Lathrop Wells Volcanic Center using the Cosmogenic ^{36}Cl Method. Zreda et al. (1993) obtained ages for the Lathrop Wells volcanic center using the cosmogenic ^{36}Cl method. They collected samples from: (1) the surface of a lava flow south of the main cone (*the western lobe of the Ql1a subunit), (2)* the summit of the main cone (*the Qs3 unit),* and (3) volcanic bombs from an alluvial plateau west of the main cone (*the stratigraphic identity of the third sample set is problematic. The most likely stratigraphic correlation is with units Qs1 or Qs2, the latter being the most likely correlation. There is a possibility the samples could be correlated with unit Qs3. The stratigraphic 'identity of the samples could only be tested from petrography descriptions combined with major- and trace element data; see Chapter 2).* The first site yielded corrected ages of 73 to 93 ka. The ages of the third site ranged from 78 to 96 ka. The cosmogenic ^{36}Cl ages of the second site were less suitable for dating both because of their location on an unstable landform and the presence of inseparable secondary minerals in one dated sample. These samples yielded ages of 83 ± 9.2 ka for the altered sample and 68 ± 5.7 ka for the second sample. Zreda et al. (1993) noted that the ages from the three sites are statistically indistinguishable and can be combined to give an average age of 81 ± 7.9 ka, their preferred estimate of the eruption age of the center. They note that this age falls between bracketing U/Th ages on carbonate above and below the volcanic rocks and is younger than but overlaps in distribution with ^{40}Ar/^{39}Ar ages for the center (Turrin et al. 1991). Zreda et al. (1993) noted the similarity of their ages to a ^{40}Ar/^{39}Ar isochron age (107 ± 31 ka) reported by Turrin et al. (1992) and argue that their data are inconsistent with but do not *preclude* multiple, time-separate eruptions at the Lathrop Wells volcanic center.

The work by Zreda et al. (1993) is a valuable contribution to assessing the age of the Lathrop Wells volcanic center. Their age determinations are consistent generally with the results of cosmogenic ^{3}He ages and permissive with the observation that K-Ar and ^{40}Ar/^{39}Ar age determinations may be slightly old (see Chapter 2). Moreover their results apply a largely independent method that is different from conventional radiometric dating methods (although related indirectly through calibrations of production rates). There are however, several important limitations of the method and analyzed samples that require the resulting ages to be applied with caution. First, the ^{36}Cl method requires corrections for production rates, thermal neutron activation of ^{35}Cl, surface geometry, and secondary alteration. Second, the unknown stratigraphic correlation of the sample collected from an alluvial surface west of the cone complicates interpretations of ages. Third, the presence of inseparable secondary minerals in one sample from the summit cone is problematic. The samples were collected in scoria oxidized and altered by basaltic volcanic gases that tend to be highly enriched in halogens (Olmez et al. 1986; Crowe et al. 1987; Miller et al. 1990). Fourth, and probably the most significant concern, trenching studies at the Lathrop Wells center have shown that the samples collected from the western lava site were covered by at least 1.8 m of scoria-fall deposits. The resulting ages ***must*** *be interpreted as* ***minimum*** *ages (see Chapter 2). We note that the cosmogenic ^{36}Cl ages, like the cosmogenic ^{3}He ages, yield tightly clustered ages, a result that can be interpreted traditionally as indicating an uncomplicated surface exposure history. However, field relations show unquestionably that the sample collection sites were covered by fall-deposits, which have to complicate the surface exposure history. Finally, Zreda et al. (1993) did not recognize or sample the youngest volcanic event at the Lathrop Wells center, unit Qs4..*

2. Geophysical Investigations of Buried Volcanic Centers: Studies by the U.S. Geological Survey. Langenheim et al. (1993) described five dipolar aeromagnetic anomalies in alluvial deposits of the Amargosa Valley, south of the Yucca Mountain site. Anomaly B located south of the town of Amargosa Valley and the largest of the anomalies, was evaluated using gravity and ground magnetic data. Three different two-dimensional magnetic models were constructed to fit the observed magnetic field. The first

model fits the longer wavelengths of the anomaly and is wedge-shaped, comparable to a basaltic scoria cone (depth to top of 150 m). The two alternative models fit the short wavelength part of the anomaly and are represented by either lava flows or sills, or a dike swarm. The depth to the top of the body for these two models ranges from 50 to 250 m. The apparent lack of a gravity anomaly associated with the aeromagnetic anomaly could indicate either that the body may be a tuff, or if it is a basalt, the volume is small. The depth to basement near anomaly B from an electrical resistivity is approximately 800 m and suggests that the causative body for the anomaly is within alluvial deposits.

The aeromagnetic anomaly was drilled in 1991 by a private company (Harris et al. 1992). Basalt cuttings at the depths predicted from the geophysical studies were obtained and dated by the $^{40}Ar/^{39}Ar$ method. The resulting age is 3.85 ± 0.05 Ma (see Chapter 2).

3. Assessment of Volcanic Hazards for the Yucca Mountain site by Golder Associates Using the Repository Integration Program (RIP). Wallman et al. (1993) described the results of applying the RIP for classes of disruptive events. The RIP uses a stochastic simulation approach that incorporates model and parameter uncertainty in performance assessment. They examined disruptive events judged to be both credible (likely to occur) and significant (having potential impact on system performance) for seismic and volcanic events. The volcanic events assessed are direct disruption of a repository and a volcanic event downgradient of a repository that affects the water table. They modeled E1 as a uniform distribution with a range from 3.0×10^{-6} to 5.0×10^{-5} events yr^{-1}, setting the upper bound to high values to avoid underestimating recurrence rates. The E2 was modeled through simulation using FracMan, a program for generating three-dimensional fracture networks. Multiple structural models were considered and estimates of E2 ranged from 6.0×10^{-3} to 2.6×10^{-2}. A disruption probability for E3 was assigned for a subset of dikes modeled in the estimates of E2 where the dikes were near vertical (±30°). The E3 was assigned as a uniform distribution with a range of 0.0 to 0.05. Dike lengths were treated as a uniform distribution varying between 500 and 5500 m. Dike driving pressure (excess of lithostatic) was assumed to vary between 2 and 20 mPa. Dike orientations were modeled by two triangular distributions, and dike thickness assumed the maximum displacement of crack walls (elastic medium) for appropriate dike lengths and driving pressures. Magma eruption volume was treated as an exponential distribution with an expected value of 1.1×10^8 m^3 and maximum of 10^9 m^3. A dike intersecting a repository was evaluated through assumptions of the disruption of waste packages, surface eruption of waste, and transfer of radionuclides from pathways to the surface. The calculations assumed waste is uniformly distributed through a repository and has an equal likelihood of incorporation into magma as country rock (lithic fragments). The same assumptions were made for radionuclide pathways. The probability of eruption once a dike reached the repository was treated as a triangular distribution with a minimum of 0.5 and expected and maximum value of 1.0. The dike damming effect assumed the primary effect would be a rise of the water table, and a maximum rise of 345 m was assumed.

The results of 500 realizations of the RIP model using the described assumptions for volcanism showed that volcanic disruptive events have no visible effect on cumulative releases, which are dominated by ^{14}C releases during waste package corrosion. Releases were also evaluated for distributions assuming volcanic events occur in each realization allowing assessment of the effects of individual disruptive events. All calculations show that disruption of the potential site by volcanism does not result in significant consequences.

The calculated release consequences for disruptive volcanic events show small effects on repository performance, comparable to the studies of Link et al. (1983). The study provides bounding calculations because event probabilities and descriptors were all chosen to ***not underestimate*** *volcanic*

effects. The acceptance or rejection of these calculations are dependent on assessments of the viability of the modeling for the base case release calculations.

4. Alternative Calculations of the Probability of Magmatic Disruption of the Potential Repository: Work by the Center for Nuclear Waste Regulatory Analyses. Connor and Hill (1993) presented alternative estimations of the probability of magmatic disruption of the potential repository site at Yucca Mountain. They summarized previously published recurrence rates of volcanism, and estimated recurrence rates using a repose-time method or maximum likelihood estimator. Connor and Hill (1993) argued that if the uncertainty of the ages of volcanic events is included in estimates, the recurrence rate is known only to about $7 \pm 3 \times 10^{-6}$ event yr^{-1}. *(Their calculations were based on 1992 geochronology data and did not include the results of recent geochronology data summarized in Chapter 2).* They examined recurrence rates using the Weibull-Poisson distribution and noted the strong dependency of β and θ *(fitting parameters for the Weibull model)* on the time interval of calculations. Specifically, they recognized that β is <1 *(waning volcanism)* for most estimates of recurrence rates using time intervals tied to the volcanic record. Connor and Hill (1993) emphasized the uncertainty of recurrence rate estimates and urged use of ranges of expected recurrence rates. They also examined spatial variations in the recurrence rate and assessed models of spatially random distribution of events. A Clark-Evans and Hopkins F test was used to reject the hypothesis of homogeneous Poisson distribution of events. *This is not a surprising conclusion. The distribution of volcanic events in the YMR was never inferred to be random. The point of confusion is with the spatial distribution models of Crowe et al. (1982). They defined distribution zones for combinations of Quaternary, and Pliocene and Quaternary volcanic events and assumed, for simplicity of calculations, that the distribution of events* ***within the zones*** *was random. The individual zones are defined by the distribution of volcanic events and that distribution is assumed to be structurally controlled.*

Connor and Hill (1993) used a near-neighbor method to assess the recurrence rate per unit area. They estimated the probability of magmatic disruption of the potential site using a nonhomogeneous Poisson distribution. They obtained disruption probabilities that ranged from 0.8 to 3.4×10^{-8} events yr^{-1} using Quaternary recurrence rates and 6.9 to 9.2×10^{-9} events yr^{-1} for recurrence rates averaged over the Miocene. Connor and Hill (1993) argued that volcanic centers form clusters and this clustering should be included in "robust" probability models because the Yucca Mountain site is located on a probability gradient.

There are several assumptions in the probability estimates that need to be more carefully described before applying a NHPP model to the YMR. These are a more clear definition of cluster model and the basis for, combining the two episodes of the basalt (see discussions in Chapter 3). However, these points are not significant because the resulting estimated probability range of Connor and Hill (1993) ***is virtually identical to probability ranges obtained through application of homogeneous Poisson distribution models.*** *The continuing debate contrasting homogeneous versus nonhomogeneous distribution models is not significant unless the different approaches yield different probability distributions (see Chapter 7). The reason the probability estimates are similar is because of the limited number of volcanic events. No probability model can be considered* ***"robust"*** *that is applied to or describes the small data set of volcanic events in the YMR. The choice of different time distribution models for the time patterns of volcanic events is actively debated in the geologic literature (Crowe et al. 1992b). This debate will not be solved using the data set for the YMR. The spatial distribution of volcanic events is almost certainly nonrandom. The nonhomogeneous distribution model of Connor and Hill (1993) is an important and useful contribution to probabilistic volcanic risk assessment. Their*

model would be preferred for assessments of the spatial distribution of volcanic events in large volcanic fields where the number of events is >30 (for example, the Lunar Crater volcanic field).

5. An Alternative Method for Calculating the Probability of Dikes Intersecting a Repository: Continuing Studies by Golder Associates Inc. Wallmann (1993) assessed the probability that a volcanic event will disrupt the potential repository at Yucca Mountain (E2) **given that a volcanic event has occurred (E1).** He used the computer code FracMan to simulate intrusion of the repository by basaltic dikes. He varied both the dike size and orientation using multiple distribution forms and multiple models for the spatial distribution of dike centers (Poisson and cluster models). Dikes were modeled as rectangular, planar features with a length, height, and orientation. Each dike was located within a model volume that represented alternative conceptual models for the structural controls of basaltic volcanism in the YMR. The models included the **lower part** of the CFVZ (Crowe and Perry 1989), the AMRV (Smith et al. 1990), and the Lathrop Wells chain model (Smith et al. 1990). A bivariate normal distribution was used to specify dike orientation and simulation modeling was adopted to model the propagation of dikes away from a center. The propagation direction of dikes was assumed to follow the maximum stress direction (N 20° E) but the dikes could propagate either NNE or SSW. Because of the uncertainty in dike propagation directions, the dike length distribution used was twice the mean dike length and each dike feature was represented as two dikes propagating in opposite directions. The location of dike centers was selected as a Poisson distribution for most simulations. However, a series of simulations were generated using a location model described by a Levy Flight algorithm. A base case was defined for dike generation regions and all other simulations were normalized to that case. A repository horizon or traceplane was simulated as a 12-km^2 area located 300 m below the surface. Each set of simulation parameters were run for 10 iterations using 10,000 fractures per iteration (20,000 dikes). The total number of intersections of the traceplane was summed for each iteration. The resulting disruption probabilities were highest for the Lathrop Wells chain model and lowest for the CFVZ. Varying the mean and standard deviation of the strike had the greatest effect on the CFVZ. Increasing dike length and height increased the disruption probabilities for all models. The cluster model results show that a cluster model by itself will not increase significantly the probability of repository disruption without a mechanism to focus the location of future clusters near or adjacent to the potential repository. Combining the simulation results for E2 with E1 (Poisson process, event count during 4.7 Ma) shows that the event rate for each structural model must be adjusted for the specific model or the probability of magmatic disruption is overestimated.

The probability estimates of magmatic disruption for the event recalibrated models (Wallmann 1993, Fig. 9) are in close agreement with published probability estimates (1 to 3 x 10^{-8} events yr^{-1}). An important conclusion of this work is that the probability of magmatic disruption of the Lathrop Wells chain model falls between values calculated for the AMRV and CFVZ when the event rate is recalibrated. A logical extension of this work would be to expand the simulation modeling to include the thirteen sets of structural models described in Chapters 3 and 7.

6. Continuing Field and Computational Studies of the Effects of Magmatic Activity on the Yucca Mountain site. Valentine et al. (1993) completed the second in a series of papers describing progress on studies of the effects of magmatic activity on a potential repository. The emphasis of their work is on E3, the probability that a given magmatic event will cause release of waste to the accessible environment in quantities that exceed the regulatory limits. Work on E3 is divided into three parts: (1) $E3_e$, or eruptive effects, (2) $E3_s$, or subsurface effects, and (3) Magma system dynamics. Valentine et al. (1993) initiated studies to examine the abundance of xenoliths in volcanic deposits of small basaltic centers. Basalt centers of similar size, composition, and eruptive style of basalt centers in the YMR were studied to evaluate the abundance and depth of derivation of crustal xenoliths. Geologic studies were described at the Alkali Buttes centers in New Mexico. These consist of erosional remnants of 4–5 basaltic vents that

probably formed a single landform prior to erosion. Deposits of the centers were formed by hydrovolcanic and mixed hydrovolcanic and magmatic eruptions. Lithic abundance data for the centers are grouped according to their eruption facies and included only the megascopic component (>1 cm). Most deposits show a general decrease in lithic abundance with increasing depth of derivation (incorporation in magma). That trend is reversed for lithic fragments derived from the Glorieta sandstone which may have acted as a fracture-dominated aquifer. Additionally, the incorporation of fragments of the Glorieta sandstone may have been influenced by the mechanical properties of the rock. Total lithic contents decrease upward in stratigraphic position and parallel an inferred decrease in the relative importance of hydrovolcanic eruptive processes. Three main entrainment mechanisms have been identified at analog basalt centers. These are: (1) spalling of rock into the tip of a propagating dike, (2) dike wall erosion by shear from flowing magma, and (3) inclusion of wall rock material between a main dike and subparallel offshoots. Field evidence from the Paiute Ridge analog site in the Half Pint range indicates sills do **not** result from processes related to neutral buoyancy. Instead, the sills appear to form where asperities caused local locking along fault planes and a resulting reorientation of principle stresses. The software package MESHGEN has been developed to build three-dimensional tetrahedral meshes for the stratigraphy of the Yucca Mountain site and will be used for flow and transport calculations that encompass the potential repository boundary.

7. Continuing Revisions of the Probability of Magmatic Disruption of the Potential Yucca Mountain: The First Results of Simulation Modeling. Crowe et al. (1993) compiled the range of estimated values for the probability of magmatic disruption of the repository and bounded these data using logical numerical limits for the recurrence rate (E1) and spatial and structural models of the distribution of volcanic events (E2). They used risk simulation to assess the uncertainty of the cumulative probability distributions. The RIP was used to test the applicability of the code to assess system responses or sensitivity to volcanic events. Estimates (midpoint, maximum, minimum) of E1 were combined through risk simulation to calculate the distribution of E1 in probability space. The minimum bound was taken from regulatory guidance (5×10^{-7} events yr^{-1} or no volcanic events in the Quaternary). The maximum bound was defined by recurrence rates in large-volume, very active basaltic volcanic fields in the Basin and Range province. The midpoint estimates were used from multiple alternate models of E1 including time-series analysis, homogeneous, modified homogeneous, and nonhomogeneous Poisson models, and regression analysis of magma volume versus time. The E1 was modeled using Latin hypercube simulation sampling of a modified triangular distribution. The median (50 percentile) estimates ranged from 5.2 to 8.4×10^{-6} events yr^{-1}.These estimates are more dependent on probability bounds than midpoint estimates. The E2 was assessed as multiple spatial and structural models (24 alternative models) of the distribution of basaltic volcanic events. Bounds were estimated using simple geometric constraints. The E2 was modeled using Latin hypercube simulation sampling of a normal distribution with a mean or 4.3×10^{-3} and a standard deviation of 3.5×10^{-3}. The cumulative probability distribution of the magmatic disruption of a potential repository (Pr_{md} = Pr[E2 given E1]Pr[E1] was obtained by integrating the E1 probability distribution using quartile values from the simulation runs and multiplying by the probability distribution for E2. The median estimate of the cumulative probability distribution for Pr_{md} is 2.6×10^{-8} events yr^{-1}. This distribution was recalculated by revising E1 for specific models of E2. The 50% estimate for the revised distribution of Pr_{md} is 9.5×10^{-9} events yr^{-1} . These results support previous conclusions that the potential repository site at Yucca Mountain is not disqualified solely on the basis of the risk of volcanism. The uncertainty of the probability estimations is sufficiently large that volcanic events must be considered for their potential effects on the performance of a waste isolation system. The RIP computer code was used to compare releases of a simulated repository without volcanic events to releases for simulations using time histories including volcanic disruptive events. Resulting release simulations show that performance modeling can be used to assess the sensitivity of volcanic effects on the potential repository site.

V. References

Baer, G., and Z. Reches, "Mechanics of Emplacement and Tectonic Implications of the Ramon Dike System, Israel," *Journal Geophysical Research* **96**, 11,895-11,910 (1991).

Carr, W. J., "Volcano-Tectonic History of Crater Flat, Southwestern Nevada, as Suggested by New Evidence From Drill Hole USW-VH-1 and Vicinity," U.S. Geological Survey Open-File Report 82-457, 23 pp. (1982).

Carr, W. J., "Regional Structural Setting of Yucca Mountain, Southwestern Nevada, and Late Cenozoic Rates of Tectonic Activity in Part of the Southwestern Great Basin, Nevada and California," U.S. Geological Survey Open-File Report 84-854, 109 pp. (1984).
Carr, W. J., and L. D. Parrish, "Geology of Drill Hole USW VH-2, and Structure of Crater Flat, Southwestern Nevada," U.S. Geological Survey Open-File Report 85-475, 41 pp. (1985).

Champion, D. E., "Volcanic Episodes Near Yucca Mountain as Determined by Paleomagnetic Studies as Lathrop Wells, Crater Flat, and Sleeping Butte, Nevada," in *Proceedings, High Level Radioactive Waste Management, Las Vegas, Nevada* (American Nuclear Society, La Grange Park, Illinois, 1991), pp. 61-67.

Condit, C. D., L. S. Crumpler, J. C. Aubele, and W. E. Elston, "Patterns of Volcanism Along the Southern Margin of the Colorado Plateau; The Springerville Volcanic Field," *Journal Geophysical Research* **94**, 7975-7986 (1989).

Connor C. B., and B. E. Hill, "Estimating the Probability of Volcanic Disruption of the Candidate Yucca Mountain Repository Using Spatially and Temporally Non Homogeneous Poisson Models," in *Proceedings Site Characterization and Model Validation Focus'93 Symposium Volume* (American Nuclear Society, La Grange, Illinois, 1993), pp. 174-181.

Crowe, B. M., "Disruptive Event Analysis: Volcanism and Igneous Intrusion," Battelle Pacific Northwest Laboratory Report PNL-2882M, 28 pp. (1980).

Crowe, B. M., "Volcanic Hazard Assessment for Disposal of High-Level Radioactive Waste," in *Active Tectonics: Impact on Society* (National Academy Press, Washington, DC., 1986), Chap. 16, pp. 247-260.

Crowe, B. M., "Basaltic Volcanic Episodes of the Yucca Mountain Region," in *Proceedings High-Level Radioactive Waste Management Conference, Las Vegas, Nevada* (American Nuclear Society, La Grange Park Illinois, 1990), pp. 65-73.

Crowe, B. M., and K. A. Sargent, "Major-Element Geochemistry of the Silent Canyon-Black Mountain Peralkaline Volcanic Centers, Northwestern Nevada Test Site: Applications to an Assessment of Renewed Volcanism," U.S. Geological Survey Open-File Report 79-296, 25 pp. (1979).

Crowe, B. M., and W. J. Carr, "Preliminary Assessment of the Risk of Volcanism as a Proposed Nuclear Waste Repository in the Southern Great Basin," U.S. Geological Survey Open-File Report 80-375, 15 pp. (1980).

Crowe, B. M., M. E. Johnson, and R. J. Beckman, "Calculation of the Probability of Volcanic Disruption of a High-Level Radioactive Waste Repository Within Southern Nevada, USA," *Radioactive Waste Management* **3**, 167-190 (1982).

Crowe B. M., D. T. Vaniman, and W. J. Carr, "Status of Volcanic Hazard Studies for the Nevada Nuclear Waste Storage Investigations," Los Alamos National Laboratory Report LA-9325-MS (1983a).

Crowe, B. M., S. Self, D. Vaniman, R. Amos, and F. Perry, "Aspects of Potential Magmatic Disruption of a High-Level Radioactive Waste Repository in Southern Nevada," *Journal Geology* **91**, 259-276 (1983b).

Crowe, B. M., K. H. Wohletz, D. T. Vaniman, E. Gladney, and N. Bower, "Status of Volcanic Hazard Studies for the Nevada Nuclear Waste Storage Investigations," Los Alamos National Laboratory Report LA-9325-MS, Vol. II (1986).

Crowe, B. M., D. L. Finnegan, W. H. Zoller, and W. V. Boynton, "Trace Element Geochemistry of Volcanic Gases and Particles From 1983-1984 Eruptive Episodes of Kilauea Volcano," *Journal Geophysical Research* **92,** 13,708-13,714 (1987).

Crowe, B., C. Harrington, L. McFadden, F. Perry, S. Wells, B. Turrin, and D. Champion, "Preliminary Geologic Map of the Lathrop Wells Volcanic Center," Los Alamos National Laboratory Report LA-UR-88-4155 (1988).

Crowe, B. M. and F. V. Perry, "Volcanic Probability Calculations for the Yucca Mountain Site: Estimation of Volcanic Rates," in *Proceedings Nuclear Waste Isolation in the Unsaturated Zone Focus '89, Symposium Volume* (American Nuclear Society, La Grange Park, Illinois, 1989), pp. 326-334.

Crowe, B. M., B. Turrin, S. Wells, F. Perry, L. McFadden, C. Renault, D. Champion, and C. Harrington, "Volcanic Hazard Studies for the Yucca Mountain Project," *Waste Management '89* **1,** 485-492 (1989).

Crowe, B. M., and F. V. Perry, "Preliminary Geologic Map of the Sleeping Butte Volcanic Centers," Los Alamos National Laboratory Report LA-12101-MS, 11 pp. (1991).

Crowe, B., R. Morley, S. Wells, J. Geissman, E. Mcdonald, L. McFadden, F. Perry, M. Murrell, J. Poths, and S. Forman, "The Lathrop Wells Volcanic Center: Status of Field and Geochronology Studies," in *Proceedings High-Level Radioactive Waste Management Conference, Las Vegas, Nevada* (American Nuclear Society, La Grange Park Illinois, 1992a), pp. 1997-2013.

Crowe, B. M., R. Picard, G. Valentine, and F. V. Perry, "Recurrence Models of Volcanic Events: Applications to Volcanic Risk Assessment," in *Proceedings High-Level Radioactive Waste Management Conference, Las Vegas, Nevada* (American Nuclear Society, La Grange Park Illinois, 1992b), 2344-2355.

Crowe, B.M., G. Valentine, R. Morley, and F.V. Perry, "Recent Progress in Volcanism Studies: Site Characterization Activities for the Yucca Mountain Site Characterization Project," *Waste Management '92* **2,** 376-382 (1992c).

Crowe, B. M., F. V. Perry, G. A. Valentine, P. C. Wallmann, and R. Kossik, "Simulation Modeling of the Probability of Magmatic Disruption of the Yucca Mountain Site," in *Proceedings Site Characterization and Model Validation Focus'93 Symposium Volume* (American Nuclear Society, La Grange Park, Illinois, 1993), pp. 182-191.

DOE (U.S. Department of Energy), "Environmental Assessment: Yucca Mountain Site, Nevada Research and Development Area, Nevada," Office of Civilian Radioactive Waste Management report DOE/RW-0073, (1986).

DOE (U.S. Department of Energy), "Site Characterization Plan, Yucca Mountain Site, Nevada Research and Development Area, Nevada," Office of Civilian Radioactive Waste Management report DOE/RW-0199, (1988).

Dueker, K., and E. Humphreys, "Upper-Mantle Velocity Structure of the Great Basin," *Geophysical Research Letter* **17**, 1337-1330 (1991).

Evans, J. R., and M. Smith III, "Teleseismic Tomography of the Yucca Mountain Region: Volcanism and Tectonism," in *Proceedings High-Level Radioactive Waste Management Conference, Las Vegas, Nevada* (American Nuclear Society, La Grange Park Illinois, 1992), pp. 2371-2380.

Farmer, G. L., F. V. Perry, S. Semken, B. Crowe, D. Curtis, and D. J. DePaolo, "Isotopic Evidence on the Structure and Origin of Subcontinental Lithospheric Mantle in Southern Nevada," *Journal Geophysical Research* **94,** 7885-7898 (1989).

Fedotov, S. A., "Magma Rates in Feeding Conduits of Different Volcanic Centers," *Journal Volcanology Geothermal Research* **9**, 379-394 (1981).

Frey, F. A., W. S. Wise, M. O. Garcia, H. West, S. T. Kwon, and A. Kennedy, "Evolution of Mauna Kea, Hawaii: Petrologic and Geochemical Constraints on Postshield Volcanism," *Journal Geophysical Research* **95**, 1271-1300 (1990).

Harris, A. G., J. E. Repetski, J. L. Clayton, J. A. Grow, M. D. Carr, and T. A. Davis, "Results From 1991 Wildcat Wells Near Yucca Mountain, Nevada," *Geological Society America Abstracts* **24**, 17 (1992).
Ho, C. H., "Bayesian Analysis of Basaltic Volcanic Eruptions," *Journal Volcanology Geothermal Research* **43**, 91-98 (1990).

Ho, C. H., "Time Trend Analysis of Basaltic Volcanism for the Yucca Mountain Site," *Journal Volcanology Geothermal Research* **46**, 61-72 (1991).

Ho, C. H., "Risk Assessment for the Yucca Mountain High-Level Nuclear Waste Repository Site: Estimation of Volcanic Disruption," *Mathematical Geology* **24**, 347-364 (1992).

Ho, C. H., E. I. Smith, D. L. Feuerbach, T. R. Naumann, "Eruptive Probability Calculation for the Yucca Mountain Site, USA: Statistical Estimation of Recurrence Rates," *Bulletin Volcanology* **54**, 50-56 (1991).

Jones, J. H., B. P. Wernicke, G. L. Farmer, J. D. Walker, D. S. Colman, L. W. McKenna, and F. V. Perry, "Variations Across and Along a Major Continental Rift: An Interdisciplinary Study of the Basin and Range Province, Western USA," *Tectonophysics* **213**, 57-96 (1992).

Kane, M. F., and R. E. Bracken, "Aeromagnetic Map of Yucca Mountain and Surrounding Regions, Southwest Nevada," U.S. Geological Survey, Open-File Report 83-616, 19 pp. (1983).

Klein, F. W., "Patterns of Historical Eruptions as Hawaiian Volcanoes," *Journal Volcanology Geothermal Research* **12**, 1-35 (1982).

Langenheim, V. E., K. S. Kirchoff-Stein, and H. W. Oliver, "Geophysical Investigations of Buried Volcanic Centers Near Yucca Mountain, Southwest Nevada," in *Proceedings High-Level Radioactive Waste Management Conference, Las Vegas, Nevada* (American Nuclear Society, La Grange Park Illinois, 1993), pp. 1840-1846.

Link, R., S. E. Logan, H. S. Ng, F. A. Rockenbach, and K. J. Hong, "Parametric Studies of Radiological Consequences of Basaltic Volcanism," Sandia National Laboratories Report SAND 81-2375, 219 pp. (1983).

McKee, E. H., D. C. Noble, and S. I. Weiss, "Very Young Silicic Volcanism in the Southwestern Great Basin: the Late Pliocene Mt. Jackson Dome Field, Southwestern Esmeralda County, Nevada," *EOS Transactions* **70**, 1420 (1989).

Miller, T. L., W. H. Zoller, B. M. Crowe, and D. L. Finnegan "Variations in Trace Metal and Halogen Ratios in Magmatic Gases Through an Eruptive Cycle of the Pu'u O'o Vent, Kilauea, Hawaii: July-August 1985," *Journal Geophysical Research* **95**, 12,607-12,615 (1990).

Miyashiro, A. "Nature of Alkalic Volcanic Rock Series," *Contributions Mineralogy Petrology* **66**, 91-104 (1978).

Naumann, T. R., D. L. Feuerbach, and E. I. Smith, "Structural Control of Pliocene Volcanism in the Vicinity of the Nevada Test Site, Nevada: An Example From Buckboard Mesa," *Geological Society America Abstracts* **23**, 82 (1991).

Olmez, I., D. L. Finnegan, and W. H. Zoller, "Iridium Emissions From Kilauea Volcano," *Journal Geophysical Research* **91**, 653-662 (1986).

Perry, F. V., and B. M. Crowe, "Geochemical Evidence for Waning Magmatism and Polygenetic Volcanism as Crater Flat, Nevada," in *Proceedings High-Level Radioactive Waste Management Conference, Las Vegas, Nevada* (American Nuclear Society, La Grange Park Illinois, 1992), pp. 2344-2355.

Rosenbaum, J. G., M. R. Hudson, and R. B. Scott, "Paleomagnetic Constraints on the Geometry and Timing of Deformation as Yucca Mountain, Nevada," *Journal Geophysical Research* **96**, 1963-1980 (1991).

Rubin, A. M., and D. D. Pollard, "Origins of Blade-Like Dikes in Volcanic Rift Zones," U.S. Geological Survey Professional Paper 1350, pp. 1449-1470 (1987).

Sheridan, M. F., "A Monte Carlo Technique to Estimate the Probability of Volcanic Dikes," in *Proceedings High-Level Radioactive Waste Management Conference, Las Vegas, Nevada* (American Nuclear Society, La Grange Park Illinois, 1992), pp. 1840-1846.

Sinnock, S., and R. G. Easterling, "Empirically Determined Uncertainty in Potassium-Argon Ages for Plio-Pleistocene Basalts From Crater Flat, Nye County, Nevada," Sandia National Laboratories, Albuquerque, New Mexico, SAND82-2441, pp. 3-17 (1982).

Smith, E. I., D. L. Feuerbach, T. R. Naumann, and J. E. Faulds, "The Area of Most Recent Volcanism Near Yucca Mountain, Nevada: Implications for Volcanic Risk Assessment," in *Proceedings High-Level Radioactive Waste Management Conference, Las Vegas, Nevada* (American Nuclear Society, La Grange Park Illinois, 1990), pp. 81-90.

Spence, D. A., and D. L. Turcotte, "Magma-Driven Propagation of Cracks," *Journal Geophysical Research* **90**, 575-580 (1985).

Turrin, B. D., and D. E. Champion, "$^{40}Ar/^{39}Ar$ Laser Fusion and K-Ar Ages From Lathrop Wells Nevada, and Cima, California: The Age of the Latest Volcanic Activity in the Yucca Mountain Area," in *Proceedings High-Level Radioactive Waste Management Conference, Las Vegas, Nevada* (American Nuclear Society, La Grange Park Illinois, 1991), pp. 68-75.

Turrin, B. D., D. Champion, and R. J. Fleck, "$^{40}Ar/^{39}Ar$ Age of the Lathrop Wells Volcanic Center, Yucca Mountain, Nevada," *Science* **253**, 654-657 (1991).

Turrin, B. D., D. E. Champion, and R. J. Fleck, "Measuring the Age of the Lathrop Wells Volcanic Center as Yucca Mountain," *Science* **257**, 556-558 (1992).

Valentine, G. A., B. M. Crowe, and F. V. Perry, "Physical Processes and Effects of Magmatism in the Yucca Mountain Region," in *Proceedings High-Level Radioactive Waste Management Conference, Las Vegas, Nevada* (American Nuclear Society, La Grange Park Illinois, 1992), pp. 2344-2355.

Valentine, G. A., K. R. Groves, C. W. Gable, F. V. Perry, and B. M. Crowe, "Effects of Magmatic Activity on the Potential Yucca Mountain Repository: Field and Computational Studies," in *Proceedings Site Characterization and Model Validation Focus'93 Symposium Volume* (American Nuclear Society, La Grange Park, Illinois, 1993), pp. 167-173.

Vaniman, D. T., and B. M. Crowe, "Geology and Petrology of the Basalts of Crater Flat: Applications to Volcanic Risk Assessment for the Nevada Nuclear Waste Storage Investigations," Los Alamos National Laboratory Report LA-8845-MS, 67 pp. (1981).

Vaniman, D. T., B. M. Crowe, and E. S. Gladney, "Petrology and Geochemistry of Hawaiite Lavas From Crater Flat, Nevada," *Contributions Mineralogy Petrology* **80**, 241-357 (1982).

Walker, G. P. L., "Gravitational (Density) Controls on Volcanism, Magma Chambers and Intrusions," *Australian Journal Earth Sciences* **36**, 149-165, (1989).

Wallmann P. C., "A Technique for Calculation of the Probability of Dikes Intersecting a Repository," in *Proceedings Site Characterization and Model Validation Focus'93 Symposium Volume* (American Nuclear Society, La Grange Park, Illinois, 1993), pp. 192-199.

Wells, S. G., L. D. McFadden, C. E. Renault, B. D. Turrin, and B. M. Crowe, "A Geomorphic Assessment of Quaternary Volcanism in the Yucca Mountain Area, Nevada Test Site, Southern Nevada," *Geological Society America Abstracts With Programs* **20**, 242 (1988).

Wells, S. G., L. D. McFadden, C. E. Renault, and B. M. Crowe, "Geomorphic Assessment of Late Quaternary Volcanism in the Yucca Mountain Area, Southern Nevada: Implications for the Proposed High-Level Radioactive Waste Repository," *Geology* **18**, 549-553 (1990).

Wells, S. G., L. D. McFadden, C. E. Renault, and B. M. Crowe, "Reply on Geomorphic Assessment of Late Quaternary Volcanism in the Yucca Mountain Area, Southern Nevada: Implications for the Proposed High-Level Radioactive Waste Repository," *Geology* **19**, 661-662 (1991).

Wells, S. G., B. M. Crowe, and L. D. McFadden, "Measuring the Age of the Lathrop Wells Volcanic Center of Yucca Mountain," *Science* **257**, 555-558 (1992).

Wood, C. A., "Morphometric Analysis of Cinder Cone Degradation," *Journal Volcanology Geothermal Research* **8**, 137-160 (1980).

Zreda, M. G., F. M. Phillips, P. W. Kubik, P. Sharma, and D. Elmore, "Cosmogenic ^{36}Cl Dating of a Young Basaltic Eruption Complex, Lathrop Wells, Nevada," *Geology* **21**, 57-60 (1993).

CHAPTER 7: VOLCANIC RISK ASSESSMENT FOR THE YUCCA MOUNTAIN SITE

I. Summary

Chapter 7 presents the status of volcanic risk assessment for the Yucca Mountain site focusing on estimating the occurrence probability of magmatic disruption of a potential repository. Probabilistic risk assessment is conducted through evaluating the most likely, minimum, and maximum estimates of a range of alternative models of the geologic record of basaltic volcanism in the Yucca Mountain region (YMR). The purpose of these estimates is to explore the scientific basis for constraining and defining the distribution of data for a conditional probability model of repository disruption by magmatic processes. These studies provide the background foundation for formal probabilistic assessment of volcanic risk for the Yucca Mountain site in future reports by the Department of Energy (DOE).

The risk of future volcanism for the Yucca Mountain site is assessed as a conditional probability: *Prdr = Pr(E3 given E2,E1)Pr(E2 given E1)Pr(E1),* where E1 denotes the recurrence rate of volcanic events, E2 denotes the probability of intersection of specified areas, and E3 is the probability of exceeding regulatory releases through volcanic eruptions or through changes in the waste isolation system. This conditional probability is expressed mathematically as an exponential or modified exponential equation on the basis of multiple assumptions. First, we assume a homogeneous, modified homogeneous, or nonhomogeneous Poisson distribution of volcanic events in time and space. Second, the recurrence rate (E1) and the disruption probability (E2) are estimated by extrapolation of past patterns of volcanic events (geologic record). Third, the most current site characterization data for the Yucca Mountain region are used to identify and describe past volcanic events. Finally, alternative models of eruption patterns, the chronology, and the structural controls of volcanic centers are incorporated systematically in risk simulation to attempt to bound uncertainty.

The strategy for probabilistic assessment of the risk of future volcanism is defined by evaluation of four questions: (1) Is igneous activity a concern for the Yucca Mountain site? (2) What is the range of possible future volcanic events? (3) What is the occurrence probability of each type of volcanic or magmatic activity? (4) Where could future volcanic events occur? The presence of five Quaternary volcanic centers in the vicinity of Yucca Mountain is the primary basis for identifying the presence of the potentially adverse condition of future igneous activity in the YMR. The range of possible future volcanic events includes the formation of a new volcanic center (λ_v), the formation of a cluster of volcanic centers (λ_c), magmatic intrusions with or without eruptions (λ_i), polygenetic eruptions at an existing volcanic center (λ_p), and intracluster volcanic events (λ_{ce}). Current site characterization information combined with simple logic require that $\lambda_i > \lambda_v > \lambda_c$, that $\lambda_i \approx \lambda_{v,}$ and λ_i ,$\lambda_{v,,}$ and λ_c are all $>10^{-8}$ events yr^{-1}.

Past eruptions of Pliocene and Quaternary volcanic centers in the YMR were predominately mixed hawaiian and strombolian with minor hydrovolcanic eruptions. The occurrence frequency of hydrovolcanic eruptions is estimated to be <10%, particularly for areas of deep groundwater. There is a high probability (>95%) that future volcanic activity will occur within the distribution area of past volcanic events (the YMR), a high probability (> 90%) that future events will occur within the Crater Flat volcanic zone (CFVZ), and a lesser probability of occurring in a northeast-trending structural zone (67%). Future volcanic events are about 6 times more likely to occur in an alluvial valley or range front than in a range interior.

Four time intervals are used to assess recurrence models of volcanic events (E1). One interval of emphasis is the Quaternary epoch; both the current geologic definition (1.6 million years [Ma]) and the regulatory definition (2.0 Ma) are used. A more appropriate and preferred approach is to identify time intervals for probabilistic assessment using cycles of volcanic activity in the YMR (volcanic record). Two intervals are emphasized. The first is the duration of the Younger postcaldera basalt cycle (4.8 Ma). The second is a somewhat arbitrary interval in the Quaternary that corresponds to a time of possible increased frequency of volcanic events (1.0 Ma). The volcanic events λ_i, λ_v, and λ_c are defined from the perspective of their impact on a geologic repository located about 300 m below the surface. A volcanic event is assumed to consist of the rapid emplacement of 1 to 3 dikes that feed surface volcanic eruptions. Any volcanic vent or center spaced over 5 km distance from another volcanic vent or center is presumed to represent a separate volcanic event. Events spaced less than 5 km are inferred to represent a single event unless field, geochronology, or geochemical data indicate the vents formed from time-distinct events or separate pulses of magma. Polygenetic volcanism represents a special subclass of volcanic events. A *polygenetic episode* is defined as an eruption at a preexisting volcanic center that is separated in time from the preceding *volcanic event* by an interval exceeding the residence time of basaltic magma in the shallow crust (decades). It is dependent on the occurrence of a preceding event defined as the formation of a new volcanic center and is therefore a subclass of λ_c. Probabilistic assessment of polygenetic episodes will be considered in future volcanism studies.

The most current data obtained from site characterization studies for the Pliocene and Quaternary volcanic record of the YMR are used in probabilistic risk assessment. The Quaternary volcanic record of the YMR includes three groups of volcanic centers. The Quaternary basalt of Crater Flat consists of one cluster event or two to five center events. Each event is estimated to be 1.0 ± 0.1 Ma. Polygenetic eruptive activity may have occurred at the Red Cone and Black Cone centers. The basalt of Sleeping Butte is treated as two individual centers formed in one cluster event and one or two center events. Existing geochronology data give a mean age of 350 ± 50 thousand years (ka) but are not considered to be definitive. A Pleistocene episode of polygenetic activity may have occurred at the Hidden Cone center. The Lathrop Wells volcanic center is treated as a single-event volcanic center with three associated polygenetic episodes. The initiating event is estimated to be about 100 to 130 ka. The first polygenetic episode followed at 80 to 90 ka, the second at 40 to 60 ka, and the youngest at 4 to 9 ka. The estimated uncertainty of the initiating event and first polygenetic episode is ± 35 ka, and the uncertainty of the second polygenetic episode is ± 40 ka. The uncertainty of the youngest polygenetic episode cannot be estimated with current data. Pliocene volcanic centers include the basalt of Thirsty Mesa (4.8 ± 0.13 Ma), the aeromagnetic anomaly of the Amargosa Valley (3.85 Ma), the aeromagnetic anomalies (two anomalies) of central Amargosa Valley (undrilled but presumed to be the same age as the aeromagnetic anomaly of the Amargosa Valley), the basalt of southeast Crater Flat (3.74 ± 0.10 Ma), and the basalt of Buckboard Mesa (2.9 ± 0.13 Ma).

Revised estimates of E1, the recurrence rate of volcanic events, are examined systematically using time-series analysis, homogeneous Poisson and nonhomogeneous Poisson models, and magma-output rates. Time-series analysis is limited by the small number of Pliocene and Quaternary volcanic events. Some bounds on estimates can be approximated by assessing event repose times. The *minimum* repose interval during the last 4.8 Ma is 200 ka and is equivalent to a recurrence rate of 5.2×10^{-6} events yr^{-1}. The mean estimate of the recurrence rate is 1000 ± 570 ka ($n = 6$) and provides little useful information. Homogeneous Poisson recurrence rates are examined for four time intervals, using event, cluster, and stress-dike event counts; estimates are obtained for the *minimum*, *most likely* and *maximum* recurrence rates. The mean recurrence rate for the *most likely* recurrence models is $3.5 \pm 1.3 \times 10^{-6}$ events yr^{-1}; the mean of all *minimum* recurrence rates is $2.0 \pm 0.6 \times 10^{-6}$ events yr^{-1} and the *minimum* or best case estimate is 1.5×10^{-6} events yr^{-1}. The mean of the *maximum* recurrence rates is $4.6 \pm 4.3 \times 10^{-6}$ events yr^{-1} and the

maximum or worst case recurrence rate is 8.0×10^{-6} events yr^{-1}. The mean recurrence rate for the *most likely* recurrence models using nonhomogeneous Poisson models is $4.6 \pm 1.8 \times 10^{-6}$ events yr^{-1}. The mean of the *minimum* recurrence rate is $3.0 \pm 1.2 \times 10^{-6}$ events yr^{-1} and the minimum or best case recurrence rate is 1.4×10^{-6} events yr^{-1}. The mean of the *maximum* recurrence rate is $5.5 \pm 2.4 \times 10^{-6}$ events yr^{-1}, and the *maximum* or worst case recurrence rate is 8.4×10^{-6} events yr^{-1}. The β (fitting parameter for the Weibull distribution) is < 1 for all recurrence models using intervals based on volcanic cycles and is consistent with *waning* volcanism during both the last 4.8 Ma and the last 1.0 Ma. Volumes of volcanic eruptions during the last 4.8 Ma (Dense Rock Equivalent) have decreased by greater than a factor of 30. Simple linear regression fits of magma volume versus time are unsatisfactory. Regression coefficients for different combinations of plots of magma volume versus time indicate strong correlations (squared multiple $R > 0.86$ for all but two cases). Linear regression models show that the basalt of Thirsty Mesa is an outlier. Residual plots show linearity and curvilinear structure. A log normalized regression model provides improved regression fits but the basalt of Sleeping Butte is an outlier and there is structure to the regression residuals. Future work will examine event location and magma chemistry as variables in multiple regression. Two linear regression cases give marginally acceptable fits and have slopes (magma-output rates) of 270 and 300 $m^3\ yr^{-1}$. These rates are used to calculate event recurrence times using different estimates of the volume of representative volcanic events. The only geological reasonable recurrence times are obtained for the mean volume of the *smallest* volume Quaternary eruptive events because of the 30-fold decrease in magma volumes through time. The mean estimate of the event recurrence rate is 3.4×10^{-6} events yr^{-1} for *preferred* models; *minimum* recurrence rates are 3.2×10^{-6} events yr^{-1} and *maximum* recurrence rates are 5.3×10^{-6} events yr^{-1}. Simulation modeling is used to assess recurrence rates for the YMR. The *median* estimates for eight recurrence models and five simulations using different boundary conditions (*minimum* and *maximum*) and distribution assumptions (trigen and normal distributions) vary from 3.6×10^{-6} events yr^{-1} to 5.5×10^{-6} events yr^{-1}.

Revised estimates of E2, the disruption probability, are examined systematically using spatial distribution models, structural models, and comparison with analog basaltic volcanic fields. Twenty-five spatial distribution models are evaluated. Eleven models are unlikely to result in repository disruption; three additional models are judged to have a low likelihood of resulting in repository disruption. The median estimate of the disruption probability for 14 spatial models (*including* the three unlikely models) is $3.1 \pm 1.5 \times 10^{-3}$ (dimensionless ratio). The median estimate for the 14 spatial models of the disruption probability is 4.6×10^{-4} if the models are weighted for the likelihood of volcanic events in range interiors. Seventeen structural models are used to estimate E2; four of the models include the Yucca Mountain site, one is judged to have a moderate likelihood of extending to the site, and the remaining 12 models are judged to have a low or improbable likelihood of extending to the potential site. The median estimate of the disruption probability for all models is $4.6 \pm 4.4 \times 10^{-3}$. The median estimate is 6.9×10^{-4} if the disruption probability is weighted for the likelihood of volcanic events in range interiors. The median estimate of intersection models (models that include the Yucca Mountain site) is $3.1 \pm 1.1 \times 10^{-3}$ ($4.7 \pm 1.6 \times 10^{-4}$ for range interiors). Structural models inferring northeast-trending structural controls of volcanic events *do not yield significantly higher* estimates for the disruption probability. Simple spatial analyses of the distribution of volcanic events in the Cima and Lunar Crater volcanic fields show that the degree of dispersion of volcanic events orthogonal to the elongation direction of the fields is comparable to the observed dispersion of vents in the YMR. If these fields are overlain on the YMR with their long dimension oriented parallel to the CFVZ, the observed dispersion of events in the analog fields would not result in penetration of the Yucca Mountain site. Simulation modeling is used to assess the variability in E2. A simulation matrix is constructed using five sets of model estimations for E2 and two subclasses for each model. The mean estimates of intersection models range from 3.1 to 4.6×10^{-3}; the mean estimates of the range interior models range from 4.7 to 7.7×10^{-4}.

The cumulative probability distributions for E1 and E2 are combined through risk simulation to give the cumulative probability distribution for the probability of magmatic disruption of the repository (Pr[E2 given E1]Pr[E1]). Two sets of simulation matrices were evaluated. The first uses two distribution curves for E2 (intersection and range intersection) and a range of distribution models for E1. The second uses a single distribution curve for E1 and varies distribution models for E2. The mean estimates for the first simulation matrix range from 2.2 to 2.6 x 10^{-8} events yr^{-1} for intersection models. The mean estimates of the second matrix range from 1.3 to 2.2 x 10^{-8} events yr^{-1} for intersection models and 1.9 to 3.4 x 10^{-9} events yr^{-1} for the range intersections models. However, the minimum and maximum estimates are much more variable for the second simulation matrix. The *maximum* estimates for the second matrix of the probability of magmatic disruption of the repository are the *largest* calculated for the YMR. Careful examination of the data shows that they result from spatial and structural models that have a very low likelihood of intersecting the potential repository site. Judgment is required to decide whether these models should be incorporated into probability estimates. A final set of estimations of the probability of magmatic disruption of the repository is evaluated for specific models of the probability of disruption (E2), because some spatial and structural models *exclude* volcanic events. A probability matrix was assembled and E1 recalculated for each spatial and structural model. The median estimate for all models using the revised estimates for E1 is 1.8 ± 1.6 x 10^{-8} events yr^{-1} (intersection models) and 2.7 ± 2.1 x 10^{-9} events yr^{-1} (range interior models) or smaller by 17% to a factor of 4 than the estimates of E1 that are not adjusted for specific spatial and structural models.

II. Introduction

Chapter 7 of this volcanism status report presents the results of volcanic hazard and volcanic risk assessment for the Yucca Mountain site current to the preparation of this report. The assessment builds on the data and methods for probability estimates from published studies (Crowe and Carr 1980; Crowe et al. 1982, 1983; Crowe 1986; Crowe et al. 1989; Crowe and Perry 1989; Smith et al. 1990; Ho et al. 1991; Wallmann et al. 1992; Crowe et al. 1992; Ho 1992; Connor and Hill 1993; Wallmann et al. 1993; Crowe et al. 1993) and adds the most recent results for data collected from site characterization studies. The term *volcanic hazard* refers to the perception of a peril or jeopardy from future volcanic events. The term *risk* is used to denote an attempt to quantify the magnitude of a volcanic hazard through either estimation of event probabilities or event consequences. The term *risk assessment* denotes formal evaluation of the probability of event occurrence combined with the consequences of that event. Most volcanism studies for the Yucca Mountain site have focused on estimating the *occurrence probability* of magmatic disruption of a repository; only a few studies have combined the occurrence probability with assessments of the *consequences* of a volcanic event (volcanic risk assessment). We use the formal definitions of these terms throughout this chapter to avoid confusion, and to discriminate between probabilistic assessment (occurrence probability) and *risk assessment* (occurrence probability combined with event consequences). The term *risk* is used when either the occurrence probability or consequences of a volcanic event have been determined; its usage does not require definition of both occurrence probability *and* consequences. Some authors use the term *hazard* to refer to the probability that a specific area will be affected by a volcanic eruption (Scandone et al. 1993). We prefer to use the term *volcanic hazard* less specifically, and use *probabilistic assessment* or *occurrence probability* to refer to probabilistic studies.

The primary emphasis of past volcanism studies was on gathering and evaluating data that would facilitate assessment of the potential disqualification of the Yucca Mountain site from the hazards of future volcanic activity (Crowe and Carr 1980; Crowe et al. 1982), recognizing that the DOE has the final responsibility for the assessment. The past assessments were based primarily on attempts to estimate the

occurrence probability of future volcanic events. One of the purposes of this report is to refine the occurrence probability of volcanic events for specific areas required for studies of the performance of the potential repository system and to aid the DOE in their continuing assessment of the Yucca Mountain site. To accomplish this task, a conditional probability model is described for future volcanic events in the Yucca Mountain region (YMR), and the logic of assessing the probability model through volcanism studies is presented. These studies are designed to test underlying assumptions and meet the data requirements of the conditional probability model. The volcanic record of the YMR that is applied to the volcanic model is defined carefully to avoid confusion in probability estimations. Assumptions needed to apply the volcanic record of the YMR to the probability model are described, and the basis for the assumptions is discussed from the perspective of the underlying volcanic processes. Probability estimations are assembled for a range of alternative recurrence and structural models of basaltic volcanism. The uncertainty of the probability range is defined by calculating cumulative probability distributions through simulation modeling. The cumulative probability distributions for the occurrence probability and the probability of disruption are integrated for the potential repository area, the controlled area, and the YMR. These probability distributions represent the best approximations, from a scientific perspective and using current data, of the likelihood of future volcanic events. These numbers *may differ* from those used by the DOE in formal assessments of the suitability of the Yucca Mountain site from a regulatory perspective.

This chapter of the volcanism status report focuses on revising assessments of the occurrence probability of magmatic disruption of a potential repository, the controlled area encompassing a potential repository, and the YMR. We use a slightly different perspective than past studies, including past studies by ourselves and other workers. Past volcanism studies attempted primarily to bound the occurrence probability of volcanic events. This was accomplished through identification of a range of values that could be assigned to attributes of the probabilistic assessment. If there was uncertainty involving assignment of data values, *conservative* values or values that would *not* underestimate risk were used (Crowe and Carr 1980; Crowe et al. 1982). Many assessments emphasized worst case or maximum estimates of volcanic occurrence probabilities (for example, Crowe and Carr, 1980; Crowe et al. 1982; Smith et al. 1990; Ho et al. 1991; Ho 1992; Connor and Hill 1993). In contrast, we initiate a perspective of assessing attribute values for probabilistic risk assessment that includes *most likely*, *minimum,* and *maximum* values for a range of alternative models of the geologic record of basaltic volcanism in the YMR. The identification of most likely values (midpoint estimates) avoids the addition of nonsystematic bias toward worst case calculations that are built unavoidably into calculations when only conservative attribute values are used. This bias results primarily from the absence of a standard definition of "conservatism" in the assignment of probability values. The choice of what constitutes "reasonable" levels of conservatism in assigning attribute values varies dramatically with the perspective of the assignee. This is especially true for an issue like assessing risk for a potential site for storage of high-level radioactive waste. The political and scientific sensitivities of the issue can lead to dramatic differences in probabilistic assessments for technical issues that could potentially disqualify the site. In contrast, assigning mean or most likely values for probability attributes are better defined. These values are chosen as unbiased descriptors of the central tendency of data distributions. They can be expressed as means, medians, or other appropriate univariate statistical descriptors. The uncertainty of estimates of the occurrence probability of volcanic events is assessed using simulation modeling incorporating the midpoint, minimum, and maximum estimates of probabilistic attributes (Crowe et al. 1993). Our primary goal in this work is to explore the range of probability estimates that can be supported scientifically from systematic examination of multiple alternative models of the volcanic record in the YMR.

The traditional and most common approach for defining volcanic hazards is to study the past record of volcanism at and around a site of interest (here the use of the term hazard refers to the perception of a peril or danger). These studies employ standard geological methods (field mapping, geochronology,

petrology, geochemistry, and geophysics). Information from the conventional studies is used to make subjective judgments about the hazards of future volcanism. This generally involves identifying the eruptive styles of past volcanic events, the area affected by past volcanic activity, and the range of hazards represented by similar future events. A general but not universal assumption of these studies is that future volcanic activity will follow the same patterns as past volcanic activity. This approach has utility for historically active volcanoes. Recent growth in world population has lead in the last several decades to occupation of land surrounding the flanks of many active volcanoes and created the need, often in a crisis situation, to assess volcanic hazards. However, that is a very different assessment than the probabilistic volcanic assessment conducted for the YMP. There is a higher degree of predictability for hazard assessment at historically active volcanoes. Generally, historically active polygenetic volcanoes are fed from a shallow magma chamber with an established magma feeder system. Alerts to impending eruptive activity or a volcanic crisis develop when there are changes in the volcano from movement of magma or introduction of new pulses of magma in a magma chamber or magma feeder system. The continued existence of the chamber through periodic magma replenishment results in a high chance that future volcanic activity will occur at or near the same vent areas. Often, eruptive patterns of new volcanic events are similar to past volcanic eruptions. The time perspective of volcanic hazard studies is months to years to decades.

The conventional approaches to volcanic hazard studies are not easily applied to the issue of defining risk for the long-term isolation of high-level radioactive waste. Here, the task of identifying the nature of a future volcanic hazard is obvious. It is the simple recognition that future volcanic activity could disrupt a buried repository and spread radionuclides to the accessible environment. A more pertinent and difficult question is how can the risk of the perceived volcanic hazard be quantified? The risk in most cases is not from another eruption at an existing volcano but from the birth of a new volcano that could erupt through or near a repository. The added uncertainties are that the volcanic risk is more difficult to define with respect to the timing and location of a future volcanic event and the risk must be defined for 10,000 yr.

Past basaltic volcanic activity in the YMR was characterized by the intermittent formation of spatially isolated, small-volume basalt centers of Pliocene and Quaternary age (Crowe 1986; Crowe and Perry 1989; Crowe 1990). The geochemistry of these lavas almost certainly is inconsistent with storage of magma in a shallow crustal magma chamber (see Chapter 4, this report). The basalts are aphyric to sparsely porphyritic and probably ascended rapidly from a depth below the plagioclase stability field (Perry and Crowe 1992). The most likely event from the perspective of volcanic hazards is the formation of a new pulse of magma that ascends through country rock beneath the YMR and intrudes or erupts at an uncertain location. There are unique problems in evaluating recurrence rates and predicting the spatial location for these type of future volcanic events (see Chapter 3). First, there is a limited number of past volcanic events (seven Quaternary volcanic centers). The record of events is insufficient to describe using conventional univariate statistics or to test null or alternative hypotheses using accepted measures of statistical significance. We can only approximate time-distribution models and attempt to construct probability calculations that do not underestimate risk (Crowe et al. 1993). Second, volcanic centers tend to occur within a narrow northwest-trending zone called the CVFZ (Crowe and Perry 1989). The most likely location of future events is in this zone. During the last 4.8 Ma, there were 19 volcanic events in the zone and only one event outside of the zone. The Pliocene basalt of Buckboard Mesa is located in the Timber Mountain caldera about 37 km northeast of the Yucca Mountain site; it is the only Plio-Quaternary center that occurs outside of the CFVZ. This raises a small but finite possibility that events could occur *outside* the CFVZ and possibly within Yucca Mountain (see Smith et al. 1990). Third, within the CFVZ, the location of subsequent volcanic events bears no simple relation to the location of preceding volcanic events (Crowe et al. 1993). Sites of successive volcanic events jump to new locations with no systematic patterns

to either their jump directions or jump lengths. The only observed pattern is a higher likelihood for events to remain within the CFVZ. Fourth, new volcanic events occur either as individual centers or as clusters of centers (Crowe and Perry 1989) and the lengths of the clusters vary from 2 to 13 km. The clusters tend to be aligned northeast, parallel to the maximum compressive-stress direction (Crowe et al. 1986; Crowe 1990). Locally, this direction is coparallel to faults in Yucca Mountain (Crowe and Carr 1980; Smith et al. 1990). The spatial patterns of Pliocene and Quaternary volcanic activity in the YMR lack the spatial predictability of repeated volcanic eruptions of a stratavolcano fed from a shallow and long-lived magma chamber.

A preferred strategy for attempting to quantify the risk of future volcanic events is to use a probabilistic approach; it has several distinct advantages over standard volcanic hazard studies. First, a probabilistic approach attempts to quantify a problem and provides a more objective basis for judging acceptable or unacceptable risks. In contrast, hazard studies identify zones where future volcanic events might occur with subjective descriptions of the nature of the hazard. Second, a probabilistic approach brings a structured formalism to the problem. This allows a complex issue like predicting the risk of future volcanism to be subdivided into logical sections with set rules for combining the results of each section. Precise answers cannot always be given for each aspect of a probabilistic approach, but the probabilities can generally be bounded and decisions made whether the bounding data are acceptable or unacceptable. Third, an often unappreciated advantage of a probabilistic approach is flexibility. The importance of alternative models or different data interpretations can be assessed by examining how they change the probability distributions. Volcanic studies for the Yucca Mountain site require working with a small data set. The limitations of the data set make it likely, if not expected, that there will be alternative perspectives or models of the nature and risk of future volcanic activity. Moreover, by virtue of the limited data, it is very difficult to conclusively prove or disprove alternative models. Instead, the different models become important only if they change the probability distributions. Fourth, probabilistic studies are iterative. Once formulated, they can be refined readily with the addition of new data from site characterization studies. The results of the assessment can be upgraded continuously as new data are gathered. In fact, the test for judging the importance of new site characterization data is a determination of whether the new data change the probability distribution. Finally, the most important advantage of a probabilistic approach is it allows the data to be more readily assessed against the regulatory requirements for licensing of a repository.

There are three parts to this chapter of the volcanism status report. First, the probability models are described. The logic of application of the probability models to volcanic risk assessment for the Yucca Mountain site is presented. Much of the confusion and differences in assessing the probability of magmatic disruption of the Yucca Mountain site results from a lack of consistency in applying a probabilistic approach and stating clearly the assumptions used for that assessment. Second, the data set used for the probabilistic assessment is defined, the assumptions used in the data set are described, and the underlying physical models controlling interpretations of the record of basaltic magmatism are discussed. These data are applied to estimations of revised values of the probability of magmatic disruption of a potential repository located beneath the surface of Yucca Mountain. The midpoint, maximum, and minimum values of the distribution of probability attributes are estimated. Simulation modeling is conducted using these values to define the uncertainty of probability assessments. This section of the volcanism status report constitutes the formal initiation of the systematic process of probabilistic studies described in Study Plan 8.3.1.8.1.1, Probability of Magmatic Disruption of the Repository. The purpose of presenting these numbers is, again, to provide a scientifically defensible basis for probabilistic assessment of future volcanic events. The actual application of the data presented in this report to formal assessments of the Yucca Mountain site will be undertaken by the DOE.

The probabilistic estimates presented in this report are not final. There is always the possibility that new discoveries from continuing site characterization studies may change the results of the assessment of the risk of volcanism. However, the basic data and approach used for assessing the risk of volcanism (occurrence probability combined with consequences) for the Yucca Mountain site were described as early as 1980 (Crowe and Carr 1980) and formalized in 1982 (Crowe et al. 1982). Continuing reviews, evaluations, and questioning of these assessments have occurred for more than a decade. Reviews of the probability studies have focused on identifying differences in assumptions used to make probability calculations. In almost all cases, the different assumptions do not result in significantly changed probability distributions. There is and will continue to be a virtually unconstrained number of methods that can be used to construct volcanic probability calculations for the Yucca Mountain site. Because of the limited data set used for the calculations, there never will be complete agreement on the best or even the more appropriate method to use. Given this uncertainty, the only realistic test of the significance of alternative models is whether they lead to probability distributions that differ significantly from existing estimations.

III. Probability Model

The probability of magmatic disruption of a repository and release of radionuclides to the accessible environment *(Prdr)* is defined as a conditional probability:

$$Prdr = Pr(E3 \text{ given } E2,E1)Pr(E2 \text{ given } E1)Pr(E1), \qquad (7.1)$$

where *E1* denotes the recurrence rate of volcanic events in the YMR, *E2* denotes the probability that the future magmatic event intersects a specified area, and *E3* denotes the probability that magmatic disruption leads to rapid release of radionuclides to the accessible environment in quantities that exceed the regulatory requirements. This probability can be expressed mathematically as (Crowe et al. 1982):

$$\Pr[\text{no eruptive event before time } t] = exp(-\lambda tpr), \qquad (7.2)$$

where λ is the recurrence rate of volcanic events, p is the probability that an event is disruptive, and r is the probability that the radionuclide releases to the accessible environment exceed the regulatory requirements for licensing a repository. The λ can be defined in a number of ways (see following section on the definition of volcanic events). For this report, the volcanic event of emphasis is defined as the rate of formation of new volcanic centers, volcanic clusters, or magmatic intrusions. The p is defined as a/A where a is the area of concern (repository, controlled area, or YMR) and A is the area of the established volcanic rate or λ.

A basic assumption used in most applications of the probability model is a homogeneous or modified homogeneous Poisson distribution of the volcanic events in time and space (Crowe et al. 1982; Crowe 1986). A Poisson random variable with parameter $\lambda > 0$ has a probability density function (Devore 1987; Tuckwell 1988; Evans et al. 1993)

$$f(x) = \frac{e^{-\lambda}\lambda^{x}}{x!} \qquad (7.3)$$

The probability density function can be integrated over *(x1,x2)* to obtain the probability of X

$$\Pr\{x_1 < X < x_2\} = \int_{x_1}^{x_2} f(x)dx. \qquad (7.4)$$

A Poisson random variable has mean $E(X) = \lambda$ and variance = λ, (Tuckwell 1988; Evans et al. 1993). The Poisson distribution is a special case of the binomial distribution when n, the number of trials, becomes very large, and p, the event probability, becomes very small. The Poisson distribution is easier to calculate than the binomial distribution because $np = \lambda$, and λ is the rate of occurrence of events (Davis 1986). Critical assumptions of the Poisson distribution are that the events occur independently, they are exponentially distributed through time t, and the probability of more than one event occurring at the same time is vanishingly small (Davis 1986; Devore 1987). The rate parameter or intensity (λ) of a homogeneous Poisson process (HPP) is assumed to be independent of its interval or time; for a nonhomogeneous Poisson process (NHPP), λ is assumed to be a function of t, denoted as $\lambda(t)$ (Tuckwell 1988; Ho 1991). The versatility of application of the Poisson process is that individual nonPoisson processes often become Poisson when considered together (Tuckwell 1988; Olkin et al. 1994).

Crowe et al. (1992) reviewed recurrence models for volcanic events and discussed the rationale for choosing a simple Poisson model for probabilistic volcanic risk assessment for the YMR. Briefly, the model is conceptually simple, assumptions using this model are well defined, and potential errors can be constrained. The simple Poisson model is widely used in many volcanism studies (for example, De la Cruz–Reyna 1991; Scandone et al. 1993). The Poisson model is particularly appropriate and may be conservative for the case of the YMR where multiple lines of evidence indicate patterns of volcanism may be waning over the last 4.8 Ma (Vaniman and Crowe 1981; Crowe et al. 1982; Crowe et al. 1992; Perry and Crowe 1992). Finally, a homogeneous Poisson distribution is used because the data set (number of past volcanic events) is too limited to apply statistical tests to select or justify use of other distribution models. The limited data set means that application of other distribution models can neither be proved nor disproved. Basically, a homogeneous Poisson model is used because it requires the fewest assumptions in probabilistic estimations.

There has been and continues to be debate in the geologic literature concerning the suitability or nonsuitability of the use of homogeneous Poisson distribution for modeling volcanic recurrence rates. Clearly this debate will not be resolved using the limited data set of Pliocene and Quaternary volcanic events in the YMR. A far more important issue than a debate over a choice of distribution models is whether probabilistic assessments can be structured using a homogeneous Poisson model (or any other model) so that they do not *underestimate* the risk of volcanism. The choice of homogeneous or nonhomogeneous Poisson distribution models has received lengthy discussion (Ho et al. 1991; Ho 1991, 1992; Connor and Hill 1993). This discussion continues *despite* minor differences in the probability estimates of magmatic disruption of the potential repository for nonhomogeneous Poisson distribution models compared to homogeneous Poisson models. Again, this tangential debate cannot be resolved with the small data set of volcanic events in the YMR. It diverts attention from the more important topic: the interpretation of the meaning of the probability estimates. To attempt to limit debate over the choice of distribution models, and to emphasize the more important issue of the interpretation of probability estimates, we present and discuss the application of nonhomogeneous Poisson models for the volcanic record of the YMR.

Several geologic assumptions are required to apply a probabilistic approach to the Yucca Mountain site. First, the past record of basaltic volcanic activity in the YMR is assumed to be the most reliable indicator of the rates and nature of future volcanic events. This means that the record of basaltic volcanism in the YMR is used as the primary basis for estimating and bounding future recurrence rates of volcanic activity. This assumption is supported by the consistency of the record of volcanism in the region for the last 10 Ma. All post-late Miocene volcanic centers formed from the eruption of small volumes ($\leq$1 km^3 of basaltic magma (Crowe 1990), except the basalt of Thirsty Mesa (3 km^3). The small-volume volcanic

activity occurred at spatially isolated centers comprising scoria and spatter cones, fissure systems, and associated lava flows. The primary emphasis of probabilistic assessment is on the last 4.8 Ma, the youngest cycle of the Postcaldera basaltic volcanic episodes (Crowe 1990; see Chapters 2 and 3).

Second, we assume there has been a sufficiently detailed study of the YMR to identify all Quaternary volcanic centers. This assumption is based on several lines of evidence and may be changed pending the results of further site characterization studies. Quaternary basaltic volcanic centers are conspicuous geomorphic landforms in arid regions of the southwest United States (Dohrenwend et al. 1986). They persist as prominent landforms for long periods of time. For example, Pliocene basalt centers in Crater Flat (3.7 Ma) are readily identified by the presence of scoria deposits with exposed feeder dikes (Vaniman and Crowe 1981; Crowe et al. 1983). The Pliocene and Quaternary basalt centers in the YMR can be identified through visual inspection of aerial photographs and even satellite photographs. Detailed geologic mapping has been completed of the areas near and surrounding the Yucca Mountain site. The presence and location of Quaternary volcanic centers in the region have long been recognized and their identifications have remained unchanged for several decades. Third, detailed drape aeromagnetic surveys were completed for the YMR (Kane and Bracken 1983; Langenheim et al. 1991, 1993). Basaltic volcanic rocks have high magnetic susceptibility and are identified easily among the generally nonmagnetic Paleozoic rocks, and the alluvial fill of the basins flanking Yucca Mountain (Kane and Bracken 1983). Surface Pliocene and Quaternary volcanic centers form prominent anomalies in aeromagnetic data (Crowe and Carr 1980; Kane and Bracken 1983; Crowe et al. 1986; Langenheim et al. 1991; 1993). The detection of buried basalt centers or basalt intrusions may be more difficult in volcanic bedrock where the country rock has higher magnetic susceptibility. We are developing field and laboratory experiments to test the depth and resolution of detection of basalt intrusions through application of aeromagnetic, ground magnetic, and geophysical studies which will be conducted for continuing site characterization studies. However, undetected basalt centers are not expected to be a major problem for two reasons. First, a basaltic event must ascend to depths at or near a repository to adversely affect the waste isolation system (300 m). Basalt magma at these depths typically exsolves volatiles, and the volatile exsolution provides a strong driving force, pushing the magma toward eruption (Wilson and Head 1981). Second, we have examined basalt intrusions at all known sites of intrusions in the YMR (Crowe et al. 1986; Crowe 1990; Valentine et al. 1992). Every *known* site *in the YMR where intrusions are observed* is associated with a site or sites of surface volcanic rocks formed from contemporaneous eruptions. The recognition of Pliocene and Quaternary volcanic activity when they are recorded in the geologic record by eruptions is not a difficult task. Third, the existence of undetected basalt intrusions requires that they are either deep, small, or a combination of both. As the depth of an intrusion below the surface increases and the size decreases, the likely effect of these bodies on a waste isolation system decreases.

The issue of undetected basalt centers or intrusions has been raised repeatedly in informal and formal comments by the Nuclear Regulatory Commission (NRC). The possibility of undetected features is an issue that obviously must be considered in site characterization studies. Moreover, it is an issue that is a difficult to assess (by definition). Existing geophysical data provide partial control for this issue. Six aeromagnetic anomalies have been identified in the YMR that could be buried basalt centers or intrusions (Crowe and Carr 1980; Kane and Bracken 1983; Crowe et al. 1986). Three of these sites have been drilled and shown not to be produced by Quaternary basaltic volcanic rocks (see Chapter 2). Additional geophysical studies are planned to assess the presence of undetected features. New data will be incorporated, if required, in future revisions of volcanic probabilistic assessment. Probabilistic assessment of volcanism for the Yucca Mountain site follows an iterative approach. Each step of probability assessment of volcanism is evaluated on the basis of *existing information*. Conclusions at each step are as reliable as the current status of the site characterization studies. The conclusions apply obviously only to

data used for an assessment. As new information is obtained, it is easy to reassess and evaluate the probabilistic estimates.

Finally, we assume that the observations and interpretations of the geologic record are reliable, an assumption that is difficult to quantify. Here there are three sources of uncertainty. First, and by far the largest area of uncertainty, is differences in opinion concerning interpretations of the geologic record. Experience has shown already that a range of differences exists in interpretation of existing site data for the record of basaltic volcanism. There is controversy concerning eruptive models for individual volcanic centers (Turrin et al. 1991). Different interpretations of the structural controls of sites of basaltic volcanism have been presented (Smith et al. 1990). There is even some disagreement over the definition of what constitutes a volcanic event (Ho et al. 1991; Ho 1992; Connor and Hill 1993). The limited number of volcanic events in the YMR makes it difficult to resolve or discriminate conclusively different interpretations. Thus, different interpretations of the geologic record have to be resolved through using multiple alternative models in probabilistic assessment. This will be a source of uncertainty in all stages of probabilistic evaluations. Second, the primary method for dating of Quaternary basaltic volcanic rocks is the K-Ar method. The method becomes increasingly less precise with decreasing age of the rocks. However, this problem can be mitigated partly by using multiple chronology methods. Additionally, we assign multiple models for the age of volcanic events where there is uncertainty in age determinations. Third, the reliability of interpreting the record of basaltic volcanism decreases with increasing age of the volcanic centers. This is because older centers are progressively more modified and parts of the record of volcanic events are eroded or covered. To reduce this uncertainty, we have attempted to reconstruct original volumes, have drilled exploratory holes, and used aeromagnetic and ground magnetic data to estimate the areal extent of buried basalt units (Crowe et al. 1983a,b). Additionally, we accommodate this uncertainty by varying the assumptions of the eruptive models and the volume determinations for the probability calculations.

IV. Strategy For Assessing The Volcanism Issue

There are two fundamental questions that must be answered to determine if volcanism is a significant issue with respect to a potential repository at Yucca Mountain. These are:

1. What are the probability and consequences of a range of future volcanic scenarios that could affect either the waste isolation system of a repository, or the repository itself?

2. Should the Yucca Mountain site be disqualified solely on the basis of the risk of future volcanism? *(Note: We use the term disqualification in reference to the risk of future disruptive volcanic events that could eliminate the Yucca Mountain site from further consideration as a site for isolation of high-level radioactive waste. Volcanism data described in this report will be one of multiple data sets the DOE will use to determine whether the site should or should not be disqualified. The suitability of the site is a more complicated and broader issue.)*

Assessment of both of these questions requires information from two classes of volcanic events. The first is what is referred to as the eruptive events. This is a category of volcanic activity that includes eruptive events. These events could lead to immediate releases of magma-transported radioactive waste at the surface. Eruptive processes are rapid, and represent a potentially catastrophic threat to the isolation system of a repository compared to the required 10,000-yr isolation period. The eruption event requires intersection or near-intersection of a potential repository for ascending magma to incorporate *directly* radioactive waste prior to eruption. Establishing the occurrence probability of magmatic disruption of the repository and surrounding area is the *primary emphasis* of this report.

The second category of volcanism events is disruption or modification of the repository or isolation system from the effects of intrusions accompanied or not accompanied by an eruption. Here, emplacement of magma into or through the controlled area or immediate vicinity of the repository could result in changes in the long term performance of the natural barriers of a waste isolation system. This is a more complicated problem than a determination of the occurrence probability of an eruptive event. It requires identifying the occurrence probability of the event and the range of secondary or coupled processes caused by the intrusion of magma into or near a repository. The effects of these events must be projected over the required isolation period of a repository. The probability of an intrusive event is defined somewhat differently than the eruptive event because of a potentially larger or more complicated subsurface geometry of an intrusive event. The significance of this second category will be evaluated through a combination of estimating their occurrence probabilities and the consequences of their induced effects. Again, the emphasis of this report is on the occurrence probabilities of *eruptive* events.

The logic of assessing the volcanism issue is illustrated on figure 7.1. Volcanism studies have sequential decision points that determine the priority of site characterization studies. The decision points determine whether the scenario categories need studies only of the occurrence probability, or whether the consequences or releases must also be assessed (Fig. 7.1). The primary basis for decisions is an assessment of whether the initiating volcanic events can or cannot be shown to have a probability of occurrence of less than 1 in 10,000 in 10,000 years (10^{-8} yr^{-1}). This criterion, which was part of Appendix B of 40 CFR191, is currently under review, and may or may not continue to apply. If this criterion is changed or removed, we will reassess the logic of volcanic studies on the basis of the revised regulations. At this phase of study, the 10^{-8} yr^{-1} criterion is used only to establish priorities in *volcanism studies.*

If volcanic events have an occurrence probability of $<10^{-8}$ yr^{-1}, they will be judged not to be an issue that could lead to disqualification of the Yucca Mountain site *(Note: the judgment of nondisqualification may or may not eliminate the events from consideration for their contribution to the cumulative releases from the waste isolation system. This decision will be based on assessments of the overall performance of a waste isolation system).*

If the events have an occurrence probability of $>10^{-8}$ yr^{-1}, a two-step logic sequence will be used to assess the significance of the events. First, the occurrence probability will be evaluated that the event will occur and will result in immediate releases to the accessible environment that exceed regulatory requirements. If the occurrence probability of exceeding allowable releases is $<10^{-8}$ yr^{-1}, the event will be judged *not* to be an issue that could lead to disqualification of the Yucca Mountain site. If the occurrence probability of exceeding allowable releases is $>10^{-8}$ yr^{-1}, studies will be undertaken to establish the contribution of volcanic-driven releases to the cumulative releases from the waste isolation system. Studies of the release component of magmatic-induced radiological releases are *not the subject of this volcanism report.* Volcanism studies for Study Plan 8.3.1.8.1.2, Physical Processes of Magmatism and Effects on the Potential Repository, provide the information needed to identify and evaluate the secondary effects of magmatic activity on the waste isolation system. The calculation of the radiological releases from secondary or coupled effects of magmatic activity will be undertaken as part of performance assessment studies.

There are several key questions that must be answered to assess the data needed for evaluating the risk of future volcanism. The first is whether igneous activity is a concern for the Yucca Mountain site (Fig. 7.1)? The DOE has established that the presence of five Quaternary volcanic centers in the vicinity of Yucca Mountain is a potentially adverse condition and requires assessment as a part of site characterization activities (DOE 1986, 1988). The affirmative answer to that question means that the probability of a future

volcanic event in the Yucca Mountain region is >5 x 10^{-7} events yr^{-1}, or one igneous event in the Quaternary (Crowe et al. 1993; the calculation uses a definition of 2.0 Ma for the Quaternary period as recommended by the NRC).

The next questions are interlinked. First, what is the range of possible future volcanic events? Second, what is the probability of each type of volcanic event? The latter question must be answered first, because the recurrence probability may differ for different volcanic events. The λ is defined as the recurrence rate of volcanic events. It is divided into subsets, including: (a) λv, the recurrence rate for formation of a *new* volcanic center, (b) λc, the recurrence rate for the formation of *clusters* of volcanic centers, and (c) λi, the recurrence rate for formation of magmatic *intrusions*. Defining the recurrence probability for these three subsets is a goal of this volcanism status report. Other subsets of λ that will require additional study include λp, the probability of polygenetic volcanic events (formerly called polycyclic events; Crowe et al. 1988, 1992a) and λce, the probability of formation of intracluster events, given the initiation of a future cluster event (λc).

Current site characterization information combined with simple logic requires that $\lambda i > \lambda v > \lambda c$. This follows from:

1. The number of volcanic clusters in the Pliocene and Quaternary in the YMR is less than the number of volcanic events (Crowe and Perry 1989; Crowe et al. 1994).

2. Magma rises through the crust along intrusive feeder dikes or more complex intrusive forms (Crowe et al. 1983b; Valentine et al. 1992). Therefore each volcanic event must be accompanied by at least one intrusive event.

3. The acceptance of (2) requires that λi must be $\geq \lambda v$.

Interpretation of current site data (described above) leads to the conclusion that $\lambda i \cong \lambda v$. However, this conclusion is regarded as preliminary for two reasons. First, as noted above, every known locality in the YMR where basaltic intrusive rocks of Cenozoic age have been identified is associated with contemporaneous surface basaltic volcanic rocks. A cautionary note with that statement is that exposure of intrusive rocks requires considerable erosion (generally >100 meters). Erosion of the Pliocene and Quaternary age volcanic centers is insufficient to assess whether there are extensive intrusive rocks (intrusions larger than simple feeder dikes) associated with these centers. Aeromagnetic data for Crater Flat and the Amargosa Valley show that there is no evidence of basaltic intrusions extending beyond the dimensions of surface outcrops of Quaternary basalt centers (Kane and Bracken 1983). However, intrusions are possible directly beneath the centers where their aeromagnetic signature could be masked by the surface volcanic rocks. Second, there are an insufficient number of sites where intrusions are exposed to assess the frequency of occurrence of *extensive* intrusive rocks (intrusions of more complex geometry than linear feeder dikes) below the Pliocene and Quaternary basalt centers of the YMR. There are six sites of Cenozoic basaltic volcanism in the southwest Nevada volcanic field (a notably larger area than the YMR) where at least part of the country rock beneath basalt centers are exposed. Basaltic intrusions more complicated than simple feeder dikes have been identified at two of those sites. These are the Paiute Ridge area of the Half Pint Range (Crowe et al. 1983; Valentine et al. 1993) and the southern center of the basalt

Fig. 7.1 Diagram of logic used to study the risk of volcanism for the YMR.

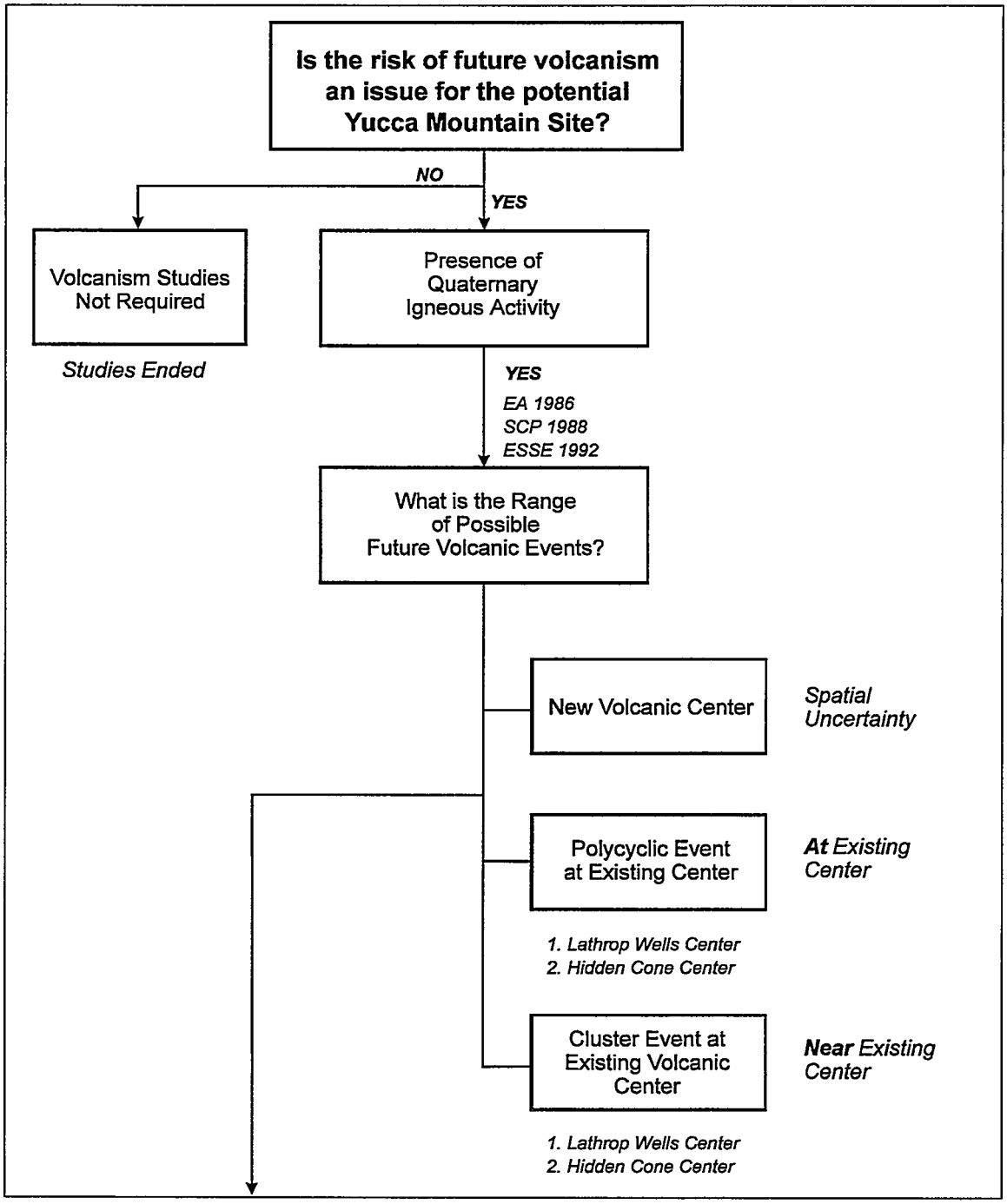


Fig. 7.1 (cont.)

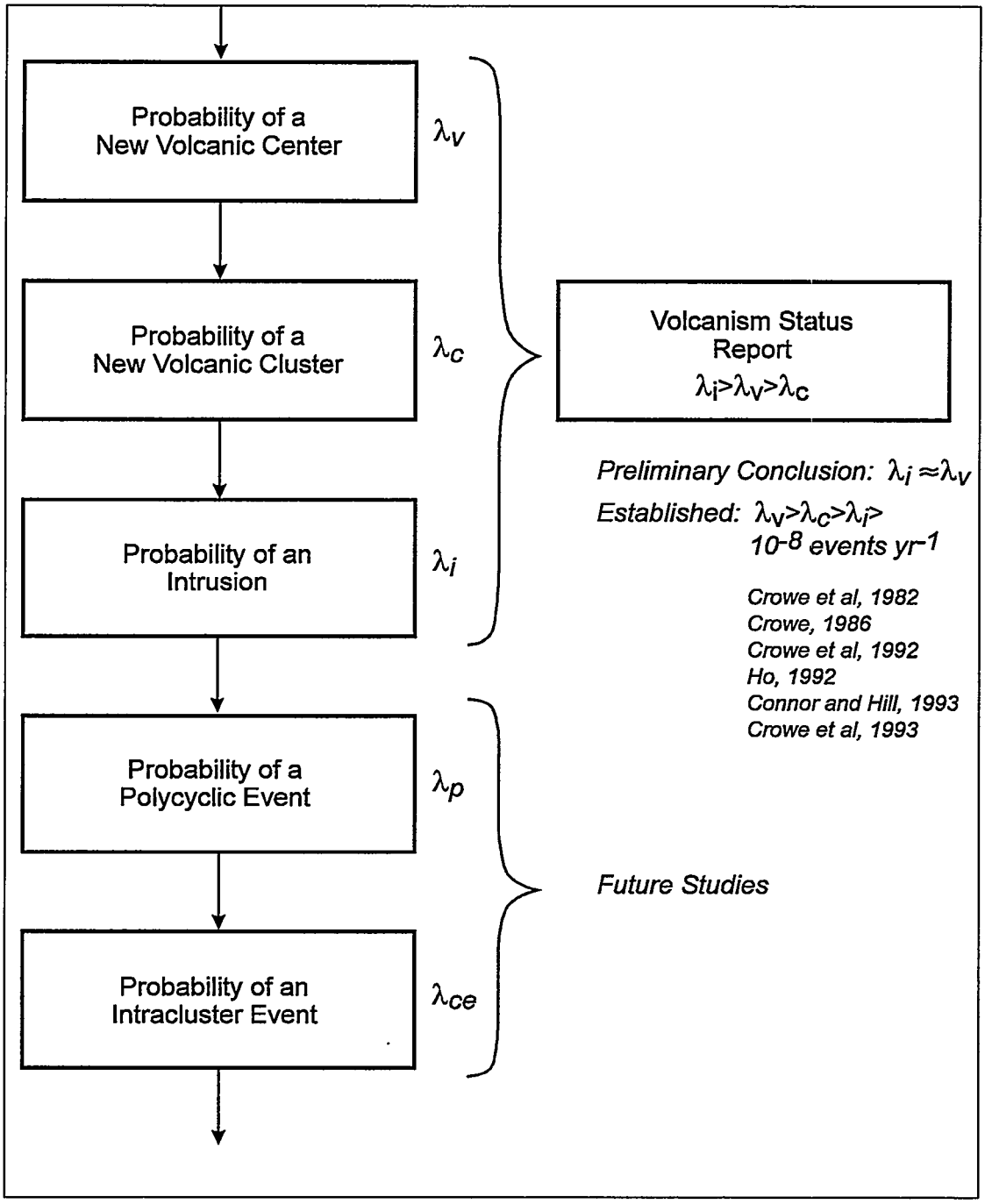

Probability of a New Volcanic Center
λ_V
Probability of a New Volcanic Cluster
λ_C
Probability of an Intrusion
λ_I
Probability of a Polycyclic Event
λ_P
Probability of an Intracluster Event
λ_{CE}
Volcanism Status Report
$\lambda_I > \lambda_V > \lambda_C$
Preliminary Conclusion: $\lambda_I \approx \lambda_V$
Established: $\lambda_V > \lambda_C > \lambda_I >$ 10^{-8} events yr^{-1}
Crowe et al, 1982
Crowe, 1986
Crowe et al, 1992
Ho, 1992
Connor and Hill, 1993
Crowe et al, 1993
Future Studies

Fig. 7.1 (cont.)

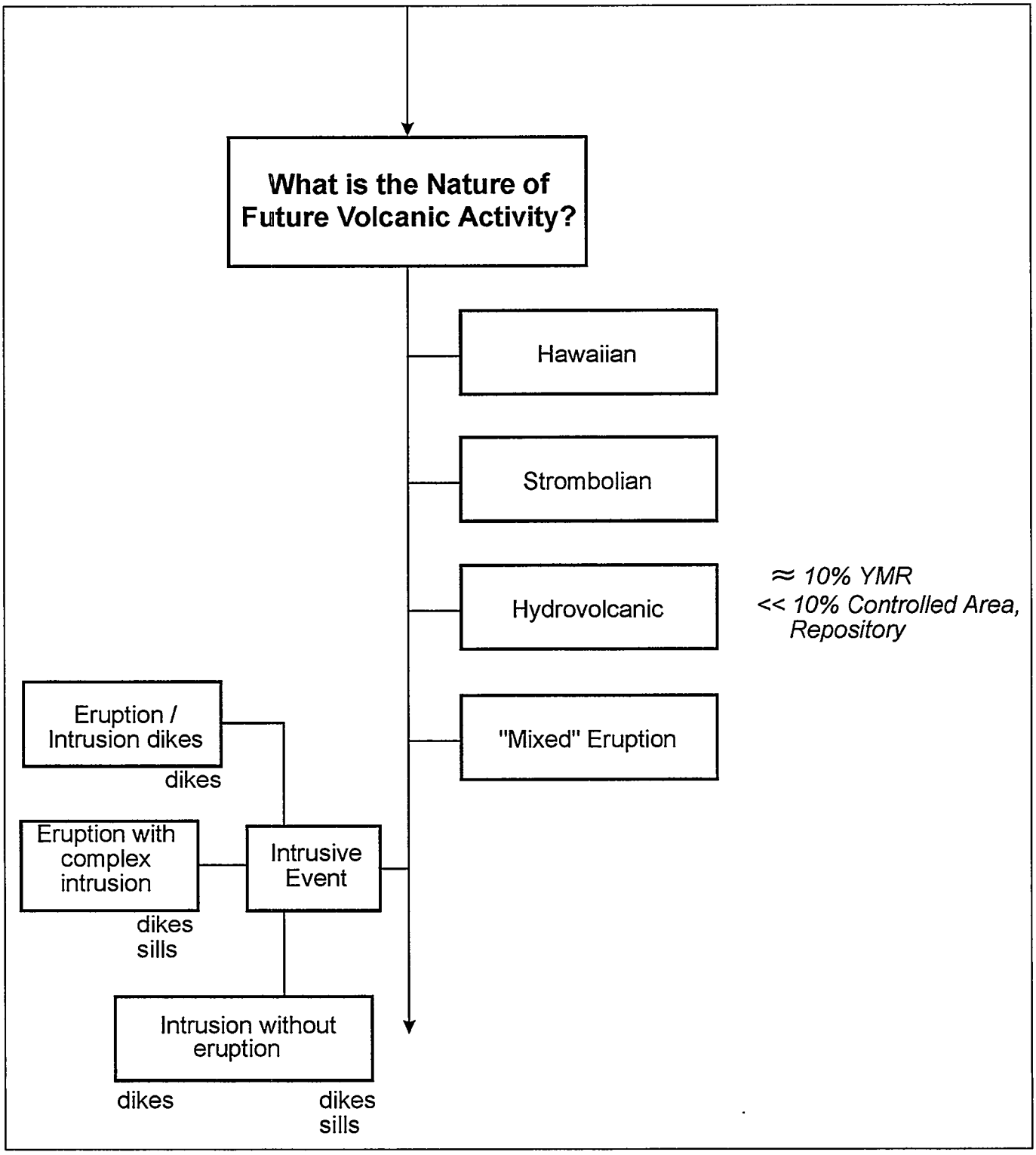

What is the Nature of Future Volcanic Activity?
Hawaiian
Strombolian
Hydrovolcanic
"Mixed" Eruption
≈ 10% YMR
<< 10% Controlled Area, Repository
Eruption / Intrusion dikes
dikes
Eruption with complex intrusion
dikes
sills
Intrusive Event
Intrusion without eruption
dikes
dikes
sills

Fig. 7.1 (cont.)

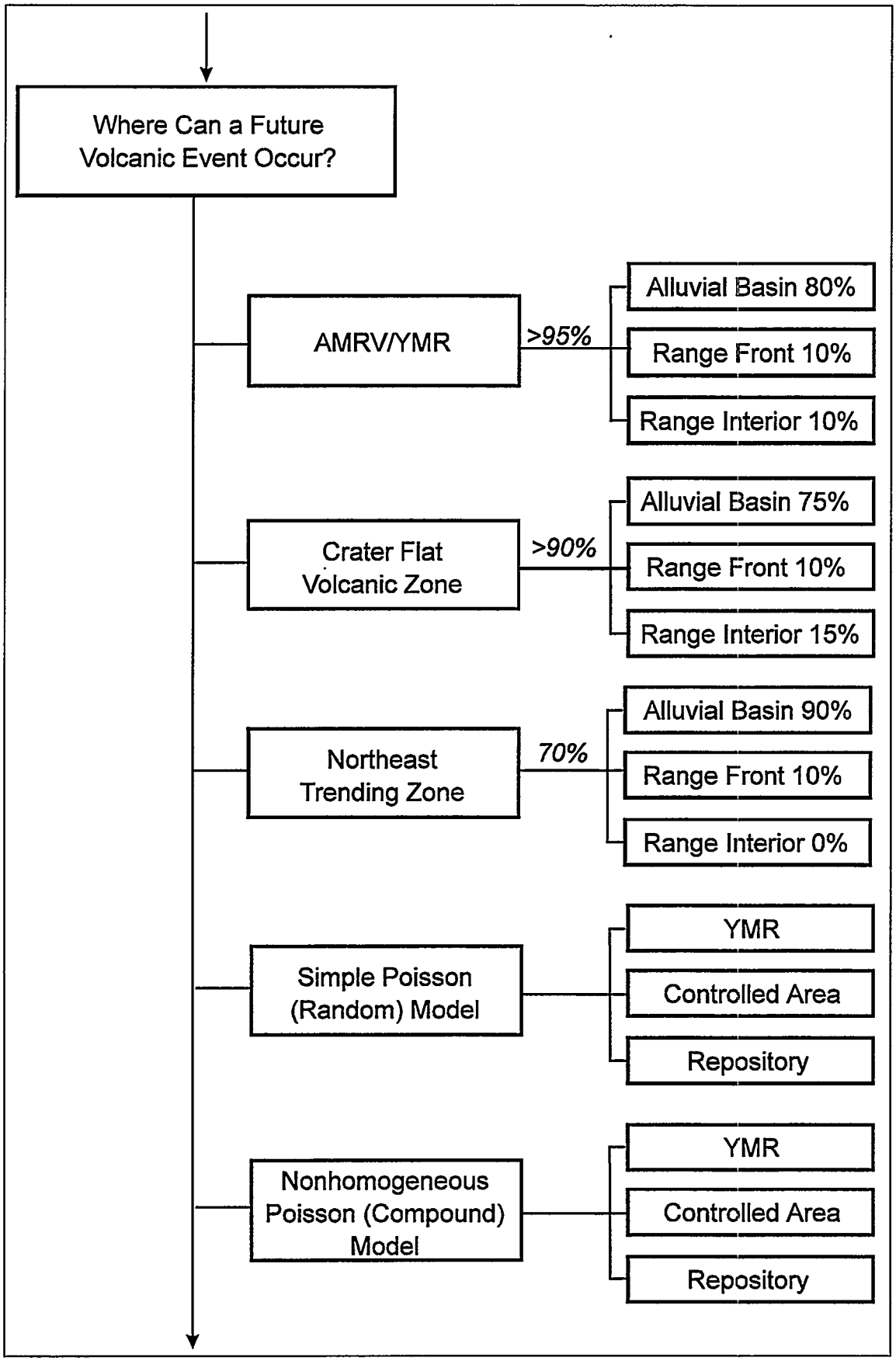
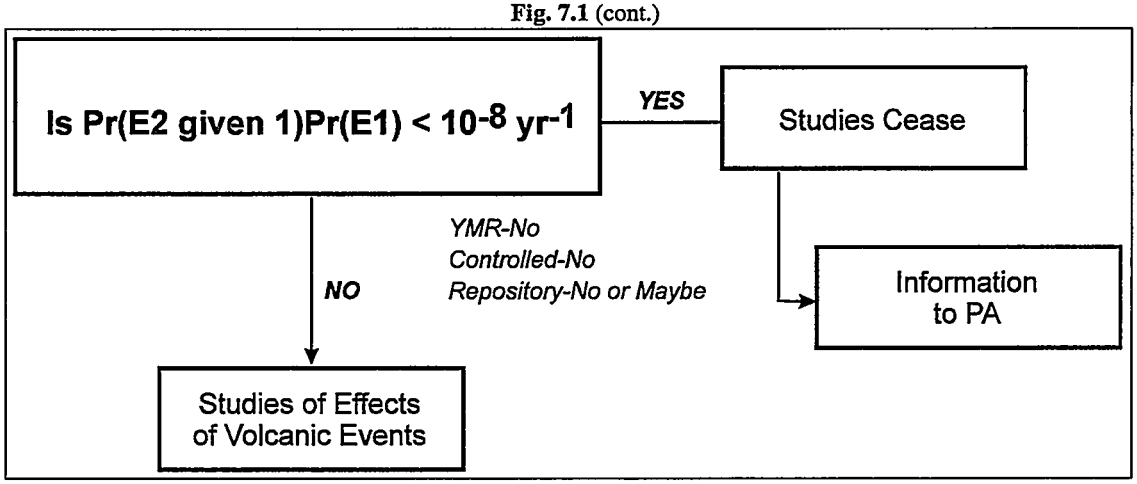

Where Can a Future Volcanic Event Occur?
AMRV/YMR
>95%
Alluvial Basin 80%
Range Front 10%
Range Interior 10%
Crater Flat Volcanic Zone
>90%
Alluvial Basin 75%
Range Front 10%
Range Interior 15%
Northeast Trending Zone
70%
Alluvial Basin 90%
Range Front 10%
Range Interior 0%
Simple Poisson (Random) Model
YMR
Controlled Area
Repository
Nonhomogeneous Poisson (Compound) Model
YMR
Controlled Area
Repository

Fig. 7.1 (cont.)



of Nye Canyon. These conclusions will continue to be tested through ongoing field and geophysical studies. They are an important part of planned studies for Study Plan 8.3.1.8.1.2, Physical Processes of Magmatism and Effects on the Potential Repository. The conclusions will be changed if required by new data. *Because $\lambda i \cong \lambda v$, the remaining discussion will only mention λv recognizing that the described assessments may or may not apply to both events.*

By definition (the presence of Quaternary igneous activity in the YMR):

$$\lambda v, \lambda c, \lambda i > 10^{-8} \text{ events yr}^{-1}. \qquad (7.5)$$

The next important question is what type of volcanic activity can occur? This must be answered by examination of the volcanic record. Table 7.1 is a compilation of the predominant eruptive style of Pliocene and Quaternary basaltic volcanic centers in the YMR. Eruptive activity at basaltic volcanic centers in the YMR has been mostly mixed hawaiian and strombolian, with locally important hydrovolcanic eruptions. Further, there are some general patterns, in time and space, for the occurrence of different types of volcanic eruptions. Pliocene volcanic eruptions were mostly of hawaiian type, with higher eruption volumes (>0.5 km^3) and a low ratio of pyroclastic deposits/lava compared to the total erupted volume (Crowe et al. 1983b). Quaternary eruptions were of mixed hawaiian-strombolian type, volumes were low (<0.1 km^3), the morphology of lava flows are consistent with low effusion rates, and the ratio of pyroclastic deposits/lava volumes for these eruptions was greater than the Pliocene eruptions. Hydrovolcanic eruptions occurred at one center (Lathrop Wells center) and are possible at some of the Quaternary and Pliocene basalt centers of Crater Flat. The volume of hydrovolcanic deposits is minor at all centers (<0.05 km^3). The groundwater table is relatively shallow at the Lathrop Wells volcanic center (< 100 m) where hydrovolcanic eruptions occurred in three of the four eruptive episodes.

Future eruptions in the YMR would be expected to form small volumes of predominantly blocky aa lava, and the pyroclastic component would be expected to be of mixed hawaiian-strombolian type with strombolian eruptions dominating. The occurrence frequency of hydrovolcanic eruptions is estimated to be <10% (very approximate estimate) and may be even less for areas of deep groundwater, like Yucca Mountain (<<10%). Smith and Luedke (1984) estimated that hydrovolcanic eruptions occur in about 10% of volcanic eruptions in the western United States. Hasenaka and Carmichael (1985) noted that hydrovolcanic centers (tuff rings or tuff cones) form <3% of the Michoacan-Guanajuao volcanic field of central Mexico (22 of 913 basaltic volcanic centers). There is a relatively high probability

Table 7.1 Eruption characteristics of Pliocene and Quaternary volcanic centers in the YMR.

Volcanic Center	Events	Lava Eruptions	Effusion Rate	Hawaiian	Pyroclastic Strombolian	Eruptions Hydrovolcanic
Basalt of Thirsty Mesa	1 to 3	Mesa or Shield	High	90%	10%	None
Pliocene basalt, SE Crater Flat	1 to 5	Aa lava sheets	Moderate	70%	30%	Minor?
Basalt of Buckboard Mesa	1	Mesa/Aa lava sheet	High	70%	30%	None
Quaternary Crater Flat	1 to 5	Blocky aa	Low	30%	70%	Minor?
Sleeping Butte	1 to 2	Blocky aa	Low	30%	70%	None
Lathrop Wells	1	Blocky aa	Low	20%	75%	5%

(estimated to be >95%; Table 7.2) that any future event will occur within the distribution area of past volcanic events. Figure 7.2 illustrates the basis for this assumption. The spatial area defined by the locations of the sequence of three sets of Pliocene volcanic events in the YMR (4.8 to 2.9 Ma) outline an irregular polygon bounded on the northwest by the basalt of Thirsty Mesa, on the south and southeast by the aeromagnetic anomalies in the Amargosa Valley, and on the north and northeast by the basalt of Buckboard Mesa (Fig. 7.2). All subsequent volcanic events (3 sets of Quaternary volcanic events) occurred near or within the bounds of that area (Fig. 7.2). The area encompassed by the distribution of Pliocene and Quaternary volcanic events on Figure 7.2 is designated as the YMR; it is slightly larger than but similar to the Area of Most Recent Volcanism (AMRV) of Smith et al. (1990). Second, based on the past record, there is a >90% probability that a future volcanic event will occur within the CFVZ (Table 7.2; Fig. 7.2). There have been 19, possibly 20, volcanic events (see following section for a definition of a volcanic event) in the YMR during Pliocene and Quaternary. One volcanic event, or 5%, occurred *outside* the CFVZ. Third, if an event did occur outside the CFVZ, it would probably occur within a less-well defined, northeast-trending zone (Carr 1990; Smith et al. 1990). Of the 20 Pliocene and Quaternary volcanic events in the YMR, 15, or 75%, are in the northeast-trending zone, and 5 events, or 25%, are outside the northeast-trending zone; the CFVZ is a more consistent predictor of sites of volcanic activity than the northeast-trending zone (Table 7.2). Finally, the distribution of past events suggests that a future event is about six times more likely to occur in an alluvial valley or along a range front than in a range interior (75% of the centers occur in alluvial basins, 10% along range fronts, and 15% occur in a range interior) (Table 7.2).

A second approach to assessing recurrence rates and locations of future volcanic events is to use homogeneous and nonhomogeneous Poisson distribution models to describe the events. Multiple recurrence and structural models are used to assess the probability of a volcanic event in the YMR, the

Table 7.2 Structural and Topographic Setting of Pliocene and Quaternary volcanic centers/events in the YMR.

Geologic Unit	CFVZ	Other	NE Zone	Other	Alluvial Basin	Range Front	Range Interior
Thirsty Mesa #1	1			1			1
Thirsty Mesa #2	1			1			1
Thirsty Mesa #3	1			1			1
Amargosa Valley	1		1		1		
Undrilled Anomaly	1		1		1		
Undrilled Anomaly	1		1		1		
Anomaly CF	1		1		1		
Buckboard Mesa*		1	1		1		
Crater Flat 3.7#1	1		1		1		
Crater Flat 3.7#2	1		1		1		
Crater Flat 3.7#3	1		1		1		
Crater Flat 3.7#4	1		1		1		
Crater Flat 3.7#5	1		1		1		
Makani Cone	1		1		1		
Black Cone	1		1		1		
Red Cone	1		1		1		
Little Cones	1		1		1		
Little Black Peak	1			1	1		
Hidden Cone	1			1		1	
Lathrop Wells	1		1			1	
Totals	19	1	15	5	15	2	3
Group % CFVZ	95%	5%	--	--	75%	10%	15%
Group % NESZ	--	--	67%	33%	94%	6%	--

* The basalt of Buckboard Mesa has been classified by some workers as in a range-interior setting. However, the unit occurs in the moat zone of the Timber Mountain caldera, a basin-setting.

controlled area, and the potential repository block. We first examine the probability equations for a homogeneous Poisson distribution of events. The likelihood of the first option, a future volcanic or intrusive event in the YMR is:

$$Pr_o = 1 - exp(-\lambda tp), \qquad (7.6)$$

where Pr_o is the probability of intrusion or eruption in the YMR. The variables λ and p are defined using homogeneous distribution models. Further, the variable p is significant for the equation only for events close to the boundary of the controlled area. This variable drops out of the equation as the area of the event occurrence YMR gets large because a/A is $\cong 1$ as a approaches A. For this case, the annual probability of a volcanic event occurring in the YMR approaches λ, the recurrence rate of volcanic events. We have already established that λ is $>10^{-8}$ yr^{-1}. Therefore Pr_o is $>10^{-8}$ yr^{-1} for all cases of this option of the probability estimations. The significance of volcanic eruptions or magmatic intrusions in the YMR should be assessed through evaluation of secondary radiological releases. While this evaluation has not yet been completed, an obvious relationship is that *rs*, the probability of secondary releases exceeding the regulatory requirements associated with a volcanic event or intrusion in the YMR, decreases with increasing distance of the event from the repository. At some standoff-distance (d_s) from the repository, the likelihood of secondary effects resulting in radiological releases that exceed the regulatory requirements approaches 0. For these cases, the conditional probability of an eruptive or intrusive event occurring outside the controlled area *and* resulting in secondary releases that exceed the regulatory requirements is $<<10^{-8}$ yr^{-1}. One of the

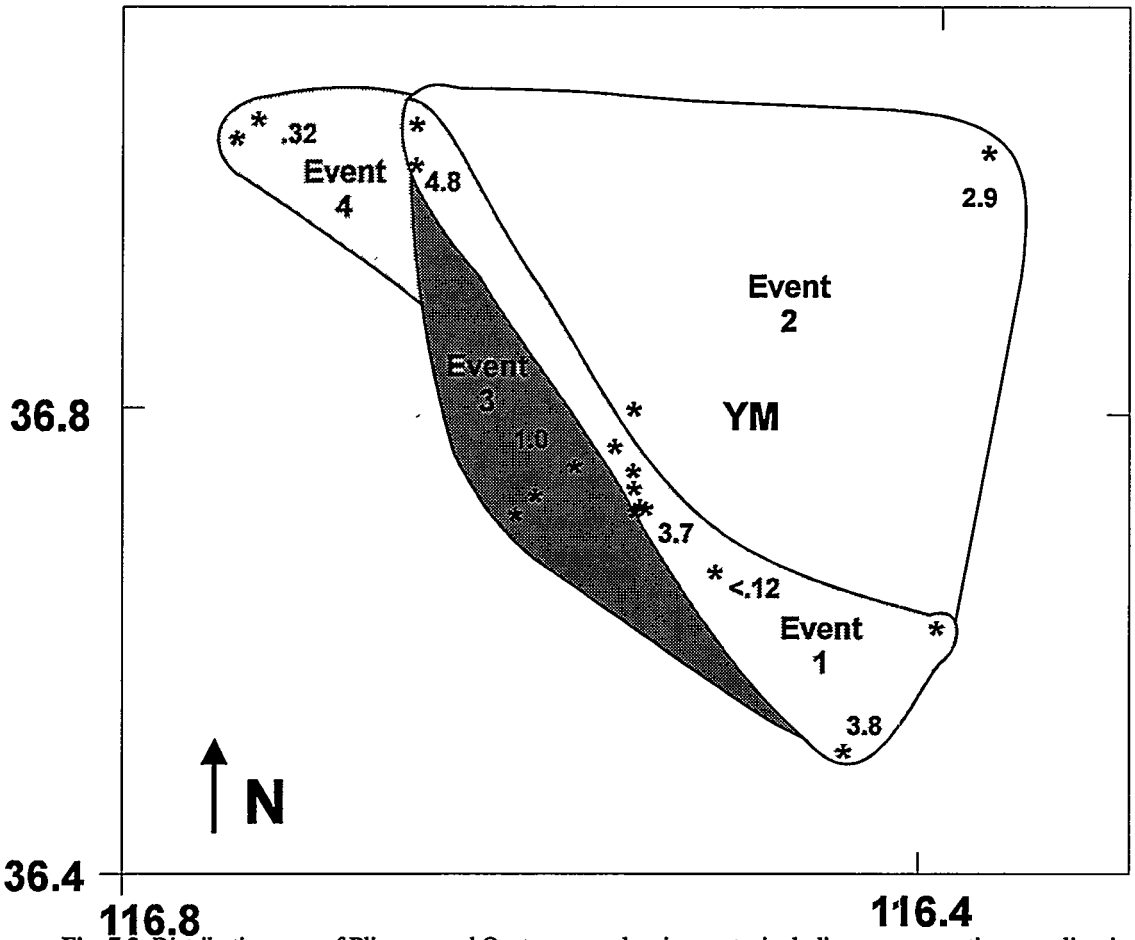


Fig. 7.2 Distribution area of Pliocene and Quaternary volcanic events, including aeromagnetic anomalies, in the YMR. Event areas are defined as the areas that enclose successive volcanic events. The four Pliocene volcanic Events (basalt of Thirsty Mesa, aeromagnetic anomalies of Amargosa Valley, basalt of southeast Crater Flat, and the basalt of Buckboard Mesa) define an irregular polygon that encloses the Yucca Mountain site (area of event 1 and event 2 of Fig. 7.2). All subsequent volcanic events are in or adjacent to the irregular polygon (Events areas for Events 3 and 4). The YM is the approximate location of the Yucca Mountain site.

goals of the studies of the secondary effects of magmatic processes on the waste isolation system is to identify the distances and directions where this relationship is satisfied.

The second option using homogeneous Poisson models is the likelihood of a future volcanic event in the controlled area:

$$Pr_{ca} = 1 - exp(-\lambda tp), \qquad (7.7)$$

where Pr_{ca} is the probability of intrusion or eruption through the controlled area and p is the a/A where a is the controlled area. The controlled area is larger than the area of the repository by slightly greater than a factor of ten.

The third option is a future volcanic event penetrating the repository. The likelihood of a future volcanic event penetrating the repository is:

$$Pr_d = 1 - exp(-\lambda tp), \tag{7.8}$$

where Prd is the probability of intrusion or eruption through the repository and p is a/A where a is equal to the area of the repository and A is the area of the volcanic recurrence rate. The value of a is likely to be somewhat larger than the area of the repository for the general case of linear feeder dikes because some events could be centered outside of the repository and have feeder dikes that extend into the repository (Crowe et al 1982; Connor and Hill 1993). Generally, this is a relatively small effect and is ignored in the probability estimations (Crowe et al 1982). It can be assessed easily by expanding the area of the repository. The dike effect is more important for assessing the consequences of volcanic events than their occurrence probabilities. We treat a simply as the area of the repository.

Finally, nonhomogeneous Poisson models can be applied to the three areas (YMR, controlled area, and the repository) using the same form of the above equations. However, λ is replaced in the equations with (λt), following the Weibull process models of Ho (1991, 1992). The distribution function of a Weibull process is (Tuckwell 1988; Evans et al. 1993)

$$F(t) = 1 - \exp^{(-\lambda t^{\rho})}, \tag{7.9}$$

which by differentiation gives the Weibull density function

$$f(t) = (\lambda\rho)t^{\rho-1}\exp^{(-\lambda tp)}, \tag{7-10}$$

where λ and ρ are distribution parameters and are ≥ 0. Ho (1991, 1992) uses a slightly different form of the Weibull process where

$$\lambda(t) = (\frac{\beta}{\theta})(\frac{t}{\theta})^{\beta-1}, \tag{7.11}$$

and β and θ are parameters of the Weibull distribution (WEI[θ,β]).

The DOE has judged in previous documents that the site is not disqualified solely because of the occurrence probability of magmatic disruption of the repository (DOE 1986, 1988; Younker et al. 1992). A primary goal of this report is to continue to reassess the basis for that judgment.

If Pr_d is $<10^{-8}$ yr^{-1}, the direct effects of repository disruption and eruption are not an important issue. A critical question for assessing this relationship is what constitutes an acceptable value of the probability of magmatic disruption of the repository. Is it the most likely value? Is it a confidence interval about the most likely value? Is it a determined percentage on a cumulative probability distribution? The answers to these questions are not provided in current regulatory guidelines for disposal of high-level radioactive waste.

If Pr_d is $>10^{-8}$ yr^{-1}, assessments will be conducted of the probability of direct releases of radioactive waste to the assessable environment by a volcanic eruption. This relationship is modeled as:

$$Pr_{dr} = 1 - exp(-\lambda tpr), \qquad (7.12)$$

where Pr_{dr} is the probability that radiological releases carried by future volcanic eruptions exceed regulatory requirements and r is the probability that volcanic eruptions release radionuclides to the accessible environment. This relationship does not apply to the probability of volcanic intrusion because this event may not result in direct releases of radionuclides to the accessible environment (*Note: An assessment of r for both extrusive and intrusive events is being conducted as part of Study Plan 8.3.1.8.1.2, Physical Processes of Magmatism and Effects on the Potential Repository).*

If $Pr_{dr} > 10^{-8}$ yr^{-1}, radiological releases from a volcanic event could exceed the regulatory requirements. The studies to establish that evaluation are described in Study Plan 8.3.1.8.1.2. Important parts of the effects studies are an evaluation of the abundance and depth of derivation of lithic fragments in basaltic volcanic deposits (Valentine et al. 1992, 1993). If these studies indicate that $Pr_{dr} > 10^{-8}$ yr^{-1} the recommendation will be made to the DOE that the radiological releases from volcanic events should be included as part of assessments of the cumulative releases from the waste isolation system over a 10,000-yr period. The logic of the choices of the studies required for assessment of Pr_{dr} is critically dependent on r. If $r < 1$ and > 0.1, identification, evaluation, and modeling of eruptive scenarios will probably be undertaken (see Study Plan 8.3.1.8.1.2, the logic is based on the assumption that the probability of repository disruption is $\approx 10^{-8}$ yr^{-1}. Crowe et al. 1980; Ho 1992; Connor and Hill 1993; Crowe et al. 1993). The information obtained from eruption modeling will be provided for assessments of the performance of the waste isolation system. If r is <0.1, the releases associated with the eruptive scenarios may not require study because of a low occurrence probability. Volcanism studies are tasked with developing the logic of bounding possible values of r, using a probabilistic approach. The formal selection, application, and evaluation of estimated values for the conditional probability of the eruptive events will be implemented by the DOE.

V. Revised Probability Calculations

A. Volcanic Record: Assumptions and Physical Models

This part of Chapter 7 attempts to define the current understanding of the record of basaltic volcanism in the YMR so it can be applied consistently to the probabilistic assessment of the recurrence rate (E1), the disruption probability (E2), and the probability of magmatic disruption of the repository and related areas (Pr[E2 given E1]). The most current data from site characterization studies are used to make revised estimations of the probability of magmatic disruption of the Yucca Mountain site. Data on the geology and chronology of Pliocene and Quaternary volcanic centers are taken from Crowe (1990), Wells et al. (1990), Smith et al. (1990), Turrin et al. (1991, 1992), Crowe et al. (1992, 1993), and from Chapters 2 and 3 of this report.

We acknowledge without extended discussion that there is not a single accepted definition of the number of past volcanic events in the YMR. Multiple models of E1 are used including center models, cluster models, and a Quaternary accelerated model. Likewise, there is not a single, universally accepted model for the structural control of the location of basaltic volcanic events. The small number of past volcanic events makes it difficult to either prove or disprove structural models of volcanism. Instead, we take the approach that it is more important to identify and evaluate the minimum, maximum, and most likely values of the conditional probability of magmatic disruption of the repository for a range of alternative models. For E1, minimum values are defined as the smallest number of volcanic events required to produce the record of observed Pliocene and Quaternary volcanic activity. Maximum values of E1 are

defined as the largest number of volcanic events required to produce the observed volcanic record. The most likely values are defined as the number of volcanic events required to produce the volcanic record using *reasonable* constraints from multiple lines of geologic, geochemical, and geophysical evidence. The selection of these values is somewhat subjective and requires judgment. However, by careful identification of the assumptions used to define the recurrence and structural models for the YMP, with *justification and documentation for the selections,* it is possible to narrow the range of alternative probability estimates. The systematic approach used for this assessment, and the description of alternate event models, should help identify *why* specific probabilistic assessments are chosen and why there are differences in probability estimates.

The best perspective for judging the results of probability assessments and ensuring they are neither underestimated nor overestimated is through comparison with the geologic record. We use two criteria in assessing both the validity and applicability of probability estimates. First, they should include evaluations of a full range of recurrence (E1) and structural (E2) models. In some cases, estimates of the conditional probability of repository disruption are formulated *only for the worst or worse* cases (for example, Ho et al. 1991; Ho 1992; Connor and Hill 1993). This is not necessarily incorrect, but the calculations should be identified clearly as worse or worst case calculations. Second, events and models used in probability estimations should be physically plausible. In some cases, published probability estimates are correct mathematically but physically implausible from the perspective of volcanic processes (for example, the *worst* case estimations of Ho [1992]).

The process of assembling probabilistic estimates for volcanic risk assessment requires making some judgmental decisions, particularly with the limited data sets of volcanic events in the YMR. We attempt to identify areas where judgment is required and try to both justify and present a range of alternative options for the judgments. In almost all cases the range of alternative options is large, and as a result, there are many equally viable methods for assembling probability estimates. Four approaches are used to constrain the variability in judgmental options for estimating probabilities. First, the methods and approaches used for the calculations must be compatible with the record of volcanic activity in the YMR. Second, the assumptions used for probability estimations must be consistent with and supported by conceptual understanding of the physical processes of volcanic activity. Third, we emphasize the numerical range of probability estimates, not the *different* ways of making the calculations. It is not necessary to discriminate alternative assumptions if they result in similar ranges of probability estimates. Finally, Study Plan 8.3.1.8.1.1 calls for review and refinement of probability estimations by an external group using formal methods of expert judgment. The purpose of an external review is to provide an independent assessment of probability estimates and ensure a full range of alternative assumptions are incorporated into the estimates.

1. Time Perspective of Probability Calculations. The first aspect of assembling probability calculations is identifying a time criterion for the probabilistic assessment. Regulatory guidelines by the NRC require an assessment of disruptive events during the Quaternary (1.6 Ma geologic definition; 2 Ma NRC definition). A more consistent assumption using a geologic perspective is to assess the record of volcanism for intervals corresponding to volcanic cycles (Crowe and Perry 1989). Here the suggested interval for the examination of the volcanic record in the YMR is 4.8 Ma. This is the period corresponding to the YPB, the youngest and present volcanic cycle for basaltic volcanism in the YMR (Crowe 1990; see Chapters 2 and 3). The YMR, as noted earlier, is defined as the area of distribution of Pliocene and Quaternary volcanic rocks and aeromagnetic anomalies suspected as buried volcanic centers or intrusive rocks (Fig. 7.2).

An area of misunderstanding or misinterpretation in past assessments of recurrence rates (E1) for the YMR is the use of an arbitrary or undocumented period of time, *t*, for the probability assessment. During the past 4.8 Ma, volcanic activity in the YMR has occurred episodically. There have been brief periods of volcanic activity separated by long periods of inactivity. Unrealistically small recurrence times can result from narrowing the period of assessment to intervals closely bracketing the time or times of volcanic activity. Equally, vanishingly small recurrence rates can be obtained by estimating recurrence rates during intervals of limited or no volcanic activity. Neither approach gives realistic recurrence rates. What is more important and a fundamental requirement for making probability estimations is to provide justification for selection of the interval used for probability calculations. Ideally, the justification should be based on volcanic processes or the geologic record. In a following section, we illustrate why intervals defined on the basis of the volcanic record provide the most realistic estimations of recurrence rates of volcanic events.

Crowe and Perry (1989) reviewed methods for assessing the time sensitivity of the record of volcanic events. They noted that plots of cumulative magma volume or magma volume versus time provide a basis for evaluating the evolutionary stages of volcanic activity through time. The slope of the curve, or the magma-output rate (Kuntz et al. 1986), is a sensitive indicator of changes in rates of magma production (Crowe and Perry 1989). It is used frequently to assess the historic behavior of active volcanoes (Wadge 1987; Shaw 1987). Crowe and Perry (1989) noted that the magma output rate shows characteristic changes through time in response to evolutionary patterns of basaltic volcanic fields (time scale of millions of years).

We use the last 4.8 Ma as the preferred interval for estimating volcanic recurrence rates because this interval corresponds to an established volcanic cycle in the record of volcanism in the YMR. Additionally, the recurrence rates are calculated for the last 2 Ma and 1.6 Ma to correspond to the NRC regulations and the geologic definition of the Quaternary period. To bound maximum recurrence rates, we assess recurrence rates for the last 1.0 Ma. an interval of possible increased frequency of volcanic events (Vaniman and Crowe 1981; Connor and Hill 1993; Crowe et al. 1993).

2. Definition of Volcanic Events. The second aspect of assessing the volcanic record, and an additional source of confusion in published estimates of the probabilistic assessment of volcanism, is defining a volcanic event. The definition of volcanic events used in the probability assessment conducted for this report includes λv, λc, and λi. Each involves the birth of a new volcanic center or an episode of intrusion of basaltic magma in the shallow crust. These events have spatial variability in their locations and therefore represent a finite risk of forming at or near the potential repository.

A volcanic event is defined from the perspective of its impact on a repository for underground storage of radioactive waste. The primary magmatic event of concern is the rise of a new pulse of magma through a repository. Figure 7.3 is a schematic block diagram of a typical dike-fed, eruptive event. The flow of magma moves upward initially along a near-vertical, sheetlike dike or dikes. As magma nears the surface and erupts, magma flow is concentrated in a near-circular conduit that becomes the predominant eruptive site or main vent. Multiple conduit sites can occur along the fissure (Fig. 7.3). Additionally, dikes can branch from the main dike at depth and form separate vents at the surface. From the perspective of the repository, the key variables in consideration of a volcanic event are the depth of formation of branching of dikes, the depth of expansion of dikes into conduit, and the depth of magma fragmentation associated with eruption (Fig. 7.3). Events occurring well *above* the depth of the repository will have a smaller effect on the repository with respect to the incorporation and surface dispersal of radioactivity. Events occurring *below* the repository could increase the geometric area of waste-magma contact, and potentially, the volume of dispersed radioactivity, either through eruptions or through secondary or coupled effects.

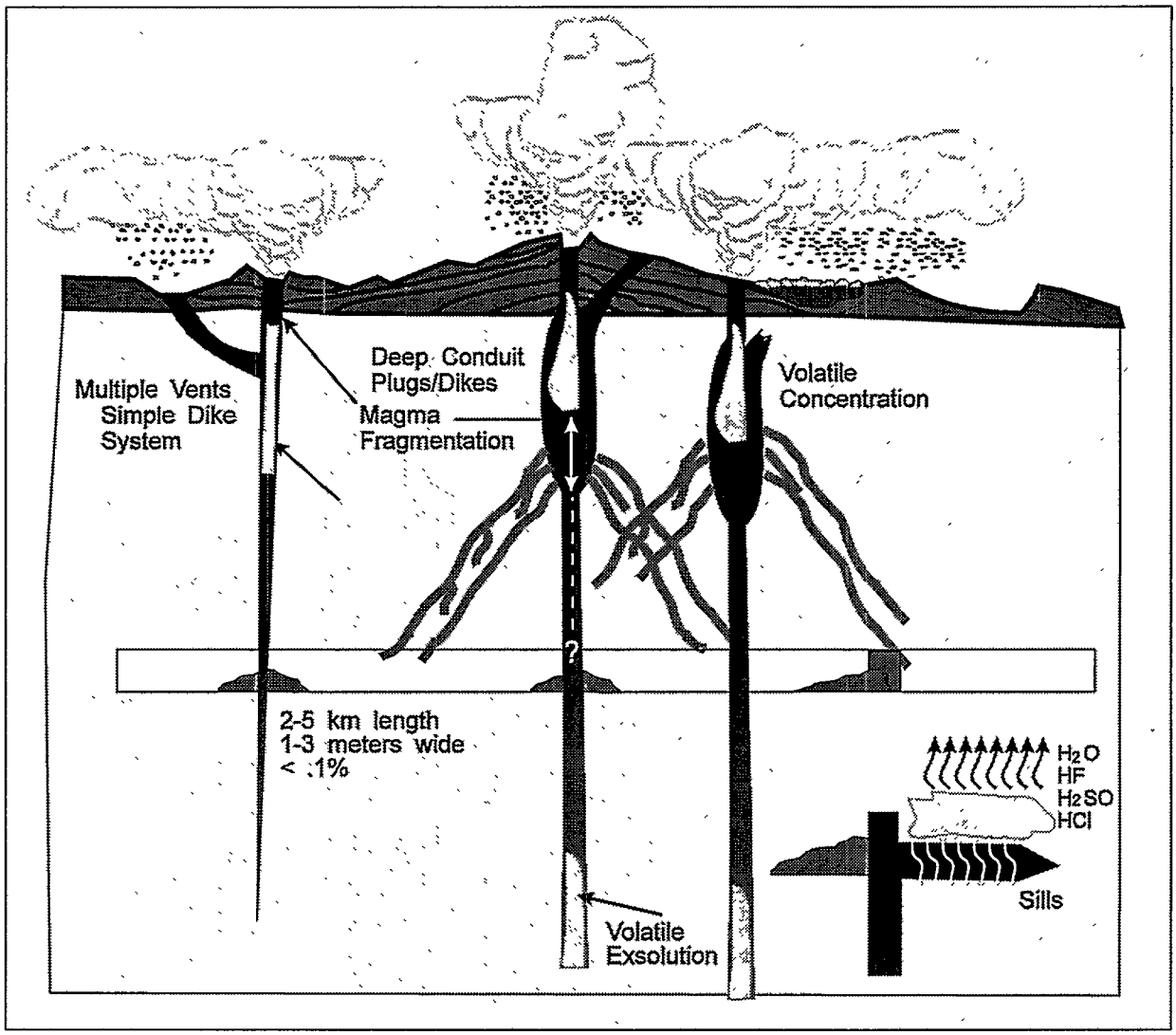


Fig. 7.3 Schematic cross section of a volcanic event penetrating a repository.

The rise and eruption of magma can lead to the formation of a single volcanic center such as the Lathrop Wells volcanic center or a cluster of multiple centers like the basalt of Sleeping Butte (Crowe and Perry 1991). A basaltic volcanic center is defined as a group of closely spaced vents that form a spatially distinct volcanic landform. Generally, a volcanic center consists of one main eruptive vent with a moderate-sized scoria cone and multiple satellite vents of smaller dimensions associated with the main cone (Crowe 1986). Individual volcanic *centers* are formed by the rise and eruption of a pulse of magma from single or multiple contemporaneous dikes. We use the term *volcanic center* to correspond to a *single* volcanic event. Multiple *vents* at a volcanic center are not necessarily counted as multiple volcanic *events.* Multiple *vents* can be formed by the rise of single *pulse* of magma. Multiple *vents* can also form as polygenetic episodes, a special subset of volcanic events that is not counted as a spatially unique volcanic *event* (see following discussion).

We assume a volcanic event (new volcanic center) is formed from the rapid emplacement of 1 to 3 dikes that feed surface volcanic eruptions. More than one dike is probably required because the geometry of vent zones and fissures at volcanic centers cannot easily be satisfied by a single dike. This is illustrated

by the distribution of fissure vents associated with the first chronostratigraphic unit of the Lathrop Wells volcanic center. The distribution of the vents defines three partly overlapping fissure systems (see Chapter 2). The spacing of the fissures requires that eruptions were fed from multiple dikes; a single feeder dike could not easily have produced the three fissures. Moreover, geochemical data suggest the fissures erupted magma of slightly different compositions (see Chapters 2 and 4). One of the goals of Study Plan 8.3.1.8.1.2 is to evaluate whether basalt magma ascends as dike swarms or whether a single feeder dike branches to form multiple feeder dikes.

The identification of volcanic events can be bounded approximately by the dimensions of feeder dikes. Dikes typically have aspect ratios ranging from 10^{-2} to 10^{-3} and widths of 1 to 5 m (see Chapter 5). Any volcanic vent or center spaced over 5 km distance (an arbitrary distance) from another center probably require a spatially separate feeder dike. They would be counted therefore, as separate volcanic *events*. Any vents spaced closer than 5 km are inferred to represent single *events* unless field or geochronology data indicate the vents formed from time-separate or geochemically distinct *events*. They could be classified as single or multiple volcanic *events*, or polygenetic *episodes* associated with a previous volcanic *event*. These definitions are generally useful but cannot always discriminate unambiguously the number of volcanic events. In ambiguous cases, multiple approaches are used to define volcanic events. For example, the Quaternary basalt of Crater Flat consists of four separate volcanic centers (see Chapter 2). These could be identified as four distinct volcanic *events*, a single cluster *event*, or combinations of volcanic *events* and cluster *events*. *Because of the potential ambiguities, we attempt to carefully define the usage and assumptions in the definitions of volcanic events in the following probability estimations.* It is unlikely that there will be complete agreement with all assumptions used in the probability estimations for the volcanism status report. Again, by carefully identifying and describing the basis for assumptions, we hope to at least clarify or possibly reduce areas of disagreement over different probability estimations.

3. Polygenetic Volcanism. Polygenetic volcanism (Crowe et al. 1989; Wells et al. 1990; Perry and Crowe 1992) represents a special subcase of volcanic events. A polygenetic *episode* is defined as an eruption at a preexisting volcanic center that is separated in time from the preceding *event* by an interval exceeding the residence time of basaltic magma in the shallow crust (decades). By definition, polygenetic *episodes* represent eruptions of discrete pulses of magma. Dike cooling times in the shallow crust, assuming dike widths of 5 m or less, are no more than 10 yr (Hubbert and Bruce 1990; Lister and Kerr 1991). Thus, a polygenetic *episode* is regarded as the recurrence of an eruption at an existing center where there has been no activity for a minimum of several decades. The existence and significance of polygenetic eruptions are still under investigation and have been controversial (Crowe et al. 1989; Wells et al. 1990; Whitney and Shroba 1991; Champion 1991; Turrin et al. 1991, 1992; Wells et al. 1992; Crowe et al. 1992). We regard the current field, geochemical, and geomorphic data for the Lathrop Wells center to indicate, with a high degree of confidence, that the center may have formed from multiple, time-distinct volcanic eruptions (Chapter 2). Therefore the significance of polygenetic *episodes* are considered in probabilistic assessments.

The definition of a polygenetic *episode* and its distinction from a volcanic *event* affects probabilistic assessments. Ho et al. (1991) counted polygenetic *episodes* (and in some cases, individual vents) in estimation of E1 (Ho et al. 1991, p. 54). This is not consistent with the requirement of independence of the attributes of the conditional probability. The usage results in higher cone counts and a bias toward higher values for E1. Viewed probabilistically, the polygenetic model requires that there is an increased likelihood of another eruption *at an existing volcanic center* given a previous *event* that formed a *new* volcanic center (initiating event). Thus, there is spatial uncertainty in the location of a new volcanic center. Accordingly, there is a high probability that the first event will occur in the YMR and a finite probability that the event could disrupt the potential repository site. Because a polygenetic *episode* occurs

at or near the same location as the first event, it does not have the same spatial uncertainty in location as an initiating volcanic event. If an initiating volcanic *event* passes through a repository, a subsequent polygenetic *episode* would also pass through the repository. If the initiating *event* did not pass through the repository, the subsequent polygenetic *episode* would also not pass through the repository. The probability of a polygenetic *episode* is added as a probability branch to λ, the recurrence rate of volcanic events. Thus, the critically important concept for probabilistic assessment is the recognition that a polygenetic event is *dependent* on the occurrence of a preceding event and that event is the formation of a new volcanic center.

We are still in the process of assessing the frequency of occurrence and recurrence rates of polygenetic *events* in the YMR. This will be a topic of continuing probabilistic studies (see Crowe et al. 1989). Accordingly, the following discussion is presented as a preliminary assessment of the logic and methods for assessing polygenetic volcanic eruptions.

Given a new volcanic event (formation of a new volcanic center) in the YMR, there appears to be an increased probability that subsequent events will occur at the *same* volcanic center. The frequency of occurrence of polygenetic centers and the duration between polygenetic events at a center is not well established. The results of ongoing geochronology studies at the Lathrop Wells volcanic center indicate that the time between eruptions may be on the order of 1 to 8 x 10^{-4} yr (see Chapter 2). A single polygenetic eruption at the Hidden Cone center may have occurred more than 200 ka after the initiating volcanic event (Crowe and Perry 1991) but the identification of this polygenetic event remains uncertain. Polygenetic activity is suspected at Black Cone (see Chapter 4). The time between polygenetic episodes at the center, if they exist, must be less than the analytical uncertainty of K-Ar and $^{40}Ar/^{39}Ar$ age determinations for the center (~100 ka; see Chapter 2).

A polygenetic eruption may be expressed in either of two possible forms. One form is illustrated by the Lathrop Wells and the Hidden Cone volcanic centers. These centers may have had multiple, time-separate volcanic eruptions that all occurred *at a single* preexisting volcanic center. A second possible form of polygenetic eruptions is multiple time-separate eruptions, where each separate eruption formed a distinct but temporally and spatially related volcanic center. This may be typified by the volcanic clusters of the basalt of Sleeping Butte and the Quaternary basalt of Crater Flat. Each consists of a cluster of multiple volcanic centers. In this case, subsequent events, if they are polygenetic events, are confined not to an individual center, but to a *cluster*. The spatial variability in location of a polygenetic eruption in a cluster is controlled by the *dimensions* of cluster lengths of aligned volcanic centers (2.5 to 13 km). The existence of polygenetic clusters has not been proved at any of the volcanic clusters in the YMR; it is only possible. Current chronology data are insufficiently precise to test for polygenetic activity at either the basalt of Sleeping Butte or the Quaternary basalt of Crater Flat.

At some unknown length of time (probably >100 ka), the likelihood of a polygenetic eruption must decrease. Future volcanic events would form a *new volcanic center at an unconstrained location.* The only data we currently have on the transition time between polygenetic events and the formation of a new volcanic center are that the latter must be >10 ka, and less than the typical recurrence time between successive volcanic events (200 ka to >1 Ma; see the following section on volume-predictable volcanic events).

The most likely site of a future polygenetic volcanic eruption in the YMR is either the Lathrop Wells or the Hidden Cone volcanic centers. The most recent polygenetic episodes at both centers are probably <50 ka; therefore the centers are inferred to be in a continuing stage of polygenetic activity. The most likely event in the YMR in the next 10,000 yr is, accordingly, the *recurrence of a polygenetic eruption* at either of the two centers. The recurrence rate of these type of eruptions is probably >10^{-4} and <2 x 10^{-5} yr^{-1} – it is

the *highest probability* of any identified future volcanic event in the YMR. However, the polygenetic episode would be expected to be another small-volume eruption *at* either center, or a related cluster event *near* either center. Because the Lathrop Wells center is 20 km south and the Hidden Cone is 47 km northwest of the potential repository, the disruption ratio (E2) for these events is very small. Dikes from these events are *very unlikely* to intersect the repository. Logically, a polygenetic episode is a relatively high probability event (E1), with a very low E2, and probably very low E3. We have focused volcanism studies on estimations of the highest risk event: the possibility of intersection or near intersection of the potential repository by a future volcanic event, where the event is the formation of a *new* volcanic center.

We will, in future studies, complete revised probabilistic assessments of polygenetic and *intra*cluster events. This is the only discussion provided in this volcanism status report of the logic for assessing polygenetic events. Further studies of polygenetic and intracluster events are planned also for E3, the probability of releases of radioactive waste at the surface.

B. Quaternary Volcanic Centers in the Yucca Mountain Region (Oldest to Youngest)

The following data set is used for the revised probability calculations. All data and interpretations used to generate the set are *not final.* They are regarded as the current best estimates of existing information from site characterization studies. The data set will be revised as site characterization studies continue. Quaternary volcanic centers in the YMR include (oldest to youngest):

1. **1.0 Ma Centers: Quaternary basalt of Crater Flat.** These are defined as one cluster event or two to five center events. Each volcanic center is estimated to be 1.0 ± 0.1 Ma on the basis of existing chronology data (see Table 2.2, Chapter 2). These data include the results of replicate K-Ar age determinations from separate analytical laboratories. The resolution of chronology data are insufficient to establish whether each center of the Quaternary basalt of Crater Flat did or did not form as a result of polygenetic episodes. Moreover, the age of specific centers cannot be discriminated individually on the basis of existing data (see Chapter 2). The close spacing of the Little Cone centers supports treating these cones as a single event. Alternatively, Ho (1992) and Connor and Hill (1993) treat the Little Cones center as *two* centers and as *two* volcanic events. The composite length of the arc of the four basalt centers of Crater Flat is probably too long for the complete cluster to have formed as one volcanic event. It could have been formed however, by a single dike branching from the midpoint of the volcanic cluster (see the following discussion of the dike-stress model). The volume of the Quaternary basalt of Crater Flat center is estimated to be 0.23 km^3 (DRE). *(Note: We are in the process of completing revised volume calculations for the Pliocene and Quaternary basalt centers of the YMR. Descriptions of the methods of volume calculations, the uncertainty of the calculations, and the resulting data are expected to be completed in calendar year 1995).*

   Minimum Event Model: 1 event
   Maximum Event Model: 5 events
   Most Likely Event Model: 3 events
   Polygenetic Episode: Unknown but possible at Red Cone and Black Cone

2. **0.32 Ma Centers: Basalt of Sleeping Butte.** These are treated as two individual centers formed either in *one* cluster event or as *two* center events at about 320 ka (Crowe and Perry 1991; Champion 1991; Turrin 1992, Minor et al. 1993). High precision $^{40}Ar/^{39}Ar$ age determinations have not been obtained for the basalt of Sleeping Butte under the approved Quality Assurance

program. The mean age of existing age determinations for the center is 350 ± 50 ka. We arbitrarily assign a larger uncertainty of 150 ka to the age to reflect an incomplete data set. Existing soil and geomorphic data are consistent with an age of about 350 ka (Crowe and Perry 1991). A Pleistocene polygenetic episode may have occurred at the Hidden Cone center. The uncertainty of the age assignments for the center cannot be estimated from current data. The volume of the basalt of Sleeping Butte is estimated to be 0.06 km^3 (DRE).

Minimum Event Model: 1 event
Maximum Event Model: 2 events
Most Likely Event Model: 1 event
Polygenetic Episodes: Suspected but unconfirmed at Hidden Cone

3. **0.1 Ma Center: Lathrop Wells Center.** This is treated as a *single*-event volcanic center formed by *one* initiating event followed by *three* polygenetic episodes. The initiating event (formation of a new volcanic center) is estimated at 100 to 130 ka. The first polygenetic episode followed at 80 to 100 ka (minimum age) and a second polygenetic episode occurred at about 40 to 60 ka. The youngest polygenetic episode occurred at 4 to 9 ka. The uncertainty of the age of the events and episodes can be only bounded using existing data. The first initiating event and the first polygenetic episode are estimated to have an uncertainty of ± 35 ka; the second polygenetic episode is no younger than 25 ka, and probably no older than about 85 ka. The uncertainty of the youngest episode cannot be estimated with current data. The volume of the Lathrop Wells volcanic center is estimated to be 0.14 km^3 (DRE).

Minimum Event Model: 1 event
Maximum Event Model: 1 event
Most Likely Event Model: 1 event
Polygenetic Events: Three polygenetic episodes

C. Pliocene Volcanic Events in the Yucca Mountain Region (Oldest to Youngest):

1. **4.8 Ma Centers: Basalt of Thirsty Mesa.** This lava mesa formed from lava and scoria eruptions at three coalesced vents. It can be defined as *one* cluster event or as many as *three* center events, each with an age of 4.8 ± 0.13 (2 *s*) Ma. Unpublished $^{39}Ar/^{40}Ar$ ages by the U.S. Geological Survey are consistent with this age (second laboratory verification). The volume of the basalt of Thirsty Mesa is estimated to be 3 km^3 (DRE).

Minimum Event Model: 1 event
Maximum Event Model: 3 events
Most Likely Event Model: 1 event
Polygenetic Events: Unknown

2. **3.8 Ma Center: Basalt of the Amargosa Valley.** This volcanic event is represented by the aeromagnetic anomaly located a few kilometers south of the town of Amargosa Valley. The shape, size, and continuity of the anomaly suggest it should be treated as *one* volcanic event. The age of the volcanic event is 3.85 ± 0.05 Ma. There are insufficient data to estimate the uncertainty of the age of the center. The volume of the basalt of Amargosa Valley is estimated to be between 0.2 and 0.4 km^3 from the dimensions of the aeromagnetic anomaly and comparison with surface basalt centers.

Minimum Event Model: 1 event
Maximum Event Model: 1 event
Most Likely Event Model: 1 event
Polygenetic Events: Unknown

3. **Undrilled Aeromagnetic Anomalies: Basalt of Central Amargosa Valley.** These presumed Pliocene volcanic center(s) have not been explored by drilling. For this report, the two remaining aeromagnetic anomalies are included, and they are assumed to be the same age as the drilled Amargosa Valley anomaly (3.85 Ma). The anomalies define two circular bodies (Langenheim et al. 1991, 1993) and are presumed to represent *one* cluster or *two* center events. The cluster event includes the basalt of Amargosa Valley since the three centers are aligned on a northeast trend.

Minimum Event Model: 1 event
Maximum Event Model: 2 events
Most Likely Event Model: 1 event
Polygenetic Events: Unknown

4. **3.7 Ma Centers: Basalt of Southeast Crater Flat.** This Pliocene unit consists of *one* cluster event and *three* to *five* center events (Vaniman and Crowe 1981; Crowe et al. 1983b; Champion 1991). The age of the centers is dated at 3.74 ± 0.10 Ma (average of 2 *s* errors) using replicate, high-precision $^{39}Ar/^{40}Ar$ age determinations. This age has been verified with replicate conventional K-Ar ages at multiple analytical laboratories. The volume of the basalt of southeast Crater Flat, including reconstructed volumes of eroded or buried deposits is 0.68 km^3. (*Note: A sixth center was discovered in the southern outcrops of the basalt of southeast Crater Flat in the early summer of 1994, too late to change the numerous tables and calculations of Chapter 7. This new center requires that the basalt of southeast Crater Flat consists of* ***two*** *cluster events and three to* ***six*** *center events. The description of the center is included in Chapter 2).*

Minimum Event Model: 1 event
Maximum Event Model: 5 events
Most Likely Event Model: 1 event
Polygenetic Events: Unknown

5. **2.9 Ma Center: Basalt of Buckboard Mesa.** This consists of one center erupted from a main scoria cone and associated fissure system. It is assumed to be a single cluster and single event center that formed a lava mesa in the moat zone of the Timber Mountain caldera (Crowe 1990). The age of the basalt of Buckboard Mesa is about 2.9 ± 0.13 Ma. The volume of the basalt of Buckboard Mesa is 0.92 km^3.

Minimum Event Model: 1 event
Maximum Event Model: 1 event
Most Likely Event Model: 1 event
Polygenetic Events: Unknown

D. Revised Calculations of E1: The Recurrence Rate of Volcanic Events.

This section of this volcanism status report initiates formal revisions of E1, the recurrence rate of volcanic events. We follow the logic of Study Plan 8.3.1.8.1.1, Probability of Magmatic Disruption of the

Repository, and systematically examine values for E1 using three methods: time-series analysis, homogeneous Poisson and nonhomogeneous Poisson models using cumulative counts of volcanic events for specified periods of time, and modified homogeneous Poisson models using magma-output rate. The recurrence rates are estimated for minimum, maximum, and most likely values of E1.

Table 7.3 lists, with the referenced publication, published estimates of the recurrence rate (E1) for volcanic events in the YMR. The results are taken from publications from 1980 to 1993. There are 41 published estimations of E1. The estimates range from 3.0×10^{-5} to 6.0×10^{-7} events yr^{-1}. Distribution models for the estimations include homogeneous Poisson models using event, cluster, and stress-field dike counts, modified homogeneous Poisson models using magma-output rate, and Weibull (nonhomogeneous) models using event counts (but not cluster counts). The observation periods for the calculations vary from 1.0 to 12 Ma. Descriptive statistics for the published data set (excluding the confidence interval calculations of Ho [1992]) are: $n = 39$, mean = 4.9×10^{-6}, median = 4.0×10^{-6}, minimum = 0.6×10^{-6}, maximum = 28×10^{-6}, standard deviation = 4.5×10^{-6} (all as events yr^{-1}), and skewness = 3.6. The data are strongly skewed to higher values consistent with the bias introduced from attempts to identify upper bounds in probability estimates. Most of the recurrence rates are in the range of 1 to 6×10^{-6} events yr^{-1}. The significance of numbers in this range has been debated (Ho et al 1991; Ho 1992; Connor and Hill 1993). They are not considered to be significantly different, however, given the small data set used for the calculations and the underlying uncertainties of the event models (Crowe et al. 1992, 1993).

There are some important limitations in the data summarized in Table 7.3. First, as noted earlier, most of the calculations attempt to bound the recurrence rate to determine if the risk of volcanism could result in disqualification of the Yucca Mountain site. This resulted in the introduction of nonsystematic bias in the published estimations of E1 toward higher recurrence rates (positive skewness). Assumptions used for most of the estimations were constructed to ensure that the probabilities were not underestimated. Second, no attempt was made in the different calculations to structure the results to obtain an unbiased representation of the distribution of recurrence rates. As a consequence, descriptive statistics derived from the estimations are difficult to interpret. Third, the recurrence rates were calculated with different levels of completeness of data for the ages, locations, and eruptive history of volcanic events. Generally, the more recent the calculations, the better the quality of data. Recognizing these limitations, we nonetheless employed standard methods of exploratory data analysis of the data listed in Table 7.3 (histogram, box, stem and leaf, probability plots). Three estimations of E1 were rejected as outliers in successive iterations of the evaluation of the data distribution (28×10^{-6} events yr^{-1} of Crowe et al. 1989; 11×10^{-6} events yr^{-1} from Crowe et al. [1982] and Connor and Hill [1993]). Descriptive statistics for the edited data set are: $n =$ 36, mean = 3.9×10^{-6}, median = 3.9×10^{-6}, minimum = 0.6×10^{-6}, maximum = 9.4×10^{-6}, standard deviation = 2.2×10^{-6} (*all* as events yr^{-1}), and skewness = 0.68.

1. Time-Series Analysis. One standard method for assessing patterns of volcanic events in time is to apply techniques used for sequenced or time-series analysis (Davis 1986); this approach has been applied in the volcanological literature primarily for historic eruptions of active volcanoes. There is a diverse range of methods for analyzing time-series data. The primary problem with application of any of the methods is the limited number of volcanic events in the YMR. The standard advice for using limited data sets in textbooks describing techniques for application of time-series analysis is universal: *obtain more data*. Given that the volcanic events used in the YMR data set have been acquired (recorded in the geologic

Table 7.3 Published estimates of the recurrence Rate (E1) of Volcanic Events in the YMR.

Publication	E1 (events yr^{-1} x 10^{6})	Quaternary Events	Rate Model	Interval (Ma)
Crowe and Carr 1980	4.0	6.4	Poisson Cone Count	1.8 to 2.8
Crowe et al. 1982	0.6 to 11*	1.0 to 17.6	Volume predictable	1.8 to 3.7
	9.4	15.0	Poisson Cone Count	1.8
	6.4	10.2	Poisson Cone Count	2.8
	8.0	12.8	Poisson Cone Count	3.7
Crowe et al. 1989	28*	44.8	Volume predictable	3.7
	7.0	11.2	Volume predictable	3.7
	5.0	8.0	Volume predictable	1.8
	3.2	5.1	Volume predictable	1.8
Crowe and Perry 1989	1.9	3.0	Volume predictable	1.8
	1.6	2.6	Volume predictable	1.8
Ho 1991	2.3	3.7	Weibull Episode	12
	5.0	8.0	Weibull Cycle	3.7
	6.2	9.9	Cone Count	6.0
	5.5	8.8	Weibull Cone Count	1.6
Crowe et al 1992	3.9	6.2	Poisson Cone Count	1.8
	1.7	2.7	Poisson Cluster Count	1.8
	3.5	5.6	Poisson Cone Count	3.7
	1.3	2.1	Poisson Cluster Count	3.7
	3.2	5.1	Poisson Cone Count	5.0
	1.2	1.9	Poisson Cluster Count	5.0
Ho 1992	5.0	8.0	Weibull Episode	6.0
	5.5	8.8	Weibull Episode	1.6
	1.8**	2.9	Weibull 90% CI**	1.6
	13.0**	21	Weibull 90% CI**	1.6
Connor and Hill 1993	5.4	8.6	Weibull-Poisson	1.6
	1.5	2.4	Weibull-Poisson	1.6
	11.0*	17.6	Weibull-Poisson	1.6
	2.1	3.4	Weibull-Poisson	1.2
	4.8	7.7	Weibull-Poisson	1.2
	7.0	11.2	Weibull-Poisson	1.2
Crowe et al. 1993	1.5	2.4	Poisson Cluster Count	2.0
	4.0	6.4	Poisson Cone Count	2.0
	1.7	2.7	Poisson Cluster Count	4.7
	4.3	6.9	Poisson Cone Count	4.7
	3.4	5.4	Repose	2.0
	2.1	3.4	Volume predictable	2.0
	1.5	2.4	Accelerated Cluster	1.9
	4.1	6.6	Accelerated Cone	1.9
	3.0	4.8	Accelerated Cluster	1.0
	8.0	12.8	Accelerated Cone	1.0

* outlier values ** confidence intervals

record) over the last 4.8 Ma, the prospects for obtaining more data in the immediate future are extremely limited. Accordingly, there is limited merit in applying time-series analysis. We proceed cautiously with only simple applications.

Table 7.4 lists the age, volume, cumulative volume, and the repose interval for volcanic events in the YMR. One problem noted immediately from simple examination of the data table is individual events can be identified on a center by center basis but the ages of individual centers within clusters of centers cannot be discriminated. This is illustrated on figure 7.4, a plot of the cumulative events (events defined as cluster events) versus time. The slope of the line segments between points is the rate or number of events per unit time, and the plot readily shows changes in average event rates. The slopes are slightly steeper during the Pliocene and the last 1 Ma and slightly lower during a middle period (1 to 2.9 Ma). One steep slope segment results from plotting the event for the buried basalt of the Amargosa Valley. It is so close in age to the southeast basalt of Crater Flat that it may be more appropriate to plot it with the latter unit. If center events for each cluster are added to the plot of events versus time, little additional insight is gained. (Fig. 7.5). This revised plot does underscore, however, how volcanic events tend to occur in clusters, much like clustered seismic events.

An alternative plot can be constructed to partly discriminate clustering events by changing the y-axis to magma volume. However, the problem with this approach is the older basalt units are too modified by erosion to trace the volume components to individual volcanic centers. This can be resolved partly by plotting the y-axis as the cumulative magma volume. Better event separation is obtained but the assignment of volumes for some clustered centers and the older basalt centers is arbitrary (Fig. 7.6). The data and slope segments can be divided visually into two groups: Pliocene volcanic events (higher magma-output rate) and Quaternary events (lower magma-output rate). This relationship is examined more carefully in a following section.

The event repose times vary from 200 ka to 1.9 Ma with a mean of 1000 ± 570 ka ($n = 6$; Table 7.4). The number of events is too limited to be statistically significant. However, some potentially important observations are noted from a plot of repose intervals (time between the initiation of volcanic events). First, three of the five repose periods are between 700 and 1100 ka, and the other three periods are approximately half and double those values (Fig. 7.7). Second, the minimum repose period between events

Table 7.4. Age, volume, cumulative volume and repose intervals for Pliocene and Quaternary volcanic events of the YMR.

Center	Age (Ma)	Volume (km^3)	Cumulative Volume (km^3)	Repose Interval (Ma)
Basalt of Thirsty Mesa	4.8	3.0	3.0	1.5
Amargosa Anomaly	3.8	0.3*	3.3	0.1**
Basalt of Southeast Crater Flat	3.7	0.68	3.98	1.1
Basalt of Buckboard Mesa	2.9	.92	4.90	.8
Quaternary Basalt of Crater Flat	1.0	.23	5.13	1.9
Basalt of Sleeping Butte	.32	.06	5.19	.7
Lathrop Wells Volcanic Center	.12	.14	5.33	.2
mean		*0.84*		*1.0*
std deviation		*0.11*		*0.6*

* volume of undrilled anomalies not included
** not included in repose statistics

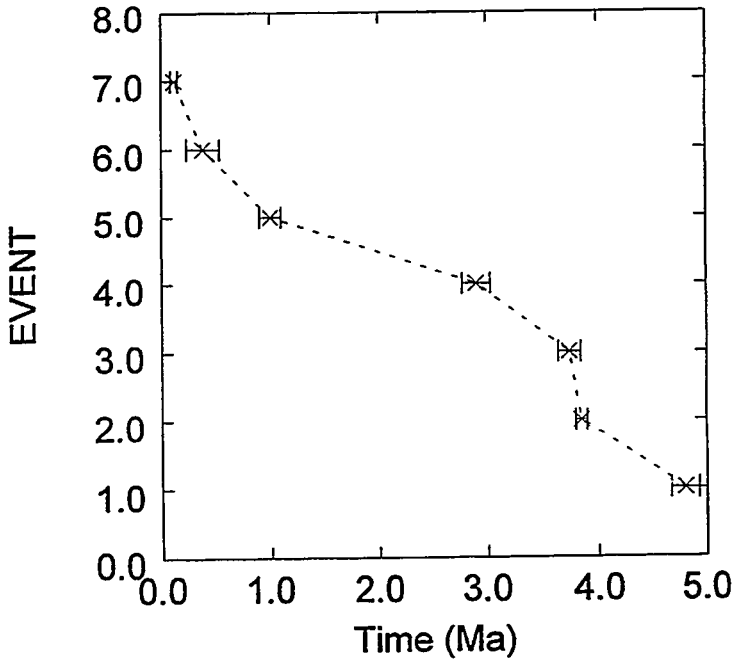


Fig. 7.4 Plot of volcanic events versus age for the Pliocene and Quaternary volcanic record of the YMR.

for the duration of the YPB (4.8 Ma) is 200 ka. If the minimum observed repose period is used as a worst case bound for predicting the next volcanic event (corrected for the time since the last eruption, the Lathrop Wells volcanic center; 9 ka) the predicted minimum time to the next event is 191 ka, which is equivalent to a recurrence rate of 5.2×10^{-6} events yr^{-1}. Third, the data can be fitted with a linear regression model with some limitations (Fig. 7.7). There are an insufficient number of data points, and the data are too dispersed for the regression model to be significant, but the slope of the regression line is consistent with a slight decrease in repose intervals through time. The data can also be fitted with a distance weighted least squares model, an undulating curve fit that declines markedly in the Quaternary. Note that this curve fit intersects the y-axis at an age of 0. This would be equivalent to a 0 repose interval, a physically unrealistic value. Intuitively, the argument that future repose intervals cannot be less than the shortest observed repose interval appears compelling. During the last 4.8 Ma, there has never been a repose period of less than 200 ka. The long interval of the observed record makes it appear unlikely that this pattern would change over the next 10,000 yr. However, from an opposite perspective, the shortest repose period preceded the youngest volcanic event in the region. Again, a consistent pattern emerges: the limited data make a range of interpretations permissive.

2. Homogeneous Poisson Models (Event Counts). Table 7.5 is a compilation of revised calculations of the recurrence rate of volcanic events using a homogeneous Poisson model for the record of volcanic events in the YMR. We attempted, in this data compilation, to provide a representation of the distribution of values by identifying models that give the minimum, most, likely and maximum values using geologically reasonable combinations of event counts.

The event count models of Table 7.5 are divided into multiple cases, where the cases are identified under the column labeled "Model". The first category includes combinations of Quaternary (2 Ma) volcanic events. The second category is the last 4.8 Ma using the recognition of the basalt cycle of the YPB (Crowe 1990). The third category examines data for the Quaternary using 1.6 Ma, the current geologic definition of the Quaternary. A fourth category examines data for an interval of decreased erupted volumes

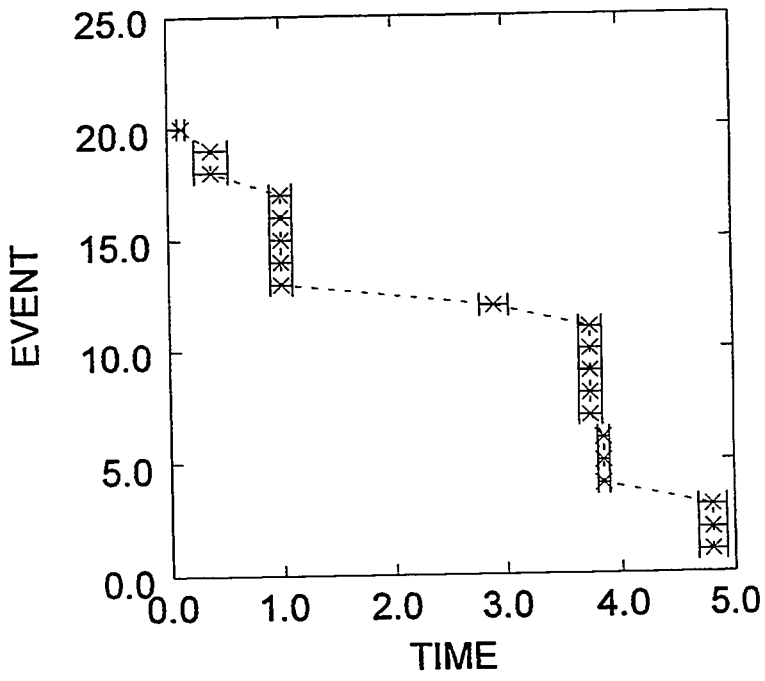


Fig. 7.5 Plot of clustered volcanic events versus age for the Pliocene and Quaternary volcanic record of the YMR.

associated with an increase in the frequency of eruptive events. The actual interval of this increased frequency of volcanic events cannot be defined precisely (Crowe et al. 1993). It must have initiated somewhere between the age of the basalt of Buckboard Mesa (2.9 Ma) and the age of the Quaternary basalt of Crater Flat (1.0 Ma). We assume this interval initiates with the age of the Quaternary basalt of Crater Flat (1.0 Ma) so that it is equivalent to the definition of a volcanic cycle. Conceptually, the interval may correspond with a time of decreased degree of partial melting resulting in a higher volatile content and a greater tendency for the magma to erupt versus stagnate in the crust (Crowe et al. 1993).

The minimum event models of Table 7.5 for both the Quaternary and YPB event counts are based on the interpretations of the paleomagnetic data of Champion (1991). He argues that all geographically adjacent volcanic centers in individual clusters have closely spaced field magnetization directions and therefore formed from a single magma pulse (monogenetic cluster model). Using these arguments, the Quaternary basalt of Crater Flat and the basalt of Sleeping Butte, for example, would be recognized as single volcanic events. This interpretation represents the *minimum* number of volcanic events (spatially and temporally distinctive magma pulses) that can be assigned to the volcanic centers of the YMR for both the Quaternary and the YPB categories.

The most likely volcanic models for Quaternary and YPB volcanic events are established through attempts to integrate all existing data for the volcanic centers. Insights provided by geologic, geochronologic, petrologic, and geophysical data are used to identify volcanic events. In some cases, the geochronologic, petrologic, and paleomagnetic data are insufficiently precise to provide convincing proof

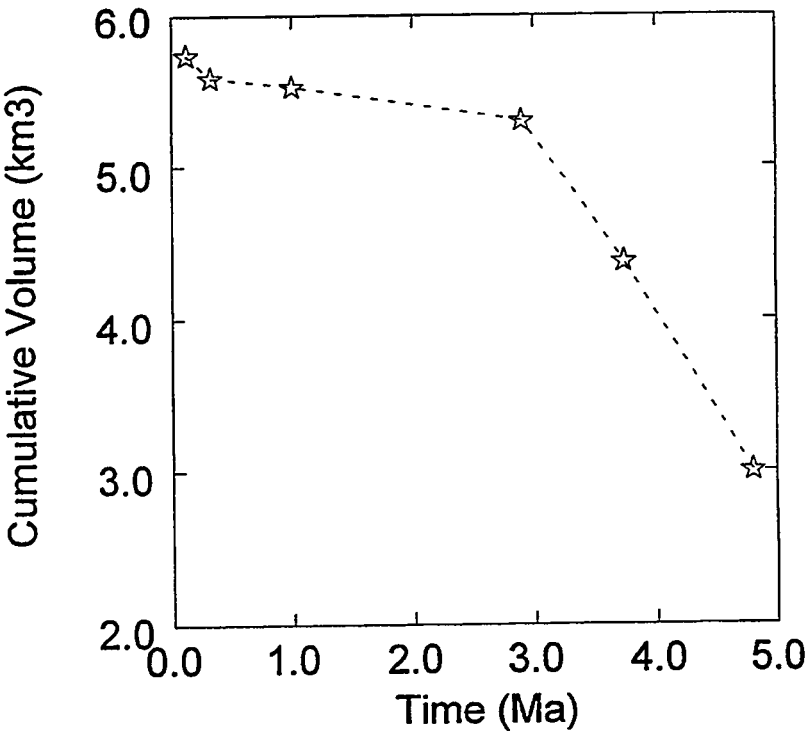


Fig. 7.6 Plot of cumulative volume versus age for the Pliocene and Quaternary volcanic record of the YMR.

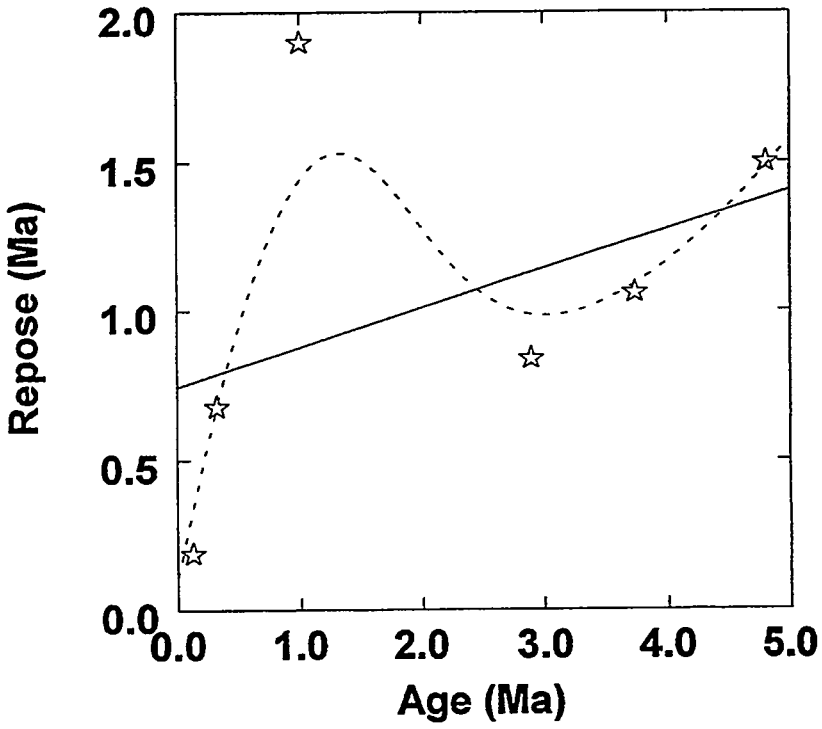


Fig. 7.7 Plot of repose interval versus age for the Pliocene and Quaternary volcanic record of the YMR.

Table 7.5 Table of Homogeneous Poisson Models for Volcanic Events (E1) in the YMR.

Interval	Model	Interval (yr.)	Minimum events yr^{-1}	Maximum events yr^{-1}	Most Likely events yr-1
Quaternary		2.00E+06			
	Poisson Events		3	8	6
	Poisson Rates		1.5E-06	4.0E-06	3.0E-06
	Stress-Dike Events		3	8	5
	Stress-Dike Rates		1.5E-06	4.0E-06	2.5E-06
Volcanic Cycle*		4.70E+06			
	Poisson Events		8	19	12
	Poisson Rates		1.7E-06	4.0E-06	2.5E-06
	Stress-Dike Events		8	10	10
	Stress-Dike Rates		1.7E-06	2.1E-06	2.1E-06
Quaternary		1.60E+06			
	Poisson Events		3	8	6
	Poisson Rates		1.9E-06	5.0E-06	3.7E-06
	Stress-Dike Events		3	6	5
	Stress-Dike Events		1.9E-06	3.7E-06	3.1E-06
Quaternary Accelerated*		1.00E+06			
	Poisson Events		3	8	7
	Poisson Rates		3.0E-06	8.0E-06	6.0E-06
	Stress-Dike Events		3	6	5
	Stress-Dike Rate		3.0E-06	6.0E-06	5.0E-06
Summary Statistics (all Models)		*Mean*	*2.0E-06*	*4.6E-06*	*3.5E-06*
		Median	*1.8E-06*	*4.0E-06*	*3.1E-06*
		Geomean	*1.9E-06*	*4.3E-06*	*3.3E-06*
		Std Deviation	*0.6E-06*	*1.7E-06*	*1.3E-06*
*Summary Statistics (Preferred Models)**		*Mean*	*2.3E-06*	*5.0E-06*	*3.9E-06*
		Median	*2.3E-06*	*5.0E-06*	*3.8E-06*
		Geomean	*2.3E-06*	*4.5E-06*	*3.6E-06*
		Std Deviation	*0.7E-06*	*2.5E-06*	*1.8E-06*

* Preferred models are models where the event counts span an interval that corresponds to cycles of volcanic activity (4.8 Ma to present; and 1.0 Ma to present).

of individual magmatic events. For example, the Quaternary basalt centers of Crater Flat can be divided into one to as many as four (possibly 5) events because the cluster length (12 km) exceeds the likely lengths of individual feeder dikes and there are distinct geochemical differences between some of the centers. Red Cone and Black Cone could be identified as one event because of their proximity and petrologic evidence of mixing of magmas from both centers (Bradshaw and Smith 1994). The Little Cones center is inferred to be a separate and *single* event because of the close spacing of the scoria cones and their small volumes. The assignments for the Sleeping Butte centers is less clear. The close spacing of the centers (2.6 km) and the paleomagnetic data (Champion 1991) are permissive with the centers representing a single volcanic event. The choice of events that correspond to the maximum estimates is established from assuming every volcanic center represents a volcanic event. This approach corresponds generally to the event assignments of Ho (1991), Ho (1992), and Connor and Hill (1993). The only differences are that Ho et al (1991)

include polygenetic episodes in their event counts. Additionally, both Ho (1992) and Connor and Hill (1993) separate the Little Cone center into *two* events. We regard this as a possible but unproven assignment, but count the center as two events in the maximum event counts to avoid controversy. The stress-field dike model for the Quaternary and YPB categories follows the logic of two observations described in Chapters 2, 3, and 5 of this volcanism status report. First, the clusters of probable near-contemporaneous basalt centers of the CFVZ are elongate north-northeast, parallel to the maximum compressive stress direction. This is the inferred direction of dike propagation in the shallow crust. Second, the clustered centers may have formed by upwelling of magma along a concealed northwest-trending structure. By inference, the magma may have diverted at shallow levels from the northwest-trending structure and was emplaced by magma-generated hydrofracture parallel to the maximum compressive stress direction. The site of upwelling is identified by the northwest alignment of basalt centers in the CFVZ, which coincides also with the location of the surface of maximum erupted magma volumes (see Chapter 3, Fig. 3.15). Magma upwelling would have an equal probability of propagating either northeast or southwest to form clustered volcanic centers. On the basis of this model, for example, the 1 Ma basalt centers of Crater Flat can be inferred to have formed by two distinct or related dikes propagating in opposite directions: one to the northeast forming Black Cone and Makani cone centers, and one to the southwest forming Red Cone and the Little Cone centers. An appealing aspect of this model is that it is consistent with the volume relations of the Quaternary basalt centers of Crater Flat. The smallest-volume centers (Makani and Little Cone centers) are located at the opposite ends of the cluster.

In most cases, there are sufficient data to make reasonable judgments about the event assignments for the model categories. These assignments will, of course, be tested and refined by acquisition of additional information from ongoing site characterization studies. There are limited data for selection of volcanic event models for the basalt of Amargosa Valley. The basalt of Amargosa Valley has been penetrated only in a single, exploratory drill hole (Harris et al. 1992). Information on the dimensions of the center are based on interpretations of aeromagnetic data (Kane and Bracken 1983; Crowe et al. 1986; Langenheim et al. 1991; 1993).

One major question concerning the listed calculations of Table 7.5 is what is a reasonable representation of the uncertainty of the homogeneous Poisson calculations? There is not a single and simple answer to that question. One method for defining the uncertainty is to examine the descriptive statistics using the data summarized in Table 7.5. Mean volcanic event rates using the combinations of homogeneous Poisson models listed in Table 7.5 are $2.0 \pm 0.6 \times 10^{-6}$ events yr^{-1} for the minimum model, $4.6 \pm 1.7 \times 10^{-6}$ events yr^{-1} for the maximum model, and $3.5 \pm 1.3 \times 10^{-6}$ events yr^{-1} for the most likely model. These ranges are equal to average recurrence intervals for volcanic events of 450 ka (minimum model), 220 ka (maximum model) and 290 ka for the most likely model. The minimum estimate of Table 7.5 is 1.5×10^{-6} events yr^{-1} (670 ka recurrence interval), and the maximum estimate is 8.0×10^{-6} events yr^{-1} (125 ka recurrence interval). A second method is to calculate univariate statistics for the most geologically reasonable sets of data from Table 7.5 (preferred models). These are the volcanic cycle (4.8 Ma) and the Quaternary accelerated (1 Ma) models. Mean recurrence rates combining the preferred models of Table 7.5 are $2.3 \pm 0.7 \times 10^{-6}$ events yr^{-1} (385 ka recurrence interval) for the minimum model, $5.0 \pm 2.5 \times 10^{-6}$ events yr^{-1} (200 ka recurrence interval) for the maximum model, and $3.9 \pm 1.9 \times 10^{-6}$ events yr^{-1} (260 ka recurrence interval) for the most likely model (data from Table 7.5). A third alternative method is to use the method of Ho (1992), who calculated a 90% confidence interval for the recurrence of Weibull-distributed volcanic events. The resulting values are 1.8×10^{-6} to 1.3×10^{-5} events yr^{-1}. Ho (1992) makes the valid argument that interval estimates are more informative than point estimates. However, he

calculated confidence intervals about a worst case recurrence estimation, *not* a midpoint estimate. Moreover, the validity of calculations of confidence intervals is limited by the sparse data.

A third and preferred approach to calculating the uncertainty of the homogeneous Poisson models is to use simulation modeling (Crowe et al. 1993). We prefer this approach because of the paradox of the volcanic record of the YMR. That paradox is the following:

> *There are only a small number of volcanic events that have occurred in the YMR during the Quaternary. The small number of events means that volcanic recurrence rates are low, but the uncertainty of calculating the rate is large. Viewed conversely, if there were more volcanic events in the YMR during the Quaternary, there would be less uncertainty in calculating the recurrence rate. However, the risk of future events, by virtue of the larger number of events,* ***would be higher.*** *The trade-off between decreased risk and increased uncertainty seems logical. Accepting the opposite view leads to two mutually illogical conclusions: (1) the best place to locate a repository would be in an active volcanic field because the recurrence rate could be calculated with increased certainty or (2) the worst place to locate a repository would be in an area of no volcanic events because the uncertainty of calculating volcanic risk would be unbounded.*

The position taken in this volcanism status report is that the record of volcanic events in the YMR cannot be used to make robust calculations of the risk of volcanism. The recurrence rate of volcanic events is low ($<10^{-5}$ events yr^{-1}), but the data sets are too limited to test for statistical significance. Therefore, it is unrealistic to attempt to define the uncertainty of homogeneous Poisson models using a conventional statistical approach.

The problem can be solved through the application of risk analysis (Newendorp 1974; Megin 1984; Clemen 1991; Meyer and Booker 1992; Crowe et al. 1993). Elements of subjective judgment are used to translate uncertain data into probability distributions. We adopt this approach and combine the different approaches for estimating E1 with risk simulation to calculate the distribution of E1 in probability space. The results of simulation modeling for E1 are described at the end of this section. Similar approaches are also used for E2 and Pr(E2 given E1)Pr(E1) in following sections.

3. Nonhomogeneous Poisson Models. We next examine the application of NHPP to the record of volcanic events in the YMR. This approach suffers from the same limitations as the time-series analyses: the small data set. Under ideal conditions, the record of volcanic events in the YMR would be tested against different distribution models using statistical tests of the goodness of fit. There are three standard fitting methods for testing data distributions. The Chi-square test compares the data fit to a hypothesized probability density function (Tuckwell 1988). The Kolmogorov-Smirnov (K-S) test is similar to the Chi-square test but does not require grouping of data and can be applied to small sample sizes (Davis 1986). The Anderson-Darling test is similar to the K-S test but is designed to detect discrepancies in the tails of distributions (Walpole and Myers 1993).

The choice of NHPP models is large and many different approaches are possible. None of the standard statistical tests provide reasonable fits to the small data set for the time-distribution of volcanic events in the YMR. Lacking goodness of fit tests, the selection of distribution models must be based on nonstatistical judgments. In fact, the sparse data set provides the primary justification for selection of simple or homogeneous Poisson distribution models, which require minimal data assumptions. Ho (1991, 1992) reviewed NHPP recurrence models for the YMR and applied an NHHP model with Weibull intensity for estimating the instantaneous recurrence rate. He used an HPP for predicting the time of future eruptive

events. The density function of a Weibull process is described in equation (7.10); the form of the nonhomogeneous intensity function applied to the Yucca Mountain data set is shown in equation (7.11). The Weibull distribution is a versatile distribution that can be fitted to a wide range of data applications although with limited theoretical justification (Devore 1987). Modeling the time distribution of volcanic events as a Weibull process avoids a major disadvantage of the Poisson process: the Poisson process assumes uniform or stationary values of the intensity parameter λ. For the application to the YMR, this means that the model is insensitive to the time-distribution of events and the uncertainty in estimating the chronology of volcanic events. In contrast, the form of the Weibull model is dependent on the *time patterns* of volcanic events (Ho 1991).

An important comparison between volcanic recurrence estimates using Weibull versus simple Poisson processes can be tested by examination of the values of β, a fitting parameter for the Weibull density function. The Weibull model is similar to the exponential distribution when $\beta \approx 1$, and therefore includes the case of the Poisson or homogeneous Poisson model (Devore 1987; Tuckwell 1988). A goodness-of-fit test can be constructed, as noted by Ho (1991), to estimate whether β is ≤ 1 or ≥ 1. Crowe et al (1992) argued that the simple Poisson model is appropriate for conditions of steady state or waning volcanism. This is equivalent in the Weibull model to $\beta \leq 1$. Therefore, the Weibull model would be a more appropriate fit to the YMR data if $\beta > 1$.

Ho (1991) obtained a β of 1.09 for an analysis of Quaternary volcanic events and values of >1 for analysis of three cases of Pliocene and Quaternary volcanic events. Careful examination of the latter calculations shows that the three cases where $\beta > 1$ are a result of how the problems were structured because of the sensitivity of β to the time-distribution of volcanic events. For one case of $\beta > 1$, Ho (1991) used a *t* of 6 Ma (Pliocene interval) and assigned the youngest possible age to the Lathrop Wells event (10 ka). This results in *no* volcanic events during the first 40% of the time interval of his calculations (6.0 to 3.7 Ma). The 6 Ma interval used in combination with the youngest possible age of the Lathrop Wells center (polygenetic episode *not* an initiating event), forces the value of β to be >1 (see equation 7.11). For the second case of $\beta > 1$, Ho (1991) used a *t* of 3.7 Ma (volcanic cycle) but he *discarded* all the 3.7 Ma events, presumably because their recalculated cumulative times are zero. This distributes all the volcanic events in the late Pliocene and Quaternary and forces β to be >1. Clearly the limited data set of volcanic events in the YMR makes discarding of data an unacceptable approach. Finally, for the third case of $\beta > 1$, Ho (1991) used a *t* of 1.6 Ma (Quaternary interval) but assigned four volcanic events to the Lathrop Wells center, *all* with ages of 10 ka. This assignment skews the distribution of events to young ages and again forces β to be >1.

Connor and Hill (1993) reviewed existing calculations and made independent estimations of the probability of magmatic disruption of the Yucca Mountain site using nonhomogeneous approaches for estimating E1 and E2. They recognized the importance of *t*, the time interval of volcanic events, and β. Connor and Hill (1993) evaluated the sensitivity of β and θ and calculated values for a range of assumptions, primarily by varying the estimated time of volcanic events. Their values of β are all <1 except for one case. That case is where they assigned the *youngest possible ages* to all Quaternary volcanic events in the YMR (β= 2.2) (Connor and Hill 1993, their Table 2).

To independently assess the sensitivity of β, and to test the Weibull versus Poisson models, we calculated the fitting parameters (WEI β, θ) for the Weibull model using all combinations of cluster and event models listed in Table 7.6. A critical assumption of this calculation is again *t*, the time of volcanic events. We follow the same models and assumptions used to construct Table 7.5 with one important exception. If *t* of the interval (0,*t*) is equal to the age of the oldest volcanic events, the cumulative times are 0 and the β is undefined. This is assumed to be the reason Ho (1991) discarded the oldest volcanic events in his calculations. A more logical approach is to assume the oldest events differ in age from *t* by the standard deviation of the replicate age determinations. For example, the assigned difference for the 4.8 Ma volcanic events is 0.13 ka where 0.13 is the standard deviation of replicate ages (see Chapter 2). The importance of this data approach cannot be understated. Ho (1991) obtained a $\beta = 2.55$ for a time interval of 3.7 Ma when the 3.7 Ma events were rejected. If the same calculations are repeated and the 3.7 Ma events are included, the $\beta = 0.68$.

Table 7.6 is a compilation of β and estimates of the recurrence rate using Ho's (1992) form of the Weibull model for the minimum, most likely, and maximum values of cluster, center, and stress-field dike events for the different combinations of *t* (2.0 Ma, 4.8 Ma, 1.6 Ma, and 1.0 Ma). The β values fall into two groups. All values of β are ≤ 1 for the preferred Quaternary accelerated and the volcanic cycle models (the β values range from 0.6 to 1.0). Thus for intervals where *t* is defined on the basis of the *volcanic record*, the Weibull model gives longer recurrence intervals than the homogeneous Poisson model. The values of β for all other data sets are >1. Examination of the data set provides the explanation for the values of β of >1. All of the calculations span intervals where the initial values of *t* coincide with a gap in the record of volcanic events (1.0 to 2.9 Ma; the interval between the Quaternary basalt of Crater Flat and the basalt of Buckboard Mesa). Because of the form of the construction of the calculations, the *distribution* of volcanic events are skewed to younger ages and therefore to higher values of β. This illustrates an important perspective: calculations of the recurrence rate using a Weibull model may not be appropriate when the interval (0,*t*) initiates during a time of no volcanic activity. Structured in this manner, the fitting parameters for recurrence rate calculations using a Weibull distribution may *overestimate* λ. This perspective gives equal insight to the homogeneous Poisson calculations. The HPP calculations may *underestimate* λ when they are constructed across a significant interval of no volcanic activity. Accordingly, the most appropriate data sets for estimating the recurrence rate of volcanic events, from a geologic and calculation perspective, are the sets for the volcanic cycle (4.8 Ma to present) and the Quaternary accelerated model (1 Ma to present).

Mean values of the recurrence rate using estimations from a Weibull distribution model are $3.0 \pm 1.2 \times 10^{-6}$ events yr^{-1}, $5.5 \pm 2.4 \times 10^{-6}$ events yr^{-1} and $4.6 \pm 1.9 \times 10^{-6}$ events yr^{-1} for respectively, the minimum, maximum and most likely values of Table 7.6. The reciprocals of these mean estimations are 330 ka (minimum), 180 ka (maximum), and 220 ka (most likely) and represent estimations of the recurrence time between volcanic events. The minimum value of all the Weibull calculations is 1.4×10^{-6} events yr^{-1} (700 ka recurrence time) and the maximum is 8.4×10^{-6} events yr^{-1} (120 ka recurrence time). Collectively, the recurrence estimations using a Weibull distribution tend to be *slightly greater* than estimations using a homogeneous Poisson distribution. However, if the sets are compared for the two preferred models (4.8 Ma volcanic cycle and 1.0 Ma accelerated interval), the mean values of the minimum, maximum, and most likely estimates using the HPP model *exceed* the NHPP estimations. The minimum, maximum, and most likely values of the preferred models using an NHPP model are, respectively, $2.1 \pm 0.8 \times 10^{-6}$, $3.4 \pm 1.3 \times 10^{-6}$, and $2.9 \pm 1.0 \times 10^{-6}$ events yr^{-1} (compare summary statistics for the preferred models for Tables 7.5 and 7.6). The reason for this reversal in the recurrence estimations is the β values for the preferred data sets are all <1.0.

Table 7.6 Nonhomogeneous recurrence models (E1) for the YMR.

Interval	Model	Interval (yr.)	Minimum events yr^{-1}	Maximum events yr^{-1}	Most Likely events yr^{-1}
Quaternary		2.00E+06			
	Events		3	8	6
	Beta		3.10	2.10	2.30
	Weibull Rate		4.6E-06	8.4E-06	6.9E-06
	Stress Dike		3	8	5
	Beta		3.1	2.10	2.10
	Weibull Rate		4.6E-06	8.4E-06	5.2E-06
Volcanic Cycle*		4.80E+06			
	Events		8	19	12
	Beta		0.84	0.72	1.00
	Weibull Rate		1.4E-06	2.9E-06	2.5E-06
	Stress Dike		8	10	10
	Beta		0.84	0.9	0.9
	Weibull Rate		1.4E-06	1.9E-06	1.9E-06
Quaternary Rate		1.60E+06			
	Events		3	8	6
	Beta		1.7	1.4	1.7
	Weibull Rate		3.2E-06	7.0E-06	6.4E-06
	Stress Dike		3	6	5
	Beta		1.7	1.7	1.8
	Weibull Rate		3.2E-06	6.4E-06	5.6E-06
Quaternary Accelerated*		1.00E+06			
	Events		3	8	6
	Beta		0.94	0.60	0.70
	Weibull Rate		2.8E-06	4.8E-06	4.2E-06
	Stress Dike		3	6	5
	Beta		0.94	0.70	0.60
	Weibull Rate		2.8E-06	4.2E-06	3.0E-06
Summary Statistics (all models)		*Mean*	*3.0E-06*	*5.5E-06*	*4.6E-06*
		Median	*3.0E-06*	*5.6E-06*	*4.7E-06*
		Geomean	*2.8E-06*	*4.9E-06*	*4.0E-06*
		Std Deviation	*1.2E-06*	*2.4E-06*	*1.9E-06*
*Summary Statistics (Preferred Models)**		*Mean*	*2.1E-06*	*3.4E-06*	*2.9E-06*
		Median	*2.1E-06*	*3.5E-06*	*2.7E-06*
		Geomean	*2.0E-06*	*3.2E-06*	*2.8E-06*
		Std Deviation	*0.8E-06*	*1.3E-06*	*1.0E-07*

* Preferred models are models with event counts spanning intervals that correspond to cycles of volcanic activity (4.8 Ma to present; 1.0 Ma to present)

4. Volume-Predictable Recurrence Rates. Crowe et al. (1982) developed an alternative approach for estimating the recurrence rate of volcanic events. They examined magma-output rates from a plot of the erupted volume of magma versus time for basaltic volcanic events of the YMR. The slope of the curve on this plot is the magma-output rate. Crowe and Perry (1989) noted that there are several limitations of a homogeneous Poisson model based on event counts that can be overcome by application of volume-predictable recurrence rates. First, vent counts record only the recognition of a volcanic event. Their magnitude, commonly expressed as the volume of the event, is not accounted for through a vent count. A

large-volume eruption is given an equal weight in an event count as a small-volume eruption. Second, the previous discussion of homogeneous and nonhomogeneous Poisson event counts show they can overestimate or underestimate recurrence rates, dependent on the observation period. This problem can be overcome by constructing vent counts over an interval that is tied to the geologic record. Crowe and Perry (1989) noted that an alternative approach, which is based on a process-based perspective of basaltic volcanism, is to construct time-volume curves of volcanic activity.

Estimations of recurrence rates for volcanic centers and fields using a time-volume relationship have been determined frequently in the geological literature. Bacon (1982) noted that time-volume behavior of basaltic and rhyolitic volcanism in the Coso volcanic field of eastern California exhibited time-predictable behavior. He discussed analogs between the volcanic events of the Coso volcanic field and slip-predictable behavior observed for some types of earthquake sequences. Kuntz et al. (1986) described volume-predictable eruptions of the Great Rift in the Snake River plains of Idaho. They identified a change in magma-output rates on the basis of a change in slope of the curve of magma-volume versus time. Wadge (1982) described steady-state (volume-predictable) behavior of many polygenetic volcanoes. He used the slope of a time-volume curve to define the effusion rate of volcanoes and speculated that the steady-state behavior was probably controlled by the magma-supply rates. Volume-predictable behavior was documented for historical eruptions of the volcanoes of Kilauea, Mauna Loa, and Piton de la Fournaise (King 1989; Stieltjes and Moutou 1987). Theoretical support for a volume-predictable behavior of volcanoes controlled by magma-supply rate was provided by Shaw (1980, 1987).

Estimation of magma-output rates for the basaltic volcanic record of the YMR has been established through examination of plots of magma volume through time (Crowe et al. 1982, 1989; Crowe and Perry 1989). Published estimations range from 210 to 33 $m^3\ yr^{-1}$. The variability in the estimated output rates is a result of different observation periods and different models of the age and volume of the volcanic centers. Crowe and Perry (1989) noted that the calculations of the magma-output rate for the YMP are especially sensitive to assumptions concerning the volume of the scoria-fall sheet associated with each volcanic center.

The major limitations in estimating magma-output rates in the YMR are the small number of Pliocene and Quaternary volcanic events (sparse data set), the difficulty of reconstructing eruption volumes for Pliocene volcanic events, and the variability and uncertainty in establishing the chronology of some volcanic events. We are still reassessing the eruption volumes of volcanic events. Moreover, the chronology of volcanic events has not been completed for all Quaternary and Pliocene volcanic events. Therefore, estimations of the magma-output rate through time remain preliminary. However, an important test of the models of Crowe et al. (1982, 1989) and Crowe and Perry (1989) is how the simple regression model of time (independent variable) versus magma volume (dependent variable) is affected by adding data not used in previous regression calculations. The important new data include the recognition of the Pliocene-age, basalt center of Thirsty Mesa (4.8 Ma; 3 km^3), the drilling, dating, and volume estimates for the aeromagnetic anomalies of the Amargosa Valley (Chapter 2), and changes in the estimated ages of individual volcanic centers using the most current geochronology data. Exploratory data analyses of the revised data set (Table 7.4) reveal several important features. First, the volume data are not randomly distributed. The large volume basalt center of Thirsty Mesa is an outlier and skews the distribution of volume data toward larger values. Second, an influence diagram of volume-time data shows the correlation between volume and age is strongly influenced by the large volume of the basalt of Thirsty Mesa. Any regression analyses of the data set will be weighted heavily by this data point.

Figure 7.8 is a plot of magma volume versus time and includes the most current data for volcanic events in the YMR. Visually, the fit to a linear model is not satisfactory. There is considerable dispersion from the regression curve, and the y-intercept occurs at negative values of magma volume (an unrealistic fit

physically). The regression fit can be improved somewhat by modifying the data using geologic constraints. The aeromagnetic anomalies of the Amargosa Valley are close in age to the basalt of Crater Flat and can be plotted as a single volume-age point. Figure 7.9 is a revised plot with the two units combined. The fit of the linear regression curve (solid line) is improved but still remains unsatisfactory; the y-intercept is negative, and some of the points are still dispersed off the regression curve. Visually, the data distribution is curvilinear in the x,y plane and may be better fit with a transformed or nonlinear regression model. Two approaches are used to further test the data. First, the dashed line of Figure 7.9 is the regression fit obtained using distance weighted least squares of volume-time data. Visually the fit is much improved, and the data distribution is consistent with an exponential decline in magma eruption rates through time. Second, to test for intrinsic linearity, the volume (y-axis data) was log transformed and fitted by regression using linear smoothing. Figure 7.10 is a plot of the linear regression fit obtained using a regression model of the form

$$E_v = a + b\ln(age) + \varepsilon \quad (7.13)$$

where E_v is the volume, a is a constant, b is the slope, and ε is a random variable representing the regression prediction error. Visually the fit of the log-regression curve is much improved (Fig. 7.10). However, the linear fit is best for the Pliocene data points, and the data are more dispersed for the Quaternary data points. The fit is worse for the basalt of Sleeping Butte. We next examine the suitability of output coefficients and the residuals for a series of regression calculations.

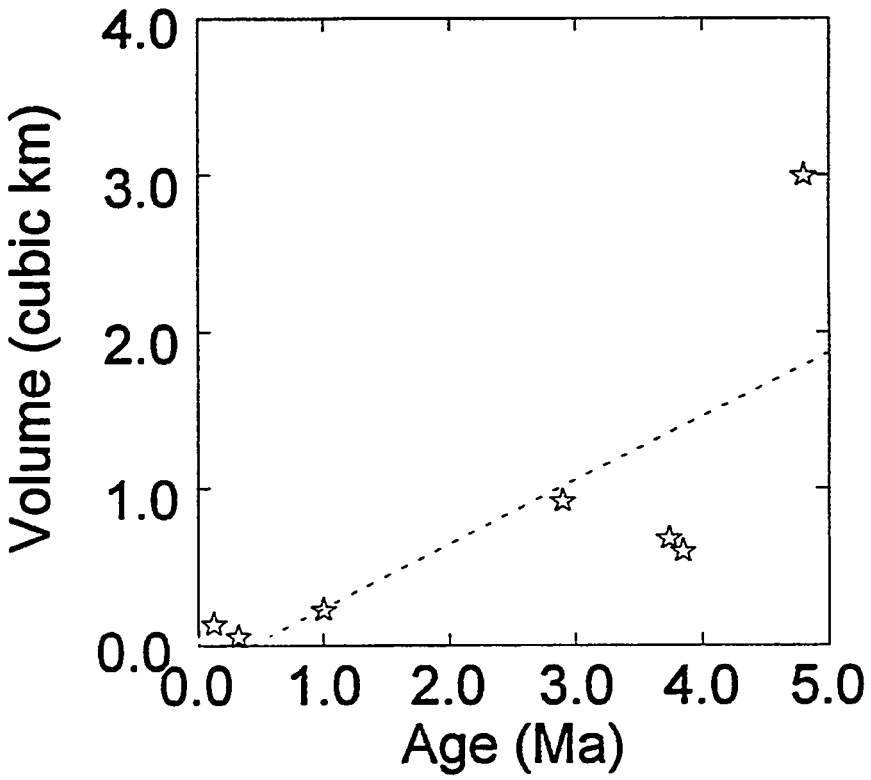


Fig. 7.8 Bivariate plot of magma volume (DRE) versus age for the Pliocene and Quaternary volcanic events of the YMR. The dashed line is the least squares, linear-regression fit to the data points. Symbols noted by stars represent volcanic events.

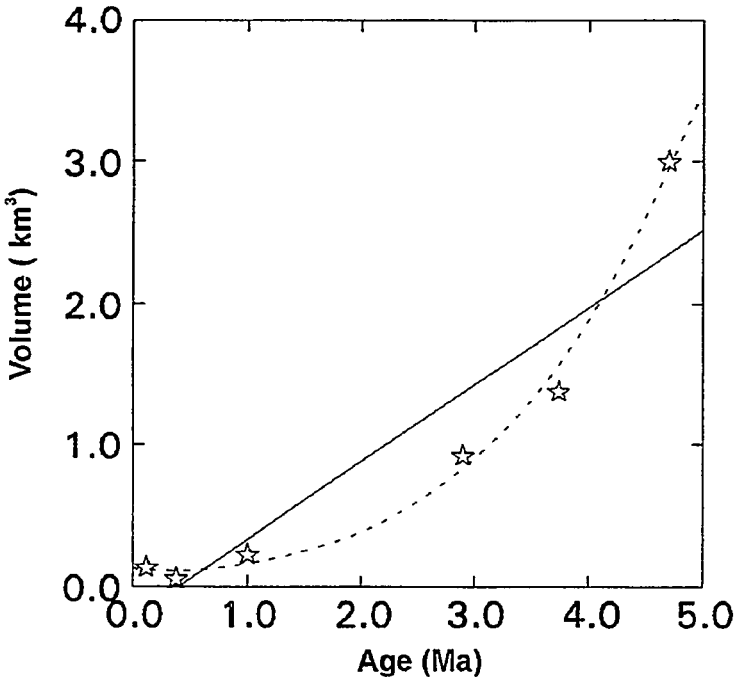


Fig. 7.9 Bivariate plot of magma volume (DRE) versus age for the Pliocene and Quaternary volcanic events of the YMR with the basalt of southeast Crater Flat combined with the aeromagnetic anomalies of the Amargosa Valley. The solid line is the linear-regression curve, the dashed line is fitted by distance weighted least squares.

Table 7.7 shows the regression results of the simple linear models using different combinations of the data set of Table 7.4. Table 7.8 is the regression residuals for each of the regression cases of Table 7.7. The regression coefficients (multiple R and squared multiple R) are >0.86 for all regression cases except cases 1 and 6 and indicate a strong correlation between the volume of volcanic events and the event age. The most significant regression fits are for cases 3 and 4 (using two-tailed *P* estimates). The slope or magma-output rate derived from all regression fits ranges from 140 to 750 $m^3\ yr^{-1}$. These are higher estimates than previous calculations and reflect the addition in the regression calculations of the large-volume Pliocene volcanic events. Careful examination of the residuals shows that the regression fits are generally unsatisfactory (Table 7.8). The studentized residuals show that the data point for the basalt of Thirsty Mesa is an outlier for regression cases 1 and 2, the Lathrop Wells data point is an outlier for case 3, and the Sleeping Butte data point is an outlier for the log-normalized regression (case 7). Plots of residuals versus event age, and residuals versus estimated values, show linearity and curvilinear structure. The patterns suggest the data distribution does not meet assumptions of the regression model because the distribution of the error variable ε is nonrandom. The patterns of the residuals suggest an added variable or quadratic term is needed in the regression model. The log-normalized model improves the fit of the residuals but also shows linear and curvilinear patterns on plots of residuals versus the age (sequencing of residuals) of data points. The three point regression model of the Quaternary events gives a low value of multiple R (Table 7.7).

The difficulties with the regression calculations require caution in interpreting the results. Additional site characterization data will be obtained that may change the regression analysis. Revised volume estimations will be completed for all volcanic centers. Changes in estimated magma volumes may be important particularly for the log-transformed regression analyses that shows the basalt of Sleeping Butte as an outlier. We plan to reassess whether a previously mapped western lava lobe may be part of the

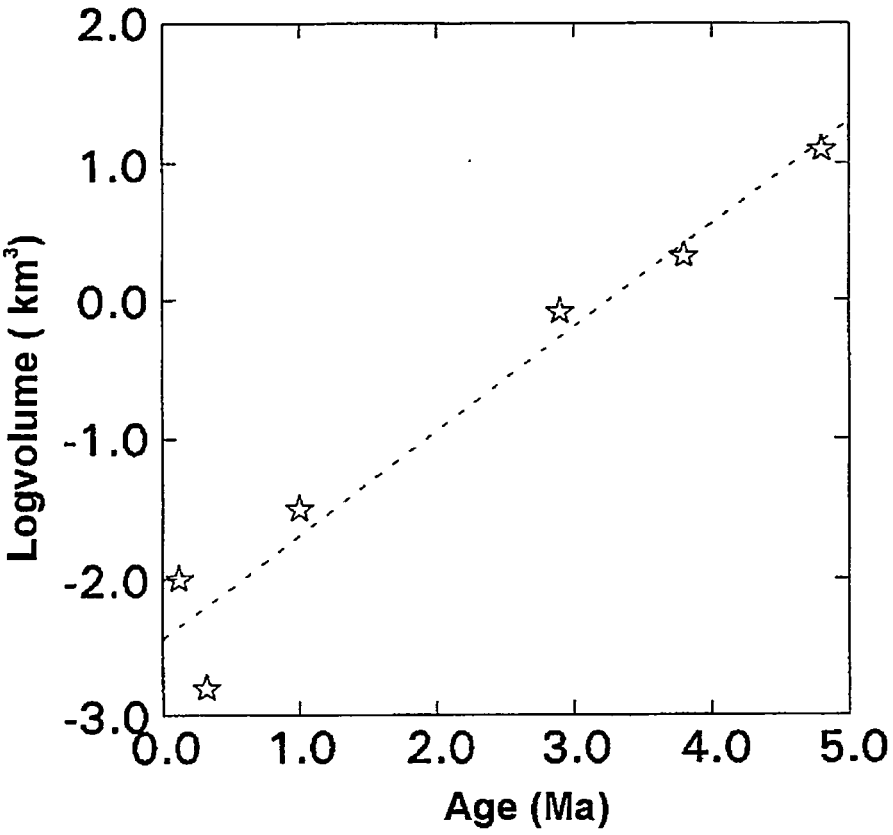


Fig. 7.10 Plot of log-transformed magma volume (DRE) versus age for the Pliocene and Quaternary volcanic events of the YMR with the basalt of southeast Crater Flat combined with the aeromagnetic anomalies of the Amargosa Valley. The solid line is the linear-regression curve of the volume-transformed data.

Hidden Cone center (see Chapter 2). Incremental addition of this lava volume may move the volume point for the basalt of Sleeping Butte closer to the log-transformed regression curve (Fig. 7.10). We will also examine whether better regression fits can be obtained using multiple regression models. There are strong bivariate correlations between magma volume and the location of basalt centers (see Chapter 3). Moreover, there are systematic variations in magma chemistry with time that correlate with erupted volumes. It may be possible to examine these data as additional variables in multiple regression models.

Until further data are available, the only marginally significant regression results are for cases 3 and 4 of Table 7.7. The magma-output rate is used for these cases (270 and 300 $m^3\ yr^{-1}$) for estimations of volume-predictable recurrence rates. Table 7.9 is a compilation of representative magma volumes of the volcanic events for the YMR. These values are divided by the magma-output rates to yield the predictor variable, the generation time to produce a future volcanic event. The generation time is calculated as different combinations of the mean, median, and geometric mean of the magma volumes of volcanic events during the Quaternary and the YPB. The event recurrence rate is the reciprocal of generation time. The calculation for the recurrence time to the next volcanic event using the magma-output rate is given by:

$$Ne = (Rv/Op) - Lt, \qquad (7.14)$$

Table 7.7 Results of simple regression fits for seven combinations (cases) of Pliocene and Quaternary volcanic centers of the YMR.

Regression	Model	N	Multiple R	Squared Multiple R	Variable	Coeff	Std Error	T	P (2 tail)
Case 1	All Events	7	0.78	0.61	Constant	-0.17	0.44	-0.39	0.716
					Volume	0.41	0.14	2.80	0.038
Case 2	Case 1 with SE CF and Aeromag Anomalies Combined	6	0.93	0.86	Constant	-0.19	0.30	-0.66	0.545
					Volume	0.53	0.10	4.97	0.008
Case 3	Case 2 without Thirsty Mesa	5	0.98	0.97	Constant	-0.02	0.07	-.31	0.780
					Volume	0.34	0.03	10.57	0.002
Case 4	Case 3 Without Undrilled Aeromag Anomalies	5	0.98	0.96	Constant	0.03	0.07	0.44	0.940
					Volume	0.26	0.03	8.61	0.003
Case 5	Case 4 without SE Crater Flat	4	0.96	0.96	Constant	0.01	0.07	0.09	0.940
					Volume	. 30	0.04	6.96	0.020
Case 6	Quaternary Volcanic Centers	3	0.76	0.58	Constant	0.08	0.07	1.04	0.487
					Volume	0.14	0.12	1.17	0.451
Case 7	All Events, Aeromag Combined Log-Transformed Volume	6	0.97	0.95	Constant	-2.43	0.28	-9.75	0.001
					Volume	0.75	0.10	8.45	0.001

Table 7.8 Regression residuals for the seven regression cases of Table 7.7.

Regression Model	Volcanic Events	Estimate	Residual	Leverage	Cook	Student	Sepred
Case 1							
	Thirsty Mesa	1.79	1.21	.41	1.67	8.33	.47
	Aeromag Anom	1.40	-.80	.24	.25	-1.37	.36
	SE Crater Flat	1.35	-.67	.23	.16	-1.07	.35
	Buckboard Mesa	1.01	-.09	.15	.00	-.12	.29
	Quat Crater Flat	.24	-.01	.23	.00	- .01	.35
	Sleeping Butte	-.04	.10	.34	.01	.15	.43
	Lathrop Wells	-.12	.26	.38	.07	.42	.45
Case 2							
	Thirsty Mesa	2.37	.63	.53	2.19	8.49	.34
	SE Crater Flat	1.83	-.45	.31	.30	-1.23	.26
	Buckboard Mesa	1.35	-.43	.20	.13	-1.03	.21
	Quat Crater Flat	.34	-.11	.24	.01	-.22	.23
	Sleeping Butte	- .03	.09	.34	.01	.20	.28
	Lathrop	- .13	.27	.38	.17	.69	.29
Case 3							
	SE Crater Flat	1.30	.08	.64	1.26	1.33	.10
	Buckboard Mesa	.99	-.07	.35	.17	-.73	.06
	Quat Crater Flat	.33	-.10	.24	.16	-1.04	.05
	Sleeping Butte	.09	-.03	.36	.03	-.28	.07
	Lathrop Wells	.02	.12	.41	.72	2.07	.07
Case 4	SE Crater Flat	1.04	-.06	.63	.92	-1.06	.08
	Buckboard Mesa	.81	.11	.36	.50	1.75	.06
	Quat Crater Flat	.30	-.07	.24	.10	-.74	.05
	Sleeping Butte	.11	-.05	.36	.13	-.61	.06
	Lathrop Wells	.06	.08	.41	.39	1.07	.06
Case 5							
	Buckboard Mesa	.90	.03	.93	9.55	1.43	.09
	Quat Crater Flat	.31	-.08	.25	.16	-.95	.05
	Sleeping Butte	.10	-.04	.37	.10	-.44	.06
	Lathrop Wells	.04	.10	.44	.71	2.88	.06
Case 6							
	Quat Crater Flat	.22	.01	.97	15.4	.	.08
	Sleeping Butte	.12	-.06	.39	.32	.	.05
	Lathrop Wells	.09	.05	.64	.88	.	.06
Case 7	Thirsty Mesa	1.16	-.06	.53	.03	-.19	.27
	SE Crater Flat	.40	-.09	.31	.02	-.24	.21
	Buckboard Mesa	-.27	.19	.20	.04	.51	.17
	Quat Crater Flat	-1.69	.19	.24	.05	.54	.18
	Sleeping Butte	-2.20	- .60	.34	1.00	-8.24	.22
	Lathrop Wells	-2.35	.35	.38	.45	1.30	.23

Table 7.9 Age, Cumulative Volume, Magma-Output Rates, Magma-Generation Rates, and Event Rates for Pliocene and Quaternary Volcanic Centers

EVENT MODELS	AGE (Ma)	VOLUME	CUMVOL	MOR* ($m^3\ yr^{-1}$)			
Event: Case I							
Thirsty Mesa	4.8	3.0E+09	3.0E+09	305	GR** (mean)	GR (geomean)	GR (median)
Amargosa Valley	3.8	3.0E+08	3.3E+09	268	2.5E+06	1.2E+06	9.7E+05
CF3.7	3.7	6.8E+08	4.0E+09		2.8E+06	1.4E+06	1.1E+06
Buckboard	2.9	9.2E+08	4.9E+09		ER*** (mean)	ER (geomean)	GR (median)
CF1.0	1.0	2.3E+08	5.1E+09		4.0E-07	8.2E-07	1.0E-06
Sleeping Butte	.32	5.9E+07	5.2E+09		3.5E-07	7.2E-07	9.0E-07
Lathrop Wells	.12	1.4E+08	5.3E+09				
Mean	*7.6E+08*	*Median*	*3.0E+08*				
Geomean	*3.8E+08*	*Std Deviation*	*1.0E+09*				
Event: Case II					GR (mean)	GR (geomean)	GR (median)
CF1.0	1.0	2.3E+08	2.3E+08	305	4.6E+05	4.0E+05	4.5E+05
Sleeping Butte	.32	5.9E+07	2.9E+08	268	5.2E+05	4.5E+05	5.1E+05
Lathrop Wells	.12	1.4E+08	4.3E+08		ER (mean)	ER (geomean)	ER (median)
Mean	*1.4E+08*	*Median*	*1.4E+08*		2.2E-06	2.5E-06	2.2E-06
Geomean	*1.2E+08*	*Std Deviation*	*8.5E+07*		1.9E-06	2.2E-06	1.9E-06
Event: Case III					GR (mean)	GR (geomean)	GR (median)
CF-North	1.0	1.7E+08	1.7E+08	305	2.7E+05	2.1E+05	1.9E+05
CF-South	1.0	6.0E+07	2.3E+08	268	3.1E+05	2.3E+05	2.1E+05
Hidden	.32	3.5E+07	2.6E+08		ER (mean)	ER (geomean)	ER (median)
Black Peak	.32	2.4E+07	2.9E+08		3.7E-06	4.9E-06	5.3E-06
Lathrop	.12	1.4E+08	4.3E+08		3.2E-06	4.2E-06	4.6E-06
Mean	*8.6E+07*	*Median*	*6.0E+07*				
Geomean	*6.5E+07*	*Std Deviation*	*6.5E+07*				
*MOR : Magma Output Rate					*Preferred Models*	*Generation Rate*	*Event Rate*
**GR= Generation Rate					*Preferred mean*	*2.9E+05*	*3.4E-06*
***ER = Event Rate					*Preferred median*	*2.0E+05*	*5.0E-06*
					Preferred geomean	*2.2E+05*	*4.5E-06*

where *Ne* is the predicted time to the next volcanic event, *Rv* is the representative volume of a volcanic event, *Op* is the magma output rate, and *Lt* is the time since the last volcanic event (Crowe et al. 1982). The time of the last event is the age of the youngest volcanic event at the Lathrop Wells volcanic center and is estimated to be 9 ka (see Chapter 2).

A difficult attribute to characterize for the magma-volume calculations is the representative volume of a future volcanic event. Table 7.9 compiles magma volumes, the magma-output rates from regression analyses, and generation-time and event-time estimations for three sets of data. These include the YPB volcanic events (4.8 Ma and younger), volcanic events ≤1 Ma, and the smallest-volume events (event = volcanic center) of the Quaternary volcanic record (≤2.0 Ma). Examination of the predicted generation times of representative events for the YPB data set shows that all values exceed 1 Ma, a physically unrealistic value (Table 7.9). Figure 7.9, the plot of magma volume versus time for all volcanic events of the YPB provides an explanation for the long magma-generation times. The volume of erupted magma has decreased exponentially through time. The volume of erupted magma for a representative volcanic event has decreased by more than a factor of *30* since the Pliocene. Averaging the volume of volcanic events for the Pliocene and Quaternary gives mean values that are unrealistically large compared to the volume of volcanic events of the late Quaternary.

A second approach to estimating recurrence times using magma-volume plots is to use the volume of Quaternary eruptive events to establish the representative eruptive volume. This results in decreased estimated magma-generation times but the intervals are still consistently greater than 4×10^6 yr. These generation times give estimated event rates of $\leq 2.5 \times 10^{-6}$ events yr^{-1}. These estimates are equal to the minimum homogeneous and nonhomogeneous Poisson rates derived from counts of volcanic events (Tables 7.5 and 7.6). Projection of these rates for the Quaternary and YPB intervals gives low predicted numbers of volcanic events compared to the observed geologic record.

A third approach is to use representative volumes of the smallest Quaternary volcanic events (data set III of Table 7.9). Here, event rates are equal to and slightly greater (3.2 to 5.3×10^{-6} events yr^{-1}) than the homogeneous and nonhomogeneous Poisson event count rates of Tables 7.5 and 7.6.

5. Simulation Modeling: E1 the Recurrence Rate. This part of Chapter 8 uses risk simulation to define and assess the distribution of E1 in probability space. Representative estimates for E1 are selected from the data tables for E1 (Table 7.5 and 7.6). These estimates are used systematically in simulation modeling to generate cumulative probability distribution curves. There are nearly an infinite number of approaches that can be used in risk modeling. No single approach is likely to gain complete acceptance. We attempt to bound the problem by producing a range of probability distribution curves using midpoint estimates for the range of models of the recurrence rate. We also explore the sensitivity of the risk modeling by systematically varying the bounding assumptions used to describe the distributions.

An upper bound for E1 is established from the regulatory guidelines of 10 CFR60 (Fig. 7.11). An adverse condition is defined as the presence of igneous activity in the Quaternary, or 2 Ma using the regulatory definition. Formulated probabilistically, the risk of volcanism becomes a concern for siting a potential repository when there is at least one volcanic event in the Quaternary (1 event/2×10^6 yr. or $\approx 5 \times 10^{-7}$ events yr^{-1}) (*regulatory perspective* of Fig. 7.11). An upper bound to rates of volcanic events can be defined by event rates in large-volume, very active basaltic volcanic fields of the Basin and Range province, selecting fields in analogous tectonic settings as the YMR. The fields used for the rate bounds are the Lunar Crater volcanic field in central Nevada (Scott and Trask, 1971; Crowe et al. 1992, 1993) and the

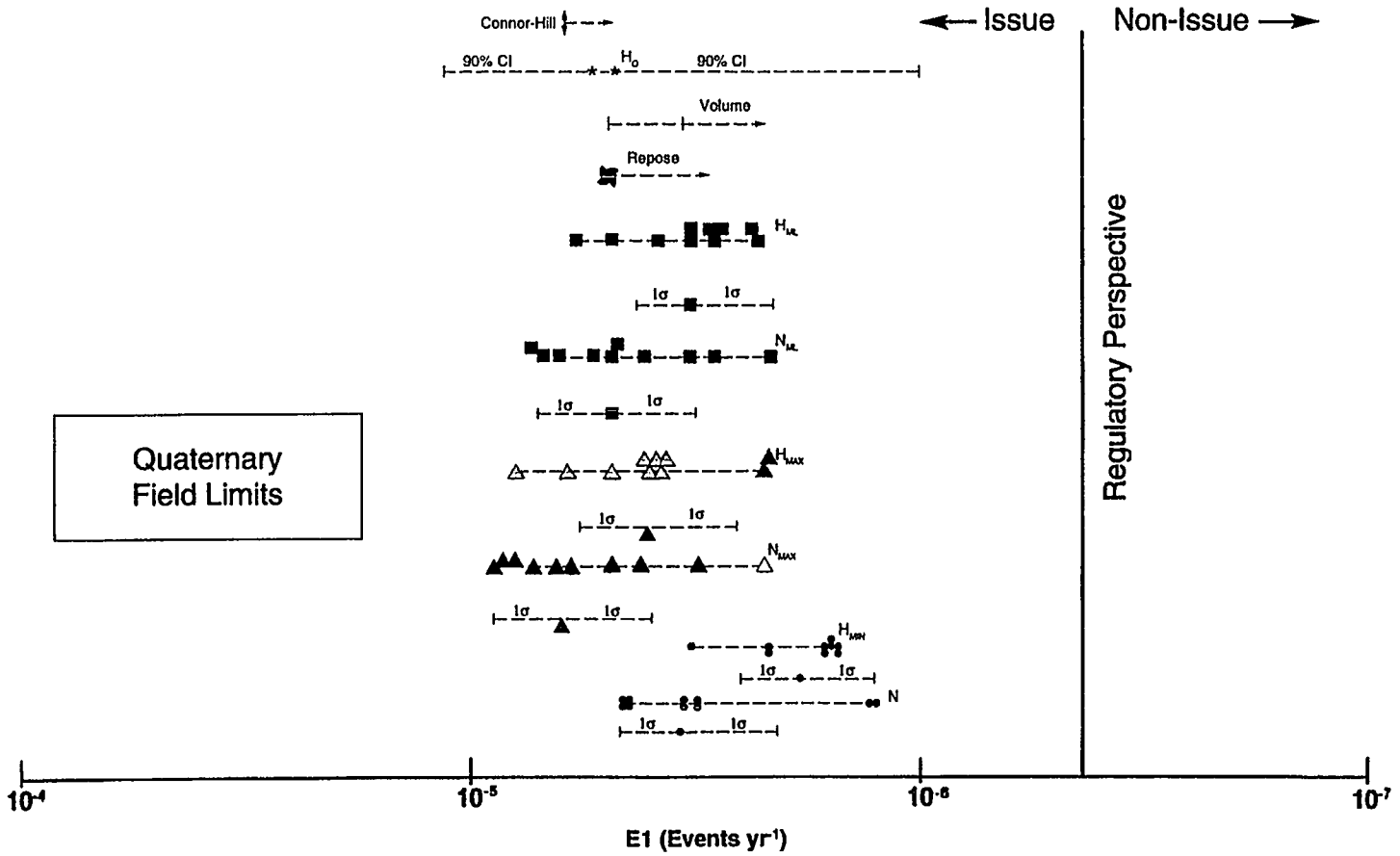


Fig. 7.11 Distribution of estimates of E1 in probability space. The x-axis is a log scale. The y-axis has no scale and is used only to distribute the overlapping estimates of E1. The estimations of E1 from this report are shown as the range of values and as their mean values. N: minimum estimates for nonhomogeneous Poisson models, H_{min}: minimum estimates for homogeneous Poisson models, N_{max}: maximum estimates for nonhomogeneous Poisson models, H_{max}: maximum estimations for homogeneous Poisson models, N_{ml}: most likely estimates for nonhomogeneous Poisson models, H_{ml}: most likely estimates for homogeneous Poisson models; Repose: time-series repose estimates of E1, Volume: volume-predictable estimates of E1 from regression calculations, Ho: E1 estimates (worse case) and confidence intervals from Ho (1992), Connor-Hill: Worse case (vertical arrow) estimates of E1 from Connor and Hill (1993).

Cima volcanic field (Dohrenwend et al 1986; Wilshire 1991; Crowe et al. 1992; 1993). The Yucca Mountain site is *not* located in a major volcanic field. Therefore, logically, the recurrence rates in the YMR must be *less* than rates in major basaltic volcanic fields. The Lunar Crater field has a maximum of 82 vents occurring in 28 clusters of probable Quaternary age (Crowe et al. 1992). A cluster is defined as a closely aligned group of volcanic vents that could be fed from a *single dike system.* They are identified primarily from structural alignments and proximity of individual vents. The Cima volcanic field has 29 vents in 22 clusters, all of inferred Quaternary age. Translating these vent and cluster counts into event counts gives Quaternary recurrence rates of 4.5×10^{-5} to 1.1×10^{-5} events yr^{-1} (we assume a homogeneous Poisson model for the fields because the chronology of the events is too poorly constrained to test other distribution models). These rates are shown in the box labeled volcanic field limits on Fig. 7.11.

Table 7.10 is a matrix of E1 values assembled for simulation modeling. The matrix is divided into columns representing five simulation conditions; the rows represent eight different approaches used to estimate E1. Crowe et al. (1993) showed that the median (50% estimates) from cumulative probability distributions for E1 is sensitive to the selection of probability bounds and is somewhat insensitive to midpoint estimates. The five simulation models of Table 7.10 assign different values for the upper and lower bounds of assumed distributions for E1. There is insufficient information (limited number of volcanic events in the geologic record) to define precisely the shape of the probability distribution curve between the upper and lower bounds of Figure 7.11. The most logical choice for a distribution form for E1 is the triangular distribution (boundary values constrained, midpoints estimated). However, because the distribution bounds for E1 can be defined (their values are >0 on a probability distribution curve), the triangular distribution is not appropriate (Newendorp 1974). We use a trigen distribution model for most of the modeling simulations. This is a modified form of the triangular distribution and allows input of upper, lower, and midpoint estimates. The midpoint estimate is the most likely value, and the upper and lower estimates are chosen from values that are >0 and bracket the midpoint estimate (lower bound < midpoint < upper bound).

Simulation 1 of Table 7.10 uses midpoint estimates of E1 from the summary statistics and estimates of Tables 7.5, 7.6, and 7.9; the 25 and 75 percentiles of the distribution curve are assigned from the *minimum* and *maximum* values of the probability tables. Simulations 2 through 4 use the same midpoint estimates as simulation 2 but the upper and lower estimates of the distribution are used from the probability bounds of Fig. 7.11) (lower bound = regulatory perspective; upper bound = volcanic field limits). The lower estimate of 5×10^{-7} events yr^{-1} is assigned a fixed value of 10% in all the simulations. An upper bound of 1.1×10^{-5} events yr^{-1} is assigned a 1, 5, and 10 percentile value, respectively, for simulations two through 4. Simulation 5 uses a normal distribution and values for the mean and standard deviation are taken from Tables 7.5, 7.6, and 7.9. The cross-column variation in the simulation matrix reflects differences in the distribution assumptions (trigen and normal) and boundary assumptions for the distributions.

The eight rows of the E1 simulation matrix vary in the assignment of midpoint estimates for the trigen distribution. Row 1 uses mean values from the summary statistics for the most likely estimates of E1 for all homogeneous Poisson models from Table 7.5. Row 2 uses most likely estimates for homogeneous Poisson models from the summary statistics of the preferred models (corresponding to volcanic cycles of the 4.8 and 1.0 Ma intervals). Row 3 is identical to row 1 but assigns the most likely estimates from summary statistics for all nonhomogeneous Poisson models (Table 7.6). Row 4 is identical to Row 2 but derives the most likely estimates from the summary statistics of the preferred models of the nonhomogeneous distribution. Row 5 assigns the midpoint estimates for E1 from repose calculations.

Table 7.10 Simulation matrix, expected values and matrix statistics for E1, the recurrence rate.

Model	Min	Most Likely	Max	Min(all)	Max(all)				
Homogeneous: All	2.1E-06	3.6E+00	4.6E-06	1.5E-06	8.0E-06				
Homogeneous: Pref	2.3E-06	4.1E-06	5.0E-06	1.7E-06	8.0E-06				
Nonhomogeneous: All	3.0E-06	4.4E-06	5.5E-06	1.4E-06	8.4E-06				
Nonhomogeneous: Pref	2.1E-06	2.9E-06	3.4E-06	1.4E-06	4.8E-06				
Repose			5.3E-06						
Volume-Predict	1.0E-06	3.2E-06	5.3E-06						
Distribution Boundaries	quartiles	10%/1% limits	10%/5% limits	10%/10% limits	Normal (1 σ)				
Risk Simulations	Sim1	Sim2	Sim3	Sim4	Sim5	*Mean*	*Median*	*Geomean*	*Std Dev*
Homogeneous: All	4.8E-06	4.4E-06	4.9E-06	5.4E-06	3.6E-06	*4.6E-06*	*4.8E-06*	*4.6E-06*	*6.8E-07*
Homogeneous: Pref	4.8E-06	4.1E-06	5.0E-06	5.5E-06	4.1E-06	*4.8E-06*	*4.8E-06*	*4.8E-06*	*5.2E-07*
Nonhomogeneous: All	4.8E-06	4.6E-06	5.1E-06	5.6E-06	4.5E-06	*4.9E-06*	*4.8E-06*	*4.9E-06*	*4.4E-07*
Nonhomogeneous: Pref	4.8E-06	4.3E-06	4.8E-06	5.4E-06	2.9E-06	*4.4E-06*	*4.8E-06*	*4.3E-06*	*9.3E-07*
Repose		4.7E-06	5.2E-06	5.7E-06		*5.2E-06*	*5.2E-06*	*5.2E-06*	*4.7E-07*
Volume	2.8E-06	4.4E-06	4.9E-06	5.4E-06	3.4E-06	*4.5E-06*	*4.6E-06*	*4.5E-06*	*1.1E-06*
Minimum		4.0E-06	4.6E-06	5.2E-06	2.2E-06	*4.0E-06*	*4.3E-06*	*3.8E-06*	*1.3E-06*
Maximum		5.3E-06	5.7E-06	6.1E-06	4.5E-06	*5.4E-06*	*5.5E-06*	*5.5E-06*	*6.7E-07*
Ho (1992)	7.0E-06								
Mean	*4.4E-06*	*4.5E-06*	*5.0E-06*	*5.5E-06*	*3.6E-06*				
Median	*4.8E-06*	*4.5E-06*	*5.0E-06*	*5.5E-06*	*3.6E-06*				
Geomean	*4.3E-06*	*4.5E-06*	*5.0E-06*	*5.5E-06*	*3.5E-06*				
Std Deviation	*8.8E-07*	*3.8E-07*	*3.1E-07*	*2.5E-07*	*8.4E-07*				

Simulations 1 - 4: Trigen distribution. Simulation 1: min-max from Tables 7.5 and 7.6. Simulations 2-4: min-max from Fig. 7.11
Simulations 5: Normal distribution. Median and standard deviation from Tables 7.5 and 7.6.

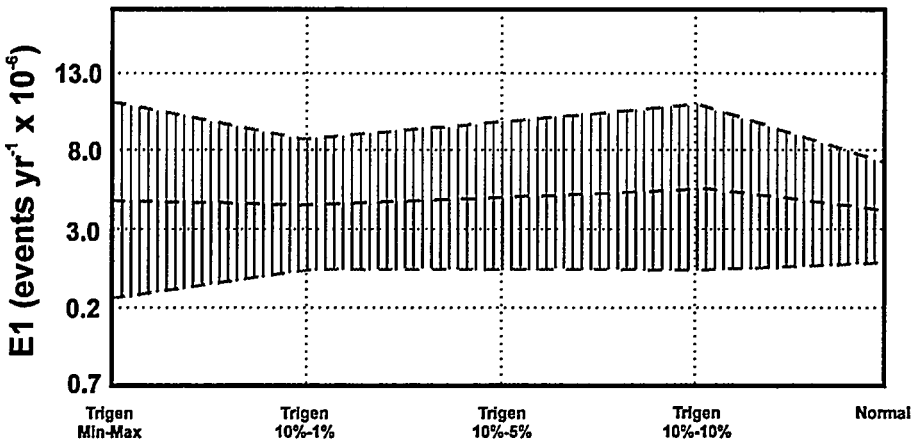
However, because only the minimum repose interval was used in the calculations, row 5 estimates are biased toward higher or maximum recurrence rates. The most likely estimates of rows 6 and 7 were obtained from the summary statistics for the *minimum* and *maximum* recurrence rate estimates using all homogeneous and nonhomogeneous Poisson models. Finally, row 9 uses the midpoint estimates and the 90% confidence intervals from the most recent calculations of Ho (1992). These midpoint estimates and confidence limits are biased toward higher probabilities for E1 because they were derived from a *worse case estimate,* and the confidence intervals are centered about that estimate (instead of a midpoint estimate). The distribution of Ho (1992) is shown primarily for comparison, and its distribution assumptions are not varied across the simulation matrix.

Table 7.11 lists summary output (mean, 10%, 90%) for the risk simulations using the simulation matrix of Table 7.10. The simulations were run for 10,000 iterations using the Latin Hypercube sampling method. The simulations evaluated for the preferred model using a homogeneous Poisson distribution (Table 7.11) show only minor variance (Fig. 7.12). Simulation 1 shows the widest distribution because of the assignment of 25% values for the upper and lower bounds. The cumulative distribution curves for simulations 2 through 4 are shifted systematically toward higher probability values reflecting the progressive skewing of the distribution toward the upper probability bounds (1, 5, and 10% lower bound). The distribution curve for simulation 5 has the smallest uncertainty because the data were modeled as a normal distribution (Fig. 7.12). Figure 7.13 is the same plot as Figure 7.12 but uses a nonhomogeneous Poisson distribution for the preferred model. The uncertainty again is smallest for simulation 5 because it is modeled as a normal distribution. Also, simulation 5 has the smallest mean estimate because β is <1 for the nonhomogeneous Poisson distribution (Fig. 7.13). The range of the mean estimates (Table 7.11) for the cross-column simulations are 2.2×10^{-6} (minimum models) to 6.1×10^{-6} events (maximum models). The range of mean estimates for the preferred data sets using homogeneous and nonhomogeneous recurrence models is 2.9×10^{-6} to 5.5×10^{-6} events yr^{-1}. This is judged to be a small degree of variation given the limited data sets and the uncertainty of the assumptions used for the probabilistic estimates.

Additional insight into the cumulative probability distribution curves for E1 is provided by examining simulation summaries for individual columns of the simulation matrix. Figure 7.14 shows the mean estimates and the 10 and 90 percentile estimates for simulation 3 for eight recurrence models (homogeneous and nonhomogeneous preferred, repose, volume, minimum, and maximum). For comparison, the mean estimate and confidence limits from the worst case estimate of Ho (1992) are shown. The mean estimates and the uncertainly bands are mostly uniform except for the estimate of Ho (1992) and the latter show similar uncertainty bands but are skewed toward higher mean estimates. The similarity in model variation is illustrated also by Fig. 7.15, which is identical to Fig. 7.14 except the output of the simulations are shown as cumulative distribution curves. The curves are tightly clustered and there is little difference between all recurrence models except for the minimum and maximum models (Fig. 7.15). The median estimates (50 percentile values) range from 3.3×10^{-6} (volume model) to 7.0×10^{-6} events yr^{-1} (Ho model). The cumulative probability distribution curve for the estimates of Ho (1992) is, as noted above, centered about a worse case estimate. The simulation modeling shows, similar to Figs.7.12 and 7.13, that there is limited variation in cumulative probability curves for a range of model assumptions of the recurrence rate (E1). The simulation modeling leads to the conclusion that the recurrence rate is well bounded and requires little additional work other than assessment of alternative models using results from continuing site characterization studies.

Table 7.11 Results of simulation modeling using the simulation matrix of Table 7.10.

Homogeneous Poisson: All Models						Homogeneous Poisson: Pref Models					
Cell:	Sim1	Sim2	Sim3	Sim4	Sim5		Sim1	Sim2	Sim3	Sim4	Sim5
10Perc	-1.1E-06	4.99E-07	4.99E-07	4.99E-07	2.08E-06	*10Perc*	-1.3E-06	4.99E-07	4.99E-07	4.99E-07	9.45E-07
Mean	4.79E-06	4.41E-06	4.93E-06	5.45E-06	3.62E-06	*Mean*	4.77E-06	4.52E-06	5.02E-06	5.52E-06	4.15E-06
90Perc	1.11E-05	8.59E-06	9.78E-06	1.1E-05	5.16E-06	*90Perc*	1.1E-05	8.66E-06	9.82E-06	1.1E-05	7.35E-06
Nonhomogeneous : Poisson All Models						Nonhomogeneous Poisson: Pref Models					
Cell:	Sim1	Sim2	Sim3	Sim4	Sim5		Sim1	Sim2	Sim3	Sim4	Sim5
10Perc	-1.3E-06	4.99E-07	5E-07	4.99E-07	1.65E-06	*10Perc*	-9.2E-07	4.99E-07	4.99E-07	5E-07	1.64E-06
Mean	4.76E-06	4.58E-06	5.07E-06	5.57E-06	4.46E-06	*Mean*	4.82E-06	4.28E-06	4.82E-06	5.36E-06	2.9E-06
90Perc	1.09E-05	8.7E-06	9.84E-06	1.1E-05	7.27E-06	*90Perc*	1.12E-05	8.51E-06	9.74E-06	1.1E-05	4.16E-06
Repose Models						Volume Models					
	Sim1	Sim2	Sim3	Sim4	Sim5		Sim1	Sim2	Sim3	Sim4	Sim5
10Perc		4.99E-07	4.99E-07	4.99E-07		*10Perc*	-2E-06	5E-07	4.99E-07	4.99E-07	2.42E-06
Mean		4.73E-06	5.19E-06	5.67E-06		*Mean*	2.82E-06	4.38E-06	4.9E-06	5.43E-06	3.43E-06
90Perc		8.81E-06	9.89E-06	1.1E-05		*90Perc*	7.41E-06	8.57E-06	9.77E-06	1.1E-05	4.44E-06
Minimum Models						Maximum Models					
	Sim1	Sim2	Sim3	Sim4	Sim5		Sim1	Sim2	Sim3	Sim4	Sim5
10Perc		5E-07	5E-07	4.99E-07	2.15E-06	*10Perc*		5E-07	4.99E-07	4.99E-07	2.06E-06
Mean		4.04E-06	4.62E-06	5.2E-06	2.25E-06	*Mean*		5.33E-06	5.68E-06	6.06E-06	4.5E-06
90Perc		8.37E-06	9.68E-06	1.1E-05	2.35E-06	*90Perc*		9.35E-06	1.01E-05	1.1E-05	6.93E-06

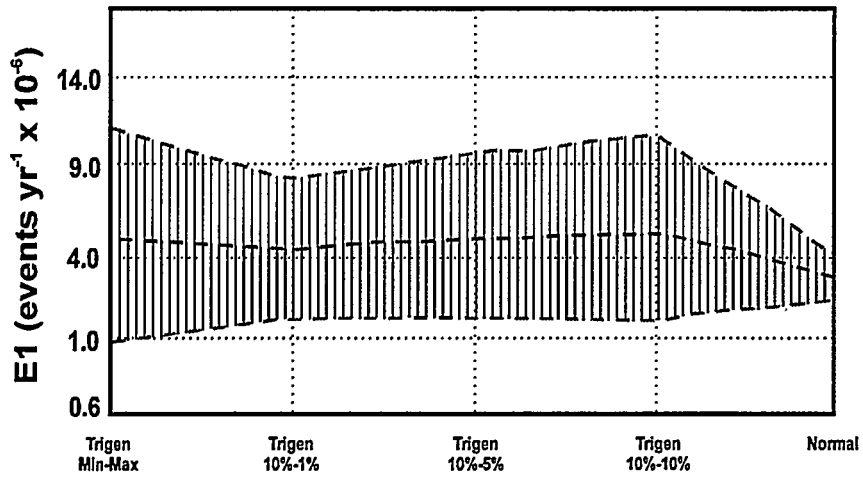


Top ---- 90 per %

Center ---- 50 Per %

Bottom ---- 10 per %

Fig. 7.12 Results of simulation modeling of the column variation of the simulation matrix of Table 7.10 for the homogeneous Poisson distribution models. The Figure shows the variations in the recurrence rate on the y-axis plotted against the mean , 90, and 10 percentile estimates. This Figure illustrates the variability of the simulation results according to different distribution assumptions and the maximum and minimum bounds for the simulations.



Top ---- 90 per %

Center ---- Mean

Bottom ---- 10 per %

Fig. 7.13 Results of simulation modeling of the column variation of the simulation matrix of Table 7.10 for the nonhomogeneous Poisson distribution model.

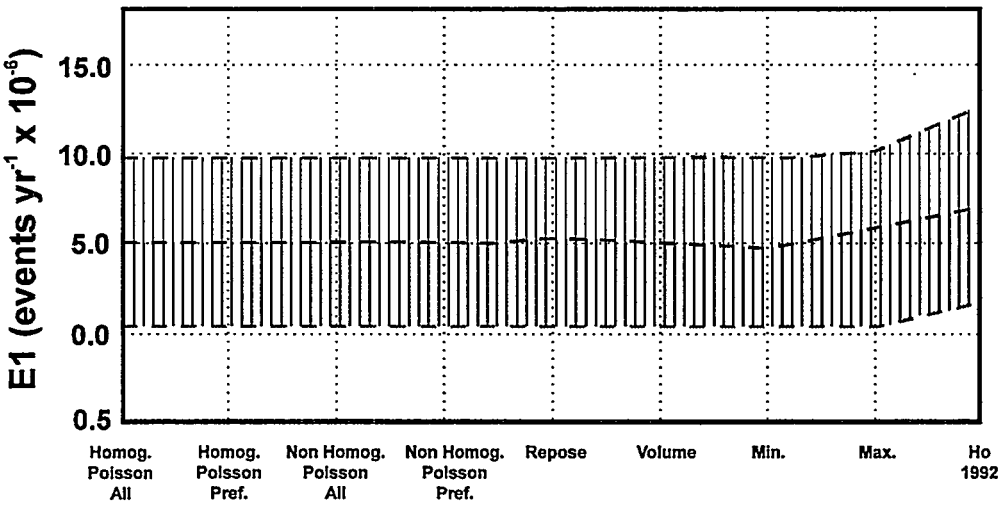


Fig. 7.14 Results of simulation modeling showing the row variation in the simulation matrix of Table 7.10 for simulation three (trigen distribution, upper bound is 10%, lower bound is 5%). This figure examines the variability of the simulation results using different models of the recurrence rate.

E. Revised Calculations of E2: the Disruption Probability

The second variable of the conditional probability of magmatic disruption of the potential repository is E2, the probability of magmatic disruption of a specified area. The primary area of concern is the potential repository or exploratory block. However, additional attention is given to the controlled area and the YMR in order to assess the occurrence probability of magmatic penetration of the waste isolation system of a geologic repository. The disruption probability, like E1 the recurrence rate, is difficult to quantify because of the small number of volcanic centers in the region. The small number of widely distributed events means that there is considerable uncertainty in calculating E2, and as a result an unconstrained number of models that can be proposed for the spatial distribution of volcanic activity. Further, by virtue of the small number of events, it is difficult to prove or disprove convincingly alternative structural models. Crowe and Carr (1980) and Crowe et al. (1982) attempted to bound the disruption probability using spatial fitting models established from the distribution of volcanic events. Smith et al. (1990) presented alternative models of E2, assuming the distribution of volcanic vents in Crater Flat and vicinity are controlled by local northeast-trending faults. Sheridan (1992) used Monte Carlo simulation to model the distribution of volcanic dikes in the YMR using the geometry of the volcanic field, the dike geometry (aspect ratio, orientation), and structural controls as constraints for the modeling. Wallmann et al. (1992) and Wallmann (1993) also used stochastic models of dike dimensions and orientation for sets of structural models to establish probabilistic estimates of repository disruption. Connor and Hill (1993) used cluster models (near-neighbor linking) to examine controls on the distribution of volcanic events in the YMR.

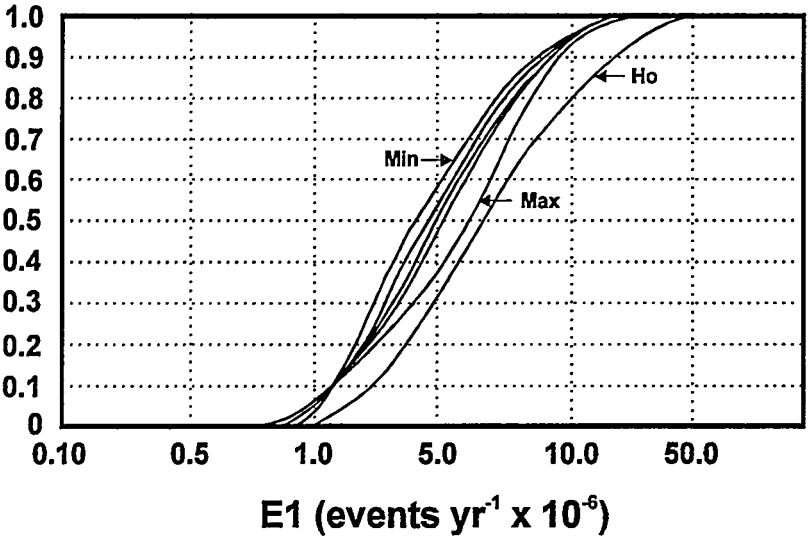


Fig. 7.15. Results of simulation modeling showing the row variation in the simulation matrix of Table 7.10 for simulation 3 (trigen distribution, upper bound is 10% , lower bound is 5%). This Figure is identical to Fig. 7.14 but presents the simulation results as cumulative probability distributions.

Expected Values:

Homogeneous $5.0E^{-6}$
Nonhomogeneous $4.8E^{-6}$
Repose $5.2E^{-6}$
Volume $4.9E^{-6}$
Minimum $4.6E^{-6}$
Maximum $5.7E^{-6}$
Ho(1992) $7.0E^{-6}$

There is considerable variability in the structural and topographic setting of Pliocene and Quaternary volcanic centers in the YMR (see Chapter 3). Some centers are located on ring-fracture zones of known or inferred caldera complexes; others occur along existing faults or at the intersection of fault systems. Alternatively, the local stress field may control the location and distribution of clusters of volcanic centers of similar age. The frequency of occurrence of basalt centers is higher in topographic basins compared to range fronts or range interiors (Table 7.2). Volcanic events tend to occur in age-correlated clusters (Crowe and Perry 1989). The patterns of the *sequenced distribution of the location* of volcanic events in the YMR are variable and difficult to generalize. There is a tendency for the events to occur in the CFVZ and possibly secondarily in the NESZ. As a consequence, it is more difficult to limit or bound constraints on the disruption probability (E2) than the recurrence rate of volcanic events (E1).

The approach followed in this section of this volcanism status report is to place priority on integrating observational data obtained from field, chronology, and structural studies of volcanic centers. These data provide the primary constraints for development of multiple alternative distribution models. Inferences gathered from statistical analyses of the time-space distribution of volcanic events are given secondary priority for two reasons. First, the small data set is insufficient to evaluate alternative hypotheses using statistical methods of hypothesis testing. Second, the variation in the possible controls of the location of volcanic events makes the assumptions required for application of statistical methods difficult. Unless the physical meaning of statistical models are examined carefully, their use can lead to inferences or identification of patterns in event distribution that are not consistent with the geologic record. Estimating or

Table 7.12 Published values of E2, the disruption ratio.

Structural Model	Publication	Area (km2)	E2 Ratio	Comments
Fixed Circle- 25 km	Crowe and Carr 1980	1963	3.0E-03	Circle fixed at YM
Fixed Circle- 50 km	Crowe and Carr 1980	7845	1.3E-03	Circle fixed at YM
Random Circle	Crowe et al. 1982	2437	2.5E-03	Quaternary Centers
Random Ellipse	Crowe et al. 1982	4419	1.4E-03	Quaternary Centers
Random Circle	Crowe et al. 1982	2470	2.4E-03	Quaternary + Buckboard Centers
Random Ellipse	Crowe et al. 1982	1953	3.0E-03	Quaternary + Buckboard Centers
Strike Slip Quaternary	Swchweickert, 1989	1310	4.6E-03	Quaternary Centers
Strike Slip Plio-Quaternary	Swchweickert, 1989	1450	4.1E-03	Subset Plio-Quaternary Centers
CFVZ	Crowe and Perry 1989	1310	4.6E-03	Quaternary Centers
CFVZ	Crowe and Perry 1989	1450	4.1E-03	Plio-Quaternary Centers
YMR or YPB	Crowe 1990	2180	2.8E-03	Slightly Larger than AMRV; all volcanic centers
AMRV	Smith et al. 1990	1955	3.1E-03	Similar but Slightly Smaller than YMR
NE Chain Model	Smith et al. 1990	390	7.8E-04	Subset Plio-Quaternary Centers
Lathrop Chain Model	Smith et al. 1990	360	1.7E-02	One Quaternary Center
Caldera Model	Carr 1990	400	1.5E-02	Subset Plio-Quaternary Centers
NE Structural Zone	Carr 1990, Smith et al 1990	2250	2.7E-03	Subset Plio-Quaternary
Pull-apart Basin	Fridrich and Price 1992	690	8.7E-03	Subset Plio-Quaternary Centers
Stochastic Dike/NW-NE	Sheridan 1992		6.0E-03	Subset Plio-Quaternary
Stochastic Dike/NE-NE	Sheridan 1992		1.0E-02	Subset Plio-Quaternary
Lathrop Wells Dike	Sheridan 1992		5.1E-03	One Quaternary Center

Table 7.12 Published values of E2, the disruption ratio (cont.).

Structural Model	Publication	Area (km2)	E2 Ratio	Comments
Stochastic Dike	Wallman et al. 1993		2.0E-03	Bounds for Three Structural Models
Stochastic Dike	Wallman et al. 1993		5.0E-03	Bounds for Three Structural Models
Nonhomogeneous Poisson:	Connor and Hill 1993		2.0E-03	Cluster, 6-7 neighbors fitting model
Nonhomogeneous Poisson	Connor and Hill 1993		2.4E-03	Cluster, 6-7 neighbors fitting model
Nonhomogeneous Poisson	Connor and Hill 1993		2.8E-03	Cluster, 10-13 neighbors fitting model
Nonhomogeneous Poisson	Connor and Hill 1993		3.4E-03	Cluster, 10-13 neighbors fitting model
Nonhomogeneous Poisson	Connor and Hill 1993		2.7E-03	Cluster, $\lambda = 4 \times 10^{-6}$
Nonhomogeneous Poisson	Connor and Hill 1993		2.7E-03	Cluster, $\lambda = 1 \times 10^{-5}$
Nonhomogeneous Poisson	Connor and Hill 1993		3.1E-03	Cluster, $\lambda = 1.1 \times 10^{-5}$
Stress Field Dike-Q	Crowe et al. 1993	1310	4.6E-03	Quaternary Centers
Stress Field Dike-P	Crowe et al. 1993	1450	4.1E-03	Subset Plio-Quaternary Centers
Crater Flat/Buckboard	Crowe et al. 1993	1700	3.5E-03	Subset Plio-Quaternary
Crater Flat Field	Crowe et al 1993	400	1.5E-02	Subset Plio-Quaternary Centers
Disruption Simulation	Crowe et al. 1993		4.0E-03	Integration of 24 Structural Models

bounding the disruption probability for the YMR is a difficult and somewhat subjective problem. The only logical approach with the limited data set is to attempt to develop systematically a range of alternative models primarily using geological intuition and to apply methods of comparing the models using simulation modeling analogous to the approaches used in assessing E1. The important comparisons for alternative models of E2 are the similarities or differences in the cumulative probability distributions, not the strengths or weaknesses of individual models. The alternative models for E2 are grouped into three cases. including models developed from the spatial distribution of volcanic centers, models involving structural control of the location of volcanic centers, and insight from comparison with analog basaltic volcanic fields of the Basin and Range province.

1. Published Estimates of E2. Table 7.12 is a compilation of existing estimations of the disruption ratio obtained from published studies of the probability of magmatic disruption of a potential repository at Yucca Mountain. The descriptive statistics for the unedited data from Table 7.12 are: $n = 34$, maximum = 1.7×10^{-2}, minimum = 1.3×10^{-3}, mean = 4.5×10^{-3}, median = 3.7×10^{-3}, standard deviation = 3.1×10^{-3}, skewness = 2.2. The data are strongly skewed to larger or worse case values consistent with bias in the calculations introduced from attempts to bound the distribution of estimates for E2 (similar to published estimates of E1). Exploratory data analyses show that the Lathrop chain model (Smith et al. 1990) is identified as a far outside outlier, and the caldera model (Carr 1990), the Crater Flat field model (Crowe et al. 1993), and one set of the stochastic dike models (Sheridan 1992) are identified as outlier values. Rejection of these models from the data set of Table 7.12 gives the following summary statistics: $n = 30$, maximum = 7.0×10^{-3}, minimum = 1.3×10^{-3}, mean = 3.6×10^{-3}, median = 3.0×10^{-3}, standard deviation = 1.5×10^{-3}, and skewness = 0.7. The edited data remain skewed toward positive values and the median is a better statistical descriptor (more resistant to outliers) than the mean. However, the edited data distribution is much improved and approaches a normal distribution. A median estimate of $3.0 \pm 1.5 \times 10^{-3}$ represents the best approximation of published values for E2.

2. Spatial Distribution Models. Spatial distribution models were used by Crowe et al. (1982) to attempt to bound the disruption ratio, E2. They defined the area of the disruption ratio from the distribution of basalt centers used to calculate a correlated value for E1. The area was established using a spatial-fitting program to calculate minimum area circles and minimum area ellipses enclosing the volcanic centers used to calculate E1 and the potential repository. The circles and ellipses were varied using different combinations of volcanic centers and the resulting areas were compiled into a matrix of disruption ratios. Maximum and minimum estimates were identified from the data matrix and used to establish bounds for the disruption ratio. These spatial distribution models are described generally as random models and that has lead to some confusion (for example, see Connor and Hill 1993). The spatial zones are not established through assuming a homogeneous spatial distribution of volcanic events in space. Instead, the areal dimensions of individual models are established from the spatial distribution of volcanic events using different combinations of the age and location of volcanic events. The assumption is made that the distribution area of the volcanic centers is structurally controlled but there is a random distribution of volcanic events *within* the distribution area. These models presume the larger scale structural controls of the distribution of volcanic events (nonrandom spatial events) are reflected in the distribution of volcanic centers. They do not account for local structural control of individual centers (Crowe et al. 1982; Crowe 1986; Smith et al. 1990).

Davis (1986) and more recently Cressie (1991) have summarized some of the many different approaches to statistical analyses of spatial point patterns. The problem is complicated by time, t, for the case of basaltic volcanism in the YMR. Volcanic events must be examined not only for their spatial distribution but additionally for their space-time distribution (space-time point patterns, Cressie 1991).

Further, the recurrence rate for volcanic intrusions (λ_i) may vary with depth in the crust. There may be higher recurrence rates at given cross-sectional depths compared to surface rates. The three-dimensional aspect of the problem is probably not severe because we are concerned mostly with surface penetrating volcanic events (<2 km). For these events λ_v is probably $\approx \lambda_i$ (see earlier section). Finally, volcanic events exhibit spatial and temporal variability in the location, the age, the type of eruptions (hawaiian, strombolian, hydrovolcanic), and possibly magma composition (see Chapter 4). This requires analyses of multivariate spatial point processes in addition to space-time point processes (Cressie 1991). Given the complex range of methods of data analyses and the sparse data set of volcanic events, we do not attempt to apply formal methods of statistical analyses to the spatial data. Instead we attempt to systematically evaluate ranges of alternative spatial models of the distribution of volcanic events.

Fig. 7.16 is a plot of the locations (latitude and longitude converted to Mercator projections) of the Pliocene and Quaternary volcanic centers of the YMR. Simple visual examination of Fig. 7.16 shows that the centers are not randomly distributed in space. Connor and Hill (1993) used a combination of a Clark-Evans test and a Hopkins F test to reject the null hypothesis that basaltic volcanic centers in the YMR are randomly distributed, an unsurprising conclusion. Fig. 7.16 shows that basaltic volcanic centers are concentrated primarily in a northwest-trending zone extending across the middle of the YMR and confirms the statistical inference of Connor and Hill (1993); one isolated center occurs outside this zone, the basalt of Buckboard Mesa. This northwest-trending zone has been named the CFVZ (Fig. 7.16; see Crowe and Perry 1989). Secondary or small-scale distribution trends are defined by clusters of volcanic centers and are oriented approximately perpendicular to the 60- to 75-km-long, northwest-trending CFVZ. The secondary event clusters are defined by closely spaced volcanic centers (1 to 13 km) of coeval age that follow systematic trends defined by the structure of vents and vent alignments. The identified secondary distribution trends include clusters of north-trending centers (basalt of Thirsty Mesa; basalt of southeast Crater Flat) and clusters of north/northeast-trending basalt centers (aeromagnetic anomalies of the Amargosa Valley; basalt of Sleeping Butte, Quaternary basalt of Crater Flat). The secondary distribution trends probably were controlled by emplacement of feeder dikes parallel to the maximum compressive stress direction (see Chapters 3 and 5). Alternative views of the structural controls of the distribution of volcanic centers in the YMR are presented by Smith et al. (1990). They argue that the *primary trends* of volcanic centers of the YMR follow north-northeast patterns that parallel local normal faults cutting bedrock in Yucca Mountain (NESZ of Fig. 7.16).

Figure 7.17 shows bivariate plots of the distribution of volcanic events in the YMR and the distribution centroids (95% confidence) drawn for different combinations of volcanic centers. The distribution centroids are centered on the means of the mercator transformed locations (latitude and longitude). Their major axes are determined by the standard deviations of the variables, and their orientations are determined by the covariance of the variables. All distribution centroids are located in the vicinity of Crater Flat. Figure 7.17a shows the distribution centroid for all Pliocene and Quaternary volcanic centers of the YMR. Figure 7.17b shows the distribution centroid for all centers *excluding* the basalt of Buckboard Mesa (CFVZ model). Figure 7.17c includes all centers *except* the basalt of Thirsty Mesa and the basalt of Sleeping Butte (NESZ model). Exclusion of the basalt of Buckboard Mesa elongates the distribution centroid parallel to the CFVZ. Exclusion of the basalt of Thirsty Mesa and Sleeping Butte results in a near-spherical centroid "pulled" or offset toward the location of the basalt of Buckboard Mesa.

The distribution centroids are used as starting points to divide visually the Plio-Quaternary volcanic centers into clusters (Fig. 7.18). Visual methods are used because they are effective for identifying patterns on simple bivariate data plots (Sharaf et al. 1986), and the data are too sparse to obtain meaningful results

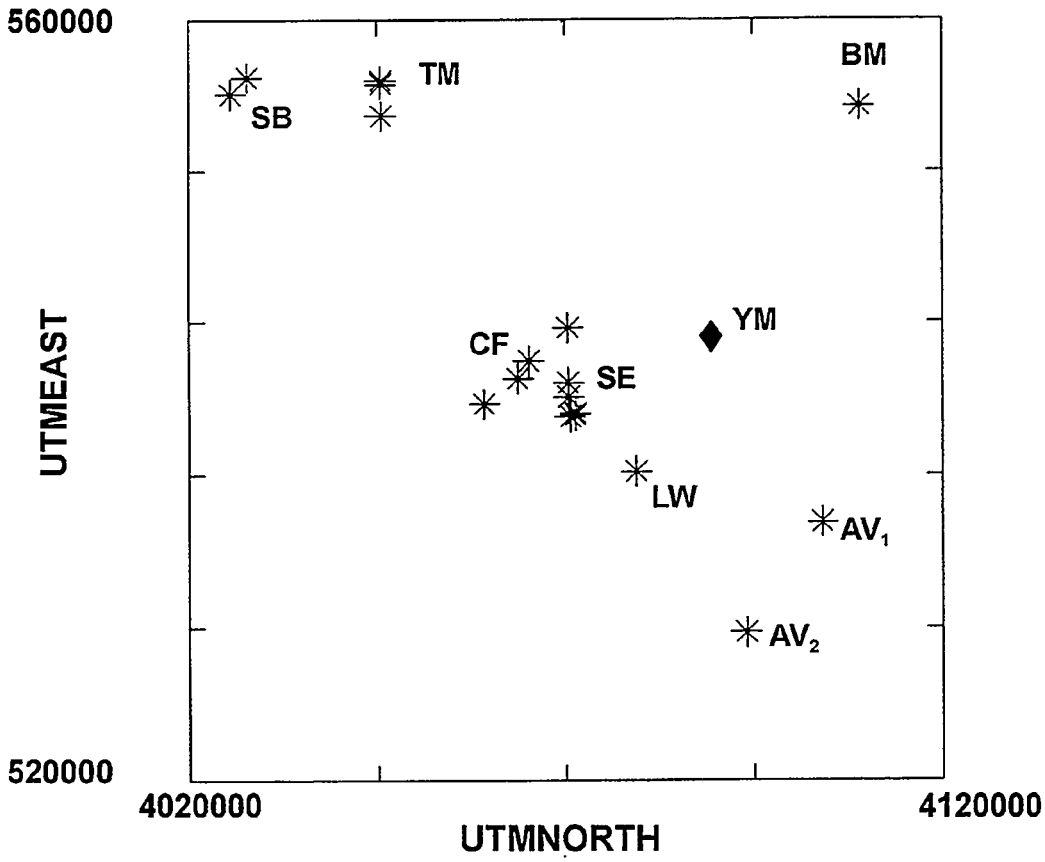


Fig. 7.16 Distribution of Pliocene and Quaternary volcanic centers in the YMR. The latitude and longitude coordinates have been converted to Mercator coordinates. The symbols on the Figure include: SB: Sleeping Butte volcanic center, TM: basalt of Thirsty Mesa, BM: basalt of Buckboard Mesa, CF: Quaternary basalt of Crater Flat, SE: basalt of southeast Crater Flat, LW: Lathrop Wells volcanic center, AV_1: aeromagnetic anomaly of Amargosa Valley (intersected in exploratory drilling), AV_2: aeromagnetic anomaly of Amargosa Valley (identified but not investigated by exploratory drilling), YM: exploratory block of Yucca Mountain

using statistical methods of cluster analyses. The first event cluster consists of basalt centers in and adjacent to Crater Flat (cluster 1: basalt of SE Crater Flat, Quaternary basalt of Crater Flat, and the Lathrop Wells volcanic centers) (Fig. 7.18a). A spatially separate cluster in the Amargosa Valley is defined by the third iteration joins cluster 1a with cluster 2a to form the CFVZ, cluster 3a with cluster 1a to form the NESZ, and cluster 2a with cluster 3a to form an east/west-trending zone (Fig. 7.18c). This same method of visual clustering is repeated using bivariate plots to assess the distribution of Quaternary volcanic centers in the YMR (Fig. 7.19). The Quaternary centroid, and three iterations of cluster definitions are shown on Figure 7.19a–c. In this case, the cluster joining ends with the definition of the Quaternary CFVZ (Fig. 7.19c).

The cluster models of Figures 7.18 and 7.19 are used to define disruption zones for E2 by simply expanding each cluster to form an irregular polygon that *encloses* the Yucca Mountain site. The clusters are expanded while attempting to maintain their geometric dimensions—they are not just expanded toward the Yucca Mountain site. The expansion presumes the fields could broaden in a northeast and southeast

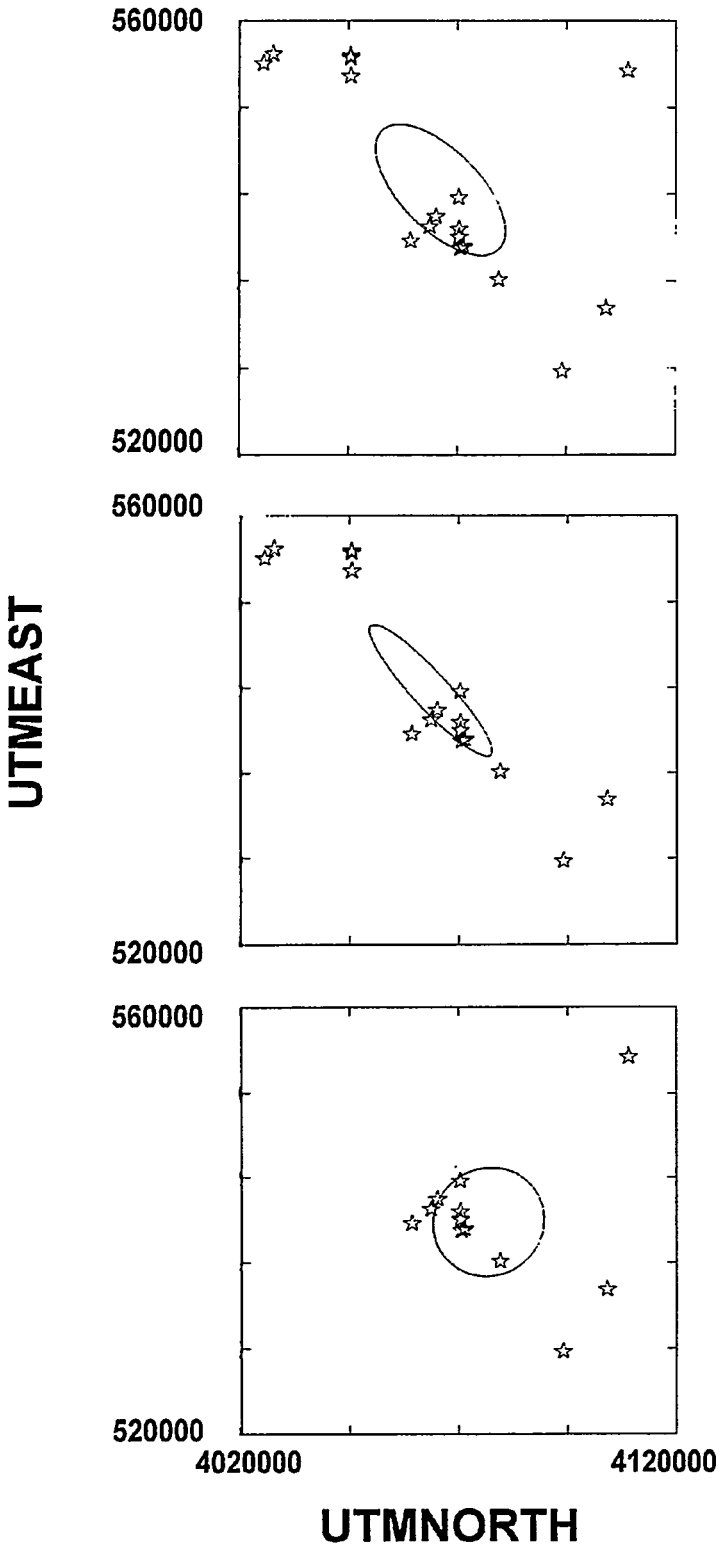


Fig. 7.17 Distribution centroids (95% confidence interval) for combinations of Pliocene and Quaternary volcanic centers in the YMR. The star symbols mark the locations of volcanic centers and are described in the caption of Figure 7.16. The top Figure is the distribution centroid using all Pliocene and Quaternary volcanic centers. The middle Figure is the same as the top Figure but *excludes* the basalt of Buckboard Mesa. The bottom Figure is the same as the top Figure but *excludes* the basalt of Thirsty Mesa and the basalt of Sleeping Butte.

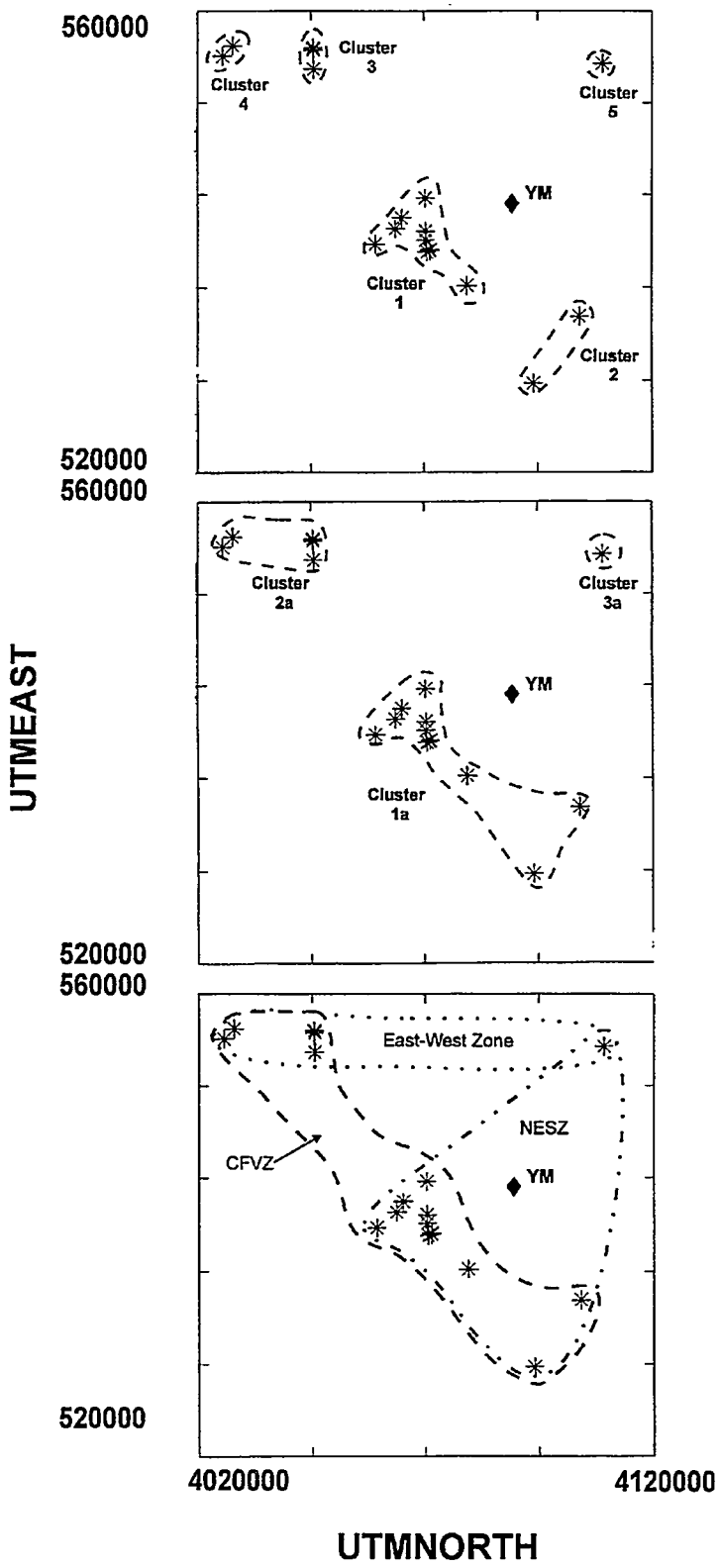


Fig. 7.18 -Cluster patterns using simple visual clustering of different combinations of Pliocene and Quaternary volcanic centers in the YMR. The top Figure joins the immediately adjacent centers. The middle Figure joins adjacent clusters identified in the top Figure. The bottom Figure joins the clusters identified in the middle Figure and results in the CFVZ, the NESZ, and an East/West zone.

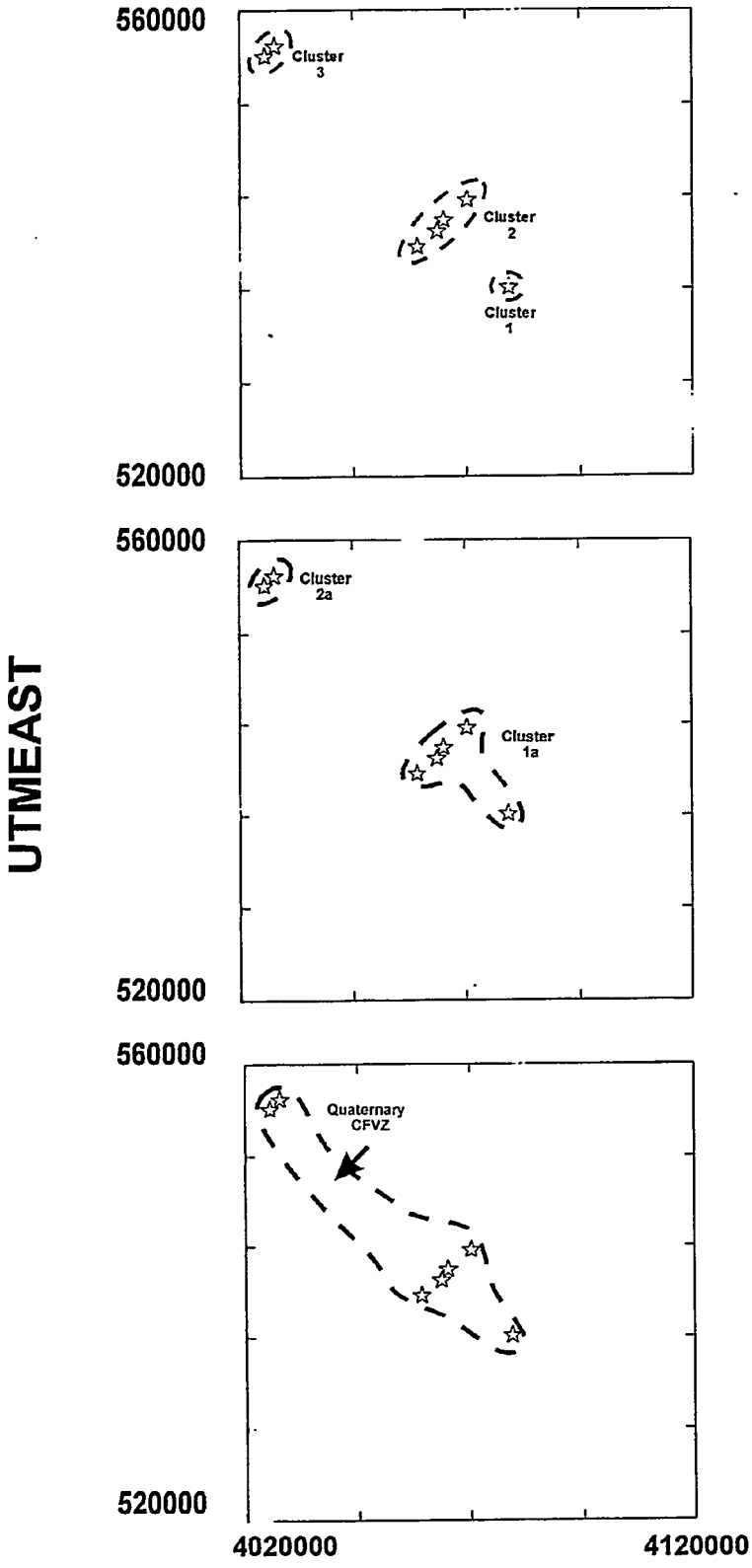


Fig. 7.19 Visual clustering of Quaternary volcanic centers in the YMR following the same steps as Figure 7.18. The clustering process ends with the definition of the CFVZ

direction (stress-field controlled) consistent with the probable elongation direction of feeder dikes and intrusions. The area of each repository-enclosing zone is listed on Table 7.13. E2 is estimated using three sets of models and assuming a 6-km^2 area of a potential repository. (*Note: the repository area (heated area of Wilson et al. 1994) is dependent on the repository thermal loading, an issue currently under consideration by the YMP. Estimations of the repository area were published during final editing of this report and could not be incorporated in the probabilistic analyses. However the repository areas vary from 2.3 to 4.6 km^2 for 114-kW/acre and 57-kW/acre cases assuming in-drift emplacement. The areas will almost certainly change as new information is obtained from underground explorations and the revised estimates will be used in future probabilistic volcanic risk assessment.)* The first model assumes a random distribution of volcanic events *in* the disruption zone. The second and third models assume the distribution of volcanic events *follows the spatial patterns* of Table 7.2: 75% of future volcanic events would occur in alluvial basins, 10% in range fronts, and 15% occur in range interiors. The areas of the structural zones listed on Table 7.13 were measured from topographic maps of the YMR (1:250,000). These areas will be recalculated more precisely using a geographic information system (GIS) when the computer programs used for the GIS are certified for the YMP.

Disruption probabilities (E2) are not calculated for all clusters defined on Figures 7.18 and 7.19. Cluster zones located more than 30 km from the potential repository block are assumed not to be capable of disrupting the potential repository; their areas and disruption ratios are not listed. Additionally, cluster 2 of the Quaternary cluster models (the Lathrop Wells center) is identified as a case where intersection is not possible. We have highlighted this *excluded* case in Table 7.13 because it may be regarded as controversial by some workers (for example, Smith et al. 1990). There are two explanations for the exclusion of the Lathrop Wells cluster. First, projection of the cluster along a north-northeast trend (stress field control) does not result in intersection of the potential repository site; the cluster extends east of the exploratory block. Second, the length of the projection of the cluster (20 km) exceeds substantially the half length of the longest observed cluster in the YMR (6.5 km) and the half length of expected dimensions of feeder dikes. Finally, three cases from Table 7.13 are judged possible but unlikely to intersect the Yucca Mountain site. This basis for this judgment is twofold. First, the required half length of projected north/northeast-trending dikes (stress-field control) required to intersect the potential repository exceeds slightly the expected maximum dimensions of feeder dikes. Second, assuming projection of north/northeast-trending dikes, intersection of the potential repository site is possible for only a part of the area of the cluster zone. Thus, we regard the assumptions required to expand these spatial models to include the potential repository site to be difficult to support. These spatial models are noted with asterisks on Table 7.13. We *included* those models in the first group of summary statistics for E2 and excluded them from the second group of summary statistics. The primary effects of *excluding* the identified cases are to decrease significantly the mean, standard deviation, and skewness and slightly decrease the median (Table 7.13). The data of Table 7.13 *including* the three marginal cases are strongly skewed toward larger values. Because of the degree of skewness, the median is a more robust indicator of the central tendency of the data. Median estimates for models of intersection, range interior models, and range front plus range interior models are, respectively, $3.1 \pm 4.5 \times 10^{-3} \times 10^{-3}$, $4.6 \pm 6.8 \times 10^{-4} \times 10^{-3}$ and $7.6 \pm 11.3 \times 10^{-4}$ (Table 7.13).

A different method for estimating E2 was developed by Connor and Hill (1993); their approach is a variant of the spatial distribution model. They related the recurrence rate (E1) per unit area in the YMR to cluster models using near-neighbor clustering routines for both the age and location of volcanic centers. An

Table 7.13 Spatial Distribution models for E2. Model 1 = Random, Model 2 = Range Interior, Model 3 = Range Interior + Range Front.

Spatial Model	Time (Ma)	Area (km2)	Model 1	Model 2	Model 3	Comments
Quat Centers (circle)	1.00	2400	2.5E-03	3.7E-04	6.2E-04	Crowe et al. 1982
Quat Centers (ellipse)	1.00	4400	1.4E-03	2.0E-04	3.4E-04	Crowe et al. 1982
Quat + BB (circle)	3.75	2500	2.4E-03	3.6E-04	6.0E-04	Crowe et al. 1982
Quat + BB (ellipse)	3.75	2000	3.0E-03	4.5E-04	7.5E-04	Crowe et al. 1982
Cluster 1*	3.75	400	1.5E-02	2.2E-03	3.7E-03	Crater Flat Volcanic Field*
Cluster 2	3.85					Intersection not possible
Cluster 3	4.80					Intersection not possible
Cluster 4	4.80					Intersection not possible
Cluster 5	2.90					Intersection not possible
Cluster 1a*	3.75	750	8.0E-03	1.2E-03	2.0E-03	Crater Flat + Amargosa*
Cluster 2a	4.80					Intersection not possible
Cluster 3a	2.90					Intersection not possible
CFVZ	4.80	1450	4.1E-03	6.2E-04	1.0E-03	Crater Flat Volcanic zone
NESZ	3.85	1200	5.0E-03	7.5E-04	1.2E-03	Northeast Structural Zone
East-west zone	4.80					Intersection not possible
Cluster 1	1.00					Intersection not possible
Cluster 2	1.00	110				Lathrop Wells cluster
Cluster 3	1.00					Intersection not possible
Cluster 1a*	1.00	400	1.E-02	2.2E-03	3.7E-03	Quaternary CF + Lathrop*
Cluster 2a	1.00					Intersection not possible
CFVZ	1.00	1310	4.6E-03	6.9E-04	1.1E-03	Crater Flat Volcanic Zone
NHPP Cluster	3.75		2.0E-03	3.0E-04	5.0E-04	Connor and Hill
NHPP Cluster	3.75		2.4E-03	3.6E-04	6.0E-04	Connor and Hill
NHPP Cluster	1.00		2.7E-03	4.0E-04	6.7E-04	Connor and Hill
NHPP Cluster	1.00		3.1E-03	4.6E-04	7.7E-04	Connor and Hill
	Summary Statistics	*Mean*	5.1E-03	7.6E-04	7.6E-04	
		Median	3.1E-03	4.6E-04	7.6E-04	
		Std Dev	4.5E-03	6.8E-03	1.1E-03	
		Skew	1.8	1.8	1.8	
	(unlikely cases excluded)	*Mean*	3.0E-03	4.5E-04	7.5E-04	
		Median	2.6E-03	3.9E-04	6.5E-04	
		Std Dev	1.2E-03	1.8E-04	2.9E-04	
		Skew	0.6	0.6	0.6	

*Spatial models noted by the asterisk are included in the first group of summary statistics but repository intersection is judged to be unlikely from geometrical constraints on the propagation of dikes from the cluster areas, and the long half length of projected dike dimensions required to achieve intersection.

important observation resulting from this approach is that both the recurrence rate (E1) and probability of repository disruption (Pr[E2 given E1]Pr[E1] are dependent on the number of near-neighbor volcanic centers used in nonhomogeneous Poisson models. Connor and Hill (1993) presented bivariate plots showing families of curves for the recurrence rate and the probability of repository disruption established using near-neighbor models. They also showed contour maps of the probability of magmatic disruption of the potential repository and argue that the probabilities vary in the YMR because of the tendency for volcanic centers to cluster. Connor and Hill (1993) did not explicitly calculate values for E2 but E2 can be

approximated by rearranging their equations and substituting values for estimates of E1 and for the probability of magmatic disruption of the repository.

The positive merits of identifying the spatial distribution models for constraining E2 are several. First, the estimations used for E2 tend to be less arbitrary than other calculational methods. The disruption probability is established by the area of irregular zones encompassing the distribution of combinations of Pliocene and Quaternary volcanic centers and the Yucca Mountain site. Second, the shapes of the distribution zones are irregular and it is therefore relatively easy to extend the zones to include the Yucca Mountain site. Third, the number of models is determined by the number of different combinations of volcanic centers. It is relatively easy to include all possible event combinations and be systematic in establishing alternative disruption models.

There are several areas of weaknesses or limitations in the spatial distribution models. First, the assumptions required to expand each distribution zone must be assessed for validity. If it is not logical to include the Yucca Mountain site in the distribution zone, the disruption model may overestimate the disruption ratio. These disruption ratios are worse cases because the ratio must be less than the estimated disruption ratio. Second, the weighing percentages used for the range interior and range front models were established for the YMR. They may be different for individual distribution models. Third, the spatial models of Connor and Hill (1993) employ multivariate cluster analyses of the location of volcanic events for the Postcaldera basalt (OPB and YPB). The number of data points used in the analyses makes the application of the statistical method marginal at best. The distribution of the OPB is spatially different from and largely unrelated to the distribution of the YPB (see Chapter 3). The means of the ages of the OPB and the YPB are statistically different (see Chapter 3). Combining the data sets in cluster analyses appears unwarranted. Moreover, Connor and Hill (1993) use only the age (partially) and the spatial location of volcanic events. They do not include all aspects of the data variance (for example, location, age, magma volume, eruption type, relationship to local structure). Their statistical analyses are underdetermined for cluster analyses, and their calculations are likely to be significantly different if extended to multivariate space. Connor and Hill (1993) also treat each volcanic event independently and weight equally spatially separated volcanic centers and volcanic centers in recognized age-correlated clusters (secondary control of the distribution of volcanic events). This treatment results in a bias of their spatial analyses to areas of clustered volcanic activity.

Perhaps the most important weakness of the spatial distribution models is the assumption that the location of past volcanic events constrains the location of future events. Careful examination of the patterns of the *sequences* of past volcanic events shows that this is not always a valid assumption (Crowe et al. 1993). Examination of the sequence of the location of past volcanic events shows that there no consistent patterns in the location of individual volcanic events *relative* to the location of the *immediately preceding* volcanic event (Fig. 7.20). There is a tendency for events to occur in the CFVZ and secondarily in the Crater Flat topographic basin. However, the jump directions or lengths of the *changes* in location of one event to the next event are not systematic. Thus, there is an inherent danger of over-interpreting the composite patterns of past events in attempts to constrain the location of future volcanic events using cluster models. Again, there is an almost unconstrained range of models that can be used in probabilistic assessments of E2. The important consideration in risk assessment is the variation in E2 for different spatial models not the relative merits of individual models. We suggest however, that approaches assuming a random distribution of volcanic events within spatial models or volcanic source zones that are defined by the distribution of volcanic centers may best model the observed spatial sequence of volcanic events in the volcanic record of the YMR.

3. Structural Models for E2. The second approach used to estimate E2 is an assessment of structural models for the location of volcanic centers in the YMR. This approach overlaps partly with the spatial distribution models but brings a slightly different perspective. The spatial distribution models are established entirely from the distribution of volcanic events. In contrast, the approach used for structural models attempts first, to identify structural features in the YMR, and second, to relate the spatial patterns of volcanic events to the structural features.

Table 7.14 lists the current range of identified structural models in the YMR and the strengths and weaknesses of each model. Two interpretations emerge immediately from examination of the structural models. First, there are two classes of models. These include: (1) structural models where the enclosing zone must be expanded to allow for intersection of the repository, and (2) structural models that include the repository and part or all of the controlled area in the zone. Most of the structural models fall into the first category. Second, the structural models cannot be considered independent of E1. Selection of some structural models eliminates individual or groups of volcanic centers from inclusion in the events used to estimate E1. This reduces the recurrence rate for most models (Wallmann et al. 1993; Wallmann 1993; Crowe et al. 1993) and is described further in the final part of Chapter 7.

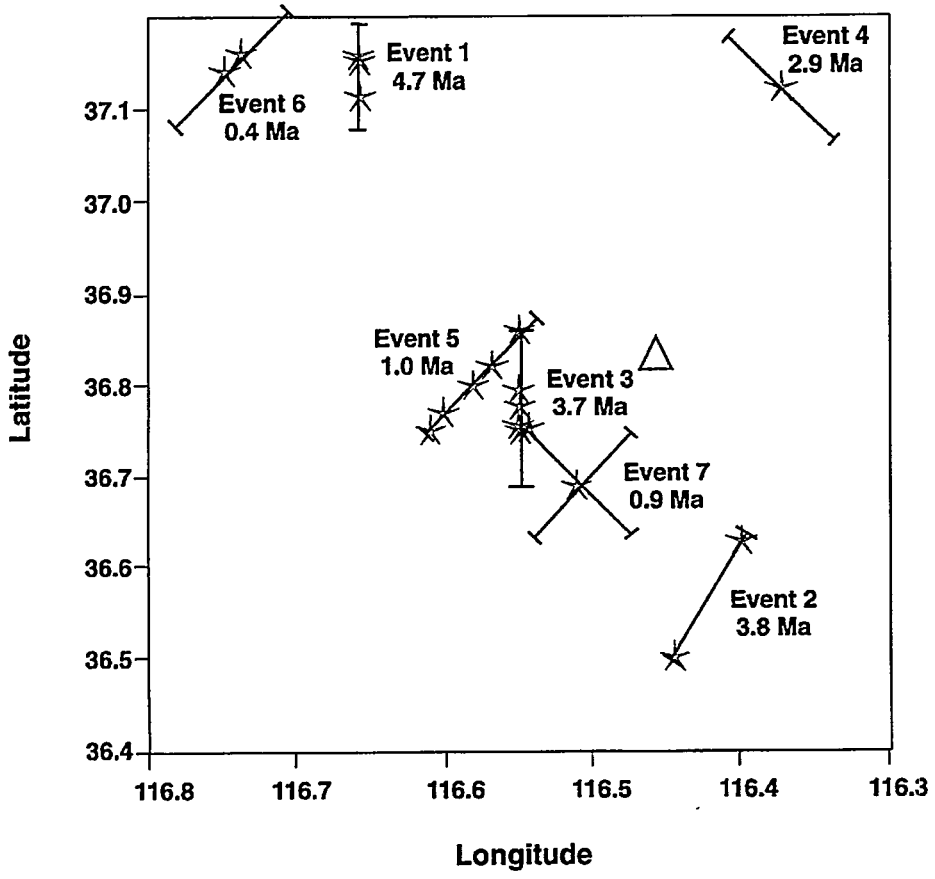


Fig. 7.20 Plot of the sequence of Pliocene and Quaternary volcanic events in the YMR. The events are plotted with brackets equal in length to the *maximum* cluster length in the YMR (13 km) and are centered at the spatial midpoint of the volcanic event or cluster. The brackets represent possible directions of expansion of clusters or dikes following the modern stress field (northeast or southwest). The orientation of the brackets is controlled by the direction of alignment of multiple centers or vent-fissure systems and these parallel the stress field with the exception of the Lathrop Wells center (northwest vent alignments). The event locations jump nonsystematically through time. The only area of overlap of successive events is in Crater Flat.

Table 7.14 Alternative structural models for the distribution of Pliocene and Quaternary volcanic centers in the YMR.

Structural Model	Evidence for Model	Evidence Against Model	Subsets or Alternative Models
Model 1: Crater Flat Volcanic Zone (Quaternary). This structural model is based on the definition of the Crater Flat volcanic zone of Crowe and Perry (1989). The dimensions of the zone are defined from the distribution of Quaternary volcanic centers.	***Supportive Evidence:*** *Northwest-trending linear distribution of volcanic vents, predominance of northwest structural trends in the Walker Lane structural zone, possible evidence of strike-slip offset of structural features in Paleozoic rocks, strike-slip pull-apart origin of Crater Flat.*	**Negative Evidence:** Small number of volcanic centers, distance of gap between Crater Flat and Sleeping Butte centers, secondary northeast alignment of vent clusters.	***Alternative Submodels:*** *The Crater Flat centers and the Sleeping Butte centers may be located in separate structural zones.*
Model 2: Crater Flat Volcanic Zone (YPB). Same as model 1 but the dimensions of the zone are defined by the distribution of the Pliocene and Quaternary volcanic centers and aeromagnetic anomalies of the Younger postcaldera basalt.	***Supportive Evidence:*** *Same as Model 1.*	**Negative Evidence:** Same as model 1, basalt of Buckboard Mesa is not included in the structural zone.	***Alternative Submodels:*** *Same as Model 1, the aeromagnetic anomalies of the Amargosa Valley may also be in separate structural zones.*
Model 3: Yucca Mountain Region. This is a non-structurally based zone defined by the distribution of Pliocene and Quaternary basalt centers of the YMR. It is similar to but slightly larger than the Area of Most Recent Volcanism of Smith et al. (1990).	***Supportive Evidence:*** *Model is based on the distribution of Pliocene and Quaternary volcanic centers in the YMR.*	**Negative Evidence:** No structural basis for model.	

Table 7.14 (cont.)

Model 4: Crater Flat Volcanic Field: This zone assumes that the major control of the occurrence of basalt centers is the local Crater Flat volcanic field, which is the primary site of Pliocene and Quaternary basaltic volcanism.	***Supportive Evidence:*** *Most Pliocene and Quaternary volcanic events have occurred in the Crater Flat basin, Crater Flat is the centroid of the distribution of units of the YPB, the Crater Flat basin may be an area of continuing extension, Crater Flat basin was a site of Miocene extension and basaltic volcanism.*	**Negative Evidence:** Other basalt centers occur outside the Crater Flat basin, the linear north-northwest alignment of basalt centers is oblique to the north-south elongation of the Crater Flat basin.	***Alternative Submodels:*** *Each group of volcanic centers may represent a separate volcanic field including the Crater Flat, Amargosa, Black Mountain and Buckboard Mesa fields.*
Model 5: Strike-Slip Structural Control: This structural model is based on the inference that the alignment of basalt centers parallels a concealed northwest-trending right-slip fault of the Walker Lane structural system (Schweickert (1989).	***Supportive Evidence:*** *Linear northwest alignment of basaltic volcanic centers, proposed offset of structural features of Paleozoic rocks, Walker Lane structural setting, clockwise rotation of field magnetization directions of the Tiva Canyon Member, coincidence of the basalt centers with zone of maximum rotation of the magnetization directions, similar structural bounds may be defined for Miocene basaltic volcanism (Older basalt of Crater Flat, aeromagnetic anomaly of VH-2).*	**Negative Evidence:** Strike-slip fault is not expressed at the surface; there is not a strong correlation between strike-slips faults and sites of Quaternary volcanism in the Great Basin part of the Basin and Range province.	***Alternative Submodels:*** *The Thirsty Mesa/Sleeping Butte centers and the aeromagnetic anomalies of the Amargosa Valley may be located on separate strike-slip faults and be unrelated to the Crater Flat basalt units.*

Table 7.14 (cont.)

Model 6: Strike Slip Structural Control: Model B. This structural model is based on the inference that the south-southeast edge of the Crater Flat basin is bounded by a north-northwest trending, right slip fault. The Pliocene and Quaternary basalt centers are inferred to have ascended along this fault zone and diverted to the northeast (maximum compressive stress direction).	***Supportive Evidence:*** *Steep gravity gradient paralleling proposed strike-slip fault, presence of north-northwest trending right-slip fault in the arcuate ridge at the south end of Crater Flat, clockwise rotation of field magnetization directions of the Tiva Canyon member, structural models of Crater Flat basin.*	**Negative Evidence:** Bare Mountain fault shows predominately dip-slip offset, basalt centers do not occur on the Bare Mountain fault, no correlation between volume of basalt centers and proximity to proposed bounding strike-slip fault.	***Alternative Submodels:*** *Same as model 5.*
Model 7: Stress-field Dike: Quaternary Centers. This structural model assumes basalt magma ascended along a concealed structure defined by the northwest orientation of vents of the CFVZ. The feeder dike or dikes diverted at shallow depths to follow the maximum compressive stress direction. The direction of dike propagation is to the north-northeast or south-southwest.	***Supportive Evidence:*** *Coincidence of the zone of maximum erupted volume of magma with the CFVZ, symmetrical distribution of vents about northwest-trending zone, cluster length of the Quaternary basalt of Crater Flat exceeds maximum likely dike length.*	**Negative Evidence:** Multiple dikes are required only for the Quaternary basalt of Crater Flat, no recognized correlation between center chemistry and proposed dike systems, does not explain the distribution of all basalt centers.	***Alternative Submodels:*** This model is a subset of the strike-slip models.

Table 7.14 (cont.)

Model 8: Stress-field Dike: Pliocene and Quaternary Centers. This model is identical to model 7. The dimensions of the structural zone are defined by the distribution of Pliocene and Quaternary volcanic centers.	***Supportive Evidence:*** *Same as model 8, aeromagnetic anomalies of Amargosa Valley may be analogous to the Quaternary basalt centers of Crater Flat, and formed basalt centers only at the ends of the dikes.*	**Negative Evidence:** Does not explain the occurrence of the basalt of Buckboard Mesa.	***Alternative Submodels:*** *May form three separate structural systems including the aeromagnetic anomalies of Amargosa Valley, the Crater Flat volcanic field, and the Thirsty Mesa/Sleeping Butte centers.*
Model 9: Chain Model. Basalt centers follow northeast-trending chains and the chains form zones of higher risk for future volcanic events (Smith et al. 1990).	***Supportive Evidence:*** *Northeast-trends of clusters of contemporaneous volcanic centers, parallelism of northeast trends of clusters to bedrock faults of Yucca Mountain, analog comparison to other basaltic volcanic fields.*	**Negative Evidence:** Risk zones are unsuccessful as predicators of future events, Quaternary basalt of the YPB do not follow existing faults, dimensions of chains from analog volcanic fields exceed maximum cluster lengths of centers in the YMR, structural trends different for alignments of the Thirsty Mesa and basalt of southeast Crater Flat (north trending), longer chains occur only in alluvial basins, Lathrop Wells and Buckboard Mesa centers do not form chains, northeast trends are secondary to northwest trends.	

Table 7.14 (cont.)

Model 10: Pull-Apart Basin: The Crater Flat basin is a pull-apart basin located at the termination of northwest-trending, strike-slip faults of the Walker Lane structural system. The basin is a combined strike-slip/extensional tectonic basin and the basalt centers concentrated along extensional structures of the basin (Fridrich and Price 1992; Fridrich et al. 1994).	***Supportive Evidence:*** *Discontinuous northwest-trending faults of the Crater Flat area, multiple basalt cycles of the Crater Flat basin (10.5 Ma and Pliocene and Quaternary), gravity data showing steep, northwest-trending gradients, clockwise rotation of field magnetization directions of the Tiva Canyon Member, Walker Lane structural setting.*	**Negative Evidence:** The occurrence of basalt centers is not confined to the pull-apart basins, limited continuity of northwest-trending fault systems.	
Model 11: Caldera Model. The Crater Flat basin is a structural depression formed by multiple, coalesced caldera collapses associated with eruption of the Crater Flat Tuff. Basalt centers are inferred to follow the ring-fracture system of the caldera complex (Carr, 1990).	***Supportive Evidence:*** *Crater Flat basin is located on the south part of the southwest Nevada volcanic field, basalt centers are located commonly along ring-fracture zones of caldera complexes, basalt of Buckboard Mesa is located on the ring-fracture of the Timber Mountain caldera, dike of Solitario Canyon and extensions may follow ring-fracture zone.*	**Negative Evidence:** Caldera origin of the basin is controversial, basalt centers occur beyond the confines of the Crater Flat basin, basalt centers occur across the caldera floor and resurgent dome and are not confined to the ring-fracture zone.	

Table 7.14 (cont.)

Model 12: Northeast Structural Zone: The YMR is located in a diffuse northeast trending, tectonic-volcanic rift zone. Sites of basaltic volcanism are more common in the zone than outside the zone; composite model proposed by Carr (1984; 1990; Kawich-Greenwater Rift zone, and Wright 1989; Amargosa Desert Rift zone).	***Supportive Evidence:*** *Northeast-trending zone of closely spaced, normal faulting, orientation of caldera centers in the southwest Nevada volcanic field, northeast trending structural trough that is delineated partly by gravity data, concentration of basaltic volcanic centers in the northeast-trending structural zone.*	**Negative Evidence:** Structural zones may be a composite of multiple different structures, basalt centers are present both in and outside the structural zone, northwest linear alignment of basalt centers occur within the northeast-trending zone.	
Model 13: Crater Flat and Buckboard Mesa Volcanic Zone: The basalt centers of Crater Flat and the basalt of Buckboard Mesa form a northeast trending zone that extends through the Yucca Mountain site (proposed by Smith et al. 1990 and Naumann et al. 1992).	***Supportive Evidence:*** *Local northeast trends of basalt vents in Crater Flat, existence of the basalt centers of Crater Flat, and Buckboard Mesa.*	**Negative Evidence:** Distance of separation between the Crater Flat basalt centers and the basalt of Buckboard Mesa, interruption of the northeast-trends by oblique structures of the Timber Mountain-Oasis Valley caldera complex, northwest-trending vent alignments of the basalt of Buckboard Mesa, no basalt centers between Crater Flat and Buckboard Mesa.	

Table 7.15 is a summary of disruption ratios (E2) established from the structural models of Table 7.14. The minimum disruption ratio (column E2 area of Table 7.15) is estimated by assuming a 6-km^2 repository area located in the structural zone. Structural models that do not include the potential repository site (12 of the 16 structural models of Table 7.14) are enlarged to include the site (column "Forced Intersection" of Table 7.15) by increasing the dimensions of each zone while still attempting to preserve the geometric shape of the zone. The directions of enlargement are preferentially to the north-northeast and south-southwest following the direction of propagation of feeder dikes in the local stress field. The column labeled "Likelihood Intersection" on Table 7.15 is a judgmental assessment of how likely the required expansion is for each model from the perspective of the structural zone and the spatial dispersion of volcanic events in the structural zone. For most cases the likelihood of intersection is low. Intersection is judged to be unlikely for four cases. Cases 4 and 4a require dike lengths that exceed representative lengths to result in intersection. Cases 10 and 10a are for structures that do not intersect the Yucca Mountain site. For one case, the caldera model (model 11 of Table 7.14), the likelihood of intersection is judged to be moderate because the inferred structure extends to the boundaries of the Yucca Mountain site. The models labeled high are structural models that include (without expansion) the Yucca Mountain site. The column labeled "E2 Intersection" on Table 7.15 is the disruption ratio (E2) for the expanded structural zone. The columns labeled "E2 Interior" and "E2 Front" are weighted values of the E2 intersection column using the frequency of occurrence of volcanic events in alluvial basins, range fronts, and range interiors (weightings are from the frequencies summarized in Table 7.2). The median estimates of E2 for forced intersection, range interior, and range front plus range interior models are respectively, $4.6 \pm 4.4 \times 10^{-3}$, $6.9 \pm 6.6 \times 10^{-4}$, and $1.1 \pm 1.1 \times 10^{-3}$ (all from Table 7.15).

Evaluation of the estimates of E2 from Table 7.15 requires some degree of subjective judgment. First, a judgment must be made about the structural viability of the geometry of structural models that are expanded to intersect the potential repository site. If the geometry of intersection is not realistic, the estimates of Table 7.15 are worse case estimates. Second, a judgment must be made of how reasonable the structural models are for the Yucca Mountain setting. The majority of structural models form zones that do not include the potential repository or the controlled area. This statement is consistent with the geologic record of the YMR. During the past 4.8 Ma, there has been intermittent basaltic volcanism in the basins of the Amargosa Valley, Crater Flat, Timber Mountain caldera depression, and the south edge of the Black Mountain highland. None of the volcanic events occurred in the potential repository or controlled area of Yucca Mountain. The required subjective judgment is whether the models are sufficiently valid to conclude that Yucca Mountain is not and will continue not to be located in the structural zones.

Four of the structural models of Table 7.15 include the Yucca Mountain site. The mean estimates of E2 for the four models (intersection, range interior, and range front plus range interior models) are respectively: $3.5 \pm 1.1 \times 10^{-3}$, $5.2 \pm 1.6 \times 10^{-4}$, and $8.7 \pm 2.7 \times 10^{-4}$. These estimates are smaller than and exhibit less variance than the median estimates for all other structural models. The data show that the northeast-trending models do not give larger estimates for the disruption ratio and are not worst or even worse case models for the YMR (compare with Smith et al. 1990; Ho 1992). The only inconsistency with that statement is for the chain model of Smith et al. (1990). There are two lines of evidence why the chain length model proposed by Smith et al. (1990) may *not* be applicable to the YMR. First, the maximum chain lengths used by Smith et al. (1990) are taken from the Reveille and Fortification volcanic fields. These fields are unrelated to the volcanic rocks and tectonic setting of the YMR. An alternative and more realistic approach is to assign a chain length for the chain model of Table 7.15 using the *longest* observed cluster length of volcanic centers in the YMR (13 km). The dispersion of volcanic vents using this cluster length is the half -length (6.5 km) since a dike could propagate *either* southwest or northeast. The 6.5-km half-length is *too short* to result in penetration of the repository using the models of Smith et al. (1990). Second, even if the assumption is accepted that longer chain lengths are feasible, penetration of the repository would result from north/northeast propagation of volcanic clusters for only a small component of the total length of the CFVZ (approximately 10% of the zone). For example, northeast projection of a long-chain length

Table 7.15 Estimations of E2 for structural models of the YMR.

Model Number	Name	Time Interval	Intersection repository	Area (km^2)	Forced Intersection	Likelihood Intersection	E2 Intersection	E2 Interior	E2 Front
Model 1	CFVZ	1.00	no	1100	1310	Low	4.6E-03	6.9E-04	1.2E-03
Model 2	CFVZ	3.85	no	1350	1450	Low	4.1E-03	6.2E-04	1.0E-03
Model 3	YMR/AMRV	4.80	yes	2180	2180	High	2.7E-03	4.1E-04	6.9E-04
Model 4	CFVZ	3.75	no	220	400	Unlikely	1.5E-02	2.2E-03	3.7E-03
Model 4a	CFVZ with AV	3.85	no	750	750	Unlikely	8.0E-03	1.2E-03	2.0E-03
Model 5	Strike Slip	1.00	no	1100	1310	Low	4.6E-03	6.9E-04	1.1E-03
Model 6	Strike Slip	4.80	no	1350	1450	Low	4.1E-03	6.2E-04	1.0E-03
Model 7	Stress-Dike	1.00	no	1100	1310	Low	4.6E-03	6.9E-04	1.1E-03
Model 8	Stress-Dike	4.80	no	1350	1450	Low	4.1E-03	6.2E-04	1.0E-03
Model 9	Chain Model	3.75	no	390	450	Low	2.7E-03	4.0E-04	6.7E-04
Model 9a	Chain Model	3.85	no	500	690	Low	7.8E-04	1.2E-04	2.0E-04
Model 10	Pull-Apart	3.75	no	390	450	Unlikely	1.3E-02	2.0E-03	3.3E-03
Model 10a	Pull-Apart	3.85	no	500	690	Unlikely	8.7E-03	1.3E-03	2.2E-03
Model 11	Caldera	3.75	no	220	400	Moderate	1.5E-02	2.2E-03	3.7E-03
Model 12	Kawich Rift	3.75	yes	1700	1700	High	3.5E-03	5.3E-04	8.8E-04
Model 12a	12 with AV	3.85	yes	2250	2250	High	2.7E-03	4.0E-04	6.7E-04
Model 13	NESZ	3.75	yes	1200	1200	High	5.0E-03	7.5E-04	1.2E-03
				Statistics	*(all models)*	*Mean*	*6.1E-03*	*9.1E-04*	*1.5E-03*
						Median	*4.6E-03*	*6.9E-04*	*1.1E-03*
						Geomean	*4.8E-03*	*7.2E-04*	*1.2E-03*
						StdDev	*4.4E-03*	*6.6E-04*	*1.1E-03*
				Statistics	*(intersection models)*	*Mean*	*3.5E-03*	*5.2E-04*	*8.7E-04*
						Median	*3.1E-03*	*4.7E-04*	*7.8E-04*
						Geomean	*3.4E-03*	*5.0E-04*	*8.4E-04*
						Std Dev	*1.1E-03*	*1.6E-04*	*2.7E-04*

(high-risk zone) following the maximum compressive stress direction from the Lathrop Wells volcanic center *does not* result in intersection of the exploratory block of the Yucca Mountain site. Smith et al. (1990) changed slightly the chain orientation to permit their high risk zone to intersect the exploratory block. Accordingly, the disruption probability of the chain models of Table 7.15 is estimated only for the areal extent of the high risk zones that can be propagated to intersect the potential repository site. These cases are highlighted on Table 7.15 because this treatment of the data could be viewed as controversial.

4. Analog Basaltic Volcanic Fields of the Basin and Range Province. Additional insight can be gained on bounds for the disruption ratio for the YMR through comparisons with the spatial distribution of volcanic centers in basaltic volcanic fields of the Basin and Range province. The analog fields used for comparison are the same as those used for the analog assessments of E1: the Lunar Crater and Cima volcanic fields. Each field has a sufficient number of centers to evaluate the spatial variability of the locations of basaltic volcanic centers. Moreover, the large number of volcanic events at both fields provides a representative assessment of the spatial dispersion of vents in a volcanic field.

Figure 7.21 is a plot of the location of volcanic vents in the Lunar Crater field. The locations are shown as x,y coordinates transposed from the latitude and longitude coordinates of the vents. Mercator projections are not used for these data because of the relatively small size of the area and because the detail of the intrafield distribution of vents is not important. What is important is the geometry of the volcanic fields, the dispersion of vents in the fields, and a comparison with the distribution of basaltic volcanic centers in the YMR.

The distribution of volcanic vents in the Lunar Crater volcanic field is structurally controlled (Fig. 7.21). There are 82 identified vents of probable Quaternary age and the vents are distributed along north northeast-trending alignments (Crowe et al. 1986) parallel to the elongation of the volcanic field (Fig. 7.21) (see also Scott and Trask 1970). The volcanic field occupies an area of about 260 km^2. Exploratory data analyses show that the locations of the vents (latitude and longitude) deviate slightly from a normal distribution, but there are no identified outliers in the data set. Several methods are used to evaluate the spatial variability of the vent distribution. The major points of interest are the *shape* of the basaltic field and the *degree of dispersion* of the vents; the detailed spatial patterns of vents is of lesser importance. Also shown on Figure 7.21 is the centroid of the vent distribution (95% confidence interval), with bivariate Gaussian ellipsoids drawn at the 90% and 95% confidence intervals. The ellipsoids are elongate parallel to the elongation direction of the volcanic field, reflecting the northeast structural control of vent locations. The width of the volcanic field is 10.5 km at the location of the vent centroid. The 90% ellipsoid bounds approximately the distribution of vents in the field (Fig. 7.21). The half-width of the 90% ellipsoid at the position of the centroid is 5.25 km (orthogonal to the field elongation). The half-width of the 95% ellipsoid at the position of the vent centroid is 7.3 km. The half-length of the ellipsoid drawn through the centroid is 29 km. These dimensions provide approximate measures of the shape and dispersion of vents in the Lunar Crater volcanic field.

There are several complicating factors that must be considered for assessing the vent distributions in the Lunar Crater volcanic field. First, construction of bivariate Gaussian ellipsoids assumes a normal distribution of volcanic vents. The actual vent distribution deviates somewhat from a normal distribution. Second, there is time-space migration in the location of eruptive vents in the Lunar Crater volcanic field. The general pattern is a decrease in the age of the centers from southwest to northeast (Scott and Trask 1971; Crowe et al. 1986; Bergman 1982). This migration should increase slightly the degree of vent dispersion parallel to the direction of vent migration but should have a minor effect on field width.

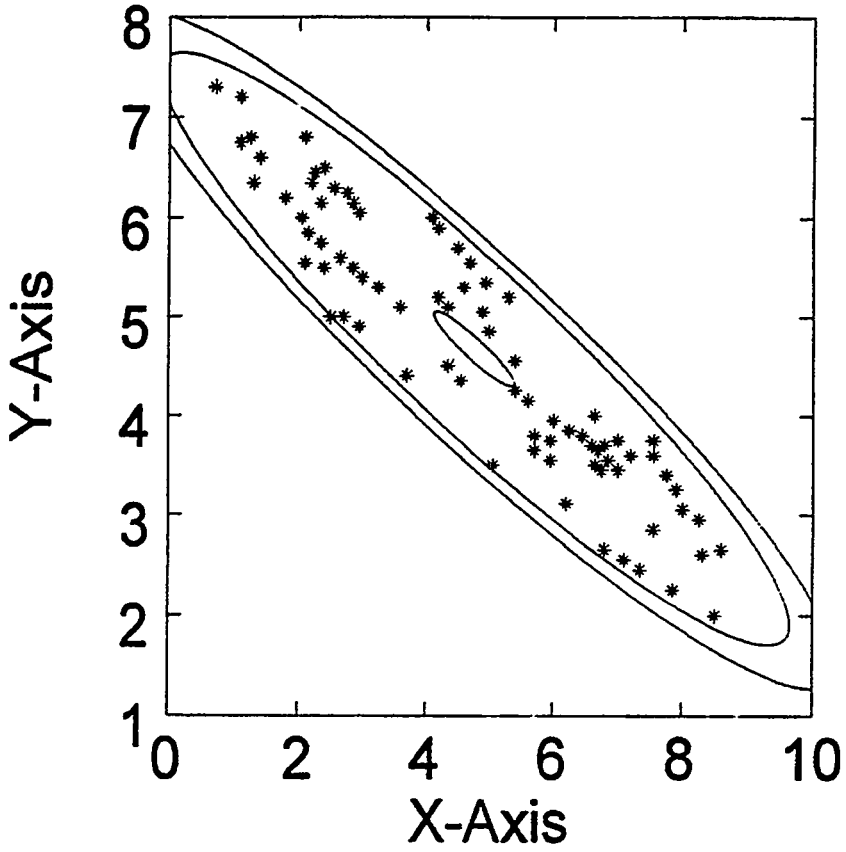


Fig. 7.21 Distribution of volcanic vents in the Lunar Crater volcanic field. The vent locations are the latitude and longitude of the vents converted to an xy grid for plotting. The data *have not* been converted to Mercator projections because of the small size of the map. The small ellipse in the center of the field is the centroid calculated from the distribution of all vents. The larger ellipses are the bivariate Gaussian ellipsoids drawn at confidence intervals of 90% and 95%

The same calculations can be made for the Cima volcanic field in the Mojave desert of California (Dohrenwend et al. 1986, Crowe et al. 1992). Figure 7.22 is similar to Figure 7.21 and shows the distribution of Quaternary volcanic vents in the southwest part of the Cima volcanic field. The centroid of the vent distribution (95% confidence interval) and bivariate Gaussian ellipsoids are drawn at the 90% and 95% confidence intervals. The distribution of volcanic events in the Cima volcanic field is less strongly controlled structurally than the Lunar Crater volcanic field. The former field is elongate slightly in a northeast direction as shown by the vent centroid and bivariate Gaussian ellipsoids. The half-width of the 90 percentile confidence interval for the bivariate Gaussian ellipsoid is 4.8 km; the half-width of the 95 percentile confidence interval drawn through the vent centroid is 5.4 km.

What is the significance of the analog comparisons of the Lunar Crater and Cima volcanic fields? The calculations are not intended to provide statistically significant descriptions of the spatial distribution of volcanic vents in the fields. However, the calculations for the Lunar Crater and Cima volcanic fields illustrate two important points that have application to the YMR. First, there are a large number of Quaternary vents in these active volcanic fields. The number of Quaternary basaltic centers in the fields exceeds the number of centers in the YMR by a factor of 4 (Cima volcanic field) to greater than a factor of 10 (Lunar Crater volcanic field). The number of vents is sufficient to assume that the vent dispersion is representative of the behavior of large, high cone density volcanic fields. Second, Figure 7.23 is a plot of the distribution of volcanic centers in the YMR and shows the half-width and half-length dimensions of the 95% bivariate Gaussian ellipsoid for the Lunar Crater volcanic field (the Cima volcanic field is not shown since it is smaller than the Lunar Crater field). The plotted dimensions of the Lunar Crater volcanic field are centered on the vent centroid drawn from the distribution of Pliocene and Quaternary volcanic centers; the long dimension of the field is oriented parallel to the CFVZ. The dispersion of vents in the Lunar Crater volcanic field is insufficient, when superimposed on the YMR, to overlap the exploratory block of the Yucca Mountain site. The width of the Lunar Crater volcanic field drawn at the 95% ellipsoid (14.6 km)

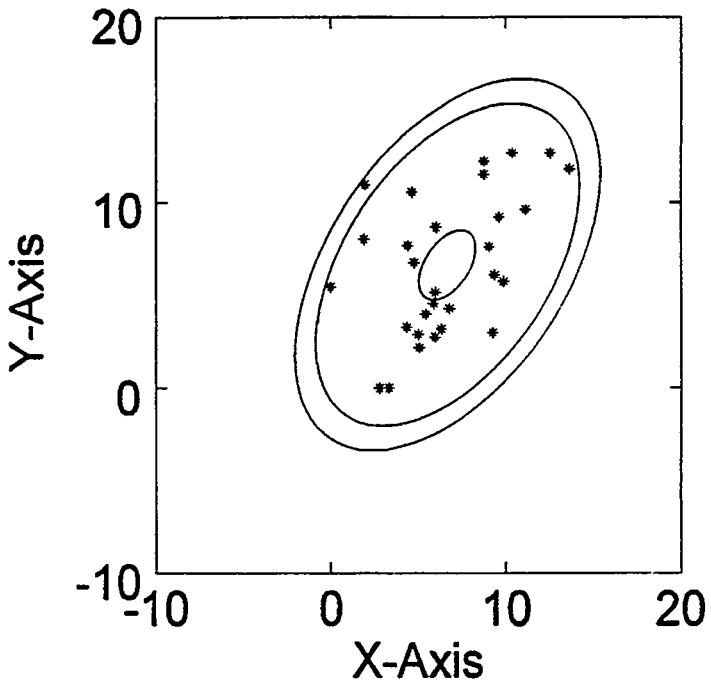


Fig. 7.22 Distribution of volcanic vents in the Cima volcanic field. The Figure is identical to Figure 7.21 but drawn for volcanic vents in the Cima volcanic field.

is only slightly greater than the degree of north-northeast dispersion of clustered volcanic centers in the YMR (longest cluster = 13 km).

5. Simulation Modeling: E2 the Disruption Probability. Risk simulation is used to attempt to define the distribution of E2 in probability space. Figure 7.24 shows the distribution of E2 (dimensionless) using different combinations of published, spatial, and structural estimates for the YMR (Tables 7.13 and 7.14). Defining limits for E2 in probability space is more difficult than for E1, and only approximate limits can be identified. The vertical line labeled "controlled area" on Figure 7.24 is the ratio of the repository area (6 km^2) to the controlled area (86 km^2). Estimates of E2 must lie to the right of that line since Pliocene and Quaternary volcanic activity is centered in Crater Flat and there has been no volcanism in the controlled area since the Miocene. The lines labeled "Cima volcanic field" and "Lunar Volcanic field" on Figure 7.24 are the disruption probability obtained by locating a 6-km^2 repository in the interior of the respective volcanic fields. Logically, the disruption ratio for the YMR should be located to the right of the disruption ratios for the Cima and Lunar fields because the potential repository site is not located *inside* the zones of *most* spatial and structural models. The potential site *is included in some spatial and structural models* but because the cone density (centers km^{-2}) in the YMR is low, these models are located well to the right of the disruption ratios for the Cima and Lunar volcanic fields (see enclosed pattern of NESZ on Figure 7.24). Finally, the vertical line labeled "Outlier" on Figure 7.24 identifies the approximate position of estimates identified as outliers using exploratory data analyses (box, stem and leaf, and probability. All disruption ratios to the left of the line are outliers or far outliers. This line provides a less subjective method for identifying natural variations in the data distribution.

The judgment could be made that the outlier values of Figure 7.24 should *not be included* in estimations of the disruption ratio (E2). Spatial models that approach or exceed the disruption ratio for the Lunar Crater and Cima volcanic fields appear unrealistic, given the greater number of basaltic centers in the volcanic fields versus the YMR. Moreover, judgments concerning the suitability of the outlier values are dependent partly on the acceptance or rejection of structural models for the tectonic setting of Yucca Mountain. The majority of geologic and structural data for the YMR appear consistent with the CFVZ being a preferential zone of Pliocene and Quaternary basaltic volcanism. The fundamental evidence in

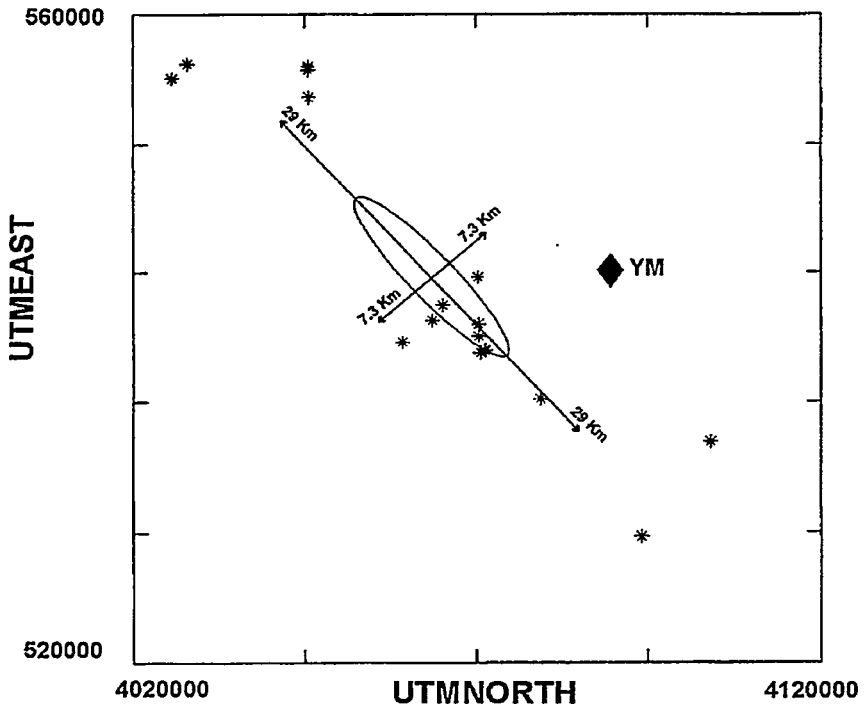
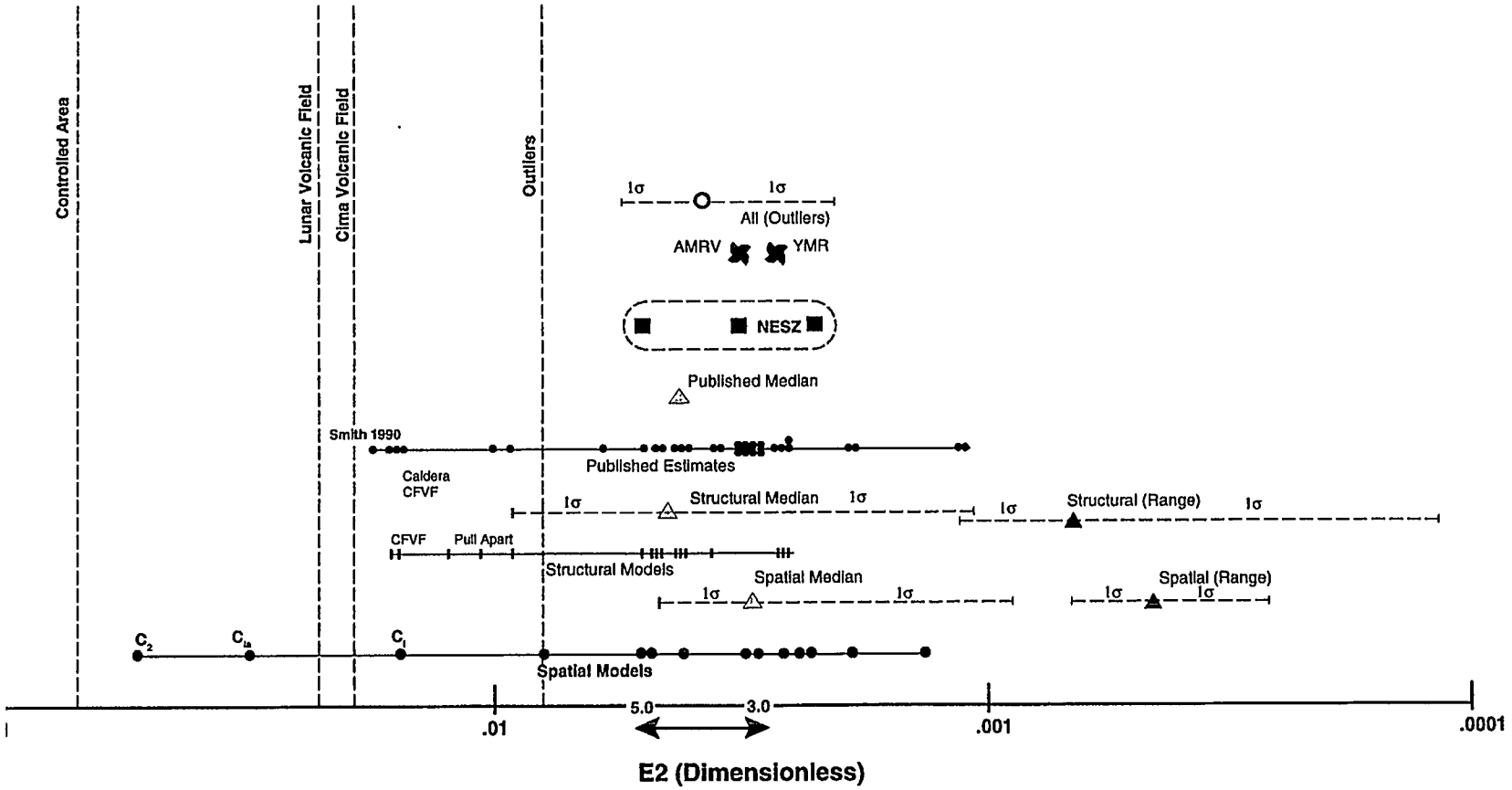


Fig. 7.23 Plot of the distribution of Pliocene and Quaternary volcanic events in the YMR (excluding the basalt of Buckboard Mesa) with the event centroid drawn at a 90% confidence interval. The Quaternary part of the Lunar Crater volcanic field is centered in the event centroid and its long axis is oriented parallel to the CFVZ.

support of the observation is simply the spatial distribution of volcanic events. Additionally, newly refined structural models of the Crater Flat basin provide increased support for the existence of a strike-slip bounded, pull-apart basin that has and should continue to bound the occurrence of basaltic volcanic activity (Fridrich et al. 1994). The significance of the pull-apart basin is twofold. First, the Yucca Mountain site is located outside the structural basin. Second, the basin boundaries appear to limit the distribution and degree of north-northeast dispersion of sites of Pliocene and Quaternary basaltic volcanism. Thus sites of basaltic volcanism, in the vicinity of Crater Flat, appear to occur only within the structural boundaries of the pull-apart basin. We have chosen to not exclude the outlier estimates of E2 from the risk analyses for two reasons. First, we prefer to *not* exclude any information at this stage of studies. Second, alternative structural models inferring northeast trends in the distribution of volcanic events, both in the orientation of age-correlated centers and in the alignment of vents, have been proposed. The evidence that these trends extend to or through the Yucca Mountain site is weak but cannot be disproved with the limited number of volcanic events in the YMR.

The disruption ratios determined from spatial and structural models group between values of 3.0 to 5.0 x 10^{-3} (Fig. 7.24). The set of structural models that include the Yucca Mountain site (labeled NESZ and AMRV on Fig. 7.24) give ratios for E2 that are also between 3.0 to 5.0 x 10^{-3}. Finally, if the estimates of all models of E2 are weighed for the tendency of basalt centers to occur in alluvial basins versus range fronts or range interiors, almost all estimates of the probability of disruption (E2) are $<10^{-3}$ (Fig. 7.24).

A simulation matrix was constructed using five sets of model estimations of E2, with each model subdivided into two cases (Table 7.16). The models include: (1) all published estimates of E2, (2) edited estimates of all published estimates (outlier estimates removed), (3) spatial models, (4) outlier edited



Fi.g. 7.24. Distribution of E2, the disruption probability in probability space. The x-axis is a log scale for E2 (dimensionless) and the y-axis has no scale. It is used to provide plotting space for the overlapping estimates of the disruption ratio. The vertical line labeled "Outliers" is the position of estimates identified as outliers using exploratory data analyses. All points to the left of the line are outliers or far outliers. The vertical lines labeled "Lunar volcanic field" and "Cima volcanic field" are the estimate of the disruption probability if a 6-km^2 repository were randomly located in the respective fields. The vertical line labeled "Controlled Area" is the ratio of the controlled area to the potential repository site.

Table 7.16 Simulation matrix for E2, the disruption probability.

Disruption Model (E2)	Median	Std Deviation	Skewness	Simulation (mean, 1 *s*)
All Published Estimates				
Intersection	4.1E-03	7.9E-03	2.2	4.1E-03
Range Interior	6.2E-04	1.3E-03	2.2	6.2E-04
All Published (no outliers)				
Intersection	3.8E-03	1.8E-03	1.3	3.8E-03
Range Interior	5.7E-04	2.6E-04	1.3	5.7E-04
Spatial Distribution Models				
Intersection	3.1E-03	1.5E-02	2.6	3.1E-03
Range Interior	4.6E-04	2.2E-03	2.6	4.6E-04
Spatial Distribution (no outliers)				
Intersection	2.8E-03	1.8E-03	1.6	2.8E-03
Range	4.3E-04	2.7E-04	1.6	4.3E-04
Structural Models				
Intersection	4.6E-03	4.4E-03	1.2	4.6E-03
Range Interior	6.9E-04	6.6E-04	1.2	6.9E-04
Intersection Models				
Intersection	3.1E-03	1.1E-03	1.3	3.1E-03
Range Interior	4.7E-04	1.6E-04	1.3	4.7E-04

data are not strongly skewed), and (6) intersection models that include the Yucca Mountain site (Tables 7.13 and 7.14). Subclasses for each model include: (1) estimates of E2 for intersection or forced intersection models and (2) estimates of E2 for range interiors. Because it is difficult to identify bounds for E2, the data are modeled as a normal distribution using the median and standard deviation estimates from the data tables. All simulations were run for 10,000 sampling iterations using the Latin-Hypercube sampling method.

The results of the simulation modeling are shown on Table 7.17. Intersection models (mean estimates) range from 4.6×10^{-3} (structural models) to 2.8×10^{-3} (outlier-removed, spatial models). Range interior models (mean estimates) range from 6.9×10^{-4} (structural models) to 4.3×10^{-4} (outlier-removed, spatial models). A subset of cumulative probability curves (intersection models) generated from the simulation modeling using the simulation matrix are shown on Figure 7.25. The cumulative probability curves for the range interior models are not shown. They are identical to the intersection models but are shifted to lower disruption ratios. The median estimates of the cumulative distribution curves cluster in a narrow range (2.8 to 4.6×10^{-3}; see expected values of Fig. 7.25). The curves differ primarily in the spread or uncertainty of the distributions (Fig. 7.26). The uncertainty is largest for the spatial model (with outliers) and smallest for the subset of intersection models that include the repository (NE models of Fig. 7.25). The 50 percentile estimate of the structural models is *larger* than the 50 percentile estimate for the spatial model

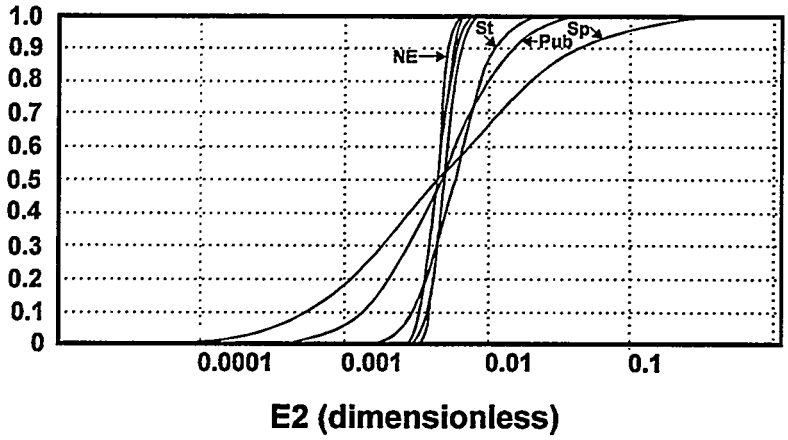
Table 7.17 Simulation results for E2, the probability of magmatic disruption.

Simulation Statistics	Published Estimates Intersection	Published Estimates Range	Published Estimates Intersection (no outliers)	Published Estimates Range (no outliers)
10 percent	-6.9E-03	-1.1E-03	1.5E-03	2.3E-04
Mean	4.1E-03	6.2E-04	3.8E-03	5.7E-04
90 percent	1.4E-02	2.4E-03	6.0E-03	9.0E-04
	Spatial Models Intersection	Spatial Models Range	Spatial Models Intersection (no outliers)	Spatial Models Range (no outliers)
10 percent	-1.6E-02	-2.4E-03	5.5E-04	8.3E-05
Mean	3.1E-03	4.7E-04	2.8E-03	4.3E-04
90 percent	2.2E-02	3.3E-03	5.1E-03	7.7E-04
	Structural Models Intersection	Structural Models Range	Direct Intersection	Direct Intersection Range
10 percent	-1.1E-03	-1.6E-04	1.8E-03	2.6E-04
Mean	4.6E-03	6.9E-04	3.1E-03	4.7E-04
90 percent	1.0E-02	1.5E-03	4.5E-03	6.8E-04

F. Probability of Magmatic Disruption of the Potential Repository . The cumulative distribution curves for E1 and E2 can be combined through risk simulation to give the cumulative distribution curves for estimates of the probability of magmatic disruption of the repository, the controlled area, and the YMR (Pr[E2 given E1]Pr[E1]). We attempt to define a range of cumulative distribution curves for the probability of magmatic disruption by assembling three sets of models. For the first model, two fixed estimates for E2 are used (intersection and range intersection) and E1 is varied using the estimates from Tables 7.5 and 7.6. For the second model, a single distribution is used for E1, and E2 is varied using the range of simulation modeling from Table 7.17. Finally, the third model examines the variability in E1 *required* by selection of individual models of E2. The exponential equation for the conditional probability of magmatic disruption is approximately linear for t = 1 to 10,000 yr so the cumulative distribution curves can be combined by multiplication.

Table 7.18 is the simulation matrix and expected values for estimations of the probability of magmatic disruption of the repository. The models used for E1 are the preferred models using homogeneous and nonhomogeneous Poisson distributions for the volcanic cycle (event and stress-dike) and Quaternary accelerated intervals (event and stress-dike). Also included in the recurrence models are the minimum and maximum estimations from Tables 7.5 and 7.6. The simulations were run for 10,000 iterations using Latin-Hypercube sampling. The recurrence estimates are modeled as trigen distributions using the most likely values for the midpoint estimate (except minimum and maximum simulations), the Quaternary field limit as the 5 percentile lower bound (1.1×10^{-5} events yr^{-1}), and the regulatory perspective as the 10 percentile upper bound (5×10^{-7} events yr^{-1}). The two fixed estimates for E2 are simulated as normal distributions (median, standard deviation) using the summary statistics for the structural models from Table 7.14. The minimum and maximum estimates used in the simulation are the maximum estimate (worst case) and minimum estimate (best case) from Tables 7.5 and 7.6. This simulation matrix is designed to examine the sensitivity of the probability of magmatic disruption to different recurrence models.

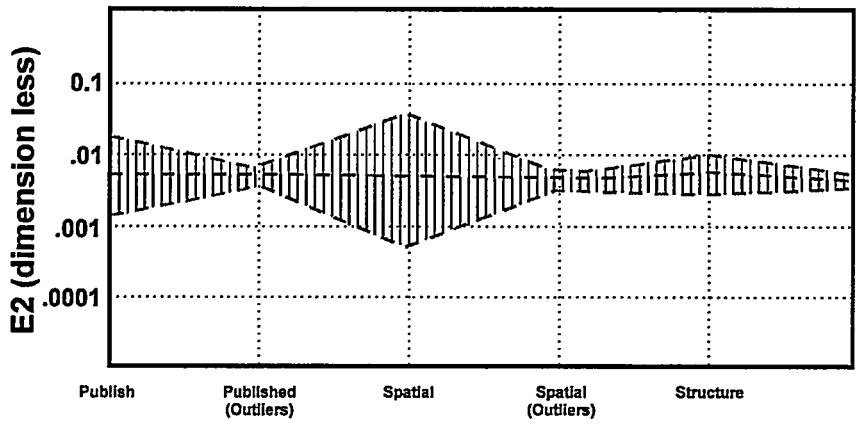
Fig. 7.25. Cumulative probability curves for E2 generated from the simulation matrix of Table 7.16.



Expected Value

All Published $4.1E^{-3}$
Published (outliers) $3.8E^{-3}$
All Spatial $3.1E^{-8}$
Spatial (outliers) $2.8E^{-3}$
Structural $4.6E^{-3}$
NE Trend $3.1E^{-3}$

Fig. 7.26 Variability in the probability of disruption for published, spatial, and structural models of E2 (published and spatial models shown with and without outliers).



Top - - - - **90 per %**

Center - - - - **Mean**

Bottom - - - - **10 per %**

Table 7.18 Simulation matrix for homogeneous and nonhomogeneous Poisson recurrence models of E1 using fixed estimates of E2.

Simulation Matrix E1 Model	Trigen Homogeneous	Trigen Nonhomogeneous	Trigen E2Intersect	Normal E2Range
Vol Cycle Event	4.8E-06	4.8E-06	4.6E-03	6.9E-04
Vol Cycle Stress Dike	4.7E-06	4.7E-06	4.6E-03	6.9E-04
Quat Accel Events	5.3E-06	5.0E-06	4.6E-03	6.9E-04
Quat Accel Stress Dike	5.2E-06	4.8E-06	4.6E-03	6.9E-04
Minimum	4.6E-06	4.6E-06	4.6E-03	6.9E-04
Maximum	5.7E-06	5.7E-06	4.6E-03	6.9E-04
Simulation Expected Values	Homogeneous Pr(intersect)	Nonhomogeneous Pr(intersect)	Homogeneous Pr(range)	Nonhomogeneous Pr(range)
Vol Cycle Event	2.2E-08	2.2E-08	3.3E-09	3.2E-09
Vol Cycle Stress Dike	2.1E-08	2.1E-08	3.2E-09	3.2E-09
Quat Accel Events	2.4E-08	2.3E-08	3.7E-09	3.4E-09
Quat Accel Stress Dike	2.4E-08	2.2E-08	3.5E-09	3.3E-09
Minimum	2.1E-08	2.1E-08	3.2E-09	3.2E-09
Maximum	2.6E-08	2.6E-08	3.9E-09	3.9E-09
Summary Statistics				
Mean	2.3E-08	2.3E-08	3.5E-09	3.4E-09
Std Deviation	0.2E-08	0.2E-08	0.3E-09	0.3E-09

Table 7.19 shows the mean, 10 percentile, and 90 percentile estimates for the risk simulation using homogeneous Poisson models. Only the homogeneous Poisson model is shown because the estimates for the nonhomogeneous model are nearly identical. The mean estimates using simulation modeling based on the probability matrix are bracketed by the minimum and maximum models of Table 7.19 (2.1×10^{-8} to 2.6×10^{-8} events yr^{-1} for intersection). There is only a narrow range of mean estimates, showing that there is limited variability in the probability of magmatic disruption with different recurrence models (E1). The mean estimates for homogeneous and nonhomogeneous Poisson models are identical ($2.3 \pm 0.2 \times 10^{-8}$ events yr^{-1}). Figure 7.27 shows the cumulative probability curves for the minimum and maximum homogeneous Poisson models of Table 7.19. This figure provides an approximation of the sensitivity or uncertainty of the probability of magmatic disruption controlled by alternative recurrence models.

Judgment is required to assess whether it is reasonable to weigh the probability of magmatic disruption by the frequency of formation of basaltic volcanic centers in range interiors. Table 7.18 shows that the mean estimates of cumulative probability curves for volcanic events in range interiors vary from 3.2×10^{-9} to 3.9×10^{-9} events yr^{-1}. The probability of magmatic disruption of the controlled area is larger than the probability of magmatic disruption of the repository by a factor of 13.5. The probability of

Table 7.19 Simulation results of homogeneous Poisson models for the probability of magmatic disruption of the repository (Pr[E2 given E1]Pr[E1]).

Simulation Results						
Homogeneous Poisson	Cycle Event	Cycle Dike	Quat Events	Quat Dikes	Minimum	Maximum
10Perc=	-2.29E-08	-2.19E-08	-2.74E-08	-2.64E-08	-2.14E-08	-3.05E-08
Mean=	2.18E-08	2.17E-08	2.46E-08	2.34E-08	2.13E-08	2.62E-08
90Perc=	8.30E-08	8.31E-08	9.21E-08	8.85E-08	8.14E-08	9.87E-08

Table 7.20 Simulation matrix for the probability of magmatic disruption of the repository using median, minimum and maximum estimates of E2 and a fixed estimate of E1.

E2 Models	E1	Intersect	Range	Minimum	Maximum
Structural	4.9E-06	4.6E-03	6.90E-04	7.8E-04	1.5E-02
Pr(disrupt)		*2.2E-08*	*3.4E-09*	*3.8E-09*	*7.3E-08*
Spatial	4.9E-06	3.1E-03	4.6E-04	1.4E-03	1.5E-02
Pr(disrupt)		*1.5E-08*	*2.2E-09*	*6.9E-09*	*7.3E-08*
Spatial (outliers)	4.9E-06	2.6E-03	3.9E-04	1.40E-03	5.0E-03
Pr(disrupt)		*1.3E-08*	*1.9E-09*	*6.9E-09*	*2.4E-08*

magmatic disruption of the YMR is greater than or equal to the probability of disruption of the controlled area.

Table 7.20 is the second simulation matrix, and it is designed to assess the variability of the probability of magmatic disruption with different estimates of E2. The simulation uses a single distribution for E1 and a range of estimates for E2. The E1 is modeled as a trigen distribution using the median estimate from the most likely value of Table 7.5. A lower bound of 1.1×10^{-5} events yr^{-1} (95 percentile) is used with an upper bound of 5.0×10^{-7} events yr^{-1} (10 percentile; simulation 3 of Table 7.5). The estimates used for E2 are the median and standard deviation from the summary statistics for the intersection, and range interior columns for the structural, the spatial, and the spatial models with outliers removed (estimates from Tables 7.13 and 7.15). The minimum and maximum estimates were assigned from the smallest and largest estimates from *all* estimates of Tables 7.13 and 7.15. A standard deviation of 50% of the estimate was assumed for the distribution models of the minimum (best case) and maximum (worst case) estimates.

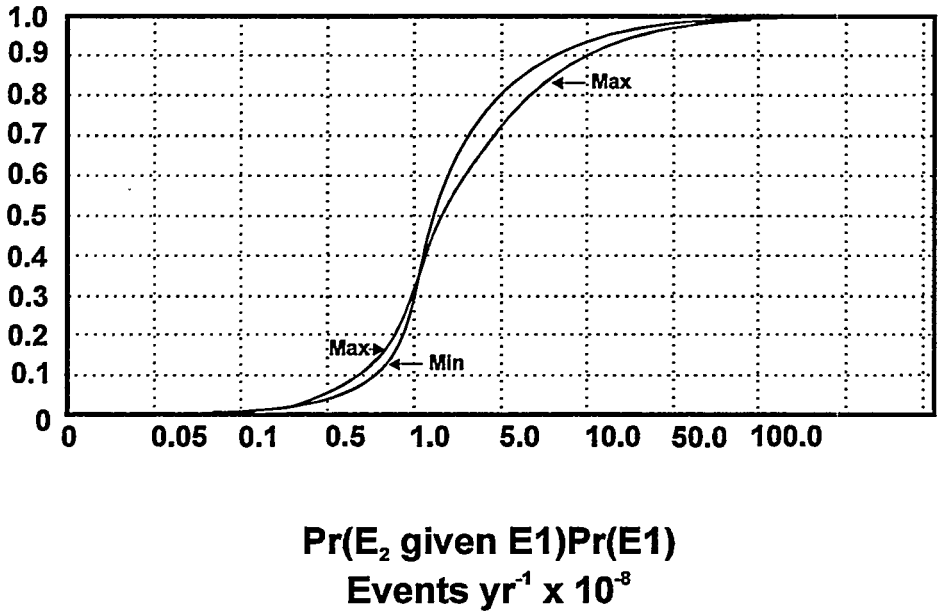


Fig. 7.27 Cumulative probability distribution curves for the simulation matrix of Table 7.18. Fixed estimates of E2 are used for intersection and range interior models for a range of homogeneous Poisson models of the recurrence rate. The probability distribution curves are not shown for nonhomogeneous Poisson models because the results are similar.

The mean estimates of the probability of magmatic disruption of the repository are similar to the estimates for the first simulation matrix (intersection and range models) (Fig. 7.28). The estimates range from 1.3 to 2.2 x 10^{-8} events yr^{-1} for the intersection models and 1.9 to 3.4 x 10^{-9} events yr^{-1} for the range intersection models (Table 7.21). However, the minimum and maximum estimates are much more variable for the second simulation matrix than the first simulation matrix (Fig. 7.28). The minimum estimates of the probability of magmatic disruption (intersection models) range from 3.8 x 10^{-9} to 6.9 x 10^{-9} events yr^{-1} (Table 7.21). The maximum estimate is identical to the range of the first simulation matrix for the spatial models with outliers removed (2.4 x 10^{-8} events yr^{-1}) (Table 7.21). However, an estimate for the probability of magmatic disruption of the repository of 7.3 x 10^{-8} events yr^{-1} was obtained from the maximum estimates (worse cases) of the structural and spatial models. This is the largest estimation of the probability of magmatic disruption of the potential repository for any previously published probability estimation (except the worst case of Ho 1992). The variability in the maximum estimates is controlled by the large values of E2 for a small set of spatial and structural models (Tables 7.13 and 7.15; Fig. 7.28). Accordingly, these models are identified as having significant effects on the sensitivity of estimations of the probability of magmatic disruption of the repository. They must be examined more carefully, and this examination leads to the consideration of the third probability matrix.

The conditional probability model used for risk assessment assumes independence of probability attributes. However, there are indirect controls placed on the recurrence rate from the selection of spatial and structural models for E2. These limits are controlled by the inclusion or exclusion of volcanic events for specific spatial or structural models of E2. This effect has not been considered in estimations of the probability of magmatic disruption *if E1 and E2 are estimated independently* (Crowe et al. 1993; Wallmann 1993). The effect on estimates of the probability of magmatic disruption is largest for disruption models that give the highest disruption probabilities (spatially restricted models) and is zero for disruption models that include all volcanic events in the YMR.

Table 7.21 Simulation results for the probability of magmatic disruption of a repository using the probability matrix of Table 7.20.

Structural Models		Intersection	Range	Minimum	Maximum
	10Perc=	-5.0E-09	-7.7E-10	1.4E-09	2.6E-08
	Mean=	2.2E-08	3.4E-09	3.8E-09	7.3E-08
	90Perc=	5.0E-08	7.5E-09	6.3E-09	1.2E-07
Spatial Models (all data)		Intersection	Range	Minimum	Maximum
	10Perc=	5.7E-09	-2.3E-09	2.4E-09	2.6E-08
	Mean=	1.5E-08	2.3E-09	6.9E-09	7.3E-08
	90Perc=	2.5E-08	6.9E-09	1.1E-08	1.2E-07
Spatial Models (all data)		Intersection	Range	Minimum	Maximum
	10Perc=	5.2E-09	7.8E-10	2.4E-09	8.7E-09
	Mean=	1.3E-08	1.9E-09	6.9E-09	2.4E-08
	90Perc=	2.0E-08	3.1E-09	1.1E-08	4.1E-08

Fig. 7.28 Cumulative probability distribution curves for the probability of magmatic disruption of the repository using a fixed estimate of E1 and varying models for E2.

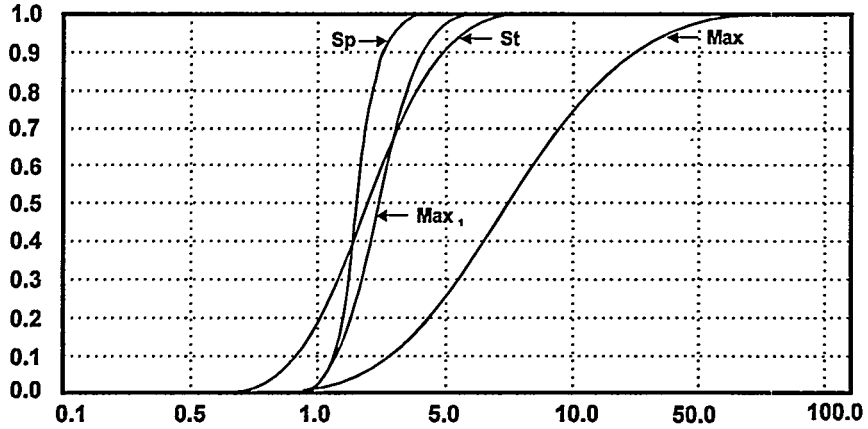


Table 7.22 is a revised probability matrix where E1 is adjusted for individual spatial and structural models for E2 (column "E1 Adjusted" of Table 7.22). The adjusted estimates of E1 are combined with estimates for E2 to give the probability of magmatic disruption of the repository. The adjustments to E1 are made by *not including* volcanic events in the recurrence rate calculations if they *are not included* in the area of the spatial or structural model used to estimate the disruption ratio. The adjusted estimates of E1 for Table 7.21 are made only for the most likely models established from homogeneous Poisson event counts. We have not re-estimated E1 for all recurrence models because the recurrence models show limited variability.

Careful examination of Table 7.22 shows two features. First, the median estimate is smaller than median estimates for the probability of magmatic disruption of the repository for E2 (Tables 7.19 and 7.21). However, the difference is small and is not significant (standard deviations overlap). Second, Table 7.22 provides a more realistic basis for identifying worse case estimates for the probability of magmatic disruption. The column labeled "Z score" is the standardized variable of the intersection column and can be used to identify data that are more than 1*s* from the median. There are two cases where the z-score is greater than 1: Cluster 1 and 1a of the spatial models. These cases are highlighted in Table 7.22, and are identified as sensitive models for the estimates of the probability of magmatic disruption of the repository.

G. Discussion: Probability of Magmatic Disruption. The conditional probability of magmatic disruption has been examined for a range of alternative models of the recurrence rate, and spatial and structural models of the distribution of volcanic centers in the YMR. The median estimates using both statistical descriptors and risk simulations are slightly greater than 10^{-8} events yr^{-1} for simple intersection models, and generally less than 10^{-8} for models weighted by the likelihood of volcanic events in range interiors. Cumulative probability distributions, constructed through simulation modeling, are presented for a range of alternative recurrence and disruption models. These curves provide the best representation of the

Table 7.22 Probability of magmatic disruption of the repository where the recurrence rate (E1) is adjusted for individual spatial and structural models of E2.

Spatial Models	E2	E1 Adjusted	Pr(E2 given E1)Pr(E1) Intersection	Z Score	Range
Cluster 1 (3.7)	*1.5E-02*	*2.6E-06*	*4.01E-08*	1.4	*6.0E-09*
Cluster 1a (3.85)	8.0E-03	2.3E-06	1.9E-08	0.0	2.8E-09
CFVZ (4.8)	4.1E-03	3.7E-06	1.5E-08	-0.1	2.3E-09
NESZ (3.85)	5.0E-03	3.6E-06	1.8E-08	0.0	2.7E-09
Cluster 1a (1.0)	*1.5E-02*	*5.0E-06*	*7.5E-08*	3.6	*1.1E-08*
CFVZ (1.0)	4.6E-03	6.0E-06	2.7E-08	0.6	4.1E-09
Structural Models					
CFVZ (1.0)	4.6E-03	6.0E-06	2.7E-08	0.6	4.1E-09
CFVZ (4.8)	4.1E-03	2.5E-06	1.0E-08	-0.5	1.5E-09
YMR (4.8)	2.7E-03	2.5E-06	6.9E-09	-0.7	1.0E-09
CFV Field (3.75)	1.5E-02	1.6E-06	2.4E-08	0.4	3.6E-09
CFV Field + AV	8.0E-03	2.3E-06	1.9E-08	0.0	2.8E-09
Strike Slip (1.0)	4.6E-03	6.0E-06	2.7E-08	0.6	4.1E-09
Strike Slip (4.8)	4.1E-03	2.3E-06	9.5E-09	-0.5	1.4E-09
Stress-Dike (1.0)	4.6E-03	2.7E-06	1.2E-08	-0.4	1.8E-09
Chain Model (3.7)	2.7E-03	1.6E-06	4.3E-09	-0.9	6.4E-10
Chain Model (3.85)	7.8E-04	2.1E-06	1.6E-09	-1.0	2.4E-10
Pull-Apart (3.7)	1.3E-02	1.6E-06	2.1E-08	0.2	3.2E-09
Pull-Apart (3.85)	8.7E-03	2.1E-06	1.8E-08	0.0	2.7E-09
Caldera (3.75)	1.5E-02	1.6E-06	2.4E-08	0.4	3.6E-09
Kawich Rift (3.7)	3.5E-03	1.6E-06	5.6E-09	-0.8	8.5E-10
Kawich Rift (3.85)	2.7E-03	2.1E-06	5.5E-09	-0.8	8.3E-10
NESZ (3.7)	5.0E-03	1.9E-06	9.4E-09	-0.6	1.4E-09
	Summary Statistics	*Mean*	*1.9E-08*		*2.9E-09*
		Median	*1.8E-08*		*2.7E-09*
		Geomean	*1.5E-08*		*2.2E-09*
		StDev	*1.6E-08*		*2.1E-09*
		Skewness	*2.2*		*2.2*
		Minimum	*1.6E-09*		*2.4E-10*
		Maximum	*7.5E-08*		*1.1E-08*

uncertainty of the data distributions. The cumulative probability distributions for the recurrence rate (E1) are bounded by regulatory perspectives and observations of rates of basaltic volcanic events in Quaternary volcanic fields. The midpoint estimates of the recurrence rate show a limited range of variation for multiple alternative models (time-series, homogeneous and nonhomogeneous Poisson, and models of magma output rate). The cumulative probability distributions for the disruption probability (E2) are more difficult to bound. The data show a relatively narrow range of median estimates but with significant variance. The data distribution for E2 is affected strongly by the existence of a subset of spatial and structural models that can be identified as outliers and give high disruption probabilities ($\approx 10^{-2}$).

What is the significance of the present status of probability studies? The data summarized in this section supports previous judgments by the DOE (EA 1986; SCP 1988; ESSE 1992) that volcanism is not a disqualifying condition for the Yucca Mountain site. The basis for that judgment is the low probability of disruption of the potential repository. The occurrence probability is sufficiently small that volcanism

scenarios have limited impact on studies of total system performance (Wilson et al. 1994). These performance studies are not final and more work will be done in future studies to examine the effects of subsurface disruption of a repository system. The median probability of disruption of a 6 km^2 repository area at Yucca Mountain using both homogeneous and nonhomogeneous Poisson recurrence models and the median estimate from disruption models is $2.3 \pm 0.8 \times 10^{-8}$ events yr^{-1}. The median estimate of the probability of magmatic disruption for models weighted by the likelihood of the occurrence of volcanic events in range interiors is $3.5 \pm 0.3 \times 10^{-9}$ events yr^{-1}. The mean probability of disruption from simulation modeling using a mean estimate of recurrence models and median estimates of disruption models is $1.7 \pm 0.5 \times 10^{-8}$ events yr^{-1} for intersection, and $2.5 \pm 0.8 \times 10^{-9}$ events yr^{-1} for intersection weighted by the likelihood of volcanic events in range interiors. Finally, the median probability of disruption of the repository is $1.8 \pm 3.2 \times 10^{-8}$ events yr^{-1} for intersection models and $2.7 \pm 4.7 \times 10^{-9}$ events yr^{-1} events yr^{-1} for range intersection models for estimates where E1 is adjusted for individual spatial and structural models. Two worse case estimates for the E1 are identified from the adjusted probability matrix, and are 7.5 to 4.0×10^{-8} events yr^{-1}. These estimates correspond to cluster models of volcanic events in Crater Flat (Pliocene and Quaternary) and the models have a low likelihood of resulting in disruption of the potential repository. They are probably not geologically viable models but are identified from the simulation modeling is worse cases.

The probability estimates exceed 10^{-8} events yr^{-1} for the controlled area and the YMR. Therefore, studies will be conducted of the effects of eruptive and intrusive activity near the potential repository site. The probability of disruption of the potential repository approaches or is less than 10^{-8} events yr^{-1} if the probability is weighted for the reduced likelihood of event occurrence in range interiors. However, studies will probably still be required of the effects of magmatic disruption of the repository for several reasons. First, the criterion identifying an occurrence probability of 10^{-8} events yr^{-1} as a critical value for probability studies is currently being reviewed. Second, it is unclear what percentile on a cumulative probability curve must be less than 10^{-8} events yr^{-1}. Is it a 50 % value or some other value? The standards for judging the significance of probability estimations are ambiguous and difficult to apply. We have emphasized mean or median estimates from the simulation modeling. However, until the standards are revised and clarified with respect to critical values of occurrence probabilities, it is very difficult to make judgments concerning the significance of probability estimates. Accordingly, we continue to assess nearly all scenarios in studies of E3.

The range of estimates of the probability of magmatic disruption for this report is nearly identical to estimates of the probability of magmatic disruption of the repository by Crowe et al. (1982) Crowe 1986; Wallmann et al. 1993; Wallmann 1993; Connor and Hill 1993; Crowe et al. 1993). The only published calculations with different probability estimates are those by Ho (1992). However, Ho's calculations cannot easily be compared with other calculations (see discussion of Chapter 6). He used recurrence rates for the YMR and applied them to an area of 75 km^2 (less than the size of the controlled area) and did not examine the variability in E1 required by assumptions used to estimate E2. The calculations of Ho (1992) are correct mathematically but are physically implausible. Justification for his worst case model would require evidence that future volcanic events, defined as the recurrence rate of formation of a new volcanic center in the YMR, could occur only in the identified 75 km^2 area. Existing data provides no obvious support for that model.

The framework calculations for probability studies are now well developed. It will be relatively easy to reassess probability estimates as new results change assumptions for models of E1 or E2. The cumulative probability distributions for the probability of magmatic disruption can be readily modified using the systematic procedures of risk simulation. Three observations and conclusions can be made using insight gained from risk simulations. First, the recurrence rate of volcanic events (E1) is relatively well constrained in probability space. The range of probability estimates using alternative recurrence models is not large and the probability of magmatic disruption does not vary significantly with different models of E1. Pending major changes in interpretations of the volcanic record of the YMR, or in assumptions used

for probability estimations, further studies of recurrence rates are judged to be a low priority for future volcanism studies. Second, simulation modeling of E2, the disruption probability, shows that the cumulative distributions are sensitive to a small number of spatial and structural models. It is logical to focus future site characterization studies on assessments of the applicability of these models. A key area of sensitivity that may require further study is the northeast boundary of the pull-apart model of Fridrich et al. (1994). Third, we have made only limited attempts to assess the likelihood of acceptance of alternative models of E1 and E2. Logically, there is a ranking that could be developed for the alternative models, and this ranking could be applied in the risk simulations. Ranking of models is probably most important for E2 and of lesser importance for E1. Ranking of models is somewhat subjective, but could logically be implemented through application of formal procedures of expert judgment. Expert judgment assessments of E1, E2 and E2 given E1 were started in late calendar year 1995 during final completion of this volcanism status report.

Some insight into the magnitude of the probability of magmatic disruption of the potential repository in the YMR can be gained by examination of analog volcanic fields. Probabilistic assessments can be compared by estimating the probability of intersection of a 6-km^2 area placed randomly in the interior of the Lunar Crater and Cima volcanic fields. The area of the Lunar Crater volcanic field (Quaternary part of the field) is about 260 km^2. The probability of intersection of a 6-km^2 area located randomly in the field is about 0.023. There are 82 vents forming 28 clusters in the Lunar Crater volcanic field. Recurrence rates (homogeneous Poisson model) for the Lunar Crater volcanic field are about 4.5 x 10^{-5} to 1.1 x 10^{-5} events yr^{-1} (Crowe et al. 1992, 1993). The probability of magmatic disruption of a 6-km^2 area randomly located in the Lunar Crater volcanic field is 1.0 x 10^{-6} to 2.5 x 10^{-7} events yr^{-1}. The area of the Quaternary part of the Cima volcanic field is about 160 km^2. The probability of intersection of a 6 km^2 area located randomly in the field is about .037. There are 28 volcanic centers forming 22 volcanic clusters in the Cima volcanic field. The recurrence rate of volcanic events (homogeneous Poisson model) in the Cima volcanic field is about 1.4 to 1.1 x 10^{-5} events yr^{-1}. The probability of disruption of a 6-km^2 area in the Cima volcanic field is about 4 to 5 x 10^{-7} events yr^{-1}. These probability estimates (4 x 10^{-7} to 1 x 10^{-6} events yr^{-1}) represent an upper bound to the disruption probability that is useful to compare with the probabilistic assessments for the YMR region. The probability of repository disruption in large and active basaltic volcanic fields is relatively low (<1 in one million per year) for two reasons. First, volcanic events even in large and active volcanic fields are infrequent. The recurrence times between volcanic events for very active basaltic volcanic fields are relatively long (20,000 to 90,000 yr) compared to the 10,000-yr isolation period of radioactive waste. Second, a volcanic event must occur in or near a potential repository to result in immediate release of radioactive waste. The Lunar Crater field has more than an order of magnitude greater number of Quaternary volcanic events than the YMR. The Cima volcanic field has more Quaternary events than the YMR by a factor of four. The potential repository site in Yucca Mountain is not located inside most spatial and structural zones. The structural models that include the potential site have a very low cone density per square kilometer. Both the disruption ratio and the probability of magmatic disruption must be less in the YMR than in the Lunar Crater and Cima volcanic fields. By comparison with analog volcanic fields, simple logic requires that the probability of magmatic disruption of the Yucca Mountain site must be less than about 5 x 10^{-7} events yr^{-1}. This limit could be inferred *without extensive* site characterization studies and its sensitivity for siting of a potential repository is dependent on the sensitivity of cumulative release models for the repository system (see for example, Wilson et al. 1994).

Finally, the probability tables and cumulative probability distributions for E1, E2, and Pr(E2 given E1)Pr(E1) are not necessarily the data that will be used in regulatory documents. They are the best estimates using site characterization data current to the completion of this report. The DOE may or may not choose to modify the probability estimates and the cumulative probability distributions in formal documents that respond to regulatory requirements for assessment of sites for geologic isolation of high-level radioactive waste.

V. References

Bacon C. R., "Time-Predictable Bimodal Volcanism in the Coso Range, California," *Geology* **10**, 65-69 (1982).

Bergman, S. C. "Petrogenetic Aspects of Alkali Basaltic Lavas and Included Megacrysts and Nodules from the Lunar Crater Volcanic Field, Nevada, USA," PhD. Dissertion, Princeton University, 432 pp. (1982).

Bradshaw, T.K., and E.I. Smith, "Polygenetic Quaternary Volcanism at Crater Flat, Nevada," Journal Volcanology and Geothermal Research **63**, 165-182 (1994).

Bruce, P. M., and H. E. Huppert, "Solidification and Melting Along Dykes by the Laminar Flow of Basaltic Magma," M. P. Ryan Ed., in *Magma Transport and Storage*, (John Wiley & Sons, New York, New York, 1990) 88-101pp.

Carr, W. J., "Regional Structural Setting of Yucca Mountain, Southwestern Nevada, and Late Cenozoic Rates of Tectonic Activity in Part of the Southwestern Great Basin, Nevada and California," U.S. Geological Survey Open-File Report 84-854, 109 pp. (1984).

Carr, W. J., "Styles Of Extension In The Nevada Test Site Region, Southern Walker Lane Belt; An Integration Of Volcano-Tectonic And Detachment Fault Models," in *Geological Society America Memoir 176: Basin and Range Extensional Tectonics near the Latitude of Las Vegas, Nevada,* B. P. Wernicke, Ed. (Geological Society America, Boulder, Colorado, 1990), pp. 283-303.

Champion, D. E., "Volcanic Episodes Near Yucca Mountain as Determined by Paleomagnetic Studies at Lathrop Wells, Crater Flat, and Sleeping Butte, Nevada," in *Proceedings High-Level Radioactive Waste Management Conference, Las Vegas, Nevada, (*American Nuclear Society, La Grange Park Illinois, 1991) pp. 61-67.

Champion, D. E., "Oral Presentation to the United States Nuclear Waste Technical Review Board," Panel on Structural Geology and Geoengineering, Meeting on Volcanism, Las Vegas, Nevada (September 14, 1992).

Clemen, R.T., *Making Hard Decisions,* (PWS-Kent Publishing Company, Boston, Massachusetts, 1991) 557pp.

Connor C. B., "Cinder Cone Clustering in the TransMexican Volcanic Belt Implications for Structural and Petrologic Models," *Journal Geophysical Research* **95**, 19,395-19,405 (1990).

Connor C. B., and B. E. Hill, "Estimating the Probability of Volcanic Disruption of the Candidate Yucca Mountain Repository Using Spatially and Temporally Non Homogeneous Poisson Models," in *Proceedings Site Characterization and Model Validation Focus'93 Symposium Volume* (American Nuclear Society, La Grange Park, Illinois, 1993)

Cressie, N. A. C., *Statistics for Spatial Data,* (John Wiley & Sons, New York, New York, 1991) 900 pp.

Crowe, B. M., "Volcanic Hazard Assessment for Disposal of High-level Radioactive Waste," in *Recent Tectonics: Impact on Society,* (National Academy Press, Washington, D.C., 1986) Chap. 16, pp. 247-260.

Crowe, B. M., "Basaltic Volcanic Episodes of the Yucca Mountain region," in *Proceedings High-Level Radioactive Waste Management Conference, Las Vegas, Nevada (*American Nuclear Society, La Grange Park Illinois 1990), pp. 65-73.

Crowe, B. M., and W. J. Carr, "Preliminary Assessment of the Risk of Volcanism at a Proposed Nuclear Waste Repository in the Southern Great Basin," U.S. Geological Survey Open-File Report 80-375, 15 p. (1980).

Crowe, B. M., M. E. Johnson, and R. J. Beckman, "Calculation of the Probability of Volcanic Disruption of a High-Level Radioactive Waste Repository Within Southern Nevada, USA," *Radioactive Waste Management* **3**, 167-190 (1982).

Crowe B. M., D. T. Vaniman, and W. J. Carr, "Status of Volcanic Hazard Studies for the Nevada Nuclear Waste Storage Investigations," Los Alamos National Laboratory report LA-9325-MS 47 p. (1983a).

Crowe, B. M., S. Self, D. Vaniman, R. Amos, and F. Perry, "Aspects of Potential Magmatic Disruption of a High-Level Radioactive Waste Repository in Southern Nevada," *Journal Geology* **91**, 259-276 (1983b).

Crowe, B. M., K. H. Wohletz, D. T. Vaniman, E. Gladney, and N. Bower, "Status of Volcanic Hazard Studies for the Nevada Nuclear Waste Storage Investigations," Los Alamos National Laboratory Report LA-9325-MS, Vol. II 101 p. (1986).

Crowe, B., C. Harrington, L. McFadden, F. Perry, S. Wells, B. Turrin, and D. Champion, "Preliminary Geologic Map of the Lathrop Wells Volcanic Center," Los Alamos National Laboratory Report LA-UR-88-4155 (1988).

Crowe, B. M., and F. V. Perry, "Volcanic Probability Calculations for the Yucca Mountain site: Estimation of Volcanic Rates," in *Proceedings Nuclear Waste Isolation in the Unsaturated Zone, Focus '89,* (American Nuclear Society, La Grange Park, Illinois, 1989) pp. 326-334.

Crowe, B. M., B. Turrin, S. Wells, F. Perry, L. McFadden, C. Renault, D. Champion, and C. Harrington, "Volcanic Hazard Studies for the Yucca Mountain Project," *Waste Management '89* **1**, 485-492 (1989).

Crowe, B. M., R. Picard, G. Valentine, and F. V. Perry, "Recurrence Models of Volcanic Events: Applications to Volcanic Risk Assessment," in *Proceedings High-Level Radioactive Waste Management Conference, Las Vegas, Nevada* (American Nuclear Society, La Grange Park, Illinois, 1992) **2**, pp. 2344-2355.

Crowe, B. M., and F. V. Perry, "Preliminary Geologic Map of the Sleeping Butte Volcanic Centers," Los Alamos National Laboratory Report LA-12101-MS, 11 pp. (1991).

Crowe, B.M. F.V. Perry, G.A. Valentine, P.C. Wallmann and R. Kossik, "Simulation Modeling of the Probability of Magmatic Disruption of the Potential Repository Yucca Mountain Site," in *Proceedings Site Characterization and Model Validation Focus'93 Symposium Volume* (American Nuclear Society, La Grange Park, Illinois, 1993), pp. 182-191.

Davis, J. C., *Statistics and Data Analysis in Geology*, (John Wiley & Sons, New York, New York, 1986), 646pp.

De la Cruz-Reyna, S. "Poisson Disrtibuted Patterns of Explosive Eruptive Activity," Bulletin Volcanology **54**, 57-67 (1991).

Delaney, P. T., "Heat Transfer During Emplacement and Cooling of Mafic Dykes," in H. C. Hall, and W. F. Fahrig (Eds.), *Mafic Dike Swarms*, Geological Association Canada Special Paper **34**, 31-46 (1987).

Delaney P. T., and D. D. Pollard, "Solidification of Basaltic Magma During Flow in a Dike," *America Journal Science* **242**, 856-887 (1982).

Devore, J. L. *Probability and Statistics for Engineering and the Sciences*, (Brooks/Cole Publishing Company, Monterey, California, 1987) 672pp.

DOE (U.S. Department of Energy), "Environmental Assessment: Yucca Mountain Site, Nevada Research and Development Area, Nevada," DOE/RW-0073, Office of Civilian Radioactive Waste Management, Washington D.C. (1986).

DOE (U.S. Department of Energy), "Site Characterization Plan, Yucca Mountain Site, Nevada Research and Development Area, Nevada," DOE/RW-0199, Office of Civilian Radioactive Waste Management, Washington D.C. (1988).

Dohrenwend, J. C., L. D. McFadden, B. D. Turrin, and S. G. Wells, "K-Ar dating of the Cima Volcanic Field, Eastern Mojave Desert, California: Late Cenozoic Volcanic History and Landscape Evolution," *Geology* **12**, 163-167 (1984).

Dohrenwend, J. C., S. G. Wells, and B. D. Turrin, "Degradation of Quaternary Cinder Cones in the Cima Volcanic Field, Mojave, Desert, California," *Geological Society America Bulletin* **97**, 421-427 (1986).

Evans, M., N. Hastings, and B. Peacock, *Statistical Distributions,* (John Wiley & Sons, New York, New York, 1993) 170 p.

Foland, K. A., and S. C. Bergman, "Temporal and Spatial Distribution of Basaltic Volcanism in the Pancake and Reveille Ranges North of Yucca Mountain," in *Proceedings, High Level Radioactive Waste Management, Las Vegas, Nevada* (American Nuclear Society, La Grange Park, Illinois, 1992) **2**, pp. 2366-2371.

Fridrich, C. and J. Price, "Tectonic framework of Crater Flat Basin, Adjacent to Yucca Mountain Nevada: A Preliminary Report," *Abstract Geological Society America* **23**, 189 (1992).

Fridrich C. J., B. M. Crowe, M. R. Hudson, V. E. Langenheim, and G. A. Thompson, "Structural Control of Basaltic Volcanism in a Region of Oblique Extension, Southwest Nevada Volcanic Field," *EOS Transactions, American Geophysical Union 1994 Fall Meeting* **75** (44), 603 (1994).

Frizzel, V. A., and J. Shulters, "Geologic Map of the Nevada Test Site," U.S. Geol. Surv., Misc. Invest. Series, Map I-2046 (1990).

Harris, A. G., J. E. Repetski, J. L. Clayton, J. A. Grow, M. D. Carr, and T. A. Davis, "Results from 1991 Wildcat Wells near Yucca Mountain, Nevada," *Geological Society America Abstracts with Programs*, **24**, 17 (1992).

Hasenaka, T., and I. S. E. Carmichael, "The Cinder Cones of Michoacan-Guanajuato, Central Mexico: Their Age, Volume, Distribution, and Magma Discharge Rate, *Journal Volcanology Geothermal Research* **25**, 105-124 (1985).

Ho, C. H., E. I. Smith, D. L. Feurbach, and T. R. Naumann, "Eruptive Probability Calculation for the Yucca Mountain Site, USA: Statistical Estimation of Recurrence Rates," *Bulletin Volcanology* **54**, 50-56 (1991).

Ho, C. H., "Time Trend Analysis of Basaltic Volcanism for the Yucca Mountain site," *Journal Volcanology Geothermal Research* **46**, 61-72 (1991).

Ho, C. H., "Risk Assessment for the Yucca Mountain High-Level Nuclear Repository Site: Estimation of Volcanic Disruption," *Mathematical Geology* **24**, 347-364 (1992).

Kane, M. F., and R. E. Bracken, "Aeromagnetic Map of Yucca Mountain and Surrounding Regions, Southwest Nevada," U.S. Geol. Survey, Open-File Report 83-616, 19 pp. (1983).

Katz, M., and A. Boettcher, "The Cima Volcanic Field," in Fiefe, D. L., and A. R. Brown (Eds.), *Geology and Mineral Wealth of the California Desert,* Santa Ana, California South Coast Geologic Society, 236-241 (1980).

King, C. Y., "Volume Predictability of Historical Eruptions at Kilauea and Mauna Loa Volcanoes," *Journal Volcanology Geothermal Research* **38**, 281-285 (1989).

Kuntz, M. A., D. E. Champion, E. C. Spiker, R. H. Lefebure, "Contrasting Magma Types and Steady-State, Volume-Predictable Basaltic Volcanism Along the Great Rift, Idaho," *Geological Society America* **97**, 579-594 (1986).

Langenheim, V. E., S. F. Carle, D. A. Ponce, and J. D. Philips, "Revision of an Aeromagnetic Survey of the Lathrop Wells Area, Nevada," U.S. Geol. Survey, Open-File Report 91-46, 17 pp. (1991).

Lister, J. R., and R. C. Kerr, "Fluid-Mechanical Models of Crack Propagation and Their Application to Magma Transport in Dykes," *Journal Geophysical Research* **96**, 10,049-10,077 (1991).

Megil, R.E., *An Introduction to Risk Analysis,* (PennWell Books, Tulsa, Oklahoma, 1984) 274pp.

Meyer, M. A., and J.M. Booker, *Eliciting and Analyzing Expert Judgement A Practical Guide*, (Academic Press, London, 1991) 452pp.

Minor, S. A., D. A. Sawyer, R. R. Wahl, V. A. Frizzel Jr., S. P. Schilling, R. G. Warren, P. P. Orkild, F. A. Coe, M. R. Hudson, R. J. Fleck M. A. Lanphere, W. C. Swadley, and J. C. Cole, "Preliminary Geologic Map of the Pahute Mesa 30' X 40' Quadrangle, Nevada," U. S. Geological Survey Open-File Report 93-299, (1993).

Nauman, T. R., D. L. Feuerbach, and E. I. Smith, "Structural Control of Pliocene volcanism in the Vicinity of the Nevada Test Site, Nevada: An Example from Buckboard Mesa," *Abstract Geological Society America* **23** (2) 82 (1991).

Newendorp, P.D. *Decision Analysis for Petroleum Exploration*, (PennWell Books, Tulsa, Oklahona, 1974) 668 pp.

Olkin, I., L.J. Gleser, and C. Derman, *Probability Models and Applications*, (McMillan College Publishing Company, New York, New York, 1994) 715 p.

Perry, F. V., and B. M. Crowe, "Geochemical Evidence for Waning Magmatism and Polygenetic Volcanism at Crater Flat, Nevada," in *Proceedings High-Level Radioactive Waste Management Conference, Las Vegas, Nevada* (American Nuclear Society, La Grange Park Illinois, 1992) **2**, pp. 2344-2355.

Peterson, D. W., "Volcanoes: Tectonic Setting and Impact on Society," in *Active Tectonics, Impact on Society,* (National Academy Press, Washington D.C., 1986) Chap. 15, 231-245.

Scandone R., G. Arganese G., F. Galdi, "The Evaluation of Volcanic Risk in the Vesuvian Area," *Journal Volcanoloogy Geothermal Research* **58,** 263-271 (1993).

Schweickert, R. A., "Evidence for a Concealed Dextral Strike-Slip Fault Beneath Crater Flat, Nevada," *Geological Society America Abstracts with Programs*, A90 (1989).

Scott, D. H., and N. J. Trask, "Geology of the Lunar Crater Volcanic Field, Nye County, Nevada," U.S. Geological Survey Professional Paper 599-I, 36 pp. (1971).

Settle, M., "The Structure and Emplacement of Cinder Cone Fields," *America Journal Science* **279**, 1089-1107 (1980).

Sharaf, M.A., D.L. Illman, and B.R. Kowalski *Chemometrics*, (John Wiley & Sons, New York, New York, 1986) 332 pp.

Shaw, H., "The Fracture Mechanisms of Magma Transport from the Mantle to the Surface," in *Physics of Magmatic Transport*, R. B. Hargraves, Ed., (Princeton University Press, Princeton, New Jersey, 1980) p. 201-264.

Shaw, H. R., "Uniqueness of Volcanic Systems," U.S. Geological Survey Professional Paper 1350, p. 1357-1394 (1987).

Sheridan, M. F. "A Monte Carlo Technique to Estimate the Probability of Volcanic Dikes,"in *Proceedings High-Level Radioactive Waste Management Conference, Las Vegas, Nevada (*American Nuclear Society, La Grange Park, Illinois, 1992) **2**, 2033-2038.

Sinnock, S. and R. G. Easterling, "Empirically Determined Uncertainty in Potassium-Argon Ages for Plio-Pleistocene Basalts from Crater Flat, Nye County, Nevada," Sandia National Laboratories, SAND82-2441, 17 pp. (1982).

Smith, E. I., D. L. Feuerbach, T. R. Naumann, and J. E. Faulds, "The Area of Most Recent Volcanism Rear Yucca Mountain, Nevada: Implications for Volcanic Risk Assessment," in *Proceedings High- Level Radioactive Waste Management Conference, Las Vegas, Nevada (*American Nuclear Society, La Grange Park, Illinois, 1990) **1**, 81-90.

Smith, R. L., and R. G. Luedke, "Potentially Active Volcanic Lineaments and Loci in Western Conterminous United States," in *Explosive Volcanism: Inception, Evolution and Hazards,* (National Academy Press, Washington DC, 1984) p. 47-66.

Stilettos, L. and P. Moot, "A Statistical and Probabilistic Study of the Historic Activity of Piton de la Furnace, Reunion Island, Indian Ocean," *Journal Volcanology Geothermal Research* **36**, 67-86 (1987).

Tuckwell H. C., *Elementary Applications of Probability Theory* (Champion and Hall, New York, New York, 1988), 255 p.

Turrin, B. D., D. Champion, and R. J. Fleck, "$^{40}Ar/^{39}Ar$ Age of the Lathrop Wells Volcanic Center, Yucca Mountain, Nevada," *Science* **253**, 654-657 (1991).

Turrin, B. D., D. E. Champion, and R. J. Fleck, "Measuring the Age of the Lathrop Wells Volcanic Center at Yucca Mountain," *Science* **257**, 556-558 (1992).

Turrin, B. C. Oral Presentation to the United States Nuclear Waste Technical Review Board, Panel on Structural Geology and Geoengineering, Meeting on Volcanism, Las Vegas, Nevada (September 15, 1992) pp. 222-273.

Valentine, G. A., B. M. Crowe, and F. V. Perry, "Physical Processes and Effects of Magmatism in the Yucca Mountain Region," in *Proceedings High- Level Radioactive Waste Management Conference, Las Vegas, Nevada* (American Nuclear Society, La Grange Park, Illinois, 1992) **3**, pp. 2344-2355.

Vaniman, D. T., and B. M. Crowe, "Geology and Petrology of the Basalts of Crater Flat: Applications to Volcanic Risk Assessment for the Nevada Nuclear Waste Storage Investigations," Los Alamos National Laboratory Report LA-8845-MS, 67 pp. (1981).

Vaniman, D. T., B. M. Crowe and E. S. Gladney, "Petrology and Geochemistry of Hawaiite Lavas From Crater Flat, Nevada," *Contributions Mineralogy Petrology* **80**, 341-357 (1982).

Wadge G., "Steady State Volcanism: Evidence from Eruption Histories of Polygenetic Volcanoes," *Journal Geophysical Research* **87**, 4035-4039 (1982).

Wallmann, P. C. I. Miller, and R. Kossik, "Assessment of Volcanic and Tectonic Hazards to High Level Radioactive Waste Repositories," in *Proceedings High- Level Radioactive Waste Management Conference, Las Vegas, Nevada* (American Nuclear Society, La Grange Park, Illinois, 1993) **4**, pp. 188-195.

Wallmann P. C., "A Technique for Calculation of the Probability of Dikes Intersecting a Repository," in *Proceedings Site Characterization and Model Validation Focus'93 Symposium Volume* (American Nuclear Society, La Grange Park, Illinois, 1993), pp. 192-199.

Walpole, R. E., and R. H. Myers, *Probability and Statistics for Engineers and Scientists,* (Macmillan Publishing Company, New York, New York, 1993) 479 pp.

Wells, S. G., L. D. McFadden, C. E. Renault, B. D. Turrin, and B. M. Crowe, "A Geomorphic Assessment of Quaternary Volcanism in the Yucca Mountain area, Nevada Test Site, Southern Nevada: Implications for the Proposed High-level Radioactive Waste Repository," *Geology* **18**, 549-553 (1990).

Wells, S. G., B. M. Crowe, and L. D. McFadden, "Measuring the Age of the Lathrop Wells Volcanic Center at Yucca Mountain," *Science* **257**, 555-558 (1992).

Whitney, J. W., and R. R. Shroba, "Comment and Reply on Geomorphic Assessment of late Quaternary Volcanism in the Yucca Mountain Area, Southern Nevada: Implications for the Proposed High-Level Radioactive Waste Repository," *Geology* **19** 661-662 (1991).

Wilshire, H. G., McGuire, A. V., Noller, J. S., and B. D. Turrin, "Petrology of Lower Crustal and Upper Mantle Xenoliths from the Cima volcanic Field, California, *Journal Petrology* **32** 169-200 (1991).

Wilson, L. and J. W. Head, "Ascent and Eruption of Basaltic Magma on the Earth and Moon," *Journal Geophysical Research* **86**, 2971-3001 (1981).

Wilson, M.L, .J. H. Gauthier, R. W. Banard, G. E. Barr, H. A. Dockery, E. Dunn, R. R. Eaton, D.C. Guerin, N.Lu, M. J. Martinez, R. Nilson, C. A.Rautman, T. H. Robey, B. Ross, E. E. Ryder, A. R. Schenker, S. A. Shannon, L. H. Skinner, W. G. Halsey, J. D. Halsey, J. D. Gansemer, L. C. Lewis, A. D.Loamont, I. R.Triay, A. Meijer, and D. E. Morris, 1994, Total-System Performance Assessment For Yucca Mountain -- SNL Second Iteration (TSPA-1993), Sandia Report Sand 93-2675.

Wood, C. A., and J. Kienle, *Volcanoes of North America*, (Cambridge University Press, Cambridge, MA, 1990) 384pp.

Wright, L. A., "Overview of the Role of Strike-Slip and Normal Faulting in the Neogene History of the Region Northeast of Death Valley, California-Nevada, "Nevada Bureau of Mines Open-File Report 89-1, (1987).

Younker, J. L., W. B., Andrews, G. A. Fasano, C. C. Herrington, S. R. Mattson, R. C. Murray, L. B. Ballou, M. A. Revelli, L. E. Shephard, W. W. Dudley, D. T. Hoxie, R. J. Herbst, E. A. Patera, B. R. Judd, J. A. Docka, and L. D. Rickertsen, "Report of the Early Site Suitability Evaluation of the Potential Repository Site at Yucca Mountain, Nevada," Science Applications International Corporation Report SAIC-91/8000 (1992).

CHAPTER 8: STATUS AND IMPLICATIONS OF FUTURE STUDIES

I. Introduction

Chapter 8 of the volcanism status report describes from three perspectives the status of information used for probabilistic volcanic risk assessment. First, remaining information requiring resolution is discussed by topic. Second, expectations of how new information may affect the assessment of probabilistic volcanic risk assessment for the Yucca Mountain site are discussed. Third, areas of controversy in volcanism studies are described and their potential effects considered on the application of results of volcanism studies to the Yucca Mountain site. This section of the volcanism status report is organized after the activity structure of volcanism study plans: 8.3.1.8.1.1, Probability of Magmatic Disruption of the Repository, and 8.3.1.8.5.1 Characterization of Volcanic Features. The activities of study plan 8.3.1.8.5.1, are described first because it is the data gathering part of the volcanism studies. A major part of continuing volcanism studies are for Study Plan 8.3.1.8.1.2, Physical Processes of Magmatism and the Effects on the Potential Repository. These studies are not described in the volcanism status report. Finally, this section is written in abbreviated form because substantial discussions of individual topics are included in other sections of the status report.

II. Study Plan 8.3.1.8.5.1, Characterization of Volcanic Features

A. Activity 8.3.1.8.1.1.1, Volcanism Drill holes

Three identified aeromagnetic anomalies in the YMR that may represent buried volcanic centers or intrusions remain to be explored by drilling. If the aeromagnetic anomalies are produced by buried centers or intrusions, determinations of their age and geochemistry is required to complete characterization of volcanism in the YMR. Two of the anomalies are in the Amargosa Valley. These anomalies are located in areas where rates of alluvial sedimentation are expected to be lower than the drilled anomaly site south of the town of Amargosa Valley. The latter site is a probable buried basalt center dated at 3.8 million years. Therefore, by comparison, the undrilled anomaly sites in the Amargosa Valley, if they are buried volcanic centers, are probably ≥3.8 Ma. In this case, the centers would have little effect on the recurrence rate of volcanic events using magma-output rates. They can have no more than about a 20% increase in the recurrence rate using homogeneous and nonhomogeneous Poisson models simply from an increase in the number of volcanic events used for the minimum, maximum, and most likely event counts. However, the alternative Pliocene and Quaternary models for the recurrence rate tables used in Chapter 7 include volcanic events assigned to the undrilled anomaly sites in Amargosa Valley. The anomalies were assumed to be 3.8 Ma. Cuttings from a water well drilled in the Amargosa Valley were described as basaltic debris and may be from one of the undrilled anomaly sites. We will attempt to determine if reliable samples of these cutting can be obtained. The anomaly site in southern Crater Flat is unusual because it is a positive anomaly. All of the surface basaltic volcanic centers in Crater Flat exhibit reversed magnetic polarity. However, the anomaly, if it is a buried basalt center, it is expected to be >3.7 Ma because 3.7-Ma centers are exposed at the surface of Crater Flat. If the positive anomaly is a Pliocene or older basalt, it would *not* have a significant effect on the probability estimations of Chapter 7 other than a minor increase in event counts. The ages of the undrilled anomalies could also affect the β value of probability estimates for nonhomogeneous Poisson distribution models. The magnitude of the effect cannot be predicted until the ages are known. However, if the anomalies are produced by buried basalt centers of Pliocene age, they principal effect will be to *decrease* the β values.

A remaining unknown for this activity is whether any of the anomaly sites could be basaltic intrusions. To date, none of the anomalies drilled with continuous coring (VH-1 and VH-2) have been shown to be intrusions. The drilling record (cuttings, not core) of the one drilled anomaly site in Amargosa Valley does not allow for assessment of intrusive versus extrusive origin. However, because the anomaly is produced by a basalt that is 3.8 Ma, the event has limited significance on volcanic risk assessment even if it is an intrusion.

Finally, the issue of recurrence of silicic volcanism will be reexamined if any drilled anomalies are produced by silicic volcanic rocks that are of Pliocene or Quaternary age. This possibility appears unlikely because of the absence of post-8-Ma silicic volcanism in the region and the small size of the undrilled anomalies.

B. Activity 8.3.1.8.5.1.2, Geochronology Studies

There are three remaining goals of continuing geochronology studies. The first is to establish the age of the basaltic volcanic centers of the Yucca Mountain region (YMR) with an acceptable degree of confidence. Second, additional geochronology data will be acquired to continue to test monogenetic versus polygenetic eruption models for the volcanic centers. Resolution of the different eruption models is not critical, however, because both models have been and will continue to be considered in Study Plans 8.3.1.8.1.1, Probability of Magmatic Disruption of the Repository and 8.3.1.8.1.2, Physical Processes of Magmatism and Effects on the Potential Repository. Probabilistic volcanic risk assessment would be simplified considerably, however, for both geochronology and consequences studies if we discover new data that disproves the polygenetic model. The third goal is to ensure that all geochronology data used for probabilistic volcanic risk assessment meets the Quality Assurance requirements of the Yucca Mountain Site Characterization Project (YMP), a requirement that has been met by all data gathered during the last six years. We next examine the status of geochronology information for individual centers of the Younger postcaldera basalt (YPB).

1. Basalt of Thirsty Mesa. Duplicate samples of basalt lava flows collected from the basal and upper parts of the basalt of Thirsty Mesa were submitted for K-Ar age determinations using the $^{40}Ar/^{39}Ar$ method. These samples yielded ages of 4.68 and 4.88 Ma, and the age determinations meet the Quality Assurance requirements of the YMP. The ages are in close agreement with unpublished age determinations by the U.S. Geological Survey. Existing ages are judged to be sufficient to meet data requirements for this center.

2. Basalt of Amargosa Valley (aeromagnetic anomaly). Samples of cuttings were collected from the exploratory drill hole that penetrated the aeromagnetic anomaly. These samples were submitted for K-Ar age determinations and yielded an $^{40}Ar/^{39}Ar$ age of 3.85 Ma. This age determination meets the Quality Assurance requirements of the YMP. An age of 4.4 Ma has been obtained for basalt cuttings from this anomaly by workers with the U.S. Geological Survey (outside the YMP). The reason for the discrepancy in the age is currently unknown and may require obtaining a duplicate age determination. The drilling of the aeromagnetic anomaly was completed by an independent company and does not meet the Quality Assurance requirements of the YMP. However, the basalt center is Pliocene in age and has limited affect on risk assessment studies. No additional geochronology work is required for this center unless we decide it is important to resolve the discrepancy between existing ages. Currently this is not assigned a high priority. Dating of the other aeromagnetic anomalies in the YMR is dependent on the volcanism drilling schedule.

3. Basalt of Southeast Crater Flat (3.7 Ma). Reproducible whole-rock, K-Ar age determinations of about 3.7 Ma have been obtained by a variety of workers at multiple analytical laboratories for the basalt

of southeast Crater Flat. The majority of data either do not meet current Quality Assurance requirements or were collected before full implementation of the current Quality Assurance program. Four new $^{40}Ar/^{39}Ar$ age determinations were obtained for this basalt center to cross-check earlier data, and are consistent with all existing nonqualified age determinations. Additionally, K-Ar age determinations of about 3.7 Ma have been obtained for the basalt of southeast Crater Flat by the State of Nevada under their approved Quality Assurance program. Both sets of new age determinations are consistent and meet the Quality Assurance requirements of the YMP. The chronology of these basalt centers is judged to have been established with sufficient confidence.

4. Basalt of Buckboard Mesa. All recognized geologic units at the basalt of Buckboard Mesa have been dated by the K-Ar method by a number of workers at independent laboratories. Results of this work are both reproducible and consistent. However, none of the age determinations either meet or were completed under a fully certified, Quality Assurance program. We have submitted samples from the basalt of Buckboard Mesa for $^{40}Ar/^{39}Ar$ age determinations under the current program controls to test and verify past data. The results of these age determination are expected in early calendar year 1995. If the new geochronology results are in agreement with past studies, we will consider the data to be sufficient to meet the geochronology data requirements for this basalt center.

5. Quaternary Basalt of Crater Flat. The Quaternary basalt centers of Crater Flat have yielded largely consistent age determinations using both the K-Ar and $^{40}Ar/^{39}Ar$ methods. These ages were obtained at independent K-Ar laboratories but are not qualified under the current Quality Assurance program. Recent results using the $^{40}Ar/^{39}Ar$ method have been obtained for basalt samples from the Black Cone and Little Cones centers and these data meet the Quality Assurance requirements of the YMP. Additional samples from Red Cone, Makani cone, and Little Cones have been submitted for age determinations and results are expected in calendar year 1995. The State of Nevada has reported ages for the Red Cone and Black Cone centers that were obtained under their Quality Assurance program. These data are consistent with all existing data except samples identified as statistical outliers (see Chapter 2 for a more complete discussion of the geochronology data for these centers). We will obtain several more sets of age determinations to complete the chronology of the Quaternary basalt of Crater Flat. The number of additional age determinations is dependent on the results of samples currently being analyzed. The identified data needs current to the completion of the volcanism status report are additional age determinations for the major lava flow groups of Red Cone, for the separate scoria cones and lava flows of Little Cones, and for independent cross-checking of current geochronology data for Makani center.

A current unresolved problem for the Quaternary basalt of Crater Flat is whether separate centers were formed by single or multiple pulses of magma. If they were formed by multiple, time-separate pulses of magma, there are insufficient data to resolve the ages of the magma pulses. The existing chronology data for the Quaternary basalt of Crater Flat are reproducible with an uncertainty of about $\pm$ 0.1 Ma (see Chapter 2). We infer from current data that if the basalt centers formed as multiple, time-separate eruptive events, the different events were formed in a span of <0.1 Ma. We do *not* anticipate being able to obtain chronology data that could resolve the ages of these events with a precision that would discriminate age differences of <0.1 Ma, but this is dependent on an evaluation of new geochronology data using the $^{40}Ar/^{39}Ar$ method. Generally, age assignments with a reproducibility of about 0.1 Ma are sufficient for probabilistic volcanic risk assessment for the YMR. We will continue to refine geochronology data to test for possible age differences between the individual centers of the Quaternary basalt of Crater Flat. New $^{40}Ar/^{39}Ar$ data obtained during the final stages of completion of the volcanism status raise the possibility that some, possibly all, units of the Little Cone center may be slightly less than 1.0 Ma. Geochemical data

published by the state of Nevada provide strong support for the inference that at least some of the eruptions of Red Cone and Black Cone were contemporaneous.

6. Basalt of Sleeping Butte. Potassium-Argon age determinations of the Sleeping Butte basaltic centers have yielded generally reproducible results consistent with preliminary information obtained on the soils and geomorphic features of the centers. However, the precision of most of the age determinations has been poor. New $^{40}Ar/^{39}Ar$ age determinations were obtained by researchers with the U.S. Geological Survey for work that is unrelated to the YMP. They obtained high precision ages of about 350 ka for both the Little Black Peak and Hidden Cones. We have submitted multiple samples from both of the centers for $^{40}Ar/^{39}Ar$ age determinations and these data should be available in calendar year 1995. If these data are consistent with existing data, most of the chronology studies will have been completed for the Sleeping Butte centers. Preliminary $^{40}Ar/^{39}Ar$ age determinations obtained during the final completion of the volcanism status report are consistent with existing $^{40}Ar/^{39}Ar$ age determinations and provide evidence of excess Ar in the analyzed samples. Uranium-Thorium disequilibrium age determinations using solid source mass spectrometry of the western lava flow from the Little Black Peak center should be completed in early 1995 and will be used to cross-check K-Ar data. However, results using the U-Th disequilibrium method at the Lathrop Wells center have been difficult to interpret, and similar problems with the method are possible for the Little Black Peak sample. Major- and trace-element geochemistry data obtained during the final stages of completion of this volcanism status report are consistent with field studies that show the Little Black Peak center is monogenetic. Additionally, the data indicate that all mapped units at the Hidden Cone center were probably formed in a single eruptive event, with the exception of the youngest event which has not yet tested with geochemical data. The only remaining geochronology problems for the Hidden Cone center are to test and attempt to constrain the age of the inferred youngest volcanic event and the stratigraphic relations, age, and geochemistry of the northwest lava flow lobe. The former will require trenching at the center to expose cross sections through the north flanks of the center. The trenching sites have been surveyed and the work will be completed when land access permits are processed. Samples of the inferred young scoria-fall event were collected and submitted for cosmogenic ^{3}He ages. We anticipate that data for these samples should be available in early calendar year 1995.

7. Lathrop Wells Volcanic Center. The results of field and geochemistry studies for the Lathrop Wells volcanic center have begun to converge. We have established with a fair degree of confidence (consistent field and geochemical data) that the center formed in four distinct eruptive or chronostratigraphic units. However, the ages of these units remain somewhat uncertain (see Chapter 2) despite application of multiple geochronology methods. We do not expect to be able to constrain the ages of the events at the center or discriminate individual events using convention K-Ar or the $^{40}Ar/^{39}$ methods. We have obtained new $^{40}Ar/^{39}Ar$ step-heating results on fragments of silicic tuff collected from multiple chronostratigraphic units, and for samples of multiple lava units. The results are too preliminary to present in the volcanism status report but do provide evidence supporting younger ages for the lava units than the data presented in Chapter 2. Further work is in progress. The U-Th disequilibrium method has yielded past results that were not completely consistent with field and stratigraphic data. However, new data obtained during the final stage of completion of this volcanism status report have revised considerably the U-Th ages. New isochron ages of about 50 ka were obtained from mineral phases with a much wider range of U/Th ratios for subunit Ql3. Moreover a U-Th isochron age of about 30 ka was obtained for groundmass phases from the main cone (subunit Qs3). These ages are consistent the with stratigraphic and geochemical data for the volcanic center, and the new $^{40}Ar/^{39}Ar$ step-heating results on fragments of silicic tuff. The U-Th disequilibrium ages will be assessed carefully and described further in future reports. The cosmogenic ^{3}He method has yielded the most consistent results for the Lathrop Wells center and we judge, pending further data evaluation, that we have an adequate data set. We do not anticipate further work using the cosmogenic ^{3}He method other than completion of samples that are being processed. We have collected

samples for additional thermoluminescence (TL) age determinations of the older chronostratigraphic units of the Lathrop Wells center and these samples are currently being analyzed by the U.S. Geological Survey. These samples will be used to test existing TL data and to evaluate geochronology data for samples collected from faults exposed in trenches around Yucca Mountain that contain layers of basalt or basalt tephra in fissures. Because of the developmental stages of many of the geochronology methods, we anticipate that geochronology data will continue to be difficult to interpret and as a result controversial. The data summarized in this volcanism status report may prove sufficient for probabilistic volcanic risk assessment. The primary goal of ongoing geochronology work is to continue to test each method for consistency and to further test monogenetic and polygenetic eruption models. We plan to complete a manuscript that summarizes the most current interpretations of the geochronology of the Lathrop Wells volcanic center in FY95.

C. Activity 8.3.1.8.5.1.3, Field Volcanism Studies

Field volcanism studies are nearly completed. Revised geologic mapping has been completed for the Lathrop Wells and Sleeping Butte volcanic centers. A revised geologic map of the Lathrop Wells center is being drafted for completion in calendar year 1995. Additionally, geologic field checking will be completed at the Hidden Cone center to evaluate a western lobe reported by investigators with the U.S. Geological Survey to be derived from the center. Revised geologic mapping has been completed for the Quaternary basalt of Crater Flat and will be combined with field studies of the centers by the State of Nevada. Final geologic mapping of the basalt of southeast Crater Flat will be completed in early calendar year 1995. Flow edges of buried lava of the basalt of southeast Crater Flat will be located using ground magnetic data and these data will be used to refine volume calculations for the volcanic unit. Final sampling and field work has been completed at the basalt of Thirsty Mesa and some of the data will be used to revise volume calculations. New field data show that thickness of the lava units of the basalt of Thirsty Mesa may have been overestimated in our calculations.

No major changes are anticipated in probabilistic volcanic risk assessment from the remaining field geologic studies. There may be minor changes in calculations of the volume of basalt units when data from the remaining geologic mapping is combined with computer-based volume calculations. We have attempted already to bound these changes by field estimations of the basaltic rocks buried by alluvium or removed by erosion. The volume predictable recurrence models have proven problematic (see Chapter 7), and these new results will probably only have a limited impact on the risk assessment studies.

D. Activity 8.3.1.8.5.1.4, Geochemistry Studies of Eruptive Sequences

Collection of samples for geochemistry studies has been largely completed for the Lathrop Wells and Sleeping Butte centers, the Quaternary basalt of Crater Flat, the basalt of southeast Crater Flat, the basalt of Buckboard Mesa, and the basalt of Thirsty Mesa. Additional geochemistry samples may be acquired from the Red Cone and Black Cone centers in Crater Flat. Additional sampling and analyses of the basaltic ash units in trenches excavated for the tectonics program will be required to attempt to identify the stratigraphic correlation of the ashes with chronostratigraphic units at the Lathrop Wells center. The first of these data were received during the final completion of this volcanism status report, and show that reproducible trace-element compositions can be obtained for these ashes. Some additional sampling and analyses of units exposed in the trenching studies of the Sleeping Butte center will be completed. Revised mapping of the basalt of Crater Flat may identify additional eruptive units that will require geochemical sampling and analysis.. Geochemical data from basalt for the remaining undrilled aeromagnetic anomalies will be needed to complete geochemical characterization for basalts of the YMR.

The primary goal of the geochemistry studies is to assess models for the generation and evolution of the basalt magmas that formed the Pliocene and Quaternary volcanic centers of the YMR and to test alternative eruption models. Magmatic models for each volcanic center will test whether geochemical variations observed at individual centers or between closely clustered centers are due to the generation and ascent of separate magma bodies or are due to the evolution of single magma bodies. Geochemical data for clustered volcanic centers will aid in possible discrimination of models of clustered (single pulse) versus individual magma pulses for the basalt of southeast Crater Flat, the Quaternary basalt of Crater Flat, and the basalt of Sleeping Butte. These data may allow discrimination of single versus multiple feeder dike models for these centers and will also be used to refine the minimum, maximum, and most likely event assignments for the recurrence tables of Chapter 7. Geochemical studies will be used to identify, through petrologic and geochemical analyses, the origin of basaltic ash exposed in multiple trenches near the Yucca Mountain site.

E. Activity 8.3.1.8.5.1.5, Evolutionary Cycles of Basaltic Volcanic Fields

This activity has just begun to be fully implemented in volcanism studies during completion of the volcanism status report. There are now sufficient data for the basalt units of Crater Flat to allow development of models of the evolution of the magma cycles of the Younger postcaldera basalt. A major and still tentative conclusion of these studies is that a variety of evidence indicates magmatic processes associated with the formation of the basalt magmas have waned since the late Miocene. A major area of future consideration for studies of this activity will be continued testing of possible models for the future patterns of basaltic volcanism in the YMR. These studies will focus primarily on the evolution of the volcanic centers of the Crater Flat volcanic zone (CFVZ) in order to examine both the variations in individual centers and the time-space-compositional patterns that could potentially impact risk assessment studies. Current models support the interpretation that magmatic processes have and may continue to decline. While this interpretation is supported by existing data, we continue to use probabilistic models based on steady state assumptions for volcanic risk assessment. We anticipate that testing of alternative evolutionary models of the CFVZ will be a major area of emphasis in future volcanism studies and a major use of this work will be in assessing whether a full range of possible alternative models have been used in evaluating recurrence rates (E1). Magmatic models for the evolution of the CFVZ will be closely integrated with the magma system dynamics studies of Study Plan 8.3.1.8.1.2 *Physical Processes of Magmatism and Effects on the Potential Repository,* in order to understand the magmatic evolution of the CFVZ from a combined physical and geochemical perspective.

III. Study Plan 8.3.1.8.1.1, Probability of Magmatic Disruption of the Repository

A. Activity 8.3.1.8.1.1.1, Age and Location of Volcanic Centers.

The activity involves collation of geochronology and field data for basaltic volcanic centers of the YMR. Potential changes in these data are described under the activities of Study Plan 8.3.1.8.5.1, Characterization of Volcanic Features. The activity will start in FY96 and use information obtained from other activities.

B. Activity 8.3.1.8.1.1.2, Evaluation of the Structural Controls of Sites of Basaltic Volcanism

The primary goal of this activity is to continue to develop and test alternative models for E2. These studies are iterative. That is, continued reevaluations will be undertaken of the models, their applications, and their effect on E2. This report implements the formal process outlined in Study Plan 8.3.1.8.1.1 to

systematically evaluate and refine the distribution of potential values for E2. Yearly updates are planned to incorporate the latest information from site characterization studies. We currently are assessing 17 structural models and 25 spatial models in assessments of E2. Stochastic modeling of dike distributions associated with the 42 alternative models will be undertaken for planned studies of E2 for the repository, controlled area, and the YMR.

An area of future development that will affect this activity is refinement of models of the structural setting of the YMR. This will be enhanced by revised field and geophysical studies of the structure of Crater Flat, Yucca Mountain, and the Amargosa Valley. We assume that the location of sites of Pliocene and Quaternary basaltic centers is reasonably well constrained. What could change through additional studies are the interpretations of how the distribution of centers can be related to the structural setting of the YMR. The mechanisms for accommodating these changes are continuing tectonic studies, yearly examinations of the alternative spatial and structural models, and yearly reassessments of the cumulative probability distributions for E2 using the framework of simulation modeling presented in Chapter 7.

Increased confidence that the distribution of values of E2 is acceptably bounded awaits more complete results of ongoing studies through the planned tectonic programs for the YMP and continued acquisition of local and regional geophysical data (see Chapter 3). Controversies concerning this activity are concerned with alternative structural models of the distribution of basalt centers. Multiple structural models are supported by reasonable interpretations of tectonic, geologic, and geophysical data. We anticipate that there may never be sufficient data to fully resolve the different structural interpretations. The controversy has been resolved and will continue to be resolved by incorporating multiple models in probabilistic calculations of E2.

C. Activity 8.3.1.8.1.1.3, Presence of Magma Bodies in the Site Vicinity

The primary goals of this activity are twofold. First, determinations must be made whether there is reasonable evidence that subsurface magma may be present beneath the YMR. Second, if magma is present, an evaluation must be conducted to assess whether the presence of magma could invalidate the use of the past record of volcanism to forecast future volcanic events for evaluations of volcanic risk.

There are two areas of controversy for this activity. First, interpretations of geophysical data using methods of teleseismic tomography support the possible existence of magma beneath parts of the Crater Flat and Amargosa Valley basins. Second, evaluations have been insufficient to date to establish whether the geophysical data available for this activity are adequately comprehensive to make reasonable assessments of the possible presence of magma bodies. Assessments of the impact of this controversy await resolution of these two questions. Currently, we regard the conclusions supporting the possible presence of subsurface magma to be inconclusive and judge that it does not invalidate the application of the probabilistic methods of risk assessment. This judgment is based on five lines of evidence. First, the spatial occurrence of the possible magma bodies is in an area that has been amagmatic during intense episodes of magmatism and extensional deformation in the Mesozoic and Cenozoic. There appears to be no compelling regional process that would lead to development of maintained magma bodies in this part of the crust. Second, there is a poor correlation between the geometry of the inferred magma body and sites of Quaternary volcanism. The inferred magma body is located mostly south of the sites of Quaternary volcanism. Third, there are a range of alternative interpretations of the anomaly, which *do not require the presence of magma bodies.* Fourth, if a magma body is present in the area south of Yucca Mountain, it may have existed for a long period of geologic time and thus require no revisions of projections of past patterns of basaltic volcanism. Fifth, no evidence of a magma body was noted in the seismic reflection line across the Amargosa Valley. To date, permissive but not compelling evidence has been obtained for the

existence of magma bodies beneath the YMR. Two sets of ongoing studies will provide additional information on the issue of the possible presence of magma bodies. First, the seismic refraction/reflection line across Crater Flat will test the existence of the proposed teleseismic anomalies. Second, the planned upgrade to the seismic net for the YMR will provide an opportunity to acquire higher resolution teleseismic data. Once the upgraded net is in operation for a period of time, the higher resolution teleseismic data will allow reassessment of the existence and origin of the low-velocity anomalies. The seismic line across Crater Flat was completed successfully during final revisions of the volcanism status report (late calendar year 1994).

The issue of the possible presence of magma in the crust beneath the region is regarded as a potentially important issue. If evidence is obtained that invalidates current conclusions or if the present data are regarded as inconclusive, this issue will be reassessed and additional methods of gathering definitive data will be proposed. This issue will continue to be carefully evaluated during the site characterization process. There is a potential major impact on the program if crustal magma is discovered in the Yucca Mountain area. This discovery could invalidate the use of the geologic record to bound future volcanic processes if the processes that produced the magma are active and could effect the site during the next 10,000 yr. We will inform the DOE of progress in these areas in the yearly updates to the probabilistic volcanic risk assessment.

D. Activity 8.3.1.8.1.1.4, Revised Probability Calculations and Assessment.

The report completes the first phase of formal assessment of the probability of magmatic disruption (eruption or intrusion) (Pr[E2 given E1]Pr[E1]) of the repository, the controlled area, and the YMR. Future work will focus on yearly updates of the probability assessment including revision of the data matrices developed for the simulation model of E1 and E2 and the methods for combining E1 and E2 into the probability of magmatic disruption. Future work will focus on several areas. First, we will continue site characterization studies that could lead to the identification of new volcanic centers. Second, we will continue to develop structural models of the Yucca Mountain setting. Third, we will extend probabilistic studies to include evaluation of polygenetic and clustered polygenetic activity. Fourth, we will apply formal methods of expert judgment to attempt to further refine the probability distribution of E1, E2, and E2 given E1 using an approach that is largely independent of existing volcanism studies. The expert judgment studies were initiated in early FY95 during final completion of the volcanism status report.

The distribution of estimates for the recurrence rate of volcanic events is probably the best constrained variable of the conditional probability model. Alternative models by a range of workers outside the YMP have not resulted in significantly different distributions for E1. Recurrence rates using homogeneous and nonhomogeneous Poisson distribution models have been shown to be similar (see Chapter 7). We judge that studies of E1 are nearly complete. It is always possible that there could be changes in or new distribution models developed for the recurrence rate of volcanic events and it is difficult to anticipate the results of new breakthroughs in volcanic recurrence models. We have scheduled annual updates of probabilistic models and if changes are noted, they will be examined on a case by case basis. We hope that the formal presentation of recurrence models in this volcanism status report may stimulate further analyses of conceptual models of volcanic processes in the YMR.

Discovery of new Quaternary volcanic centers is not expected because known Quaternary centers form conspicuous constructional landforms. The only possible sites of buried Quaternary centers might be along the trace of the Fortymile Wash or at the east side of the Bare Mountain front where alluvial sedimentation rates should be higher. However, drape aeromagnetic data and exploratory drilling of aeromagnetic sites in Crater Flat revealed no evidence of buried Pliocene or Quaternary basalt or silicic

centers. We conclude that current data are sufficiently compelling to argue that further site characterization studies are *unlikely* to discover new sites of Quaternary basaltic volcanism in areas of alluvial fill or Paleozoic rocks (non-magnetic or weakly magnetic rocks). The only anticipated changes would be if new geophysical data leads to identification of *unanticipated* sites of basaltic volcanism or if subsurface exploration associated with construction of the Exploratory Studies Facility encounters basaltic dikes of Quaternary age. Data will be acquired in FY95 to allow assessment of the depth of detection of basalt intrusions in a variety of rock types and the results of this work will be incorporated in the annual probability updates.

It is less easy to constrain the possibilities of discovery of new Pliocene volcanic centers. The presently undrilled aeromagnetic anomalies (two, possibly three, sites) are judged likely to be Pliocene (or older) volcanic centers. This impact has been constrained somewhat already by assessing the impact of discovery of new Pliocene centers on estimation of recurrence rates (see Chapter 7). Thus, discovery of new volcanic centers of Pliocene age would have a limited effect on time-trend models because of the Pliocene age of the events. Additionally, the effect on volume-predictable models would be limited because of the marked decline in erupted volume through time. The effect on cone counts is more direct. Identification of new events will have a 5% to 20% increase on minimum and maximum event models dependent on the number of newly identified centers. Identification of at least five or more *new* centers is required to have a significant effect on the cumulative probability distributions for the recurrence rate of volcanic events.

Changes in the alternative models of the structural controls of volcanic activity are more likely because of the preliminary stage of tectonic studies of the Yucca Mountain site. The most important potential change would result from identification of structural models that could *increase* the likelihood of a future volcanic event occurring in or near the repository. Identification of new structural models that do *not include* the repository are unlikely to change the distribution of E2 because of the large number of existing alternative models identified in current probabilistic estimates. The only anticipated changes would be if new models are developed that change current concepts of expected or anticipated sites of future basaltic volcanism. One area of development is assessment of the structural controls of the north-east edge of the pull-apart tectonic model of Crater Flat. This edge appears to have controlled the northeast extent of basaltic volcanic rocks during the late Miocene, Pliocene, and Quaternary. The seismic reflection/refraction line crossed this structural edge in east-central Crater Flat and interpretations of the result of this line may prove useful in assessing structural models.

Aspects of the probabilistic assessment of the occurrence of future volcanism require judgment in assumptions and in the application of data. We have attempted to carefully identify these areas in the discussions in Chapter 7 and to use full ranges of alternative models in probabilistic assessments. We anticipate, from past experience, that there will always be some areas of disagreement in our assessments. For this reason, we have initiated in late 1994, an external assessment of probabilistic volcanic hazard and probabilistic risk assessment using expert judgment to identify, constrain, and reduce bias for the judgmental aspects of the studies. Formal methods of expert judgment will be used to establish independent estimations of the probability distribution for E1, E2, and the probability of magmatic disruption of the repository, the controlled area, and the YMR. Expert judgment studies were underway during final editing of this report.

1. Areas of Controversy. There are several areas of controversy involving probabilistic assessment of volcanism. These include: (1) completeness of the data set used for probabilistic assessment, (2) selection of probability distribution models, (3) the use of conservative or worst case assumptions in

probability calculations, and (4) uncertainty of probability calculations. The impact of these topics is discussed in their respective order.

a. Completeness of the Data Set. The issue of the completeness of the data set used for probabilistic assessments will always be of concern. It is easy to develop arguments that any data set is never complete and there can always be future advancements in methods of data collection and development of alternative data interpretations. For example, the rapidly evolving development of new chronology methods and refinements of existing methods will lead invariably to refined and hopefully improved age determinations. What we have emphasized throughout this volcanism status report is the iterative nature of probability calculations. The structured approach used in probabilistic volcanic risk assessment allows for efficient recalculation of probability estimates. There is no inherent danger in conducting probability calculations with an evolving data set. The issue of data completeness is in reality more correctly identified as an issue of when probability studies provide reasonable confidence that a problem has been estimated and bounded. Currently the concept of "reasonable assurance" is at best only a vaguely defined and largely subjective regulatory concept and makes judgments of data sufficiency extremely difficult. The primary basis for judgments of reasonable assurance should be developed logically from sensitivity studies of the probability distributions and their impacts on the performance of the waste isolation system. The bounds for establishing the probability of magmatic disruption of the repository were estimated in 1982. Succeeding work has provided better constraints on the probability distribution but has not resulted in modifications of the probability range. Current results from performance assessment studies suggest that eruptive effects of future volcanic events are not significant largely because of their low occurrence probability. Further work is required and is ongoing on the subsurface effects of magmatic activity on an underground repository system.

b. Time-Distribution Models. A mildly controversial issue for probabilistic volcanic risk assessments is the choice of time-distribution models for volcanic events. We have used both homogeneous and nonhomogeneous Poisson models for estimating the distribution of volcanic events in Chapter 7. Work to date (see Chapter 7) shows that alternative distribution models do *not change significantly* the resulting probability estimations.

c. Conservative or Worse Case Probability Assumptions. A third area of controversy in probability calculations is the approach used to choose values for assumptions to support or conduct the probability estimations. A common approach is to use conservative or worse case assumptions. These assumptions provide a measure of confidence that the probability values will not be underestimated. Moreover, this approach has merit, particularly for attempts to bound the probability of events. An often unappreciated problem with this approach, however, is that it introduces an element of nonsystematic bias in probabilistic assessment. There is not a standard definition of what constitutes *conservatism* in selection of attribute values. Different workers can select widely different values under the general guideline of maintaining conservatism. A second problem with the selection of worse case values is propagation of conservatism. Probabilistic assessment using conservative assumptions for attributes of conditional probabilities can lead to propagation of assumptions to a point where the calculated values are not physically plausible for the modeled events or processes.

We argue that a more reasonable approach to probabilistic assessment is through assignment of values measuring the central tendency of data attributes. Underestimation of probability results can be avoided by sensitivity analyses of affects of probability distributions for volcanic events in assessments of total system performance.

d. Uncertainty of Probability Calculations. The final area of controversy in probabilistic assessment is evaluating the uncertainty of the probability assessments. This falls directly into the area of the data paradox for the YMR. *The small number of past volcanic events in the YMR results in a low risk of future volcanic activity but a relatively large uncertainty in calculating that risk. Conversely, if there were more volcanic events, there would be a reduced uncertainty of estimating volcanic risk but an increased risk.*

The probabilistic assessments for volcanism for the YMR can never be regarded as robust statistical calculations. Instead they are attempts to constrain or bound a problem using a structured probabilistic approach. Uncertainty in probability estimates is assessed by presenting the values as *probability distributions.* The significance of the defined uncertainty is assessed by comparison of the data to the regulatory standards for licensing a repository, a responsibility of the Department of Energy.

CHAPTER 9: CONCLUSIONS

Chapter 1

1. An assessment of the risk of future volcanism is one of a number of issues that must be resolved to assess the suitability of the Yucca Mountain site for disposal of high-level radioactive waste.

2. The absence of post-Miocene silicic volcanism in the Yucca Mountain region (YMR) is the basis for the conclusion that the risk of recurrence of silicic volcanism is negligible. Final resolution of this issue requires completion of drilling of aeromagnetic anomalies suspected to be buried centers, or intrusions (probably of basaltic but possibly of silicic composition).

3. The risk of future basaltic volcanism is an event of concern for the Yucca Mountain site. Such an event could directly penetrate a repository and erupt at the surface releasing radioactive waste elements. An additional concern is an eruptive event near the repository that could degrade the isolation system of an underground repository primarily from the subsurface effects of the dike feeder system. An intrusive event (dikes or sills) near or beneath a repository but without an accompanying eruption could also degrade a waste isolation system of a repository . However, the combination of the relatively shallow depth of burial of a repository (300 m), and regional geologic evidence that all exhumed shallow basalt intrusions were accompanied by eruptive events indicate this event scenario may be unlikely.

4. The timing or location of a future basaltic volcanic eruption in the Yucca Mountain region cannot be predicted with certainty. The risk (occurrence probability combined with disruption effects) can be estimated and bounded using methods of probabilistic volcanic risk assessment.

5. This volcanism status report summarizes the current status of a range of volcanism studies all in support of assessment of the occurrence probability of magmatic disruption of the potential repository site, the controlled area surrounding the site, or the Yucca Mountain region (YMR). Information presented in the report is current to April 1994.

Chapter 2

1. The period of most voluminous silicic volcanism in the YMR occurred 15 to 11 million years (Ma). The YMR marks the southern limit of the spread of time-transgressive silicic volcanism. A transition to fundamentally basaltic volcanism occurred in the YMR about 12 to 10 Ma.

2. Field and geochronology data for the YMR show that basaltic volcanic centers in the YMR are divided into two episodes. These are: (1) the basalt of the Silicic episode (BSE) (12 to 8.5 Ma) that occurred during the waning stage of large-volume silicic volcanism of the Timber Mountain–Oasis Valley caldera complex and (2) small-volume, Postcaldera basalt (9.0 Ma to Quaternary) that formed at scattered localities in the YMR. The recurrence of a future basaltic volcanic eruption of the Postcaldera basalt episode represents the primary hazard of future volcanism for the Yucca Mountain site.

3. The Postcaldera basalt episode is divided into two cycles including the Older postcaldera basalt (OPB) and the Younger postcaldera basalt (YPB). The OPB (9.0 to 6.3 Ma) occurs primarily north and east of the Yucca Mountain site. The YPB (4.8 to <0.1 Ma) occurs mostly west and

southwest of the Yucca Mountain site except for the basalt of Buckboard Mesa that is located in the northeast part of the ring-fracture zone of the Timber Mountain caldera.

4. The OPB consists of the basalt of Rocket Wash (8.0 Ma), the basalt of Pahute Mesa (~ 9 Ma), the basalt of Paiute Ridge (8.5 Ma), the basalt of Scarp Canyon (8.7 Ma), and the basalt of Nye Canyon (6.3 to 7.2 Ma). Each basalt unit consists of individual centers or clusters of centers of coeval age, associated lava flows, and locally dikes and sills.

5. The YPB consists of two sites of single centers (basalt of Buckboard Mesa, the Lathrop Wells center) and five sites of clustered centers (basalt of Thirsty Mesa, basalt of Amargosa Valley, southeast basalt of Crater Flat, Quaternary basalt of Crater Flat, and basalt of Sleeping Butte). All but one of the seven Plio-Quaternary basalt sites (basalt of Buckboard Mesa) occur in a narrow northwest-trending zone called the Crater Flat volcanic zone (CFVZ). Basalt centers *in* the CFVZ tend to form as north/south- or northeast-trending, aligned clusters of centers. The direction of alignment of the centers parallels the maximum compressive stress direction.

6. The oldest and largest volume basaltic volcanic center of the YPB is the basalt of Thirsty Mesa, a Pliocene center (4.8 Ma). It occurs at the northwest end of the CFVZ. The center formed a small lava mesa surmounting a plateau surface upheld by outflow sheets of the Thirsty Canyon Tuff. The vents for the lava mesa are three coalesced (north/south-trending) and now partly eroded scoria-spatter cones.

7. A negative aeromagnetic anomaly was drilled by a private company who encountered basalt interbedded with alluvial deposits (150 m depth). Cuttings from the basalt were dated at 3.8 Ma and are similar in age to the basalt of southeast Crater Flat. Two structurally related (northeast-trending alignment) aeromagnetic anomalies (one negative, one positive) in the central Amargosa Valley are suspected to be buried basalt of similar age as the drilled aeromagnetic anomaly. The basalt of southeast Crater Flat comprises six north-trending, deeply dissected scoria cones marking the vents for the associated lavas. Five of the vents form a partly coalesced cluster of vents in the northwest part of the outcrop area of the basalt of southeast Crater Flat. The vents are marked by dike swarms in scoria and lava ponds in elongate fissure vents. The sixth center, a dissected scoria cone, occurs in southern Crater Flat at the south end of outcrops of faulted sheets of aa lava flows. The lavas of the basalt of southeast Crater Flat are the most extensive of the YPB. New $^{40}Ar/^{39}Ar$ age determinations are consistent with an age of about 3.7 Ma for the basalt of southeast Crater Flat.

8. The basalt of Buckboard Mesa formed along the ring-fracture zone of the northeast part of the Timber Mountain caldera. Nearly 1 km^3 of aphyric to sparsely porphyritic lava vented from a small scoria cone (Scrugham Peak), and an associated fissure extending from the southeast base of the scoria cone. The lava ponded in topographic lows along ancestral branches of Fortymile Wash, and the lava surface now forms a topographically inverted, high-standing mesa-surface. A single major flow lobe is observed at most outcrops except in two boreholes and northwest of Scrugham Peak two lava-flow units are observed. The age of the basalt of Buckboard Mesa is about 2.9 Ma.

9. The Quaternary basalt of Crater Flat consists of an arcuate northeast-trending alignment of four basalt centers in central Crater Flat. The southern center (Little Cones) consists of two separate scoria cones of small dimensions. The southwest cone is breached on the south side and several small satellite vents, mostly buried by alluvium, are present south of the southern scoria cone.

Potassium-Argon age determinations of a feeder dike in satellite cone scoria exposed southeast of the southern cone yielded ages of about 1.0 Ma.

10. The Red Cone and Black Cone centers form the middle centers of the Quaternary basalt of Crater Flat and are eroded volcanic landforms that had similar eruptive histories. Both consist of a main scoria cone with a summit crater filled by deposits of spatter, lava blocks, and scoria. The main scoria cones of both centers are flanked by scattered eroded scoria mounds; some may have been the eruptive vents for blocky aa lava flows that surround the scoria cone and mounds. Potassium-Argon age determinations for the Red Cone center range from 0.84 to 1.5 Ma. Published and unpublished K-Ar age determinations for the Black Cone center range from 0.8 to 1.1 Ma. Newly obtained, high-precision $^{40}Ar/^{39}Ar$ ages for Black Cone are about 1.0 Ma.

11. The Makani cone is the northern center of the basalt of Crater Flat and is the most deeply eroded of all centers of the Quaternary basalt of Crater Flat. It consists of an eroded scoria cone flanked on the southwest and northeast by small lava lobes. Potassium-Argon ages for the Makani center range from 1.1 to 1.7 Ma.

12. Areas of continuing controversy for the Quaternary basalt of Crater Flat are the chronology and eruptive history of the individual centers. Paleomagnetic data support the inference that all centers formed contemporaneously. However, this interpretation is limited by assumptions of the variability of the geomagnetic field and the quantity and reliability of the data have not been reconciled with evidence of geochemical diversity in the lava and scoria units. Exploratory data analyses show that the K-Ar determinations for the centers are not distributed normally and contain outliers. Removal of the outliers results in a near-normal data distribution, with a mean age of all centers of 1.0 ± 0.1 Ma (one *s*).

13. The basalt of Sleeping Butte consists of two small-volume basalt centers located at the northwest end of the CFVZ, 47 km northwest of the Yucca Mountain site. Each center consists of a main scoria cone flanked to the south and east by small satellite cones. The Little Black Peak cone, the southeast center, is a symmetrical cone that erupted western and eastern lobes of small-volume, blocky aa lava flows from radial dikes. It is inferred to be a monogenetic center with an age of about 320 thousand years (ka). The Hidden Cone center is an asymmetrical cone formed on the north-facing slope of Sleeping Butte. Multiple lobes of lava flows vented from radial dike sets on the northeast flank of the main cone. The lava of the center has yielded imprecise and variable K-Ar ages of 0.22 to 0.32 Ma. Newly obtained and more precise $^{40}Ar/^{39}Ar$ age determinations are consistent with an age of about 0.32 to 0.38 Ma. The Sleeping Butte center may have been mantled by a late Pleistocene scoria-fall eruptive event (polygenetic center) but this event has not been verified through geochronology studies.

14. The Lathrop Wells basalt center is located near the intersection of several sets of northwest-trending faults and the southeast-trending Stagecoach Road fault. The center consists of a large main scoria cone and multiple sets of predominately northwest-trending fissures marked by paired or individual accumulations of spatter, bombs, and scoria. The center was formed during four eruptive phases marked by four chronostratigraphic units that have been identified by their combined field and geomorphic relations, and geochemical compositions.

15. Chronostratigraphic unit I of the Lathrop Wells center consists of four groups of lava flows and local pyroclastic deposits that crop out along multiple, northwest trending fissures located south, beneath, north, and northeast of the main cone. The fissures mark scoria and spatter deposits

of eruptive events that were modified considerably by erosion and pedogenic processes prior to deposition of chronostratigraphic unit II. The age of the lava and scoria deposits of chronostratigraphic unit I are between 85 and 95 ka and may possibly be as old as 135 ka.

16. Chronostratigraphic unit II consists of the largest volume lavas, local fissure deposits, and a widespread scoria-fall sheet containing interbedded hydrovolcanic (pyroclastic surge) deposits. The lava sequence erupted from a northwest-trending fissure that parallels a northwest-trending fault offsetting the Timber Mountain Tuff. Existing chronology data cannot discriminate the age of chronostratigraphic unit II from chronostratigraphic unit I. The respective deposits can be discriminated by their spatially separate eruptive vents, stratigraphic relations, different degrees of erosional modification and pedogenic alteration, and distinct geochemical compositions. The age of chronostratigraphic unit II may be bracketed between 80 and 107 ka. Chronostratigraphic unit II is inferred to be the source of primary fall and surge deposits overlying alluvium several kilometers north of the main cone and reworked basaltic tephra identified in multiple fault trenches flanking Yucca Mountain.

17. Chronostratigraphic unit III of the Lathrop Wells center consists of most of the main scoria cone and possibly one site of small-volume lobes of blocky aa lava flows extruded from a vent northwest of the main cone. The inferred age of this unit may be bracketed between 40 and 65 ka and must be younger than the deposits of chronostratigraphic unit I. Present geochronology data cannot rule out the possibility that the deposits could be as old as chronostratigraphic unit II but they are inferred to be younger on the basis of contrasts in erosion of surfaces formed by deposits of chronostratigraphic units II and III.

18. Chronostratigraphic unit IV consists of very small-volume and local scoria-fall and hydrovolcanic deposits interbedded with multiple soils with horizon development that occur just southeast of the south flank of the main cone. The deposits have now mostly been removed by commercial quarrying of the scoria deposits. The identification of the deposits and the interpretation of their primary origin is aided by their distinct major- and trace-element geochemistry. The age of the deposits of chronostratigraphic unit IV is Holocene.

19. Potassium-Argon and $^{40}Ar/^{39}Ar$ age determinations for chronostratigraphic units I, II, and III of the Lathrop Wells volcanic center contain outliers, are skewed toward older ages, and exhibit a positive correlation between percentage radiogenic Ar and age. Excess Ar has been noted in olivine phenocrysts and may be present in other phases, notably ubiquitous matrix glass. The radiometric age determinations must be interpreted cautiously and are probably maximum ages.

20. Uranium-Thorium disequilibrium isochron ages for lavas from chronostratigraphic units I and III are about 125 to 135 ka. Interpretations of the ages are limited by the small degree of U-Th fractionation in measured phases and uranium enrichment in olivine of one isochron. The ages are consistent with K-Ar and $^{40}Ar/^{39}Ar$ age determination and reproducible for separate sample sites. The ages are inconsistent with field and stratigraphic relations of the analyzed chronostratigraphic units.

21. Cosmogenic ^{3}He age determinations of surface samples have been obtained for multiple stratigraphic units of the Lathrop Wells volcanic center. Multiple samples of lava flow surfaces of chronostratigraphic unit I give closely grouped ages for individual sample sites (81 to 96 ka) but must be *minimum* ages because the sites were covered by at least 2 m of scoria-fall deposits of chronostratigraphic unit II. Lava sites of chronostratigraphic unit II give reproducible ages of 82 to

100 ka. Bombs collected from the surface of the main scoria cone (chronostratigraphic unit III) show more variability in their cosmogenic ^{3}He surface exposure ages (28 to 63 ka). A cosmogenic ^{3}He age of a shielded sample from the excavated interior of a buried Ql1c lava gave an age of about 5 ka consistent with assumptions for the ^{3}He method. A secondary finding of studies of the noble gas components of the lavas of the Lathrop Wells center is the presence of excess ^{40}Ar released during crushing of olivine under vacuum.

22. Thermoluminescence age determinations for samples collected from buried soils interbedded with tephra of chronostratigraphic unit IV give reproducible and stratigraphically consistent ages of about 4 to 9 ka (Holocene) for the deposits. An age of about 25 to 30 ka for volcaniclastic deposits baked by overlying lava of chronostratigraphic unit II is significantly younger than results for other chronology methods and is probably anomalous.

23. Geomorphic data for the volcanic units of the Lathrop Wells center can be used to discriminate some of the deposits of the Lathrop Wells center and requires a time break between chronostratigraphic units I, II, and III.

24. Studies of the development of soils show that volcanic landforms of the Lathrop Wells center have weakly developed calcic soils (weakly developed vesicular A and B horizons) and closely resemble Holocene soils in the Silver Lake area of the Cima volcanic field in California. Soil development on chronostratigraphic unit III is inconsistent with K-Ar and U-Th disequilibrium ages of >100 ka. Scoria deposits of the Lathrop Wells center are *not stable landforms* conducive to the preservation of soils; soils provide constraints only on the minimum age of the respective deposits.

25. Paleomagnetic data have been obtained for the Lathrop Wells center to augment nonqualified (Quality Assurance requirements) paleomagnetic data. Each sampling site consisted of 8 to 12 independently oriented samples with at least one specimen per site subjected to progressive alternating field magnetization. Interpretation of the data is complicated by difficulty in sampling intact material and overprint by lightning strikes. A new sampling method was developed to analyze field magnetic directions of cone scoria. Studies show that satellite spatter cones record coherent field magnetic directions. In contrast, scoria clasts from the main cone show random variations in magnetic directions consistent with cooling prior to deposition. Deposits of the center have recorded field magnetization directions that are within the expected range of paleosecular field variation about the latest Quaternary spin-axis direction. These data provide at best only a limited opportunity to discriminate time-distinctive eruptive events. There is no indication of a single volcanic event that occurred during a period of unusual geomagnetic activity.

Chapter 3

1. Yucca Mountain developed as a physiographic feature through a combination of deposition of large volume ignimbrites from the Timber Mountain–Oasis Valley caldera complex and subsequent uplift and tilting along extensional faults. It is located at the north edge of a conspicuously amagmatic zone that exhibited *no* volcanism during Cenozoic extension. The tectonic framework of the area has been affected by detachment faulting; however these fault systems, if present, are no longer active. The Crater Flat basin that borders Yucca Mountain to the west may be a caldera depression possibly associated with the eruption of the Crater Flat Tuff. Alternatively, the basin may be a pull-apart in the Kawich-Greenwater rift zone. Other alternative structural models are

that the basin is the site of a northwest-trending, strike-slip fault or was formed by combined extension and right-slip associated with development of a half-graben.

2. The BSE is distributed in a broad northwest trending zone paralleling the Walker Lane structural system and is spatially associated with Miocene caldera complexes. Postcaldera basalt is temporally or spatially distinct from silicic volcanism centers and forms two distinct episodes. The OPB occurs mostly along basin and range faults and at the intersection of basin and range faults with ring-fracture zones of the Miocene caldera complexes. The youngest unit of the OPB, the basalt of Nye Canyon, forms a northeast-trending cluster of centers that is largely independent of local structural features.

3. The YPB occurs in a 70-km-long, northwest-trending zone named the Crater Flat volcanic zone (CFVZ) with one basalt center, the basalt of Buckboard Mesa, occurring outside of the zone. The OPB and YPB are temporally and spatially distinct. The distribution centroid of the OPB is located in the northeast part of the Timber Mountain caldera. The distribution centroid of the YPB overlaps with the Crater Flat basin. The t-test shows that the means of event-assigned ages of the two basalt cycles are different with a p-value of <0.0005.

4. The basalt centers of the YPB (except the basalt of Buckboard Mesa) show a preferential *northwest-trending* distribution (nonrandom). The locations of the centers are correlated spatially using least squares regression fits of the latitude and longitude coordinates. This regression fit coincides with the trend of a three-dimensional surface fitted by distance weighted least squares to vent locations and eruption volume but this surface is obtained for a limited data set. A secondary trend of *clustered centers* is north-northeast is parallel to the maximum compressive stress direction. This secondary trend is inferred to represent the direction of propagation of feeder dikes in the shallow crust. The YPB is inferred to have formed by repeated pulses of basalt magma that followed northwest-trending structures at depth and diverted at shallow levels to form northeast-trending dikes. An alternative structural model assumes the secondary north-northeast trends are controlled by basin-range faults of the Yucca Mountain block.

5. A local seismic net has been installed and maintained for the YMR since 1979. Earthquakes in the region are distributed in an east/west zone and show strike-slip and dip-slip offsets. Earthquake clusters are difficult to relate to surface faults. Yucca Mountain is located in a zone of low seismicity. There may be a negative correlation between sites of Quaternary basaltic volcanism and seismicity. Strain-field modeling shows that off-fault location of seismicity is expected. The seismic gap in the Yucca Mountain area is coincident with a region of modeled low shear strain.

6. Gravity data for the YMR show a gravity high associated with Bare Mountain and a gravity low centered in Crater Flat and extending to the west margin of Yucca Mountain.

7. Drape aeromagnetic and local ground magnetic data have been obtained for the YMR. These data reveal multiple anomaly sites, some of which are correlated with Pliocene and Quaternary sites of basaltic volcanism. Other anomaly sites are inferred to represent buried basalt centers or intrusive bodies. Three of these anomalies have been explored by drilling. Two anomaly sites are the results of buried basalt. These are a large reversed anomaly in western Crater Flat and large reversed anomaly directly south of the town of Amargosa Valley. The third anomaly site, a broad positive magnetic anomaly in Crater Flat, is unexplained but is not associated with sites of surface or buried Pliocene and Quaternary basaltic volcanism. Two aeromagnetic anomalies in the Amargosa Valley and a third, small, positive anomaly 1 km south of Little Cones will be studied

by exploratory drilling. Additional aeromagnetic and ground magnetic experiments are planned to assess the detectability of buried basalt centers or intrusions in different types of country rock.

8. Seismic reflection and refraction data for the Amargosa Valley reveal a bright spot in the profile. It is interpreted to represent a focusing of energy from the midcrust by low-velocity basin fill. Teleseismic topographic data reveal the presence of a low-velocity anomaly in Crater Flat and the Amargosa Valley. One interpretation of the anomaly is that it is formed by magma. However, other interpretations are possible and the magmatic interpretation is inconsistent with geologic, seismic, heat flow, and magnetic data for the region.

9. Sites of Quaternary basaltic centers cannot be related consistently to prevailing shallow structural features. The most consistent relations of the sites are with deep-seated structural features that are inferred to be passive features promoting the ascent of basalt magma. Basalt centers are more common in alluvial basins than range interiors.

Chapter 4

1. Basalt magma erupted in the Pliocene and Quaternary in the YMR almost certainly was derived from the upper mantle by partial melting of hydrous peridotite.

2. A transition to basaltic volcanism in the western United States was probably not associated with increased rates of extension. Instead, the time-space distribution of basaltic volcanism is more consistent with increases in mean crustal density resulting from cooling of the crust after the cessation of subduction.

3. Basalt erupted in the Great Basin and Basin and Range province during the last 5 Ma tends to be more nepheline normative, have higher MgO contents, and may show a decrease in erupted volumes compared with basalt erupted >5 Ma. The younger group of basalts probably reflects smaller degrees of partial melting at greater mantle depths than the older group of basalts. The younger basalt group may show greater volatile enrichments and more frequent eruptions since they are more likely to ascend quickly through the crust.

4. Basalt of the southern Great Basin was derived from lithospheric mantle despite being erupted in a region of active extension during the last 10–15 Ma. Ascent of melt may not be favored by the tectonic setting of the YMR.

5. Basaltic volcanic fields in the *interior* of the Basin and Range province show characteristic patterns of time-composition variation in their evolution. The intensity of mantle melting with these fields was never great enough to produce large volumes of tholeiitic basalt. The relatively long lifetime and small volume of the basalt of the YMR result in one of the lowest eruptive rates in a volcanic field in the southwest United States.

6. Pliocene lavas of the Crater Flat area contain phenocrysts of plagioclase, olivine, and clinopyroxene. The Quaternary lavas tend to lack plagioclase phenocrysts and probably fractionated at high pressure in the lower crust or upper mantle.

7. Major- and trace-element compositional variations among the volcanic units of the Lathrop Wells volcanic center are incompatible with fractional crystallization from a single magma. Preliminary modeling of compositional variations leads to a preferred model of separate unrelated

magma batches to account for geochemical variations observed at the center. The eruption of each of these magma batches requires a new episode of dike intrusion. Once a new volcanic center is established, there is a tendency for subsequent magmas to ascend and erupt at the same location for long periods of time (0.1 Ma).

Chapter 5

1. Basalt magma in the YMR ascended from the upper mantle and crust through the processes of melt segregation and propagation as dikes. The initial rise and segregation of magma were driven by buoyancy of the melt phase. The equations for two-phase flow accompanied by matrix deformation and compaction have been developed but not applied to all boundary conditions. Computer modeling of modified forms of the equations suggest the presence of solitary-wave solutions or solitons. They may contribute to episodic volcanic activity for areas of low melt production, or they may degrade from nonlinearity, diffusion, or overprint by processes of magma ascent.

2. Extraction of magma into conduits by melt-fracture requires that the melt pressure exceeds the yield pressure of country rock. This occurs at depths as great as 50 km. The form of magma transport has been modeled from a perspective of rock mechanics and the dynamics of magma transport. The latter requires consideration of elastic deformation of the country rock and processes of fracture, magma flow, and volatile exsolution at the dike tip.

3. Magma in the form of dikes will rise until it erupts, solidifies, or reaches the level of neutral buoyancy (LNB). The location of the LNB in the YMR may occur at the base of low-density basin fill at 4 to 5 km. Alternatively, the combined low flux of magma and processes such as crack-rate propagation, magma-gas content, or concentrations of volatiles in the dike tip may negate the controls of the LNB.

4. Dikes in the region probably followed northwest-trending structure at depth and diverted at shallow depths to follow the direction of maximum compressive stress direction (north-northeast).

Chapter 6

1. Volcanism studies for the Yucca Mountain Site Characterization Project began in 1979. The methods of probabilistic risk assessment were developed in the early part of the 1980's. Petrology and geochemical studies of the basalt of Crater Flat were published in 1981 and 1982. The first evidence of a long-lived controversy concerning the interpretation of whole-rock, K-Ar age determinations for the Lathrop Wells center was identified in 1983. The first status report on volcanism studies was published in 1983. Reports on the results of drill holes in Crater Flat were published in 1984 and 1985. The second status report on volcanism studies was completed in 1986. Volcanism studies were summarized in the Environmental Assessment in 1986.

2. A three-part strategy for volcanism studies was formalized in the Site Characterization Plan in 1988. The chronology of the Lathrop Wells center was reassessed and a revised geologic map of the center was completed in 1988. The concept of polygenetic volcanism and the implications of a revised age of the Lathrop Wells center were assessed for probabilistic volcanic risk assessment in 1989. A summary paper on recurrence rates of volcanic events was completed in 1989. The paper identified the CFVZ. The results of regional isotopic and trace-element studies of basalt in the southern Great Basin were published in a separate paper in 1989.

3. Study Plan 8.3.1.8.5.1, Characterization of Volcanic Features, was prepared and released in 1990. The first technical overviews of the volcanism program by the state of Nevada were completed in 1990. The first in a series of papers describing alternative views by the U.S. Geological Survey of the chronology and eruptive models of basalt centers was presented in 1991. A geologic map and report for the Sleeping Butte center were completed in 1991. The first in a series of alternative interpretations of probabilistic models of the recurrence rate of volcanic events by the state of Nevada was published in 1991. Study Plan 8.3.1.8.1.1, Probability of Magmatic Disruption of the Repository, was prepared and released in 1991. The long-awaited resumption of surface disturbing activities for the YMP occurred in 1991.

4. Summary papers on the volcanic stratigraphy and chronology of the Lathrop Wells volcanic center, the recurrence rate of volcanic events, the patterns of temporal and geochemical variation of basaltic magma in the Crater Flat area, and the consequences of magmatic disruption of the potential repository were published in 1992. The results presented in these papers were augmented by completion of over 60 shallow trenches. Several papers advocating use of nonhomogeneous Poisson distributions of volcanic events in time were published by the state of Nevada in 1992. Stochastic models of disruption of the repository by basalt dikes were published in 1992.

5. In 1993, a paper was published on the cosmogenic ^{36}Cl ages of the Lathrop Wells volcanic center. Geophysical investigations of buried volcanic centers were summarized by the U.S. Geologic Survey in 1993. The Repository Integration Program was used to assess the consequences of volcanic disruptive events for the Yucca Mountain site in 1993.

6. Alternative probability models using nonhomogeneous Poisson distribution models for the spatial patterns of volcanic events in the YMR were published by the Center for Nuclear Waste Regulatory Analysis in 1993. A paper was published in 1993 on stochastic modeling of the probability of intersection of the Yucca Mountain site by dikes using alternative structural models. Risk simulation modeling was used to evaluate cumulative probability distributions for E1, E2, and E2 given E1 in 1993. A paper was published on the preliminary results of studies of the abundance and depth of derivation of lithic fragments in basalt eruptions in 1993.

Chapter 7

1. Probabilistic assessments of E1, E2, and E2 given E1 have been reevaluated for the potential repository, the controlled area, and the YMR. The emphasis of these revised estimates is to provide unbiased assessments of the most likely, minimum, and maximum values for ranges of alternative recurrence and structural models.

2. The probability of magmatic disruption of a repository and release of radionuclides to the accessible environment is defined as a conditional probability that includes the recurrence rate of volcanic events in the YMR, the probability of magmatic disruption of a specified area, and the probability that magmatic disruption leads to *rapid* release of radionuclides to the accessible environment in quantities that exceed regulatory requirements. The probability is expressed mathematically as a modified exponential equation.

3. A basic assumption used in applications of many cases of the probability model is a homogeneous Poisson distribution of the volcanic events in time and space. The model is conceptually simple, required assumptions are well defined, and potential errors can be identified and constrained.

4. Because of the continuing debate concerning the applicability of the homogeneous Poisson model, nonhomogeneous Poisson models were also assessed. These models show minor differences in probability estimates compared to homogeneous Poisson distribution models of E1.

5. Required assumptions of probabilistic models are the use of the volcanic record to forecast future events, use of multiple alternate recurrence and structural models, identification of all Quaternary volcanic centers in the YMR, and reliability of the observations and interpretations of the geologic record of the YMR. The uncertainty of these assumptions is mitigated by using multiple alternative models of the volcanic record.

6. The strategy for assessing the risk of future volcanism for the YMR is to ask a series of questions for the YMR. First, has there been Quaternary igneous activity in the YMR? (*answer: yes).* Second, what is the range of possible future volcanic events? (*answer: formation of a* ***new volcanic center****, a polygenetic event at an* ***existing*** *center, and a* ***cluster event*** *associated with an* ***existing*** *center).* The second question is assessed by estimating the probability of formation of a new volcanic center, volcanic cluster, or intrusion (*topics of this volcanism status report).* Remaining studies to be conducted are the probability of a polygenetic event or cluster. Third, what is the likely nature of future volcanic activity? (*answer: hawaiian, strombolian, hydrovolcanic or mixed eruptions of combinations of the three types).* Fourth, where can a future volcanic event occur? (*answer: the YMR and most likely in the CFVZ*). Finally, is the probability of magmatic disruption $<10^{-8}$ yr^{-1}? *(answer: no for the YMR, no for the controlled area, and no or maybe for the potential repository).* Studies of the effects of eruptive and subsurface processes of magmatism will be required for the volcanism issue. These studies are *not* described in this volcanism status report.

7. Current site characterization information combined with simple logic require that the probability of an intrusion is greater than or equal to the probability of formation of a new volcanic center which is greater than the probability of formation of a new volcanic cluster. All events have rates that are $>10^{-8}$ events yr^{-1}.

8. Volcanic events have occurred more frequently in the CFVZ than in a northeast-trending structural zone. Basalt centers occur more frequently in alluvial basins than along range fronts or in range interiors.

9. The time perspective for probability estimations is the Quaternary (1.6 Ma), the regulatory definition of the Quaternary (2.0 Ma), and volcanic cycles defined from studies the geologic record of volcanic events (4.8 and 1.0 Ma). Volcanic events are defined from the perspective of their effects on a buried repository. Polygenetic volcanism represents a special subclass of volcanic events and will be assessed in future studies. The geologic record as currently assessed from data presented in Chapter 2 is used to define minimum event, maximum event, and most likely event models for probability estimations.

10. The recurrence rate of volcanic events in the YMR is examined systematically using time-series analysis, homogeneous and nonhomogeneous Poisson distribution models, and relations of magma volume versus time. Because of limited data (volcanic events), the only useful information from time-series analysis is the magma-repose intervals through time. Event repose times range from 200 ka to 1.9 Ma with a mean of 1000 ± 570 ka ($n = 6$). Repose intervals decline slightly through time (4.8 Ma to present) and the minimum repose interval is 200 ka for the last two volcanic events

(the Sleeping Butte and Lathrop Wells centers). The minimum repose interval is equivalent to a recurrence rate of 5.2×10^{-6} events yr^{-1} .

11. The recurrence rate using homogeneous Poisson models ranges from 1.5 to 8.0×10^{-8} events yr^{-1}. Mean event rates are 3.5 to 4.0×10^{-6} event yr^{-1}. The recurrence rates using homogeneous Poisson distribution models are lower for arbitrary time intervals than for volcanic cycles. The preferred models are for volcanic cycles (geologic plausibility). The recurrence rate using nonhomogeneous Poisson distribution models (Weibull distribution) range from 1.4 to 8.4×10^{-8} events yr^{-1}. Mean rates are 2.9 to 4.6×10^{-6} events yr^{-1}. The nonhomogeneous rates are similar to the homogeneous rates. Recurrence rates are *slightly lower* for the volcanic cycle models because the β values (fitting parameter for the Weibull distribution) are ≤ 1. Regression-fit models treating magma volume as the dependent variable and event time as the independent variable are generally unsatisfactory (residuals are nonrandom) for both simple, exponential, and log-transformed regression models. Further studies will examine multiple regression models. Marginally significant results are obtained for several cases and these models are used for estimations of volume-predictable recurrence rates by calculating magma generation times for the volume of representative volcanic events. Resulting recurrence times are $>10^6$ yr because of the marked decrease in magma volume versus time (decrease by greater than a factor of 30). The only geologically plausible recurrence rates are for the *smallest* volume events. These yield event rates of 3.4 to 5.0×10^{-8} events yr^{-1}.

12. Risk simulation is used (trigen and normal distributions, Latin Hypercube sampling, 10,000 iterations) to define the distribution of the recurrence rate in probability space. The sensitivity of the recurrence rate is assessed by using model dependent midpoints and varying the bounding assumptions used to describe the distributions. Calculated probability distributions for the recurrence rate show that the uncertainty of the distributions is determined mostly by the assumptions used to bound the distribution models.

13. Estimating or bounding the disruption probability for the YMR is difficult because of the small number of Pliocene and Quaternary volcanic centers. Priority is placed on multiple alternative models rather than on statistical analyses of the time-space distribution of volcanic events. Spatial distribution models are identified from alternative combinations of distribution areas for sets of volcanic events in the Yucca Mountain region. The distribution of events *in* distribution areas is assumed to be random for simplicity of probability estimations. The disruption probability can also be weighted by the occurrence of volcanic events in alluvial basins, range fronts, and range interiors. Volcanic events occur preferentially in the CFVZ but the location of successive events is not systematic with respect to both their jump lengths and directions. The location of past volcanic events does not constrain uniquely the location of future volcanic events. Structural models for the disruption probability are constructed by first identifying structural features of the YMR, and second, relating the spatial patterns of volcanic events to the structural features. Two classes of models are identified: models that exclude the Yucca Mountain site and models that include the Yucca Mountain site. Most structural models fall into the first class. The median estimate of E2 using spatial models is 3.1×10^{-3} and 4.6×10^{-3} for structural models. Analog basaltic volcanic fields in the Basin and Range province show that the spatial dispersion of volcanic events long-lived and very active basaltic volcanic fields is similar to the spatial dispersion of vents in the YMR. Risk simulation (normal distribution, Latin Hypercube sampling, 10,000 iterations) is used to evaluate the distribution of E2 in probability space. Bounds for the distribution are defined by comparison to active volcanic fields, exploratory data analysis (identification of outliers), and

testing the spatial and structural models for geologic plausibility. The uncertainty of E2 is largest for spatial models that include outliers and smallest for intersection models that include the Yucca Mountain site. The median estimates of E2 for structural models are larger than the median estimates for spatial models but the uncertainty of the spatial models is larger.

14. The probabilities of magmatic disruption of the potential repository, the controlled area, and the YMR are estimated through risk simulation using multiple sets of simulation matrices. Alternative models of the recurrence rate have limited controls on the uncertainty of the probability of magmatic disruption. Alternative models of the disruption probability result in considerable more variability in the probability of magmatic disruption of the repository but each model must be considered for effects on the recurrence rate. The median estimate of the probability of magmatic disruption is about 2.0×10^{-8} events yr^{-1}, closely similar to previously published estimates. The sets of worse case estimations are reduced to two, and these models are controlled by spatial models of E2.

15. Ranking of the suitability of models of E2, and to a lesser degree E1, may be important to further refine the probability of magmatic disruption. This ranking could be implemented efficiently through application of formal procedures of expert judgment.

Chapter 8

1. Three to five aeromagnetic anomalies remain to be evaluated by exploratory drilling. The anticipated results from the drilling exploration are not expected to change the record of *Quaternary* volcanic events in the YMR. Remaining uncertainties are whether any of the anomalies are produced by buried silicic volcanic rocks or silicic intrusive rocks.

2. Additional age determinations may be required to assess the age of the buried basalt center of the Amargosa Valley. The basalt of Buckboard Mesa, Little Cones, Red Cone, Makani cone, and the Sleeping Butte centers will be dated by high precision $^{40}Ar/^{39}Ar$ methods under Quality Assurance controls. Only minor changes in chronology are expected for these centers. Further studies will be undertaken to establish the chronology of a possible late Pleistocene scoria-fall event at the Hidden Cone center. These results will test polygenetic models for the center. The chronology of the Lathrop Wells center will be further studied through completion of step-heating, $^{40}Ar/^{39}Ar$ ages for tuff lithic fragments from chronostratigraphic units I, II, and III.

3. Revised geologic mapping will be completed for the basalt of southeast Crater Flat and the Makani and Little Cones centers. Revised volume calculations will be completed using the results of the geologic mapping.

4. Future geochemistry studies will focus on the major-, trace-element and isotopic compositions of Pliocene and Quaternary volcanic units of the CFVZ. The data will be used to test eruptive models and models of magma genesis. These data may prove especially important for assessing multiple versus single-pulse models of magma origins. Data from the geochemical studies will also provide iterative tests of the completeness of alternative models used in recurrence rate estimations.

5. A major area of future geochemistry studies will be in testing and developing alternative models for future patterns of evolution of basaltic volcanism in the YMR.

6. Annual reassessments of E2 will be conducted incorporating results of structural controls of sites of basaltic volcanism and tectonic studies of the YMR.

7. Assessment of the possible presence of magma bodies in the YMR will be accomplished by evaluation of results of planned geophysical studies including a seismic reflection/refraction line across Crater Flat and Yucca Mountain and teleseismic studies utilizing planned upgrades to the seismic net. Future studies will be planned, if required, pending the results of these studies.

8. The first phase of formal assessment of the probability of magmatic disruption has been completed. The framework calculations and simulation matrices will be used to facilitate yearly updates incorporating results of continuing site characterization studies. Formal methods of expert judgment will be used to further refine E1, E2, and E2 given E1. Probability estimations will be made for the recurrence of polygenetic activity at an existing center or from a cluster associated with an existing volcanic center. The uncertainty of probability calculations will continue to be assessed through simulation modeling. This approach will be extended to studies of E3. Cumulative probability distributions will be assessed and provided as input into performance assessment studies.